

R. G. Wilkins

مدرسۀ شیمی - دانشکدۀ شیمی - دانشگاه تهران

# **Kinetics and Mechanism of Reactions of Transition Metal Complexes**



© VCH Verlagsgesellschaft mbH, D-6940 Weinheim (Federal Republic of Germany), 1991

Distribution:

VCH, P. O. Box 101161, D-6940 Weinheim (Federal Republic of Germany)

Switzerland: VCH, P. O. Box, CH-4020 Basel (Switzerland)

United Kingdom and Ireland: VCH (UK) Ltd., 8 Wellington Court, Cambridge CB1 1HZ (England)

USA and Canada: VCH, Suite 909, 220 East 23rd Street, New York, NY 10010-4606 (USA)

ISBN 3-527-28389-7 (VCH, Weinheim)

ISBN 1-56081-198-6 (VCH, New York)

Ralph G. Wilkins

# **Kinetics and Mechanism of Reactions of Transition Metal Complexes**

2nd Thoroughly Revised Edition



Weinheim · New York · Basel · Cambridge

Prof. Ralph G. Wilkins  
University of Warwick  
Dept. of Chemistry  
Coventry CV4 7AL  
Great Britain

This book was carefully produced. Nevertheless, author and publisher do not warrant the information contained therein to be free of errors. Readers are advised to keep in mind that statements, data, illustrations, procedural details or other items may inadvertently be inaccurate.

1st edition 1974  
2nd edition 1991

Published jointly by  
VCH Verlagsgesellschaft mbH, Weinheim (Federal Republic of Germany)  
VCH Publishers, Inc., New York, NY (USA)

Editorial Director: Karin von der Saal  
Production Manager: Elke Littmann

Library of Congress Card No. applied for.

A CIP catalogue record for this book is available  
from the British Library.

Deutsche Bibliothek Cataloguing-in-Publication Data:  
Wilkins, Ralph G.:  
Kinetics and mechanism of reactions of transition metal  
complexes / Ralph G. Wilkins. – 2., thoroughly rev. ed. –  
Weinheim ; New York ; Basel ; Cambridge : VCH, 1991  
ISBN 3-527-28389-7 (Weinheim ...) brosch.  
ISBN 3-527-28253-X (Weinheim ...) Gb.  
ISBN 1-56081-198-6 (New York) brosch.  
ISBN 1-56081-125-0 (New York) Gb.

© VCH Verlagsgesellschaft mbH, D-6940 Weinheim (Federal Republic of Germany), 1991

Printed on acid-free and low chlorine paper.

All rights reserved (including those of translation into other languages). No part of this book may be reproduced in any form – by photoprinting, microfilm, or any other means – nor transmitted or translated into a machine language without written permission from the publishers. Registered names, trademarks, etc. used in this book, even when not specifically marked as such, are not to be considered unprotected by law.

Composition: Filmsatz Unger und Sommer GmbH, D-6940 Weinheim. Printing and bookbinding: Konrad Tritsch, Graphischer Betrieb, D-8700 Würzburg. Cover design: TWI, Herbert J. Weisbrod, D-6943 Birkenau. Printed in the Federal Republic of Germany



## Preface

Seventeen years is a long time between editions of a book. In order to add some of the vast amount of new material which has been published in that time, I have needed to abridge the older edition and in so doing apologise to oldtimers (myself included!) whose work may have been removed or modified. Nevertheless, the approach used is unchanged. In the first three chapters I have dealt with the acquisition of experimental data and discussed use for building up the rate law and in the deduction of mechanism. In the second part of the book, the mechanistic behavior of transition metal complexes of the Werner type is detailed, using extensively the principles and concepts developed in the first part.

There are noticeable changes from the first edition. The past decade or so has seen a marked increase in the use of photolytic and nmr methods, pressure effects and so on, to discover the intimate details of mechanism. These developments have been incorporated. So too, the growing interest in the biological aspects of inorganic chemistry has not been ignored. On the other hand, photochemical behavior and organometallic compounds are used for illustrative purposes only. I have succumbed to the use of SI units for energy, recognizing that much of the past (and a sizeable amount of the present) literature do not employ these. I shall never forget the factor 4.184 which converts old to new. I have increased the number of problems threefold and provided a section containing hints on their solution.

I would like to thank Dave Pennington for his careful examination of Chapter 5, Steve Davies for producing the structures, Ellen Foley and Merlin Callaway for valient typing and the staff of VCH, especially Michael Weller and Karin von der Saal, for their kind help in the production of the book. Many copyright holders gave permission to reproduce material. All these people have my sincere thanks. At the end of course, errors that remain are my responsibility alone.

My especial thanks go to my wife, Pat. She critically read the whole manuscript and gave much encouragement and understanding from the beginning. The book would never have appeared without her support and I dedicate it to her, with much love.

Ralph G. Wilkins, June 1991  
Wappenbury, England

# Contents

<b>Ligands and Complexes</b> . . . . .	<b>XIII</b>
<b>1 The Determination of the Rate Law</b> . . . . .	<b>1</b>
1.1 The Rate of a Reaction and the Rate Law . . . . .	1
1.2 The Rate Law Directly from Rate Measurements . . . . .	2
1.2.1 Initial-Rate Method . . . . .	3
1.2.2 Critique of the Initial-Rate Method . . . . .	4
1.2.3 Steady-State Approach . . . . .	5
1.3 Integrated Forms of the Rate Expression . . . . .	5
1.4 Monophasic Unidirectional Reactions . . . . .	7
1.4.1 Zero-Order Dependence . . . . .	7
1.4.2 First-Order Dependence . . . . .	8
1.4.3 Second-Order Dependence . . . . .	10
1.4.4 Conversion of Pseudo to Real Rate Constants . . . . .	11
1.5 Monophasic Reversible Reactions . . . . .	13
1.5.1 Conversion of Reversible to Unidirectional Reactions . . . . .	15
1.6 Multiphasic Unidirectional Reactions . . . . .	16
1.6.1 Concurrent Reactions . . . . .	17
1.6.2 Consecutive Reactions with no Elements of Reversibility . . . . .	18
1.6.3 Two-Step Reactions with an Element of Reversibility . . . . .	23
1.6.4 Reaction Schemes Associated with (1.98) . . . . .	24
1.6.5 Two-Step Reactions with Total Reversibility . . . . .	27
1.7 Recapitulation . . . . .	31
1.8 Relaxation Kinetics . . . . .	32
1.8.1 Single-Step Reactions . . . . .	32
1.8.2 Multistep Reactions . . . . .	33
1.9 Exchange Kinetics . . . . .	38
1.10 The Inclusion of $[H^+]$ Terms in the Rate Law . . . . .	41
1.10.1 One Monoprotic Reactant, One Acid-Base Equilibrium . . . . .	41
1.10.2 Two Acid-Base Equilibria . . . . .	43
1.10.3 The Effect of High Acid Concentration . . . . .	47
1.11 Kinetics and Thermodynamics . . . . .	49
1.12 Concluding Remarks . . . . .	50
References . . . . .	50
Problems . . . . .	56

<b>2</b>	<b>The Deduction of Mechanism</b> . . . . .	65
2.1	The Rate Law and Mechanism . . . . .	65
2.1.1	First-Order Reactions . . . . .	67
2.1.2	Second-Order Reactions . . . . .	68
2.1.3	Third-Order Reactions . . . . .	69
2.1.4	Even Higher-Order Reactions . . . . .	72
2.1.5	Negative-Order Reactions . . . . .	72
2.1.6	Fractional-Order Reactions . . . . .	73
2.1.7	The Inclusion of $[H^+]$ Terms in the Rate Law . . . . .	75
2.2	Further Checks of Mechanism . . . . .	80
2.2.1	The Detection and Study of Intermediates . . . . .	80
2.2.2	The Determination of Bond Cleavage . . . . .	84
2.3	Activation Parameters, Thermodynamic Functions and Mechanism . . . . .	87
2.3.1	The Effect of Temperature on the Rate of a Reaction . . . . .	87
2.3.2	The Variation of $E_a$ or $\Delta H^\ddagger$ with Temperature . . . . .	89
2.3.3	The Effect of Pressure on the Rate of a Reaction . . . . .	90
2.3.4	The Variation of $\Delta V^\ddagger$ with Pressure . . . . .	91
2.3.5	Activation Parameters and Concentration Units . . . . .	91
2.3.6	Reaction Profiles . . . . .	91
2.4	Free Energy of Activation and Mechanism . . . . .	93
2.5	Linear Free-Energy Relationships – $\Delta G^\ddagger$ and $\Delta G$ . . . . .	96
2.5.1	Hammett Relationship . . . . .	99
2.5.2	Taft Relationship . . . . .	101
2.5.3	Brønsted Relationship . . . . .	101
2.5.4	Swain-Scott Relationship . . . . .	103
2.6	Enthalpy of Activation and Mechanism . . . . .	104
2.7	Entropy of Activation and Mechanism . . . . .	105
2.7.1	$\Delta S^\ddagger$ and the Charge of the Reactants . . . . .	105
2.8	Volume of Activation and Mechanism . . . . .	106
2.8.1	$\Delta H^\ddagger$ and $\Delta S^\ddagger$ Values – The Isokinetic Relationship . . . . .	108
2.8.2	$\Delta S^\ddagger$ and $\Delta V^\ddagger$ Values . . . . .	109
2.8.3	Use of All Parameters . . . . .	110
2.9	Medium Effects on the Rate . . . . .	110
2.9.1	The Effect of Electrolytes . . . . .	110
2.9.2	The Effect of Electrolytes – Medium or Mechanistic? . . . . .	115
2.9.3	The Solvent Effect and Mechanism . . . . .	116
	References . . . . .	118
	Problems . . . . .	123
<b>3</b>	<b>The Experimental Determination of the Rate of Reaction</b> . . . . .	131
3.1	Essential Preliminaries . . . . .	131
3.1.1	Reactant Species in Solution . . . . .	131
3.1.2	Stoichiometry of Reaction . . . . .	133
3.1.3	The Nature of the Products . . . . .	133

3.1.4	The Influence of Impurities . . . . .	134
3.1.5	The Control of Experimental Conditions . . . . .	134
3.2	The Methods of Initiating Reaction and their Time Ranges . . . . .	135
3.3	Flow Methods . . . . .	136
3.3.1	Continuous Flow . . . . .	137
3.3.2	Quenched Flow . . . . .	138
3.3.3	Stopped Flow . . . . .	139
3.4	Relaxation Methods . . . . .	140
3.4.1	Temperature Jump . . . . .	141
3.4.2	Pressure Jump . . . . .	141
3.4.3	Electric-Field Jump . . . . .	143
3.4.4	Ultrasonic Absorption . . . . .	144
3.5	Large Perturbations . . . . .	145
3.5.1	Flash or Laser Photolysis . . . . .	145
3.5.2	Pulse Radiolysis . . . . .	148
3.5.3	Comparison of Large Perturbation Methods . . . . .	151
3.6	Competition Methods . . . . .	151
3.7	Accessible Rate Constants Using Rapid Reaction Methods . . . . .	151
3.8	The Methods of Monitoring the Progress of a Reaction . . . . .	153
3.9	Spectrophotometry . . . . .	154
3.9.1	Ultraviolet and Visible Regions . . . . .	154
3.9.2	Infrared Region . . . . .	158
3.9.3	Fluorescence . . . . .	159
3.9.4	Polarimetry . . . . .	160
3.9.5	Nmr Region . . . . .	161
3.9.6	Nmr Line Broadening . . . . .	163
3.9.7	Epr Region . . . . .	169
3.9.8	Epr Line Broadening . . . . .	170
3.10	Non-Spectrophotometric Methods . . . . .	171
3.10.1	[H <sup>+</sup> ] Changes . . . . .	171
3.10.2	Cationic and Anionic Probes . . . . .	173
3.10.3	Conductivity . . . . .	173
3.10.4	Thermal Changes . . . . .	174
3.10.5	Pressure Changes . . . . .	174
3.10.6	Electrochemical Methods . . . . .	174
3.11	Batch Methods . . . . .	175
3.12	Competition Methods . . . . .	176
3.12.1	Stern-Volmer Relationship . . . . .	177
3.12.2	Isotope Fractionation . . . . .	178
3.13	The Study of Transients . . . . .	178
3.13.1	Spectral Properties of Transients . . . . .	179
3.13.2	Thermodynamic Properties of Transients . . . . .	180
3.13.3	Chemical Reactivity of Transients . . . . .	180
	References . . . . .	181
	Problems . . . . .	192

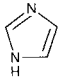
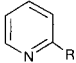
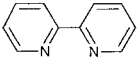
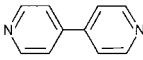
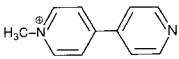
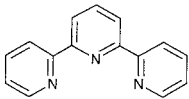
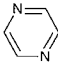
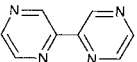
<b>4</b>	<b>Substitution Reactions</b>	199
4.1	The Characteristics of Substitution Reactions	199
4.1.1	Solvated Metal Ions	200
4.1.2	Representation of Substitution Mechanisms	201
4.2	Substitution in Octahedral Complexes	201
4.2.1	Solvent Exchange with Metal Ions	202
4.2.2	The Interchange of Different Unidentate Ligands	205
4.2.3	Outer Sphere Complexes	206
4.2.4	Characteristics of the Various Mechanisms	207
4.2.5	The Limiting First-Order Rate Constant	208
4.2.6	Second-Order Rate Constants	210
4.2.7	Summary	211
4.3	Accelerated Substitution of Unidentate Ligands	212
4.3.1	H <sup>+</sup> -Assisted Removal	212
4.3.2	Metal Ion-Assisted Removal	213
4.3.3	Ligand-Assisted Removal	214
4.3.4	Base-Assisted Removal	215
4.3.5	The Quest for Five Coordinate Intermediates	217
4.4	Replacement Reactions Involving Multidentate Ligands	219
4.4.1	The Formation of Chelates	219
4.4.2	Effect of [H <sup>+</sup> ] on the Rates of Substitution in Chelate Complexes	221
4.4.3	Metal Ion-Assisted Dechelation	222
4.4.4	Ligand-Assisted Dechelation	223
4.5	Replacement Reactions Involving Macrocycles	224
4.5.1	Azamacrocycles	226
4.5.2	Crown-Ethers and Cryptands	227
4.5.3	Porphyrins	229
4.6	Substitution in Square-Planar Complexes	232
4.6.1	The Kinetics of Replacement Involving Unidentate Ligands	232
4.6.2	Activation Parameters	235
4.7	Ligand Effects on the Rate	236
4.7.1	Effect of Entering Ligand	236
4.7.2	Effect of Leaving Group	237
4.7.3	Effect of Ligands Already Present	237
4.7.4	Effect of Solvent	238
4.7.5	Reaction Pathways	238
4.7.6	Chelation in Square-Planar Complexes	240
4.8	Substitution in Tetrahedral Complexes	242
4.9	Substitution in Five-Coordinate Complexes	243
4.10	Substitution in Organized Surfactant Systems	244
4.11	Substitution in Metalloproteins	245
	References	246
	Problems	252

<b>5</b>	<b>Oxidation-Reduction Reactions</b>	257
5.1	General Characteristics	257
5.2	Classification of Redox Reactions	258
5.3	Characterization of Mechanism	259
5.4	Outer Sphere Reactions	262
5.4.1	The Applications of the Marcus Expression	269
5.5	Inner Sphere Redox Reactions	269
5.6	The Bridging Ligand in Inner-Sphere Redox Reactions	270
5.7	Some Other Features of Redox Reactions	272
5.7.1	Mixed Outer- and Inner-Sphere Reactions	275
5.7.2	Two-Electron Transfer	276
5.7.3	Redox Catalyzed Substitution	276
5.7.4	Stereoselectivity	277
5.8	Intramolecular Electron Transfer	279
5.8.1	Between Two Metal Centers	279
5.8.2	Metal Complexes with Reducible Ligands	282
5.8.3	Induced Electron Transfer	284
5.9	Electron Transfer in Proteins	285
5.10	The Future	288
	References	288
	Problems	292
<b>6</b>	<b>The Modification of Ligand Reactivity by Complex Formation</b>	299
6.1	The Metal as a Collecting Point Reactant	299
6.1.1	Neighboring Group Effects	300
6.1.2	Template Chemistry	301
6.1.3	Collecting Reactant Molecules	303
6.2	Promotion of Reaction within the Metal-Bound Ligand	305
6.3	Hydrolysis of Coordinated Ligands	308
6.3.1	Carboxylate Esters: $-\text{CO}_2\text{R} \rightarrow -\text{CO}_2\text{H}$	308
6.3.2	Amides and Peptides: $-\text{CONHR} \rightarrow -\text{CO}_2\text{H}$	311
6.3.3	Nitriles: $-\text{CN} \rightarrow -\text{CONH}_2$	313
6.3.4	Phosphate Esters: $\text{ROPO}_3^{2-} \rightarrow \text{PO}_4^{3-}$	314
6.3.5	Other Groups	317
6.4	The Acidity of Coordinated Ligands	317
6.4.1	Coordinated Water	318
6.4.2	Coordinated Ammonia and Amines	320
6.4.3	Other Coordinated Ligands	320
6.5	Electrophilic Substitution in Metal Complexes	322
6.6	Masking Effects	322
6.7	Disturbance of Reaction Stoichiometry	323
6.8	Molecular Strain Alterations	323
6.9	Function of the Ligand	324
6.10	Conclusions	325

References . . . . .	325
Problems . . . . .	328
<b>7 Isomerism and Stereochemical Change . . . . .</b>	<b>337</b>
7.1 Conformational Isomerism . . . . .	334
7.2 Configurational Isomerism . . . . .	335
7.2.1 Planar, Tetrahedral . . . . .	336
7.2.2 Planar, Square Pyramidal . . . . .	336
7.2.3 Planar, Octahedral . . . . .	337
7.2.4 Tetrahedral, Octahedral . . . . .	338
7.3 Spin Equilibria in Octahedral Complexes . . . . .	339
7.4 Linkage Isomerism . . . . .	340
7.4.1 Rearrangement Studies . . . . .	341
7.5 Geometrical and Optical Isomerism . . . . .	343
7.6 Octahedral Complexes . . . . .	343
7.6.1 Complexes of the Type $M(AA)_3$ . . . . .	343
7.6.2 Complexes of the type $M(AA_1)_3$ . . . . .	348
7.6.3 Complexes of the Type $M(L_1)(L_2)$ . . . . .	351
7.6.4 Complexes of the Type $M(AA)_2X_2$ and $M(AA)_2XY$ . . . . .	351
7.6.5 Isomeric Forms As Biological Probes . . . . .	354
7.7 Four-Coordinated Complexes . . . . .	355
7.7.1 Optical Isomerism in Tetrahedral Complexes . . . . .	355
7.7.2 Geometrical Isomerism in Square Planar Complexes . . . . .	356
7.8 Five-, Seven- and Eight-Coordinated Complexes . . . . .	359
7.9 Inversion and Proton Exchange at Asymmetric Nitrogen . . . . .	360
References . . . . .	365
Problems . . . . .	368
<b>8 A Survey of the Transition Elements . . . . .</b>	<b>373</b>
References . . . . .	424
Problems . . . . .	433
<b>Problems – Hints to Solutions . . . . .</b>	<b>443</b>
<b>Index . . . . .</b>	<b>455</b>

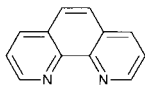
# Ligands and Complexes

## Ligand Abbreviations

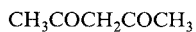
$\text{NH}_2(\text{CH}_2)_x\text{NH}_2$	en ( $x=2$ ); tn ( $x=3$ )	
$\text{NH}_2(\text{CH}_2)_2\text{NH}(\text{CH}_2)_2\text{NH}_2$	dien	
$\text{NH}_2(\text{CH}_2)_2\text{NH}(\text{CH}_2)_2\text{NH}(\text{CH}_2)_2\text{NH}_2$	trien	sal <sub>2</sub> trien
$\text{N}[(\text{CH}_2)_x\text{NH}_2]_3$	tren ( $x=2$ ); trpn ( $x=3$ )	
$\text{NH}(\text{CH}_2\text{CO}_2)_2^-$	ida <sup>2-</sup>	
$\text{N}(\text{CH}_2\text{CO}_2)_3^-$	nta <sup>3-</sup>	
$[\text{^-OCOCH}_2]_2\text{N-X-N}[\text{CH}_2\text{COO}^-]_2$	edta <sup>4-</sup> ( $\text{X}=(\text{CH}_2)_2$ ); pdta <sup>4-</sup> ( $\text{X}=\text{CH}(\text{CH}_3)\text{CH}_2$ ); cydta <sup>4-</sup> ( $\text{X}=1,2\text{-cyclohexyl}$ )	
	imid	
	py ( $\text{R}=\text{H}$ ); pic <sup>-</sup> ( $\text{R}=\text{CH}_2\text{CO}_2^-$ )	
	2,2'-bpy	
	4,4'-bpy	
	mbpy <sup>+</sup>	
	tpy	
	pz	
	bpz	



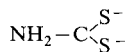
XIV Ligands and Complexes



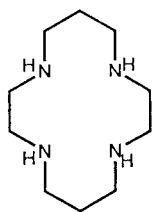
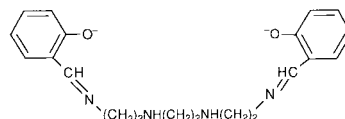
phen



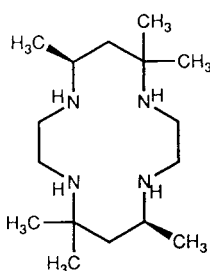
acacH



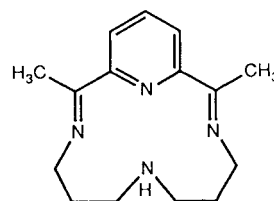
dtc<sup>2-</sup>



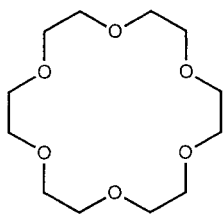
[14]ane-1,4,8,11-N<sub>4</sub>  
[14]aneN<sub>4</sub> or cyclam



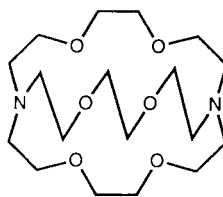
rac-(5,12)-Me<sub>6</sub>[14]aneN<sub>4</sub>  
tet b



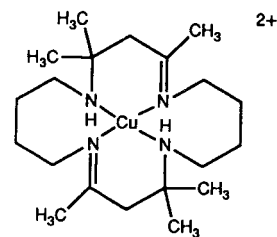
Me<sub>2</sub>pyo[14]trieneN<sub>4</sub>



[18]crown-6

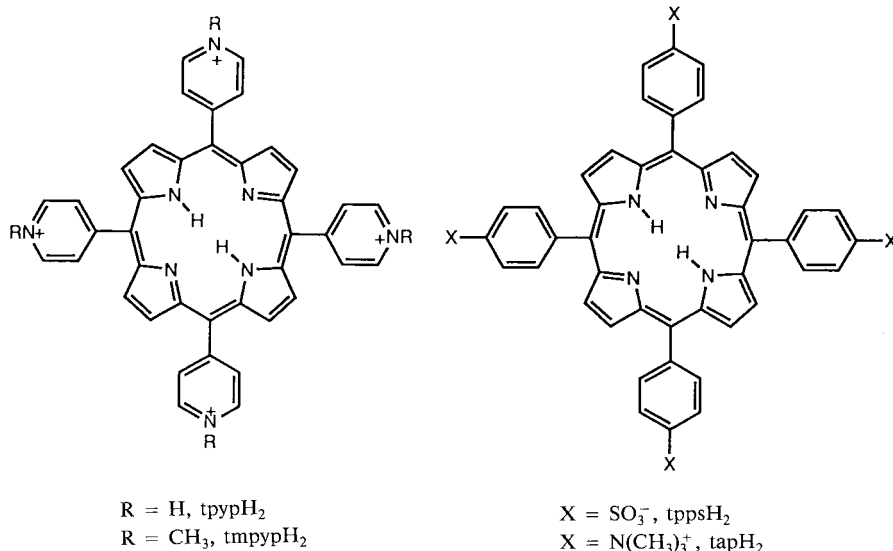


cryptand 2<sub>0</sub>2<sub>0</sub>2<sub>0</sub>  
(the numbers indicate the oxygens on each strand of the macrocyclic ligand)

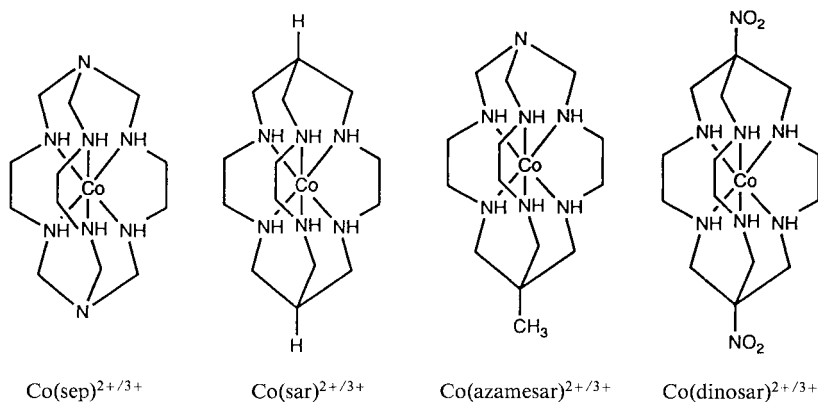


Cu(trans-(CH<sub>3</sub>)<sub>6</sub>[18]dieneN<sub>4</sub>)<sup>2+</sup>

*Some commonly used macrocycles.* – The number in brackets indicates the size of the ring. The terms ane and ene denote saturated and unsaturated rings respectively. The number of ligating atoms is indicated by a subscript. A trivial name is often used (G. A. Melson in *Coordination Chemistry of Macrocyclic Compounds*, Ed. G. A. Melson, Plenum, New York, 1979, Chapter 1; *Comprehensive Coordination Chemistry*, Ed. G. Wilkinson, Pergamon, Oxford, 1987. Several chapters in Vol. 2 (Ligands)).



*Some Useful Water-Soluble Porphyrins*



*Some Caged Cobalt Complexes* — The synthesis of these macrocycles is based on both the metal template effect as well as metal-ion activation of the imine moiety to nucleophilic attack, which initiates encapsulation (Chap. 6). A large variety of groups can replace  $\text{NO}_2$  in  $\text{Co}(\text{dinosar})^{3+}$  yielding complexes with a wide range of properties. Again, trivial abbreviations are employed e.g. sep replaces 1,3,6,8,10,13,16,19-octaazabicyclo[6.6.6]eicosane. A. M. Sargeson, *Pure Appl. Chem.* 56, 1603 (1984).

# Chapter 1

## The Determination of the Rate Law

The single most important factor that determines the rate of a reaction is concentration – primarily the concentrations of the reactants, but sometimes of other species that may not even appear in the reaction equation. The relation between the rate of a reaction and the concentration of chemical species is termed the rate law; it is the cornerstone of reaction mechanisms. The rate law alone allows much insight into the mechanism. This is usually supplemented by an examination of other factors which can also be revealing. (For these, see Chap. 2)

### 1.1 The Rate of a Reaction and the Rate Law

The rate, or velocity, of a reaction is usually defined as the change with time  $t$  of the concentration (denoted by square brackets) of one of the reactants or of one of the products of the reaction; that is,

$$\text{rate} = V = -d[\text{reactant}]/dt = n \times d[\text{product}]/dt \quad (1.1)$$

The negative sign arises because there is a loss of reactant. The value of  $n$  is often 1, but a value other than unity arises when one molecule of the reactant produces other than one molecule of the product. Rates are usually expressed in moles per liter per second, which we shall designate  $\text{M s}^{-1}$ , although  $\text{dm}^{-3} \text{ mol s}^{-1}$  is also a popular abbreviation. The rate law expresses the rate of a reaction in terms of the concentrations of the reactants and of any other species in solution, including the products, that may affect the rate.<sup>1</sup>

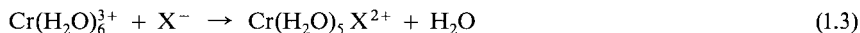
Suppose that the rate of a reaction depends only on the concentrations of A and B. The proportionality factor  $k$  relating rate to the concentrations of [A] and [B] in the rate law, or rate expression,

$$V = k [\text{A}]^a [\text{B}]^b \quad (1.2)$$

is usually termed the *rate constant*, although it is sometimes referred to as the *specific rate*, or *rate coefficient*. Although the latter terms are in some respects preferable, since the proportionality factor is rarely invariant, the term *rate constant* is used in most of the literature and it is unlikely that it will be replaced. The values of  $a$  and  $b$  in (1.2) determine the *order of the reaction*. If  $a = 1$ , the reaction is termed *first-order* in A, and if  $a = 2$ , the reaction is *second-*

order in A. These are the most frequently encountered orders of reaction. The overall order of the reaction is  $(a + b)$ . The rate may be independent of the concentration of A, even if it participates in the overall stoichiometry. In this case,  $a = 0$ , and the reaction is *zero-order* in A. The concentration of A does not then feature in the rate law.

The formation of a number of chromium(III) complexes  $\text{Cr}(\text{H}_2\text{O})_5\text{X}^{2+}$  from their constituent ions  $\text{Cr}(\text{H}_2\text{O})_6^{3+}$  and  $\text{X}^-$ ,



where  $\text{X}^-$  represents a unidentate ligand, obeys the two-term rate law (the coordinated water being usually omitted from the formula)

$$V = d[\text{CrX}^{2+}]/dt = k_1[\text{Cr}^{3+}][\text{X}^-] + k_2[\text{Cr}^{3+}][\text{X}^-][\text{H}^+]^{-1} \quad (1.4)$$

over a wide range of concentration of reactants and acid.<sup>2</sup> Symbols such as  $a$  and  $b$  instead of  $k_1$  and  $k_2$  may be used in (1.4), since these quantities are often composite values, made up of rate and equilibrium constants. To maintain both sides of (1.4) dimensionally equivalent,

$$V = \text{M s}^{-1} = k_1 \times \text{M}^2 = k_2 \times \text{M} \quad (1.5)$$

$k_1$  and  $k_2$  must obviously be expressed in units of  $\text{M}^{-1} \text{s}^{-1}$  and  $\text{s}^{-1}$  respectively. This simple application of dimension theory is often useful in checking the correctness of a complex rate law (see 1.121 and Probs. 1, Chap. 1 and Chap. 2).

If we consider specifically the formation of  $\text{CrBr}^{2+}$ , the rate law

$$d[\text{CrBr}^+]/dt = 3.0 \times 10^{-8} [\text{Cr}^{3+}][\text{Br}^-] + 3.6 \times 10^{-9} [\text{Cr}^{3+}][\text{Br}^-][\text{H}^+]^{-1} \quad (1.6)$$

holds at 25.0°C, and an ionic strength of 1.0 M.<sup>2</sup> The majority of kinetic determinations are carried out at a constant ionic strength by the addition of an “unreactive” electrolyte which is at a much higher concentration than that of the reactants. At high acid concentrations ( $>1 \text{ M}$ ), the first term in (1.6) is larger than the second, and the reaction rate is virtually acid-independent. At lower acid concentrations ( $\sim 10^{-2} \text{ M}$ ), the second term dominates and the rate of reaction is now inversely proportional to  $[\text{H}^+]$ . This emphasizes the importance of studying the rate of a reaction over as wide a range of concentrations of species as possible so as to obtain an extensive rate law.

## 1.2 The Rate Law Directly from Rate Measurements

If the rate of a reaction can be measured at a time for which the concentrations of the reactants are known, and if this determination can be repeated using different concentrations of reactants, it is clear that the rate law (1.2) can be deduced directly. It is not often obtained in this manner, however, despite some distinct advantages inherent in the method.

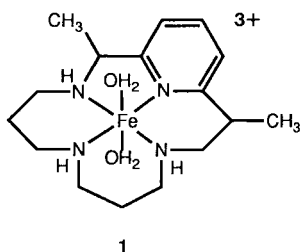
### 1.2.1 Initial-Rate Method

The rate of reaction is measured at the commencement of the reaction, when the concentrations of the reactants are accurately known, indeed predetermined.

The decomposition of  $\text{H}_2\text{O}_2$  (1.7)



is catalyzed by many metal complexes and enzymes.<sup>3</sup> The rate law for catalysis by an iron(III) macrocycle complex **1** has been deduced by measuring the initial rates  $V_0$  of oxygen production.<sup>3</sup> A selected number from many data are shown in Table 1.1.



**Table 1.1.** Initial Rate Data for the Catalyzed Decomposition of  $\text{H}_2\text{O}_2$  by an Fe(III) Macrocycle at  $25^\circ\text{C}$ <sup>3</sup>

Run	$[\text{H}_2\text{O}_2]_0$ M	Fe(III) mM	$[\text{H}^+]$ $10^5 \text{ M}$	$[\text{OAc}]_T$ M	$10^3 \times$ Initial Rate $10^3 \text{ M s}^{-1}$	$10^3 k^a$ $\text{s}^{-1}$
1	0.18	0.41	2.45	0.05	54	5.0
2	0.18	0.74	2.45	0.05	85	4.4
3	0.18	1.36	2.45	0.05	160	4.5
4	0.12	0.66	2.45	0.05	37	5.0
5	0.18	0.66	2.45	0.05	78	4.5
6	0.36	0.66	2.45	0.05	306	4.5
7	0.18	0.66	1.0	0.05	191	4.9
8	0.18	0.66	2.45	0.05	86	4.8
9	0.18	0.66	11.5	0.05	24	6.5
10	0.18	0.66	2.45	0.02	233	5.2
11	0.18	0.66	2.45	0.05	86	4.8
12	0.18	0.66	2.45	0.17	26	4.9

<sup>a</sup> Obtained from  $k = V_0 [\text{H}^+] [\text{OAc}]_T [\text{Fe(III)}]^{-1} [\text{H}_2\text{O}_2]_0^{-2}$ , a rearrangement of (1.8). Note the units of  $k$ .

It is apparent from these data that within experimental error the initial rate is proportional to the initial concentration of iron(III) complex, (Runs 1–3) to the square of the initial  $\text{H}_2\text{O}_2$  concentration  $[\text{H}_2\text{O}_2]_0$  (4–6) and inversely dependent on both  $\text{H}^+$  (7–9) and total acetate  $[\text{OAc}]_T$  (10–12) concentrations. A rate law involving the initial rate  $V_0$ ,

$$V_0 = +d[\text{O}_2]/dt = k [\text{Fe(III)}] [\text{H}_2\text{O}_2]_0^2 [\text{H}^+]^{-1} [\text{OAc}]_T^{-1} \quad (1.8)$$

applies therefore and values of  $k$  calculated on this basis are reasonably constant. They are shown in the last column of Table 1.1. Raw initial rate data are also included in papers dealing with the  $\text{Cr(VI)-I}^-$  reaction,<sup>4</sup> and the reaction of pyridoxal phosphate with glutamate in the presence of copper ions.<sup>5</sup> See Prob. 2.

Initial reaction rates are often estimated from the steepest tangents to absorbance/time traces. These initial gradients (absorbance units/sec) are easily converted into  $\text{M s}^{-1}$  units by using the known molar absorptivities of products and reactants. Alternatively, absorbance ( $D$ )/Time ( $T$ ) plots can be fit to a function (1.9) leading to (1.10) and (1.11)

$$F(D) = C_1 + C_2T + C_3T^2 + C_4T^3 \dots \quad (1.9)$$

$$d[D]/dt = C_2 + 2C_3T + 3C_4T^2 \quad (1.10)$$

$$\text{At } T = 0, \quad d[D]/dt = C_2 \quad (1.11)$$

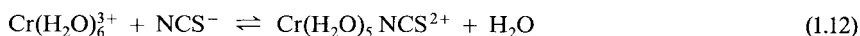
as illustrated in the study of the reaction of  $\text{H}_2\text{O}_2$  with 1,3-dihydroxybenzene in the presence of  $\text{Cu(II)}$  ions,<sup>6(a)</sup> and in the disproportionation of  $\text{Mn(VI)}$ .<sup>6(b)</sup>

## 1.2.2 Critique of the Initial-Rate Method

The merits and difficulties in the use of this method are summarized:

(a) The initial-rate method is useful in the study of reactions complicated by side reactions or subsequent steps. The initial step of hydrolytic polymerization of  $\text{Cr(III)}$  is dimerization of the monomer. As soon as the dimer is formed however, it reacts with the monomer or with dimer to form trimer or tetramer, respectively. Initial rates (using a pH stat, Sec. 3.10.1 (a)) are almost essential in the measurement of dimer formation.<sup>7</sup>

The reverse reaction in (1.12)



is unimportant during the early stages of the forward reaction when the products have not accumulated. A small initial loss of free thiocyanate ion can be accurately monitored by using the sensitive  $\text{Fe(III)}$  colorimetric method. The reverse reaction can be similarly studied for the initial rate of thiocyanate ion appearance by starting with  $\text{Cr(H}_2\text{O)}_5\text{NCS}^{2+}$  ions.<sup>8</sup>

(b) Complicated kinetic expressions and manipulations may be thus avoided. The initial-rate method is extensively employed for the study of enzyme kinetics and in enzyme assay (Prob. 3), simplifying the kinetics (see Selected Bibliography). Obviously the method cannot cope with the situation of induction periods or initial burst behavior. Furthermore a complex rate law, giving a wealth of mechanistic information, may now be disguised (for an example see Ref. 9). Despite this the initial-rate approach can be useful for distinguishing between two similar reaction schemes e.g. (1.13) and (1.14) (Sec. 1.6.4(d)).



in which A plus B yields D either *via* C or directly. The resolution otherwise requires very accurate relaxation data.<sup>10</sup>

(c) Two obvious disadvantages of the method are that many individual runs must be carried out to build up a rate law and a sensitive monitoring technique is required in order to obtain accurate concentration/time data for the first few percentage of the reaction. While nothing can be done about the first point, the advent of very sensitive computer-linked monitoring devices is ameliorating the sensitivity problem.

### 1.2.3 Steady-State Approach

In the steady-state approach to determining the rate law, solutions containing reactants are pumped separately at a constant flow rate into a vessel (“reactor”), the contents of which are vigorously stirred. After a while, products and some reactants will flow from the reactor at the same total rate of inflow and a steady state will be attained, in which the reaction will take place in the reactor with a *constant concentration of reactants*, and therefore a *constant rate*. This is the basis of the stirred-flow reactor, or capacity-flow method.<sup>11</sup> Although the method has been little used, it has the advantage of a simplified kinetic treatment even for complex systems.

## 1.3 Integrated Forms of the Rate Expression

Consider a reaction that proceeds to completion in which the concentration of only one reactant, A, changes appreciably during the reaction. This may arise because (1) there is only one reactant A involved – for example, in a stereochemical change; (2) all the other possible reactants are in much larger ( $\geq$  tenfold) concentration than A; or (3) the concentration of one of the other reactants may be held constant by buffering, or be constantly replenished, as it would be if it were acting in a catalytic role. Attention needs to be focused therefore only on the change of concentration of A as the reaction proceeds, and we can, for the present, forget about the other reactants. Now,

$$-d[A]/dt = k[A]^a \quad (1.15)$$

The manner in which [A] varies with time determines the order of the reaction with respect to A. Since it is usually much easier to measure a concentration than a rate, the form (1.15) is integrated.<sup>12</sup> The three situations  $a = 0$ , 1, and 2 account for the overwhelming number of kinetic systems we shall encounter, with  $a = 1$  by far the most common behavior.

$a = 0$ , zero-order in A:

$$-d[A]/dt = k \quad (1.16)$$

$$[A]_t = [A]_0 - kt \quad (1.17)$$

$a = 1$ , first order in A:

$$-d[A]/dt = k[A] \quad (1.18)$$

$$\log [A]_t = \log [A]_0 - kt/2.3 \quad (1.19)$$

or now increasingly common,

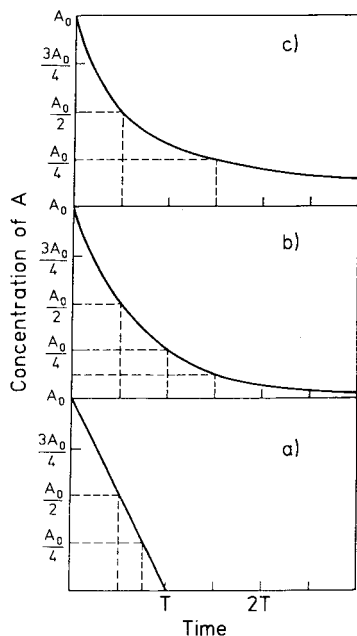
$$\ln[A]_t = \ln[A]_0 - kt \quad (1.19a)$$

$a = 2$ , second-order in A:

$$-d[A]/dt = k[A]^2 \quad (1.20)$$

$$\frac{1}{[A]_t} = \frac{1}{[A]_0} + kt \quad (1.21)$$

The differential (rate) forms are (1.16), (1.18) and (1.20), and the corresponding integrated forms are (1.17), (1.19) (or (1.19a)) and (1.21). The designations  $[A]_0$  and  $[A]_t$  represent the concentrations of A at zero time and time  $t$ . Linear plots of  $[A]_t$ ,  $\ln[A]_t$  or  $[A]_t^{-1}$  vs time therefore indicate zero-, first-, or second order dependence on the concentration of A. The important characteristics of these order reactions are shown in Fig. 1.1. Notwithstanding the appearance of the plots in 1.1(b) and 1.1(c), it is not always easy to differentiate between first- and second-order kinetics.<sup>13,14</sup> Sometimes a second-order plot of kinetic data might be mistaken for successive first-order reactions (Sec. 1.6.2) with similar rate constants.<sup>15</sup>



**Fig. 1.1** The characteristics of (a) zero- (b) first- and (c) second-order reactions. In (a) the concentration of A decreases linearly with time until it is all consumed at time  $T$ . The value of the zero-order rate constant is given by  $A_0/T$ . In (b) the loss of A is exponential with time. The plot of  $\ln[A]_t$  vs time is linear, the slope of which is  $k$ , the first-order rate constant. It obviously does not matter at which point on curve (b) the first reading is taken. In (c) the loss of A is hyperbolic with time. The plot of  $[A]_t^{-1}$  vs time is linear with a slope equal to  $k$ , the second-order rate constant.

In the unlikely event that  $a$  in (1.15) is a non-integer, the appropriate function must be plotted. In general, for (1.15),  $a \neq 1$ <sup>12</sup> (see Prob. 8)

$$\frac{1}{[A]_t^{a-1}} - \frac{1}{[A]_0^{a-1}} = (a - 1)kt \quad (1.22)$$



It should be emphasized that in the case that A is in deficiency over other reactants, B etc., then  $k$ , relating to loss of A, is a pseudo rate constant and the effect of the other reactants on the rate must still be assessed separately (Sec. 1.4.4).

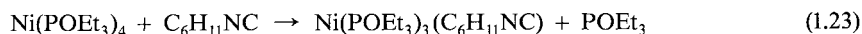
## 1.4 Monophasic Unidirectional Reactions

We shall first consider some straightforward kinetics, in which the loss of A, in the treatment referred to above, is monophasic and the reaction is unidirectional, that is, it leads to  $\geq 95\%$  loss of A.

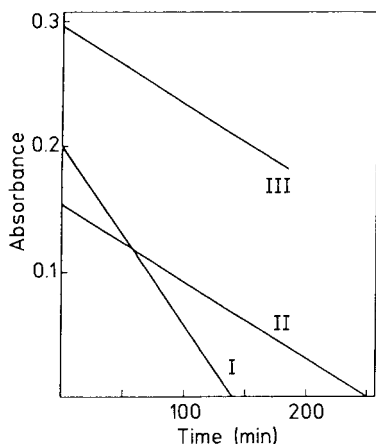
### 1.4.1 Zero-Order Dependence

It is impossible to conceive of a reaction rate as being independent of the concentration of *all* the species involved in the reaction. The rate might, however, very easily be independent of the concentration of one of the reactants. If this species, say A, is used in deficiency, then a pseudo zero-order reaction results. The rate  $-d[A]/dt$  will not vary as [A] decreases, and will *not* depend on the initial concentration of A.

In the substitution reaction



the loss of  $\text{C}_6\text{H}_{11}\text{NC}$  has been followed in the presence of excess Ni complex.<sup>16</sup> The linear plot of absorbance, which is proportional to isonitrile concentration, vs time indicates a reaction zero-order in isonitrile (Fig. 1.2).



**Fig. 1.2** Zero-order kinetic plots for reaction (1.23). Concentrations of  $\text{Ni}(\text{POEt}_3)_4$  are 95 mM(I), 48 mM(II) and 47 mM(III). Those of  $\text{C}_6\text{H}_{11}\text{NC}$  are 6.5 mM(I), 5.0 mM(II) and 9.7 mM(III).<sup>16</sup>

The slope of the zero-order plot (when absorbance is converted into concentration) is  $k, \text{M s}^{-1}$ . The value of  $k$  is found to be proportional to the concentration of  $\text{Ni}(\text{POEt}_3)_4$ , which is used in excess (Fig. 1.2),<sup>17</sup>

$$-d[\text{Ni}(\text{POEt}_3)_4]/dt = -1/2d[\text{C}_6\text{H}_{11}\text{NC}]/dt = k = k_1[\text{Ni}(\text{POEt}_3)_4] \quad (1.24)$$

The reaction is therefore overall first-order, with a first-order rate constant  $k_1 (\text{s}^{-1})$ . The zero-order situation is not often encountered (Prob. 4). A number of examples are compiled in Ref. 18 and one is shown in Fig. 8.3.

### 1.4.2 First-Order Dependence

First-order reactions are extremely common and form the bulk of reported kinetic studies. The rate of loss of the reactant A decreases as the concentration of A decreases. The differential form (1.18) leads to a number of equivalent integrated expressions, in addition to (1.19) and (1.19a):

$$[\text{A}]_t = [\text{A}]_0 \exp(-kt) \quad (1.25)$$

$$\ln([\text{A}]_0/[\text{A}]_t) = kt \quad (1.26)$$

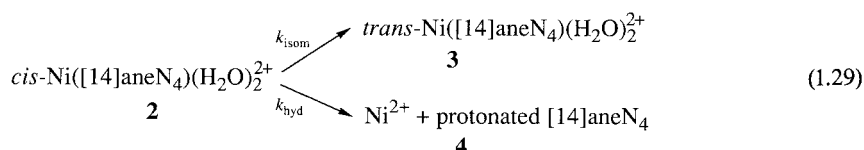
$$-d \ln [\text{A}]_t / dt = k \quad (1.27)$$

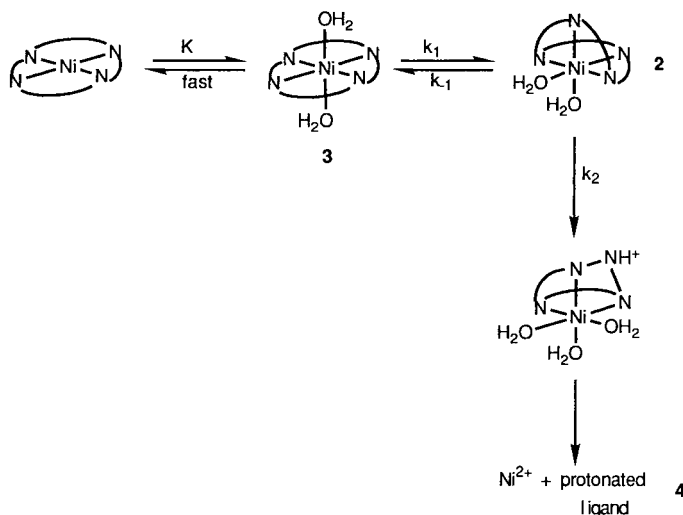
Important quantities characteristic of a first-order reaction are  $t_{1/2}$ , the half-life of the reaction, which is the value of  $t$  when  $[\text{A}]_t = [\text{A}]_0/2$ , and  $\tau$ , the relaxation time, or mean lifetime, defined as  $k^{-1}$ .

$$k = 0.693/t_{1/2} = 1/\tau \quad (1.28)$$

The latter is invariably used in the relaxation or photochemical approach to rate measurement (Sec. 1.8), and is the time taken for A to fall to  $1/e$  ( $1/2.718$ ) of its initial value. Half-lives or relaxation times are constants over the complete reaction for first-order or pseudo first-order reactions. The loss of reactant A with time may be described by a single exponential but yet may hide two or more concurrent first-order and/or pseudo first-order reactions.

The change in the absorbance at 450 nm when  $\text{cis-Ni}([\text{14}] \text{aneN}_4)(\text{H}_2\text{O})_2^{2+}$  (for structure see "Ligands and Complexes") is plunged into 1.0 M  $\text{HClO}_4$  is first-order (rate constant =  $k$ ). It is compatible with concurrent isomerization and hydrolysis (1.29)





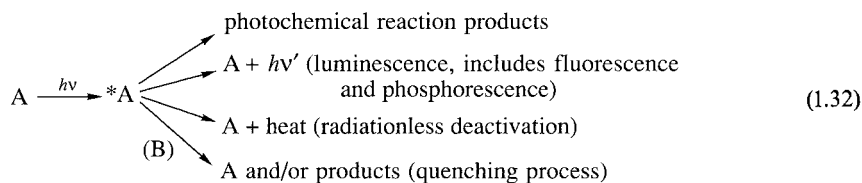
For this system

$$-d[2]/dt = k[2] = (k_{\text{isom}} + k_{\text{hyd}})[2] \quad (1.30)$$

Estimation of the amounts of **3** and **4** produced from the final absorbance change<sup>19</sup> allows determination of both  $k_{\text{isom}}$  and  $k_{\text{hyd}}$ .<sup>20</sup> See also Ref. 21.

$$k_{\text{isom}}/k_{\text{hyd}} = [3]/[4] \quad (1.31)$$

Concurrent first-order changes invariably arise from the decay of an excited state \*A which can undergo a number of first-order changes. In the presence of an excess of added B, pseudo first-order transformations can also occur:



The analysis of the immediate products or the isolation of one of the steps is essential in order to resolve the complexity.<sup>22</sup>

The reaction of a mixture of species A and A<sub>1</sub> which interconvert rapidly compared with the reaction under study, can also lead to a single first-order process. In order to resolve the kinetic data, information on the  $A \rightleftharpoons A_1$  equilibrium is essential. When the relative amounts of A and A<sub>1</sub> are pH-controlled however (Sec. 1.10.1) or when the products of reaction of A and A<sub>1</sub> differ and do not interconvert readily, resolution is also in principle possible.

### 1.4.3 Second-Order Dependence

Second-order kinetics play an important role in the reactions of complex ions. Two identical reactants may be



involved. Eqn (1.21) is modified slightly to (1.34). By convention, the

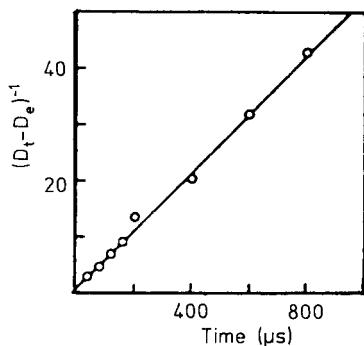
$$\frac{1}{[A]_t} - \frac{1}{[A]_0} = 2kt \quad (1.34)$$

second-order rate constant for (1.33) is designated  $2k$ , because two identical molecules disappear for each encounter leading to reaction.<sup>23</sup> Reaction (1.33) is a key step in the process of dimerization or disproportionation of A and is often observed when a transient radical A is produced by photolysis or pulse radiolysis. Flash photolysis of hexane solutions of CO and  $M_2(\text{CO})_{10}$  ( $M = \text{Mn}$  or  $\text{Re}$ ) produces  $M(\text{CO})_5^\bullet$  radicals. At the termination of



the flash the radicals recombine in a second-order manner to regenerate  $M_2(\text{CO})_{10}$  with a rate law<sup>24,25</sup>

$$-d[M(\text{CO})_5^\bullet]/dt = 2k[M(\text{CO})_5^\bullet]^2 \quad (1.36)$$



**Fig. 1.3** Second-order kinetic plot for decay of  $\text{Re}(\text{CO})_5^\bullet$  obtained by flash photolysis of  $120 \mu\text{M}$   $\text{Re}_2(\text{CO})_{10}$  with  $10 \text{ mM}$  CO in isooctane. (CO slows further reactions of  $\text{Re}(\text{CO})_5^\bullet$ ) At  $\lambda = 535 \text{ nm}$ , the molar absorbance coefficient,  $\epsilon_M$  of  $\text{Re}(\text{CO})_5^\bullet$  is  $1.0 \times 10^3 \text{ M}^{-1} \text{ cm}^{-1}$ . Since therefore from Beer-Lambert law  $(D_t - D_e) = [A]\epsilon_M l$ , where  $D$ 's are optical absorbances and  $l$  is the path length ( $10 \text{ cm}$ ), the slope of Fig. 1.3 is  $2k/\epsilon_M l$  and  $2k$  therefore equals  $(5.3 \times 10^3)(10^3)(10) = 5.3 \times 10^9 \text{ M}^{-1} \text{ s}^{-1}$ . Ref. 25. Reproduced with permission of the Journal of the American Chemical Society. © 1982, American Chemical Society.

The appropriate absorbance function vs time is linear (Fig. 1.3).<sup>25</sup> The values of  $k$  are  $9.5 \times 10^8 \text{ M}^{-1} \text{ s}^{-1}$  ( $M = \text{Mn}$ ) and  $3.7 \times 10^9 \text{ M}^{-1} \text{ s}^{-1}$  ( $M = \text{Re}$ ).<sup>24,25</sup> The second-order decay of  $\text{Cr}(\text{V})$  affords another example, of many, of the type (1.33).<sup>26</sup>

Second-order reactions between two dissimilar molecules A and B are invariably studied under pseudo first-order conditions (Sec. 1.4.4) because this is by far the simpler procedure. If however this condition cannot be used because, for example, both reactants absorb heavily

or low concentrations of *both* reactants must be used because of high rates, then for the reaction



$$-d[A]/dt = k_1[A][B] \quad (1.38)$$

Integration results in

$$\frac{1}{[B]_0 - [A]_0} \frac{\ln [A]_0[B]_t}{[B]_0[A]_t} = k_1 t \quad (1.39)$$

with subscripts  $t$  and  $0$  representing time  $t$  and  $0$ , respectively. Applications of this equation are given in Refs. 27–29 and include the treatment of flow traces for the rapid second-order reaction between Eu(II) and Fe(III).<sup>27</sup> A simplified form of (1.39) equivalent to (1.21) arises when the starting concentrations of A and B are equal. This condition  $[A]_0 = [B]_0$  must be set up experimentally with care<sup>30</sup> although in rare cases equal concentrations of A and B may be imposed by the conditions of their generation.<sup>31</sup> (Sec Prob. 9.)

#### 1.4.4 Conversion of Pseudo to Real Rate Constants

Having obtained the exponent  $a$  in (1.15) by monitoring the concentration of A in deficiency we may now separately vary the concentration of the other reactants, say B and C, still keeping them however in excess of the concentration of A. The variation of the pseudo rate-constant  $k$  with  $[B]$  and  $[C]$  will give the order of reaction  $b$  and  $c$  with respect to these species,<sup>32</sup> leading to the expression

$$k = k_1 [B]^b [C]^c \quad (1.40)$$

and therefore the full rate law

$$-d[A]/dt = k_1 [A]^a [B]^b [C]^c \quad (1.41)$$

We can use this approach also to examine the effects on the rate, of reactants that may not be directly involved in the stoichiometry (for example,  $H^+$ ) or even of products. It is the most popular method for determining the rate law, and only rarely cannot be used.

Considering just one other reactant B, we generally find a limited number of observed variations of  $k (= V/[A]^a)$  with  $[B]^b$ . These are shown as (a) to (c) in Fig. 1.4. Nonlinear plots of  $k$  vs  $[B]^b$  signify complex multistep behavior (Sec. 1.6.3).

(a) The rate and value of  $k$  may be independent of the concentrations of other reactants (Fig. 1.4(a)). This situation may occur in a dimerization, rearrangement or conformational change involving A. It may also arise in the solvolysis of A since the reaction order with respect to solvent is indeterminable, because its concentration cannot be changed.

(b) The value of  $k$  may vary linearly with  $[B]^b$ , and have a zero intercept for the appropriate plot (Fig. 1.4(b)). This conforms to a single-term rate law

$$-d[A]/dt = k [A]^a = k_3 [A]^a [B]^b \quad (1.42)$$

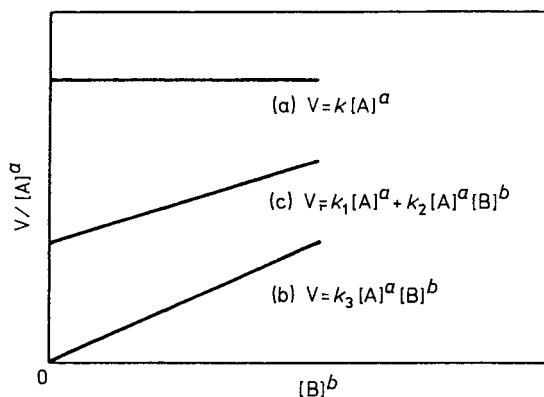
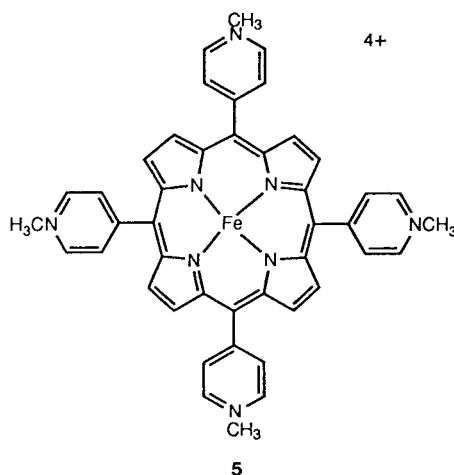


Fig. 1.4 Common variations of  $V/[A]^a$  with  $[B]^b$ .



In the oxidation of  $\text{Fe(II)P}^{4+}$  (5) by excess  $\text{O}_2$  there is a second-order loss of  $\text{Fe(II)}$ . The second-order rate constant  $k$  is linearly dependent on  $[\text{O}_2]$  with a zero intercept for the  $k/[\text{O}_2]$  plot. An overall third-order rate law therefore holds.<sup>14</sup>

$$-d[\text{Fe(II)P}^{4+}]/dt = k_1[\text{Fe(II)P}^{4+}]^2[\text{O}_2] \quad (1.43)$$

When  $a = b = 1$  in (1.42) the overall reaction is second-order. Even a quite small excess of one reagent (here B) can be used and pseudo first-order conditions will still pertain.<sup>33</sup> As the reaction proceeds, the ratio of concentration of the excess to that of the deficient reagent progressively increases so that towards the end of the reaction, pseudo first-order conditions certainly hold. Even if  $[\text{B}]$  is maintained in only a two-fold excess over  $[\text{A}]$ , the error in the computed second-order rate constant is  $\leq 2\%$  for 60% conversion.<sup>34</sup>

(c) The value of  $k$  may be linear with respect to  $[\text{B}]^b$  but have a residual value at zero  $[\text{B}]$  (Fig. 1.4(c)). This behavior is compatible with concurrent reactions of A. The oxidation of  $\text{Fe(phen)}_3^{2+}$  by excess  $\text{Tl(III)}$  conforms to this behavior leading to the rate law

$$-d[\text{Fe}(\text{phen})_3^{2+}]/dt = k[\text{Fe}(\text{phen})_3^{2+}] = k_1[\text{Fe}(\text{phen})_3^{2+}] + k_2[\text{Fe}(\text{phen})_3^{2+}][\text{Tl}(\text{III})] \quad (1.44)$$

The second-order redox reaction, giving rise to the rate constant  $k_2$ , is accompanied also by loss of the iron(II) complex by hydrolysis, which leads to the  $k_1$  term. The latter can be more accurately measured in the absence of Tl(III).<sup>35</sup> The kinetics of substitution of many square-planar complexes conform to behavior (c), see Sec. 4.6. It is important to note that an intercept might be accurately defined and conclusive only if low concentrations of B are used. In the base catalyzed conversion



$$-d[\text{Co}(\text{NH}_3)_5\text{ONO}^{2+}]/dt = (k_1 + k_2[\text{OH}^-])[\text{Co}(\text{NH}_3)_5\text{ONO}^{2+}] \quad (1.46)$$

the  $k_1$  term can be established only if low  $\text{OH}^-$  concentrations of 0.01–0.1 M are used.<sup>36</sup>

## 1.5 Monophasic Reversible Reactions

The only reactions considered so far have been those that proceed to all intents and purposes (>95%) to completion. The treatment of *reversible* reactions is analogous to that given above, although now it is even more important to establish the stoichiometry and the thermodynamic characteristics of the reaction. A number of reversible reactions are reduced to pseudo first-order opposing reactions when reactants or products or both are used in excess



of A and X. The order with respect to these can then be separately determined. The approach to equilibrium for (1.47) is still first-order, but the derived first-order rate constant  $k$  is the sum of  $k_1$  (the forward rate constant) and  $k_{-1}$  (the reverse rate constant):

$$\ln \frac{[\text{A}]_0 - [\text{A}]_e}{[\text{A}]_t - [\text{A}]_e} = kt = (k_1 + k_{-1})t \quad (1.48)$$

This equation resembles (1.26) but includes  $[\text{A}]_e$ , the concentration of A at equilibrium, which is not now equal to zero. The ratio of rate constants,  $k_1/k_{-1} = K$ , the so-called *equilibrium constant*, can be determined independently from equilibrium constant measurements. The value of  $k$ , or the relaxation time or half-life for (1.47), will all be independent of the direction from which the equilibrium is approached, that is, of whether one starts with pure A or X or even a nonequilibrium mixture of the two. A first-order reaction that hides concurrent first-order reactions (Sec. 1.4.2) can apply to reversible reactions also.

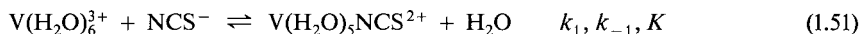
The scheme



can be reduced to (1.47) by using B in excess, and creating thereby a pseudo first-order reversible reaction. The rate law that arises is<sup>37</sup>

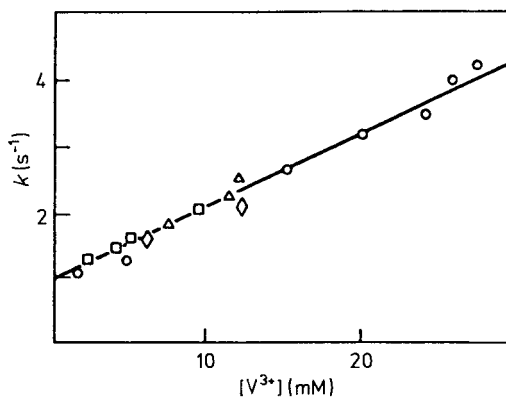
$$V = k[A] = (k_1[B] + k_{-1})[A] \quad (1.50)$$

where  $k_1[B]$  and  $k_{-1}$  are the forward and reverse first-order rate constants. Such a situation arises in the interaction of  $V(H_2O)_6^{3+}$  with  $SCN^-$  ions,



which is studied using a large excess of  $V^{3+}$  ions, although an equilibrium position is still attained. A plot of the pseudo first-order rate constant  $k$  for the approach to equilibrium vs  $[V^{3+}]$  is linear (Fig. 1.5).<sup>38</sup> The slope is  $k_1$  and the intercept is  $k_{-1}$ :

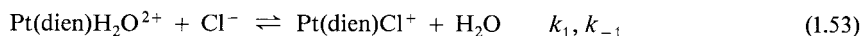
$$k = k_1[V^{3+}] + k_{-1} \quad (1.52)$$



**Fig. 1.5** Plot of  $k$  ( $s^{-1}$ ) vs  $[V^{3+}]$  for reaction (1.51) at 25°C.  $[H^+] = 1.0$  M (circles); 0.50 M (triangles); 0.25 M (diamonds) and 0.15 M (squares).<sup>38</sup>

It is not always easy to obtain an accurate value for  $k_{-1}$  from such a plot. However, combination of  $k_1$  with  $K (= k_1/k_{-1})$  obtained from spectral measurements, yields a meaningful value for  $k_{-1}$ . The plots in Fig. 1.5 show the independence of the values of  $k_1$  and  $k_{-1}$  on the acid concentrations in the range 0.15 to 1.0 M. There are slight variations to this approach, which have been delineated in a number of papers.<sup>39</sup>

Since the  $k$  vs  $[B]$  plot illustrated in Fig. 1.5 is identical to that obtained with unidirectional concurrent first- and second-order reactions of A (Fig. 1.4(c)) confusion might result if the equilibria characteristics are not carefully assessed. The pseudo first-order rate constant  $k$  for the reaction



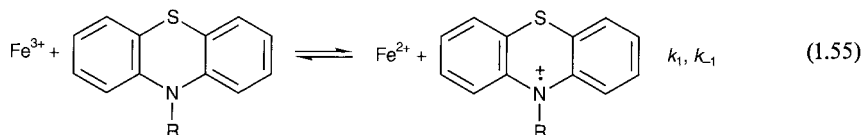
has been determined using excess  $[Cl^-]$ . The variation of  $k$  with  $[Cl^-]$  resembles that shown in Fig. 1.4(c), i. e.

$$k = a + b[Cl^-] \quad (1.54)$$



The results were interpreted as a two-term rate law for an irreversible reaction,  $b$  representing the second-order rate constant for attack by  $\text{Cl}^-$  ion and  $a$  an unusual dissociative path (Sec. 4.6). More recent work indicates that at the low  $[\text{Cl}^-]$  concentrations used, reaction (1.53) is reversible and Eqn. (1.54) is better interpreted in terms of a reversible reaction as depicted in (1.53) in which in (1.54),  $b = k_1$  and  $a = k_{-1}$ .<sup>40</sup> As a check the value of  $b/a = K$  is close to that estimated for reaction (1.53).

The conversion of second-order reversible reactions to reversible first-order kinetics by using all but one of the reactants and all but one of the products in excess is a valuable ploy. The reversible reaction



is studied by using excess  $\text{Fe}^{3+}$  and  $\text{Fe}^{2+}$ . The plot of  $\ln(D_e - D_t)$  vs time is linear, where  $D_e$  and  $D_t$  represent the absorbance of the highly colored radical at equilibrium and time  $t$ , respectively. The slope of this plot is  $k_{\text{obs}}$ , which from (1.48) is given by

$$k_{\text{obs}} = k_1 [\text{Fe}^{3+}] + k_{-1} [\text{Fe}^{2+}] \quad (1.56)$$

Thus a plot of  $k_{\text{obs}}/[\text{Fe}^{2+}]$  vs  $[\text{Fe}^{3+}]$  is linear with slope  $k_1$  and intercept  $k_{-1}$ .<sup>41</sup> For other examples of this approach see Refs. 42 and 43. The full treatment for



is quite tedious<sup>41,44,45</sup> as it is for (1.58) Prob. 10<sup>46,47</sup>



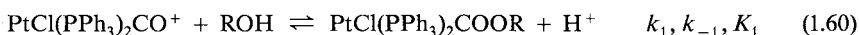
and (1.59)<sup>48,49</sup>



but simplified approaches,<sup>45,49,50</sup> relaxation treatment and computers<sup>51</sup> have largely removed the pain.

### 1.5.1 Conversion of Reversible to Unidirectional Reactions

An often useful approach is to eliminate the elements of reversibility from a reaction and force it to completion, either by the use of a large excess of reactant or by rapid removal of one of the products. A good illustration is afforded by the study of



Since the equilibrium quotient  $K_1$  is small, a nonnucleophilic base is added to the reaction mixture to react with liberated protons and drive the reaction to completion (left to right). Using an excess of ROH then ensures simple unidirectional pseudo first-order (rate constant  $k_f$ ) kinetics:

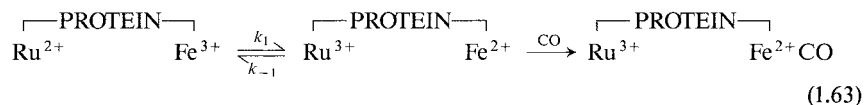
$$-d \ln [\text{PtCl}(\text{PPh}_3)_2\text{CO}^+]/dt = k_f = k_1[\text{ROH}] \quad (1.61)$$

The reverse reaction also gives simple first-order (rate constant  $k_r$ ) kinetics when studied with excess  $\text{HClO}_4$ :

$$-d \ln [\text{PtCl}(\text{PPh}_3)_2\text{COOR}]/dt = k_r = k_{-1}[\text{H}^+] \quad (1.62)$$

It was verified that  $k_1/k_{-1}$  equaled  $K_1$ , determined in a separate experiment.<sup>52</sup> For another example, see Ref. 53.

The reversible first-order reaction (1.47) can be converted into an irreversible  $\text{A} \rightarrow \text{X}$  process by scavenging X rapidly and preventing its return to A. Thus the intramolecular reversible electron transfer in modified myoglobin (Sec. 5.9)



can be converted into a unidirectional process controlled by  $k_1$ , by carrying out the experiments in the presence of CO which binds strongly to the ferrous heme.<sup>54</sup>

Care should be exercised that excess of one reactant does in fact promote irreversible reaction if this is the desired object, otherwise invalid kinetics and mechanistic conclusions will result. Consideration of the reduction potentials for cytochrome-c Fe(III) and  $\text{Fe}(\text{CN})_6^{3-}$  (0.273 V and 0.420 V respectively) indicates that even by using a  $10^2$ – $10^3$  fold excess of  $\text{Fe}(\text{CN})_6^{4-}$ , reduction of cytochrome-c Fe(III) will still not be complete. An equilibrium kinetic treatment is therefore necessary.<sup>45</sup>

## 1.6 Multiphasic Unidirectional Reactions

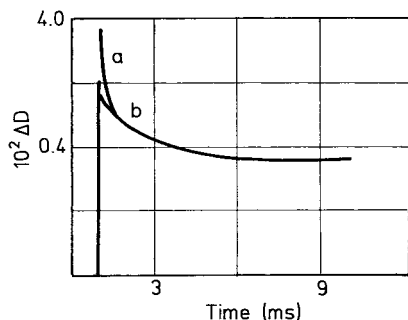
Attention is now directed to reactions that show a nonlinear plot of the appropriate function or that have rate laws that are altered with changes in the concentration of the species involved in the reaction. Such deviations are usually associated with concurrent and consecutive reactions.

### 1.6.1 Concurrent Reactions

A single species A (produced for example by radiolytic or photolytic means) may often disappear by concurrent first- (or pseudo first-) order ( $k_1$ ) as well as by a second order process ( $2k_2$ ) already alluded to (Sec. 1.4.3). Thus

$$-d[A]/dt = k_1[A] + 2k_2[A]^2 \quad (1.64)$$

At higher concentrations of A, the second-order process is more important and loss of A is second-order. As the concentration of A decreases, so the first term in (1.64) becomes dominant and decay of A is a purely first-order process (it may, for example, represent decomposition by solvent<sup>24</sup>) (Fig. 1.6).<sup>55</sup> The rate curve may be analyzed by a relatively straightforward linearizing method.<sup>23</sup>

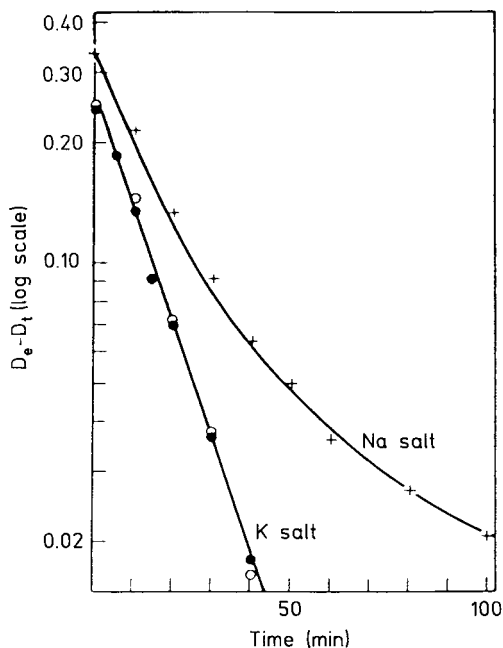


**Fig. 1.6** Decay of  $(\text{NH}_3)_5\text{Co}(\text{mbpy})^{3+}$  at pH 7.2 and  $25^\circ\text{C}$ . The transient was generated by using equivalent amounts ( $10\ \mu\text{M}$ ) of  $(\text{NH}_3)_5\text{Co}(\text{mbpy})^{4+}$  and  $\text{CO}_2^-$ . The decay of the transient was nicely second-order up to 85% reaction (a). After this, when the Co(III) radical concentration is small ( $1\text{--}2\ \mu\text{M}$ ), there is a slight deviation for the expected second-order plot (not shown) and a first-order reaction (b) remains ( $k = 5.4 \times 10^2\text{s}^{-1}$ ).<sup>55</sup> The difference between the (steep) second-order decay and the (extrapolated) first-order loss is apparent.

If a mixture of A and B undergoes parallel first-order or pseudo first-order reactions to give a common product C, and A and B do not interconvert readily compared with the reaction under study,

$$[C]_e - [C]_t = [A]_0 \exp(-k_1 t) + [B]_0 \exp(-k_2 t) \quad (1.65)$$

where  $k_1$  and  $k_2$  are the first-order rate constants for conversion of A and B, respectively.<sup>12</sup> The resultant semilog plot of  $[C]$  vs time will in general be curved, and can be dissected algebraically or by a computer program.<sup>56</sup> The hydrolysis of the anions in the complexes  $\text{Na}[\text{Co}(\text{medta})\text{Br}]$  and  $\text{K}[\text{Co}(\text{medta})\text{Br}]$  has been examined (medta = N-methyl-ethylene-diaminetriacetate). For the semilog plots the Na salt gives marked curvature, whereas the plot of the K salt is linear over four half-lives (Fig. 1.7). It is considered that the sodium salt is a mixture of isomers, in which the bromine is either in an equatorial or an axial position of the cobalt(III) octahedron. The biphasic plot can be separated into a fast component and a slow one. Significantly, the fast portion matches exactly the semilog plot for the K salt, which is considered isomerically pure.<sup>57</sup> A similar concurrent hydrolysis pattern has been observed with other complex ions.<sup>58</sup> It is not always easy to distinguish concurrent from consecutive reactions, as we shall see in the next section.



**Fig. 1.7** Semilog plot of optical absorbance at 540 nm vs time for hydrolysis of  $\text{Co}(\text{medta})\text{Br}^-$  at  $78.8^\circ\text{C}$  and pH 2.6. Mixture of isomers (+); fast component derived from mixture by subtraction of slow component (o); experimental points for fast isomer (•).<sup>57</sup>

## 1.6.2 Consecutive Reactions with no Elements of Reversibility

Consecutive reactions figure prominently in Part II. Since complex ions have a number of reactive centers, the product of one reaction may very well take part in a subsequent one. The simplest and very common, but still surprisingly involved, sequence is that of two irreversible first-order (1.66) or pseudo first-order (with X and Y in large excess) (1.67) reactions,



$$k_1 = k_1'[\text{X}]; \quad k_2 = k_2'[\text{Y}] \quad (1.68)$$

If  $k_1 \gg k_2$  then both steps in (1.66) can be analyzed separately as described previously. If  $k_2 \gg k_1$ , then only the first step is observed and

$$-d[\text{A}]/dt = d[\text{C}]/dt = k_1[\text{A}] \quad (1.69)$$

The only way for determining  $k_2$  will be through isolation and separate examination of B (see later). If B is not isolable however and its properties are unknown, real difficulties might arise.<sup>59</sup>

The rate equations for (1.66) are

$$-d[A]/dt = k_1[A] \quad (1.70)$$

$$d[B]/dt = k_1[A] - k_2[B] \quad (1.71)$$

$$d[C]/dt = k_2[B] \quad (1.72)$$

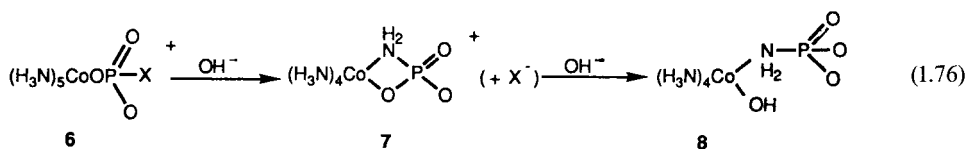
Integrating these equations, and assuming  $[A] = [A]_0$ , and  $[B] = [C] = 0$  at  $t = 0$ , we obtain the concentrations of A, B and C at any time  $t$  in terms of the concentration,  $[A]_0$ :

$$[A] = [A]_0 \exp(-k_1 t) \quad (1.73)$$

$$[B] = \frac{[A]_0 k_1}{k_2 - k_1} [\exp(-k_1 t) - \exp(-k_2 t)] \quad (1.74)$$

$$[C] = [A]_0 \left[ 1 - \frac{k_2}{k_2 - k_1} \exp(-k_1 t) + \frac{k_1}{k_2 - k_1} \exp(-k_2 t) \right] \quad (1.75)$$

Often  $k_1$  will be comparable in value to  $k_2$  and in this event the distribution of A, B and C with time is illustrated for example by the stepwise hydrolysis of a cobalt(III) complex **6**, ( $X = -OC_6H_3(NO_2)_2$ )



Stepwise Hydrolysis of a Cobalt (III) Phosphate Complex ( $X = -OC_6H_4(NO_2)_2$ )

The concentrations of **6**, **7** and **8** are determined by integration of their characteristic  $^{31}\text{P}$  nmr spectra (Sec. 3.9.5) and their variations with time are shown in Fig. 1.8.<sup>60</sup> These curves illustrate some general features of the system (1.66). At the maximum concentration of **7**,

$$d[7]/dt = 0 \quad (1.77)$$

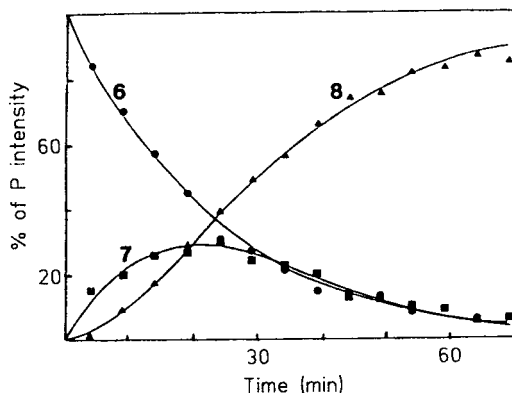
and

$$k_1[6] = k_2[7] \quad (1.78)$$

Since the relative concentrations of **6** and **7** are easily assessed at the maximum concentration of **7**, the ratio  $k_1/k_2$  can be determined even if this is quite close to unity. It can be shown<sup>61</sup> that the time for the concentration of **7** to reach a maximum ( $t_{\max}$ ) is given by (1.79), Prob. 11,

$$t_{\max} = \frac{\ln(k_1/k_2)}{k_1 - k_2} \quad (1.79)$$

(1.78) and (1.79) can be used to determine rate constants for consecutive reactions.<sup>62,63</sup> There is a lag period in the buildup of **8**, the inflection in the **[8]**/time curve corresponding to  $[7]_{\max}$ . For another example where A, B and C in (1.66) are all monitored, see Ref. 64.



**Fig. 1.8** Distribution of 6, 7 and 8 vs time from integrated  $^{31}\text{P}$  nmr spectra in 0.35 M  $\text{OH}^-$ ,  $\mu = 1.0$  M at  $5^\circ\text{C}$ . Signals (ppm) are at 6.5 (6), 22–31 (7, dependent on  $[\text{OH}^-]$ ) and 7.1 ppm (8).<sup>60</sup> (Reprinted with permission from P. Hendry and A. M. Sargeson, *Inorg. Chem.* **25**, 865 (1986). © 1986, American Chemical Society)

Such systems as (1.66) or (1.67) appear to have been examined mainly by spectral methods, and so discussion will center around this monitoring method. The occurrence of steps with similar rates is indicated by the lack of isobestic points (Sec. 3.9.1) over some portion of the reaction. In addition the appropriate kinetic plots are biphasic although perhaps only slightly so, or only at certain wavelengths. Data obtained at a wavelength that monitors only the concentration of A will give a perfect first-order plot (or pseudo first-order in the presence of excess X) rate constant  $k_1$  (1.73). Considering the optical absorbance  $D_t$  of the reacting solution at time  $t$ , in a cell of path length 1 cm,

$$D_t = \varepsilon_A[A] + \varepsilon_B[B] + \varepsilon_C[C] \quad (1.80)$$

where  $\varepsilon_A$  is the molar absorptivity of A and so on (Sec. 3.9.1). By substituting (1.73) through (1.75) into (1.80) and rearranging terms, it is not difficult to derive the expression<sup>65,66</sup>

$$D_t - D_e = a_1 \exp(-k_1 t) + a_2 \exp(-k_2 t) \quad (1.81)$$

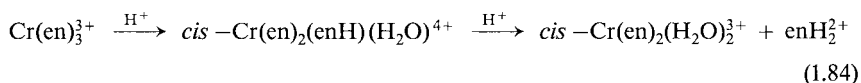
where  $D_e = \varepsilon_C[A]_0$  and  $a_1$  and  $a_2$  are composed of rate constants and molar absorptivities:<sup>67</sup>

$$a_1 = \varepsilon_A[A]_0 + \frac{\varepsilon_B[A]_0 k_1}{k_2 - k_1} + \frac{\varepsilon_C[A]_0 k_2}{k_1 - k_2} \quad (1.82)$$

$$a_2 = \frac{k_1[A]_0(\varepsilon_B - \varepsilon_C)}{k_1 - k_2} \quad (1.83)$$

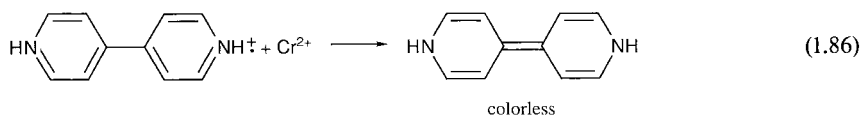
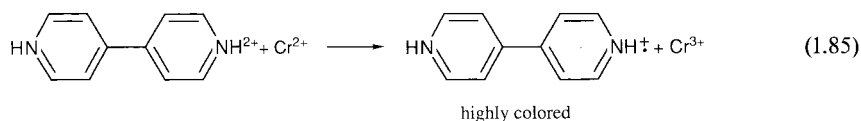
It is not always easy by inspection to be certain that two reactions are involved. The use of a semi-log plot helps<sup>68–70</sup> since it shows better the deviation from linearity that a biphasic reaction demands but a computer treatment of the data is now the definitive approach.<sup>71–77</sup> Less apparent is the fact that having resolved the curve into two rate constants  $k_{\text{fast}}$  and  $k_{\text{slow}}$  we cannot simply assign these to  $k_1$  and  $k_2$  respectively (in 1.66) without additional information since (1.81) is derived without specifying a  $k_{\text{fast}}/k_1$  or  $k_{\text{fast}}/k_2$  condition.<sup>71,78</sup> The most popular method for resolving this ambiguity is by resorting to spectral considerations. The spectrum of the intermediate B (which is a collection of  $\varepsilon_\nu$  at various wavelengths) can be

calculated from (1.81), (1.82) and (1.83) on the two premises that (a)  $k_{\text{fast}} = k_1$  and  $k_{\text{slow}} = k_2$  or (b)  $k_{\text{fast}} = k_2$  and  $k_{\text{slow}} = k_1$ . One of the two spectra estimated by this means will usually be much more plausible than the other (which may even have negative molar absorptivities!) and the sequence which leads to the unreasonable spectrum for B can be discarded. An approach of this type was first made<sup>79</sup> in a study of



and has since been adopted on numerous occasions.<sup>70,73,76,80</sup> In the majority of cases the fast and slow rate constants are assigned to  $k_1$  and  $k_2$  indicating fast formation of a relatively weakly absorbing intermediate.<sup>70,73,76,80</sup> A few instances are known however<sup>61,81</sup> where the reverse pertains i.e. a highly absorbing intermediate arises which decays rapidly compared with its formation. Now  $k_{\text{fast}} = k_2$ .

An intense purple-blue species forms within a few seconds when  $\text{Cr}^{2+}$ , in excess, is added to 4,4'-bipyridinium ion,  $\text{bpyH}_2^{2+}$ . The color fades slowly over many minutes. The formation and disappearance of the intermediate,  $k_{\text{fast}}$  and  $k_{\text{slow}}$  respectively, are assigned to  $k_2$  and  $k_1$  respectively from considerations of the assessed spectrum of the intermediate.<sup>81</sup> The reactions involved are



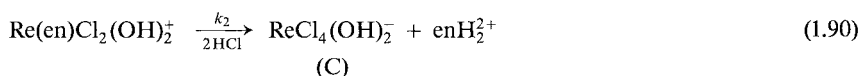
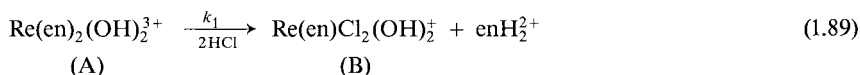
and the rate equations are

$$V = a [\text{Cr}^{2+}] [\text{bpyH}_2^{2+}] \quad (1.87)$$

$$V = \{b + c [\text{Cr}^{2+}] [\text{H}^+]\} [\text{bpyH}_2^{2+}] \quad (1.88)$$

The radical intermediate is always less than 1% of  $\text{bpyH}_2^{2+}$  but shows up because of its high absorbance.

If the spectrum of an intermediate is known, a choice of observation wavelength may allow isolation of each stage. In the reaction (A)  $\rightarrow$  (C) using concentrated HCl:



examination at 395 or 535 nm (where  $\varepsilon_B = \varepsilon_C$ ) gives  $-d[A]/dt$  and hence a value for  $k_1$ . Observation at 465 nm (where  $\varepsilon_A = \varepsilon_B$ ) allows a value for  $k_2$  to be obtained after a short induction period. Absorbance changes at 685 nm ( $\varepsilon_A = \varepsilon_C$ ) reflect  $d[B]/dt$ , and specifically allow an estimate of  $t_{\max}$ , the time for the concentration of B to reach a maximum. A confirmation of  $k_1$  and  $k_2$  is then possible by using (1.79).<sup>82</sup>

Finally we return to the situation mentioned at the beginning of the section of a system of two consecutive reactions still yielding a single linear plot of  $\ln(D_t - D_e)$  vs time. A condition which is not obvious is (1.91) which emerges from (1.81)<sup>65,78,83-85</sup>

$$\frac{k_1}{k_2} = \frac{\varepsilon_C - \varepsilon_A}{\varepsilon_B - \varepsilon_A} \quad (1.91)$$

This may appear to be an unlikely situation to encounter until one recalls that there are a number of reactions involving two isolated and independently reacting centers. One might then anticipate that statistically  $k_1 = 2k_2$  and that  $\varepsilon_B = 1/2(\varepsilon_A + \varepsilon_C)$ . These are precisely the conditions demanded by (1.91). It is worth noting that in this case the observed first-order rate constant is  $k_2$ .

Eight-iron ferredoxin contains two 4-Fe-clusters separated by about  $12 \text{ \AA}$ . Each cluster can undergo a one-electron redox reaction (r and o represent the reduced and oxidized forms)

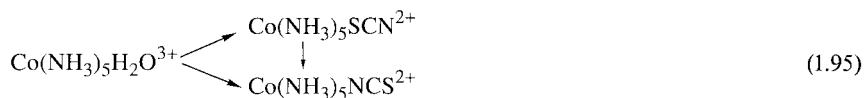


Oxidation of 8-Fe(rr) to 8-Fe(oo) by a number of one-electron oxidants gives a single first-order process. After ruling out the more obvious reasons for this observation, it is concluded that condition (1.91) holds,<sup>86</sup> one often referred to as "statistical kinetics". For other examples, see Refs. 87 and 88. Even if (1.91) is not strictly satisfied, linear plots may still be obtained.<sup>84,88</sup>

Further complexities may be anticipated. For example in the consecutive reaction (1.66), direct conversion of A to C may occur as well as conversion that proceeds via B



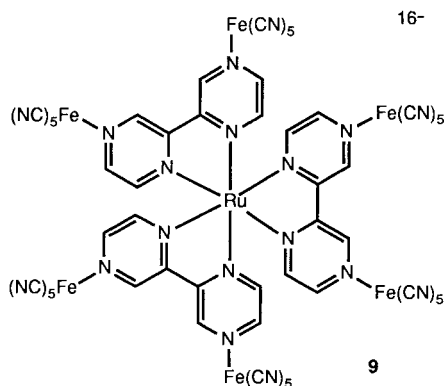
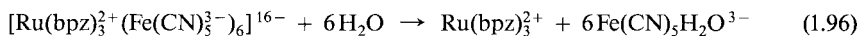
The  $\text{SCN}^-$  anation of  $\text{Co}(\text{NH}_3)_5\text{H}_2\text{O}^{3+}$  has only recently been recognized to form  $(\text{NH}_3)_5\text{CoSCN}^{2+}$  in parallel with the stable N-bonded  $\text{Co}(\text{NH}_3)_5\text{NCS}^{2+}$ . The system has been fully analyzed and illustrates well the difficulties in detecting biphasic behavior.<sup>89</sup>



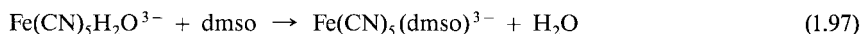
For another example, see Ref. 90.



As the number of reaction steps increases so, of course, does the complexity. A novel example is the six consecutive steps for hydrolysis of a cyanobridged polynuclear complex **9**<sup>91</sup>



The successive rate constants vary only from  $1.3 \times 10^{-3} \text{ s}^{-1}$  to  $4.6 \times 10^{-4} \text{ s}^{-1}$  at  $\mu = 0.1 \text{ M}$  and the multistep kinetics are analyzed with a computer. A large excess of dmsO is used to aid the dissociation of the polynuclear complex by reacting irreversibly with the product,  $\text{Fe}(\text{CN})_5\text{H}_2\text{O}^{3-}$



The ambiguities which have been alluded to in this section may sometimes be circumvented by changing the conditions, the concentrations of excess reactants, temperature, pH and so on.

### 1.6.3 Two-Step Reactions with an Element of Reversibility

Suppose that an irreversible reaction between A and B leading to >95% product or products, designated D, is examined in the usual way. One of the reactants, B, is held in excess and the loss of A monitored. It is likely that the loss will be a first-order process (rate constant  $k$ ). At low concentrations of B (but still  $\gg [A]$ ), the value of  $k$  may be proportional to the concentration of B. At higher concentrations of B however this direct proportionality may disappear and eventually  $k$  will become independent of [B]. Obviously, a second-order reaction at low reactant concentrations has lost its simplicity at higher reactant concentrations and eventually turned over to first-order in A alone. Such a situation is accommodated by a rate law of the form

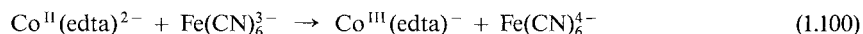
$$V = \frac{-d[A]}{dt} = k[A] = \frac{a[A][B]}{1 + b[B]} \quad (1.98)$$

This behavior is sometimes referred to as saturation kinetics. When  $b[B] < 1$ , the observed second-order is easily understood (rate constant =  $a$ ). When  $b[B] \sim 1$  there is a mixed-order

and eventually, when  $b[B] > 1$ , the reaction is first-order in A, rate constant =  $a/b$ . The  $k$  vs  $[B]$  plot is described by a hyperbola and (1.98) can be treated directly by a computer program. A favorite approach in the past, and still useful, is to convert (1.98) into a linear form (1.99). A plot of  $k^{-1}$  vs  $[B]^{-1}$

$$\frac{1}{k} = \frac{1}{a[B]} + \frac{b}{a} \quad (1.99)$$

yields  $1/a$  (slope) and  $b/a$  (intercept). An example of the rate law (1.98) is shown in the redox reaction (1.100).<sup>92</sup>  $\text{Co}(\text{edta})^{2-}$  (= B) is used in excess and  $a = 4.5 \text{ M}^{-1} \text{ s}^{-1}$  and  $b = 831 \text{ M}^{-1}$  at  $25^\circ\text{C}$ .



### 1.6.4 Reaction Schemes Associated with (1.98)

There are a number of possible schemes which may explain the rate behavior associated with (1.98). A single step can be ruled out. At least two consecutive or competitive reactions including one reversible step must be invoked.

(a) Consider the scheme



which is a very important one in chemistry.<sup>93</sup> If we do not see deviations from a single first-order process it is likely that the first reversible step is much more rapid than the second. At higher concentrations of B the rapid formation of substantial amounts of C may be discernable. If the first step is the more rapid one, C will be in equilibrium with A and B throughout the reaction and

$$\frac{[\text{C}]}{[\text{A}][\text{B}]} = \frac{k_1}{k_{-1}} = K_1 \quad (1.102)$$

will be continually maintained. We shall be monitoring the loss of both A and C or the equivalent gain in one of the products (D).

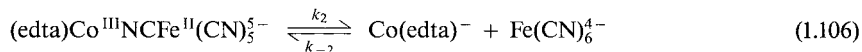
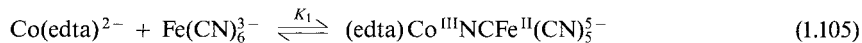
$$d[\text{D}]/dt = k([\text{A}] + [\text{C}]) = k_2[\text{C}] = k_2K_1[\text{A}][\text{B}] \quad (1.103)$$

From (1.102) and (1.103),

$$k = \frac{k_2K_1[\text{B}]}{1 + K_1[\text{B}]} \quad (1.104)$$

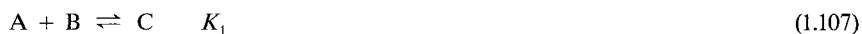
which is of the form (1.98) with  $a = k_2K_1$  and  $b = K_1$ . In reaction (1.100), C would represent some adduct, now believed to be a cyano bridged  $\text{Co}(\text{III})\text{Fe}(\text{II})$  species, with a formation con-

stant  $K_1 = b = 831 \text{ M}^{-1}$ . This adduct would break down to products with a rate constant  $k_2 = a/b = 5.4 \times 10^{-3} \text{ s}^{-1}$



The rate constant  $k_{-2}$  can be ignored at present.

(b) A related scheme to that of (a) is one in which A and B react directly to form D, but are also in a rapid “dead-end” or nonproductive equilibrium to give C (competitive reactions)



whence

$$k = \frac{k_3[\text{B}]}{1 + K_1[\text{B}]} \quad (1.110)$$

This is again equivalent to (1.98). In the reaction (1.100), the reactants still form the adduct,  $K_1$  remains  $831 \text{ M}^{-1}$ , but the reactants interact separately to give products with a rate constant  $k_3 = a = 4.5 \text{ M}^{-1} \text{ s}^{-1}$ .

(c) There is yet another possible explanation for the observed data namely the sequence



A very useful simplification that can often be made in these systems is to assume that the intermediate C is in a small “steady-state” concentration. Therefore

$$\pm d[\text{C}]/dt = 0 \quad (1.113)$$

$$k_4[\text{A}] \text{ (gain of C)} = k_{-4}[\text{C}] + k_5[\text{C}][\text{B}] \text{ (loss of C)} \quad (1.114)$$

$$d[\text{D}]/dt \simeq k[\text{A}] = k_5[\text{C}][\text{B}] = \frac{(k_5 k_4 / k_{-4}) [\text{A}][\text{B}]}{1 + (k_5 / k_{-4}) [\text{B}]} \quad (1.115)$$

which is (1.98) with  $a = (k_5 k_4 / k_{-4})$  and  $b = (k_5 / k_{-4})$ . In (1.100),  $\text{Fe}(\text{CN})_6^{4-}$  would rearrange to a reactive form with a rate constant,  $k_4 = a/b = 5.4 \times 10^{-3} \text{ s}^{-1}$ .

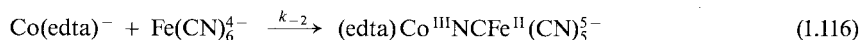
The ratio  $k_5/k_{-4} = 831 \text{ M}^{-1}$  but the analysis can be taken no further without knowledge of the equilibrium constant for (1.111) ( $k_4/k_{-4}$ ).

(d) Distinguishing Schemes (a), (b) and (c)

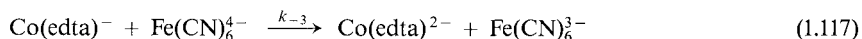
It is relatively easy to spot behavior (c). Plots of  $k$  vs  $[\text{B}]$  are non-linear with  $[\text{B}] \gg [\text{A}]$  but will always remain linear with  $[\text{A}] \gg [\text{B}]$ .<sup>94</sup> Saturation kinetics will arise with (a) and (b)

whether A or B is the reagent used in excess. Secondly, the value of  $k_4$  calculated with scheme (c) will be independent of the nature of B. Finally the value of chemical intuition cannot be underestimated in resolving these problems. Two different reactive forms of  $\text{Fe}(\text{CN})_6^{4-}$  are unreasonable (although not impossible) thus tending to rule out Scheme (c) for reaction (1.100). The scheme (c) is more likely to operate for example in the reactions of proteins. The  $\text{A} \rightleftharpoons \text{C}$  transformation in (1.111) would represent a conformational change. Such a mechanism is favored in the oxidation of blue copper proteins.<sup>94</sup>

It is often however very difficult to distinguish between schemes (a) and (b).<sup>95</sup> With scheme (a) there will be an induction period in the appearance of products as C is being built-up, see also Fig. 1.8. This will not be the case with scheme (b) since production of D starts directly from A and B. By examining very carefully the reaction progress at very early times while (1.107) is being set up, it may be possible to distinguish between the two schemes.<sup>96-99</sup> Once the rapid equilibrium has been established however the steady-state kinetics are identical for (a) and (b). Arguments over which of the two schemes is preferred must then be based on chemical or rate considerations, and these are usually equivocal. However they can be used to distinguish (a) and (b) in the reactions (1.100) using the following reasoning.<sup>100</sup> The overall equilibrium constant for (1.100) can be estimated from oxidation potential data. The value (20) is equal to  $K_1 k_2 / k_{-2}$  for (a) and  $k_3 / k_{-3}$  for (b) where  $k_{-2}$  and  $k_{-3}$  are second-order rate constants for the steps



or



This means that either  $k_{-2}$  or  $k_{-3}$  is  $0.21 \text{ M}^{-1} \text{ s}^{-1}$ . This is a reasonable value for a second-order redox process which (1.117) represents, but is very unlikely for  $k_{-2}$  since formation of the bridged adduct must involve  $\text{Co}^{\text{III}}\text{-O}$  bond cleavage in  $\text{Co}(\text{edta})^-$  and such a process would be expected to be much slower (Ch. 4). For this, and other reasons<sup>101,102</sup> mechanism (b) is strongly preferred.

Since the propensity to form adducts in chemistry is high and these adducts undergo a variety of reactions, the rate law (1.98) is quite common. This is particularly true in enzyme kinetics.<sup>103</sup> In reality, these reaction schemes give biphasic first-order plots but because the first step is usually more rapid, for example between A and B in (1.101) we do not normally, nor do we need to, examine this step in the first instance.<sup>104-106</sup> The value of  $K_1$  in (1.107) obtained kinetically can sometimes be checked directly by examining the rapid preequilibrium before reaction to produce D occurs. In the reactions of Cu(I) proteins with excited Cr and Ru polypyridine complexes, it is considered that (a) and (b) schemes may be operating concurrently.<sup>107</sup>

Finally, we consider a straightforward example of three consecutive steps as in the scheme



$$V = k_3 [\text{E}] [\text{B}] = \frac{k_1 k_2 k_3 [\text{A}] [\text{B}]^3}{k_2 k_3 [\text{B}]^2 + k_{-1} k_3 [\text{B}] [\text{D}] + k_{-1} k_{-2} [\text{D}]} \quad (1.121)$$

This rate equation is derived by assuming a steady-state treatment in which

$$d[C]/dt = d[E]/dt = 0 \quad (1.122)$$

or alternatively the Christiansen formulation is applied.<sup>108</sup> The inclusion of the concentration of product D in (1.121) indicates that D features in a reversible step that occurs prior to or at the rate-determining stage. Deliberate addition of the product D and observation of retardation of the rate will show whether this scheme is plausible.

This oxidation of inorganic reductants by Cr(VI) show a variety of behaviors based on scheme (1.118–1.120) (A = Cr(VI); C = Cr(V); E = Cr(IV); F = Cr(III); B = reduced form and D = oxidized form of reductant). With B = Ag(I) or Ce(III), the rate law (1.121) is obeyed, indicating that the rate-determining step (1.120) involves Cr(IV).<sup>109,110</sup>

### 1.6.5 Two-Step Reactions with Total Reversibility

The scheme



forms an important basis for understanding the kinetics of many reactions.<sup>111–113</sup> Although the addition of the reverse terms  $k_{-1}$  or  $k_{-2}$  (or even worse both) to (1.66) complicates the treatment considerably, some complexity can usually be removed by various subterfuges. The two steps are unlikely to be both purely first-order and any or even all of the rate constants may be functions of the concentrations of other reagents D – G. Provided these are maintained in



excess of A, B or C, the treatment of (1.124) is based on (1.123) with  $k_1 = k'_1[D]$ ,  $k_{-1} = k'_{-1}[E]$  etc. and  $k'_1$ ,  $k'_{-1}$  etc. the second-order rate constants for A reacting with D etc. We shall see that with the system (1.123) or (1.124) identical results are obtained whether pure A, pure C, or a mixture is the starting condition, or an equilibrium mixture is perturbed (Sec. 1.8.2).

Biphasic kinetics will in principle be observed with (1.123). The associated first-order rate constants  $k_1$  and  $k_{11}$  are related to the rate constants of (1.123) by the relationships (Sec. 1.8.2)

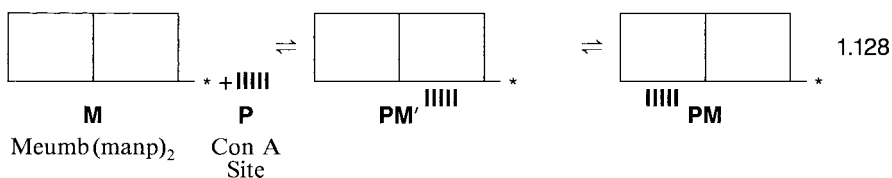
$$k_1 + k_{11} = k_1 + k_{-1} + k_2 + k_{-2} \quad (1.125)$$

$$k_1 k_{11} = k_1 (k_2 + k_{-2}) + k_{-1} k_{-2} \quad (1.126)$$

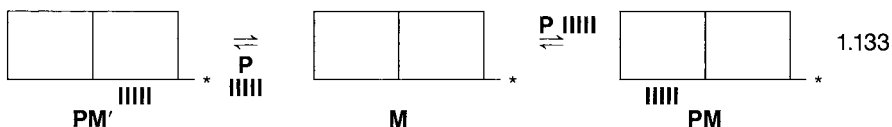
Only if  $K_1 (= k_1/k_{-1})$  and  $K_2 (= k_2/k_{-2})$  are known, are all the rate constants calculable. This necessity is removed if one of the steps is pseudo first-order, e.g. A reacts with D in the first step, as we shall now discover.

The interaction of excess concanavalin A<sup>114</sup> (P) with the chromogenic disaccharide p-nitrophenyl-2-O- $\alpha$ -D-mannopyranosyl- $\alpha$ -D-mannopyranoside(M) **10**(a) displays a spectral-time course shown in Fig. 1.9.<sup>115</sup> It is clearly biphasic and

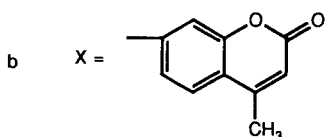
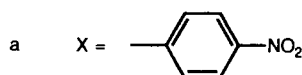
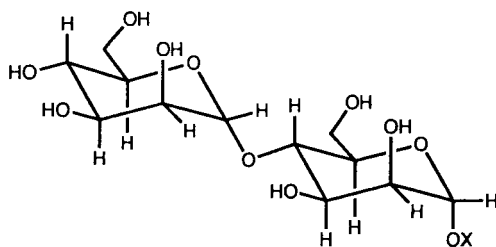
*Concanavalin A* (Con A) – There is a binding site for a single *D*-mannopyranosyl (manp) group not far from the Ca, Mn binuclear site in Con A. Carbohydrate binding is the basis of important biological properties of the protein. The interaction can be probed by attaching a nitrophenyl or a methylumbelliferyl group (Meumb) to the sugar and using spectral or fluorescence monitoring, respectively. A single phase attends the Con A reaction with Meumb-manp, but with the disaccharide Meumb(manp)<sub>2</sub> interaction is biphasic. The two mechanisms may be represented as either



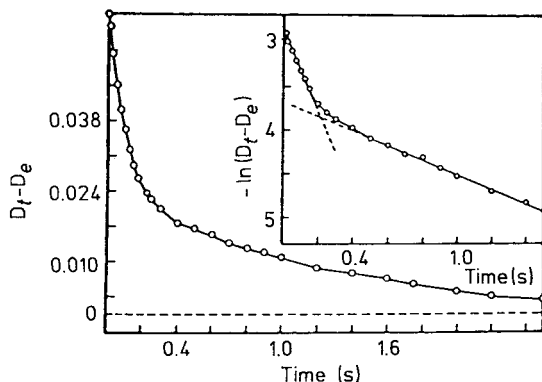
in which binding is followed by an isomerization, or by:



now binding occurs simultaneously with groups on both internal and terminal residues. The asterisk represents the chromophoric group of the disaccharide.



**10**



**Fig. 1.9** Time dependence of absorbance obtained after mixing Con A (200  $\mu\text{M}$ ) and **10** (a) (20  $\mu\text{M}$ ). The semi-log plot of the data (inset) shows even clearer the biphasic nature of the reaction.<sup>115</sup> Reprinted with permission from T. J. Williams, J. A. Shafer, I. T. Goldstein and T. Adamson, *J. Biol. Chem.* **253**, 8538 (1978).

is analyzed by

$$D_t - D_e = \alpha \exp(-k_I t) + \beta \exp(-k_{II} t) \quad (1.127)$$

where  $\alpha$  and  $\beta$  ( $= D_0 - D_e - \alpha$ ) are composite parameters. One reaction scheme related to (1.123) with A reacting with D in the first step (therefore  $k_1$  is a second-order rate constant) is



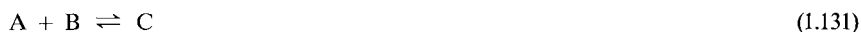
in which there is a conformational change of the protein-sugar adduct  $PM'$  subsequent to its more rapid formation. It is easy to see from (1.125) and (1.126) that

$$k_I + k_{II} = k_1 [P] + k_{-1} + k_2 + k_{-2} \quad (1.129)$$

$$k_I k_{II} = k_1 (k_2 + k_{-2}) [P] + k_{-1} k_{-2} \quad (1.130)$$

From the slopes and intercepts of the two plots of  $(k_I + k_{II})$  vs  $[P]$  and  $k_I k_{II}$  vs  $[P]$  in excess, all four rate constants can, in principle, be extracted.

However as was seen in Sec. 1.6.4 another scheme is possible



which applied to the present system yields



This is a fundamentally different mechanism. The two adducts  $PM$  and  $PM'$  are initially formed at relative rates equal to  $k_4/k_{-3}$ . In the slow phase  $PM$  and  $PM'$  equilibrate and their relative concentrations are controlled by the equilibrium constant  $k_3 k_4 / k_{-3} k_{-4}$ . For the scheme (1.133) by substituting  $k_3 + k_{-4}$  for  $k_1 + k_{-2}$  and  $(k_{-3} + k_4) [P]$  for  $k_{-1} + k_2$  in (1.125) and (1.126) one obtains

$$k_1 + k_{11} = k_3 + k_{-4} + (k_{-3} + k_4) [P] \quad (1.134)$$

$$k_1 k_{11} = k_3 k_{-4} + (k_3 k_4 + k_{-3} k_{-4}) [P] \quad (1.135)$$

Comparison of (1.129) and (1.130) with (1.134) and (1.135) shows that the schemes cannot easily be distinguished kinetically. Considerations of spectral changes accompanying the two phases and values of  $\alpha$  and  $\beta$  for the two schemes, as well as chemical considerations, strongly support the second interpretation. Both spectral and fluorescence monitoring (using **10 (b)**) and the techniques of stopped-flow (starting with P and M) and temperature-jump (starting with an equilibrium mixture of P, M, \*PM and PM) have been applied with similar results to this important interaction. The references 115–118 should be consulted for detailed analyses of the system.

The reaction of metal ion  $M^{n+}$  with the keto, enol tautomeric mixture of acetylacetonate (acacH) in acidic aqueous solution has been treated by a similar approach to that outlined above (see Prob. 16).



Simplifications ease the extraction of accurate values for the rate constants. For example, the keto, enol interconversion may sometimes be ignored, and  $k_{-2} \gg k_1$  and  $k_2 \gg k_{-1}$  are justifiable assumptions.<sup>119–121</sup>

A very important scheme in transition metal chemistry is illustrated by



which arises if the mechanism for interchange of B and C on A is dissociative in character (Sec. 4.2.2). Specifically we might consider the interchange of  $O_2$  and CO coordinated to an iron respiratory protein e.g. myoglobin (PFe)



The steady-state assumption is widely applied since the concentration of adduct-free myoglobin, PFe is very small.

$$\pm d[PFe]/dt = 0 \quad (1.141)$$

A single first-order reaction is observed and

$$d[PFe(CO)]/dt = -d[PFe(O_2)]/dt = k_{\text{obs}} ([PFe(CO)]_e - [PFe(CO)]_t) \quad (1.142)$$



where

$$k_{\text{obs}} = \frac{k_1 k_2 [\text{CO}] + k_{-1} k_{-2} [\text{O}_2]}{k_2 [\text{CO}] + k_{-1} [\text{O}_2]} \quad (1.143)$$

Further simplification may be possible, dependent on the relative values of the four terms in (1.143).<sup>122</sup> Care must be taken to ensure that both  $[\text{O}_2]$  and  $[\text{CO}] \gg [\text{PFe}(\text{O}_2)]$ , so that the concentrations of  $\text{O}_2$  and  $\text{CO}$  remain approximately constant throughout the reaction. The interchange



may be similarly treated.<sup>123</sup>

The schemes considered are only a few of the variety of combinations of consecutive first-order and second-order reactions possible including reversible and irreversible steps.<sup>124</sup> Exact integrated rate expressions for systems of linked equilibria may be solved with computer programs. Examples other than those we have considered are rarely encountered however except in specific areas such as oscillating reactions or enzyme chemistry, and such complexity is to be avoided if at all possible.

## 1.7 Recapitulation

At this stage we ought to restate briefly the sequences necessary in the construction of the rate law.

1. Decide the reactant (A) whose concentration is most conveniently monitored. Use A in deficiency and determine whether it is totally (>95%) consumed in all the experimental conditions envisaged. If it is not, the reaction is reversible, and should be allowed for in the kinetic treatment.

2. Determine the order of the reaction with respect to A. The value of  $[\text{A}]$ ,  $\ln [\text{A}]$ , or  $[\text{A}]^{-1}$  will probably be linearly related to time, indicating zero-, first-, or second-order, respectively. All other reactants are maintained in constant concentration.

3. Repeat the experiments with different concentrations of the other reactants B, and so on, varied one at a time. Thus determine the order with respect to these also. Plots of  $\log k_{\text{obs}}$  vs  $\log [\text{B}]$ , and so on, are sometimes useful in giving the reaction orders as slopes (Prob. 5).

4. If complexity is suspected from the kinetic behavior, the effect of products and of possible impurities and the occurrence of side reactions should be considered. Later we shall see that medium composition (Sec. 2.9), temperature and pressure (Sec. 2.3) are other important parameters that affect rate. The rate law incorporating these effects is obtained by further experiments of the type indicated in step 3.

## 1.8 Relaxation Kinetics

With the availability of perturbation techniques for measuring the rates of rapid reactions (Sec. 3.4), the subject of relaxation kinetics – rates of reaction near to chemical equilibrium – has become important in the study of chemical reactions.<sup>125</sup> Briefly, a chemical system at equilibrium is perturbed, for example, by a change in the temperature of the solution. The rate at which the new equilibrium position is attained is a measure of the values of the rate constants linking the equilibrium (or equilibria in a multistep process) and is controlled by these values.

### 1.8.1 Single-Step Reactions

Consider a simple equilibrium, second-order in the forward direction and first-order in the reverse:



After the perturbation, let the final equilibrium concentrations be represented by A, B, and C. At any time  $t$  after the perturbation is imposed, and before the final equilibrium is reached, let the concentrations of A, B, and C be  $(A - a)$ ,  $(B - b)$ , and  $(C - c)$ . Thus  $a$ ,  $b$ , and  $c$  represent deviations from the final equilibrium concentrations. It is apparent from the stoichiometry of the system that

$$a = b = -c \quad (1.146)$$

At time  $t$ ,

$$d(C - c)/dt = k_1(A - a)(B - b) - k_{-1}(C - c) \quad (1.147)$$

At final equilibrium,

$$dC/dt = 0 = k_1 AB - k_{-1} C \quad (1.148)$$

Since the perturbations are small, the term  $ab$  can be neglected for (1.147); then combination of (1.146), (1.147) and (1.148) gives

$$-dc/dt = [k_1(A + B) + k_{-1}]c \quad (1.149)$$

Similarly,

$$-da/dt = [k_1(A + B) + k_{-1}]a \quad (1.150)$$

The shift to the new equilibrium as a result of the perturbation, the *relaxation* of the system, is therefore a first-order process with a first-order rate constant  $k = \tau^{-1}$  (1.28) made up of  $k_1(A + B) + k_{-1}$ .

A treatment similar to that above can be applied to other single equilibria. If the stoichiometry condition akin to (1.146), the zero net rate condition at final equilibrium as in (1.148), and the neglect of squared terms in the deviation concentrations are applied to the rate equation similar to (1.147), it is found that there is always a linear relation of the form

$$-da/dt = ka \quad (1.151)$$

with a value for  $k$  characteristic of the system (Table 1.2), Prob. 12.

**Table 1.2.** Values of Relaxation Rate Constants ( $k$ ) for Various Single Equilibria

System	$k$
$A \rightleftharpoons B$	$k_1 + k_{-1}$ <sup>a</sup>
$2A \rightleftharpoons B$	$4k_1[A] + k_{-1}$
$A + B \rightleftharpoons C$	$k_1([A] + [B]) + k_{-1}$
$A + C \rightleftharpoons B + C$	$(k_1 + k_{-1})[C]$
$A + B \rightleftharpoons C + D$	$k_1([A] + [B]) + k_{-1}([C] + [D])$

<sup>a</sup> the symbols  $k_1$ ,  $k_{-1}$  represent the forward and reverse rate constants for all systems; [A], [B], [C] and [D] represent the final equilibrium concentration of these species.

Thus the determination of the relaxation times for a number of different reactant concentrations (estimated *in situ* or from a knowledge of the equilibrium constant) will give both the reaction order and the associated rate constants. It should be noted that the concentrations in (1.149) are equilibrium ones. Algebraic manipulation allows the determination of the rate constants for some systems in Table 1.2 without a knowledge of equilibrium constants. For  $2A \rightleftharpoons B$ , it can be easily deduced that a plot of  $k^2$  vs  $[A]_0$  is linear with a slope of  $8k_1k_{-1}$  and an intercept  $k_{-1}^2$ . The value  $[A]_0$  is the stoichiometric concentration =  $[A] + 2[B]$ ,<sup>126-128</sup> see Prob. 13. Normally, changes in concentration from the perturbation are held to  $< 10\%$  of the total concentration, an amount which is usually easily monitored. It is perhaps surprising that perturbations imposed can be larger than this for single- and multistep reactions, virtually without loss of the first-order relaxation features.<sup>14,129-132</sup> In any event, analysis of the last portion of a trace arising from a large perturbation will be a valid procedure.

If in the relaxation systems listed in Table 1.2 one of the reactants A or B and one of the products C or D is in large excess, that is if pseudo first-order conditions obtain, the relaxation expression is identical with the rate law obtained starting from pure reactants (1.148). For conditions other than these however, the simplified treatment with relaxation conditions is very evident, as can be seen, for example, in the simple expression for the first-order relaxation rate constant for the  $A + B \rightleftharpoons C + D$  scheme compared with the treatment starting from only A and B, and when pseudo first-order conditions cannot be imposed.<sup>41</sup>

## 1.8.2 Multistep Reactions

One does not often encounter the simple scheme involving only first-order reactions such as (1.152)



However, consider the very common and important two-step mechanism (1.153).



This can be reduced to (1.152) when  $[B] \gg [A]$ . The difficult situation to analyze arises when the rates associated with the two steps in (1.153) are similar and in addition  $[A]_0 \sim [B]_0$  and the reduction to (1.152) cannot be made. This case will be treated first. The objective is to express  $da/dt$  and  $dc/dt$  each in terms of  $a$  and  $c$ , which are the deviations from equilibrium concentrations symbolized A, B, C, and D. These provide the basis for the two relaxation times observable with the system. Now

$$a = b = -(c + d) \quad (1.154)$$

$$d(A - a)/dt = -k_1(A - a)(B - b) + k_{-1}(C - c) \quad (1.155)$$

$$-da/dt = k_1(A + B)a - k_{-1}c \quad (1.156)$$

$$d(C - c)/dt = k_1(A - a)(B - b) - k_{-1}(C - c) - k_2(C - c) + k_{-2}(D - d) \quad (1.157)$$

$$k_{-2}D = k_2C \quad (1.158)$$

$$-dc/dt = -k_1(A + B)a + k_{-1}c + k_2c + k_{-2}(a + c) \quad (1.159)$$

$$-dc/dt = -(k_1(A + B) - k_{-2})a + (k_{-1} + k_2 + k_{-2})c \quad (1.160)$$

Equations (1.156) and (1.160) are of the forms

$$-da/dt = \alpha_{11}a + \alpha_{12}c \quad (1.161)$$

$$-dc/dt = \alpha_{21}a + \alpha_{22}c \quad (1.162)$$

Making the substitution  $a = Xe^{-kt}$  and  $c = Ye^{-kt}$  gives

$$kXe^{-kt} = \alpha_{11}Xe^{-kt} + \alpha_{12}Ye^{-kt} \quad (1.163)$$

$$kYe^{-kt} = \alpha_{21}Xe^{-kt} + \alpha_{22}Ye^{-kt} \quad (1.164)$$

or<sup>133</sup>

$$(\alpha_{11} - k)a + \alpha_{12}c = 0 \quad (1.165)$$

$$(\alpha_{22} - k)c + \alpha_{21}a = 0 \quad (1.166)$$

Solving for  $k$  by eliminating  $a$  and  $c$  gives

$$k^2 - (\alpha_{11} + \alpha_{22})k + \alpha_{11}\alpha_{22} - \alpha_{12}\alpha_{21} = 0 \quad (1.167)$$

The two first-order rate constants  $k_1$  and  $k_{11}$  associated with this scheme are given by

$$2k_1 = \alpha_{11} + \alpha_{22} + [(\alpha_{11} + \alpha_{22})^2 - 4(\alpha_{11}\alpha_{22} - \alpha_{12}\alpha_{21})]^{1/2} \quad (1.168)$$

and

$$2k_{11} = \alpha_{11} + \alpha_{22} - [(\alpha_{11} + \alpha_{22})^2 - 4(\alpha_{11}\alpha_{22} - \alpha_{12}\alpha_{21})]^{1/2} \quad (1.169)$$

and

$$\alpha_{11} = k_1(A + B) \quad (1.170)$$

$$\alpha_{12} = -k_{-1} \quad (1.171)$$

$$\alpha_{22} = k_{-1} + k_2 + k_{-2} \quad (1.172)$$

$$\alpha_{21} = k_{-2} - k_1(A + B) \quad (1.173)$$

These are cumbersome equations to use but (1.168) and (1.169) can be computer treated. Alternatively, it is easily deduced that

$$k_1 + k_{11} = k_1(A + B) + k_{-1} + k_2 + k_{-2} \quad (1.174)$$

and

$$k_1k_{11} = k_1(k_2 + k_{-2})(A + B) + k_{-1}k_{-2} \quad (1.175)$$

From plots of  $(k_1 + k_{11})$  vs  $[A + B]$  and  $k_1k_{11}$  vs  $[A + B]$ , all rate constants can be determined (see Sec. 1.6.5).<sup>134</sup>

This treatment yields the time course of the relaxation which is of most concern to us, but ignores the relative magnitudes of the relaxations (contained in the X and Y terms in (1.163)). These latter are complex functions of reaction enthalpies and absorbance coefficients, but can yield equilibrium constants for the two steps.<sup>135,136</sup> However, relaxation data are much less used for thermodynamic than kinetic information.

A common simplification arises when the bimolecular step in (1.153) equilibrates rapidly compared with the unimolecular step (it may, for example, be a proton-base reaction). This means that the change in concentrations of A, B, and C due to the first process in (1.153) will have occurred before D even starts to change. The relaxation time  $\tau_1$  associated with it will therefore be the same as if it were a separated equilibrium:

$$\tau_1^{-1} = k_1 = k_1(A + B) + k_{-1} \quad (1.176)$$

The changes of concentration of C and D resulting from the second equilibrium are however coupled to the first, and the associated relaxation time  $\tau_{11}$  might be expected to be a more complex function. It is however fairly easily derived.

$$d(D - d)/dt = k_2(C - c) - k_{-2}(D - d) \quad (1.177)$$

from which

$$dd/dt = k_2c - k_{-2}d \quad (1.178)$$

Now we must express  $c$  in terms of  $d$ , so that an equation relating  $dd/dt$  and  $d$  only may be obtained. Since the first equilibrium is always maintained, compared with the second,

$$k_1(A - a)(B - b) = k_{-1}(C - c) \quad (1.179)$$

$$k_1(Ab + Ba) = k_{-1}c \quad (1.180)$$

Since

$$-a = -b = c + d \quad (1.181)$$

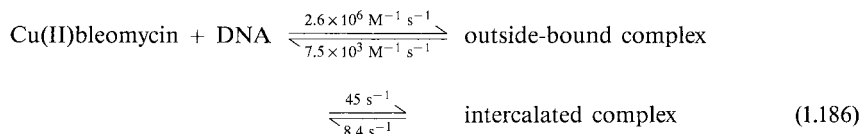
$$-k_1(A + B)(c + d) = k_{-1}c \quad (1.182)$$

$$c = \frac{-k_1(A + B)d}{k_1(A + B) + k_{-1}} \quad (1.183)$$

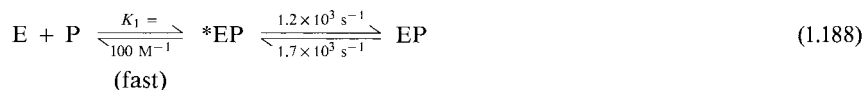
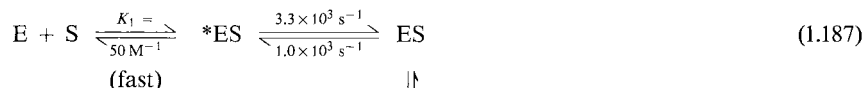
$$\frac{dd}{dt} = \frac{-k_1k_2(A + B)d}{k_1(A + B) + k_{-1}} - k_{-2}d \quad (1.184)$$

$$\tau_{II}^{-1} = k_{II} = k_{-2} + \frac{k_1k_2(A + B)}{k_1(A + B) + k_{-1}} \quad (1.185)$$

Equations (1.176) and (1.185) can be derived from the general expression (1.167) by using the relationship  $k_1(A + B) + k_{-1} \gg k_{-2} + k_2$  and making the approximation  $(1 - x)^{1/2} \sim 1 - x/2$ . The approximate approach is often used when the direct product of a bimolecular reaction undergoes a slower change (isomerization or conformational reaction). Both fast and slow relaxations are analyzed by (1.176) and (1.185) using Fig. 1.10(a) which indicates the variation of  $k_I$  and  $k_{II}$  with  $[A] + [B]$  on the basis that  $k_I > k_{II}$  ( $K_I = k_1/k_{-1}$ ). Examples of its occurrence are in the reactions<sup>137</sup>

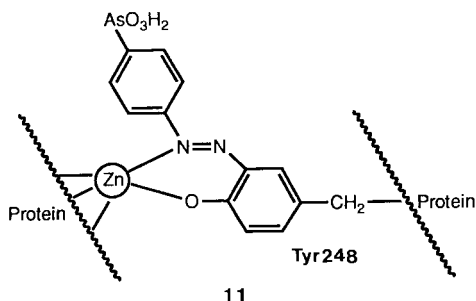


and<sup>138</sup>



Reaction (1.187) represents the binding of the substrate (S), Gly-L-Phe and (1.188) is binding of the product (P), L-Phe, to a colored derivative of carboxypeptidase (Chap. 8. Zn) ((E), arsanilazotyrosine-248 labelled) II. Only the slow step has been analyzed (starting in either direction) and it conformed to (1.185). Values for  $K_I$  (which equals  $k_1/k_{-1}$  in (1.153)),  $k_2$  and  $k_{-2}$  for the formation of both ES and EP are obtained. The two directions are isolable because the conversion of ES to EP is relatively slow ( $k_{\text{cat}} = 0.01 \text{ s}^{-1}$ ).<sup>138</sup>

The relaxation approach has played an important role in our understanding of the mechanisms of complex formation in solution (Chap. 4)<sup>139,140</sup> The use of computer programs has now eased the study of multiple equilibria. For example, four separate relaxation effects with  $\tau$ 's ranging from 100  $\mu\text{s}$  to 35 ms are observed in a temperature-jump study of the reactions of  $\text{Ni}^{2+}$  with flavin adenine dinucleotide (fad) (Eqn. (8.121)). The complex relaxation

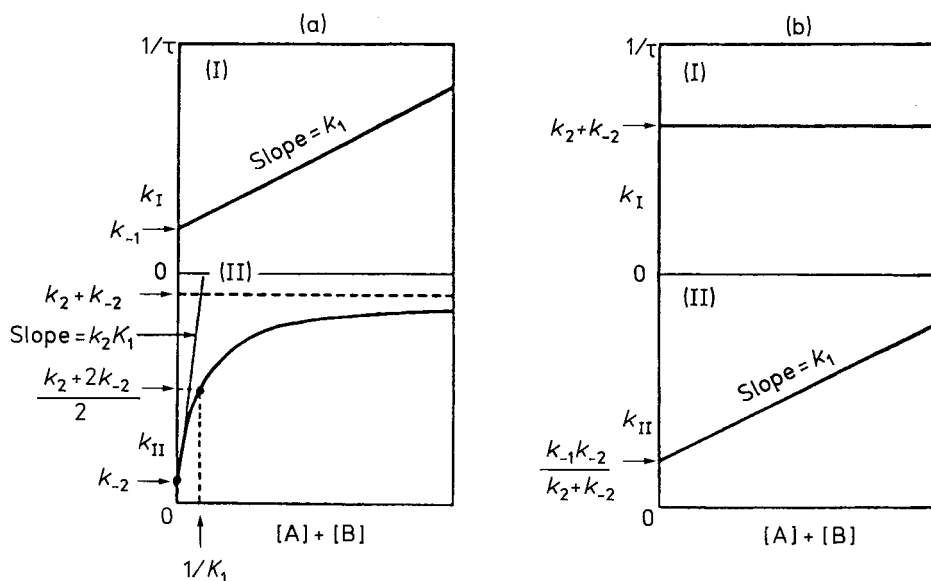


equations may be computer-analyzed and the associated four steps rationalized in terms of initial phosphate attachment to  $\text{Ni}^{2+}$  followed by intramolecular binding of the other two ligand sites of the coenzyme.<sup>141,142</sup>

Only rarely is the situation encountered when the first step in (1.153) is *slower* than the second transformation. It is easily recognized from the dependence of  $k_1$  and  $k_{II}$  on  $[A] + [B]$ , Fig. 1.10(b).<sup>143</sup> The difficulties of distinguishing Scheme (1.153) from (1.189):



have been already alluded to and the relaxation approach to this problem thoroughly examined.<sup>144</sup> Comprehensive tables of rate expressions for a variety of schemes both possible and unlikely in practice are collected in the texts by Bernasconi and Hiromi (Prob. 14).



**Fig. 1.10** Dependence of  $k_1$  and  $k_{II}$  on  $[A] + [B]$  for the sequential reactions  $A + B \rightleftharpoons C \rightleftharpoons D$  for (a)  $A + B \rightleftharpoons C$  the more rapid and (b)  $C \rightleftharpoons D$  the more rapid step.<sup>143</sup>

## 1.9 Exchange Kinetics

Somewhat in the same vein as relaxation kinetics, there is a simplicity about the manipulation of isotopic exchange results that makes the method an important and useful tool for studying mechanism. When AX and BX, both containing a common atom or group of atoms X, are mixed, there will be a continual interchange of X between the two environments that may range from extremely rapid to negligibly slow. This exchange will go undetected unless we tag AX or BX with some labeled X, which we denote by \*X:



Consider a mixture of AX and BX at chemical equilibrium. When, for example, radioisotopes are used as tracers, they are injected into the equilibrium mixture in the form of a very small amount of B\*X. At various times, either (BX + B\*X) or (AX + A\*X) is separated from the mixture and analyzed. When nmr line broadening is used to monitor the exchange the tracer is already present e.g.  $^1\text{H}$  or  $^{17}\text{O}$  (or an additional amount can be added) and the exchange is monitored *in situ* and assessed from the shape of the nmr signals (Sec. 3.9.6). If the concentration of (AX + A\*X) is  $a$  and the concentration of (BX + B\*X) is  $b$ , and the fraction of exchange at time  $t$  is  $F$ , it is not difficult to show that the gross or overall rate of X transfer between AX and BX,  $V_{\text{exch}}$  ( $\text{M s}^{-1}$ ) is given by<sup>145</sup>

$$V_{\text{exch}} = \frac{-ab \ln(1 - F)}{(a + b)t} = k_{\text{obs}} \frac{ab}{(a + b)} \quad (1.191)$$

$F$  will equal  $x/x_e$  where  $x$  and  $x_e$  represent the mole fractions of A\*X at sampling and equilibrium times. The rate of exchange will be identical in both directions in (1.190) and be always first-order, comparable to the situation with relaxation kinetics, a relationship which has been explored.<sup>146</sup> The equation (1.191) is modified slightly when isotope effects are included.<sup>147</sup> The rate of exchange will depend on the concentrations  $a$ ,  $b$ ,  $[\text{H}^+]$ , and so on, in a manner that determines the rate expression. The exchange rate is measured with different concentrations of AX, BX,  $[\text{H}^+]$  etc., and the rate law is constructed exactly as in the initial-rate or stationary-state methods (Prob. 17). A popular method for treating (1.191) has been by the use of a plot of  $-\ln(1 - F)$  vs time. For a single exchange process this will be linear, from the slope of which  $k_{\text{obs}}$  is obtained.

The exchange of Mn between  $\text{MnO}_4^-$  and  $\text{MnO}_4^{2-}$  has been followed using the  $^{54}\text{Mn}$  radioisotope and quenched-flow methods (Sec. 3.3.2).<sup>148</sup> The results are shown in Table 1.3, from which it is apparent that

$$V_{\text{exch}} = k [\text{MnO}_4^-] [\text{MnO}_4^{2-}] \quad (1.192)$$

Even complex rate laws may be easily constructed by examining the dependence of  $V_{\text{exch}}$  on the concentrations of the various species in solution. The rate of exchange of Ni between  $\text{Ni}^{2+}$  and  $\text{Ni}(\text{edta})^{2-}$  obeys the rate law

$$V_{\text{exch}} = k_1 [\text{Ni}^{2+}] [\text{Ni}(\text{edta})^{2-}] + k_2 [\text{Ni}^{2+}] [\text{Ni}(\text{edta})^{2-}] [\text{H}^+] + k_3 [\text{Ni}(\text{edta})^{2-}] [\text{H}^+] + k_4 [\text{Ni}(\text{edta})^{2-}] [\text{H}^+]^2 + k_5 [\text{Ni}(\text{edta})^{2-}] [\text{H}^+]^3 \quad (1.193)$$



**Table 1.3.** Dependence of  $^{54}\text{Mn}$  Exchange Rate on Concentrations of  $\text{MnO}_4^{2-}$  and  $\text{MnO}_4^-$  at  $0.1^\circ\text{C}$  in  $0.16\text{ M NaOH}$ 

$10^5 \times [\text{MnO}_4^{2-}]$ M	$10^5 \times [\text{MnO}_4^-]$ M	$t_{1/2}$ exch s	$10^6 \times V_{\text{exch}}$ $\text{M s}^{-1}$	$10^{-2} \times k$ $\text{M}^{-1} \text{s}^{-1}$
4.3	4.8	10.6	1.5	7.2
4.1	4.8	11.2	1.4	7.0
4.6	9.7	6.6	3.3	7.3
4.5	14.6	5.3	4.5	6.8
4.3	19.4	4.3	5.7	7.6
4.2	24.3	3.2	7.8	7.3
4.1	34.0	2.5	10.2	6.5
1.0	9.7	9.2	0.69	7.3
2.3	9.5	9.0	1.4	6.5
4.6	9.7	6.6	3.3	7.3
10.1	9.7	4.9	6.9	7.1
19.7	9.7	3.1	15	7.9
33.0	337	0.25	830	7.5
195	188	0.26	2550	7.0
29	381	0.25	750	6.8
			Average	$7.1 \pm 0.3$

The five terms simply represent paths through which exchange can occur (Sec. 4.4.3).<sup>149</sup>

If there is more than one exchanging atom of X in the interacting molecules, for example  $\text{AX}_n$  exchanging with  $\text{BX}_m$ , the rate expression (1.191) is modified accordingly, with  $a$  and  $b$  replaced by  $na$  and  $mb$  respectively. This applies only when the  $n\text{X}$  or  $m\text{X}$  atoms are equivalent. In basic solution the vanadium(V) ion,  $\text{VO}_4^{3-}$  exchanges oxygen with solvent  $\text{H}_2\text{O}$ . The plot of  $\ln(1 - F)$  is linear with time for at least four half-lives and it can be shown that all four oxygens in  $\text{VO}_4^{3-}$  exchange, from the distribution of  $^{18}\text{O}$  between  $\text{VO}_4^{3-}$  and  $\text{H}_2\text{O}$  at equilibrium. They are thus equivalent.<sup>150</sup>

$$V_{\text{exch}} = k_{\text{obs}} \frac{4 [\text{VO}_4^{3-}] [\text{H}_2\text{O}]}{4 [\text{VO}_4^{3-}] + [\text{H}_2\text{O}]} \quad (1.194)$$

and since  $[\text{H}_2\text{O}] \gg 4 [\text{VO}_4^{3-}]$

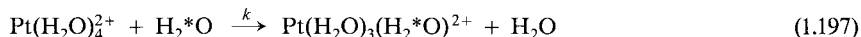
$$V_{\text{exch}} = 4k_{\text{obs}} [\text{VO}_4^{3-}] \quad (1.195)$$

A special and important type of exchange arises when one of the exchanging species is the solvent. The rate of exchange of solvent molecules, S, between free and metal-coordinated solvent has been studied for a large variety of metal ions and solvents.<sup>151</sup> A good deal of confusion has arisen over the definition and meaning of the exchange rate constant in such systems. It has been recently shown,<sup>152,153</sup> surprisingly, that the rates of isotopically labelled solvent exchange of all  $n$  ligands in  $\text{MS}_n^{2+}$  and of a particular one of these  $n$  ligands are the same. Previous division of  $k_{\text{exch}}$  by a statistical factor of  $n$  should not have been carried out.<sup>154</sup> This

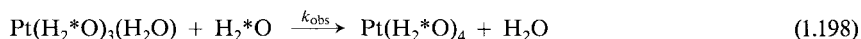
can be illustrated by reference to the exchange of  $\text{H}_2\text{O}$  between  $\text{Pt}(\text{H}_2\text{O})_4^{2+}$  and free solvent, Fig. 1.11.<sup>155</sup> From (1.191)

$$V_{\text{exch}} = k_{\text{obs}} \frac{4[\text{Pt}(\text{H}_2\text{O})_4^{2+}][\text{H}_2\text{O}]}{4[\text{Pt}(\text{H}_2\text{O})_4^{2+}] + \text{H}_2\text{O}} \sim 4k_{\text{obs}}[\text{Pt}(\text{H}_2\text{O})_4^{2+}] = k[\text{Pt}(\text{H}_2\text{O})_4^{2+}] \quad (1.196)$$

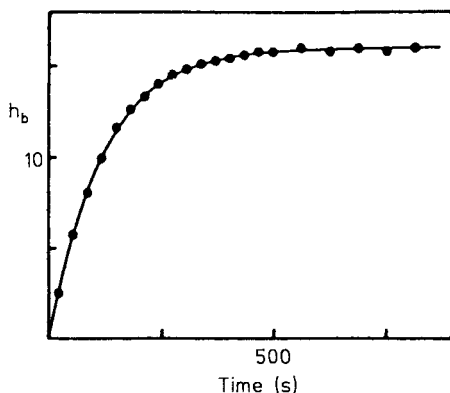
$k$  is the rate constant for exchange of any  $\text{H}_2\text{O}$  molecule



while  $k_{\text{obs}}$  is the rate constant for exchange of a particular

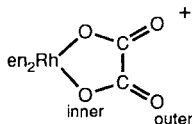


ligand and equals  $\tau_{\text{exch}}^{-1}$  ( $\tau_{\text{exch}} = 116$  s from Fig. 1.11).  $k$  therefore equals  $4k_{\text{obs}}$ .



**Fig. 1.11** Increase with time of height  $h_b$  (arbitrary units) of the  $^{17}\text{O}$  nmr signal from coordinated water in  $\text{Pt}(\text{H}_2\text{O})_4^{2+}$  when treated with  $^{17}\text{O}$ -enriched water. Fast injection of 0.7 g of  $\text{Pt}(\text{H}_2\text{O})_4(\text{ClO}_4)_2$  (0.58 M) and  $\text{HClO}_4$  (3.5 M) into 0.55 g of 20%  $^{17}\text{O}$ -enriched water at  $50.6^\circ\text{C}$  was employed.<sup>155</sup> Reprinted with permission from L. Helm, L. I. Elding and A. E. Merbach, *Inorg. Chem.* **24**, 1719 (1985). © 1985, American Chemical Society.

When the molecule contains more than one type of exchanging atom, but the associated exchange rates differ widely, there is no problem in treating this system as separate single exchange steps (see the markedly different oxygen exchange types in  $\text{Mo}_3\text{O}_4(\text{H}_2\text{O})_9^{4+}$ , **6** in Chap. 8<sup>156</sup>). However when the exchange rates are similar, their resolution and treatment is much more complex. This has been a vexing problem in the study of oxygen exchange between  $\text{H}_2\text{O}$  and metal-coordinated oxalate. There are two kinetically distinct types of coordinated oxygen in  $\text{Rh}(\text{en})_2\text{C}_2\text{O}_4^+$  (**12**). The slower exchange is attributed to inner/outer oxygen interchange which is presumed to occur before inner oxygens can exchange with solvent.



**12**

The rate processes differ only slightly and the treatment resembles that for Sec. 1.8.2.<sup>157</sup>

In recent years there have been relatively few studies of isotopic exchange using radioisotopes,<sup>158</sup> many more using  $^{18}O$  labelling<sup>159</sup> and a large number probed, both qualitatively and quantitatively by using the nmr method,<sup>151</sup> which has the decided advantage that *in situ* monitoring can be used (Chap. 3). Two overriding values of exchange reactions cannot be overemphasized. They *must* take place if a kinetic path exists (i.e. thermodynamics are not a consideration) and the associated very small driving force makes them easier to interpret than net chemical changes.

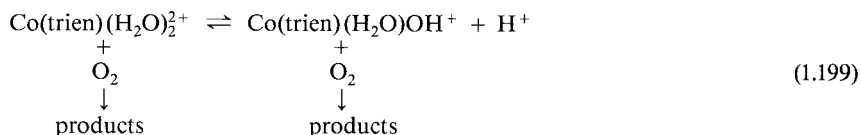
## 1.10 The Inclusion of $[H^+]$ Terms in the Rate Law

So far only the reactants directly involved in a reaction have been considered in their contribution to the rate law. Added “inert” cations and anions can sometimes contribute in a profound way by modifying the major reactants (e.g. by ion pairing) but usually the effects of their concentrations on the rates of reactions are best accommodated by the general theories of the effect of ionic strength on the reaction rate (Sec. 2.9.1).

Many reaction rates are affected by the pH of the solution. The modification of the rate as the pH is changed can be ascribed to formation of different species with different reactivities. Thus, the oxygen exchange between oxyions and water is faster in acid because of the enhanced reactivity of protonated oxyions. It is therefore essential that as wide a range of pH as possible be studied so as to detail a full reaction scheme, and thus delineate the reactive forms of the reactants. In no area is this recognized as important as in enzyme kinetics.<sup>103</sup> Assigning  $[H^+]$  terms in the rate law presents little problem, the rate constant for the reaction being simply measured at a number of hydrogen ion concentrations. The  $[H^+]$  may be in excess over that of other reagents, or alternatively the solutions may be buffered. In both cases, no change of pH occurs during the reaction. Since this is such an important parameter in its effect on rates, we shall discuss in some detail the most common types of behavior (rate/pH profiles) encountered. The determination of rate constants at even a few pH values can often indicate the extent and type of  $H^+$  (or  $OH^-$ ) involvement. It may in certain cases be necessary to separate a “medium” from a “mechanistic” effect of  $[H^+]$  on the rate (Sec. 2.9.2).

### 1.10.1 One Monoprotic Reactant, One Acid-Base Equilibrium

If the profile of the observed or the intrinsic rate constant plotted against pH resembles the profile for an acid-base titration curve, this strongly suggests that one of the reactants is involved in an acid-base equilibrium in that pH range. Such behavior is fairly common and is illustrated by the second-order reaction between the Co(II)-trien complex and  $O_2$  (Fig. 1.12).<sup>160</sup> The limiting rate constants at the higher and low acidities correspond to the acidic and basic forms of the Co(II) reactant, probably,



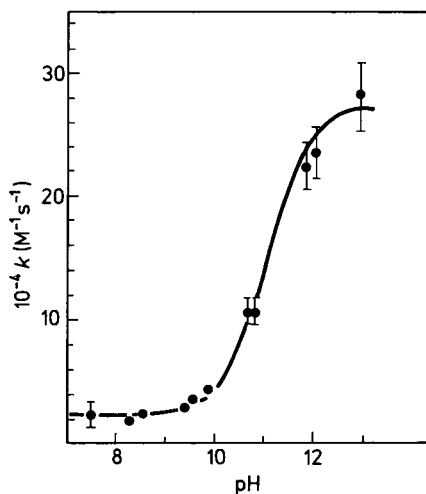
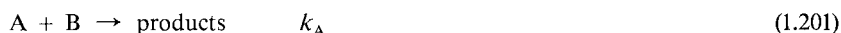


Fig. 1.12 The pH dependence of the first stage of the reaction between Co(II)-trien complex and  $\text{O}_2$ . The solid line represents Eqn. (1.207) with  $K_{\text{AH}} = 6 \times 10^{-12} \text{M}$ , which is a spectrally determined value.<sup>160</sup>

The rate law and the general reaction scheme associated with this system are easily derived. Consider the reaction of an acid AH and its conjugate base A with a substrate B (any charges are omitted from these for convenience):



Invariably, the total concentration of A and AH is monitored, and so the rate expression is formulated in terms of  $([\text{A}] + [\text{AH}])$

$$-d([\text{AH}] + [\text{A}])/dt = k([\text{AH}] + [\text{A}])[\text{B}]^n \quad (1.203)$$

where  $k$  is the experimental rate constant, first-order if  $n = 0$ , second-order if  $n = 1$ , and so on. The rate is also the sum of the contributions of AH and A.

$$-d([\text{AH}] + [\text{A}])/dt = k_{\text{AH}}[\text{AH}][\text{B}]^n + k_{\text{A}}[\text{A}][\text{B}]^n \quad (1.204)$$

Combining (1.203) and (1.204), we obtain

$$k = (k_{\text{AH}}[\text{AH}] + k_{\text{A}}[\text{A}])/([\text{AH}] + [\text{A}]) \quad (1.205)$$

Using

$$K_{\text{AH}} = [\text{A}][\text{H}^+]/[\text{AH}] \quad (1.206)$$

yields

$$k = (k_{\text{AH}}[\text{H}^+] + k_{\text{A}}K_{\text{AH}})/([\text{H}^+] + K_{\text{AH}}) \quad (1.207)$$

The full curve of Fig. 1.12 is drawn in accordance with (1.207). Considering limits, we find  $k = k_{AH}$  when  $[H^+] \gg K_{AH}$  and  $k = k_A$  with  $[H^+] \ll K_{AH}$ . The full S-shaped profile will be observed in reactions of acid/base pairs where both forms are attainable and show different reactivities. Examples are hydroxy and aqua complexes as typified by the example shown in (1.199),  $O_2^-$  and  $HO_2^-$ ,<sup>161,162</sup>  $CN^-$  and  $HCN$ ,  $Au(NH_3)_4^+$  and  $Au(NH_3)_3NH_2^+$ ,<sup>163</sup> and others. In rare cases, an unknown  $pK_{AH}$  may be determined kinetically (Prob. 20).

When one of the forms predominates over the pH range of investigation, yet the other form is much more reactive, only one limiting rate constant is obtained.

$$[A] \gg [AH]; [H^+] \ll K_{AH},$$

$$k = k_A + (k_{AH}[H^+])/K_{AH} \quad (1.208)$$

$$[AH] \gg [A]; [H^+] \ll K_{AH},$$

$$k = k_{AH} + (k_A K_{AH})/[H^+] \quad (1.209)$$

Such behavior is more common than the full rate/pH profile of (1.207). Equation (1.208) is observed in acid catalysis<sup>164-166</sup> and (1.209) in base catalysis.<sup>167</sup> The rate constant for the reaction of only one of the two forms can be obtained directly, that is,  $k_A$  in (1.208) and  $k_{AH}$  in (1.209). Ancillary information on  $K_{AH}$  is required to assess the rate constant of the acid-base partner. The absence of reliable data on  $K_{AH}$  can pose a problem in assessing the missing rate constant.<sup>167</sup>

Observation of the semblance of an S-shaped profile has been used to estimate the  $pK_{AH}$  value for an acid/base pair which may be difficult to obtain directly. This may be as the result of one of the pairs being unstable (polynuclear formation or hydrolysis, for example).<sup>168,169</sup> This approach must however be used with care since the errors are likely to be larger than when the whole, or a goodly portion, of the curve is defined.<sup>164,165</sup> See Problem 18.

A serious ambiguity in the interpretation of the rate law,

$$V = k[A][B][H^+]^n \quad (1.210)$$

exists when A and B are both basic and  $n$  is one or greater (acid hydrolysis). The actual species involved in the rate determining step, AH with B or BH with A in the case of  $n = 1$  cannot usually be assessed on the basis of kinetics but may sometimes be differentiated by resort to plausibility (Sec. 2.1.7). A similar problem arises when we consider reaction between AH and BH and  $n = -1$  in (1.210) (base hydrolysis).

## 1.10.2 Two Acid-Base Equilibria

When the sigmoidal shape of the rate constant/pH profile associated with (1.207) or the simpler derivatives (1.208) or (1.209) give way to a bell-shape or inverted bell-shape plot, the reactions of at least three acid-base-related species (two equilibria) have to be considered. This may involve acid-base forms of (a) one reactant or (b) two different reactants.

(a) Diprotic reactant A. Consider the scheme

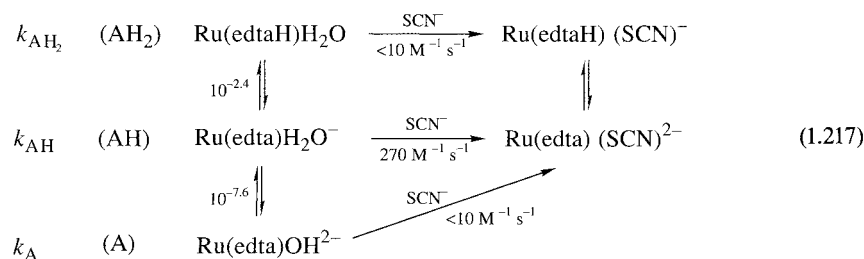


in which the rate constants may be first-order or pseudo first-order. Usually the products from the three steps are identical or at least pH-related. The observed rate constant  $k$  at any  $[\text{H}^+]$  can be shown by reasoning similar to that used in developing (1.207) to be:

$$k = \frac{k_{\text{AH}_2}[\text{H}^+]^2 + k_{\text{AH}}K_{\text{AH}_2}[\text{H}^+] + k_{\text{A}}K_{\text{AH}}K_{\text{AH}_2}}{[\text{H}^+]^2 + K_{\text{AH}_2}[\text{H}^+] + K_{\text{AH}}K_{\text{AH}_2}} \quad (1.216)$$

If the species AH reacts more rapidly or more slowly than either A or  $\text{AH}_2$ , a bell shape or inverted bell shape respectively results for the  $k/\text{pH}$  profile.

The ruthenium(III) complex of edta in which the ligand acts only as a five-coordinate species and in which an acetate arm remains free, exists in three pH-related forms:

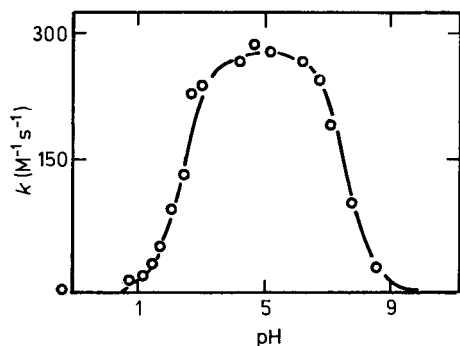


The second-order rate constants for thiocyanate anation vs pH are shown in Fig. 1.13. The full line represents (1.216) with the values shown in scheme (1.217).<sup>170</sup> This profile had been earlier recognized in the ring closure of the three analogous pH-related forms of Co(III)-edta to give  $\text{Co}(\text{edta})^-$  in which the edta is completely coordinated.<sup>171</sup> In the Co(III) case the reactivities of the three forms are much closer. A plot of  $k \{ [\text{H}^+]^2 + K_{\text{AH}_2}[\text{H}^+] + K_{\text{AH}}K_{\text{AH}_2} \}$  vs  $[\text{H}^+]$  is a quadratic curve from which  $k_{\text{AH}_2}$ ,  $K_{\text{AH}}$  and  $k_{\text{A}}$  can be obtained.<sup>172,173</sup>

If the predominant form of the reactant is AH in the pH region under examination, that is  $K_{\text{AH}_2} \gg [\text{H}^+] > K_{\text{AH}}$ , then only the middle term of the denominator in (1.216) is important. Thus

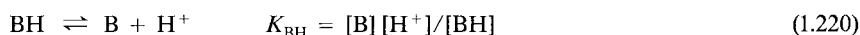
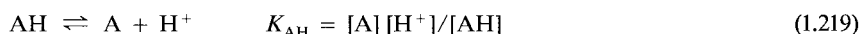
$$k = (k_{\text{AH}_2}[\text{H}^+]/K_{\text{AH}_2}) + k_{\text{AH}} + (k_{\text{A}}K_{\text{AH}}/[\text{H}^+]) \quad (1.218)$$

This describes the behavior of a number of complexes towards hydrolysis, for example  $\text{CrX}^{2+}$  (Sec. 4.3.1).



**Fig. 1.13** The pH dependence of the reaction between the Ru(III)-edta complex and  $SCN^-$  at  $25^\circ C$  ( $\mu = 0.2 M$ ).<sup>170</sup> Reprinted with permission from T. Matsubara and C. Creutz, *Inorg. Chem.* **18**, 1956 (1979). © (1979) American Chemical Society.

(b) Two protic reactants. Suppose now that we have two reactants both of which may be involved in an acid-base equilibrium



In principle (but not often in practice) four reactions are possible, their importance dependent on pH



All four products are likely to be the same or at least pH-related. The apparent second-order association rate constant  $k$  is given by

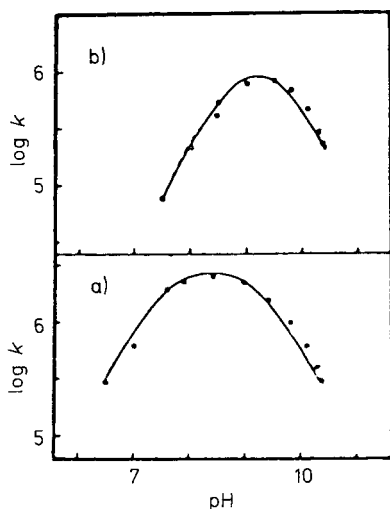
$$k(A + AH)(B + BH) = k_A^B[A][B] + k_{AH}^B[AH][B] + k_A^{BH}[A][BH] + k_{AH}^{BH}[AH][BH] \quad (1.225)$$

By using (1.219) and (1.220) and a little algebraic manipulation one obtains (1.226)

$$k = \frac{k_A^B}{[1 + ([H^+]/K_{AH})][1 + ([H^+]/K_{BH})]} + \frac{k_{AH}^B K_{BH}/K_{AH}}{[1 + [H^+]/K_{AH}][1 + (K_{BH}/[H^+])]} + \frac{k_A^{BH}}{[1 + ([H^+]/K_{AH})][1 + (K_{BH}/[H^+])]} + \frac{k_{AH}^{BH}}{[1 + (K_{AH}/[H^+])][1 + (K_{BH}/[H^+])]} \quad (1.226)$$

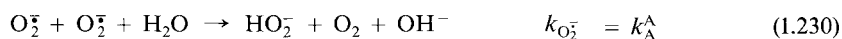
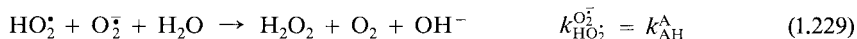
The full equation (1.226) reduces to (1.207) when  $K_{BH}$  is small, that is when B is aprotic. The observed rate constant  $k$  approaches limiting values of  $k_{AH}^{BH}$  at high  $[H^+]$  and  $k_A^B$  at low  $[H^+]$ . The total profile resembles a bell-shape or inverted bell-shape which may be symmetrical with either a maximum or a minimum at  $k \sim k_A^{BH}$  or  $k_{AH}^B K_{BH}/K_{AH}$  and at  $[H^+] = (K_{AH} K_{BH})^{1/2}$ . The bell-shape behavior is beautifully illustrated in Fig. 1.14.<sup>174</sup> It is clear from

the kinetic form that it is not easy to distinguish the reaction of AH with B from A with BH or a mixture of both. The calculated values of  $k_A^{BH}$  and  $k_{AH}^B$  from (1.226) do however differ by a factor of  $K_{BH}/K_{AH}$  and this ratio may be sufficiently different from unity to transform the calculated value of either  $k_A^{BH}$  or  $k_{AH}^B$  above the diffusion-controlled limit, and therefore unacceptable (Prob. 19).<sup>174,175</sup> Similarly we can guess that the combination of aquacobalamin with  $CNO^-$  is the correct reactive pair (rather than hydroxocobalamin with HCNO) since the hydroxo form is much less reactive than the aqua form with an aprotic ligand such as  $SCN^-$  ion.<sup>176</sup> For a final example see Ref. 163.



**Fig. 1.14** (a) The pH dependence of the rate constants for the association of carbonic anhydrase B (E) and p-nitrobenzenesulfonamide (S). The reaction is monitored by using stopped-flow and the quenching of a tryptophan fluorescence in the protein which occurs when sulfonamides bind. The full line fits Eqn. (1.226) with  $k = 3.5 \times 10^6 M^{-1} s^{-1}$ ,  $pK_E = 7.5$  and  $pK_S = 9.3$ .<sup>174</sup> The plot in (b) refers to a similar interaction with the carboxymethylated derivative of carbonic anhydrase (Prob. 19). Aromatic sulfonamides are powerful inhibitors of the action of the enzyme and are useful probes of the site characteristics.

An interesting situation arises when the molecules A and B are identical. Now we are considering two protic species reacting with one another leading perhaps to disproportionation<sup>162,177</sup> or dimerization<sup>178</sup>

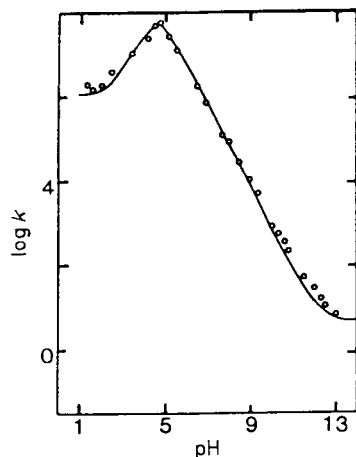


The  $k/pH$  profile is shown in Fig. 1.15 and is consistent with (1.231)<sup>177</sup>

$$k = \frac{k_{HO_2} + k_{HO_2}^{O_2^-} (K_{HO_2}/[H^+])}{(1 + K_{HO_2}/[H^+])^2} + k_{O_2^-} \quad (1.231)$$

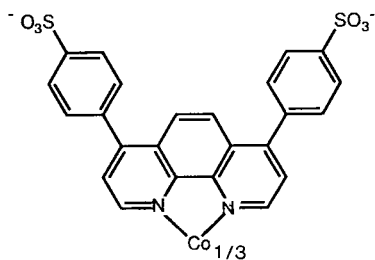
with  $k_{HO_2} = 11.0 \times 10^5 M^{-1} s^{-1}$ ,  $k_{HO_2}^{O_2^-} = 18 \times 10^7 M^{-1} s^{-1}$ ,  $k_{O_2^-} = 5.0 M^{-1} s^{-1}$  and  $K_{HO_2} = 2.2 \times 10^{-5} M$ .<sup>177,179</sup> The expression (1.231) is derived from (1.225) assuming  $A = B$ ,  $k_A^B \approx 0$ , and  $K_{AH} = K_{BH}$ . For another example, examine the pH profile for dimerization of the  $Fe(III)-tppsH_2^{4-}$  complex. The most effective combination again is of the acid form ( $Fe(tpps)H_2O^3^-$ ) with the basic one, ( $Fe(tpps)(OH)^{4-}$ ), giving a bell shaped  $k/pH$  profile.<sup>178</sup>





**Fig. 1.15** Second-order superoxide disproportionation constant vs pH at 25°C. Potassium superoxide (~1 mM) in pH  $\geq 12$  was mixed in a stopped-flow apparatus with buffers at various pH's and the change in absorbance at 250 nm monitored. The decays were second-order and data were treated in a similar manner to that described in Fig. 1.3.<sup>177</sup> The full line fits Eqn. (1.231) using the parameters given in the text. Reprinted with permission from Z. Bradić and R. G. Wilkins, *J. Am. Chem. Soc.* **106**, 2236 (1984). © (1984) American Chemical Society.

Finally, we cite an interesting example of the care which must be shown in interpreting pH effects, probably more relevant to protein studies, but a lesson for all kineticists. Investigation of the oxidation of the reduced form of the iron protein, HIPIP<sub>R</sub> (*Chromatium vinosum*) by  $Fe(CN)_6^{3-}$  indicated a near invariance of the second-order rate constant in the pH range 5–10 at  $\mu = 0.2M$ . However, there is a changing charge on the HIPIP as the pH changes and this will by itself likely lead to rate changes (Sec. 2.9.6). The valid procedure is to determine the rate constants at each pH at various ionic strengths and use the value extrapolated to zero ionic strength to assess the pH effect. More marked changes with pH are then observed.<sup>180</sup> The problem appears less important in the corresponding oxidation of HIPIP<sub>R</sub> by  $Co^{III}(bpdS)^{3-}$ , **13**, because the negative charge of the oxidant is more diffuse and electrostatic and ionic strength effects appear much less important.<sup>181</sup>



**13**

### 1.10.3 The Effect of High Acid Concentration

In higher acidity, the rate constant may correlate better with  $h_0$  (the Hammett-Dearyup acidity scale) than with the stoichiometric concentration of  $H^+$ . Since nearly all the studies involve hydrolysis reactions, the depletion of the reagent water may be an important consideration also.<sup>182</sup>

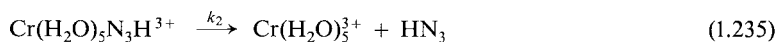
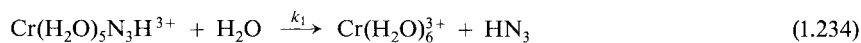
These points are illustrated nicely in the study of the aquation of  $\text{CrN}_3^{2+}$  in 1-11 M  $\text{HClO}_4$ .<sup>183</sup> The loss of  $\text{CrN}_3^{2+}$  monitored at 270 nm is first-order (rate constant =  $k$ ). The  $-\log k$  vs  $-H_0$  ( $\log h_0$ ) profile is reproduced in Fig. 1.16. It is marked by a linear dependence at lower acidities, a short plateau, and a decrease in  $k$  with increasing acidity at  $[\text{HClO}_4] > 8.0$  M, at which point there is decreasing value for  $a_w$ , the activity of water. This behavior conforms to a rate law of the form

$$-d \ln [\text{CrN}_3]_{\text{T}}/dt = k = \frac{h_0}{K_1 + h_0} (k_1 a_w + k_2) \quad (1.232)$$

where  $[\text{CrN}_3]_{\text{T}} = [\text{CrN}_3^{2+}] + [\text{CrN}_3\text{H}^{3+}]$ , and the  $h_0[K_1 + h_0]^{-1}$  term allows for substantial protonation of  $\text{CrN}_3^{2+}$ :

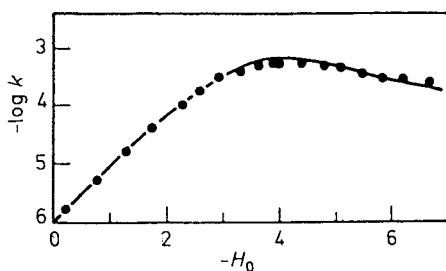
$$K_1 = [\text{CrN}_3^{2+}] h_0 / [\text{CrN}_3\text{H}^{3+}] \quad (1.233)$$

The  $k_2$  term must be included since a plot of  $k(K_1 + h_0) h_0^{-1}$  vs  $a_w$ , although linear (slope  $k_1$ ), has a positive intercept ( $k_2$ ) at  $a_w = 0$ . A simple mechanism consistent with this rate law is



with  $k_1 = k_1^0 f_{3+} / f_{\neq}$  and  $k_2 = k_2^0 f_{3+} / f_{\neq}$ . The ratios of activity coefficients may remain constant even when the reaction medium changes.

Information on the kinetics of complex ion reactions in high acid is sparse, partly because of the instability problems, but also because of the difficulties in the interpretation of results in such a complex medium.

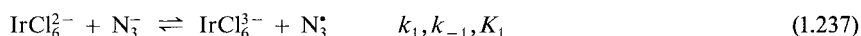


**Fig. 1.16** The variation of  $-\log k$  with  $-H_0$  for the hydrolysis of  $\text{CrN}_3^{2+}$  in 1-11 M  $\text{HClO}_4$ . The line is calculated from Eqn. (1.232).<sup>183</sup>

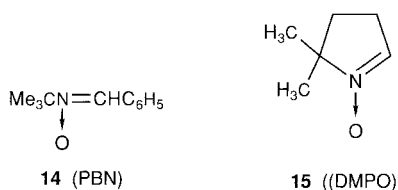
## 1.11 Kinetics and Thermodynamics

We have seen how a comparison of the equilibrium constant estimated from kinetic data for the forward and reverse directions (i.e.  $K = k_f/k_r$ ) with that obtained by measurements on the equilibrated system, may be used to provide strong support (or otherwise) for a particular reaction scheme (see also Chap. 8 Pd(II)). The kinetic approach may be useful also for providing information on thermodynamic data not otherwise easily available.

The interaction



has been used to assess the oxidation potential for the  $\text{N}_3^*$ ,  $\text{N}_3^-$  couple. Reaction (1.237) can be studied in the forward direction by stopped-flow mixing of the reactants in the presence of the spin-trap pbn, **14** or dmpo, **15**, which forces the reaction to completion ( $2\text{N}_3^* \rightarrow 3\text{N}_2$ ) and obviates complicating slow reactions of  $\text{N}_3^*$ . The value of  $2k_1$  is  $1.6 \times 10^2 \text{M}^{-1}\text{s}^{-1}$  at  $\mu = 1.0\text{M}$  and  $25^\circ\text{C}$  (the factor 2 enters because the pbn,  $\text{N}_3^*$  adduct is probably rapidly oxidized by  $\text{IrCl}_6^{2-}$ ). Reaction (1.237) is studied in the reverse direction by measuring the rate of the reaction of pulse-radiolytically generated  $\text{N}_3^*$  with added  $\text{IrCl}_6^{2-}$  (Sec. 3.5.2). The value of  $k_{-1}$  is  $5.5 \times 10^8 \text{M}^{-1}\text{s}^{-1}$  with the same conditions as for  $k_1$ . This means that  $K_1$  is  $1.5 \times 10^{-7}$  and since  $E^0$  for the  $\text{IrCl}_6^{2-}/\text{IrCl}_6^{3-}$  couple is 0.93 V that for  $\text{N}_3^*/\text{N}_3^-$  is 1.33 V.<sup>184</sup> This is in good agreement with values obtained by cyclic voltametry and by examining an equilibrium involving  $\text{Br}_2^*$  and  $\text{N}_3^-$  using pulse radiolysis.<sup>185</sup> The oxidation potentials for a number of couples involving radicals have been determined by kinetic methods.<sup>186-188</sup>



**Spin-Trapping Reagents** – These can scavenge short-lived radicals to produce free radical nitroxides of longer lifetime. The short-lived radical can thus be prevented from interfering kinetically (as in this case) or be characterised by the epr of the nitroxide.

Non-statistical successive binding of  $\text{O}_2$  and  $\text{CO}$  to the four heme centers of hemoglobin (“cooperativity”) has been thoroughly documented. It is difficult to test for a similar effect for  $\text{NO}$  since the equilibrium constants are very large ( $\approx 10^{12}\text{M}^{-1}$ ) and therefore difficult to measure accurately. It is found that the four successive formation rate constants for binding  $\text{NO}$  to hemoglobin are identical. In contrast, the rate constant for dissociation of the first  $\text{NO}$  from  $\text{Hb}(\text{NO})_4$  is at least 80 times less than that for removal of  $\text{NO}$  from the singly bound entity  $\text{Hb}(\text{NO})$ . This demonstrates cooperativity for the system, and shows that it resides in the dissociation process.<sup>189</sup> The thermodynamic implications of any kinetic data should therefore always be assessed.

## 1.12 Concluding Remarks

It is important in building up the rate law that a wide range of concentrations of species involved in the reaction be examined so that a complete picture can be obtained. By extending the concentrations of reactants used, additional rate terms have been revealed in the reaction of Fe(II) with Cr(VI),<sup>190</sup> and Fe(II) with  $\text{Co}(\text{C}_2\text{O}_4)_3^{3-}$  Ref. 191, and the rate law confirmed in the reaction of  $\text{Co}(\text{CN})_5^{3-}$  with  $\text{H}_2$  (by increasing the concentration with high pressure).<sup>192</sup> In addition, a thorough study of the effect on the rate of reactants such as electrolytes, products and so forth is essential. Other variables, temperature and pressure particularly, will be explored in the next chapter.

It would be blatantly untrue to suggest that the rate behavior of all complex-ion reactions could be fitted into categories contained in this chapter. There are many complicated reaction schemes that require solution by computer and this is becoming increasingly straightforward. It is also true that many complicated reactions can be reduced in complexity by judicious choice of reaction conditions and by so doing become amenable to the type of treatment outlined above.

## References

1. The concentration of a species is usually determined *in situ* using some physical property which is linearly dependent on its concentration. By far the most utilized is the uv/vis absorbance (see (1.80) and (3.21)).
2. F.-C. Xu, H. R. Krouse and T. W. Swaddle, *Inorg. Chem.* **24**, 267 (1985); J. H. Espenson, *Inorg. Chem.* **8**, 1554 (1969) for Table and References.
3. A. C. Melnyk, N. K. Kildahl, A. R. Rendina and D. H. Busch, *J. Amer. Chem. Soc.* **101**, 3232 (1979). Full details are given for converting  $\text{O}_2$ -pressure-time profiles into initial rates of  $\text{O}_2$  evolution in terms of  $\text{Ms}^{-1}$ .
4. K. E. Howlett and S. Sarsfield, *J. Chem. Soc. A*, 683 (1968); D. C. Gaswick and J. H. Krueger, *J. Amer. Chem. Soc.* **91**, 2240 (1969).
5. M. E. Farago and T. Matthews, *J. Chem. Soc. A*, 609 (1969).
6. (a) R. H. Dinius, *Inorg. Chim. Acta* **99**, 217 (1985); (b) D. G. Lee and T. Chen, *J. Amer. Chem. Soc.* **111**, 7534 (1989).
7. F. P. Rotzinger, H. Stunzi and W. Marty, *Inorg. Chem.* **25**, 489 (1986).
8. C. Postmus and E. L. King, *J. Phys. Chem.* **59**, 1216 (1955).
9. K. W. Hicks and J. R. Sutter, *J. Phys. Chem.* **75**, 1107 (1971).
10. R. O. Viale, *J. Theor. Biol.* **31**, 501 (1971).
11. J. E. Taylor, *J. Chem. Educ.* **46**, 742 (1969).
12. No attempt will be made to derive the integrated form for these and subsequent differential equations. This is found in a number of places including Moore and Pearson, Harris and particularly in Capellos and Bielski. Neither do we intend to say much about computer treatment of raw kinetic data except that this is largely replacing their algebraic manipulation (K. B. Wiberg, B5, Chap. 16).
13. R. A. Scott and H. B. Gray, *J. Amer. Chem. Soc.* **102**, 3219 (1980).
14. G. A. Tondreau and R. G. Wilkins, *Inorg. Chem.* **25**, 2745 (1986).
15. F. G. Halaka, G. T. Babcock and J. L. Dye, *J. Biol. Chem.* **256**, 1084 (1981).
16. M. Meier, F. Basolo and R. G. Pearson, *Inorg. Chem.* **8**, 795 (1969).

17. The factor 1/2 enters into (1.24) because a second substitution which consumes another molecule of isonitrile, rapidly follows each first stage. The rate of loss of  $C_6H_{11}NC$  is therefore twice that of  $Ni(POEt_3)_4$ .
18. H. Ogino, M. Shimura, N. Yamamoto and N. Okubo, *Inorg. Chem.* **27**, 172 (1988).
19. The product **3** is in rapid equilibrium with planar  $Ni([14]aneN_4)^{2+}$  and it is the changing absorbance of the planar complex at 450 nm ( $\epsilon = 50M^{-1}cm^{-1}$ ) which monitors the change in concentration of **3**.  $k_{hyd} = k_2$ ;  $k_{isom} \sim k_{-1}$ .
20. E. J. Billo, *Inorg. Chem.* **23**, 236 (1984).
21. D. A. Kamp, R. L. Wilder, S. C. Tang and C. S. Garner, *Inorg. Chem.* **10**, 1396 (1971).
22. A. Juris, V. Balzani, F. Barigelletti, S. Campagna, P. Belser and A. von Zelewsky, *Coordn. Chem. Revs.* **84**, 85 (1988).
23. M. S. Matheson and L. M. Dorfman, *Pulse Radiolysis*, M.I.T. Press, Cambridge, Mass. 1969, Chap. 5.
24. R. W. Wegman, R. J. Olsen, D. R. Gard, L. R. Faulkner and T. L. Brown, *J. Amer. Chem. Soc.* **103**, 6089 (1981).
25. W. K. Meckstroth, R. T. Walters, W. L. Waltz, A. Wojcicki and L. M. Dorfman, *J. Amer. Chem. Soc.* **104**, 1842 (1982).
26. M. Krumpolc and J. Rocek, *Inorg. Chem.* **24**, 617 (1985).
27. D. W. Carlyle and J. H. Espenson, *J. Amer. Chem. Soc.* **90**, 2272 (1968).
28. J. Barrett and J. H. Baxendale, *Trans. Faraday Soc.* **42**, 210 (1956).
29. S. C. Chan and S. F. Chan, *J. Chem. Soc. A*, 202 (1969).
30. B12, p. 44.
31. R. C. Young, T. J. Meyer and D. G. Whitten, *J. Amer. Chem. Soc.* **98**, 286 (1974); R. Berkoff, K. Krist and H. D. Gafney, *Inorg. Chem.* **19**, 1 (1980).
32. The values of  $b$  and  $c$  may sometimes be assessed by using log-log plots. Thus for (1.40)

$$\log k = \log k_1 + b \log [B] + c \log [C]$$

the slope of the  $\log k/\log [B]$  plot ( $[C]$ , constant) is  $b$ . Although hardly used, the method is useful when the rate law contains several terms involving  $[H^+]$  raised to various powers, J. P. Birk, *J. Chem. Educ.* **53**, 704 (1976); *Inorg. Chem.* **17**, 504 (1978). (See Prob. 5 and Fig. 8.8.)

33. J. L. Jensen, R. C. Kanner and G. R. Shaw, *Int. J. Chem. Kinetics* **22** 1211 (1990).
34. J. Rawlings, S. Wherland and H. B. Gray, *J. Amer. Chem. Soc.* **99**, 1968 (1977).
35. J. Burgess, *J. Chem. Soc. A*, 3123 (1968).
36. W. G. Jackson, G. A. Lawrance, P. A. Lay and A. M. Sargeson, *J. Chem. Educ.* **58**, 734 (1981).
37. D. Meyerstein, *Inorg. Chem.* **14**, 1716 (1975).
38. B. R. Baker, N. Sutin and T. J. Welch, *Inorg. Chem.* **6**, 1948 (1967).
39. F. Below, Jr., R. E. Connick and C. P. Coppel, *J. Amer. Chem. Soc.* **80**, 2961 (1958); J. H. Espenson and D. F. Dustin, *Inorg. Chem.* **8**, 1760 (1969); W. F. Pickering and A. McAuley, *J. Chem. Soc. A*, 1173 (1968).
40. J. K. Beattie, *Inorg. Chim. Acta* **76**, L69 (1983).
41. E. Pelizzetti and E. Mentasti, *Inorg. Chem.* **18**, 583 (1979).
42. R. F. Pasternack and E. G. Spiro, *J. Amer. Chem. Soc.* **100**, 968 (1978).
43. D. H. Macartney and N. Sutin, *Inorg. Chem.* **22**, 3530 (1983).
44. B. Bosnich, F. P. Dwyer and A. M. Sargeson, *Aust. J. Chem.* **19**, 2051, 2213 (1966).
45. J. Butler, D. M. Davies and A. G. Sykes, *J. Inorg. Biochem.* **15**, 41 (1981); N. Ohno and M. A. Cusanovich, *Biophys. J.* **36**, 589 (1981).
46. D. B. Rorabacher, T. S. Turan, J. A. Defever and W. G. Nickels, *Inorg. Chem.* **8**, 1498 (1969).
47. M. Moriyasu and Y. Hashimoto, *Bull. Chem. Soc. Japan* **53**, 3590 (1980).
48. C. K. Poon and M. L. Tobe, *J. Chem. Soc. A*, 2069 (1967).
49. E. L. King, *Int. J. Chem. Kinetics* **14**, 1285 (1982).
50. D. Cummins and H. B. Gray, *J. Amer. Chem. Soc.* **99**, 5158 (1977).

51. T. R. Crossley and M. A. Slifkin, *Prog. React. Kinetics* **5**, 409 (1970).
52. J. E. Byrd and J. Halpern, *J. Amer. Chem. Soc.* **93**, 1634 (1971).
53. T. W. Kallen and J. E. Earley, *Inorg. Chem.* **10**, 1149 (1971).
54. R. J. Crutchley, W. R. Ellis, Jr. and H. B. Gray, *J. Amer. Chem. Soc.* **107**, 5002 (1985).
55. K. Tsukahara and R. G. Wilkins, *Inorg. Chem.* **28**, 1605 (1989).
56. S. W. Provencher, *J. Chem. Phys.* **64**, 2772 (1976); S. W. Provencher, *Biophys. J.* **16**, 27 (1976).
57. M. H. Evans, B. Grossman and R. G. Wilkins, *Inorg. Chim. Acta* **14**, 59 (1975).
58. D. H. Busch, *J. Phys. Chem.* **63**, 340 (1959); P. Krumholz, *Inorg. Chem.* **4**, 609 (1965).
59. These problems may be circumvented if one or both of the steps is multi-order, since the associated pseudo first-order rate constant is modified by changes in concentrations of the excess reagent.
60. P. Hendry and A. M. Sargeson, *Inorg. Chem.* **25**, 865 (1986).
61. E. T. Gray, Jr., R. W. Taylor and D. W. Margerum, *Inorg. Chem.* **16**, 3047 (1977).
62. A. Haim and N. Sutin, *J. Amer. Chem. Soc.* **88**, 5343 (1966).
63. R. W. Hay and L. J. Porter, *J. Chem. Soc. A*, 127 (1969); R. G. Pearson, R. E. Meeker and F. Basolo, *J. Amer. Chem. Soc.* **78**, 709 (1956).
64. Z. Bradić, K. Tsukahara, P. C. Wilkins and R. G. Wilkins in *Bioinorganic Chemistry* 85, A. V. Xavier, ed. VCH, Weinheim, 1985, p. 337.
65. D. A. Buckingham, D. J. Francis and A. M. Sargeson, *Inorg. Chem.* **13**, 2630 (1974).
66. B8, p. 66.
67. Generally,  $P_t - P_e = A_1 \exp(-a_1 t) + A_2 \exp(-a_2 t)$  where  $P$  is a measured property, and  $A_1$ ,  $A_2$ ,  $a_1$  and  $a_2$  are constants.
68. K. R. Ashley and R. E. Hamm, *Inorg. Chem.* **5**, 1645 (1966).
69. J. H. Espenson and T-H. Chao, *Inorg. Chem.* **16**, 2553 (1977).
70. N. E. Dixon, W. G. Jackson, M. J. Lancaster, G. A. Lawrance and A. M. Sargeson, *Inorg. Chem.* **20**, 470 (1981).
71. N. W. Alcock, D. J. Benton and P. Moore, *Trans. Faraday Soc.* **66**, 2210 (1970).
72. J. C. Pleskowicz and E. J. Billo, *Inorg. Chim. Acta* **99**, 149 (1985).
73. J. Hoch and R. M. Milburn, *Inorg. Chem.* **18**, 886 (1979).
74. G. M. Clore, A. N. Lane and M. R. Hollaway, *Inorg. Chim. Acta*, **46**, 139 (1980).
75. S. A. Jacobs and D. W. Margerum, *Inorg. Chem.* **23**, 1195 (1984).
76. M. Shimura and J. H. Espenson, *Inorg. Chem.* **23**, 4069 (1984).
77. A. Ekstrom, L. F. Lindoy, H. C. Lip, R. J. Smith, H. J. Goodwin, M. McPartlin and P. A. Tasker, *J. Chem. Soc. Dalton Trans.* 1027 (1979).
78. W. G. Jackson, J. MacB. Harrowfield and P. D. Vowles, *Int. J. Chem. Kinetics*, **9**, 535 (1977).
79. E. Jørgensen and J. Bjerrum, *Acta Chem. Scand.* **13**, 2075 (1959).
80. A. N. Singh, E. Gelerinter and E. S. Gould, *Inorg. Chem.* **21**, 1232; 1236 (1982).
81. A. J. Miralles and A. Haim, *Inorg. Chem.* **19**, 1158 (1980).
82. J. H. Beard, J. Casey and R. K. Murmann, *Inorg. Chem.* **4**, 797 (1965).
83. D. B. Vanderheiden and E. L. King, *J. Amer. Chem. Soc.* **95**, 3860 (1973).
84. J. R. Chipperfield, *J. Organomet. Chem.* **137**, 355 (1977).
85. K. Jackson, J. H. Ridd and M. L. Tobe, *J. Chem. Soc. Perkins II* 611 (1979).
86. F. A. Armstrong, R. A. Henderson and A. G. Sykes, *J. Amer. Chem. Soc.* **102**, 6545 (1980).
87. W. Marty and J. H. Espenson, *Inorg. Chem.* **18**, 1246 (1979).
88. M. C. Pohl and J. H. Espenson, *Inorg. Chem.* **19**, 235 (1980).
89. W. G. Jackson, S. S. Jurisson and B. C. McGregor, *Inorg. Chem.* **24**, 1788 (1985).
90. D. J. MacDonald and C. S. Garner, *Inorg. Chem.* **1**, 20 (1962).
91. H. E. Toma and A. B. P. Lever, *Inorg. Chem.* **25**, 176 (1986).
92. D. Huchital and R. G. Wilkins, *Inorg. Chem.* **6**, 1022 (1967).
93. F. M. Beringer and E. M. Findler, *J. Amer. Chem. Soc.* **77**, 3200 (1955), where this scheme is fully analyzed.

94. A. G. Lappin in *Metal Ions in Biological Systems*, H. Sigel, ed. M. Dekker, NY, 1981, 13, p. 15–71; N. Al-Shatti, A. G. Lappin and A. G. Sykes, *Inorg. Chem.* **20**, 1466 (1981).
95. A. M. Martin, K. J. Grant and E. J. Billo, *Inorg. Chem.* **25**, 4904 (1986).
96. B11, p. 88.
97. J. Halpern, *J. Chem. Educ.* **45**, 372 (1968).
98. R. B. Martin, *J. Chem. Educ.* **62**, 789 (1985), for a useful treatment of the two schemes.
99. R. B. Martin, *Inorg. Chem.* **26**, 2197 (1987).
100. L. Rosenheim, D. Speiser and A. Haim, *Inorg. Chem.* **13**, 1571 (1974).
101. B. T. Reagor and D. H. Huchital, *Inorg. Chem.* **21**, 703 (1982).
102. G. C. Seaman and A. Haim, *J. Amer. Chem. Soc.* **106**, 1319 (1984).
103. I. H. Segel, *Enzyme Kinetics*, Wiley-Interscience, NY, 1975. P. C. Engel, *Enzyme Kinetics*, Chapman and Hall, London, 1977. M. Dixon, E. C. Webb, C. J. R. Thorne and K. F. Tipton, *Enzymes*, Third Ed. Academic, NY, 1979. K. F. Tipton and H. B. F. Dixon, *Methods in Enzymol.* **63**, 183 (1979).
104. When the two steps have comparable rates, the situation is more complex, see Refs. 98, 105, and 106.
105. R. L. Reeves and L. K. J. Tong, *J. Amer. Chem. Soc.* **84**, 2050 (1962).
106. R. L. Reeves, G. S. Calabrese and S. A. Harkaway, *Inorg. Chem.* **22**, 3076 (1983).
107. B. S. Brunschwig, P. J. DeLaive, A. M. English, M. Goldberg, H. B. Gray, S. L. Mayo and N. Sutin, *Inorg. Chem.* **24**, 3743 (1985).
108. J. A. Christiansen, *Z. Phys. Chem.* **339**, 145 (1936); **378**, 374 (1937).
109. J. H. Espenson, *Acc. Chem. Res.* **3**, 347 (1970).
110. R. D. Cannon, *Electron Transfer Reactions*, Butterworth, London, 1980, p. 63–68.
111. The kinetic analysis of (1.123) has been fully discussed in a number of texts in the Selected Bibliography.
112. First treated by T. M. Lowry and W. T. John, *J. Chem. Soc.* 2634 (1910).
113. F. A. Matsen and J. J. Franklin, *J. Amer. Chem. Soc.* **72**, 3337 (1950); E. S. Lewis and M. D. Johnson, *J. Amer. Chem. Soc.* **82**, 5399 (1960).
114. I. J. Goldstein and C. E. Hayes, *Adv. Carbohydrate Chem. Biochem.* **35**, 127 (1978).
115. T. J. Williams, J. A. Shafer, I. J. Goldstein and T. Adamson, *J. Biol. Chem.* **253**, 8538 (1978).
116. A. Van Landschoot, F. G. Loontjens, R. M. Clegg and T. M. Jovin, *Eur. J. Biochem.* **103**, 313 (1980).
117. T. J. Williams, L. D. Homer, J. A. Shafer, I. J. Goldstein, P. J. Garegg, H. Hultberg, T. Iversen and R. Johansson, *Arch. Biochem. Biophys.* **209**, 555 (1981).
118. F. G. Loontjens, R. M. Clegg and A. Van Landschoot, *J. Bioscience*, **5**, Supplement 1, 105 (1983).
119. R. G. Pearson and O. P. Anderson, *Inorg. Chem.* **9**, 39 (1970).
120. M. R. Jaffe, D. P. Fay and N. Sutin, *J. Amer. Chem. Soc.* **93**, 2878 (1971).
121. M. J. Hynes and M. T. O'Shea, *Inorg. Chim. Acta* **73**, 201 (1983).
122. E. Antonini and M. Brunori, *Hemoglobin and Myoglobin in their Reactions with Ligands*, North-Holland, Amsterdam, 1971, p. 197 for the derivation of (1.143).
123. J. M. Malin, H. E. Toma and E. Giesbrecht, *J. Chem. Educ.* **54**, 385 (1977).
124. J. K. Beattie, M. B. Celap, M. T. Kelso and S. M. Nesić, *Aust. J. Chem.* **42**, 1647 (1989) treat the interconversion of the geometrical isomers of  $\text{Co}(L\text{-ala})_2(\text{NO}_2)_2^-$  in terms of the scheme  $A \rightarrow B \rightleftharpoons C$ ;  $B \rightarrow D$ ;  $C \rightarrow D$ .
125. For a general treatment of relaxation kinetics see B4; G. Schwarz in B6, Chap. II, and G. W. Gastellan, *Ber. Bunsenges. Phys. Chem.* **67**, 898 (1963).
126. B4, p. 15.
127. R. Koren and G. G. Hammes, *Biochemistry* **15**, 1165 (1976).
128. M. Krishnamurthy and J. R. Sutter, *Inorg. Chem.* **24**, 1943 (1985).
129. B4, Chap. 5.
130. B13, p. 198.
131. R. Brouillard, *J. Chem. Soc. Faraday Trans. I* **76**, 583 (1980) this paper fully analyzes the degree that an equilibrium may be shifted in a chemical relaxation for a single step reaction.

132. J. P. Bertigny, J. E. Dubois, R. Brouillard, *J. Chem. Soc. Faraday Trans. I* **79**, 209 (1983), treat a two-step system, following up Ref. 131.
133. The most elegant way to tackle the simultaneous equations (1.165) and (1.166) is by determinants, see B4, p. 27.
134. B. Havsteen, *J. Biol. Chem.* **242**, 769 (1967); M. Eigen, *Quart. Rev. Biophysics* **1**, 1 (1968).
135. M. M. Palcic and H. B. Dunford, *Arch. Biochem. Biophys.* **211**, 245 (1981).
136. B4, Chap. 6.
137. L. F. Povirk, M. Hogan, N. Dattagupta and M. Buechner, *Biochemistry* **20**, 665 (1981). Cu(II)bleomycin can be used as a model for Fe(II)bleomycin which is an antitumor antibiotic that catalyses the degradation of DNA, J. Stubbe, *Biochemistry* **27**, 3893 (1988).
138. L. W. Harrison and B. L. Vallee, *Biochemistry* **17**, 4359 (1978).
139. H. Brintzinger and G. G. Hammes, *Inorg. Chem.* **5**, 1286 (1966).
140. G. G. Hammes and J. I. Steinfeld, *J. Amer. Chem. Soc.* **84**, 4639 (1962).
141. J. C. Thomas, C. M. Frey and J. E. Stuehr, *Inorg. Chem.* **19**, 501; 505 (1980).
142. J. Bidwell, J. Thomas and J. Stuehr, *J. Amer. Chem. Soc.* **108**, 820 (1986).
143. B13, p. 207.
144. B13, p. 211.
145. Eqn. (1.191) is usually referred to as the McKay equation (H. A. C. McKay, *Nature (London)* **142**, 497 (1938)) although inklings of the relationship had been recognized. J. N. Wilson and R. G. Dickenson, *J. Amer. Chem. Soc.* **59**, 1358 (1937).
146. E. L. King, E. B. Fleischer and R. D. Chapman, *J. Phys. Chem.* **86**, 4273 (1982).
147. L. Melander and W. H. Saunders, Jr., *Reaction Rates of Isotopic Molecules* Wiley, NY, 1980, p. 115.
148. J. C. Sheppard and A. C. Wahl, *J. Amer. Chem. Soc.* **79**, 1020 (1957).
149. C. M. Cook, Jr., and F. A. Long, *J. Amer. Chem. Soc. A*, **80**, 33 (1958).
150. R. K. Murmann, *Inorg. Chem.* **16**, 46 (1977).
151. A. E. Merbach, *Pure Appl. Chem.* **54**, 1479 (1982); **59**, 161 (1987).
152. L. Mønsted and O. Mønsted, *Acta Chem. Scand.* **A34**, 259 (1980).
153. A. E. Merbach, P. Moore, O. W. Howarth and C. H. McAteer, *Inorg. Chim. Acta* **39**, 129 (1980).
154. T. W. Swaddle, *Adv. Inorg. Bioinorg. Mechs.* **2**, 95 (1983).
155. L. Helm, L. I. Elding and A. E. Merbach, *Inorg. Chem.* **24**, 1719 (1985).
156. K. R. Rodgers, R. K. Murmann, E. O. Schlemper and M. E. Shelton, *Inorg. Chem.* **24**, 1313 (1985); D. T. Richens, L. Helm, P.-A. Pittet, A. E. Merbach, F. Nicolò and G. Chapuis, *Inorg. Chem.* **28**, 1394 (1989).
157. N. S. Rowan, R. M. Milburn and T. P. Dasgupta, *Inorg. Chem.* **15**, 1477 (1976) and references therein.
158. A. Nagasawa, H. Kido, T. M. Hattori and K. Saito, *Inorg. Chem.* **25**, 4330 (1986).
159. H. Gamsjager and R. K. Murmann, *Adv. Inorg. Bioinorg. Mechs.* **2**, 317 (1983).
160. F. Miller and R. G. Wilkins, *J. Amer. Chem. Soc.* **92**, 2687 (1970), and unpublished results.
161. P. Natarajan and N. V. Raghavan, *J. Amer. Chem. Soc.* **102**, 4518 (1980).
162. B. H. J. Bielski, D. E. Cabelli, R. L. Arudi and A. B. Ross, *J. Phys. Chem. Ref. Data* **14**, 1041 (1985).
163. B. Brønnum, H. S. Johansen and L. H. Skibsted, *Inorg. Chem.* **27**, 1859 (1988).
164. R. Langley, P. Hambright, K. Alston and P. Neta, *Inorg. Chem.* **25**, 114 (1986).
165. P.-I. Ohlsson, J. Blanck and K. Ruckpaul, *Eur. J. Biochem.* **158**, 451 (1986).
166. M. M. Palcic and H. B. Dunford, *J. Biol. Chem.* **255**, 6128 (1980).
167. I. Rapaport, L. Helm, A. E. Merbach, P. Bernhard and A. Ludi, *Inorg. Chem.* **27**, 873 (1988).
168. J. M. Malin and R. C. Koch, *Inorg. Chem.* **17**, 752 (1978).
169. J. E. Sutton and H. Taube, *Inorg. Chem.* **20**, 4021 (1981).
170. T. Matsubara and C. Creutz, *Inorg. Chem.* **18**, 1956 (1979).
171. A. W. Shimi and W. C. E. Higginson, *J. Chem. Soc.* 260 (1958).
172. H. Igino, K. Tsukahara and N. Tanaka, *Inorg. Chem.* **19**, 255 (1980).



173. The addition of a further protonated species  $\text{AH}_3^{3+}$  to the reaction scheme can be treated in a similar manner to that already considered. It is applied in the reaction of leghemoglobin with  $\text{H}_2\text{O}_2$ , D. Job, B. Zeba, A. Puppo and J. Rigaud, *Eur. J. Biochem.* **107**, 391 (1980).
174. P. W. Taylor, R. W. King and A. S. V. Burgen, *Biochemistry* **9**, 3894 (1970).
175. R. W. King and A. S. V. Burgen, *Proc. Roy. Soc. London, B*, **193**, 107 (1976); S. Lindskog in *Zinc Enzymes*, T. G. Spiro, ed. Wiley-Interscience, NY, 1983.
176. W. C. Randall and R. A. Alberty, *Biochemistry* **6**, 1520 (1967).
177. Z. Bradić and R. G. Wilkins, *J. Amer. Chem. Soc.* **106**, 2236 (1984).
178. A. A. El-Awady, P. C. Wilkins and R. G. Wilkins, *Inorg. Chem.* **24**, 2053 (1985).
179. These values are in excellent agreement with those collected from a compilation of previous studies<sup>162</sup> except for that of  $k_{\text{O}_2^-}$ .
180. B. A. Feinberg and W. V. Johnson, *Biochem. Biophys. Res. Commun.* **93**, 100 (1980).
181. I. K. Adzami, D. M. Davies, C. S. Stanley and A. G. Sykes, *J. Amer. Chem. Soc.* **103**, 5543 (1981).
182. H. L. Chum and M. E. M. Helene, *Inorg. Chem.* **19**, 876 (1980).
183. T. C. Templeton and E. L. King, *J. Amer. Chem. Soc.* **93**, 7160 (1971).
184. M. S. Ram and D. M. Stanbury, *Inorg. Chem.* **24**, 4233 (1985); *J. Phys. Chem.* **90**, 3691 (1986).
185. Z. B. Alfassi, A. Harriman, R. E. Huie, S. Mosseri and P. Neta, *J. Phys. Chem.* **91**, 2120 (1987); see also M. R. De Felippis, M. Faraggi and M. H. Klapper, *J. Phys. Chem.* **94**, 2420 (1990).
186. B. W. Carlson and L. L. Miller, *J. Amer. Chem. Soc.* **105**, 7453 (1983).
187. S. Goldstein and G. Czapski, *Inorg. Chem.* **24**, 1087 (1985).
188. D. M. Stanbury, *Adv. Inorg. Chem.* **33**, 69 (1989).
189. E. G. Moore and Q. H. Gibson, *J. Biol. Chem.* **251**, 2788 (1976).
190. D. R. Rosseinsky and M. J. Nicol, *J. Chem. Soc. A*, 2887 (1969).
191. R. D. Cannon and J. S. Stillman, *J. Chem. Soc. Dalton Trans.* 428 (1976).
192. J. Halpern and M. Pribanić, *Inorg. Chem.* **9**, 2616 (1970).

### Selected Bibliography

- B1. J. D. Atwood, *Inorganic and Organometallic Reaction Mechanisms*, Brooks/Cole, Monterey, California, 1985.
- B2. C. H. Bamford, C. F. H. Tipper and R. G. Compton eds. *Comprehensive Chemical Kinetics*, Vols 1–29, Elsevier, Amsterdam, 1969–1989.
- B3. S. W. Benson, *The Foundations of Chemical Kinetics*, McGraw-Hill, NY, 1960.
- B4. C. F. Bernasconi, *Relaxation Kinetics*, Academic, New York, 1976.
- B5. C. F. Bernasconi, ed. *Investigation of Rates and Mechanisms of Reactions*, Fourth Edition, Part I. *General Considerations and Reactions at Conventional Rates*, Wiley, NY, 1986.
- B6. C. F. Bernasconi, ed. *Investigation of Rates and Mechanisms of Reactions*, 4th Edition, Part II. *Investigation of Elementary Reaction Steps in Solution and Fast Reaction Techniques*, Wiley, NY, 1986.
- B7. C. Capellos and B. H. J. Bielski, *Kinetic Systems*, Wiley-Interscience, NY, 1972.
- B8. J. H. Espenson, *Chemical Kinetics and Reaction Mechanisms*, McGraw-Hill, NY, 1981.
- B9. H. J. Fromm, *Initial Rate Kinetics*, Springer-Verlag, NY, 1975.
- B10. G. G. Hammes, *Principles of Chemical Kinetics*, Academic, NY, 1978.
- B11. L. P. Hammett, *Physical Organic Chemistry*, 2nd Edition, McGraw-Hill, NY, 1970.
- B12. G. M. Harris, *Chemical Kinetics*, Heath, Boston, 1966.
- B13. K. Hiromi, *Kinetics of Fast Enzyme Reactions*, Wiley, NY, 1979.
- B14. D. Katakis and G. Gordon, *Mechanisms of Inorganic Reactions*, Wiley-Interscience, NY, 1987.
- B15. K. J. Laidler, *Chemical Kinetics*, 3rd Edition, Harper and Row, NY, 1987.

- B16. J. W. Moore and R. G. Pearson, *Kinetics and Mechanism*, 3rd Edition, Wiley, NY, 1981.  
 B17. R. van Eldik, ed., *Inorganic High Pressure Chemistry. Kinetics and Mechanism*, Elsevier, Amsterdam, 1986.  
 B18. H. Strehlow and W. Knoche, *Fundamentals of Chemical Relaxation*, Verlag Chemie, Weinheim, 1977.

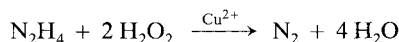
## Problems

1. The conventional equation of transition state theory is expressed as Eq. (2.119)

$$k = kT/h \exp(-\Delta G^\ddagger/RT)$$

where  $k$  is Boltzmann's constant and  $h$  is Planck's constant. Show that this is dimensionally incorrect and suggest how a correction might be made. R. D. Cannon, *Inorg. Reaction Mechs.* Vol. 6, p. 6; see also J. R. Murdoch, *J. Chem. Educ.* **58**, 32 (1981) and B14, p. 59.

2. The reaction



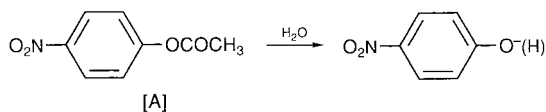
has been studied by measuring the initial rate of production of  $\text{N}_2$  gas at  $25^\circ\text{C}$  with the following results (total volume of solution = 300 ml)

$\text{N}_2\text{H}_4$ mM	$\text{H}_2\text{O}_2$ mM	$\text{Cu}^{2+}$ $\mu\text{M}$	pH	Initial rate of $\text{N}_2$ production ml of $\text{N}_2$ /min
16	65	1.23	9.5	7.3
33	65	1.23	9.7	7.4
131	65	1.23	10.0	7.4
33	33	1.23	9.8	3.6
33	131	1.23	9.0	15.0
65	131	1.23	9.7	15.0
33	65	0.33	9.7	1.95
33	65	1.3	9.7	8.3
33	65	1.64	9.7	10.4
33	65	2.46	9.7	16.2

Determine the rate law, the value of any rate constants (using M and seconds units) and after reading Chap. 2 suggest a mechanism. Is the principle of initial rate being complied with?

C. R. Wellman, J. R. Ward and L. P. Kuhn, *J. Amer. Chem. Soc.* **98**, 1683 (1976).

3. A method for the assay (enzyme activity) of carbonic anhydrase (Chap. 8. Zn(II)) uses the catalysis at pH 7.0 of the hydrolysis reaction



The initial rate is measured at 348 nm which is an isosbestic point for the product mixture of phenolate/phenol ( $\epsilon = 5.5 \times 10^3 \text{ M}^{-1} \text{ cm}^{-1}$ ;  $\text{p}K_a = 7.1$ ). The initial rate is easily determined from the linear absorbance ( $D$ ) vs. time plot, with the following results

[A]	[Enzyme]	Rate
mM	$\mu\text{M}$	$\Delta D/20 \text{ sec}$ in 1 cm cell
1.1	21	0.80
0.4	21	0.30
1.1	10.5	0.41

Show that  $V = k [\text{Enzyme}] [\text{A}]$  and determine the values of  $k$ . Estimate the percentage of A which has reacted in the 20 seconds period and thus rationalize the linearity of this plot.

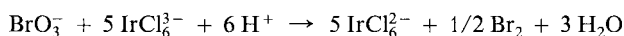
4. The  $\text{Ag}^+$  catalyzed oxidation of  $\text{VO}_3^+$  by  $\text{S}_2\text{O}_8^{2-}$  can be studied by examining  $d[\text{VO}_3^+]/dt$  at 455 nm. The loss of  $\text{VO}_3^+$  absorbance is *linear* with time, when  $\text{Ag}^+$  and  $\text{S}_2\text{O}_8^{2-}$  are used in large excess. The following data are obtained at  $20^\circ\text{C}$  and  $[\text{HClO}_4] = 0.95 - 1.05 \text{ M}$ ,  $[\text{VO}_3^+]_0 = 1.2 \text{ mM}$  and  $[\text{VO}_2^+]_0 = 3 \text{ mM}$

$[\text{S}_2\text{O}_8^{2-}]_0$ mM	$[\text{Ag}^+]_0$ mM	$10^6 \times \text{slope}^a$ $\text{Ms}^{-1}$
9.5	23	1.35
9.5	45	2.5
9.2	89	4.7
4.6	89	2.3
19	45	5.1

<sup>a</sup> From  $[\text{VO}_3^+]$  vs time plot

Deduce the rate law and suggest a likely mechanism. See also Chap. 8, Prob. 7. R. C. Thompson, *Inorg. Chem.* **22**, 584 (1983).

5. The reduction of  $\text{BrO}_3^-$  by  $\text{IrCl}_6^{3-}$



using excess  $\text{BrO}_3^-$  and  $\text{H}^+$  conformed to the rate law

$$-d[\text{IrCl}_6^{3-}]/dt = k [\text{IrCl}_6^{3-}]$$

The values of  $k$  with different concentrations of  $\text{BrO}_3^-$  and  $\text{H}^+$  are shown in the Table (selected data) at  $25^\circ\text{C}$ ,  $\mu = 0.50 \text{ M}$ :

$[\text{H}^+]$ M	$[\text{BrO}_3^-]$ mM	$10^2 \times k$ $\text{s}^{-1}$
0.05	5.0	0.19
0.10	0.80	0.16
0.10	20.0	1.1
0.30	0.50	0.36
0.30	0.80	0.49
0.40	0.80	0.78
0.40	3.0	2.4
0.40	5.0	4.4
0.50	5.0	6.5
0.50	10.0	12.4

Try a  $\log k / \log [\text{BrO}_3^-][\text{H}^+]^2$  plot and from the result, deduce the rate law (which turns out to be a common one for the reduction of  $\text{BrO}_3^-$  by a number of complexes).

J. P. Birk, *Inorg. Chem.* **17**, 504 (1978).

6. The following data were obtained for the decay of methyl radicals in the presence of argon diluent in a flash photolysis experiment.

time ( $\mu\text{s}$ )	0	10	20	30	40	50
$[\text{CH}_3\cdot]$ $\mu\text{M}$	1.25	0.95	0.80	0.65	0.57	0.50

Determine the order of the reaction and evaluate the rate constant.

7. The reduction of the Cu(II) protein, azurin, with excess dithionite,  $\text{S}_2\text{O}_4^{2-}$  was monitored at 625 nm (first-order loss of azurin) at pH 9.2 and  $25^\circ\text{C}$  with the following results

$\text{S}_2\text{O}_4^{2-}$ mM	$k_{\text{obs}}$ $\text{s}^{-1}$
1.0	5.5
2.5	10
5.0	16
7.5	20
10	24
15	32
20	39
25	43

Determine the relationship between  $k_{\text{obs}}$  and  $[\text{S}_2\text{O}_4^{2-}]$  and  $[\text{S}_2\text{O}_4^{2-}]^{1/2}$ . Thus determine the rate law. Calculate the rate constants using the value of  $1.4 \times 10^{-9} \text{ M}$  for the equilibrium constant for  $\text{S}_2\text{O}_4^{2-} \rightleftharpoons 2 \text{SO}_3^-$ .

D. O. Lambeth and G. Palmer, *J. Biol. Chem.* **248**, 6095 (1973).

Z. Bradić and R. G. Wilkins, *J. Amer. Chem. Soc.* **106**, 2236 (1984).

Generally similar results are reported by G. D. Jones, M. G. Jones, M. T. Wilson, M. Brunori, A. Colosimo and P. Sarti, *Biochem. J.* **209**, 175 (1983).

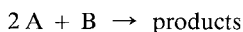
8(a). The Cu(II) catalyzed oxidation by  $O_2$  of ascorbic acid (in excess) shows linear plots of  $[O_2]^{1/2}$  vs time. What is the order of the reaction with respect to  $O_2$ ?

R. F. Jameson and N. J. Blackburn, *J. Chem. Soc. Dalton Trans.* 9 (1982).

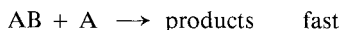
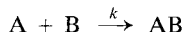
(b). The reaction in hexane at  $0^\circ C$  of  $Co_2(CO)_8$  with  $PPh_3$  (in excess) shows linear plots of  $\{[Co_2(CO)_8]_t^{-1/2} - [Co_2(CO)_8]_0^{-1/2}\}$  vs time. What is the order of the reaction with respect to  $Co_2(CO)_8$ ?

M. A.-Halabi, J. D. Atwood, N. P. Forbus and T. L. Brown, *J. Amer. Chem. Soc.* **102**, 6248 (1980).

9. Consider a reaction that has the stoichiometry



but that is second-order, with a probable mechanism



Show that a plot of  $\ln[(2b - x)/a - x]$  against  $t$  should be linear with the characteristics

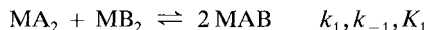
$$\text{Slope} = (2b - a)k \quad \text{Intercept} = \ln(2b/a)$$

where  $a$  and  $b$  are the initial concentrations of A and B and  $x$  is the amount of A that has been consumed at time  $t$ .

The situation is encountered in the second-order reaction of  $Mn(III) = A$  with  $p\text{-}C_6H_4(OH)_2 = B$ .

G. Davies and K. Kustin, *Trans. Faraday Soc.* **65**, 1630 (1969).

10. The reversible reaction ( $K_1 = 4.0$ )



was studied by using  $[MA_2]_0 = [MB_2]_0 = A_0$  and following  $-d[MA_2]/dt$  or  $d[MAB]/dt$ . Show

$$-\ln(1 - (2[MAB]/[MA_2]_0)) = k_1[MA_2]_0 t$$

and

$$-\ln(1 - ([MAB]/[MA_2]_0)) = k_1[MA_2]_0 t$$

How are the equations modified when  $K \neq 4$  and when  $K$  approaches an infinite value (i.e. the reaction is irreversible)? Equal concentrations of  $MA_2$  and  $MB_2$  are still assumed.

M. Moriyasu and Y. Hashimoto, *Bull. Chem. Soc. Japan* **53**, 3590 (1980); **54**, 3374 (1981); J. Stach, R. Kirmse, W. Dietzsch, G. Lassmann, V. K. Belyaeva and I. N. Marov, *Inorg. Chim. Acta* **96**, 55 (1985).

11. In the sequence  $A \xrightarrow{k_1} B \xrightarrow{k_2} C$  show that a maximum of B,  $[B]_{\max}$ , will occur at a time  $t_{\max}$  given by

$$t_{\max} = \frac{\ln(k_2/k_1)}{(k_2 - k_1)}$$

that  $[B]_{\max}$  will have a value

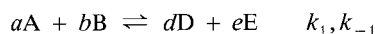
$$[B]_{\max} = [A]_0 \exp(-k_2 t_{\max})$$

and that when  $k_2 \gg k_1$

$$[B]_{\max} = [A]_0 k_1/k_2$$

E. T. Gray, Jr., R. W. Taylor and D. W. Margerum, *Inorg. Chem.* **16**, 3047 (1977).

12. A general rate equation has been derived for reactions with a single relaxation time. Consider:

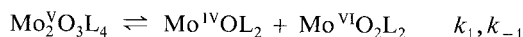


show

$$\tau^{-1} = k_1 [A]_e^a [B]_e^b [(a^2/[A]_e) + (b^2/[B]_e)] + k_{-1} [D]_e^d [E]_e^e [(d^2/[D]_e) + (e^2/[E]_e)]$$

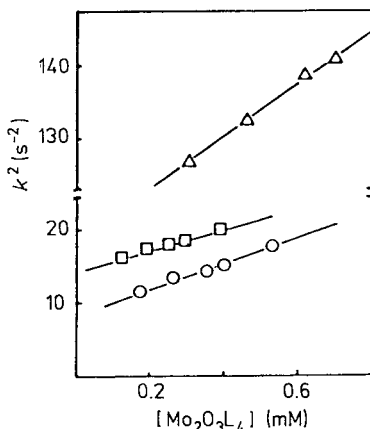
E. L. King, *J. Chem. Educ.* **56**, 580 (1979).

13. The equilibrium



in 1,2-dichloroethane (L = XYCN<sub>2</sub>Et<sub>2</sub>, XY = SSe or SeSe) has been perturbed by a 1:1 (volume) dilution with 1,2-dichloroethane in a flow apparatus. The relaxation is a single first-order process (rate constant =  $k$ ). The figure shows plots of  $k^2$  vs  $[\text{Mo}_2\text{O}_3\text{L}_4]_0$  (the concentration of  $\text{Mo}_2\text{O}_3\text{L}_4$  if the equilibrium were shifted completely to left). Estimate the values of  $k_1$  and  $k_{-1}$ .

T. Matsuda, K. Tanaka and T. Tanaka, *Inorg. Chem.* **18**, 454 (1979).

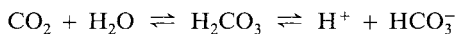


Problem 13. Plots of  $k^2$  vs  $[\text{Mo}_2\text{O}_3\text{L}_4]_0$  in 1,2-dichloroethane at 25°C. L = Et<sub>2</sub>NCS<sub>2</sub>(O), Et<sub>2</sub>NCSSe( $\square$ ), Et<sub>2</sub>NCSe<sub>2</sub>( $\Delta$ ). Reprinted with permission from T. Matsuda, K. Tanaka and T. Tanaka, *Inorg. Chem.* **18**, 454 (1979). © (1979) American Chemical Society.

14. Derive the expression for the relaxation times for

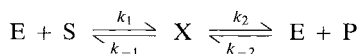


This system is fully discussed and analyzed in the early pressure-jump work on



S. Ljunggren and O. Lamm, *Acta Chem. Scand.* **12**, 1834 (1958).

15. For the Michaelis-Menten scheme involving interaction of enzyme (E) with substrate (S) or product (P):



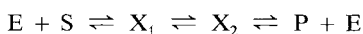
show using steady-state conditions for X and  $[S]_0 \gg [E]_0$  that

$$\frac{-d[S]}{dt} = \frac{[V_s/K_s][S] - [V_p/K_p][P]}{1 + [S]/K_s + [P]/K_p}$$

where

$$\begin{aligned} V_s &= k_2[E]_0 \\ V_p &= k_{-1}[E]_0 \\ K_s &= (k_{-1} + k_2)/k_1 \\ K_p &= (k_{-1} + k_2)/k_{-2} \end{aligned}$$

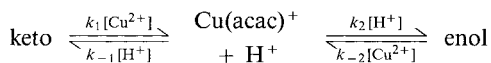
Convince yourself that (a) this equation reduces to (1.104) when initial-rate measurements,  $[P] = 0$ , are used and (b) the same form of equation results when a number of intermediates arises as in



which is a more realistic portrayal of enzyme behavior.

B10, p. 220–222.

16. The reaction of Cu(II) ion with acetylacetonone (acacH) to form the mono complex  $\text{Cu}(\text{acac})^+$  in methanol is interpreted in terms of the scheme



where the keto and enol represent those forms of acetylacetonone. The reaction is studied by mixing a solution containing  $\text{Cu}^{2+}$  and  $\text{H}^+$  with one containing acacH and  $\text{H}^+$  in a stopped flow apparatus. Two reactions are seen,  $k_1$  and  $k_{11}$  with the following conditions:

total [acacH] = 0.1 mM, [H<sup>+</sup>] = 1.09 mM, 25°C

[Cu <sup>2+</sup> ] mM	$k_1$ s <sup>-1</sup>	$k_{II}$ s <sup>-1</sup>
1.18	28	1.64
1.41	36	2.21
1.65	41	2.26
1.88	43	2.64
2.12	50	2.55
2.35	53	2.76
1.18	28	1.77
1.65	37	2.02
2.35	50	3.10

Treating the system as a relaxation with all pseudo first-order rate constants, deduce the expressions for  $k_1 + k_{II}$  and  $k_1 k_{II}$  in terms of the component rate constants and hence determine the values of  $k_1$ ,  $k_{-1}$ ,  $k_2$  and  $k_{-2}$ .

R. G. Pearson and O. P. Anderson, *Inorg. Chem.* **9**, 39 (1970).

17. Determine the rate law for the exchange of Ag between Ag(I) and Ag(II) in 5.9 M HClO<sub>4</sub> at 0°C. Use the accompanying data, obtained by the quenched-flow method. Suggest a mechanism for the exchange.

[Ag <sup>I</sup> ], mM	[Ag <sup>II</sup> ], mM	$t_{1/2}$ exch, s
2.2	0.64	0.77
3.7	1.4	0.35
3.6	1.5	0.34
3.9	1.2	0.42
6.8	2.2	0.26
7.6	1.9	0.34
10.0	1.3	0.49
9.7	2.0	0.29
10.6	1.8	0.32
15.5	1.4	0.45
17.7	1.2	0.51
24.1	1.3	0.54
30.3	1.2	0.60

B. M. Gordon and A. C. Wahl, *J. Amer. Chem. Soc.* **80**, 273 (1958).

18. The reduction of Mn(III) myoglobin by dithionite (in excess) obeys the rate law at 25°C,  $\mu = 0.45$  M (Na<sub>2</sub>SO<sub>4</sub>)

$$-d[\text{Mn(III)Myo}]/dt = k_{\text{obs}}[\text{Mn(III)Myo}]$$

$$\text{where } k_{\text{obs}} = k[\text{S}_2\text{O}_4^{2-}]^{1/2}$$

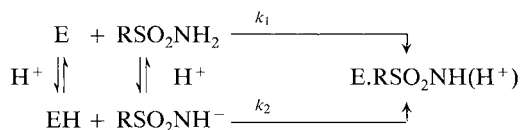


pH	$k, M^{-1/2}s^{-1}$	pH	$k, M^{-1/2}s^{-1}$
5.3	33	6.9	1.6
5.5	21	7.0	1.3
5.7	15	7.1	1.2
5.8	12	7.3	0.76
5.9	10	7.5	0.72
6.0	7.5	7.7	0.75
6.1	6.0	7.8	0.60
6.3	4.6	7.9	0.58
6.4	3.2	8.0	0.51
6.6	2.7	8.4	0.47
6.7	1.9	8.6	0.47

Plot  $k$  vs pH and see if there is a  $pK$  associated with the protein (assume dithionite is aprotic in this pH range). Deduce the expression relating  $k$  and  $[H^+]$ .

R. Langley, P. Hambricht, K. Alston and P. Neta, *Inorg. Chem.* **25**, 114 (1986).

19. Aromatic sulfonamides are specific inhibitors of carbonic anhydrase (E). The apparent second-order rate constants for association of p-nitrobenzenesulfonamide with (a) carbonic anhydrase-B and (b) the carboxymethylated derivative of the enzyme are shown against pH in Figure 1.14. Estimate using equations (1.225) and (1.226) the values for  $pK_E$ ,  $pK_s$  and  $k_1$  and  $k_2$  for the two possible schemes shown for both carbonic anhydrase-B and the carboxymethylated derivative. (It is uncertain whether the bound inhibitor is ionized in the product.)



$pK_E$  and  $pK_s$  are the ionization constants for the enzyme (or derivative) and sulfonamide respectively. Suggest which is the likely path.

P. W. Taylor, R. W. King and A. S. V. Burgen, *Biochemistry* **9**, 3894 (1970); S. Lindskog in *Zinc Enzymes*, T. G. Spiro, ed., Wiley-Interscience, NY 1983.

20. The second-order rate constant for oxidation of  $\text{Fe}(\text{CN})_6^-$  by  $\text{OH}^\bullet$  radicals, produced by low-intensity-pulse radiolysis of water, varies with pH as in the accompanying table. Determine the  $\text{p}K$  for acid dissociation of the  $\text{OH}^\bullet$  radical in aqueous solution. (This is difficult to obtain by any other method.)

pH	$10^{-10} \times k$ $\text{M}^{-1}\text{s}^{-1}$
neutral	1.2
11.94	0.49
12.10	0.36
12.57	0.19
13.07	0.06

J. Rabani and M. S. Matheson, *J. Amer. Chem. Soc.* **86**, 3175 (1964).

21. The second-order rate constant for the reaction of a hydrogen atom with a hydroxide ion to give an electron and water (hydrated electron) is  $2.0 \times 10^7 \text{M}^{-1}\text{s}^{-1}$ . The rate constant for the decay of a hydrated electron to give a hydrogen atom and hydroxide ion is  $16 \text{M}^{-1}\text{s}^{-1}$ . Both rate constants can be determined by pulse radiolytic methods. Estimate, using these values, the  $\text{p}K_a$  of the hydrogen atom. Assume the concentration of water is  $55.5 \text{M}$  and that the ionization constant of water is  $10^{-14} \text{M}$ .  
W. L. Jolly, *Modern Inorganic Chemistry*, McGraw Hill, NY, 1984, p. 239.

# Chapter 2

## The Deduction of Mechanism

We are concerned in this chapter with the mechanism of a reaction, that is, the detailed manner in which it proceeds, with emphasis on the number and nature of the steps involved. There are several means available for elucidation of the mechanism, including using the rate law, and determining the effect on the rate constant of varying the structure of reactants (linear free energy relations) and of outside parameters such as temperature and pressure. Finally chemical intuition and experiments are often of great value. These means will be analyzed.

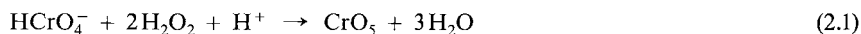
### 2.1 The Rate Law and Mechanism

The kineticist should always strive to get as complete (and accurate!) a rate law as conditions will allow. The mechanism that is suggested to account for the rate law is, however, a product of the imagination, and since it may be one of several plausible mechanisms, it might very well turn out to be incorrect. Indeed, it is impossible to prove any single mechanism but so much favorable data may be amassed for a mechanism that one can be fairly certain of its validity.

Some general rules exist for deducing the mechanism from a rate law, and the subject is hardly a magical one.<sup>1</sup> Probably the most important single statement is that *the rate law gives the composition of the activated complex – nothing more nor less – but yields no clue about how it is assembled*. Once this is appreciated, many of the problems and ambiguities that have arisen on occasion are easily understood, though not necessarily resolved.

For the moment, we can consider the activated complex as a type of “intermediate” (although not isolatable) reached by the reactants as the highest energy point of the most favorable reaction path. The activated complex is in equilibrium with the reactants and is commonly regarded as an ordinary molecule, except that movement along the reaction coordinate will lead to decomposition. The activated complex can be assumed to have the associated properties of molecules, such as volume,<sup>2</sup> heat content,<sup>3</sup> acid-base behavior,<sup>4</sup> entropy,<sup>5</sup> and so forth. Indeed, formal calculations of equilibrium constants involving reactions of the activated complex to form another activated complex can be carried out (Sec. 5.6 (b)).<sup>6</sup>

Consider the formation of CrO<sub>5</sub> from Cr(VI) and H<sub>2</sub>O<sub>2</sub> in an acid medium.<sup>7,8</sup>



The reaction is third-order:

$$d[\text{CrO}_5]/dt = k [\text{HCrO}_4^-] [\text{H}_2\text{O}_2] [\text{H}^+] \quad (2.2)$$

From the rate law, the composition of the activated complex must therefore be

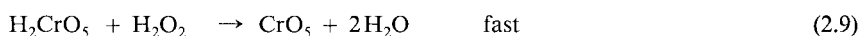
$$[\text{HCrO}_4^-, \text{H}_2\text{O}_2, \text{H}^+, (\text{H}_2\text{O})_n]^\ddagger \quad (2.3)$$

although we do not know how the various groups are assembled. The activated complex might arise, for example, from a rate-determining step (rds)<sup>9</sup> involving  $\text{H}_2\text{CrO}_4$  reacting with  $\text{H}_2\text{O}_2$ ,  $\text{HCrO}_4^-$  reacting with  $\text{H}_3\text{O}_2^+$ , or even, in principle,  $\text{CrO}_4^{2-}$  reacting with  $\text{H}_4\text{O}_2^{2+}$ . Also involved in the step will be an unknown number of solvent molecules.

Any reagent that appears as part of the reaction stoichiometry but does not feature in the rate law must react in a step that follows the rate-determining one. It is clear from the stoichiometry of (2.1) that one  $\text{H}_2\text{O}_2$  molecule must react after the rds. In light of these various points, two possible mechanisms would be



and



Activated complexes will be associated with all three steps of each mechanism since each step is in principle a separable reaction. The important activated complex is that produced in the rds. This is as far as we can go at present, using the rate law, but we shall return to this problem later (Sec. 2.1.7 (c)).

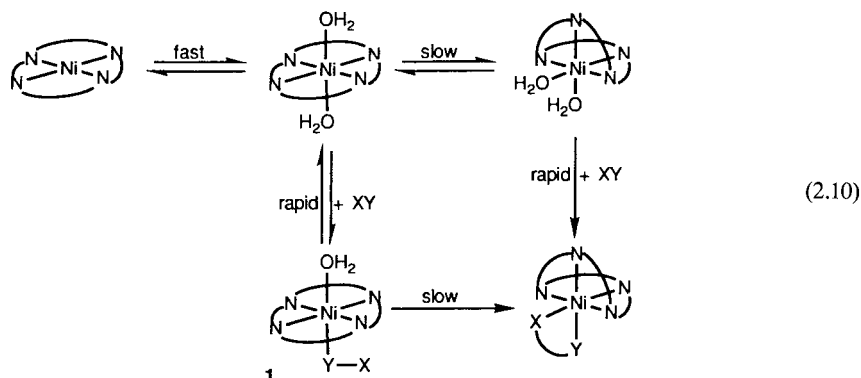
It is clear that many reactions, particularly those without simple stoichiometry, will have mechanisms containing several steps, one or more of which may include reversible equilibria (consider for example (1.118) to (1.120)). The number of separate terms in the rate law will indicate the number of paths by which the reaction may proceed, the relative importance of which will vary with the conditions. The complex multi-term rate laws, although tedious to characterize, give the most information on the detailed mechanism.

We shall discuss in the following sections the mechanisms that might be associated with the common rate laws. We have already referred to reaction schemes (mechanisms) in discussing rate laws in Chap. 1. Indeed, experienced kineticists often have some preconceived notions of the mechanism before they plan a kinetic study. Certainly in principle, however, the rate law can be obtained before any thoughts of mechanism arise.

### 2.1.1 First-Order Reactions

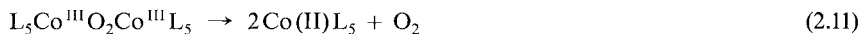
As well as the obvious example involving one reactant (even with this solvent may be involved) a number of reactions between A and B that might have been expected to be second-order, first-order in A and in B, turn out to be first-order only (say in A). Obviously some feature of A, not directly connected with the main reaction with B, must be determining the rate. The product of this rds,  $A_1$ , must react more readily with B than A does. It is possible to check the correctness of this idea by independent study of the  $A \rightarrow A_1$  interconversion. An isomerization within a complex may limit the rate of its reaction with another reagent.

The reaction of planar Ni ( $[14]aneN_4$ ) $^{2+}$  represented as shown in (2.10) with a number of bidentate ligands (XY) to produce *cis*-octahedral Ni ( $[14]aneN_4$ ) XY $^{2+}$  is first-order in nickel complex and  $[OH^-]$  and independent of the concentration of XY.<sup>10</sup> In the preferred mechanism, the folding of the macrocycle (base-catalyzed *trans*  $\rightarrow$  *cis* isomerization) is rate determining, and this is followed by rapid coordination of XY:



In an alternative mechanism a monodentate intermediate (**1**) is in rapid equilibrium with reactants and it undergoes at high  $[XY]$  rate-determining ring closure. Such a type of mechanism is believed to operate for Ni(trien) $^{2+}$  interacting with XY.<sup>11</sup> Reasons for the preferred mechanisms are given.<sup>10</sup> The isomerization may take the form of a conformational change in a metalloprotein.<sup>12</sup>

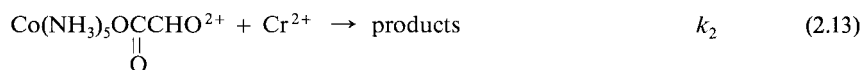
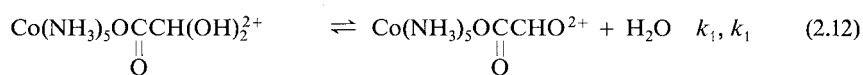
The reactivity of a dimer may be limited by its fragmentation. The rates of a number of reactions of cobalt(III) peroxo species (any charges omitted) are limited by their breakdown (rds)



The scavenging of  $Co(II)L_5$  or  $O_2$  by added reagent follows rapidly. The rate law does not therefore include the concentration of the added reagent,<sup>13,14</sup> except in certain instances.<sup>15</sup> Finally, the first-order dominance of a reaction between A and B may only become apparent at higher concentrations of B (Sec. 1.6.3).

The reaction of  $Co(III)$  complexes with  $Cr^{2+}$  is almost universally a second-order process (Chap. 5). The reaction of  $Co(NH_3)_5OCOCH(OH)_2^{3+}$  with  $Cr^{2+}$  is second-order at low concentrations of reductant, but becomes almost independent of  $[Cr^{2+}]$  when the concentration

is high.<sup>16</sup> The glyoxalate is hydrated in the complex (>98% from nmr measurements) and the rate behavior can be understood on the basis of the scheme



for which a rate law of the form (1.115) applies:

$$V = -d[\text{Co}^{\text{III}}]/dt = \frac{k_1 k_2 [\text{Co}^{\text{III}}] [\text{Cr}^{2+}]}{k_{-1} + k_2 [\text{Cr}^{2+}]} \quad (2.14)$$

At high  $[\text{Cr}^{2+}]$ ,

$$V = k_1 [\text{Co}^{\text{III}}] \quad (2.15)$$

This explanation is supported by nmr rate data for the dehydration of hydrated pyruvic acid, which is similar to glyoxalate. For this at 25°C

$$k_1 = 0.22 + 1.25 [\text{H}^+] \quad (2.16)$$

compared with

$$k_1 = 0.075 + 0.64 [\text{H}^+] \quad (2.17)$$

for the glyoxalate complex from the reduction data.<sup>16</sup>

## 2.1.2 Second-Order Reactions

These are among the most commonly encountered reactions, and can be either between two different reagents or two identical species, as in disproportionation reactions of radicals.

The distinguishing of a single step



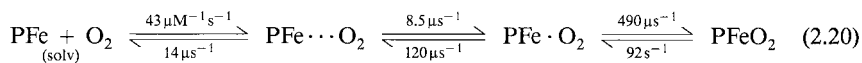
from a stepwise mechanism



may prove very difficult (Sec. 5.5).

An excellent example of a “simple” second-order reaction being far from simple is the interaction of small molecules e.g.  $\text{O}_2$ ,  $\text{CO}$  or  $\text{NO}$  with deoxymyoglobin (PFe). Examination

using flow, T-jump and flash photolysis methods shows up an excellent second-order reaction between ligand dissolved in the solvent and the heme iron center. This however disguises a much more complicated mechanism:



<b>2</b>	<b>3</b>	<b>4</b>	<b>5</b>
separated reactants in solution	O <sub>2</sub> embedded in protein but distant from Fe	“Geminate” state – O <sub>2</sub> embedded in protein near heme but not Fe bound	O <sub>2</sub> bound to Fe

Irradiation of PFeO<sub>2</sub> in solutions by short, very intense, laser pulses produces transients such as 3 and 4. Absorbance changes following the production of 3 and 4 are ascribed to their decay and rate parameters can be estimated as shown in the Scheme. Note the units in (2.20) which are occasionally used for large rate constants. The mechanism shown is certainly a simplified one.<sup>17, 18</sup>

*Geminate recombination and quantum yield.* – The hemoprotein adducts are photoactive, light breaking the iron-ligand bond. The quantum yields (unliganded protein molecules formed/quanta absorbed) however vary widely being about 0.5 to 1.0 for CO, 0.05 for O<sub>2</sub> and quite low, 0.001 for NO adducts. These differences can be rationalized in terms of geminate recombination. This represents the return of the photolyzed ligand to the iron site from a nearby site and therefore not actually getting into solution. It is shown that a high fraction of NO, much less O<sub>2</sub> and very little CO, recombines with heme after short-time laser pulse photolysis. This accounts for the order of quantum yields above, which relate to the complete removal of the ligand into the solution on sustained photolysis. The rate constant for binding generally decreases NO > O<sub>2</sub> ≫ CO (M. P. Mims, A. G. Porras, J. S. Olson, R. W. Nobel and J. A. Peterson, *J. Biol. Chem.* **258**, 14219 (1983)). The rds for NO binding is diffusion of NO into the protein, whereas with the other ligands attachment to the metal is also an important rate-controlling step. These points emerge from the geminate recombination studies (Q. H. Gibson, *J. Biol. Chem.* **264**, 20155 (1989)).

### 2.1.3 Third-Order Reactions

An activated complex containing three species (other than solvent or electrolyte), which attends a third-order reaction, is not likely to arise from a single termolecular reaction involving the three species. Third- (and higher-) order reactions invariably result from the combination of a rapid preequilibrium or preequilibria with a rds, often unidirectional. Such reactions are

fairly common in transition metal chemistry because of the stepwise nature of metal complex-ligand interactions. A third-order rate law,

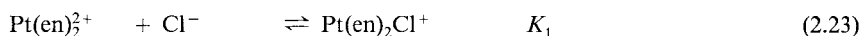
$$V = k [A] [B] [C] \quad (2.21)$$

is usually best understood as arising from a rate-determining reaction of the binary product, say AB, of a rapid preequilibrium, with the third reactant C.

The Pt(II)-catalyzed substitution of Pt(IV) complexes was first established in 1958.<sup>19</sup> The rate of exchange of chloride between  $\text{Pt}(\text{en})_2\text{Cl}_2^{2+}$  and  $\text{Cl}^-$  ions is *extremely* slow, but the rate is markedly enhanced in the presence of  $\text{Pt}(\text{en})_2^{2+}$  ions. The third-order exchange law

$$V_{\text{exch}} = k [\text{Pt}(\text{en})_2\text{Cl}_2^{2+}] [\text{Pt}(\text{en})_2^{2+}] [\text{Cl}^-] \quad (2.22)$$

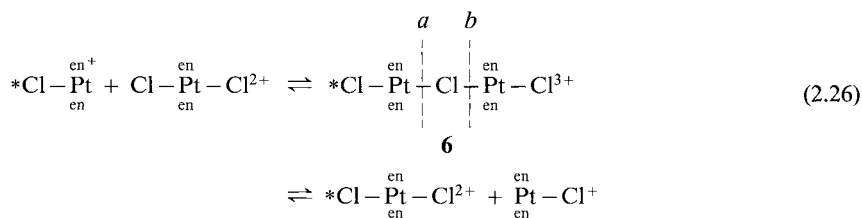
can be beautifully rationalized by the mechanism



for which

$$k = K_1 k_2 \quad (2.25)$$

Exchange is visualized as occurring through a symmetrical intermediate or transition state **6**, which allows for interchange of Cl between Pt(II) and Pt(IV). Breakage of the Cl bridge at *a* produces the original



isotopic distribution, while cleavage at *b* leads to exchange. It should be noted that this mechanism leads also to exchange of both Pt and en between Pt(II) and Pt(IV), catalyzed by  $\text{Cl}^-$  ion. All these exchanges have been studied and the existence of similar values of *k* from  $\text{Cl}^-$  exchange ( $12\text{--}15 \text{ M}^{-2}\text{s}^{-1}$ ), Pt exchange ( $11 \text{ M}^{-2}\text{s}^{-1}$ ), and en exchange ( $16 \text{ M}^{-2}\text{s}^{-1}$ , all data at  $25^\circ\text{C}$ ) is striking evidence for the correctness of the mechanism. These original studies have led to substantial developments in the chemistry of substitution in Pt(IV),<sup>20</sup> and modification of the mechanism with certain systems.<sup>21</sup>

A third-order rate law of the form

$$V = k [A]^2 [B] \quad (2.27)$$

perhaps suggests (although there are other possibilities, as we shall see) that a dimer  $\text{A}_2$  is rapidly formed, in small quantities, from the monomer A, and that it is this dimer that reacts



with B in the rate-determining step. Such a situation may apply in the  $H_2$  reduction of  $Co(CN)_5^{3-}$  (Ref. 22)



for which the rate law

$$-d[Co(CN)_5^{3-}]/dt = 2k_1 [Co(CN)_5^{3-}]^2 [H_2] - 2k_{-1} [Co(CN)_5H^{3-}]^2 \quad (2.29)$$

suggests a mechanism



The rate law (2.27) is not helpful in detailing the sequence leading to the formation of the activated complex, only that it consists of two molecules of A and one of B.

Reaction of Vitamin  $B_{12r}$  ( $B_{12r}$ ) with organic iodides (RI) in aqueous solution

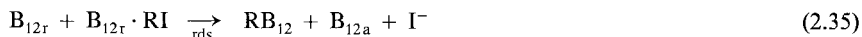


*Vitamin  $B_{12}$  (cyanocobalamin)* – This has a central Co(III) bound to four N's of a corrin ring, a methylbenzimidazole group (which is attached to the corrin ring) and a  $CN^-$  group. When the  $CN^-$  is replaced by  $H_2O$  or  $OH^-$ , aquacobalamin ( $B_{12a}$ ) and hydroxocobalamin ( $B_{12b}$ ) result. Reduced derivatives are  $B_{12r}$  also termed cob(II)alamin and  $B_{12s}$  (cob(I)alamin). The redox interconversion of the Co(III), Co(II) and Co(I) derivatives is of key importance, D. Lexa and J.-M. Saveant, *Accs. Chem. Res.* **16**, 235 (1983).

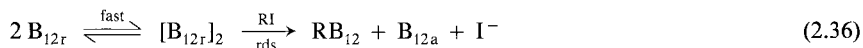
occurs with the rate law

$$V = k [B_{12r}]^2 [RI] \quad (2.33)$$

Associated mechanisms consistent with this rate law include



or



or



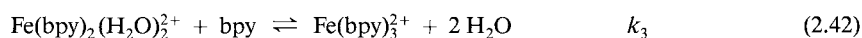
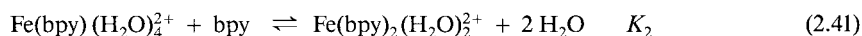
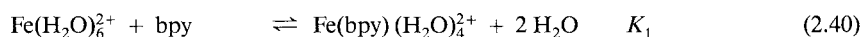
(2.37) involves the disproportionation of Co(II) in  $B_{12r}$ . For chemical reasons, the first mechanism is preferred.<sup>23</sup>

### 2.1.4 Even Higher-Order Reactions

In the formation of the highly colored  $\text{Fe}(\text{bpy})_3^{2+}$  ion from  $\text{Fe}^{2+}$  ion and excess bipyridine (bpy) in acid solution, the following rate law has been demonstrated

$$d[\text{Fe}(\text{bpy})_3^{2+}]/dt = k[\text{Fe}^{2+}][\text{bpy}]^3 \quad (2.39)$$

with  $k = 1.4 \times 10^{13} \text{M}^{-3} \text{s}^{-1}$  and temperature-independent from  $0^\circ\text{C}$  to  $35^\circ\text{C}$ .<sup>24</sup> This rate law follows from (2.40)–(2.42), with  $K_1$  and  $K_2$  associated with rapid pre-equilibria and (2.42) the rds.



On this basis,  $k$  is a composite rate constant

$$k = K_1 K_2 k_3 \quad (2.43)$$

Since  $K_1 K_2$  is  $10^8 \text{M}^{-2}$  at  $25^\circ\text{C}$ ,  $k_3$  is calculated as  $1.4 \times 10^5 \text{M}^{-1} \text{s}^{-1}$ . The latter is a reasonable value from our knowledge of the substitution reactions of iron(II); see Table 4.1. For another example, see Ref. 25.

### 2.1.5 Negative-Order Reactions

The inclusion in the rate law of a simple inverse dependence on the concentration of a species (negative-order reactions) usually indicates that this reagent features as the product of a rapid step preceding the rate-determining step. This is illustrated by the multiterm rate law that governs the reaction of Fe(III) with V(III) in acid,<sup>26</sup>

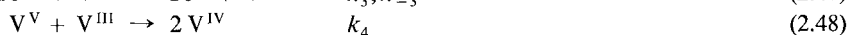
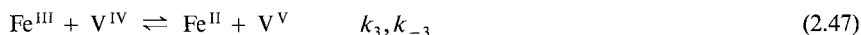


$$-d[\text{Fe}^{\text{III}}]/dt = -d[\text{V}^{\text{III}}]/dt = k_1[\text{Fe}^{\text{III}}][\text{V}^{\text{III}}] + k_2[\text{Fe}^{\text{III}}][\text{V}^{\text{III}}][\text{V}^{\text{IV}}][\text{Fe}^{\text{II}}]^{-1} \quad (2.45)$$

At high initial  $[\text{Fe}(\text{II})]$ , the term in  $k_2$  is negligible and the  $k_1$  term represents a straightforward second-order (acid-dependent) reaction,

$$k_1 = k + k'[\text{H}^+]^{-1} + k''[\text{H}^+]^{-2} \quad (2.46)$$

From experiments at high initial  $[\text{V}(\text{IV})]$ , the second term becomes important and is then easily measurable. For this term a possible mechanism is

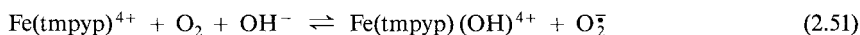
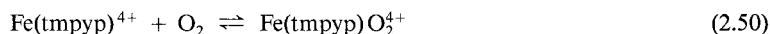
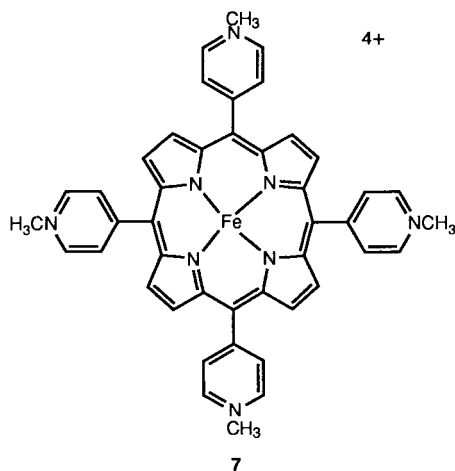


The stationary-state approximation,  $d[V(V)]/dt = 0$ , leads to

$$\frac{-d[V^{III}]}{dt} = \frac{k_3 k_4 [Fe^{III}] [V^{III}] [V^{IV}]}{k_{-3} [Fe^{II}] + k_4 [V^{III}]} \quad (2.49)$$

and if  $k_{-3} [Fe(II)] \gg k_4 [V(III)]$ , the observed rate term is obtained with  $k_2 = k_3 k_4 / k_{-3}$ . The value of  $k_3 / k_{-3}$  equals the equilibrium constant for reaction (2.47) and can be independently determined. From this, and the  $k_2$  value obtained experimentally,  $k_4$  can be calculated. A later direct determination of the rate constant for the V(III), V(V) reaction gave a value (and pH dependence)<sup>27</sup> in good agreement with that obtained indirectly, thus affording strong support for the correctness of the mechanism.

The lack of retardation by added Fe(III) (tmpyp)OH<sup>4+</sup> on the rate of the Fe(II)tmpyp<sup>4+</sup> (7) reaction with O<sub>2</sub> indicates that Fe(III) porphyrin is *not* formed in the first step, i. e. (2.50) rather than (2.51) is the better description for the first step in the overall reaction<sup>28</sup>



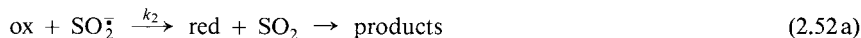
See also Chap. 8. Fe(II).

### 2.1.6 Fractional-Order Reactions

A fractional order may arise when a reaction with a multiterm rate law (containing no fractional orders) is examined over only a small range of concentrations (see (1.6.3)). Such an origin can be easily detected, since it disappears when the rate law is fully resolved.

Monomer, polymer equilibria can be the basis of a genuine fractional order. Many reductions by dithionite S<sub>2</sub>O<sub>4</sub><sup>2-</sup> of oxidants (ox) to produce reductants (red) contain in the rate law a term which includes a square root dependence on the S<sub>2</sub>O<sub>4</sub><sup>2-</sup> concentration (often this is the

only term). This arises from the presence of very small amounts of the radical  $\text{SO}_2^{\cdot-}$  in equilibrium with  $\text{S}_2\text{O}_4^{2-}$ :



It is not too difficult to show<sup>29-31</sup>

$$V = -d[\text{S}_2\text{O}_4^{2-}]/dt = \frac{2k_1[\text{S}_2\text{O}_4^{2-}]}{1 + (1 + a[\text{S}_2\text{O}_4^{2-}])^{1/2}} \quad (2.53)$$

where

$$a = \frac{16k_1k_{-1}}{k_2^2[\text{ox}]^2} \quad (2.54)$$

Two limits are immediately obvious,

$$a[\text{S}_2\text{O}_4^{2-}] \ll 1, \quad V = k_1[\text{S}_2\text{O}_4^{2-}] \quad (2.55)$$

and

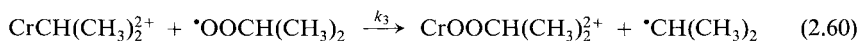
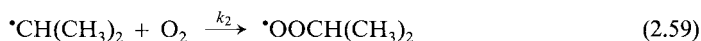
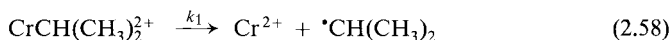
$$a[\text{S}_2\text{O}_4^{2-}] \gg 1, \quad V = 1/2k_2(k_1/k_{-1})^{1/2}[\text{S}_2\text{O}_4^{2-}]^{1/2}[\text{ox}] \quad (2.56)$$

The latter behavior is usually observed. Similar kinetics apply with the  $\text{Cr}_2(\text{OAc})_6^{2-}/\text{Cr}(\text{OAc})_3^-$  system.<sup>31</sup> (Chap.8. Cr(II)).

Fractional orders such as 3/2 often hint at a chain mechanism. The autoxidation of  $(\text{H}_2\text{O})_5\text{CrCH}(\text{CH}_3)_2^+$  leads to a number of products. Log (initial rate) vs log (initial concentration of organochromium cation) plots give a 3/2 slope. The rate is independent of  $[\text{H}^+]$  and  $[\text{O}_2]$  and the rate law is therefore

$$-d[\text{CrCH}(\text{CH}_3)_2^+]/dt = k_{\text{obs}}[\text{CrCH}(\text{CH}_3)_2^+]^{3/2} \quad (2.57)$$

A consistent mechanism is:



With a steady state approximation for the chain-carrying intermediates in (2.59) and (2.60) and the assumption of long chain length<sup>32</sup>

$$k_{\text{obs}} = \frac{k_3k_1^{1/2}}{(2k_4)^{1/2}} \quad (2.62)$$

see also Refs. 33 and 34.

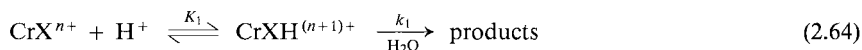
### 2.1.7 The Inclusion of $[H^+]$ Terms in the Rate Law

There are problems in correctly ascribing  $[H^+]$  terms in the rate law to a mechanism for the reaction. First, it must be decided whether a medium effect rather than a distinctive reaction pathway might be responsible for the variation of rate with  $[H^+]$ , particularly if this is a small contribution. This is an important point that we shall deal with later (Sec. 2.9.2). Secondly, even when it has been established that the pH term has a mechanistic basis, there may be an ambiguity in the interpretation of the rate law. On occasion, such ambiguity has been quite severe and has led to much discussion.

(a) *Positive Dependence on  $[H^+]$* . Inclusion of an  $[H^+]^n$ ,  $n \geq 1$ , term in the rate law can usually be explained by the operation of a rate-determining reaction of a protonated species. Usually there is a likely basic site on one of the reactants for protonation, and the greater reactivity of the protonated species compared with the unprotonated form can usually be rationalized (see Sec. 4.3.1). A two-term rate law for the acid hydrolysis of  $CrX^{n+}$  (see (1.208)),

$$-d \ln [CrX^{n+}]/dt = k + k' [H^+] \quad (2.63)$$

has been noted with a number of basic ligands,  $F^-$ ,  $N_3^-$ , and so forth. The terms can be attributed to reactions of protonated and unprotonated forms of the complex



with  $k = k_0$  and  $k' = K_1 k_1$ . The depletion of the reagent water will be an important consideration in high acid concentrations if water features in the activated complex. The rate of hydrolysis might then decrease with an increase of (high) perchloric acid concentration and

$$V \sim k [\text{complex}] a_w \quad (2.66)$$

where  $a_w$  represents the activity of water. Linear rate dependencies on the activity of water are observed in the hydrolysis of  $CrOCOCH_3^{2+}$  in 6–8 M  $HClO_4$ <sup>35</sup>, of  $CrClO_4^{2+}$  in 5–10 M  $HClO_4$ <sup>36</sup> and of  $Co(NH_3)_5OPO_3H_3^{3+}$  in  $>5$  M  $HClO_4$ .<sup>37</sup>

(b) *Negative Dependence on  $[H^+]$* . Inclusion of an  $[H^+]^n$  term in the rate law, where  $n$  is a negative integer, can be attributed to a proton being a product of a preequilibrium step (see Sec. 2.1.5), and therefore arising from the rate-determining reaction of a deprotonated species. It is often likely to occur when one of the reactants is acidic.

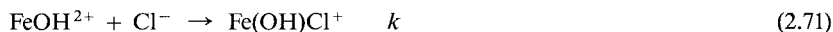
The formation of  $FeCl^{2+}$  from  $Fe^{3+}$  and  $Cl^-$  ions in acid solution obeys the rate law (compare with (1.6))<sup>38</sup>

$$d [FeCl^{2+}]/dt = k_1 [Fe^{III}] [Cl^-] + k_2 [Fe^{III}] [Cl^-] [H^+]^{-1} \quad (2.67)$$

The first term simply represents the reaction between the fully hydrated iron(III) ion,  $Fe(H_2O)_6^{3+}$ , abbreviated  $Fe^{3+}$ , the predominant iron species, and chloride ion, with an associated activated complex  $[FeCl(H_2O)_n]^\ddagger$ .



Inclusion of the  $[\text{H}^+]^{-1}$  term is reasonably ascribed to the reaction of  $\text{Fe}(\text{H}_2\text{O})_5\text{OH}^{2+}$ , abbreviated  $\text{FeOH}^{2+}$ , with  $\text{Cl}^-$  ions in the slow step:



for which

$$k_2 = kK_wK \quad (2.73)$$

The similar rate laws for the reactions of Fe(III) with a number of aprotic ligands can be rationalized in the same manner. The rate constants for ligation of  $\text{Fe}^{3+}$  and  $\text{FeOH}^{2+}$  are shown in Table 2.1. The exchange of water with Fe(III) and other trivalent transition metal ions, Cr(III), Rh(III), as well as Al(III) and Ga(III), Eqn. 4.5, proceeds via  $\text{M}(\text{H}_2\text{O})_6^{3+}$  as well as by  $\text{M}(\text{H}_2\text{O})_5\text{OH}^{2+}$ , so that here also an  $[\text{H}^+]^{-1}$  term features in the rate law.

**Table 2.1** Rate Constants ( $k$ ,  $\text{M}^{-1}\text{s}^{-1}$ ) for Reactions of  $\text{Fe}^{3+}$  and  $\text{FeOH}^{2+}$  with Ligands at 25°C

Ligand	$\text{Fe}^{3+}$	$\text{FeOH}^{2+}$	Ref.
$\text{Cl}^-$	9.4	$1.1 \times 10^4$	41
$\text{NCS}^-$	127	$1.0 \times 10^4$	41
HF	11.4	—	41
$\text{HN}_3$	4.0	—	41
Ambiguous			
$\text{CrO}_4^{2-}$	$5 \times 10^7$		
$\text{HCrO}_4^-$		$9.2 \times 10^3$	42
$\text{F}^-$	$5 \times 10^3$		
HF		$3.2 \times 10^3$	41
$\text{N}_3^-$	$1.6 \times 10^5$		
$\text{HN}_3$		$6.3 \times 10^3$	41
$\text{SO}_4^{2-}$	$4 \times 10^3$		
$\text{HSO}_4^-$		$2.4 \times 10^4$	41
$\text{RCON}(\text{O}^-)\text{R}_1$	$\sim 10^9$		
$\text{RCON}(\text{OH})\text{R}_1$		$\sim 10^3$	45
$\text{H}_2\text{PO}_4^-$	$6.8 \times 10^4$		
$\text{H}_3\text{PO}_4$		$9.2 \times 10^6$	43

(c) *Proton Ambiguity*. Acid-catalyzed reaction between species A and B, both of which are basic, leads to interpretive difficulties

$$V = k[\text{A}][\text{B}][\text{H}^+] \quad (2.74)$$

since we are uncertain whether A or B takes the proton into the activated complex. The rate law for the oxidation of hydrazinium ion by Cr(VI) takes the form of (2.74). The reactant pair  $\text{N}_2\text{H}_5^+$  and  $\text{CrO}_2\text{H}^{3+}$  are preferred over  $\text{N}_2\text{H}_6^{2+}$  and  $\text{CrO}_2^{2+}$  for chemical reasons.<sup>39</sup>

We can now return to the reaction considered at the beginning of this chapter. The third-order rate constant  $k$  will equal  $K_1 k_1$  on the basis of (2.4) and  $K_2 k_2$  if mechanism (2.7) is correct. It is possible to make rough estimates of the values (at 4°C) of  $k_1$  ( $2.5 \times 10^4 \text{ M}^{-1} \text{ s}^{-1}$ ) and  $k_2$  ( $\sim 5 \times 10^8 \text{ M}^{-1} \text{ s}^{-1}$ ) from the values of  $K_1$  ( $0.1 \text{ M}^{-1}$ ),  $K_2$  ( $\sim 2 \times 10^{-5} \text{ M}^{-1}$ ) and  $k$  ( $5 \times 10^3 \text{ M}^{-2} \text{ s}^{-1}$ ). The improbably high value for  $k_2$  is one of the reasons that the first mechanism is preferred.<sup>7,8</sup> Deviation from a first-order dependence on  $[\text{H}^+]$  occurs at high acidity since a stage is being reached where  $\text{H}_2\text{CrO}_4$  is in significant concentration (see (1.98)).<sup>40</sup> Even here and in the limiting region, where the rate is independent of  $[\text{H}^+]$  because  $\text{H}_2\text{CrO}_4$  is the major chromium species and its concentration is pH-independent, it is not difficult to see that the concentration products  $[\text{H}_2\text{CrO}_4][\text{H}_2\text{O}_2]$  and  $[\text{HCrO}_4^-][\text{H}_3\text{O}_2^+]$  are still kinetically indistinguishable.

*Diffusion-controlled reaction* – The maximum rate of a reaction between two species 1 and 2 of charge  $z_1$  and  $z_2$  is controlled by the rate at which the reactants come together (diffusion-controlled). The second-order rate constant  $k_1$  ( $\text{M}^{-1} \text{ s}^{-1}$ ) for this interaction is given by

$$k_1 = \frac{4 \times 10^{-3} \pi N (d_1 + d_2) a U(a)}{kT [\exp(U(a)/kT) - 1]}$$

The maximum rate for the reverse reaction (unimolecular dissociation  $k_{-1}$ ,  $\text{s}^{-1}$ ) is via separation by diffusion of the two molecules

$$k_{-1} = \frac{3 (d_1 + d_2) U(a)}{kT [\exp(U(a)/kT) - 1] a^2} \cdot \left[ \exp\left(\frac{U(a)}{kT}\right) \right]$$

$U(a)$  is the Debye-Hückel interionic potential

$$U(a) = \frac{z_1 z_2 e^2}{aD} - \frac{z_1 z_2 e^2 \kappa}{D(1 + \kappa a)}$$

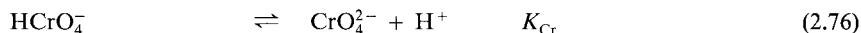
$$\kappa^2 = \frac{8 \pi N e^2 \mu}{1000 D k T}$$

$d_1$  and  $d_2$  are the diffusion coefficients of 1 and 2 in  $\text{cm}^2 \text{ s}^{-1}$ ;  $e$  is the charge on an electron in esu units;  $D$  is the dielectric constant of the medium;  $k$  is Boltzmann's constant in ergs;  $N$  is Avogadro's number and  $a$  is the distance in cm of closest approach of the ions ( $r_1 + r_2$ ), all at  $T$  (in K). The ratio  $k_1/k_{-1}$  is a diffusion-controlled equilibrium constant and equals the theoretically-deduced outer-sphere formation constant,  $K_0$  in (4.17). See G. Q. Zhou and W. Z. Zhong, *Eur. J. Biochem.* **128**, 383 (1982).

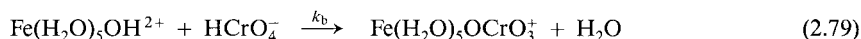
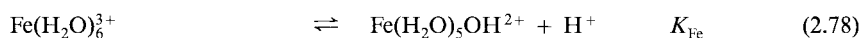
Obviously, ambiguity can also arise in the interpretation of the rate law

$$V = k [\text{AH}] [\text{BH}] [\text{H}^+]^{-1} \quad (2.75)$$

where both AH and BH are acidic. In the reaction of Fe(III) with ligands that can take part in acid-base equilibria, interpretive difficulties arise.<sup>41</sup> With  $\text{HCrO}_4^-$ , for example, the term  $k_2 [\text{Fe(III)}] [\text{HCrO}_4^-] [\text{H}^+]^{-1}$  can arise from reaction of  $\text{Fe}(\text{H}_2\text{O})_6^{3+}$  with  $\text{CrO}_4^{2-}$ ,

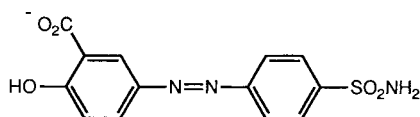


or from  $\text{Fe}(\text{H}_2\text{O})_5\text{OH}^{2+}$  interacting with  $\text{HCrO}_4^-$ ,



In Scheme (2.76, 2.77),  $k_2 = K_{\text{Cr}} k_a$  and in Scheme (2.78, 2.79),  $k_2 = K_{\text{Fe}} k_b$ . Since  $K_{\text{Cr}} = 3 \times 10^{-7} \text{M}$  and  $K_{\text{Fe}} = 1.7 \times 10^{-3} \text{M}$ , the observed value of  $k_2$ ,  $15 \text{ s}^{-1}$ , leads to values for  $k_a$  of  $5 \times 10^7 \text{ M}^{-1} \text{ s}^{-1}$  and for  $k_b$  of  $9.2 \times 10^3 \text{ M}^{-1} \text{ s}^{-1}$ , all at  $25^\circ\text{C}$ . The calculated value of  $k_b$  seems much more reasonable than the calculated value of  $k_a$  which is inordinately high. Thus  $\text{FeOH}^{2+}$ ,  $\text{HCrO}_4^-$  as the kinetically active pair is therefore preferred.<sup>42</sup> Table 2.1 shows a selected number of examples that may be resolved similarly.<sup>41</sup> It is exceptional for  $\text{Fe}(\text{H}_2\text{O})_6^{3+}$  to be the preferred reactant.<sup>43,44</sup>

The reactions of Cr(III),<sup>46</sup> Al(III)<sup>47</sup> and Ga(III)<sup>48</sup> have been rationalized in a manner similar to that used for the reactions of Fe(III). Although the hydroxy form  $\text{MOH}^{2+}$  is the minor species present in the acid medium used in such studies (typically 1–2%), its enhanced reactivity compared with  $\text{M}^{3+}$ , both in substitution and redox reactions, will ensure its participation in the overall rate. We encountered the problem of the interpretation of (2.75) in Chap. 1 (Sec. 1.10.2). The rate constant for reaction of the acid form of bovine carbonic anhydrase with deionized p-(salicyl-5-azo)benzenesulfonamide is calculated as  $10^{10} \text{ M}^{-1} \text{ s}^{-1}$ . This appears to be slightly too large a value for such a reaction. For this reason then, the alternative (kinetically equivalent) reaction of the deprotonated enzyme reacting with **8** containing the uncharged sulfonamide group ( $2.2 \times 10^7 \text{ M}^{-1} \text{ s}^{-1}$ ) is preferred.<sup>49</sup> A special problem arises when one of the acidic partners is water. Does the activated complex now arise from an rds between AH and  $\text{OH}^-$ , or between  $\text{A}^-$  and  $\text{H}_2\text{O}$ , or even from the reaction of  $\text{A}^-$  alone? This ambiguity has been particularly vexing in the study of the base hydrolysis of cobalt(III) complexes, and was a point of discussion for many years (see Sec. 4.3.4).<sup>50</sup>





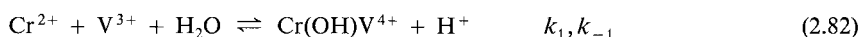
Finally, when the rate law indicates that there is more than one activated complex of importance, the composition but not the order of appearance of the activated complexes in the reaction scheme is defined by the rate law. Haim<sup>6</sup> has drawn attention to this in considering the reduction of V(III) by Cr(II) in acid solution.<sup>51</sup> The second-order rate constant  $k$  in the rate law

$$d[\text{Cr}^{\text{III}}]/dt = k [\text{Cr}^{\text{II}}] [\text{V}^{\text{III}}] \quad (2.80)$$

is dependent on  $[\text{H}^+]$ :

$$k = \frac{a}{b + [\text{H}^+]} \quad (2.81)$$

The limiting forms of the rate law yield the compositions of the activated complexes. These will be, at low  $[\text{H}^+]$ ,  $[\text{VCr}^{5+}]^\ddagger$ , and at high  $[\text{H}^+]$ ,  $[\text{VCr}(\text{OH})^{4+}]^\ddagger$ . Thus two mechanisms are possible. In one of these,  $[\text{VCr}^{5+}]^\ddagger$  precedes  $[\text{VCr}(\text{OH})^{4+}]^\ddagger$  (mechanism 1):

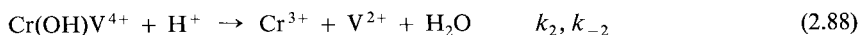


for which

$$\frac{d[\text{Cr}^{3+}]}{dt} = \frac{k_1 k_2 [\text{V}^{3+} [\text{Cr}^{2+}]]}{k_2 + k_{-1} [\text{H}^+]} \quad (2.85)$$

which is of the required form with  $a = k_1 k_2 / k_{-1}$  and  $b = k_2 / k_{-1}$  (with  $k_{-2}$  ignored).

In the other scheme,  $[\text{VCr}^{5+}]^\ddagger$  occurs after  $[\text{VCr}(\text{OH})^{4+}]^\ddagger$  in the reaction sequence (mechanism 2)



$$\frac{d[\text{Cr}^{3+}]}{dt} = \frac{k_1 k_2 K [\text{V}^{3+}] [\text{Cr}^{2+}]}{k_{-1} + k_2 [\text{H}^+]} \quad (2.89)$$

Equation (2.89) is of the form (2.81) with  $a = k_1 K$  and  $b = k_{-1} / k_2$  (with  $k_{-2}$  ignored). Indirect arguments for the validity of the second mechanism have been presented.<sup>6</sup> At high acidity,  $[\text{H}^+] > 0.5 \text{ M}$ , the concentration and thus contribution of the very reactive  $\text{VOH}^{2+}$  is so reduced that an outer sphere

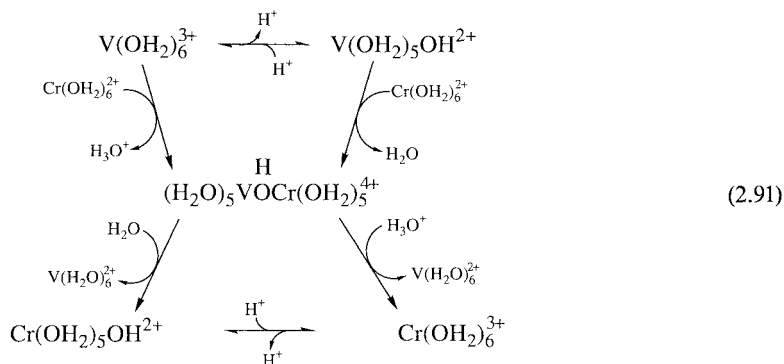


reaction becomes detectable.<sup>52</sup>

An alternative presentation of the mechanisms in (2.82)–(2.84) and (2.86)–(2.88) is shown in (2.91).<sup>6</sup> This depiction is popular in the complex mechanisms encountered in metallo-enzyme chemistry.

Mechanism 1

Mechanism 2



## 2.2 Further Checks of Mechanism

So far we have assigned mechanisms mainly on the basis of the rate law. This can give only a somewhat crude picture, detailing at the most the number of the steps involved. Some evidence for the correctness of the mechanism can be obtained by consideration of the rate constants for these steps. In the reaction of  $\text{Co(edta)}^{2-}$  with  $\text{Fe(CN)}_6^{3-}$ , for example, the formation of a “dead-end” complex is preferred (Sec. 1.6.4(d)). The outer sphere redox reaction which results from this interpretation, (direct reaction of  $\text{Co(edta)}^{2-}$  with  $\text{Fe(CN)}_6^{3-}$ ) is also supported by agreement of the rate constant with that calculated using Marcus theory (Sec. 2.5).<sup>53,54</sup> Distinguishing an “active” from a “dead-end” complex, i.e. scheme (1.101) from scheme (1.107) and (1.108) is a vexing problem, particularly in the interaction of small inorganic reactants with proteins.<sup>55</sup> Solutions to these problems and finer mechanistic detail can often be produced by subsidiary experiments, usually chemical in nature, as will now be detailed.

### 2.2.1 The Detection and Study of Intermediates<sup>56</sup>

(a) *Direct.* It may happen that the form of the rate law can be accommodated only by a mechanism where intermediates are postulated. Therefore, strong evidence for such a mechanism is the detection of these intermediates. In some cases this may present little difficulty since the intermediate may accumulate in relatively large amounts and therefore be easily detected during the course of the reaction.  $\text{V}^{2+}$  mixed with  $\text{VO}^{2+}$  produces a more rapid loss of  $\text{V}^{2+}$  than a gain of  $\text{V}^{3+}$ , the ultimate product. In concentrated solution, an intermediate brown color (ascribed to  $\text{VOV}^{4+}$ ) can actually be discerned.<sup>57</sup> Much more dif-

difficult is the support for intermediates of fleeting existence. Then special means must often be used, involving sophisticated equipment and techniques. The mode and power of the approach is well illustrated by the work on detecting the  $\text{HO}_2^\bullet$  radical in aqueous solution.

The kinetics of the Ce(III)-Ce(IV) exchange reaction catalyzed by  $\text{H}_2\text{O}_2$ <sup>58</sup> and a later study of the kinetics of the Ce(IV) reaction with  $\text{H}_2\text{O}_2$  in  $\text{H}_2\text{SO}_4$  by stopped-flow methods,<sup>59</sup> argues for the following mechanism for the Ce(IV)- $\text{H}_2\text{O}_2$  reaction,



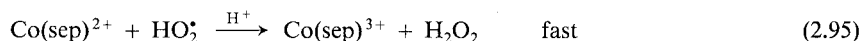
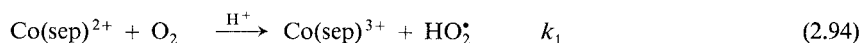
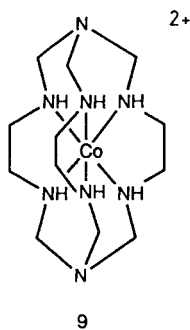
in which  $k_1 = 1.0 \times 10^6 \text{M}^{-1} \text{s}^{-1}$  and  $k_2/k_{-1} = 13$ . It is apparent from these results that a sizable amount of  $\text{HO}_2^\bullet$  should be produced, at least for a short while, by mixing large amounts of  $\text{H}_2\text{O}_2$  (0.1 M) with small amounts of Ce(IV) ( $10^{-3} \text{M}$ ), which are used up in step (2.92) and thus cannot remove  $\text{HO}_2^\bullet$  in step (2.93). If this is carried out in an efficient mixer, and the mixed solutions examined within 10 ms by electron spin resonance (esr), then  $\text{HO}_2^\bullet$  is detected in the flow tube.<sup>60</sup>

The trapping of reactive intermediates at low temperatures in a rigid medium prevents them from reacting, and allows a leisurely examination. This, combined with esr examination, has been important in studies of certain metalloproteins, e.g. nitrogenase.<sup>61</sup>

(b) *Indirect.* By far the most usual approach for sensing the presence of intermediates is to add reagents ("scavengers") which will react rapidly and effectively with an intermediate, but not the reactants. Either the rate law may be modified, perhaps only slightly, or new products may result to the exclusion of, or in addition to, the normal product.

The species  $\text{O}_2^-$  or the form in acid,  $\text{HO}_2^\bullet$ , is often considered a logical immediate product of reactions of  $\text{O}_2$ . It has been indirectly detected by scavenging additives modifying the reaction.<sup>62</sup>

$\text{Co}(\text{sep})^{2+}$  (9) reacts with  $\text{O}_2$  in acid solution with an assumed mechanism



based on a rate law

$$-d[\text{Co}(\text{sep})^{2+}]/dt = 2k_1[\text{Co}(\text{sep})^{2+}][\text{O}_2] \quad (2.96)$$

If the reaction is carried out in the presence of  $\text{Cu}^{2+}$  the rate is reduced by a factor of approximately two. This is excellent evidence for the intermediacy of  $\text{HO}_2^*$  since this would react with  $\text{Cu}^{2+}$  at a close to diffusion-controlled rate

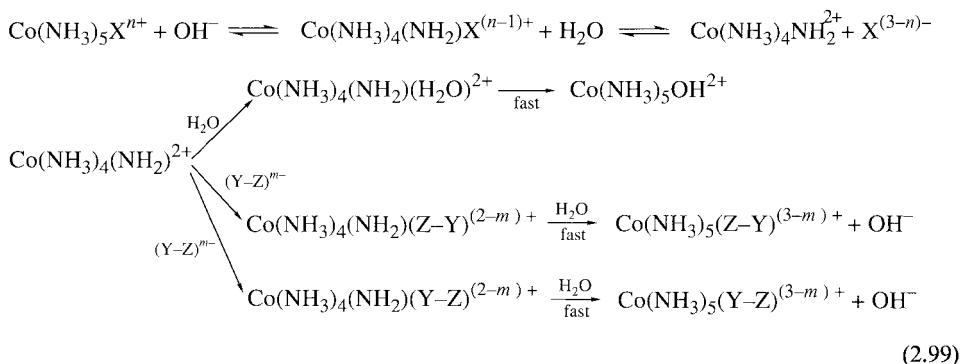


This reaction would replace (2.95) and a modified rate law would operate<sup>63</sup>

$$-d[\text{Co}(\text{sep})^{2+}]/dt = k_1[\text{Co}(\text{sep})^{2+}][\text{O}_2] \quad (2.98)$$

Transient radicals  $\text{R}^*$  can be visualized by reacting with diamagnetic spin traps  $\text{T}$  to form a persistent spin adduct  $\text{RT}$  which can be analyzed leisurely by esr,<sup>64,65</sup> (Sec. 1.11).

Competition experiments, in which the intermediate is scavenged by two reactants and the amount and nature of products examined, have played an important role in establishing the mechanism for base hydrolysis of cobalt(III) complexes. The intermediate produced in the base hydrolysis of  $\text{Co}(\text{NH}_3)_5\text{X}^{n+}$ ,  $n = 3, 2$  or  $1$  is  $\text{Co}(\text{NH}_3)_4(\text{NH}_2)^{2+}$  if the  $D_{\text{cb}}$  mechanism is correct (Sec. 4.3.4). Normally this intermediate is considered to react with  $\text{H}_2\text{O}$  to produce  $\text{Co}(\text{NH}_3)_5\text{OH}^{2+}$  but if another nucleophile  $(\text{Y}-\text{Z})^{m-}$  is also present and this can attack the intermediate also, then  $\text{Co}(\text{NH}_3)_5(\text{Y}-\text{Z})^{(3-m)+}$  and  $\text{Co}(\text{NH}_3)_5(\text{Z}-\text{Y})^{(3-m)+}$  will also result (Scheme (2.99)). These are linkage isomers (Sec. 7.4) and are spectrally distinguishable



If a series of complexes of different charges and  $\text{X}$  groups are hydrolyzed in the presence of a constant concentration of  $(\text{Y}-\text{Z})^{m-}$  then a constant competition ratio

$$\frac{[\text{Co}(\text{NH}_3)_5(\text{Y}-\text{Z})^{(3-m)+}] + [\text{Co}(\text{NH}_3)_5(\text{Z}-\text{Y})^{(3-m)+}]}{[\text{Co}(\text{NH}_3)_5\text{OH}^{2+}]} \quad (2.100)$$

should result because a common intermediate is involved, independent of  $\text{X}$  and  $n$  in  $\text{Co}(\text{NH}_3)_5\text{X}^{n+}$ . A selection of some recent results are contained in Table 2.2<sup>66-69</sup>

The ratio of linkage isomers is remarkably constant and independent of the charge, steric bulk or reactivity of leaving group. The ratios are  $2.0 \pm 0.1$  S/N ( $\text{SCN}^-$ );  $2.0 \pm 0.2$  O/N ( $\text{NO}_2^-$ ) and  $2.3 \pm 0.3$  S/O ( $\text{S}_2\text{O}_3^{2-}$ ). For a particular entering ligand  $(\text{Y}-\text{Z})^{m-}$  the percentage total anion capture is very constant within each charge group ( $n = 1-3$ ) although it increases

**Table 2.2.** Percentage of  $(Y-Z)^{m-}$  Capture in the Base Hydrolysis of  $\text{Co}(\text{NH}_3)_5\text{X}^{n+}$  in the Presence of  $(Y-Z)^{m-}$  at 25 °C (Usually in 1.0 M  $(Y-Z)^{m-}$  and 0.1 M  $\text{OH}^-$ )<sup>66-69</sup>

<i>n</i>	X	$(Y-Z)^{m-}$			
		SCN <sup>-ab</sup>	N <sub>3</sub> <sup>-</sup>	NO <sub>2</sub> <sup>- ac</sup>	S <sub>2</sub> O <sub>3</sub> <sup>2- ab</sup>
3	OP(OCH <sub>3</sub> ) <sub>3</sub>	17.3 (11.9)	12.5	7.9 (5.0)	12.2 (8.7)
3	OS(CH <sub>3</sub> ) <sub>2</sub>	18.0 (12.0)	12.3	8.8 (5.6)	12.6 (9.1)
2	I <sup>-</sup>	13.6 ( 8.9)	10.0	4.5	11.3 (8.0)
2	Cl <sup>-</sup>	—	8.5	—	—
2	OS(O) <sub>2</sub> CF <sub>3</sub> <sup>-</sup>	13.6 ( 9.0)	9.7	7.0 (4.6)	10.8 (7.7)
1	OSO <sub>3</sub> <sup>2-</sup>	6.8 ( 3.7)	5.8	—	—

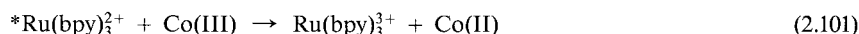
<sup>a</sup> Corrected value for subsequent reaction of  $\text{Co}(\text{NH}_3)_5(\text{Y-Z})^{(3-m)+}$ .

<sup>b</sup> Value in parenthesis is % S bound linkage isomer.

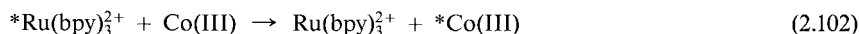
<sup>c</sup> Value in parenthesis is % O bound linkage isomer.

systematically with the charge of substrate  $3+ > 2+ > 1+$ . The conclusion is that there is a 5-coordinated intermediate which is so short-lived that it retains the original ion-atmosphere of  $\text{Co}(\text{NH}_3)_5\text{X}^{n+}$  but not the X group (Sec. 4.3.5). These experiments are very difficult to set up, carry out and analyze, but are very telling support for the  $D_{cb}$  mechanism.

In some cases the identification of the product, even without use of scavengers, can be important in the elucidation of mechanism. Thus the quenching of  $^*\text{Ru}(\text{bpy})_3^{2+}$  by cobalt(III) complexes (Eqn. 1.32, B = Co(III)) may go by electron transfer



or energy transfer



Product analysis has been useful in deciding the preferred path. Quantum yields for Co(II) production (number of molecules produced/number of quanta absorbed) measured by steady-state photolysis of  $\text{Co}(\text{NH}_3)_6^{3+}$  and  $\text{Co}(\text{en})_3^{3+}$  are 0.45 and 0.11 respectively. These show that exclusive electron transfer (when the quantum yield would be 1.0) does not occur.<sup>70</sup>

With specially designed reactants, the determination of the product structure can be very informative. Mercury(II)-catalyzed aquations of Co(III) complexes are believed to proceed via a 5-coordinated intermediate (Sec. 4.3.2). The shape of this intermediate is of interest. The Hg<sup>2+</sup>-catalyzed aquation of  $\text{Co}(\text{NH}_3)_4(\text{ND}_3)\text{X}^{2+}$  in which the ND<sub>3</sub> and X groups are *trans* to one another gives substantially *trans*- $\text{Co}(\text{NH}_3)_4(\text{ND}_3)(\text{H}_2\text{O})^{3+}$ . This is excellent evidence for a square pyramidal intermediate in the reaction. A trigonal-bipyramidal intermediate would be expected to lead to substantial scrambling of the ND<sub>3</sub> and NH<sub>3</sub> groups (Fig. 2.1).<sup>71</sup> The *definite* but very small amount (2.8 ± 0.4%) of *cis* product recently reported using <sup>15</sup>NH<sub>3</sub> instead of ND<sub>3</sub> attests to the sensitivity of current nmr machines.<sup>72</sup>

The use of highly enriched <sup>13</sup>CO and C<sup>18</sup>O and ir or nmr monitoring has been a powerful combination for studying the photochemical and thermal substitution processes of metal carbonyls and derivatives. The site of substitution and the nature of the reactive intermediates (their geometry and flexibility) have been elucidated.<sup>73</sup>

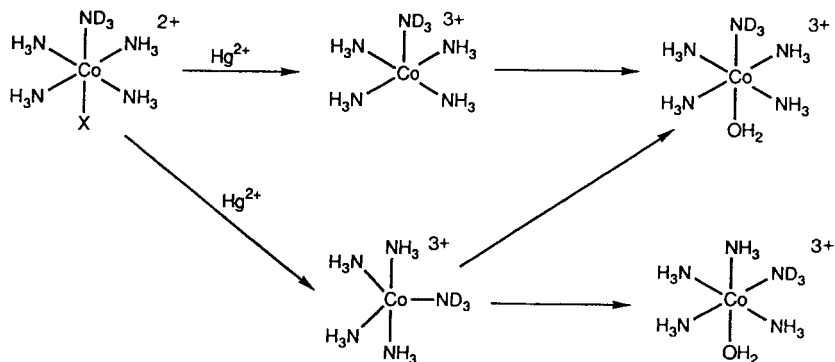
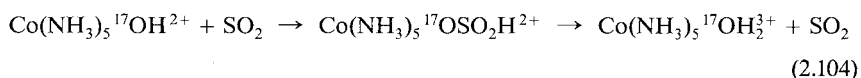
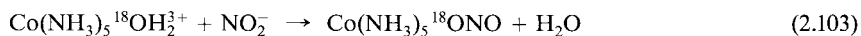


Fig. 2.1 Expected products from the Hg(II)-catalyzed aquation of  $trans\text{-Co}(\text{NH}_3)_4(\text{ND}_3)\text{X}^{2+}$  on the basis of a square-pyramid or trigonal-bipyramid intermediate.<sup>71</sup>

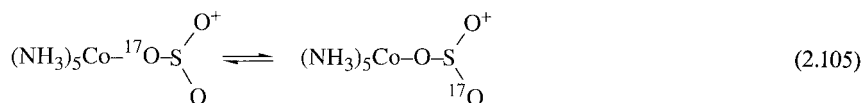
## 2.2.2 The Determination of Bond Cleavage

Obtaining definite evidence regarding the occurrence of bond cleavage is helped considerably by using isotopes. The following two examples illustrate different approaches.

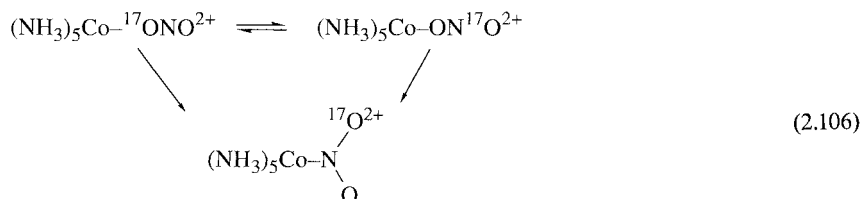
Reactions of  $\text{Co}(\text{NH}_3)_5\text{OH}^{2+}$  or  $\text{Co}(\text{NH}_3)_5\text{H}_2\text{O}^{3+}$  with certain ligands are unusually rapid (Chap. 8. Co(III)). This suggests that Co-O bond breakage does not occur during the substitution, else it likely would be very much slower. This can be verified by using isotopes e.g.<sup>74,75</sup>

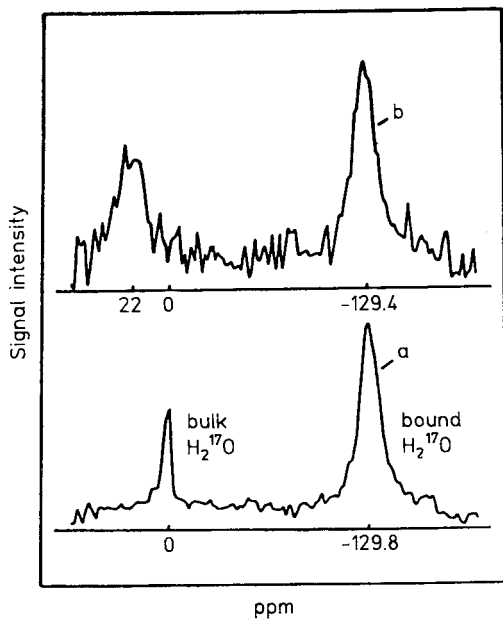


The nmr signal due to bound  $^{17}\text{OH}_2$  is unchanged after the cycle (2.104) is completed (Fig. 2.2).<sup>75</sup> This observation also rules out linkage rotation (2.105)



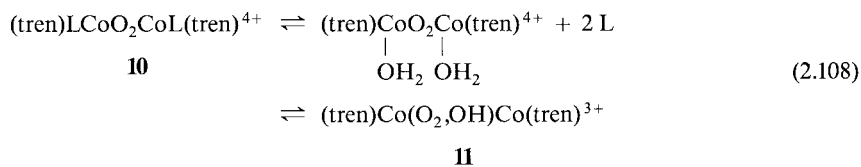
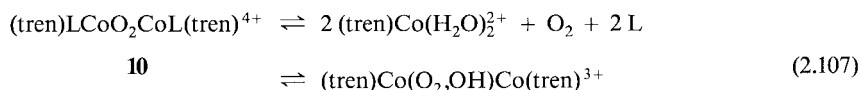
Such a rearrangement, although seemingly unlikely, does occur with the nitrito complex as demonstrated by  $^{17}\text{O}$ -nmr experiments<sup>76</sup>





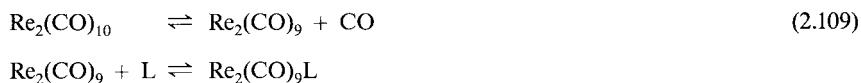
**Fig. 2.2**  $^{17}\text{O}$  nmr spectrum of  $\text{Co}(\text{NH}_3)_5^{17}\text{OH}_2^{3+}$  dissolved in  $\text{H}_2^{16}\text{O}$  (a) before and (b) after formation and acidification of sulfite complex, Eqn. (2.104). Resonance for the metal-bound water is upfield ( $-130$  ppm) relative to bulk water (0 ppm) and is markedly broader. After acidification, little intensity changes occur for the bound and bulk water, proving that the  $\text{Co}-^{17}\text{OH}_2$  bond remains substantially intact during the cycle. The broadening and shifting of the bulk water during the process results from paramagnetic  $\text{Co}^{2+}$  formed during a side redox reaction.<sup>75</sup> Reprinted with permission from R. van Eldik, J. von Jouanne, and H. Kelm, *Inorg. Chem.*, **21**, 2818 (1982).  
© (1982) American Chemical Society.

The formation of a double-bridged  $\text{Co}(\text{III})$  complex from a single peroxo-bridged complex can take place by either (2.107) or (2.108),  $\text{L} = \text{CH}_3\text{NH}_2$ ,



The first mechanism is preferred since the  $^{18}\text{O}_2$ -labelled bridged complex **10** exchanges with  $\text{O}_2$  at the same rate as the formation of the bridged product **11**.<sup>77,78</sup>

How the position of bond cleavage can be determined is illustrated by consideration of thermally initiated ligand (L) substitution in  $\text{Re}_2(\text{CO})_{10}$ . This can occur by a dissociative mechanism involving  $\text{Re}-\text{CO}$  bond breakage,

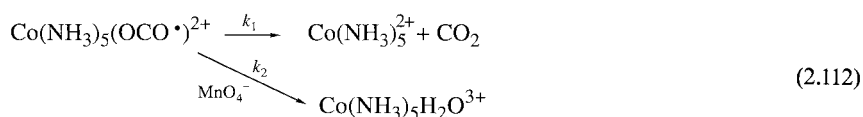


or by a radical mechanism involving metal-metal bond homolysis



The former mechanism is favored. When CO exchange ( $\text{L} = \text{CO}$ ) is studied using a mixture of  $^{185}\text{Re}_2(\text{CO})_{10}$  and  $^{187}\text{Re}_2(\text{CO})_{10}$  no  $^{185}\text{Re}^{187}\text{Re}(\text{CO})_{10}$  appears as product (analyzed by mass spectrometry). The mixture of isotopic carbonyls do however “scramble” (slowly) in the absence of L or after photolysis, showing that Re–Re bond scission is at least feasible.<sup>79</sup>

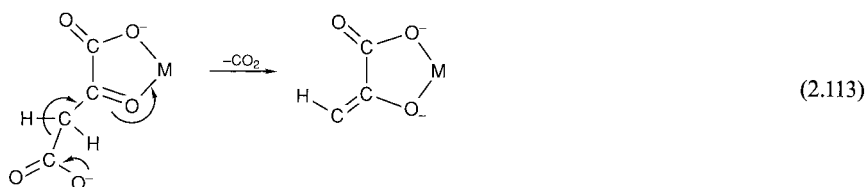
The *kinetic isotope effect* is extensively used to support mechanism.<sup>80</sup> A large deuterium kinetic isotope effect ( $k_{\text{H}}/k_{\text{D}} > 5$ ) is strong support for an X–H (or X–D) bond cleavage in the rate determining step. The 10.5 fold higher rate constant for the  $\text{MnO}_4^-$  oxidation of  $\text{Co}(\text{NH}_3)_5\text{OCHO}^{2+}$ , compared with the rate constant for  $\text{Co}(\text{NH}_3)_5\text{OCDO}^{2+}$ , supports a mechanism in which the rds is a one-electron oxidation via H atom abstraction,<sup>81</sup> for example



The first step accounts for the observed second-order kinetics and produces the large isotope effect. The second step leads to a Co(II), Co(III) mixture.<sup>82,83</sup> Even larger isotope effects have been noted (e.g. in C–H abstraction from 2-propanol by Ru(IV) compounds<sup>84,85</sup>).

It is difficult to correlate the  $k_{\text{H}}/k_{\text{D}}$  values with the operation of a hydride, proton or H atom transfer. The temperature dependence of the kinetic isotope effect, which is now easier to measure accurately, is more diagnostic of mechanism but has been applied mainly to organic systems.<sup>86</sup>

$^{13}\text{C}$  kinetic isotope effects ( $k(^{12}\text{C})/k(^{13}\text{C})$ ) are more difficult to measure accurately. The values for a variety of metal ion-catalyzed decarboxylations of oxaloacetate (2.113) are similar (1.04–1.05). This suggests that the transition state for decarboxylation (a) involves a marked breakage of the C–C bond and (b) is similar for the various metal ions, even though enhancement rates vary widely.<sup>87</sup> This apparent paradox is ascribed to an alteration of the distribution of oxaloacetate between the keto and enol forms.<sup>88</sup>





It is interesting that enzyme-catalyzed decarboxylations have a  $^{13}\text{C}$  effect of  $\sim 1.00$ , thus invoking a different mechanism.

Finally in studying isomerization reactions, one must always consider whether these are intramolecular (no bond cleavage) or intermolecular (bond cleavage). The relation between the isomerization rate constants and the dissociation rate constants will resolve whether bond cleavage accounts for isomeric change.<sup>89</sup> Other examples of the use of isotopes to detect bond breakage or bond stretching in the activated complex will occur in Part II. Determination of the fractionation factor by using isotopes can also lead to similar information (Sec. 3.12.2).

## 2.3 Activation Parameters, Thermodynamic Functions and Mechanism

So far we have considered rate laws and chemical behavior for one temperature and at normal pressures only. Much information on the mechanism of a reaction may certainly be gleaned from this information alone. However, by carrying out measurements at a number of temperatures or pressures, or in different media, one may obtain useful information, even though the form of the rate law itself rarely changes.

### 2.3.1 The Effect of Temperature on the Rate of a Reaction

The rate of a chemical reaction may be affected by temperature in several ways, but the most common behavior by far is that observed by Arrhenius some 100 years ago.<sup>90</sup> The empirical expression

$$k = A \exp(-E_a/RT) \quad (2.114)$$

relates the rate constant  $k$  to the absolute temperature  $T$  (in K). It describes the behavior of a vast number of chemical reactions amazingly well, particularly over a fairly small temperature range, but in some instances over as large a range as 100 degrees.<sup>91,92</sup> Thus a plot of  $\ln k$  vs  $T^{-1}$  is linear, with slope  $-E_a/R$  and intercept  $\ln A$ . (Fig. 2.3)<sup>91</sup>

A similar relationship is also derived by the absolute reaction rate theory, which is used almost exclusively in considering, and understanding, the kinetics of reactions in solution.<sup>93</sup> The activated complex in the *transition state* is reached by reactants in the initial state as the highest point of the most favorable reaction path on the potential energy surface. The activated complex  $\text{X}^\ddagger$  is in equilibrium with the reactants A and B, and the rate of the reaction  $V$  is the product of the equilibrium concentration of  $\text{X}^\ddagger$  and the specific rate at which it decomposes. The latter can be shown to be equal to  $kT/h$ , where  $k$  is Boltzmann's constant and  $h$  is Planck's constant:



$$V = kT[\text{X}^\ddagger]/h = kTK_c^\ddagger[\text{A}][\text{B}]/h \quad (2.116)$$

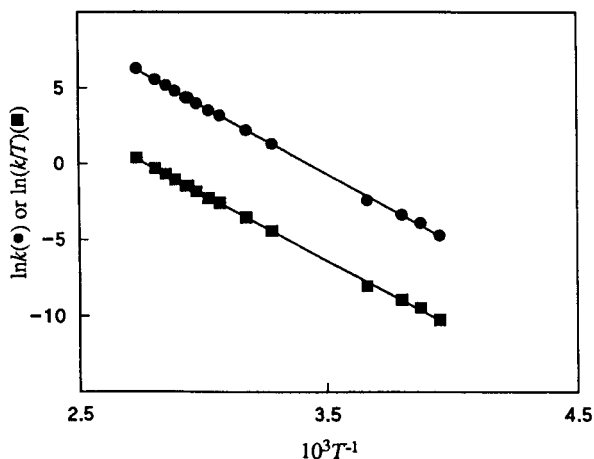


Fig. 2.3 Arrhenius (●) and Eyring (■) plots of data for the exchange of a single dmsol molecule with  $\text{Ga}(\text{dmsol})_6^{3+}$  in  $\text{CD}_3\text{NO}_2$ . Nmr line-broadening was used for the higher temperatures and stopped-flow nmr experiments for the lower temperatures.<sup>91</sup> For the Arrhenius plot, the slope and intercept (at  $T^{-1} = 0$ ) are  $-9.2 \times 10^3$  and  $+31.4$  respectively, leading to  $E_a = 76 \text{ kJ mol}^{-1}$  and  $\log A = 13.6$ . For the Eyring plot, the slope and intercept are  $-8.77 \times 10^3$  and  $+24.4$  respectively, leading to  $\Delta H^\ddagger = 73 \text{ kJ mol}^{-1}$  and  $\Delta S^\ddagger = 5 \text{ J K}^{-1} \text{ mol}^{-1}$ .

so that the experimental second-order rate constant  $k$  is given by

$$k = kTK_c^\ddagger/h \quad (2.117)$$

The formation of the activated complex may be regarded as an equilibrium process involving an “almost” normal molecule (almost, since it is short one mode of vibrational energy). The free energy of activation  $\Delta G^\ddagger$  can therefore be defined as in normal thermodynamics,

$$\Delta G^\ddagger = -RT \ln K_c^\ddagger = \Delta H^\ddagger - T\Delta S^\ddagger \quad (2.118)$$

leading to

$$k = \frac{kT}{h} \exp\left(\frac{-\Delta G^\ddagger}{RT}\right) = \frac{kT}{h} \exp\left(\frac{-\Delta H^\ddagger}{RT}\right) \exp\left(\frac{\Delta S^\ddagger}{R}\right) \quad (2.119)$$

where  $\Delta H^\ddagger$  and  $\Delta S^\ddagger$  are the enthalpy and entropy of activation. This equation strictly applies to nonelectrolytes in dilute solution and must be modified for ionic reactions in electrolyte solutions (see (2.179)).

Since  $E_a = \Delta H^\ddagger + RT$ , it is not difficult to show that

$$A = \frac{ekT}{h} \exp\left(\frac{\Delta S^\ddagger}{R}\right) \quad (2.120)$$

A plot of  $\ln(k/T)$  against  $1/T$  is linear from (2.119), with a slope,  $-\Delta H^\ddagger/R$  and an intercept  $(\ln k/h + \Delta S^\ddagger/R) = (23.8 + \Delta S^\ddagger/R)$ , Fig. 2.3. This is sometimes referred to as the Eyring relationship. Both Arrhenius and Eyring plots are used and give very similar results. The quantities  $\Delta H^\ddagger$  and  $\Delta S^\ddagger$  are almost universally preferred for discussion of solution kinetics and will be used hereafter. The agreement in the values of  $\Delta H^\ddagger$  and  $\Delta S^\ddagger$  obtained by different workers investigating the same system is not always good. Nowhere has this been more evident than in the nmr studies of solvent exchange. For example, although the rate constant at 25°C for exchange of  $\text{Ni}(\text{CH}_3\text{CN})_6^{2+}$  with solvent  $\text{CH}_3\text{CN}$  is generally reported in the relatively narrow range of  $2.0 \times 10^3$  to  $4.0 \times 10^3 \text{ s}^{-1}$ ,  $\Delta H^\ddagger$  and  $\Delta S^\ddagger$  values vary enormously.<sup>94</sup> Both positive and negative values of  $\Delta S^\ddagger$  are reported! This arises from the inaccuracy of obtaining  $\Delta S^\ddagger$  by a long extrapolation of Eyring plots to  $1/T = 0$ . This problem can be partly circumvented by using as wide a temperature range as feasible.<sup>95</sup>  $\Delta V^\ddagger$  values (see below) give similar and in some respects superior information to those of  $\Delta S^\ddagger$ , and are more accurately, but not as easily, measured.

### 2.3.2 The Variation of $E_a$ or $\Delta H^\ddagger$ with Temperature

Most investigators are content to use the best linear plots of  $\ln k$  or  $\ln(k/T)$  vs  $T^{-1}$  in estimating  $E_a$  or  $\Delta H^\ddagger$  values, and to assume that these are constants over a narrow temperature range.<sup>96</sup> It is worth examining this aspect, however, since deviations from linearity of such plots might be ascribable to complexity in the reaction mechanism.

Since the heat of a reaction  $\Delta H$  is rarely temperature-independent and since for a single step

$$\Delta H = \Delta H_f^\ddagger - \Delta H_r^\ddagger \quad (2.121)$$

it would be expected that the enthalpy of activation in the forward direction,  $\Delta H_f^\ddagger$ , or in the reverse direction,  $\Delta H_r^\ddagger$ , or both, also would generally be temperature-variant even for a simple reaction. Using a simple approach, the relationship

$$dE_a/dT = \Delta C_p^\ddagger \quad (2.122)$$

holds where  $\Delta C_p^\ddagger$  is the heat capacity of activation at constant pressure.<sup>97</sup> Values for  $\Delta C_p^\ddagger$  within the range  $-40$  to  $-120 \text{ J K}^{-1} \text{ mol}^{-1}$  (same units as  $\Delta S^\ddagger$ ) have been found for the aquation of a number of  $\text{Co}(\text{NH}_3)_5\text{X}^{2+}$  complexes.<sup>98</sup> *Marked* variation of  $E_a$  or  $\Delta H^\ddagger$  values with temperature (that is, nonlinear Arrhenius or Eyring plots) for reactions of complexes is unusual. This is perhaps surprising, since apart from the  $\Delta C_p^\ddagger$  effect many observed rate constants, and therefore associated activation parameters, are composite values. It is easily seen that even if the rate constants for the individual steps vary exponentially with respect to temperature, the composite rate constants may well not. Therefore deviations should arise in reactions involving equilibria, parallel or consecutive processes.<sup>97,99</sup> Examples are rare (Sec. 2.6<sup>100,101</sup>).

### 2.3.3 The Effect of Pressure on the Rate of a Reaction

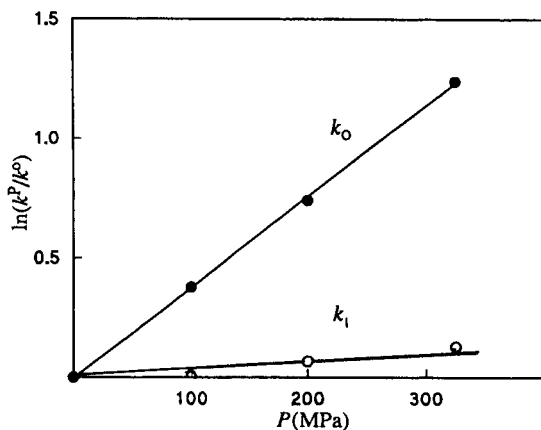
The effect of pressure  $P$  on the rate constant  $k$  for a reaction can be summarized in the simplified expression

$$\left(\frac{d \ln k}{dP}\right)_T = \frac{-\Delta V^\ddagger}{RT} \quad (2.123)$$

The volume of activation,  $\Delta V^\ddagger$ , is the partial molar volume change when reactants are converted to the activated complex.  $\Delta V_0^\ddagger$  is the volume of activation extrapolated to  $P = 0$  (if necessary).  $P$  is usually expressed in megaPascals (MPa) =  $10^6$  Pa = 10 bars = 9.87 atmospheres or  $1 \text{ J cm}^{-3}$ . At 298.2 K,  $RT = 2.48 \times 10^3 \text{ J mol}^{-1}$ . If the slope of the  $\ln(k/k_{P=0})$  vs  $P$  (MPa) is  $s$ , then  $\Delta V^\ddagger = -2.48 \times 10^3 \times s \text{ cm}^3 \text{ mol}^{-1}$  at 298.2 K. Consider the effect of pressure on the rate of water exchange ( $k_{\text{obs}}$ ) on aqueous Cr(III) perchlorate. For this reaction

$$k_{\text{obs}} = k_0 + k_1 [\text{H}^+]^{-1} \quad (2.124)$$

and  $k_0$  and  $k_1$  can be determined at a number of pressures (Fig. 2.4). From the slopes,  $\Delta V_0^\ddagger = -10 \text{ cm}^3 \text{ mol}^{-1}$  and  $\Delta V_1^\ddagger = -0.9 \text{ cm}^3 \text{ mol}^{-1}$  for the  $k_0$  and the  $k_1$  paths.<sup>102</sup> We shall consider these values in Sec. 2.8.



**Fig. 2.4** Effect of pressure on the  $k_0$  and  $k_1$  terms in (2.124) for water exchange of aqueous Cr(III) perchlorate.<sup>102</sup> Since  $\Delta V^\ddagger = -2.48 \times 10^3 \times \text{slope}$  (see text),  $\Delta V_0^\ddagger = -2.48 \times 10^3 \times (3.8 \times 10^{-3}) = -10 \text{ cm}^3 \text{ mol}^{-1}$  and  $\Delta V_1^\ddagger = -2.48 \times 10^3 \times (3.3 \times 10^{-4}) = -0.9 \text{ cm}^3 \text{ mol}^{-1}$ .

Although one of the earliest studies of pressure effects on a complex ion reaction was carried out over 30 years ago,<sup>103</sup> only the past decade has seen a concentrated number of studies of pressure effects on the rates of transition metal complex reactions. This is evidenced by the large number of recent reviews in this area. For a selection see Refs. 104–107. Instruments are now commercially available and flow, relaxation and nmr techniques have been adapted for use in high pressure kinetics (Ch. 3).<sup>108</sup> Fairly high pressures, 200–1000 MPa or 2,000–10,000 atmospheres, must be used to obtain sufficient effect on the rate.  $\Delta V^\ddagger$  values usually lie in the range  $\pm 25 \text{ cm}^3 \text{ mol}^{-1}$  and can be obtained to  $\pm 1 \text{ cm}^3 \text{ mol}^{-1}$ . The values, resulting from the slope of  $(d \ln k/dP)_T$  plots, are more likely to be accurate than those of  $\Delta S^\ddagger$ , arising from

a long extrapolation to an intercept of a  $(d \ln k/dT)_p$  plot, and with which they are sometimes compared. Although  $\Delta V^\ddagger$  is conceptually easy to understand, there is one real problem in its interpretation. This arises because  $\Delta V_{\text{obs}}^\ddagger$  can be considered as made up of two parts (a)  $\Delta V_{\text{intr}}^\ddagger$ , the intrinsic volume change when reactants are converted to the activated complex. It arises from changes in bond length, angles etc. and is diagnostic of the intimate mechanism. (b)  $\Delta V_{\text{sol}}^\ddagger$  the volume change arising from solvation effects (electrostriction of solvent). Term (b) is unfortunately not easy to assess and this creates problems when it contributes substantially to the overall  $\Delta V_{\text{obs}}^\ddagger$ . Term (b) is less important when the charges of reactants and products are the same and for this reason, exchange reactions have been popular to study for mechanistic information.

### 2.3.4 The Variation of $\Delta V^\ddagger$ with Pressure

Sometimes  $\Delta V^\ddagger$  is pressure-dependent because the compressibility of reactants and transition state is different. The most popular way of dealing with this is to use an empirical quadratic expression

$$\ln k = \ln k_{P=0} - \left( \frac{\Delta V^\ddagger}{RT} \right)_{P=0} P + \frac{\Delta \beta^\ddagger P^2}{2RT} \quad (2.125)$$

where  $\Delta \beta^\ddagger$  is the compressibility coefficient of activation. The variation of  $\Delta V^\ddagger$  with pressure appears to be, experimentally, a more important consideration than that of  $\Delta H^\ddagger$  with temperature. The expression (2.125) is often used but the value of  $\Delta \beta^\ddagger$  for interpretative purposes appears restricted at present and is often near zero.

### 2.3.5 Activation Parameters and Concentration Units

The use of accurate concentrations is vital in assessing correct rate constants and associated activation parameters. Concentrations are usually measured in terms of the number of moles of each reactant present in 1 liter of solution (M). Since liquids undergo thermal expansion or hydrostatic compression, the volume will change, leading to complications when using molarities. This can be avoided by expressing concentrations in units such as mole fractions or molalities (moles in 1 kg of solvent) which do not involve volumes. If these points are considered, an accurate value of  $\Delta V^\ddagger$  (or  $\Delta H^\ddagger$ ) can be obtained. Fortunately simple considerations<sup>109</sup> show that a true value of  $\Delta V^\ddagger$  can be obtained using (2.125) and uncorrected rate constants at various pressures based on the *molarities at atmospheric pressure*. The dilemma and analysis have been carefully reviewed.<sup>109</sup>

### 2.3.6 Reaction Profiles

Activation parameters are often composite. Consider the value of  $\Delta V_1^\ddagger$  in the exchange of Cr(III) with H<sub>2</sub>O (Sect. 2.3.3). The values of  $k_1$  and  $\Delta V_1^\ddagger$  are related to the intrinsic rate and

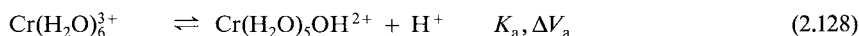
thermodynamic constants  $k_{\text{OH}}$  and  $\Delta V_{\text{OH}}^\ddagger$  (parameters for water exchange on  $\text{Cr}(\text{H}_2\text{O})_5\text{OH}^{2+}$ ) by the equations

$$k_{\text{OH}} = k_1/K_a \quad (2.126)$$

and

$$\Delta V_{\text{OH}}^\ddagger = \Delta V_1^\ddagger - \Delta V_a \quad (2.127)$$

where  $K_a$  and  $\Delta V_a$  refer to the ionization (2.128)



It is very important therefore to have information on the thermodynamic parameters, in this instance  $\Delta V_a$ . These can be measured directly by dilatometry or from the relationship:  $(d \ln K/dP)_T = -\Delta V/RT$ .<sup>108</sup> Since  $\Delta V_a = -3.8 \text{ cm}^3 \text{ mol}^{-1}$ ,  $\Delta V_{\text{OH}}^\ddagger = -0.9 + 3.8 = 2.9 \text{ cm}^3 \text{ mol}^{-1}$ , Ref. 102. We can represent the progress of this and any other reaction pictorially by a *reaction profile*, using the concept of the activated complex. The reaction profile shows, often in a qualitative but useful fashion, the change of any activation parameter ( $\Delta G^\ddagger$ ,  $\Delta H^\ddagger$ ,  $\Delta S^\ddagger$  Ref. 110 or  $\Delta V^\ddagger$  Ref. 111) as a function of the extent of the reaction (termed the reaction coordinate). Since each step in a reaction will have an associated transition state, and thus a separate reaction profile, we may have a continuous series of such profiles joining the reactants to the ultimate product.

Consider the reaction scheme



in which B is a reactive intermediate present in steady-state concentration

$$d[\text{B}]/dt = 0 = k_1[\text{A}] - (k_{-1} + k_2)[\text{B}] \quad (2.131)$$

$$d[\text{C}]/dt = k_2[\text{B}] = \frac{k_1 k_2 [\text{A}]}{k_{-1} + k_2} \quad (2.132)$$

The form of the reaction profile will depend on the relative values of the rate constants, Fig. 2.5. Several interesting points may be made.

(a) Although it is often stated that the rds is associated with the activated complex of highest energy, say  $\ddagger_1$  in Fig. 2.5(A), this may be misleading because  $\Delta G^\ddagger$  is calculated from the *rate constants*. Thus if in the first step of (2.130) another reactant D was involved, the forward rate associated with it would be  $k_1[\text{D}]$  and it is consideration of rates which determine the rds.<sup>112,113</sup>

(b) Variations in the structures of the reactants may alter the energy level of A or  $\ddagger$ , or both, and these lead to changes in  $\Delta G^\ddagger$ . In the comparison of a reaction series, it is important to bear this in mind, and it is not always easy to diagnose which behavior is leading to the rate differences within the series. This has led to controversies on the meaning of  $\Delta V^\ddagger$  values from water exchange with  $\text{M}^{2+}$  and  $\text{M}(\text{NH}_3)_5\text{H}_2\text{O}^{3+}$  Refs. 114–117.

(c) If the reaction  $A \rightarrow C$  is represented as in Fig. 2.5 moving from left to right, then the reverse reaction  $C \rightarrow A$  is simply represented by the reverse process traversed from right to left in the same diagram. This embodies the *principle of microscopic reversibility* which states that the mechanism of a reversible reaction is the same in microscopic detail in one direction as in the other, under the same conditions.<sup>118</sup>

Using the activation parameters outlined in the previous sections, we probe their value in assessing mechanism.

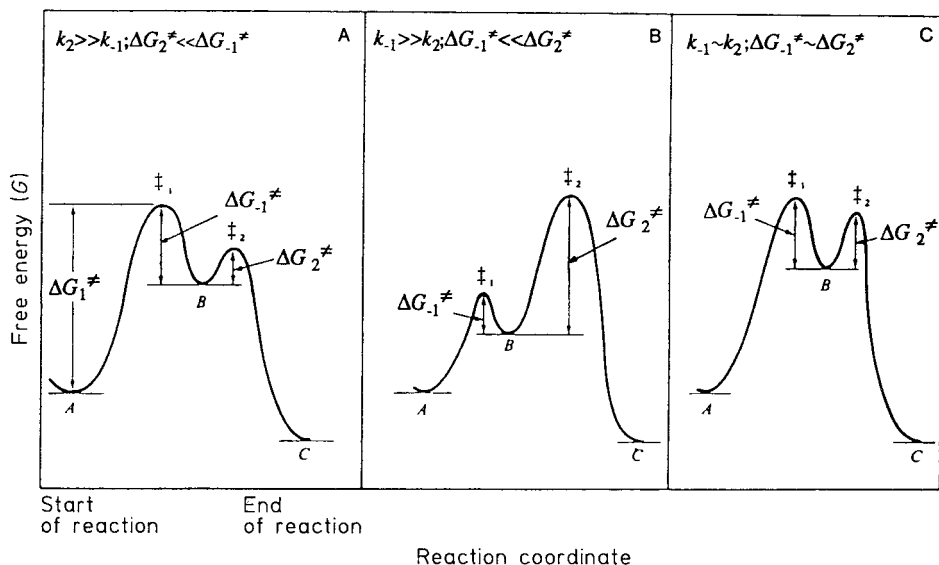
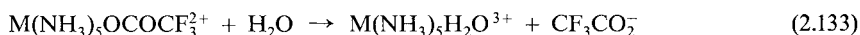


Fig. 2.5 Free energy reaction profile for (2.130) for various relative values of the associated rate constants.

## 2.4 Free Energy of Activation and Mechanism

The actual value of a rate constant for a reaction only infrequently gives a clue to its mechanism. Assessment of values within a reaction series may be more revealing, while comparisons of free energies of activation  $\Delta G^\ddagger$  with free energies for the reactions  $\Delta G$ , leading to the linear free-energy relationships (LFER), can be very useful in diagnosing mechanism.

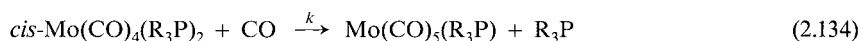
The existence of similar rate constants for a series of reactions in which there is only a change in the central metal or in the ligand in one of the reactants, suggests that a common mechanism is operative for the whole reaction series. The rate constants for aquation of a series of complexes



are similar for  $M = \text{Co}, \text{Rh}$  and  $\text{Ir}$ . This independence on metal is unusual and suggests that  $\text{C}-\text{O}$  rather than  $\text{M}-\text{O}$  bond cleavage is occurring, since the former process might be expected to be much less sensitive to the nature of  $M$  than would  $\text{M}-\text{O}$  breakage.<sup>119</sup>

Increasing steric hindrance in a reacting molecule will usually be relieved in the transition state if the mechanism is dissociative but aggravated if the reaction proceeds by an associative one. Thus the acid hydrolysis of  $\text{Co}(\text{NH}_2\text{CH}_3)_5\text{Cl}^{2+}$  proceeds 23 times faster than that of  $\text{Co}(\text{NH}_3)_5\text{Cl}^{2+}$ . This supports the assigned dissociative ( $I_d$ ) mechanism (Ch. 4).<sup>120</sup> With the  $\text{Cr}(\text{III})$  analogs, the  $\text{CH}_3\text{NH}_2$  substituted derivative reacts 33 times slower. This is used to suggest an associative ( $I_a$ ) mechanism. These assignments have independent support, particularly from  $\Delta V^\ddagger$  values (Sec. 4.2.6). The reversal of relative rates for the  $\text{Cr}(\text{III})$  complexes has been rationalized in terms of small differences in  $\text{Cr}-\text{Cl}$  bond lengths in the two complexes.<sup>121</sup> This argument has been criticized because of the small variation of  $\text{M}-\text{Cl}$  bond distances anyway in solid metal complexes.<sup>122</sup> The suggestion does however emphasize the importance of examining the ground state as well as the activated complex in rationalizing activation free energy effects.

A subtle example of steric acceleration associated with a dissociative mechanism is shown in the reaction



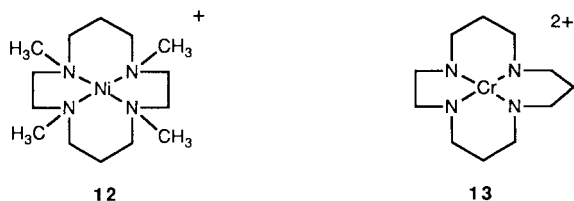
As the "size" of  $\text{R}_3\text{P}$  increases so does the value of  $k$ . A popular method of assessing the "size" of  $\text{R}_3\text{P}$  is by using Tolman's cone angle.<sup>123</sup> This is the apex angle of the cone centered on  $\text{P}$  which just encloses the van der Waals radii of the outermost atoms of  $\text{R}_3\text{P}$ . The data are shown in Table 2.3 for (2.134) in  $\text{CO}$ -saturated  $\text{C}_2\text{Cl}_4$  at  $70^\circ\text{C}$  (Ref. 124)

**Table 2.3** Effect of Tolman's Cone Angle on (2.134)

$\text{PR}_3$	Cone Angle	$k, \text{s}^{-1}$
$\text{PPhMe}_2$	$122^\circ$	$< 10^{-6}$
$\text{PPh}_2\text{Me}$	$136^\circ$	$1.3 \times 10^{-5}$
$\text{PPh}_3$	$145^\circ$	$3.2 \times 10^{-3}$

Study of the relative rate constants for reactions of a series of similar complexes  $A$  with reagents  $B$  and  $C$  may reveal deviations by a particular complex of the series  $A$  from the general pattern and therefore suggest it is reacting by an anomalous mechanism. This rarely occurs, but a general correlation suggests a common mechanism for the reactions.

The pattern for reduction of alkyl halides by  $\text{Ni}(\text{tmc})^+$  (**12**) closely resembles that by  $\text{Cr}(\text{15[ane]N}_4)^{2+}$  (**13**). This suggests a similar mechanism for both reductants. There is strong

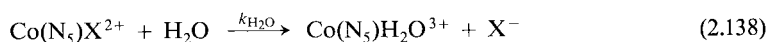
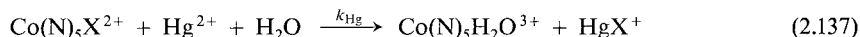




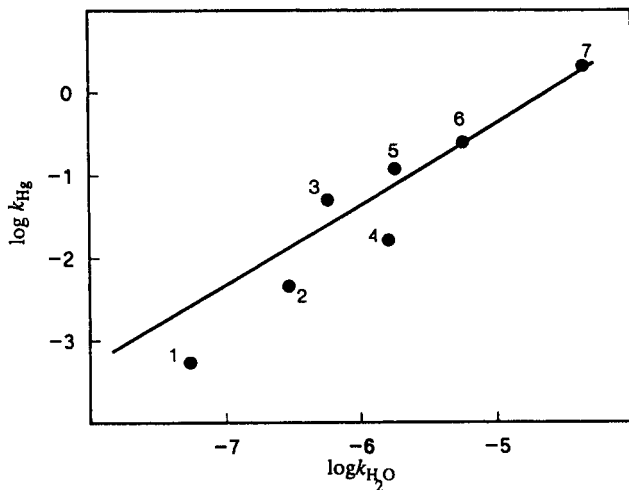
support for atom transfer for the Cr(II) reductions since inert halochromium(III) results (Sec. 5.3(a)). Therefore reductions by  $\text{Ni}(\text{tmc})^+$  are also believed to occur by atom transfer, rather than by an outer sphere mechanism.<sup>125</sup>



Finally, there is a striking linear correlation of the rate constants for the reactions (N represents a ligand with an N-donor atom, e.g.  $\text{NH}_3$ ):



For the plot of  $\log k_{\text{Hg}}$  vs  $\log k_{\text{H}_2\text{O}}$  for 34 complexes the slope is 0.96 with little scatter (Fig. 2.6). A common mechanism with a 5-coordinated intermediate is indicated.<sup>126</sup>



**Fig. 2.6** Plot of  $\log k_{\text{Hg}}$  vs  $\log k_{\text{H}_2\text{O}}$  for a number of reactions of the type (2.137) and (2.138) respectively at  $\mu = 1.0 \text{ M HClO}_4$  and  $25^\circ\text{C}$ . Only a few entries are selected from the 34 reactions tabulated in Ref. 126 but these illustrate the variety of complexes which conform to the correlation observed. Complexes: *cis*- $\text{Co}(\text{en})_2(\text{NH}_2\text{CH}_2\text{CN})\text{Cl}^{2+}$  (1), *trans*- $\text{Co}(\text{en})_2(\text{NH}_3)\text{Cl}^{2+}$  (2), *cis*- $\text{Co}(\text{en})_2(\text{imid})\text{Cl}^{2+}$  (3), *cis*- $\text{Co}(\text{en})_2(3\text{Mepy})\text{Cl}^{2+}$  (4),  $\text{Co}(\text{NH}_3)_5\text{Cl}^{2+}$  (5), *mer*- $\text{Co}(\text{dien})(\text{tn})\text{Cl}^{2+}$  (6), *cis*- $\text{Co}(\text{tn})_2(\text{C}_2\text{H}_5\text{NH}_2)\text{Cl}^{2+}$  (7). The line is the best fit for the 34 reactions, slope = 0.96.

## 2.5 Linear Free-Energy Relationships – $\Delta G^\ddagger$ and $\Delta G$

So far we have considered a limited series of rate relationships and their potential value in substantiating mechanism. We now examine more detailed linear free-energy relationships (LFER), a subject that has had full attention in organic chemistry but only recently has been exploited by the inorganic chemist.<sup>126,127</sup>

In spite of the justifiable warnings not to confuse the kinetics and thermodynamics of a reaction, there are circumstances, for example in a closely related series of reactions, in which it might be expected that the free energies of activation,  $\Delta G^\ddagger$  and reaction,  $\Delta G$  would parallel one another. There is usually no problem in measuring or estimating the equilibrium constant, and hence  $\Delta G$ , for many substitution and redox reactions by using formation constants or standard oxidation potentials. This information, together with the rate data, might then be used to test LFER. In turn, such LFER might be used to diagnose mechanism by determining the extent of bond formation or breakage in the transition state or by assessing the importance of electronic, polar, or steric effects on the rate.

Since

$$-\Delta G^\ddagger = RT \ln \frac{kh}{kT} = 2.3RT \log \frac{kh}{kT} \quad (2.139)$$

and

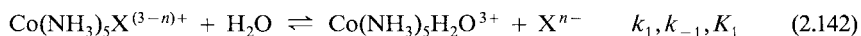
$$-\Delta G = RT \ln K = 2.3RT \log K \quad (2.140)$$

the linearity between the free energies of activation and reaction might be most easily expressed in the form

$$\log k = A \log K + B \quad (2.141)$$

Historically, the decadic log scale has been mainly used in LFER.

This idea can be tested by examining data for the aquation of a series of ions,  $\text{Co}(\text{NH}_3)_5\text{X}^{(3-n)+}$ ,



The plot of  $\log k_1$  vs  $\log K_1$  is linear over a wide range of rate constants (Fig. 2.7).<sup>128</sup> Obviously, the faster the aquation, the more the reaction goes to completion! The slope  $A$  is 1.0 and this indicates that the activated complex and the products closely resemble one another, that is, that  $\text{X}^{n-}$  has substantially separated from the cobalt and that therefore the mechanism of these reactions is dissociative ( $I_d$ ). Since  $K_1 = k_1/k_{-1}$

$$\log k_1 = \log K_1 + \log k_{-1} \quad (2.143)$$

and (2.143) is of the form (2.141) with  $A = 1.0$  and  $B = \log k_{-1}$ . The value of  $B$  is approximately constant if a dissociative mechanism applies to aquation, since the  $\text{Co}-\text{H}_2\text{O}$  bond

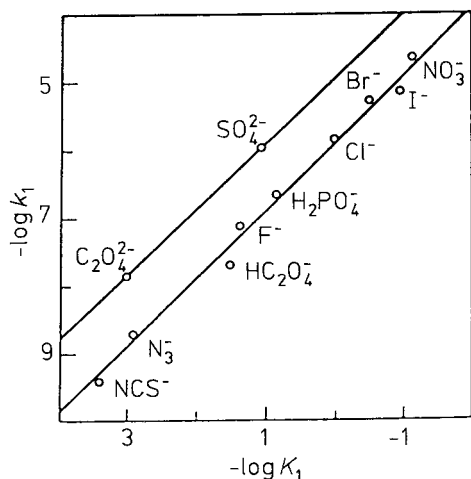
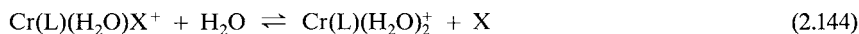
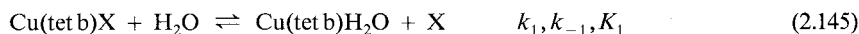


Fig. 2.7 Plot of  $\log k_1$  vs  $\log K_1$  for (2.142) at 25°C. Ref. 128.

cleavage is common to all reactions and not much influenced by the nature of  $X^{n-}$ . Such linear plots for solvolysis rate constants vs equilibrium constants with slopes near unity are reported for reactions of some Cr(III) complexes<sup>129</sup> where L is a tetradentate Schiff base (2.144), and for Li and Na

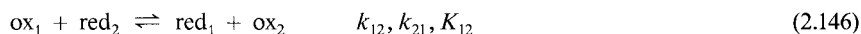


complexes of spherands and cryptands in a variety of solvents.<sup>130,131</sup> These LFER afford good evidence for a strongly dissociative mode for substitution in these reactions. By contrast, an excellent linear correlation of  $\log k_{-1}$  vs  $\log K_1$  (slope 0.94) is observed for the hydrolysis of the blue and red forms of the square pyramidal Cu(II) complex, Cu(tet b)X (Sec. 7.9).



Now, it is the forward rate constant  $k_1$  that is almost invariant (because there is a common nucleophile  $\text{H}_2\text{O}$ ), whereas  $k_{-1}$  is very sensitive to the nucleophilic character of X, i.e. it is an associative type reaction.<sup>132</sup> Selectivity would be expected to lead to curved free energy plots but these have not yet been observed.<sup>115</sup>

Undoubtedly one of the most used LFER in transition metal chemistry involves electron transfer rate constants and associated equilibrium constants in *outer sphere redox reactions*. These are an unusual class of reactions in chemistry since bonds are only stretched or contracted in the formation of the activated complex. They therefore lend themselves well to theoretical treatment. We shall have more to say about these reactions in Chap. 5. It is sufficient here to state the simple form of the LFER<sup>133</sup> with an example (Fig. 2.8).<sup>134</sup> For the reaction



$$k_{12} = (k_{11}k_{22}K_{12}f)^{1/2} \quad (2.147)$$

where

$$\log f = \frac{(\log K_{12})^2}{4 \log(k_{11}k_{22}/10^{22})} \quad (2.148)$$

and  $k_{11}$  and  $k_{22}$  refer to the isotopic exchange reactions

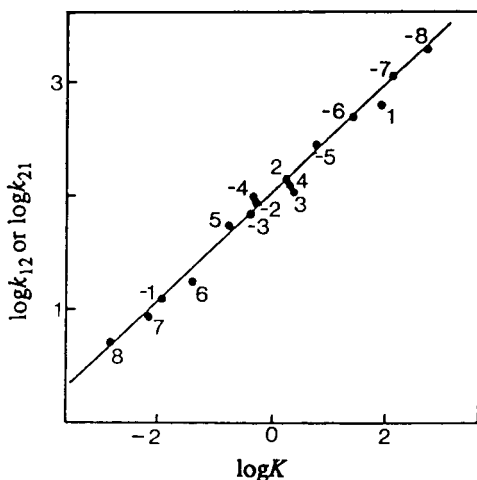
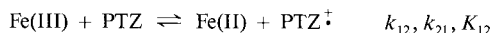


Fig. 2.8 Plot of  $\log k_{12}$  or  $\log k_{21}$  vs  $\log K$  for the reaction (1.55).



(PTZ = variety of N-alkylphenothiazines). Positive numbers use  $k_{12}$  and  $K_{12}$ . Negative numbers refer to  $k_{21}$  and  $1/K_{12}$ . X = OH, R =  $(\text{CH}_2)_3\text{N}(\text{CH}_3)_2$ (1), X = H, R =  $(\text{CH}_2)_3\text{N} \langle \bigcirc \rangle \text{NCH}_3$ (2), X =  $\text{OCH}_3$ , R =  $(\text{CH}_2)_3\text{N}(\text{CH}_3)_2$ (3), X = H, R =  $(\text{CH}_2)_3\text{N}(\text{CH}_3)_2$ (4), X = Cl, R =  $(\text{CH}_2)_3\text{N}(\text{CH}_3)_2$ (5), X = H, R =  $(\text{CH}_2)_2\text{N}(\text{C}_2\text{H}_5)_2$ (6), X = H, R =  $\text{CH}_2\text{CH}(\text{CH}_3)\text{N}(\text{CH}_3)_2$ (7), X = H, R =  $\text{CH}(\text{CH}_3)\text{CH}_2\text{N}(\text{CH}_3)_2$ (8).<sup>134</sup> The slope of Fig. 2.8 is 0.5 as expected in (2.151). Reprinted with permission from E. Pelizzetti and E. Mentasti, *Inorg. Chem.*, **18**, 583 (1979). © (1979) American Chemical Society.

Although an extended form of (2.147) is sometimes used (Eqn. 5.37) the simple one can account for a surprisingly large number of redox reactions. When the oxidizing power of  $\text{ox}_1$  and  $\text{ox}_2$  are comparable,  $f \sim 1$ , and

$$\Delta G_{12}^\ddagger = 0.50(\Delta G_{11}^\ddagger + \Delta G_{22}^\ddagger + \Delta G_{12}^0) \quad (2.151)$$

The rate constant for one reaction may have to be correlated with the equilibrium constant not for that reaction but for a related one. Rate constants for reactions of metal complexes

can be correlated with the proton affinity of one of the ligands, either in the coordinated or free state. Thus, the rate constant for  $\text{CO}_2$  uptake by a variety of metal hydroxo complexes depends on the nucleophilicity of the "bound" hydroxide ion. It therefore correlates with the O–H bond strength of the corresponding aqua complex, i.e. the  $\text{p}K_a$  of the coordinated water.<sup>135</sup> See also Figs. 6.5 and 8.4. As a second, more involved, example consider the internal electron transfer rate constant ( $k_{\text{et}}$ ) within the ion pair of  $\text{Co}(\text{NH}_3)_5\text{O}_2\text{CR}^{2+}$  with  $\text{Fe}(\text{CN})_6^{3-}$ . It is observed that  $k_{\text{et}}$  varies inversely with the  $\text{p}K_a$  of  $\text{RCO}_2\text{H}$ . It is argued that the oxidation potential of Co(III) in the complex (and therefore the rate (see above)) will increase with decreasing  $\sigma$ -donor strength of the carboxylate ligand. Decreasing  $\sigma$ -donor strength is related to decreasing  $\text{p}K_a$ .<sup>136,137</sup> This indirect approach is the basis for most LFER discussed in the next sections.

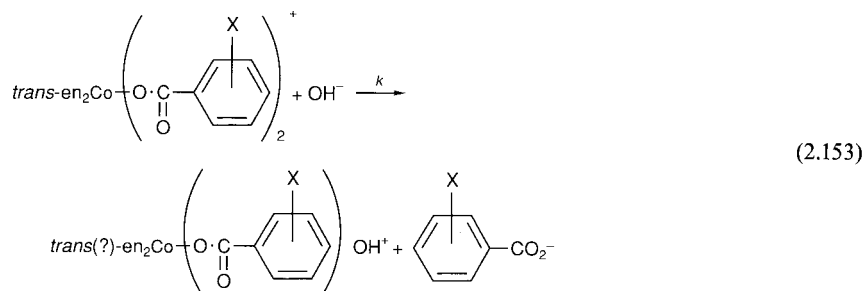
### 2.5.1 Hammett Relationship

The Hammett equation,<sup>138</sup> one of the oldest and most useful of LFER, correlates the rates of reaction of a series of *meta*- and *para*-substituted aromatic compounds with a common substrate,

$$\log \frac{k}{k^0} = \rho \log \frac{K_a}{K_a^0} = \rho \sigma \quad (2.152)$$

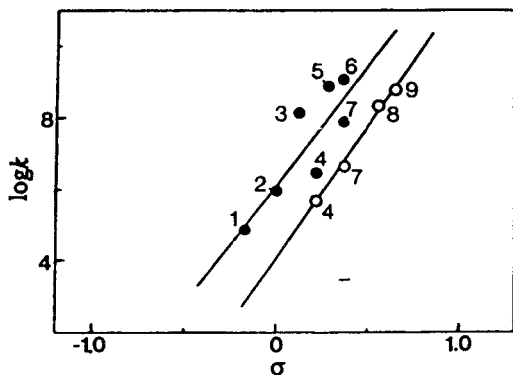
where  $k$  and  $k^0$  are the reaction rate constants for the X-substituted and unsubstituted aromatic compounds respectively, and  $K_a$  and  $K_a^0$  are the dissociation constants for the X-substituted and unsubstituted benzoic acids. This is of the general form (2.141) with  $A = \rho$  and  $B = \log k^0 - \rho \log K_a^0$ , which is a constant for a reaction series. The parameter  $\sigma$  depends on the substituent but is independent of the reaction series, whereas the value of  $\rho$  depends only on the actual reaction examined. Either  $\log k$  or  $\log(k/k^0)$  is plotted against  $\sigma$ . The slope of the line is  $\rho(\Delta \log k / \Delta \sigma)$  and is positive if  $k$  increases as the value of  $\sigma$  becomes more positive.

Second-order rate constants  $k$  for the replacement of a ring-substituted benzoate group by hydroxide ion in a number of complexes (base hydrolysis) have been carefully determined at 25°C in 40% aqueous methanol:



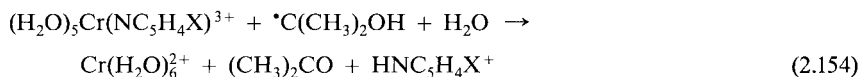
The  $\log k$  vs  $\sigma$  plot is reasonably linear with no marked deviations for seven X-substituents. The value of  $\rho$  is 0.75 and this is much smaller than that for alkaline hydrolysis of the free

esters (1.8–2.5). Acyl-oxygen fission has been established for the esters. Since  $\rho$  is a measure of the sensitivity of the reaction series to ring substitution, the smaller value of  $\rho$  with the cobalt complexes could be rationalized by the reaction site being further removed from the aromatic ring than it is in the free esters i. e. Co–O cleavage is involved for all seven reactions (2.153).<sup>139</sup>

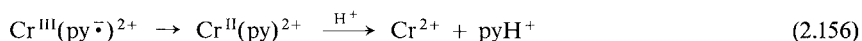
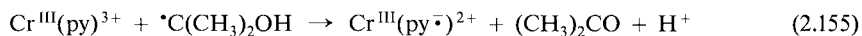


**Fig. 2.9** Plots of  $\log k$  for the reduction of  $(\text{H}_2\text{O})_5\text{Cr}(\text{NC}_5\text{H}_4\text{X})^{3+}$  (○) and  $\text{NC}_5\text{H}_4\text{XH}^+$  (●) by  $^*\text{C}(\text{CH}_3)_2\text{OH}$  vs the Hammett  $\sigma$  values for X, where X = 4–C(CH<sub>3</sub>)<sub>3</sub>(1), H(2), 3–OH(3), 4–Cl(4), 3–CONH<sub>2</sub>(5), 4–CONH<sub>2</sub>(6), 3–Cl(7), 3–CN(8) and 4–CN(9).<sup>140</sup> Reprinted with permission of A. Bakač, V. Butkovic, J. H. Espenson, R. Marcec, and M. Orhanovic, *Inorg. Chem.*, **25**, 2562 (1986). © (1986) American Chemical Society.

A comparison of the reduction of coordinated and free pyridines by a variety of reducing agents is very informative (Fig. 2.9<sup>140</sup>). Reduction of  $(\text{NH}_3)_5\text{M}(\text{NC}_5\text{H}_4\text{X})^{3+}$ , M=Co and Ru, by  $^*\text{C}(\text{CH}_3)_2\text{OH}$ ,  $\text{Ru}(\text{NH}_3)_6^{2+}$  and other strong reducing agents is known, or can be inferred, to occur by outer-sphere electron transfer to the metal. These reactions obey the Hammett LFER with  $\rho$  values of 1.1–1.9. A similar type of reduction of the free pyridines ( $\text{XC}_5\text{H}_4\text{NH}^+$  in acid) has high values of  $\rho$  of 6.6–10.3. For the reductions (X = H, 4-CN, 3-CN, 4-Cl, 3-Cl, 4-t-Bu)



of the Cr analog by  $^*\text{C}(\text{CH}_3)_2\text{OH}$ ,  $\rho = 6.6 \pm 1.9$ . This value strongly suggests that the reduction is different from that of the other complexes (above) and occurs by the “chemical” mechanism in which reduction of the Cr–NC<sub>5</sub>H<sub>4</sub>X moiety ( $\text{Cr}^{\text{III}}(\text{py})^{3+}$ ) is by electron transfer to the *pyridyl ring* (as with the free pyridines)



On the other hand, reduction of  $(\text{H}_2\text{O})_5\text{Cr}(\text{NC}_5\text{H}_4\text{X})^{3+}$  by  $\text{Ru}(\text{bpy})_3^+$  has an associated value for  $\rho$  of 1.1, the same as for the Co and Ru ammine complexes and therefore a similar mechanism.<sup>140</sup> For other applications of Hammett LFER see Refs. 141–144.

## 2.5.2 Taft Relationship

The reactivity of aliphatic compounds, where steric hindrance near the substituent site is not important, is accommodated by the Taft modification of the Hammett equation<sup>145</sup>

$$\log \frac{k}{k^0} = \sigma^* \rho^* \quad (2.157)$$

where  $\sigma^*$  is the polar substituent constant and  $\rho^*$  is a reaction constant, analogous to the Hammett functions  $\sigma$  and  $\rho$  respectively. By definition  $\sigma^* = 0.00$  for a  $\text{CH}_3$  substituent. For the oxidation of the alkyl radicals  $^*\text{CH}_n(\text{CH}_3)_{3-n}$  by  $\text{IrCl}_6^{2-}$  and  $\text{Fe}(\text{CN})_6^{3-}$  the Taft plot is shown in Fig. 2.10. The rate increase runs parallel with the increase in electron-donating power of the radicals. The oxidations by  $\text{IrCl}_6^{2-}$  are all near diffusion-controlled. Those by  $\text{Fe}(\text{CN})_6^{3-}$  have a large  $\rho^* = -13.2$ , which indicates that the activated complex has ionic character, supporting an electron transfer mechanism.<sup>146</sup> See also Ref. 147.

Problems in the use of  $\sigma^*$  have led to a modification of (2.157)

$$\log \frac{k}{k^0} = \sigma_1 \rho_1 \quad (2.158)$$

where Taft's induction factor  $\sigma_1$  is based on  $\sigma_1$  being 0.0 for an H substituent.<sup>148</sup> Recent uses of the concept in complex ion chemistry are sparse.<sup>149</sup>

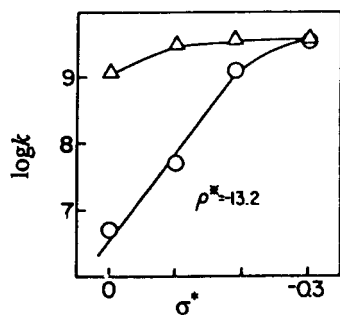


Fig. 2.10 Plots of  $\log k$  for the reactions of  $^*\text{CH}_n(\text{CH}_3)_{3-n}$  with  $\text{IrCl}_6^{2-}$  ( $\Delta$ ) and  $\text{Fe}(\text{CN})_6^{3-}$  ( $\circ$ ) vs the Taft  $\sigma^*$  parameter.<sup>146</sup> Reprinted with permission from S. Steenken and P. Neta, *J. Amer. Chem. Soc.* **104**, 1244 (1982). © 1982 American Chemical Society.

## 2.5.3 Brønsted Relationship

The earliest LFER, advanced by Brønsted, correlates the acid dissociation constant ( $K_{\text{AH}}$ ) and base strength ( $1/K_{\text{AH}}$ ) of a species with its effectiveness as a catalyst in general acid ( $k_{\text{AH}}$ ) and base ( $k_{\text{B}}$ )-catalyzed reactions respectively.<sup>150</sup> The relationships take the form

$$k_{\text{AH}} = AK_{\text{AH}}^\alpha \quad (2.159)$$

$$\log k_{\text{AH}} = \log A + \alpha \log K_{\text{AH}} \quad (2.160)$$

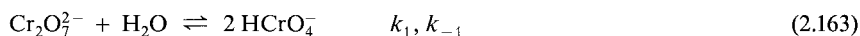
or

$$k_B = B \left( \frac{1}{K_{AH}} \right)^\beta \quad (2.161)$$

$$\log k_B = \log B - \beta \log K_{AH} \quad (2.162)$$

Equations (2.160) and (2.162) are both consistent with the generalized form (2.141). The values  $A$  and  $B$  and  $\alpha$  and  $\beta$  are constants with  $0 < \alpha, \beta < 1$ .

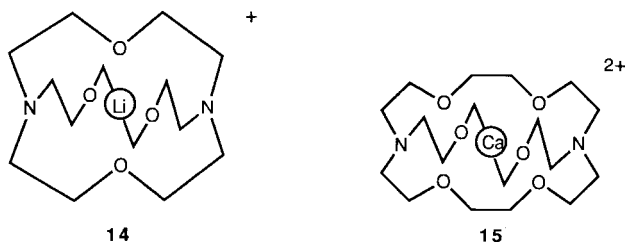
Probably the most detailed study of the acid(HA)- and base(B)-catalyzed reactions of complex ions concerns the hydrolysis of the dichromate ion:



The hydrolysis rate constant  $k$  is given by

$$k = k_1[\text{H}_2\text{O}] + \sum k_B[\text{B}] + \sum k_{AH}[\text{HA}] \quad (2.164)$$

The value of  $k_B$  has been determined for a very large number of bases. There is a reasonable correlation of  $\log k_B$  vs  $\text{p}K_{BH^+}$  in agreement with (2.162). The value of  $\beta$  is  $\sim 0.25$ , which indicates that general base catalysis holds. For specific base catalysis,  $\beta$  would equal 1, while for reactions in which solvent catalysis predominates  $\beta$  would be zero, since only the  $k_1[\text{H}_2\text{O}]$  term would then be important.<sup>151</sup>



The dissociations of the metal cryptates  $\text{Li}(2.1.1)^+$  **14** and  $\text{Ca}(2.2.2)^{2+}$  **15**, abbreviated  $\text{M}(\text{cry})^{n+}$ , are accelerated by  $\text{H}^+$  and undissociated acid HA

$$-d[\text{M}(\text{cry})^{n+}]/dt = (k_d + k_H[\text{H}^+] + k_{AH}[\text{HA}]) [\text{M}(\text{cry})^{n+}] \quad (2.165)$$

The plots of  $\log k_{AH}$  vs  $\text{p}K_{AH}$  are linear with slopes ( $\alpha$ ) of  $-0.25$  (Ca) and  $-0.64$  (Li). These values require that a rate-determining proton transfer from HA to  $\text{M}(\text{cry})^{n+}$  occur. Alternatively, dissociation of  $\text{M}^{2+}$  or  $\text{M}^+$  from an  $\text{AH} \cdots (\text{cry})\text{M}^{n+}$  adduct may be the rds. The point for  $k_H$  is well below the line, a not uncommon behavior.<sup>152</sup>

The Brønsted relationship can be strictly accurate only over a certain range of acid and base strengths. When  $k_{AH}$  has diffusion-controlled values, which of course cannot be exceeded, the linear plot of  $\log k_{AH}$  vs  $\log K_{AH}$  must level off to a zero slope, that is  $\alpha = 0$ .<sup>153</sup> As well as being reported, although rarely, in simple metal complexes,<sup>154</sup> the resultant curvature in the Brønsted plot is also shown by the zinc enzyme carbonic anhydrase (Chap. 8. Zn(II)). In



one of the steps in the overall catalysis, buffers are believed to participate as proton-transfer agents ( $\text{EZnH}_2\text{O} = \text{enzyme}$ ;  $\text{A} = \text{buffer}$ )



The variation of  $\log k_1$  with  $\text{p}K_{\text{AH}}$  of the buffer ( $\text{AH}^+$ ) is shown in Fig. 2.11.

A  $\text{p}K_{\text{AH}} = 7.6$  for the donor group on the enzyme is deduced from the curve. When the  $\text{p}K_{\text{AH}}$  of the buffer is much greater than 7.6, a saturating  $k \approx 10^9 \text{M}^{-1} \text{s}^{-1}$  is observed. When  $\text{p}K_{\text{AH}} \ll 7.6$ , the  $\log k_1$  vs  $\text{p}K_{\text{AH}}$  is of unity slope and conforms to (2.160) with  $\alpha = 1.0$ .<sup>155</sup> Similar types of plots accompany atom transfer reactions (Fig. 8.11).

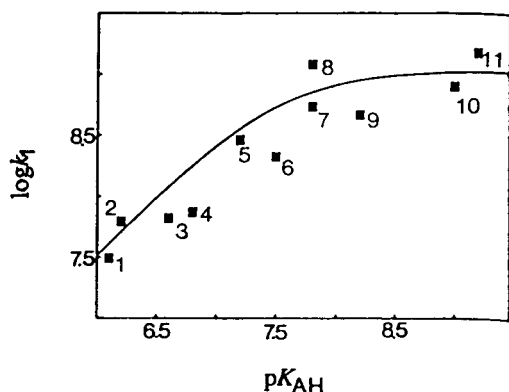
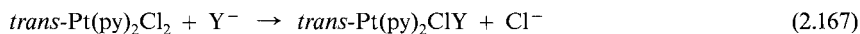


Fig. 2.11 The variation of  $\log k_1$  with  $\text{p}K_{\text{AH}}$  of the buffer for reaction (2.166). The buffers used are Mes(1), 3,5-lutidine(2), 3,4-lutidine(3), 2,4-lutidine(4), 1-Meimid(5), Hepes(6), triethanolamine(7), 4-Meimid(8), 1,2-diMeimid(9), Ted(10) and Ches(11). The curve drawn is calculated for  $k_1 = 1.1 \times 10^9 \text{M}^{-1} \text{s}^{-1}$  and a  $\text{p}K_{\text{AH}}$  for the enzyme donor group of 7.6.<sup>155</sup> Reprinted with permission from R. S. Rowlett, and D. N. Silverman, *J. Amer. Chem. Soc.* **104**, 6737 (1982). © (1982) American Chemical Society.

### 2.5.4 Swain-Scott Relationship

A completely empirical LFER can also be constructed with recourse only to kinetic data. This has been the case in the setting up of a scale of nucleophilic power for ligands substituting in square-planar complexes based on the Swain-Scott approach.<sup>156</sup> The second-order rate constants  $k_Y$  for reactions in MeOH of nucleophiles Y with  $\text{trans-Pt}(\text{py})_2\text{Cl}_2$ , chosen as the standard substrate



are compared with the rate constant for solvolysis ( $\text{Y} = \text{CH}_3\text{OH}$ )

$$k_s = \frac{k_{\text{CH}_3\text{OH}}}{[\text{CH}_3\text{OH}]} = \frac{k_{\text{CH}_3\text{OH}}}{26}$$

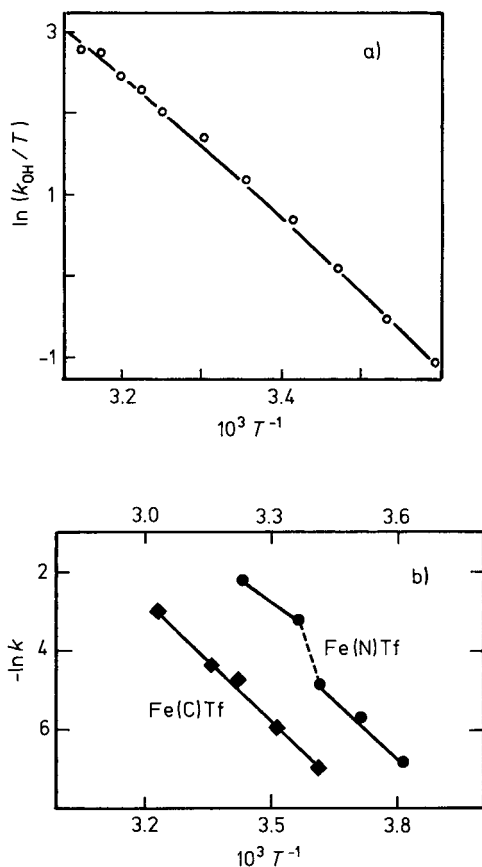
Then it is found that ( $s = 1$ ),

$$\log \frac{k_Y}{k_s} = s n_{\text{Pt}} \quad (2.168)$$

On the basis of this equation, an index of nucleophilicity  $n_{\text{Pt}}$  can be assigned to each nucleophile Y (see Table 4.13). It is found, moreover, that a plot against  $n_{\text{Pt}}$  of  $\log k_Y$ , for reaction of Y with another Pt(II) neutral substrate, is also often linear. Thus, Eq. (2.168) applies, and  $s$  is termed the nucleophilic discrimination factor (Sec. 4.7.1). Some of the departures from linearity of plots of  $k_Y$  vs  $n_{\text{Pt}}$  which have been observed, disappear if the Pt reference substrate chosen is of the same charge as the Pt reactants.<sup>157</sup> The value of  $n_{\text{Pt}}$  for a bulky nucleophile has also to be modified to allow for steric hindrance features.<sup>158</sup>

## 2.6 Enthalpy of Activation and Mechanism

As we have noted in Sec. 2.3.2, there are few authentic examples of changing  $\Delta H^\ddagger$  values with temperature that are understandable on the basis of (and therefore evidence for) a proposed mechanism. A rds in a multistep mechanism which changes with temperature might account for such behavior.



**Fig. 2.12** Examples of non-linear Arrhenius (or Eyring) plots (a)  $\ln(k_{\text{OH}})T^{-1}$  vs  $T^{-1}$  for the base hydrolysis of  $\text{trans-Co(en)}_2\text{Cl}_2^+$ . Curvature may result when  $k_{-1} \sim k_2$  and  $\Delta H_{-1}^\ddagger$  not equalling  $\Delta H_2^\ddagger$  in the conjugate-base mechanism (Sec. 4.3.4).<sup>100</sup> Reprinted with permission from C. Blakeley and M. L. Tobe, *J. Chem. Soc. Dalton Trans.* 1775 (1987). (b)  $\ln k$  vs  $T^{-1}$  for iron removal from C- and N-terminal monoferric transferrin (lower and upper scales respectively).<sup>101</sup> Transferrin contains two iron binding sites  $\approx 35 \text{ \AA}$  apart. Either of the two sites, designated C- and N-terminal, can be exclusively labelled by Fe(III) ions and these may be removed by a strong ligand such as a catechol (see Sec. 4.11). Reprinted with permission from S. A. Kretschar and K. N. Raymond, *J. Amer. Chem. Soc.* **108**, 6212 (1986). © (1986) American Chemical Society.

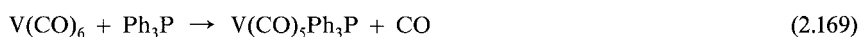
One such example may arise in the base hydrolysis of  $\text{trans-Co(en)}_2\text{Cl}_2^+$ . Figure 2.12(a) shows curvature in the  $\ln(k_{\text{OH}}/T)$  vs  $T^{-1}$  plot above 25°C. This arises from a change in the rate-determining step from formation of the 5-coordinated intermediate to deprotonation of  $\text{trans-Co(en)}_2\text{Cl}_2^+$  see (Eqn. 2.99) and Sec. 4.3.4.<sup>100</sup> Since this mechanistic change had been anticipated, great care was taken to examine for non-Arrhenius behavior. It is a salutary lesson to consider that such behavior might be more prevalent than supposed. It is always tempting to draw a straight line through the extreme points shown in Figure 2.12(a).

In Figure 2.12(b) is shown the temperature dependence of the rate constant for iron removal from N-terminal monoferric transferrin. There is an obvious break between 12 and 20°C and this is ascribed to a temperature-induced conformational change.<sup>101</sup> The effect becomes less distinct when the ionic strength is increased from 0.13 to 2.0 M,<sup>101</sup>. See also Sec. 4.11.

Negative or very small values of  $\Delta H^\ddagger$  are rare. They obviously cannot arise from a single step, and they give overwhelming evidence for a multistep process that includes a pre-equilibrium. Negative or near-zero values for  $\Delta H^\ddagger$  for a few inner-sphere and outer-sphere redox reactions indicate the occurrence of intermediates, and rule out a single step, with a single activated complex (Sec. 5.5).

## 2.7 Entropy of Activation and Mechanism

Values for  $\Delta S^\ddagger$  can be positive or negative. The same types of arguments and difficulties in understanding the magnitude and sign of  $\Delta S$  values for a reaction will be encountered in interpreting the values of  $\Delta S^\ddagger$  in the formation of the activated complex from the reactants. The interpretation of these values is easiest with “extreme” mechanisms. Thus from general considerations, one might expect large and negative values of  $\Delta S^\ddagger$  for the associative mechanisms encountered in substitution in square-planar complexes (Sec. 4.6.2) or in reactions of octahedral carbonyls



$$-d[\text{V(CO)}_6]/dt = k[\text{V(CO)}_6][\text{Ph}_3\text{P}] \quad (2.169a)$$

where  $k = 0.25 \text{ M}^{-1}\text{s}^{-1}$ ,  $\Delta H^\ddagger = 41.8 \text{ k J mol}^{-1}$  and  $\Delta S^\ddagger = -116 \text{ J K}^{-1}\text{mol}^{-1}$  in hexane at 25°C Ref. 159. Similarly, one might expect that  $\Delta S^\ddagger$  would be more positive for reactions accompanied by topological change than for similar ones that proceed with retention of configuration. This is generally observed, for example, in the aquation of *cis* and *trans* cobalt(III) complexes.<sup>160</sup> This also means that the steric course is determined in the rds and yields clues as to the structure of any five-coordinated intermediates (Sec. 4.3.5)

### 2.7.1 $\Delta S^\ddagger$ and the Charge of the Reactants

In an area of chemistry dominated by ionic reactions, it is not surprising that entropies of activation are largely charge-controlled. The reaction between unlike charged species is often at-

tended by a positive  $\Delta S^\ddagger$  because the solvent molecules are less restricted around an activated complex of reduced charge and thus are released in forming it. For the outer-sphere oxidations of *cis*-hydroxooxyvanadium(IV) chelates by negatively and positively charged oxidants e.g.



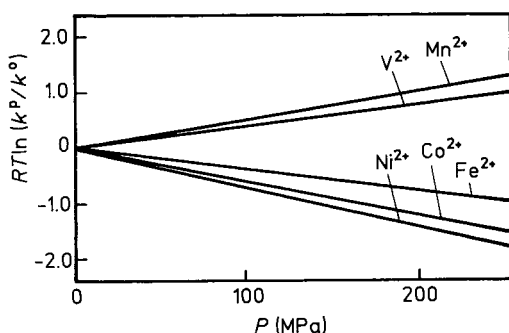
there is a linear relationship between  $\Delta S^\ddagger$  (and  $\Delta H^\ddagger$ ) and the charge product ( $z_{\text{R}}z_{\text{O}}$ ) of the redox couple ( $2n$  in (2.170)). The values of  $\Delta S^\ddagger$  ( $\text{J K}^{-1} \text{mol}^{-1}$ ) span the range  $+107$  ( $z_{\text{R}}z_{\text{O}} = -8$ ) to  $-2$  ( $z_{\text{R}}z_{\text{O}} = +4$ ).<sup>161</sup> For a number of reactions this type of behavior does not even approximately hold. Newton and Rabideau have examined a large number of redox reactions of transition and actinide ions, involving both net chemical reactions and isotopic exchange. They showed that the molar entropy of the activated complex  $S^\ddagger$  defined by

$$S^\ddagger = \Delta S^\ddagger + \sum S^0(\text{reactants}) - \sum S^0(\text{products in net activation process}) \quad (2.171)$$

is very much controlled by its charge.<sup>5,162</sup>

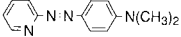
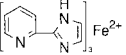
## 2.8 Volume of Activation and Mechanism

The volume of activation is probably the easiest parameter to understand conceptually. Consider again the water exchange of Cr(III), Sec. 2.3.3. The  $\Delta V^\ddagger$  value of  $-10 \text{ cm}^3 \text{mol}^{-1}$  for  $\text{Cr}(\text{H}_2\text{O})_6^{3+}$  indicates that an associative process pertains ( $I_{\text{a}}$ ) since  $\text{Cr}(\text{H}_2\text{O})_6^{3+}$  plus one  $\text{H}_2\text{O}$  will occupy more volume than the activated complex which has seven waters associated with the Cr. The volume of coordinated water has been estimated as anywhere between  $\sim 5$  and  $9 \text{ cm}^3 \text{mol}^{-1}$ , so that  $\Delta V^\ddagger \leq -9 \text{ cm}^3 \text{mol}^{-1}$  for an associative mechanism. Conversely, the value of  $+2.9 \text{ cm}^3 \text{mol}^{-1}$  for water exchange on  $\text{Cr}(\text{H}_2\text{O})_5\text{OH}^{2+}$  suggests a dissociative activation mode for the exchange.<sup>102</sup> More success in interpreting  $\Delta V^\ddagger$  values is likely for reactions in which the  $\Delta V_{\text{sol}}^\ddagger$  is small, or at least a small component of the overall  $\Delta V_{\text{obs}}^\ddagger$ . The study of the pressure effects on the rates of solvent exchange with M(III) and M(II) ions (Fig. 2.13) by nmr methods has been very rewarding,<sup>94,104,105</sup> and essential, for understanding the trend from associative to dissociative character as the d-orbitals are increasingly filled

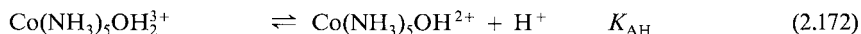


**Fig. 2.13** Effect of pressure on solvent exchange with  $\text{M}(\text{H}_2\text{O})_6^{2+}$ ,  $\text{M} = \text{V}, \text{Mn}, \text{Fe}, \text{Co}$  and  $\text{Ni}$ .<sup>105</sup> Reprinted with permission from Y. Duccomun, A. E. Merbach, *Inorganic High Pressure Chemistry*. (R. van Eldik ed.). Elsevier, Amsterdam, 1986.

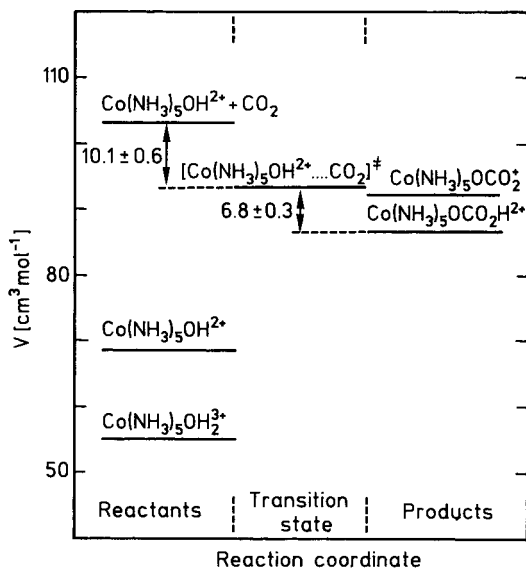
**Table 2.4.** Examples of Applications of  $\Delta V^\ddagger$  Values to the Investigation of Mechanism

Reactants	$\Delta V^\ddagger$ $\text{cm}^3 \text{mol}^{-1}$	Conclusions	Technique with high pressure	Ref.
$\text{Cr}_2\text{O}_7^{2-} + \text{base}$	Range from $-18(\text{OH}^-)$ to $-26(2,6 \text{ lutidine})$	Support $I_a$ mechanism	Stopped flow	165
Ni(II) + 	8.2( $\text{H}_2\text{O}$ ), 11.5(DMF) and 11.3(DMSO)	Similar to values of $\Delta S^\ddagger$ for solvent exchange. Support $I_d$	Laser-flash	166
$\text{M}(\text{tpps})(\text{H}_2\text{O})_2^{3-}$ + $\text{SCN}^- \rightarrow$ mono- complex	15.4(Co(III)), 8.8 (Rh(III)) and 7.4 (Cr(III))	Support $D$ , $I_d$ and $I_d$ mechanisms respectively	High pressure spectral cell in stopped-flow or spectro- photometer	167
Racemization of Cr(III) complexes	Range from 3.3 ( $\text{Cr}(\text{phen})_3^{3+}$ ) to $-16.3(\text{Cr}(\text{C}_2\text{O}_4)_3^{3-})$	Consistent with intramolecular twist mechanisms for $\text{Cr}(\text{phen})_3^{3+}$ and one-ended dissocia- tion for $\text{Cr}(\text{C}_2\text{O}_4)_3^{3-}$ for racemization	Batch technique	168
Low Spin $\xrightleftharpoons[k_{-1}]{k_1}$ High Spin 	$\Delta V_1^\ddagger = 4.9$ ; $\Delta V_{-1}^\ddagger =$ $-5.4$ (acetone); $\Delta V_1^\ddagger$ solvent dependent	Longer Fe-N and larger partial molar volumes for high spin isomer. Transi- tion state geometry intermediate be- tween spin isomers	Pulsed laser	169

(Sec. 4.2.1). The interpretation of reactions involving charges is more difficult, because of the importance of ion solvation changes.<sup>163,164</sup> All types of reactions have been studied and will be encountered in Part II. Representative examples are shown in Table 2.4.<sup>165-169</sup> It is worth reemphasizing the value of determining both  $\Delta V$  and  $\Delta V^\ddagger$  for a reaction system. The construction then of volume profiles enables a detailed description of the mechanism. The reaction steps for interaction of  $\text{CO}_2$  with  $\text{Co}(\text{NH}_3)_5\text{OH}_2^{3+}$  are considered to be

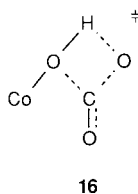


For bond formation  $\Delta V_1^\ddagger = -10.1 \text{ cm}^3 \text{mol}^{-1}$  and for bond cleavage  $\Delta V_{-1}^\ddagger = +6.8 \text{ cm}^3 \text{mol}^{-1}$  and these are considered  $\Delta V_{\text{intr}}^\ddagger$ . Comparison of these data with known  $\Delta V$  values gives a volume profile shown in Fig. 2.14.<sup>170</sup>



**Fig. 2.14** The volume profile for reaction (2.173) at 25°C, Ref. 170. The partial molar volumes of  $\text{CO}_2$ ,  $\text{Co(NH}_3)_5\text{H}_2\text{O}^{3+}$  and  $\text{Co(NH}_3)_5\text{OH}^{2+}$  were measured with a digital density apparatus. Reprinted with permission from U. Spitzer, R. van Eldik and H. Kelm, *Inorganic Chemistry*, **21**, 2821 (1982). © (1982) American Chemical Society.

The activated complex **16** is about halfway between reactants and products and there is considered to be about 50% formation or breakage in forming the activated complex in both directions<sup>170</sup>



For other examples of the use of volume profiles, see Refs. 171 (base hydrolysis of  $\text{Co(NH}_3)_5\text{X}^{n+}$ ), 172 (nickel complexing with glycolate and lactate) and general reviews.<sup>173,174</sup> We now consider the use of more than one activation parameter and any relationships between them.

### 2.8.1 $\Delta H^\ddagger$ and $\Delta S^\ddagger$ Values – The Isokinetic Relationship

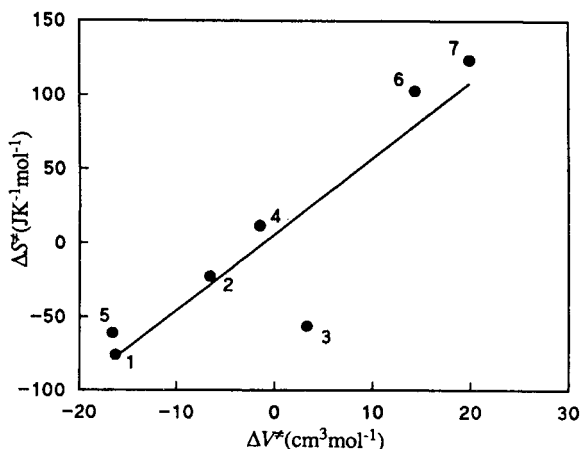
For a series of reactions of a similar type, a small range in rate constants may arise from parallel and much larger changes in  $\Delta H^\ddagger$  and  $\Delta S^\ddagger$ . This is evident from a rearrangement of (2.118)

$$\Delta H^\ddagger = T\Delta S^\ddagger + \Delta G^\ddagger \quad (2.175)$$

The slope of any linear plot of  $\Delta H^\ddagger$  vs  $\Delta S^\ddagger$  is  $T$ . This is the value of the absolute temperature at which all the reactions represented on the line occur at the same rate and is termed the *isokinetic temperature*,  $T$ . Although there are a large number of such plots recorded in the literature, the mechanistic information extractable from them is limited. Linear plots for  $\Delta H^\ddagger$  vs  $\Delta S^\ddagger$  hold for a large number of redox reactions involving actinide ions,<sup>175</sup> for substitution at Pt(II) centers, Sec. 4.6.2, interaction of  $\text{CrOH}^{2+}$  with a number of ligands,<sup>176</sup> exchange of oxoanions with  $\text{H}_2\text{O}$ ,<sup>177</sup> formation and decarboxylation of metal carbonate complexes (seventeen reactions),<sup>135</sup> reactions of Fe(III) with hydroxamic acid derivatives,<sup>144</sup> and dissociation of Ni(II) macrocycles in 1 M HCl.<sup>178</sup> A common mechanism for each reaction series is supported. Enthusiasm for the mechanistic value of the concept should be tempered by considering the following: there is a striking correlation of  $\Delta H^\ddagger$  and  $\Delta S^\ddagger$  for second-order electron transfer reactions involving a number of metalloproteins with inorganic complexes. The linear isokinetic plot does *not* depend on whether the reaction is outer- or inner-sphere, on the protein charge, or on the magnitude of the rate constant or the driving force! The charge of the inorganic reactant only is important.<sup>179</sup>

### 2.8.2 $\Delta S^\ddagger$ and $\Delta V^\ddagger$ Values

These parameters often parallel one another since they are related to similar characteristic of the system (change in number of particles involved in the reaction etc.). The catalyzed hydrolysis of  $\text{Cr}_2\text{O}_7^{2-}$  by a number of bases is interpreted in terms of a bimolecular ( $I_a$ ) mechanism, and both  $\Delta S^\ddagger$  and  $\Delta V^\ddagger$  values are negative.<sup>165</sup> In contrast the aquation of  $\text{Co}(\text{NH}_2\text{CH}_3)_5\text{L}^{3+}$  ( $\text{L}$  = neutral ligands) is attended by positive  $\Delta S^\ddagger$  and  $\Delta V^\ddagger$  values. The steric acceleration noted for these complexes (when compared with the rates for the ammonia analogs) is attributed to an  $I_d$  mechanism.<sup>117</sup> There is a remarkably linear  $\Delta V^\ddagger$  vs  $\Delta S^\ddagger$  plot for racemization and geometric isomerization of octahedral complexes when dissociative or associative mechanisms prevail, but not when twist mechanisms are operative (Fig. 2.15).<sup>180</sup> For other examples of parallel  $\Delta S^\ddagger$  and  $\Delta V^\ddagger$  values, see Refs. 103 and 181. In general  $\Delta V^\ddagger$  is usually the more easily understandable, calculable and accurate parameter and  $\Delta V^\ddagger$  is



**Fig. 2.15** Plot of  $\Delta S^\ddagger$  ( $\text{J K}^{-1} \text{mol}^{-1}$ ) vs  $\Delta V^\ddagger$  ( $\text{cm}^3 \text{mol}^{-1}$ ) for racemization and geometrical isomerization of a variety of octahedral metal complexes. Only a few entries are selected from the 27 reactions tabulated in Ref. 180. The deviation of (four) Cr(III) complexes represented by  $\text{Cr}(\text{phen})_3^{3+}$  (3) from the linear plot (best fit for 23 complexes) may indicate that these racemize by twist, and not dissociative, mechanisms. Racemization of  $\text{Cr}(\text{C}_2\text{O}_4)_3^{3-}$  (1),  $\text{Co}(\text{Ph}_2\text{dtc})_3$  (2),  $\text{Cr}(\text{phen})_3^{3+}$  (3),  $\text{Ni}(\text{phen})_3^{2+}$  (4). Geometrical isomerization of *trans*- $\text{Cr}(\text{C}_2\text{O}_4)_2(\text{H}_2\text{O})_2^-$  (5), *trans*- $\text{Co}(\text{en})_2(\text{H}_2\text{O})_2^{2+}$  (6),  $\beta\text{-Co}(\text{edda})\text{en}^+$  (7).

more likely than  $\Delta S^\ddagger$  to give consistent data for a series of reactions of similar mechanism. Thus the reaction in dmf of  $\text{Ni}(\text{dmf})_6^{2+}$  with 5 different ligands gives positive  $\Delta V^\ddagger$  values ranging from 8.8 to 12.4  $\text{cm}^3 \text{mol}^{-1}$ , whereas  $\Delta S^\ddagger$  values span the range +63 to  $-82 \text{ J K}^{-1} \text{mol}^{-1}$ . The mechanism is considered dissociative (*D*).<sup>182</sup>

### 2.8.3 Use of All Parameters

A careful compilation of as many kinetic parameters as possible can lead to overwhelming support for a mechanism. Only occasionally are such comprehensive data available. The occurrence is nicely illustrated by the exchange reaction ( $M = \text{Nb, Ta and Sb}$ ;  $X = \text{Cl and Br}$ ;  $L =$  variety of neutral ligands):



A few data (Table 2.5) are taken from a comprehensive compilation so as to illustrate the major points.<sup>104,183</sup>

**Table 2.5.** Exchange Data for (2.176) at 0°C in  $\text{CH}_2\text{Cl}_2$

$\text{MX}_5$	L	Rate Law (order)	$k$	$\Delta H^\ddagger$ $\text{kJ mol}^{-1}$	$\Delta S^\ddagger$ $\text{J K}^{-1} \text{mol}^{-1}$	$\Delta V^\ddagger$ $\text{cm}^3 \text{mol}^{-1}$
TaCl <sub>5</sub>	Me <sub>2</sub> O	1st	0.7 s <sup>-1</sup>	83	+59	+28
TaBr <sub>5</sub>	Me <sub>2</sub> O	1st	54 s <sup>-1</sup>	74	+62	+31
TaCl <sub>5</sub>	Me <sub>2</sub> S	2nd	10 <sup>3</sup> M <sup>-1</sup> s <sup>-1</sup>	22	-108	-20
TaBr <sub>5</sub>	Me <sub>2</sub> S	2nd	90 M <sup>-1</sup> s <sup>-1</sup>	29	-102	-13

With the first two entries the exchange is first-order (rate independent of [L]) and  $\Delta H^\ddagger$ ,  $\Delta S^\ddagger$  and  $\Delta V^\ddagger$  are markedly larger or more positive than with the third and fourth entries for which the rate law is second-order. Consideration of the magnitudes of the values, particularly  $\Delta V^\ddagger$ , lead the authors to assign a *D* mechanism to the first two exchanges and an *I<sub>a</sub>* (or possibly *A*) mechanism to the other two. Even steric acceleration and retardation for the two groups is observed.<sup>104,183</sup>

## 2.9 Medium Effects on the Rate

The effect of the medium on the rate of a reaction does not usually play an important role in the deduction of mechanism. However it is vital that its impact on rate is always assessed.

### 2.9.1 The Effect of Electrolytes

The rate constant for a reaction is obtained by working at constant ionic strength or alternatively by extrapolating data obtained at different ionic strengths to zero or occasionally “infinite” ionic strength.<sup>184</sup> This procedure is necessitated by the fact that ions (derived both



from the reactants and from added electrolytes) often affect the rate of a reaction. This must be allowed for, or removed by “swamping” with electrolyte, in the derivation of a true rate law. The effect of ions on the rate constant for a reaction is easily derived from the absolute reaction rate theory. Now (see Eqn. 2.117),

$$k = \frac{kT}{h} K_c^\ddagger \quad (2.177)$$

and

$$K_a^\ddagger = K_c^\ddagger \frac{f_{X^\ddagger}}{f_A f_B} \quad (2.178)$$

The terms  $K_a^\ddagger$  and  $K_c^\ddagger$  are “activity” and “concentration” equilibrium constants and  $f_{X^\ddagger}$ ,  $f_A$ , and  $f_B$  are activity coefficients of the activated complex and of the reactants. Thus,

$$k = \frac{kT}{h} K_a^\ddagger \frac{f_A f_B}{f_{X^\ddagger}} \quad (2.179)$$

This is equivalent to the earlier Brønsted-Bjerrum equation

$$k = k_0 \frac{f_A f_B}{f_X} \quad (2.180)$$

where  $k_0$  is the rate constant at zero ionic strength, and X is a “critical” complex, the forerunner of the activated complex. Now,<sup>185</sup>

$$-\log f_1 = \alpha z_1^2 F(\mu) \quad (2.181)$$

with  $\alpha = 0.52$  at 25°C and  $F(\mu)$  some function of the ionic strength  $\mu$ . Thus since the charge on  $AB^\ddagger = (z_A + z_B)$ ,

$$\log k = \log k_0 - (z_A^2 + z_B^2 - (z_A + z_B)^2) \alpha F(\mu) \quad (2.182)$$

leading to

$$\log k = \log k_0 + 2\alpha z_A z_B \mu^{1/2} \quad (2.183)$$

if the simple form  $F(\mu) = \mu^{1/2}$  is used, and

$$\log k = \log k_0 + \frac{2\alpha z_A z_B \mu^{1/2}}{1 + \mu^{1/2}} \quad (2.184)$$

if the extended form

$$F(\mu) = \frac{\mu^{1/2}}{1 + \mu^{1/2}} \quad (2.185)$$

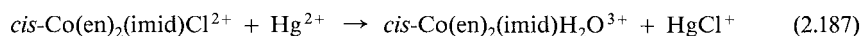
is substituted. Occasionally the expression

$$\log k = \log k_0 + \frac{2 \alpha z_A z_B \mu^{1/2}}{1 + \mu^{1/2}} - \beta \mu \quad (2.186)$$

is used where  $\alpha$  and  $\beta$  are treated as free parameters but maintained at approximate values of 0.5 and 0.1 respectively. The additional term helps correct for ion pairs.<sup>183</sup>

These equations have been used quite successfully for correlating salt effects with the rate constants for reactions involving ions, even at relatively high ionic strengths, (with the extended equation). They are the basis of the well-known Livingston and LaMer diagrams, in which plots of  $\log k$  vs  $\mu^{1/2}$  or  $\mu^{1/2}(1 + \mu^{1/2})^{-1}$  are linear, with slopes  $\sim z_A z_B$  and intercept values  $\log k_0$ .<sup>184</sup> The equations predict a positive salt effect (that is, an increasing rate constant with increasing salt concentration) when reactants have charges of the same sign and a negative salt effect when the charges are of opposite sign. For reactions between ions of unlike sign, (2.183) or (2.184) is usually reasonably obeyed, especially if uni-univalent electrolytes (often NaClO<sub>4</sub>) are used to adjust the ionic strength.<sup>126</sup> However if higher charged electrolytes are used<sup>186</sup> or reactions are carried out in nonaqueous solution, where ion-pairing is much more important,<sup>187</sup> then marked deviations from the expected behavior occur even for reactants of opposite charge. This is usually ascribed to the formation of ion pairs which will not only lead to reduction in the computed ionic strength but, more important, might very easily produce species (ion pairs) that will react with rate constants different from those for the constituent ions (for, at the least, Coulombic reasons). This effect can be accommodated by equating the observed rate constants to those for the free ions and for the ion pairs. The approach is detailed in studies of bivalent anion effects on the second-order reaction between Co(NH<sub>3</sub>)<sub>5</sub>Br<sup>2+</sup> and OH<sup>-</sup>,<sup>186,188</sup> and between FeBr<sub>4</sub><sup>-</sup> and Cl<sup>-</sup> in CH<sub>2</sub>Cl<sub>2</sub>.<sup>187</sup>

For reactions between ions of like sign, the dependence of rate constant on ionic strength is less straightforward. Now the rate is influenced by the concentration and nature of the supporting ion of opposite charge, *even at constant ionic strength*.<sup>184</sup> The ionic strength dependence of the Ru<sub>2</sub>(NH<sub>3</sub>)<sub>10</sub>pz<sup>5+</sup> - Ru(NH<sub>3</sub>)<sub>5</sub>py<sup>2+</sup> reaction does however conform very well to (2.184) when CF<sub>3</sub>SO<sub>3</sub><sup>-</sup> is used to adjust the ionic strength.<sup>189</sup> The rate constant for the reaction



is independent of [H<sup>+</sup>] from 0.3 to 1.0 M HClO<sub>4</sub> at constant ionic strength. It is however markedly dependent on the anion used to provide this medium.<sup>190</sup> The reactions of Cr<sub>2</sub>O<sub>7</sub><sup>2-</sup>, V<sub>10</sub>O<sub>28</sub><sup>6-</sup> and Mo<sub>7</sub>O<sub>24</sub><sup>6-</sup> with OH<sup>-</sup> are influenced by the cation present. The second-order rate constant (M<sup>-1</sup>s<sup>-1</sup>) for the Cr<sub>2</sub>O<sub>7</sub><sup>2-</sup>/OH<sup>-</sup> reaction changes from 7.6 × 10<sup>2</sup> (Na<sup>+</sup>) to 35 (Et<sub>4</sub>N<sup>+</sup>) at  $\mu = 1.0$  M.<sup>191</sup> These effects can be treated by the use of empirical expressions. Extended ones<sup>184</sup> such as

$$k = \frac{k_a + k_b[\text{B}] + k_c[\text{B}]^2}{1 + K_b[\text{B}] + K_c[\text{B}]^2} \quad (2.188)$$

where [B] is the formal concentration of the added ion, and  $k_a$ ,  $k_b$ ,  $k_c$ ,  $K_b$  and  $K_c$  are adjustable parameters, fit the extensive data on the effects of *cations* on the  $\text{Fe}(\text{CN})_6^{3-}$ ,  $\text{Fe}(\text{CN})_6^{4-}$  electron transfer.<sup>192</sup> A simpler form

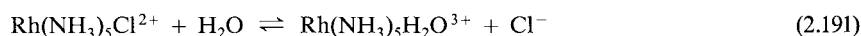
$$k = k_a + k_b [\text{B}] \quad (2.189)$$

takes care adequately of alkali metal cation effects on the manganate, permanganate exchange reaction. Activation parameters (including  $\Delta V^\ddagger$ ) values associated with the two terms are carefully analyzed.<sup>193</sup>

For the reaction between an ion and a dipolar molecule, the rate is largely uninfluenced by ionic strength. A relation of the type

$$\log k = \log k_0 - c\mu \quad (2.190)$$

sometimes holds. Thus the reversible hydrolysis



is attended by small ionic strength effects on the rate constants for the forward and large effects on the reverse direction.<sup>194</sup> The effect of ionic strength on reactions whose kinetic order is greater than two or non-simple has been considered, but is rarely used.<sup>184,195</sup>

When some dissipation of charge occurs as with larger reactants the assignment of charge to Eqn. (2.184) becomes difficult. For example, the reactions of porphyrins with peripheral charges (tpps $\text{H}_2^{2-}$  and tmpyp $\text{H}_2^{2+}$ ) give slopes for the Brønsted-Bjerrum plots of the expected sign, but with lower values than expected on the basis of (2.184). The marked effects of ionic strength on these reactions stress the importance of not using one set of conditions (e.g.  $\mu = 0.5 \text{ M}$ ) when comparing different and highly charged reactants. In addition specific salt effects of the type outlined above should be considered.<sup>195</sup>

The problem of the definition of charge and consideration of the sizes of reactants (the diameters of the reactant ions and the activated complex are assumed equal in the derivation of (2.184)) is most acute with reactions of metalloproteins. Probably the most used expression for the effect of ionic strength on such reactions is<sup>196</sup>

$$\ln k = \ln k_\infty - \frac{3.58 z_A z_B}{r_A + r_B} \left[ \frac{\exp(-\kappa r_A)}{1 + \kappa r_B} + \frac{\exp(-\kappa r_B)}{1 + \kappa r_A} \right] \quad (2.192)$$

where  $\kappa$  equals  $0.33 \mu^{1/2} \text{ \AA}^{-1}$  in  $\text{H}_2\text{O}$  at  $25^\circ\text{C}$ . The quantities  $r_A$  and  $r_B$  are the radii for the two reactants charges  $z_A$  and  $z_B$ . For proteins, molecular weight  $M$ ,  $r = 0.717 M^{1/3}$  is often used,<sup>197</sup> and  $k_\infty$  = rate constant at "infinite" ionic strength. In this latter condition the reactants are fully shielded from each other by electrolyte ions and this is an alternative approach to that of extrapolating to zero ionic strength so as to negate reactant-reactant interactions. With (2.192) also, increasing ionic strength gives increased  $k_{\text{obs}}$  for a reaction between similarly charged reactants. Agreement of (2.192) with experimental data has been observed in a number of systems, including the reaction of blue copper proteins with  $\text{Fe}(\text{edta})^{2-}$  ref. 197, cytochrome  $b_5$  (modified at the heme center) with  $\text{Fe}(\text{edta})^{2-}$  ref. 198 and a large

number of cytochromes with oxidizing and reducing anions.<sup>199,200</sup> Equations other than (2.192) and (2.184) have also been employed with variable success.<sup>199,200</sup> In many cases the use of the overall protein charge calculated from the pI value and the amino acid composition (which may range from +8 to -9<sup>200</sup>) fits the equation (2.192) and others well, particularly if low ionic strengths are used.<sup>196,199,200</sup>

*Charge on the protein* – An estimate of the charge on the protein may be made from a knowledge of the amino acid composition. At neutral pH, where the majority of the studies are carried out, the glutamates and aspartates are negative ions, the lysines are protonated, the histidines are half-protonated and the arginines are in a monocationic form. The charges on the metal ion and other ligand groups are also taken into account but are relatively unimportant. As an example, azurin (*P. aeruginosa*) has 11 Lys (11+), 1 Arg (1+), 2 His (1+), 4 Glu (4-), and 11 Asp (11-). If deprotonated amide and thiolate are ligands to the Cu(II) the metal site is zero-charged. The overall charge (2-) at pH ~7 is consistent with the pI value of 5.2. S. Wherland and H. B. Gray, in *Biological Aspects of Inorganic Chemistry*, Wiley-Interscience, New York, 1977, Chap. 10.

Equation (2.184) has rarely been used to determine the charge on one of the reactants since this is invariably known for small reactants. The value close to -6.0 for the slope of the plot of  $\log k$  against  $\mu^{1/2} (1 + \mu^{1/2})^{-1}$  for the reaction of a nickel(III) macrocycle (L) with  $\text{SO}_4^{2-}$  strongly supports a +3 charge for the complex and therefore its formulation as  $\text{Ni(L)}^{3+}$  rather than as  $\text{Ni(L)OH}^{2+}$  in the pH 3.2-4.7 range.<sup>201</sup> Charges have been assigned to  $\text{e}_{\text{aq}}^-$ ,  $\text{Cu}^+$  and  $\text{CrH}^{2+}$  on the basis of ionic strength effects on the rates of their reactions.<sup>202-204</sup> The assignment of charge with proteins is a complex subject. The charges on cytochrome  $c_{552}$  (pI = 5.5) and horse cytochrome (pI = 10.1) are negative and positive respectively in neutral pH. The effect of ionic strength on rate constants for electron transfer involving these proteins are as predicted using these charges. This tends to rule out the common heme moiety as the site for electron transfer since in that case a similar charge (that of the heme moiety) and therefore a similar effect of ionic strength on the rate constants for the two proteins might have been anticipated.<sup>200</sup> A positive patch (Sec. 5.9) on cytochrome *f* for binding of  $(\text{CN})_5\text{FeCNFe}(\text{CN})_5^-$  has been implicated by ionic strength effects.<sup>179</sup>

Ionic strength will also influence other rate parameters. Its effect on  $\Delta V^\ddagger$  is shown to be

$$\Delta V^\ddagger = -RT \left( \frac{d \ln k_0}{dP} \right) + X z_A z_B \quad (2.193)$$

X is a complex term containing  $\mu^{1/2}$ . At  $\mu = 0.1$  M,  $X = 0.62$ .  $k_0$  is the rate constant at  $\mu = 0$ . The increase of ionic strength produces a screening effect which decreases electrostriction and increases molal volumes. The effect is more important in reactions between like charges.<sup>205</sup>

### 2.9.2 The Effect of Electrolytes – Medium or Mechanistic?

The determination of the variation of the rate with the concentrations of ions in solution is the keystone to the rate law. It is apparent from the above discussion that one has to be cautioned that medium effects rather than definite reaction pathways might be responsible for this variation. For example the reaction of  $\text{Hg}^{2+}$  with *trans*- $\text{CrCl}_2^+$  studied at a constant ionic strength made up of  $\text{HClO}_4$  and  $\text{LiClO}_4$  shows decreasing values for the computed second-order rate constant ( $k$ ) with increasing concentrations of  $\text{Hg}^{2+}$ . This trend might reasonably be ascribed to the formation of appreciable amounts of an adduct such as  $\text{CrCl}_2\text{Hg}^{2+}$  (see Sec. 1.6.3 and 1.6.4). Addition of  $\text{Ba}^{2+}$  rather than  $\text{Li}^+$  to maintain the concentration of *dipositive ions constant* produces a constant  $k$  however and indicates that the variation in  $k$  observed using  $\text{Li}^+$  counter-ion, is a medium-based effect.<sup>206</sup> Distinguishing a mechanistic from a medium effect may be difficult and the problem has been most encountered when there is a relatively small influence of  $\text{H}^+$  on the rate. The dilemma arises because of the breakdown of the principle of constant ionic strength, particularly when large and highly charged ions are reactants.<sup>207</sup> The examining media  $\text{LiClO}_4 - \text{HClO}_4$  and also  $\text{LiCl} - \text{HCl}$  are particularly useful since activity coefficients of ionic species are reasonably constant in such mixtures at constant ionic strength.<sup>35</sup> Any observed  $\text{H}^+$  effects in these electrolyte media are more likely to arise from mechanistic pathways.<sup>208-210</sup> An allowance can be made for the effect of replacement by  $\text{H}^+$  of another ion, say  $\text{Na}^+$  or  $\text{Li}^+$ , in examining the effect of pH on the rate at a constant ionic strength.

The reduction of  $\text{Co}(\text{NH}_3)_5\text{H}_2\text{O}^{3+}$  ions by  $\text{Cr}(\text{II})$  has been examined in a  $\text{ClO}_4^-$  medium at  $\mu = 1.0 \text{ M}$  over an  $[\text{H}^+]$  range of 0.096–0.79 M, with the ionic medium held constant with  $\text{LiClO}_4$ .<sup>211</sup> The data (Table 2.6) could be interpreted in two ways. It could be as the result of a two-term rate law of the form

$$k = a + b [\text{H}^+]^{-1} \quad (2.194)$$

Least-square analysis yields a *negative* value for  $a = -0.72 \pm 0.14 \text{ M}^{-1}\text{s}^{-1}$  and for  $b = 3.12 \pm 0.05 \text{ s}^{-1}$ . Alternatively a single-term rate law in which the Harned correction term takes care of changing activity coefficient<sup>212</sup> could explain the data,

$$k = c [\text{H}^+]^{-1} \exp(-\beta [\text{H}^+]) \quad (2.195)$$

with  $c = 3.13 \pm 0.05 \text{ s}^{-1}$  and  $\beta = 0.25 \pm 0.05 \text{ M}^{-1}$ . The fit of Eqn. (2.195) to the data is very good (Table 2.6). The values of  $b$  and  $c$  in (2.194) and (2.195) are almost identical, so that there is no ambiguity in the rate constant for the hydroxo form in either formulation. Reactivity ascribable to the aqua form, negative in (2.194) or zero in (2.195), must in either case be very small.

One can usually be confident that  $\text{H}^+$ -containing terms in a rate law relate to a reaction pathway in a number of circumstances: (a) all the terms in the rate expression for the aquation of  $\text{Cr}(\text{H}_2\text{O})_5\text{N}_3^{2+}$

$$-d \ln [\text{CrN}_3^{2+}]/dt = k_1 [\text{H}^+] + k_0 + k_2 [\text{H}^+]^{-1} + k_3 [\text{H}^+]^{-2} \quad (2.196)$$

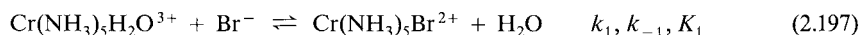
**Table 2.6.** Rate Constants for the Reduction of  $\text{Co}(\text{NH}_3)_5\text{H}_2\text{O}^{3+}$  by  $\text{Cr}^{2+}$  at Various  $[\text{H}^+]$  at  $25.1^\circ\text{C}$ <sup>211</sup>

$[\text{H}^+]$ , M	$k$ , $\text{M}^{-1}\text{s}^{-1}$	$k_{\text{calcd.}}$ , <sup>a</sup> $\text{M}^{-1}\text{s}^{-1}$
0.794	$3.39 \pm 0.03$	3.22
0.654	$4.06 \pm 0.04$	4.12
0.560	$4.83 \pm 0.03$	4.85
0.494	$5.43 \pm 0.02$	5.59
0.438	$6.53 \pm 0.04$	6.39
0.411	$7.51 \pm 0.16$	6.86
0.386	$6.72 \pm 0.21$	7.35
0.271	$10.9 \pm 0.1$	10.8
0.202	$14.9 \pm 0.1$	14.8
0.131	$23.3 \pm 0.2$	23.0
0.114	$27.1 \pm 0.3$	26.1
0.096	$31.6 \pm 2.5$	31.7

<sup>a</sup> Calculated from  $k = 3.13 [\text{H}^+]^{-1} \exp(-0.25 [\text{H}^+])$ .

can be important, contributing  $\geq 50\%$  towards the rate at different pH's, and are therefore unlikely to be due to medium effects<sup>213</sup> (b) a p*K* derived for a pH-dependent kinetic term (Sec. 1.10) agrees with a value determined spectrally<sup>35</sup> (c) the reduction of *cis*- $\text{Co}(\text{en})_2(\text{HCO}_2)_2^+$  by  $\text{Cr}^{2+}$  is *inhibited* by acid and the hydrolysis of the Co(III) complex is *enhanced* thereby. Similar p*K* values are derived in the two cases; these almost certainly cannot be due to medium effects.<sup>214</sup>

For the reaction



the value of  $K_1$  (estimated from the ratio  $k_1/k_{-1}$  ( $0.30 \text{ M}^{-1}$ )) is much larger than that determined by spectral analysis of equilibrated mixtures ( $0.02 \text{ M}^{-1}$ ) even though the ionic strengths are similar ( $\mu = 0.8\text{--}1.0 \text{ M}$  at  $25^\circ\text{C}$ ). The difference has been experimentally verified and arises from medium and specific ion effects. The value of  $K_1$  estimated at equilibrium varies with  $[\text{Br}^-]$  even if the ionic strength is maintained constant with  $\text{Br}^-/\text{ClO}_4^-$  mixtures. The discrepancy is only important because of the high reactant concentrations ( $[\text{Br}^-] \approx [\text{ClO}_4^-]$ ) which are necessary with (2.197) to effect substantial change in a reaction with a relatively small  $K_1$ .<sup>215</sup>

### 2.9.3 The Solvent Effect and Mechanism

We can arbitrarily divide solvents into three categories: *protic*, including both proton donors and acceptors; *dipolar aprotic*, solvents with dielectric constants  $>15$  but without hydrogen capable of forming hydrogen bonds; and *aprotic*, having neither acidic nor basic properties, for example,  $\text{CCl}_4$ .<sup>216</sup> These may be expected to interact in widely different ways with complex ions containing large internal charges. The effect of solvent on the rates of reactions has been extensively explored. As a means of interpreting mechanisms it has had variable success, but complex ions have proved to be valuable substrates for examining solvent structural

features.<sup>217</sup> There are basically two ways in which the solvent may be regarded, although assessing their distinction and relative importance is very difficult.

(a) The solvent may be regarded as an “inert” medium. In this case, the dielectric constant of the solvent is the most important parameter although viscosity may play an important role.<sup>218</sup> The dielectric effect can be semiquantitatively evaluated for ion-ion or ion-dipolar reactant mixtures, where electrostatic considerations dominate.

For a reaction between two ions, of charge  $z_A$  and  $z_B$ , the rate constant  $k$  (reduced to zero ionic strength) is given by

$$\ln k = \ln k_0 - \frac{e^2}{2DkT} \left[ \frac{(z_A + z_B)^2}{r_{\ddagger}} - \frac{z_A^2}{r_A} - \frac{z_B^2}{r_B} \right] \quad (2.198)$$

where  $k_0$  is the hypothetical rate constant in a medium of infinite dielectric constant,  $D$  is the dielectric constant, and  $r_A$ ,  $r_B$ , and  $r_{\ddagger}$  are the radii of the reactant ions A and B and the activated complex respectively.

If  $r_A = r_B = r_{\ddagger}$ , (2.198) becomes

$$\ln k = \ln k_0 - \frac{z_A z_B e^2}{DkT r_{\ddagger}} \quad (2.199)$$

and in a reaction between an ion  $z_A$  and a polar molecule (that is,  $z_B = 0$ ), (2.198) becomes

$$\ln k = \ln k_0 + \frac{z_A^2 e^2}{2DkT} \left[ \frac{1}{r_A} - \frac{1}{r_{\ddagger}} \right] \quad (2.200)$$

There should be a linear plot of  $\log k$  vs  $1/D$  with a negative slope if the charges of the ions are of the same sign and with a positive slope if the ions are oppositely charged. For the reaction of an ion and a polar molecule (common with solvolysis reactions), the linear plot of  $\log k$  vs  $1/D$  will have a positive slope irrespective of the charge of the ion since  $(1/r_A - 1/r_{\ddagger})$  is positive.

These expressions appear more applicable to nonpolar solvents or mixtures than to polar solvents. The nature of the solvation process (and the radii and so forth of the solvated reactants) may stay approximately constant in the first situation but almost certainly will not in the second. The function  $(D_{\text{op}}^{-1} - D_s^{-1})$  features in the reorganisation term  $\lambda_0$  which is used for estimating rate constants for redox reactions (Eqn. 5.23).  $D_{\text{op}}$  is the optical dielectric constant and  $D_s$  the static dielectric constant (= refractive index<sup>2</sup>).

(b) The solvent may act as a nucleophile and an active participator in the reaction. It is extremely difficult to assess the function of the solvent in solvolysis reactions. Some attempts to define the mechanism for the replacement of ligand by solvent in octahedral complexes have been made using mixed solvents (Sec. 4.2.1) or the solvating power concept.<sup>219</sup>

The rate of solvolysis ( $k_s$ ) of *tert*-butyl chloride in a particular solvent S compared with the rate ( $k_0$ ) in 80% v/v aqueous ethanol is used as a measure of that solvent's ionizing power,  $Y_s$ :

$$Y_s = \log \frac{k_s}{k_0} \quad (2.201)$$

For any other substrate acting by an  $S_N1$  mechanism, it might be expected that

$$\log \frac{k_s}{k_0} = mY_s \quad (2.202)$$

where  $m$  depends on the substrate, and equals 1.0 for  $t$ -BuCl. It has not proved very useful as diagnostic of mechanism e.g. for Hg(II)-assisted reactions.<sup>220</sup> More data and patterns of behavior are required before the concept is likely to be more valuable.

## References (B refers to Selected Bibliography)

- (a) J. F. Bunnett in B5, Chap. IV, From Kinetic Data to Reaction Mechanism  
(b) J. H. Espenson in B5, Chap. VII, Homogeneous Inorganic Reactions.
- R. van Eldik in B17, Chap. 1.
- D. A. House and H. K. J. Powell, *Inorg. Chem.* **10**, 1583 (1971).
- J. L. Kurz, *Acc. Chem. Res.* **5**, 1 (1972).
- T. W. Newton and S. W. Rabideau, *J. Phys. Chem.* **63**, 365 (1959).
- A. Haim, *Prog. Inorg. Chem.* **30**, 299 (1983).
- P. Moore, S. F. A. Kettle and R. G. Wilkins, *Inorg. Chem.* **5**, 466 (1966).
- S. Funahashi, F. Uchida and M. Tanaka, *Inorg. Chem.* **17**, 2784 (1978).
- One useful definition of the rds is that for which a change in rate constant produces the largest effect on the overall rate, W. J. Ray, *Biochemistry*, **22**, 4625 (1983).
- E. J. Billo, *Inorg. Chem.* **23**, 2223 (1984).
- R. K. Steinhaus and B. I. Lee, *Inorg. Chem.* **21**, 1829 (1982).
- D. V. Stynes, S. Liu and H. Marcus, *Inorg. Chem.* **24**, 4335 (1985).
- Y. Sasaki, K. Z. Suzuki, A. Matsumoto and K. Saito, *Inorg. Chem.* **21**, 1825 (1982) and previous work cited.
- S. Fallab, *Adv. Inorg. Bioinorg. Mechs.* **3**, 311 (1984).
- S. C. F. Au-Yeung and D. R. Eaton, *Inorg. Chem.* **23**, 1517 (1984).
- H. J. Price and H. Taube, *J. Amer. Soc.* **89**, 269 (1967).
- Q. H. Gibson, *Biochem. Soc. Trans.* **18**, 1 (1990); R. G. Wilkins, in *Oxygen Complexes and Oxygen Activation by Transition Metals*, A. E. Martell, ed. Plenum, 1988, p. 49.
- K. A. Jongeward, D. Magde, D. J. Taube, J. C. Marsters, T. G. Traylor and V. S. Sharma, *J. Amer. Chem. Soc.* **110**, 380 (1988) also use a four-state model, with higher rate constants for some steps.
- F. Basolo, P. H. Wilks, R. G. Pearson and R. G. Wilkins, *J. Inorg. Nucl. Chem.* **6**, 161 (1958).
- W. R. Mason, *Coordn. Chem. Revs.* **7**, 241 (1972).
- L. Drougge and L. I. Elding, *Inorg. Chim. Acta* **121**, 175 (1986).
- J. Halpern and M. Pribanić, *Inorg. Chem.* **9**, 2616 (1970).
- H. U. Blaser and J. Halpern, *J. Amer. Chem. Soc.* **102**, 1684 (1980).
- J. H. Baxendale and P. George, *Trans. Faraday Soc.* **46**, 736 (1950).
- G. Kramer, J. Patterson, A. Poë and L. Ng, *Inorg. Chem.* **19**, 1161 (1980).
- W. C. E. Higginson and A. G. Sykes, *J. Chem. Soc.* 2841 (1962).
- N. A. Dougherty and T. W. Newton, *J. Phys. Chem.* **68**, 612 (1964).
- G. A. Tondreau and R. G. Wilkins, *Inorg. Chem.* **25**, 2745 (1986).
- Derived in B8, p. 79–80.
- For the derivation in a similar scheme  $Mn_2(CO)_{10} \rightleftharpoons 2 Mn(CO)_5^{\ddagger}; Mn(CO)_5^{\ddagger} + O_2 \rightarrow \text{products}$ ; see J. P. Fawcett, A. Poë and K. R. Sharma, *J. Amer. Chem. Soc.* **98**, 1410 (1976).



31. L. W. Wilson and R. D. Cannon, *Inorg. Chem.* **24**, 4366 (1985) and earlier references.
32. For the derivation for a related scheme see B8, p. 135.
33. A. S. Goldman and J. Halpern, *J. Amer. Chem. Soc.* **109**, 7537 (1987) for rate laws containing  $+1/2$  and  $-1/2$  exponents.
34. M. A. -Halabi, J. D. Atwood, N. P. Forbus and T. L. Brown, *J. Amer. Chem. Soc.* **102**, 6248 (1980).
35. E. Deutsch and H. Taube, *Inorg. Chem.* **7**, 1532 (1968).
36. K. M. Jones and J. Bjerrum, *Acta Chem. Scand.* **19**, 974 (1965).
37. S. F. Lincoln and D. R. Stranks, *Aust. J. Chem.* **21**, 67 (1968).
38. The second term could also be expressed as  $(k_2/K_w)[\text{Fe(III)}][\text{Cl}^-][\text{OH}^-]$ . In keeping with the tendency of expressing the rate law in terms of the predominant species, the form shown is preferred for data in acid medium.
39. S. L. Bruhn, A. Bakač and J. H. Espenson, *Inorg. Chem.* **25**, 535 (1986).
40. M. Orhanović and R. G. Wilkins, *J. Amer. Chem. Soc.* **89**, 278 (1967).
41. D. Seewald and N. Sutin, *Inorg. Chem.* **2**, 643 (1963).
42. J. H. Espenson and S. R. Helzer, *Inorg. Chem.* **8**, 1051 (1969).
43. R. B. Wilhelmy, R. C. Patel, and E. Matijević, *Inorg. Chem.* **24**, 3290 (1985).
44. K. Ishihara, S. Funahashi and M. Tanaka, *Inorg. Chem.* **22**, 194 (1983); with Fe(III) complexing with 4-isopropyltropolone, the assessment is made on the basis of  $\Delta V^\ddagger$  values.
45. C. P. Brink and A. L. Crumbliss, *Inorg. Chem.* **23**, 4708 (1984).
46. J. H. Espenson, *Inorg. Chem.* **8**, 1554 (1969).
47. B. Perlmutter-Hayman and E. Tapuhi, *Inorg. Chem.* **16**, 2742 (1977).
48. A. Campisi and P. A. Tregloan, *Inorg. Chim. Acta* **100**, 251 (1985).
49. P. W. Taylor, R. W. King, and A. S. V. Bergen, *Biochemistry* **9**, 3894 (1970).
50. R. G. Pearson, *J. Chem. Educ.* **55**, 720 (1978).
51. J. H. Espenson, *Inorg. Chem.* **4**, 1025 (1965); A. Adin and A. G. Sykes, *J. Chem. Soc. A* 351 (1968).
52. F. P. Rotzinger, *Inorg. Chem.* **25**, 4870 (1986).
53. D. H. Huchital and J. Lepore, *Inorg. Chem.* **17**, 1134 (1978).
54. J. Phillips and A. Haim, *Inorg. Chem.* **19**, 1616 (1980).
55. A. G. Sykes, *Chem. Soc. Revs.* **14**, 283 (1985).
56. M. L. Bender in *Investigation of Rates and Mechanisms of Reactions, Part I*, S. L. Friess, E. S. Lewis and A. Weissberger, eds. Interscience, NY, 1961, Chap. 25.
57. T. W. Newton and F. B. Baker, *Inorg. Chem.* **3**, 569 (1964).
58. P. B. Sigler and B. J. Masters, *J. Amer. Chem. Soc.* **79**, 6353 (1957).
59. G. Czapski, B. H. J. Bielski and N. Sutin, *J. Phys. Chem.* **67**, 201 (1963).
60. E. Saito and B. H. J. Bielski, *J. Amer. Chem. Soc.* **83**, 4467 (1961).
61. R. N. F. Thorneley and D. J. Lowe, in *Molybdenum Enzymes*, T. G. Spiro, ed. Wiley-Interscience, NY, 1985, Chap. 5.
62. D. S. Sigman, *J. Amer. Chem. Soc.* **102**, 5421 (1980).
63. A. Bakač, J. H. Espenson, I. I. Creaser and A. M. Sargeson, *J. Amer. Chem. Soc.* **105**, 7624 (1983).
64. E. Janssen, in *Free Radicals in Biology 4*, W. A. Pryor, ed. Academic, NY, 1980, p. 115.
65. C. R. Johnson, T. K. Myser and R. E. Shepherd, *Inorg. Chem.* **27**, 1089 (1988) for studying  $\text{OH}^\bullet$  production from complexes and  $\text{H}_2\text{O}_2$  or  $\text{O}_2$ .
66. N. E. Dixon, W. G. Jackson, W. Marty and A. M. Sargeson, *Inorg. Chem.* **21**, 688 (1982). ( $\text{N}_3^-$ )
67. W. G. Jackson, M. L. Randall, A. M. Sargeson and W. Marty, *Inorg. Chem.* **22**, 1013 (1983). ( $\text{NO}_2^-$ )
68. W. G. Jackson, D. P. Fairlie and M. L. Randall, *Inorg. Chim. Acta* **70**, 197 (1983). ( $\text{S}_2\text{O}_3^{2-}$ )
69. W. G. Jackson and C. N. Hookey, *Inorg. Chem.* **23**, 668 (1984). ( $\text{SCN}^-$ )
70. Z. Khurram, W. Böttcher and A. Haim, *Inorg. Chem.* **24**, 1966 (1985).
71. D. A. Buckingham, I. I. Olsen and A. M. Sargeson, *Aust. J. Chem.* **20**, 597 (1967).
72. N. E. Brasch, D. A. Buckingham, C. R. Clark and K. S. Finnie, *Inorg. Chem.* **28**, 3386 (1989).
73. D. J. Darensbourg, *Adv. Organomet. Chem.* **21**, 113 (1982).

74. R. K. Murmann and H. Taube, *J. Amer. Chem. Soc.* **78**, 4886 (1956).
75. R. van Eldik, J. von Jouanne and H. Kelm, *Inorg. Chem.* **21**, 2818 (1982).
76. W. G. Jackson, G. A. Lawrance, P. A. Lay and A. M. Sargeson, *J. Chem. Soc. Chem. Commun.* 70 (1982).
77. S. Fallab, H. P. Hunold, M. Maeder and P. R. Mitchell, *J. Chem. Soc. Chem. Commun.* 469 (1981).
78. S. Fallab and P. R. Mitchell, *Adv. Inorg. Bioinorg. Mech.* **3**, 311 (1984).
79. N. J. Coville, A. M. Stolzenberg and E. L. Muetterties, *J. Amer. Chem. Soc.* **105**, 2499 (1983).
80. W. H. Saunders, Jr., in B5, Chap. VIII.
81. J. P. Candlin and J. Halpern, *J. Amer. Chem. Soc.* **85**, 2518 (1963).
82. H. Taube, *Electron Transfer Reactions of Complex Ions in Solution*, Academic, NY, 1970, p. 92.
83. N. V. Breznjak and M. Z. Hoffman, *Inorg. Chem.* **18**, 2935 (1979).
84. M. S. Thompson and T. J. Meyer, *J. Amer. Chem. Soc.* **104**, 4106 (1982).
85. J. T. Chen and J. H. Espenson, *Inorg. Chem.* **22**, 1651 (1983).
86. H. Kwart, *Acc. Chem. Res.* **15**, 401 (1982).
87. C. B. Grissom and W. W. Cleland, *J. Amer. Chem. Soc.* **108**, 5582 (1986).
88. D. L. Leussing and M. J. Emly, *J. Amer. Chem. Soc.* **106**, 443 (1984).
89. J. N. Armor and H. Taube, *J. Amer. Chem. Soc.* **92**, 2561 (1970).
90. S. Arrhenius, *Z. Phys. Chem.* **4**, 226 (1889).
91. A. E. Merbach, P. Moore, O. W. Howarth and C. H. McAteer, *Inorg. Chim. Acta* **39**, 129 (1980).  
The wide temperature range used to study the  $\text{Ga}(\text{dmsO})_6^{3+}$ -dmsO exchange improves markedly the accuracy of the derived activation parameters.
92. J. V. Beitz, J. R. Miller, H. Cohen, K. Wieghardt, and D. Meyerstein, *Inorg. Chem.* **19**, 966 (1980).  
The formation and breakdown of the radical anion  $\text{Co}(\text{NH}_3)_5(\text{p-NO}_2\text{C}_6\text{H}_4\text{CO}_2^-)^{2+}$  obeys Arrhenius from 200 to 300 K in 50%  $\text{H}_2\text{O}$ /ethyleneglycol.
93. For a full account see B11, Chap. 5, and B20, pp. 62–73, 109; also S. Glasstone, K. J. Laidler and H. Eyring, *The Theory of Rate Processes*, McGraw-Hill, NY, 1941; M. M. Kreevoy and D. G. Truhlar, in B5, Chap. 1.
94. K. E. Newman, F. K. Meyer and A. E. Merbach, *J. Amer. Chem. Soc.* **101**, 1470 (1979); A. E. Merbach, *Pure Appl. Chem.* **59**, 161 (1987).
95. C. H. McAteer and P. Moore, *J. Chem. Soc. Dalton Trans.* 353 (1983).
96. G. Kohnstam, *Adv. Phys. Org. Chem.* **5**, 121 (1967), for a discussion of heat capacities of activation and their uses in mechanistic studies.
97. J. R. Hulett, *Quart. Rev.* **18**, 227 (1964).
98. W. E. Jones, R. B. Jordan and T. W. Swaddle, *Inorg. Chem.* **8**, 2504 (1969).
99. J. F. Bunnett, in B5, Chap. 4.
100. C. Blakeley and M. L. Tobe, *J. Chem. Soc. Dalton Trans.* 1775 (1987). There is however no variation of  $\Delta V^\ddagger$  with temperature, which is puzzling; V. Kitamura, G. A. Lawrance and R. van Eldik, *Inorg. Chem.* **28**, 333 (1989).
101. S. A. Kretchmar and K. N. Raymond, *J. Amer. Chem. Soc.* **108**, 6212 (1986); *Inorg. Chem.* **27**, 1436 (1988).
102. F. C. Xu, H. R. Krouse, and T. W. Swaddle, *Inorg. Chem.* **24**, 267 (1985).
103. H. R. Hunt and H. Taube, *J. Amer. Chem. Soc.* **80**, 2642 (1958).
104. A. E. Merbach, *Pure Appl. Chem.* **54**, 1479 (1982).
105. Y. Ducommun and A. E. Merbach in B17, Chap. 2.
106. R. van Eldik, T. Asano and W. J. Le Noble, *Chem. Revs.* **89**, 549 (1989).
107. P. Moore, *Pure Appl. Chem.* **57**, 347 (1985).
108. M. Kotowski and R. van Eldik, *Coordn. Chem. Revs.* **93**, 19 (1989) for a succinct account of high pressure equipment used in various techniques.
109. S. D. Hamann and W. J. Le Noble, *J. Chem. Educ.* **61**, 658 (1984).
110. J. K. Beattie, M. T. Kelso, W. E. Moody and P. A. Tregloan, *Inorg. Chem.* **24**, 415 (1985).

111. Y. Ducommun, P. J. Nichols and A. E. Merbach, *Inorg. Chem.* **28**, 2643 (1989).
112. D. Kost and A. Pross, *Educ. in Chem.* **14**, 87 (1977).
113. J. R. Murdoch, *J. Chem. Educ.* **58**, 32 (1981).
114. T. W. Swaddle, *J. Chem. Soc. Chem. Commun.* 832 (1982).
115. T. W. Swaddle, *Adv. Inorg. Bioinorg. Mech.* **2**, 95 (1983).
116. P. A. Lay, *Inorg. Chem.* **26**, 2144 (1987).
117. N. J. Curtis and G. A. Lawrance, *Inorg. Chem.* **25**, 1033 (1986).
118. R. M. Krupka, H. Kaplan and K. J. Laidler, *Trans. Faraday Soc.* **62**, 2754 (1966). R. L. Burwell, Jr. and R. G. Pearson, *J. Phys. Chem.* **70**, 300 (1966).
119. F. Monacelli, F. Basolo and R. G. Pearson, *J. Inorg. Nucl. Chem.* **24**, 1241 (1962).
120. N. J. Curtis, *Inorg. Chem.* **25**, 1033 (1986).
121. P. A. Lay, *Inorg. Chem.* **26**, 2144 (1987).
122. L. Mønsted and O. Mønsted, *Coordn. Chem. Revs.* **94**, 109 (1989).
123. C. A. Tolman, *Chem. Revs.* **77**, 313 (1977). Ligand intermeshing must also be considered; H. C. Clark, *Isr. J. Chem.* **15**, 210 (1977).
124. D. J. Darensbourg and A. H. Graves, *Inorg. Chem.* **18**, 1257 (1979).
125. A. Bakac and J. H. Espenson, *J. Amer. Chem. Soc.* **108**, 713 (1986).
126. D. A. House, *Inorg. Chim. Acta*, **51**, 273 (1981).
127. E. S. Lewis in B5, Chap. 13.
128. C. H. Langford, *Inorg. Chem.* **4**, 265 (1965); A. Haim, *Inorg. Chem.* **9**, 426 (1970).
129. D. R. Prasad, T. Ramasami, D. Ramasamy and M. Santappa, *Inorg. Chem.* **21**, 850 (1982) – These unusually rapid reactions of Cr(III) are promoted by lengthening (distortion) of the axial water and thus enhancing the dissociative character. They are *not* typical of Cr(III) behavior.
130. B. G. Cox, J. Garcia-Ross and H. Schneider, *J. Amer. Chem. Soc.* **103**, 1054 (1981).
131. D. J. Cram and G. M. Lein, *J. Amer. Chem. Soc.* **107**, 3657 (1985).
132. D.-T. Wu and C.-S. Chung, *Inorg. Chem.* **25**, 4841 (1986).
133. R. Marcus, *Ann. Rev. Phys. Chem.* **15**, 155 (1964).
134. E. Pelizzetti and E. Mentasti, *Inorg. Chem.* **18**, 583 (1979).
135. R. van Eldik, D. A. Palmer, H. Kelm and G. M. Harris, *Inorg. Chem.* **19**, 3679 (1980).
136. E. Kremer, G. Cha, M. Morkevicius, M. Seaman, and A. Haim, *Inorg. Chem.* **23**, 3028 (1984).
137. S. Goldstein and G. Czapski, *Inorg. Chem.* **24**, 1087 (1985).
138. C. Hansch, A. Leo and R. W. Taft, *Chem. Revs.* **91**, 165 (1991).
139. F. Aprile, V. Cagliotti and G. Illuminati, *J. Inorg. Nucl. Chem.* **21**, 325 (1961).
140. A. Bakač, V. Butković, J. H. Espenson, R. Marcec and M. Orhanovic, *Inorg. Chem.* **25**, 2562 (1986).
141. J. P. Leslie and J. H. Espenson, *J. Amer. Chem. Soc.* **98**, 4839 (1976).
142. R. J. Mureinik, M. Weitzberg and J. Blum, *Inorg. Chem.* **18**, 915 (1979).
143. S. S. Eaton and G. R. Eaton, *Inorg. Chem.* **16**, 72 (1977).
144. C. P. Brink and A. L. Crumbliss, *Inorg. Chem.* **23**, 4708 (1984). A number of LFER are included with a short discussion of the strict statistical criteria for isokinetic relationships.
145. R. W. Taft, *J. Amer. Chem. Soc.* **75**, 4231 (1953).
146. S. Steenken and P. Neta, *J. Amer. Chem. Soc.* **104**, 1244 (1982).
147. R. S. Berman and J. K. Kochi, *Inorg. Chem.* **19**, 248 (1980).
148. D. F. DeFar, *J. Amer. Chem. Soc.* **102**, 7988 (1980).
149. H. Cohen, S. Efrima, D. Meyerstein, M. Nutkovich and K. Wiegardt, *Inorg. Chem.* **22**, 688 (1983).
150. J. N. Brønsted and K. J. Pederson, *Z. Phys. Chem.* **108**, 185 (1924).
151. R. Bahwad, B. Perlmutter-Hayman and M. A. Wolff, *J. Phys. Chem.* **73**, 4391 (1969), and references therein.
152. B. G. Cox and H. Schneider, *J. Amer. Chem. Soc.* **102**, 3628 (1980).
153. M. Eigen, *Angew. Chem. Int. Ed. Engl.* **3**, 1 (1964).
154. D. A. Buckingham, C. R. Clark and T. W. Lewis, *Inorg. Chem.* **18**, 2041 (1979).

155. R. S. Rowlett and D. N. Silverman, *J. Amer. Chem. Soc.* **104**, 6737 (1982); D. N. Silverman and S. Lindskog, *Accs. Chem. Res.* **21**, 30 (1988).
156. C. G. Swain and C. B. Scott, *J. Amer. Chem. Soc.* **75**, 141 (1953).
157. G. Annibale, L. Canovese, L. Cattalini, G. Marangoni, G. Michelon and M. L. Tobe, *Inorg. Chem.* **20**, 2428 (1981).
158. M. Becker and H. Elias, *Inorg. Chim. Acta* **116**, 47 (1986).
159. Q.-Z. Shi, T. G. Richmond, W. C. Trogler and F. Basolo, *J. Amer. Chem. Soc.* **106**, 71 (1984).
160. M. L. Tobe, *Inorg. Chem.* **7**, 1260 (1968).
161. M. Nishizawa, Y. Sasaki and K. Saito, *Inorg. Chem.* **24**, 767 (1985).
162. N. A. Daugherty and J. K. Erbacher, *Inorg. Chem.* **14**, 683 (1975).
163. J. Burgess, A. J. Duffield and R. Sherry, *J. Chem. Soc. Chem. Commun.* 350 (1980). It is difficult to rationalize  $\Delta V_{\text{obs}}^{\ddagger}$  values of  $\sim 20 \text{ cm}^3 \text{ mol}^{-1}$  with an associative mechanism for nucleophiles reacting with low spin Fe(II) diimine complexes. This value however represents a balance between contributions from  $\Delta V_{\text{intr}}^{\ddagger}$  (negative) and anion desolvation in forming activated complex (positive  $\Delta V^{\ddagger}$ ).
164. I. Krack and R. van Eldik, *Inorg. Chem.* **25**, 1743 (1986).
165. P. Moore, Y. Ducommun, P. J. Nichols and A. E. Merbach, *Helv. Chim. Acta* **66**, 2445 (1983).
166. E. F. Caldin and R. C. Greenwood, *J. Chem. Soc. Faraday Trans. I*, **77**, 773 (1981).
167. J. G. Leipoldt, R. van Eldik and H. Kelm, *Inorg. Chem.* **22**, 4146 (1983).
168. G. A. Lawrance and D. R. Stranks, *Inorg. Chem.* **16**, 929 (1977).
169. J. J. McGarvey, I. Lawthers, K. Heremans and H. Tofflund, *J. Chem. Soc. Chem. Commun.* 1575 (1984). See also J. DiBenedetto, V. Arkle, H. A. Goodwin and P. C. Ford, *Inorg. Chem.* **24**, 455 (1985).
170. U. Spitzer, R. van Eldik and H. Kelm, *Inorg. Chem.* **21**, 2821 (1982).
171. Y. Kitamura, R. van Eldik and H. Kelm, *Inorg. Chem.* **23**, 2038 (1984).
172. T. Inoue, K. Sugahara, K. Kojima and R. Shimozawa, *Inorg. Chem.* **22**, 3977 (1983).
173. A comprehensive collection of volume profiles and their value is contained in Ref. 106.
174. R. van Eldik, *Angew. Chem. Int. Ed. Engl.* **25**, 673 (1986).
175. T. W. Newton and F. B. Baker, *Adv. Chem.* **71**, 268 (1967).
176. D. Thusius, *Inorg. Chem.* **10**, 1106 (1971).
177. H. von Felten, B. Wernli, H. Gamsjäger and P. Baertschi, *J. Chem. Soc. Dalton Trans.* 496 (1978).
178. A. Ekstrom, L. F. Lindoy and R. J. Smith, *Inorg. Chem.* **19**, 724 (1980).
179. D. B.-Betts and A. G. Sykes, *Inorg. Chem.* **24**, 1142 (1985).
180. G. A. Lawrance and S. Suvachittanont, *Inorg. Chim. Acta* **32**, L13 (1979).
181. F. K. Meyer, W. L. Earl and A. E. Merbach, *Inorg. Chem.* **18**, 888 (1979).
182. P. J. Nichols, Y. Fresard, Y. Ducommun and A. E. Merbach, *Inorg. Chem.* **23**, 4341 (1984).
183. H. Vanni and A. E. Merbach, *Inorg. Chem.* **18**, 2758 (1979).
184. A. D. Pethybridge and J. E. Prue, *Inorganic Reaction Mechanisms, Part 2*, p. 327, for a comprehensive account.
185. Again we use decadic logarithms because of traditional and current usage.
186. P. B. Abdullah and C. B. Monk, *J. Chem. Soc. Dalton Trans.* 1175 (1983) and previous studies.
187. G. P. Algra and S. Balt, *Inorg. Chem.* **20**, 1102 (1981).
188. B. Perlmutter-Hayman and Y. Weissman, *J. Phys. Chem.* **68**, 3307 (1964); M. R. Wendt and C. B. Monk, *J. Chem. Soc. A*, 1624 (1969).
189. U. Fűrholz and A. Haim, *J. Phys. Chem.* **90**, 3686 (1986).
190. Despite this problem, the literature data for (2.187) and many related reactions can be converted to 1.0 M  $\text{HClO}_4$  as a standard state. The rate constants obtained ( $k_{\text{Hg}}$ ) give a more consistent LFER when  $\log k_{\text{Hg}} / \log k_{\text{H}_2\text{O}}$  for these reactions are plotted.<sup>126</sup>
191. B. W. Clare, D. M. Druskovich, D. L. Kepert and J. H. Kyle, *Aust. J. Chem.* **30**, 211 (1977).
192. R. J. Campion, C. F. Deck, P. King, Jr. and A. C. Wahl, *Inorg. Chem.* **6**, 672 (1967).

193. L. Spiccia and T. W. Swaddle, *Inorg. Chem.* **26**, 2265 (1987).
194. G. C. Lalor and G. W. Bushnell, *J. Chem. Soc. A*, 2520 (1968).
195. J. Nwaeme and P. Hambright, *Inorg. Chem.* **23**, 1990 (1984).
196. S. Wherland and H. B. Gray, *Proc. Natl. Acad. Sci. USA* **79**, 2950 (1976).
197. R. C. Rosenberg, S. Wherland, R. A. Holwerda and H. B. Gray, *J. Amer. Chem. Soc.* **98**, 6364 (1976).
198. L. S. Reid, M. R. Mauk and A. G. Mauk, *J. Amer. Chem. Soc.* **106**, 2182 (1984).
199. T. Goldkorn and A. Schejter, *J. Biol. Chem.* **254**, 12562 (1979). Figures representing four equations are presented and compared.
200. R. A. Marcus and N. Sutin, *Biochim. Biophys. Acta* **811**, 265 (1985), Table V.
201. H. Cohen, L. J. Kirschenbaum, E. Zeigerson, M. Jacobi, E. Fuchs, G. Ginzburg and D. Meyerstein, *Inorg. Chem.* **18**, 2763 (1979).
202. G. Czapski and H. A. Schwarz, *J. Phys. Chem.* **66**, 471 (1962).
203. O. J. Parker and J. H. Espenson, *J. Amer. Chem. Soc.* **91**, 1968 (1969).
204. D. A. Ryan and J. H. Espenson, *Inorg. Chem.* **20**, 4401 (1981).
205. S. Wherland, *Inorg. Chem.* **22**, 2349 (1983).
206. J. P. Birk, *Inorg. Chem.* **9**, 735 (1970).
207. In other words, there may be a relation of the form  $\log f_{\text{H}} = \log f_{\text{O}} + a [\text{H}^+]$ , where  $f_{\text{H}}$  and  $f_{\text{O}}$  are the activity coefficients of reactants and activated complex at  $[\text{H}^+] = \text{H}$  and  $\text{O}$  respectively at constant  $\mu$ . From (2.179) this will lead to a rate law,  $\log k \propto [\text{H}^+]$  from a purely medium effect (A. Pidcock and W. C. E. Higginson, *J. Chem. Soc.* 2798 (1963)).
208. J. Doyle and A. G. Sykes, *J. Chem. Soc. A*, 795 (1967); R. Davies and A. G. Sykes, *J. Chem. Soc. A*, 2831 (1968).
209. A. Ekstrom, *Inorg. Chem.* **16**, 845 (1977).
210. W. D. Drury and J. M. DeKorte, *Inorg. Chem.* **22**, 121 (1983).
211. D. L. Toppen and R. G. Linck, *Inorg. Chem.* **10**, 2635 (1971).
212. R. A. Robinson and R. H. Stokes, *Electrolyte Solutions*, Butterworths, London, 1955, Chap. 15.
213. T. W. Swaddle and E. L. King, *Inorg. Chem.* **3**, 234 (1964).
214. J. R. Ward and A. Haim, *J. Amer. Chem. Soc.* **92**, 475 (1970).
215. L. Mønsted, T. Ramasami and A. G. Sykes, *Acta Chem. Scand. A* **39**, 437 (1985).
216. M. Chastrette, M. Rajzmann, M. Chanon and K. F. Purcell, *J. Amer. Chem. Soc.* **107**, 1 (1985) increase this to nine classes of (83) solvents, based on eight different variables, dipole moments etc.
217. M. J. Blandamer and J. Burgess, *Pure Appl. Chem.* **62**, 9 (1990).
218. Consider the striking effect of glycerol in reducing the solvent exchange rate constant (Sec. 4.2(a)) of all the first row transition metal ions.
219. E. Grunwald and S. Winstein, *J. Amer. Chem. Soc.* **70**, 846 (1948).
220. R. Banerjee, *Coordn. Chem. Revs.* **68**, 145 (1985).

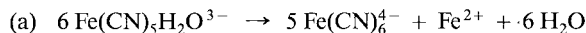
## Selected Bibliography

- B19. R. P. Bell, *The Proton in Chemistry*, 2nd edit. Chapman and Hall, London, 1973. Full discussion of Brønsted relationships.
- B20. J. E. Leffler and E. Grunwald, *Rates and Equilibria of Organic Reactions*, Wiley, NY, 1963.

## Problems

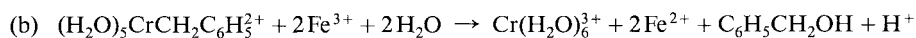
1. Suggest mechanisms for the following reactions. In each case specify the units for the rate constants (Sec. 1.1) and the composition of the activated complex(es) (Sec. 2.1). Indicate

which mechanism is likely when there is more than one and suggest additional experiments to substantiate the choice.



$$-d[\text{Fe}(\text{CN})_5\text{H}_2\text{O}^{3-}]/dt = k[\text{Fe}(\text{CN})_5\text{H}_2\text{O}^{3-}]$$

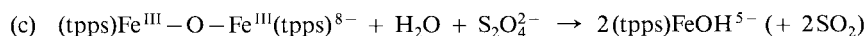
The reaction is carried out in dilute solution with exclusion of oxygen. J. A. Olabe and H. O. Zerga, *Inorg. Chem.* **22**, 4156 (1983).



$$-d[(\text{H}_2\text{O})_5\text{CrCH}_2\text{C}_6\text{H}_5^{3+}]/dt = k[(\text{H}_2\text{O})_5\text{CrCH}_2\text{C}_6\text{H}_5^{3+}]$$

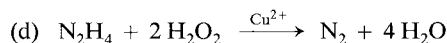
A similar rate law is obtained with  $\text{O}_2$ ,  $\text{Cu}(\text{II})$  and  $\text{Co}(\text{NH}_3)_5\text{Cl}^{2+}$  with similar values for  $k$ , but with different organic products.

R. S. Nohr and J. H. Espenson, *J. Amer. Chem. Soc.* **97**, 3392 (1975).



$$-d[(\text{tpps})\text{Fe}-\text{O}-\text{Fe}(\text{tpps})^{8-}]/dt = k[(\text{tpps})\text{Fe}-\text{O}-\text{Fe}(\text{tpps})^{8-}]$$

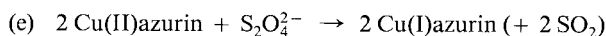
A. A. El-Awady, P. C. Wilkins and R. G. Wilkins, *Inorg. Chem.* **24**, 2053 (1985).



$$\frac{d[\text{N}_2]}{dt} = \frac{a[\text{N}_2\text{H}_4][\text{H}_2\text{O}_2][\text{Cu}(\text{II})]}{1 + b[\text{N}_2\text{H}_4]}$$

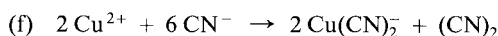
See Problem 2, Chap. 1.

C. R. Wellman, J. R. Ward and L. P. Kuhn, *J. Amer. Chem. Soc.* **98**, 1683 (1976).



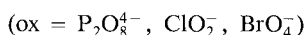
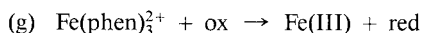
$$-d[\text{Cu}(\text{II})\text{azurin}]/dt = k_1[\text{Cu}(\text{II})\text{azurin}][\text{S}_2\text{O}_4^{2-}] + k_2[\text{Cu}(\text{II})\text{azurin}][\text{S}_2\text{O}_4^{2-}]^{1/2}$$

G. D. Jones, M. G. Jones, M. T. Wilson, M. Brunori, A. Colosimo and P. Sarti, *Biochem. J.* **209**, 175 (1983); Z. Bradić and R. G. Wilkins, *J. Amer. Chem. Soc.* **106**, 2236 (1984).



$$d[\text{Cu}(\text{CN})_2^-]/dt = k[\text{Cu}^{2+}]^2[\text{CN}^-]^6$$

J. H. Baxendale and D. T. Westcott, *J. Chem. Soc.* 2347 (1959); R. Patterson and J. Bjerum, *Acta Chem. Scand.* **19**, 729 (1965); A. Katagiri and S. Yoshizawa, *Inorg. Chem.* **20**, 4143 (1981).



$$-d[\text{Fe}(\text{phen})_3^{2+}]/dt = \frac{a[\text{Fe}(\text{phen})_3^{2+}][\text{ox}]}{b[\text{phen}] + c[\text{ox}]}$$

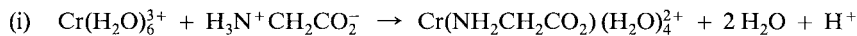
A. M. Kjaer and J. Ulstrup, *Inorg. Chem.* **21**, 3490 (1982) and references cited.



$$-d[\text{HCrO}_4^-]/dt = k [\text{HCrO}_4^-] [\text{H}^+] [\text{H}_2\text{O}_2]$$

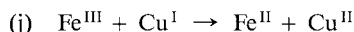
The rate law and value of  $k$  for the formation of the violet diperoxo chromium(VI) are the same as for the formation of the blue  $\text{CrO}_5$  species (Sec. 2.1)

S. N. Witt and D. M. Hayes, *Inorg. Chem.* **21**, 4014 (1982).



$$d[\text{Cr}(\text{NH}_2\text{CH}_2\text{CO}_2)(\text{H}_2\text{O})_4^{2+}]/dt = (k_2 + k_2'[\text{H}^+]^{-1})[\text{Cr(III)}]$$

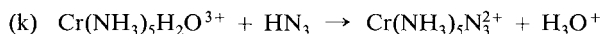
M. Abdullah, J. Barrett and P. O'Brien, *J. Chem. Soc. Dalton Trans.* 1647 (1984); *Inorg. Chim. Acta* **96**, L35 (1985).



$$-d[\text{Fe(III)}]/dt = k [\text{Fe(III)}] [\text{Cu(I)}] [\text{H}^+]^{-1}$$

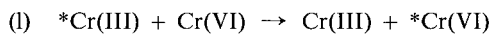
This is a common type of rate law for reactions between two acidic metal ions.

O. J. Parker and J. H. Espenson, *Inorg. Chem.* **8**, 1523 (1969).



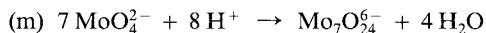
$$-d[\text{Cr}(\text{NH}_3)_5\text{H}_2\text{O}^{3+}]/dt = k [\text{Cr}(\text{NH}_3)_5\text{H}_2\text{O}^{3+}] [\text{HN}_3] [\text{H}^+]^{-1}$$

S. Castillo-Blum and A. G. Sykes, *Inorg. Chem.* **23**, 1049 (1984).



$$V_{\text{exch}} = (k_1 + k_2 [\text{H}^+]^{-2}) [\text{Cr}^{\text{(III)}}]^{4/3} [\text{H}_2\text{CrO}_4]^{2/3}$$

C. Altman and E. L. King, *J. Amer. Chem. Soc.* **83**, 2825 (1961).



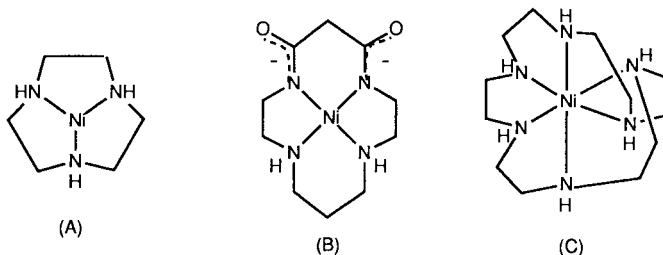
$$d[\text{Mo}_7\text{O}_{24}^{6-}]/dt = k [\text{MoO}_4^{2-}]^7 [\text{H}^+]^8$$

D. S. Honig and K. Kustin, *Inorg. Chem.* **11**, 65 (1972).

2. The dissociation of metal complexes of macrocycles is often speeded up by acid. For the nickel(II) complexes A, B and C (indicated NiL) the rate laws are

$$-d[\text{NiL}]/dt = \{k_1 + k_2 [\text{H}^+]^n\} [\text{NiL}]$$

where for A,  $n = 1$ ; B,  $k_1 = 0$ ,  $n = 2$ ; and C,  $k_1 = 0$ ,  $n = 3$ . Suggest mechanisms for these reactions.



(A) L. J. Murphy, Jr., and L. J. Zompa, *Inorg. Chem.* **18**, 3278 (1979).

(B) R. W. Hay, M. P. Pujari and F. McLaren, *Inorg. Chem.* **23**, 3033 (1984).

(C) R. W. Hay, R. Bembi, W. T. Moodie and P. R. Norman, *J. Chem. Soc. Dalton Trans.* 2131 (1982).

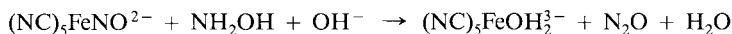
3. The oxidation of  $\text{Fe}^{2+}$  by two-equivalent oxidants produces unstable oxidation states either of iron or of the oxidant. The immediate products of oxidation by (1)  $\text{H}_2\text{O}_2$ , (2)  $\text{HOCl}$ , and (3)  $\text{O}_3$  in 0.1 M to 1.0 M  $\text{HClO}_4$  are (1)  $>99\%$   $\text{Fe}^{3+}$  (and  $\text{FeOH}^{2+}$ ), (2)  $\approx 80\%$   $\text{Fe}^{3+}$  and  $\approx 15\%$   $\text{Fe}_2(\text{OH})_2^{4+}$ , and (3)  $\approx 60\%$   $\text{Fe}^{3+}$  and  $\approx 40\%$   $\text{Fe}_2(\text{OH})_2^{4+}$ . Suggest reasons for this difference in behavior, and for the decreasing yield of  $\text{Fe}_2(\text{OH})_2^{4+}$  with increasing  $[\text{H}^+]$  in reaction (2).

T. J. Conocchioli, E. J. Hamilton and N. Sutin, *J. Amer. Chem. Soc.* **87**, 926 (1965).

4. Neither  $\text{Cr(VI)}$  nor  $\text{Fe(III)}$  can oxidize iodide ions rapidly. However a mixture of  $\text{Cr(VI)}$  and  $\text{Fe(II)}$  forms iodine rapidly from iodide ions. The oxidation of  $\text{I}^-$  is said to be induced by the  $\text{Fe(II)}-\text{Cr(VI)}$  reaction. At high  $[\text{I}^-]/[\text{Fe}^{2+}]$  ratios, the induction factor (ratio of  $\text{I}^-$  oxidized per  $\text{Fe}^{2+}$  oxidized) is 2.0. Interpret this behavior, detailing the intermediates involved.

J. H. Espenson, *Accts. Chem. Res.* **3**, 347 (1970).

5. The reaction between  $\text{Fe(CN)}_5\text{NO}^{2-}$  and  $\text{NH}_2\text{OH}$  in basic solution gives  $\text{N}_2\text{O}$  quantitatively



with a rate law

$$-d[(\text{NC})_5\text{FeNO}^{2-}]/dt = k[(\text{NC})_5\text{FeNO}^{2-}][\text{NH}_2\text{OH}][\text{OH}^-]$$

Using  $^{15}\text{N}$  and  $^{18}\text{O}$  labelled reactants show how the source of  $\text{N}_2\text{O}$  might be deduced, and suggest a mechanism for the reaction.

S. K. Wolfe, C. Andrade and J. H. Swinehart, *Inorg. Chem.* **13**, 2567 (1974).

6. Suggest a reason for the small but definite value for  $k_{\text{H}}/k_{\text{D}}$  of 2.1 for reaction of  $\text{Co(sep)}^{2+}$  (9) with  $\text{O}_2^-$ , but not with  $\text{O}_2$ . The NH groups are deuterated.

A. Bakač, J. H. Espenson, I. I. Creaser and A. M. Sargeson, *J. Amer. Chem. Soc.* **105**, 7624 (1983).

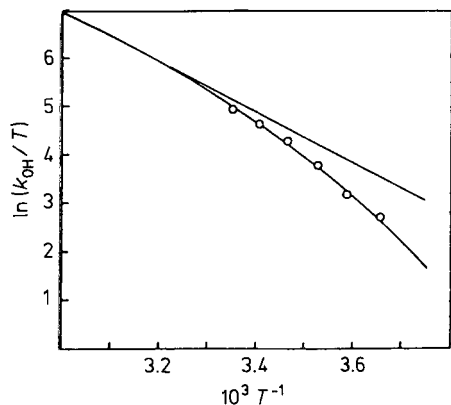


7. In general,

$$k = CT^n \exp(-U/RT)$$

so that a plot of  $\ln kT^{-n}$  vs  $1/T$  is linear with slope  $-U/R$ . Show that with various values of  $n$ : 0, 1/2 and 1 one obtains the Arrhenius expression, the Eyring expression and the expression used in the collision theory for bimolecular reactions in the gas phase.

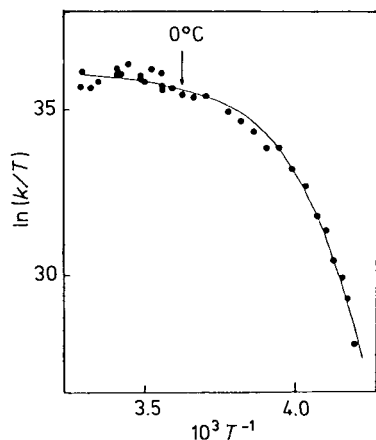
8. The plot of  $\ln k_{\text{OH}}/I$  vs  $T^{-1}$  for the base hydrolysis of *trans*-Co(*RSSR*[14]aneN<sub>4</sub>)Cl<sub>2</sub><sup>+</sup> is curved slightly (concave down). Bearing in mind the conjugate mechanism for base hydrolysis give a plausible explanation for this behavior.



Problem 8. Plot of  $\ln(k_{\text{OH}}T^{-1})$  against  $T^{-1}$  for the base hydrolysis of *trans*-Co(*RSSR*-cyclam)Cl<sub>2</sub><sup>+</sup>. Reproduced with permission from J. Lichtig, M. E. Sosa, and M. L. Tobe, *J. Chem. Soc. Dalton Trans.* 581 (1984).

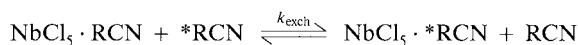
J. Lichtig, M. E. Sosa and M. L. Tobe, *J. Chem. Soc. Dalton Trans.* 581 (1984).

9. Cryokinetic studies of the plastocyanin-ferricyanide redox reactions in 50:50 v/v MeOH + H<sub>2</sub>O, pH = 7.0,  $\mu = 0.1$  M reveal an Eyring plot shown for the second-order rate constant  $k$  from 25 °C to -35 °C. The reaction is irreversible over the whole temperature range and there is no evidence for a change in the Cu(I) active site. Recalling that these reactions may involve consecutive steps, explain the deviation from a linear Eyring plot. F. A. Armstrong, P. C. Driscoll, H. G. Ellul, S. E. Jackson and A. M. Lannon, *J. Chem. Soc. Chem. Commun.* 234 (1988).



Problem 9. Eyring plot for the oxidation of PCu<sup>I</sup> by Fe(CN)<sub>6</sub><sup>3-</sup> in 50:50 v/v CH<sub>3</sub>OH-H<sub>2</sub>O, pH = 7.0,  $\mu = 0.1$  M(NaCl).

10. For the exchange reaction



there is a linear relationship between  $k_{\text{exch}}$  and  $K$  the stability constant of the adduct for a variety of R groups. What does this suggest for the mechanism of the exchange?

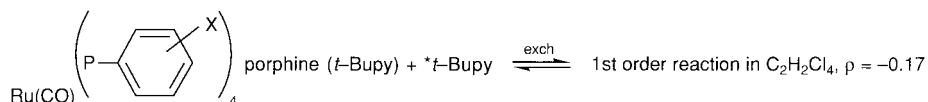
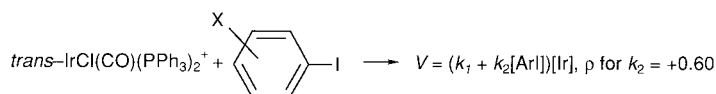
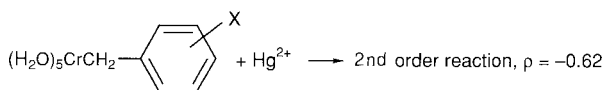
R. Good and A. E. Merbach, *Inorg. Chem.* **14**, 1030 (1975).

11. Why is there likely to be a parallelism between the dissociation rate constant for nickel(II) complexes with L and the  $\text{p}K_{\text{a}}(\text{LH}^+)$ ?

P. Moore and R. G. Wilkins, *J. Chem. Soc.* 3454 (1964).

H. Hoffmann, *Ber. Bunsenges. Phys. Chem.* **73**, 432 (1969).

12. Comment on the  $\rho$ -values for the following reactions



J. P. Leslie and J. H. Espenson, *J. Amer. Chem. Soc.* **98**, 4839 (1976).

R. J. Mureinik, M. Weitzberg and J. Blum, *Inorg. Chem.* **18**, 915 (1979).

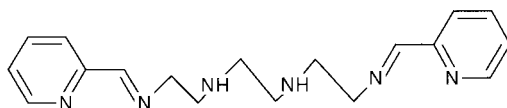
S. S. Eaton and G. R. Eaton, *Inorg. Chem.* **16**, 72 (1977).

13. Draw a reaction profile for a reaction in which a) the activated complex most resembles the reactants and b) the activated complex most resembles the products.

B17, p. 54.

14. Give a plausible explanation for

(a) a positive value for  $\Delta V^\ddagger$  (+ 13  $\text{cm}^3 \text{mol}^{-1}$  at 298 K) for the second-order reaction of  $\text{OH}^-$  ion with an iron(II) chelate,  $\text{Fe}(\text{hxsb})^{2+}$  which would be expected to be negative intrinsically.

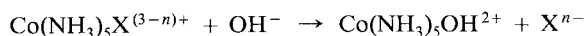


J. Burgess and C. D. Hubbard, *J. Chem. Soc. Chem. Commun.* 1482 (1983).

(b) negative and positive  $\Delta V^\ddagger$  values for dmf exchange of solvent with  $\text{Co}(\text{Me}_6\text{tren})\text{dmf}^{2+}$  and  $\text{Cu}(\text{Me}_6\text{tren})\text{dmf}^{2+}$  respectively.

S. F. Lincoln, A. M. Hounslow, D. L. Pisaniello, B. G. Doddridge, J. H. Coates, A. E. Merbach and D. Zbinden, *Inorg. Chem.* **23**, 1090 (1984).

15. The values of  $\Delta V_{\text{expl}}^\ddagger$  and  $\Delta V_0$  for the reaction



are shown in the Table. Also included are partial molar volumes  $V(\text{Co}(\text{NH}_3)_5\text{X}^{(3-n)+})$  and  $V(\text{X}^{n-})$ , all  $\text{cm}^3\text{mol}^{-1}$

$\text{X}^{n-}$	$\Delta V_{\text{expl}}^\ddagger$ <sup>a</sup>	$\Delta V_0$	$V(\text{Co}(\text{NH}_3)_5\text{X}^{(3-n)+})$ <sup>b</sup>	$V(\text{X}^{n-})$ <sup>b</sup>
$\text{Me}_2\text{SO}$	40	21	112	69
$\text{Cl}^-$	33	10	84	22
$\text{Br}^-$	33	11	89	29
$\text{SO}_4^{2-}$	22	-4	95	23

<sup>a</sup>  $\mu = 10\text{--}16$  mM, value little dependent on  $\mu$ .

<sup>b</sup> By dilatometry, data extrapolated to infinite dilution.

Consider the  $D_{\text{cb}}$  mechanism for base hydrolysis.

(a) Comment on the constancy of

$$\Delta V_{\text{expl}}^\ddagger - \Delta V_0 \text{ and its value.}$$

(b) satisfy yourself that

$$\begin{aligned} \Delta V_{\text{expl}}^\ddagger \approx & V(\text{Co}(\text{NH}_3)_4\text{NH}_2^{2+}) + V(\text{X}^{n-}) + V(\text{H}_2\text{O}) \\ & - V(\text{OH}^-) - V(\text{Co}(\text{NH}_3)_5\text{X}^{(3-n)+}) \end{aligned}$$

(c) Plot  $\Delta V_{\text{expl}}^\ddagger + V(\text{Co}(\text{NH}_3)_5\text{X}^{(3-n)+})$  vs  $V(\text{X}^{n-})$  and comment on the values of the slope and intercept. ( $V(\text{H}_2\text{O}) - V(\text{OH}^-) = 17.6 \text{ cm}^3\text{mol}^{-1}$ )

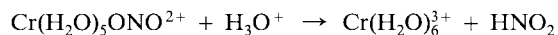
(d) What does  $\Delta V_{\text{expl}}^\ddagger$  comprise on the basis of a  $D_{\text{cb}}$  mechanism?

Y. Kitamura, R. van Eldik and H. Kelm, *Inorg. Chem.* **23**, 2038 (1984); R. van Eldik, *Angew. Chem. Int. Ed. Engl.* **25**, 673 (1986).

16. The plot of  $\log k$  vs  $\mu^{1/2}/1 + \mu^{1/2}$  for the second-order reaction between  $\text{Co}(\text{edta})^-$  and  $\text{Fe}(\text{CN})_6^{4-}$  (Sec. 1.6.3) showed an initial linear slope at low  $\mu$  of 3.8, reached a maximum at  $\mu \approx 0.1$  M and then decreased. The ionic strength was supplied by  $\text{NaClO}_4$ . Give a reasonable explanation for this behavior.

D. H. Huchital and J. Lepore, *Inorg. Chim. Acta* **38**, 131 (1980).

17. Determine the dependence of the first-order rate constant  $k$  for the reaction



on the proton concentration,  $T = 10^\circ\text{C}$ ,  $\mu = 1.0$ . (See accompanying table.)

$[\text{H}^+], \text{M}$	$10^2 k, \text{s}^{-1}$	$[\text{H}^+], \text{M}$	$10^2 k, \text{s}^{-1}$
0.0114	0.345	0.150	7.9
0.0216	0.706	0.200	11
0.030	1.16	0.300	20
0.040	1.59	0.400	31
0.050	2.07	0.500	45
0.060	2.53	0.600	59
0.080	3.50	0.700	81
0.100	4.66	0.800	104
		0.900	129
		0.993	158

Suggest a mechanism, and analyze whether medium effects are likely to be a cause of the acidity dependence.

T. C. Matts and P. Moore, *J. Chem. Soc. A*, 1997 (1969).

## Chapter 3

# The Experimental Determination of the Rate of Reaction

### 3.1 Essential Preliminaries

In determining experimentally the rate of a reaction, it is imperative to define the reaction completely, with respect to the reactants, the stoichiometry and even the products. This is preferably carried out before any detailed rate measurements are made, otherwise difficulties in understanding the rate data (particularly if these are complex) are likely to arise.

#### 3.1.1 Reactant Species in Solution

It is essential to characterize the reactant species in solution. One of the problems, for example, in interpreting the rate law for oxidation by Ce(IV) or Co(III) arises from the difficulties in characterizing these species in aqueous solution, particularly the extent of formation of hydroxy or polymeric species.<sup>1</sup> We used the catalyzed decomposition of H<sub>2</sub>O<sub>2</sub> by an Fe(III) macrocycle as an example of the initial rate approach (Sec. 1.2.1). With certain conditions, the iron complex dimerizes and this would have to be allowed for, since it transpires that the dimer is catalytically inactive.<sup>2</sup> In a different approach, the problems of limited solubility, dimerization and aging of iron(III) and (II)-hemin in aqueous solution can be avoided by intercalating the porphyrin in a micelle. Kinetic study is then eased.<sup>3,4</sup>

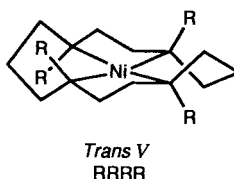
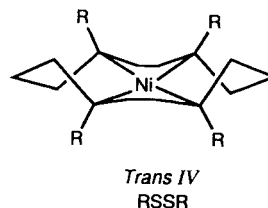
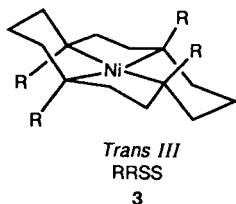
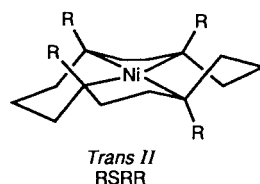
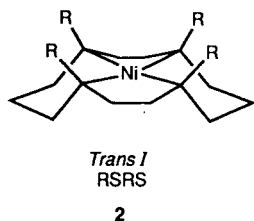
Inability or failure to characterize the reactant species may lead to problems in kinetic interpretation. In M(II)-edta complexes the degree of coordination (5- or 6-) by the ligand is uncertain. Since the mode of coordination appears sensitive to temperature and ionic strength, this may explain contradictions in the literature in the rate behavior of M(II)-edta complexes.<sup>5</sup> The ability of ligands to induce changes in protein structure has been probed by examining the reactivity of thiol groups in the protein towards organomercurials. However, ligands react with organomercurials and rate



differences may arise simply because of different reactivities of ArHgOH and ArHgL.<sup>6</sup> See Prob. 1.

It must always be considered that a reactant is in fact a mixture of species. If these species are in labile equilibrium, or have similar reactivities, their presence will not show up as multiphasic kinetics.

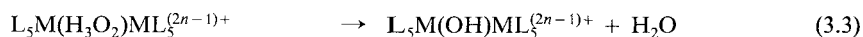
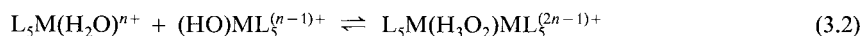
Recent  $^1\text{H}$  nmr studies of an equilibrated solution of  $\text{Ni}(\text{cyclam})^{2+}$  at  $25^\circ\text{C}$  shows that it contains in addition to  $\text{Ni}(\text{cyclam})(\text{H}_2\text{O})_2^{2+}$  (**1**) a mixture of about 15% of isomer *RSRS* **2**, and mainly *RRSS*, **3**, ((+ + + +) and (+ - - +) respectively where + indicates the H of the NH group is above the macrocycle plane). The results mean that previous studies of the  $\text{Ni}(\text{II})$  macrocycle made with the assumption of only a single planar isomer in solution have to be reassessed.<sup>7</sup> For a pair of esoteric examples of the importance and difficulties of characterization consider the following:

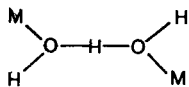


Configurational isomers of planar  $\text{Ni}(\text{cyclam})^{2+}$   
R = H and  $\text{Ni}(\text{Me}_4\text{cyclam})$ , R =  $\text{CH}_3$ .

(a) Native myoglobin exists with the heme in two different orientations (one 10%). These have the same optical spectrum but different nmr,  $\text{O}_2$  affinities and associated rate constants. Reconstituted myoglobin from apomyoglobin and heme contains equimolar mixtures of the two forms.<sup>8</sup>

(b) Some metal ions may exist in aqueous solution as dinuclear species bridged by hydrogen oxide ligands ( $\text{H}_3\text{O}_2^-$ ), **4**. These may be reactive species not easily detected but precursors to olation.<sup>9</sup>

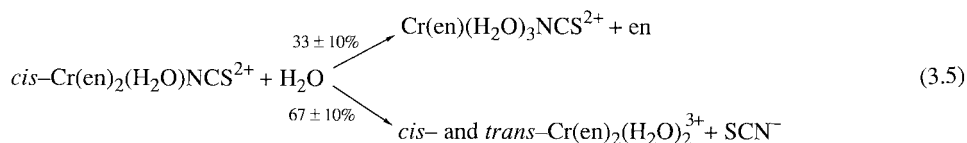
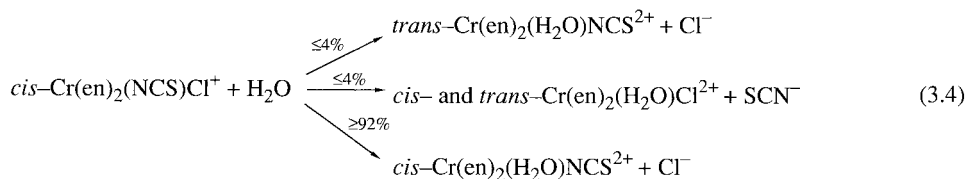




4

### 3.1.2 Stoichiometry of Reaction

The importance of knowing the stoichiometry of a reaction can be simply illustrated by considering the aquation of *cis*-Cr(en)<sub>2</sub>(NCS)Cl<sup>+</sup> ion.<sup>10</sup> Is Cl<sup>-</sup> or NCS<sup>-</sup> replaced in the initial step and is the product *cis* or *trans* or both? Does the product of this first step aquate further, and if so what groups are then replaced? Chemical and spectral analysis answers these questions. The results reveal the surprising fact that the bidentate ligand en is lost at one stage, a behavior that appears more common with amines of Cr(III)<sup>11</sup> than with Co(III), where its occurrence is only occasionally<sup>12</sup> noted.



Inconsistencies in the values of equilibrium constants obtained from measurements on systems at equilibrium with those derived from rate measurements may also reveal unexpected reaction paths.<sup>13</sup> See Chap. 8, Pd(II).

### 3.1.3 The Nature of the Products

If the rate constants for parallel reactions are to be resolved, then analysis of the products is essential (Sec. 1.4.2). This is vital for understanding, for example, the various modes of deactivation of the excited state (Sec. 1.4.2). Only careful analysis of the products of the reactions of Co(NH<sub>3</sub>)<sub>5</sub>H<sub>2</sub>O<sup>3+</sup> with SCN<sup>-</sup>, at various times after initiation, has allowed the full characterization of the reaction (1.95) and the detection of linkage isomers. Kinetic analysis by a number of groups failed to show other than a single second-order reaction.<sup>14</sup> As a third instance, the oxidation of 8-Fe ferredoxin with Fe(CN)<sub>6</sub><sup>3-</sup> produces a 3Fe-cluster, thus casting some doubt on the reaction being a simple electron transfer.<sup>15</sup>

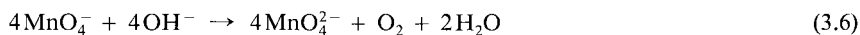
It is easily observed when a product precipitates from solution. Some reductions of Co(III) complexes yield insoluble Co(II) products. Addition of powerful ligands such as edta will complex with Co(II), maintain homogeneity and force irreversibility (Sec. 1.5.1).<sup>16</sup> It should be always checked whether the added ligand has an influence on the rate.

### 3.1.4 The Influence of Impurities

The materials used, including the solvent, should be as pure as possible. There are several instances recorded (and doubtless a number unrecognized) in which traces of impurities introduced inadvertently into a system have had catastrophic consequences.

The pseudo first-order rate constants ( $k$ ) for reaction of  $\text{Co}(\text{CN})_5\text{H}_2\text{O}^{2-}$  with  $\text{N}_3^-$  concentration in excess were reported as curved (Sec. 1.6.3) and have been interpreted for some 20 years as evidence for a 5-coordinate intermediate and a  $D$  mechanism. If however  $\text{Co}(\text{CN})_5\text{H}_2\text{O}^{2-}$  is generated in solution by aquation of  $\text{Co}(\text{CN})_5\text{Cl}^{3-}$  (rather than from  $\text{Co}_2(\text{CN})_{10}\text{O}_2^{6-}$  as in the original studies) the  $k/[\text{N}_3^-]$  plot does *not* deviate from linearity. Reasons are suggested why the latter behavior is correct and importantly, the original material could be shown to contain a slower reacting component which gives false data at higher  $\text{N}_3^-$  concentrations. The  $D$  mechanism remains a possibility however.<sup>17,18</sup> Traces of impurities in a solution of  $\text{Fe}(\text{CN})_5\text{H}_2\text{O}^{3-}$  have led to false conclusions as to the  $\text{p}K_a$  of the coordinated water.<sup>19,20</sup> The photolytic behavior of aqueous  $\text{Fe}(\text{CN})_6^{3-}$  depends on its history.<sup>21</sup> Copper(II) ion is a potent catalyst even in micromolar concentrations for a number of reactions of  $\text{Fe}(\text{CN})_6^{3-}$  ion.<sup>22</sup>

These catalytic effects are usually signaled by irreproducible behavior. If it is suspected that traces of metal ions may be causing peculiar rate effects, a strong ligand may be added to sequester the metal ion. The spontaneous decomposition of  $\text{H}_2\text{O}_2$  has been reported as  $4.7 \times 10^{-7} \text{ M}^{-1}\text{s}^{-1}$  at pH 11.6 and 35 °C. This is the lowest recorded value and is obtained in the presence of strong chelators.<sup>23</sup> In a similar way the decomposition of permanganate in alkaline solution (3.6) is markedly slowed when the reactants are extensively purified



and metal ion concentrations are reduced below  $10^{-9} \text{ M}$ .<sup>24</sup>

### 3.1.5 The Control of Experimental Conditions

Some general considerations applicable to all rate studies can be outlined.<sup>25</sup> Since the rate constants for many reactions are affected by the ionic strength of the medium (Sec. 2.9.1) it is necessary either to maintain a constant ionic strength with added electrolyte, or to carry out a series of measurements at different ionic strengths and extrapolate to infinite dilution. The former practice is usually followed and  $\text{NaNO}_3$  or  $\text{NaClO}_4$  have been popular as added salts. There are some advantages however in using the weakly-coordinating<sup>26</sup> *p*-toluenesulfonate or trifluoromethylsulfonate ions in place of perchlorate. A potential explosive hazard is avoided and problems of oxidation, e.g. with V(III),<sup>27</sup> do not arise.



Many complex-ion reactions are accompanied by a pH-change, and since the rate of these reactions is often pH-dependent, it is necessary to use buffers. A list of useful buffers for the pH region 5.5–11.0 is contained in Table 3.1.<sup>28</sup>

**Table 3.1** Some Useful Buffers for Studying Complex-Ion Reactions.<sup>28</sup>

Buffer (Acronym)	p <i>K</i> <sub>a</sub> (25°C)
2-[N-Morpholino]ethanesulfonic acid (MES)	6.1
Bis[2-hydroxyethyl]iminotris(hydroxymethyl)methane (Bis-Tris)	6.5
Piperazine-N,N'-bis[2-ethanesulfonic acid] (PIPES)	6.8
3-[N-Morpholino]propanesulfonic acid (MOPS)	7.2
N-[2-Hydroxyethyl]piperazine-N'-[2-ethanesulfonic acid] (HEPES)	7.5
N,N-bis[2-Hydroxyethyl]glycine (BICINE)	8.3
2-[N-Cyclohexylamino]-ethanesulfonic acid (CHES)	9.3
3-[Cyclohexylamino]-l-propanesulfonic acid] (CAPS)	10.4

Many of these are substantially non-nucleophilic and unlikely to effect the rate or course of the reaction, although this should always be checked. References 29 to 31 relate some problems in the use of some of these buffers. Occasionally, one of the reactants being used in excess may possess buffer capacity and this obviates the necessity for added buffer. The situation will often arise in the study of complex ion-ligand interactions when either reactant may be involved in an acid-base equilibrium.

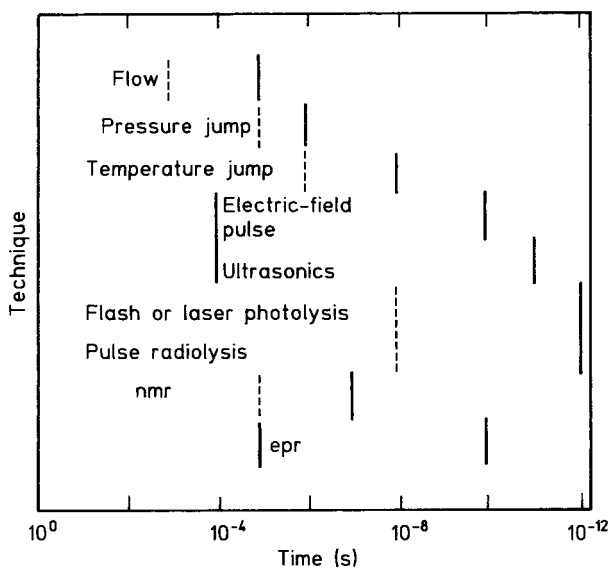
Concentrations of reactants reported usually refer to room temperature and pressure. Any changes in concentrations caused by carrying out the runs at other temperatures or pressures may be either ignored or are not relevant (Sec. 2.3.5). It is often unnecessary to maintain the reaction temperature more constant than  $\pm 0.05$  degrees. Variations in rate constants due to such a temperature fluctuation are generally well within the experimental error. It is obviously wise to exclude light or air, if it is suspected that these might interfere with the reaction. Darkened reaction vessels and apparatus for anaerobic manipulation are described.<sup>32</sup> Special equipment must be used if the reaction is carried out at elevated pressure.<sup>33</sup> A simple device for working at high temperatures (say  $>100^\circ\text{C}$ ), when continual opening of the apparatus is to be avoided, has been described.<sup>34</sup> Finally, when all the results have been gathered in, analysis of the errors, precision and accuracy associated with the study has to be made.<sup>35</sup>

## 3.2 The Methods of Initiating Reaction and their Time Ranges

Obviously the speed with which it is necessary to initiate a reaction will depend on its rate. If it is a slow process with half-lives longer than about 20 s, then the reaction can be initiated simply by mixing the reactants. Even reactions with shorter reaction times may be studied without recourse to sophisticated equipment. Simple mixing devices fitting into a spectrophotometric cuvette<sup>32,36</sup> or used to initiate and quench enzymatic reactions (down to 0.5 s

and using 20  $\mu\text{l}$  volumes)<sup>37</sup> can effectively reduce accessible reaction times. It is even possible to commence absorbance/time traces within 5 s of dissolution of a solid.<sup>38</sup> Flow and rapid mixing methods allow observation times to be as short as, and occasionally even much shorter than, milliseconds and have been considerably exploited. Relaxation methods circumvent the mixing limitations. These are extremely important for the measurement of rapid reactions but the relative simplicity of the associated kinetics (see Chap. 1) makes them also an attractive prospect for the study of slow reactions.<sup>36</sup> Any perturbation e.g. ionic strength or pH changes which alters concentrations of species at equilibrium can in principle be used, imposed by flow methods if necessary.<sup>36,39-43</sup> A special method for the rapid initiation of a reaction employs a large perturbation by a light pulse (usually with a laser) or an electron beam. Primary and secondary reducing and oxidizing radicals or excited states can be produced in very short times (even picoseconds, or less, but usually nano- or microseconds) and their physical properties and chemical reactivity (towards added substrates) can be studied.

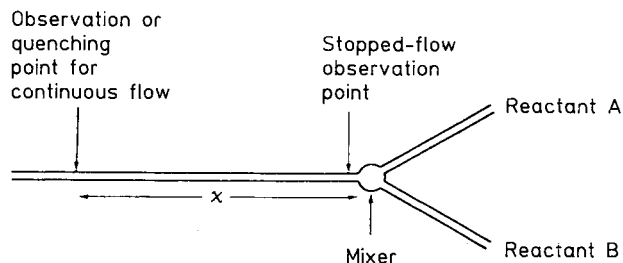
The time coverage for the various rapid-reaction techniques is shown in Figure 3.1.<sup>44</sup>



**Fig. 3.1** Time coverage for various rapid-reaction techniques. Broken lines indicate the usual shorter time limits. Full lines indicate the shorter time limits attainable in some laboratories. Unless indicated, the longer time limit is usually unlimited.<sup>44</sup>

### 3.3 Flow Methods

Comprehensive discussions of flow methods are available in the literature.<sup>45,46</sup> There are basically three ways in which the reaction solution may be treated after mixing (Fig. 3.2 and Table 3.2)



**Fig. 3.2** The operation of flow methods. The distance  $x$  and the combined flow rate govern the time that elapses between mixing and when the combined solutions reach the observation, or quenching, point. In the stopped flow method, observation is made as near to the mixer as is feasible, and monitoring occurs after the solutions are stopped. In the pulsed accelerated flow method, observation is within the mixer.

**Table 3.2** Rapid Mixing and Flow Methods

Flow-Mode	General Procedure	Characteristics
Continuous	<i>In situ</i> monitoring at a fixed point on the observation tube with various flow rates. Alternatively, the mixing chamber is incorporated into the observation tube with early monitoring	Tedious but leisurely analysis. Useful with sluggish monitoring probes. A 1–0.01 ms resolution. Large volumes of reactants used ( $\geq 5$ ml). Not commercially available.
Quenched	Mixed solutions quenched after a predetermined time controlled by the distance between the mixer and quencher and the flow rate.	Tedious but leisurely analysis. Essential for the batch method used in rapid isotopic exchange and low temperature epr monitoring. A 10–20 ms resolution. Large volumes of reactants used ( $\geq 5$ ml). Commercially available.
Stopped	Mixed solutions abruptly stopped and analyzed near mixer.	Most popular method. Easy analysis requiring rapidly responding monitor. A 1 ms resolution. Uses small ( $\approx 0.2$ ml) volumes. A number of commercial apparatus in wide variety of modes and monitoring methods.

### 3.3.1 Continuous Flow

The continuous-flow method avoids the stopping features of the stopped-flow technique which are time limiting, but suffers from the disadvantage of consuming relatively large amounts of material, even in the latest developments. There has however been a resurgence of interest in the method, using integrating observation with a very fast jet mixer which is incorporated into the observation tube. The resolution time is short ( $\leq 10 \mu\text{s}$ ) but relatively large volumes of solution are necessary.<sup>47,48</sup> The integrating observation feature has been combined with pulsed continuous flow (pulsed continuous-flow spectrometer), resulting in the use of smaller volumes of material (5 ml), enhanced optical sensitivity and short resolution times (4  $\mu\text{s}$ ).<sup>49,50</sup> It now represents a method for determining high rate constants ( $\approx 10^5 \text{ s}^{-1}$  or  $10^{10} \text{ M}^{-1}\text{s}^{-1}$ ) for irreversible reactions (which are not amenable to relaxation methods). Unfor-

tunately, the treatment of kinetic data is more involved than with the stopped-flow method.<sup>47-50</sup>

The continuous flow method is still necessary when one must use probe methods which respond only relatively slowly to concentration changes. These include pH,<sup>51</sup> O<sub>2</sub>-sensitive electrodes,<sup>52</sup> metal-ion selective electrodes,<sup>53</sup> thermistors and thermocouples,<sup>54</sup> epr<sup>55</sup> and nmr detection. Resonance Raman and absorption spectra have been recorded in a flowing sample a few seconds after mixing horseradish peroxidase and oxidants. In this way spectra of transients (compounds I and II) can be recorded, and the effect of any photoreduction by the laser minimized.<sup>56</sup>

### 3.3.2 Quenched Flow

A number of simple pieces of apparatus for using the quenched-flow method have been described.<sup>57-59</sup> Commercial stopped-flow apparatus are available in which a double mixer arrangement allows quenching of a transient produced in a first mixer with quencher from a second mixer.<sup>60-62</sup> In one apparatus the aging interval for the transient (time between first and second mixer) can be adjusted from 20 ms to 11 s. This is accomplished by altering the volume of tubing between the mixers and/or altering the flow rate. A series of quenched solutions with different "ages" are thus obtained and can be analyzed (for details, see Ref. 63). See Prob. 2. Some varied examples of the applications of quenched flow are shown in Table 3.3. Quenching can be effected by several means including rapid cooling,<sup>62</sup> precipitation of one reactant<sup>57,58,61,64</sup> or chemical destruction by adding a complexing agent or acid. The method has been particularly useful for studying fairly rapid isotopic exchange reactions (Table 3.3). Some of the reactions have also been studied without the necessity of a separation procedure, and therefore more conveniently, by nmr line-broadening methods (Sec. 3.9.6). The latter still require fairly high reactant concentrations, and with these conditions subtle medium

**Table 3.3** Some Rapid Isotopic Exchange Reactions Studied by Quenched Flow

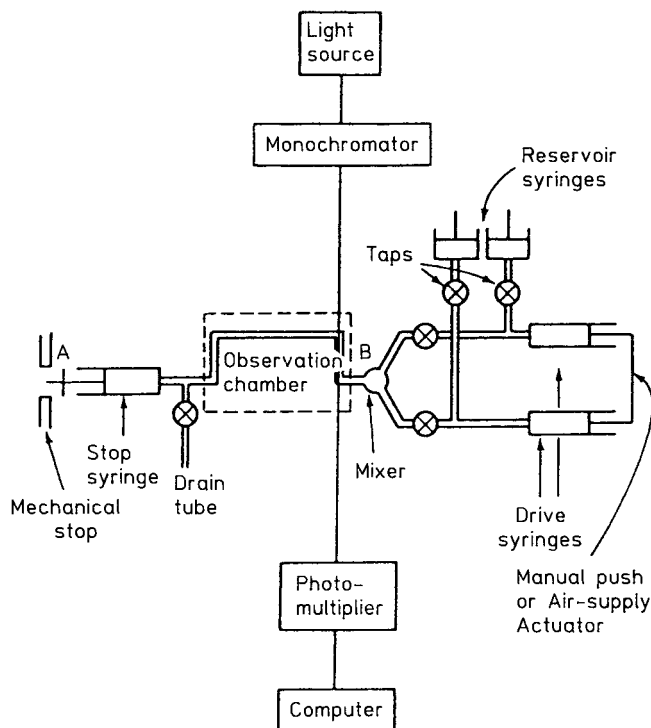
Exchanging Pair	Rate Constant M <sup>-1</sup> s <sup>-1</sup>	Temp. °C	Quenching Method	Refer- ence
<sup>54</sup> MnO <sub>4</sub> <sup>2-</sup> , MnO <sub>4</sub> <sup>-</sup> (0.16 M OH <sup>-</sup> )	7.1 × 10 <sup>2</sup>	0.0	(C <sub>6</sub> H <sub>5</sub> ) <sub>4</sub> As <sup>+</sup> coprecipitates MnO <sub>4</sub> <sup>-</sup> (in presence of ReO <sub>4</sub> <sup>-</sup> )	57
IrCl <sub>6</sub> <sup>3-</sup> , <sup>192</sup> IrCl <sub>6</sub> <sup>2-</sup>	≈ 2.3 × 10 <sup>5</sup>	25.0	2-Butanone extracts IrCl <sub>6</sub> <sup>2-</sup> (stopped flow mixing)	58
<sup>63</sup> Cu <sup>II</sup> stellacyanin, <sup>65</sup> Cu <sup>I</sup> stellacyanin	1.2 × 10 <sup>5</sup>	20.0	Cool to -120°C and epr analysis using slight differences in epr of <sup>63</sup> Cu <sup>II</sup> and <sup>65</sup> Cu <sup>II</sup> stellacyanin. Rapid mixing, reaction half times ≈ 10 msec at 0.5 mM concentra- tions.	62
VO <sub>4</sub> <sup>3-</sup> , H <sub>2</sub> <sup>18</sup> O (in 0.5 M base)	2.4 × 10 <sup>2</sup> (s <sup>-1</sup> )	0.0	Co(NH <sub>3</sub> ) <sub>6</sub> <sup>3+</sup> precipitates VO <sub>4</sub> <sup>3-</sup> . An injection device allows short t <sub>1/2</sub> 's 8-44 s.	64
IO <sub>3</sub> <sup>-</sup> , H <sub>2</sub> <sup>18</sup> O	4 term rate law	5.0	Ag <sup>+</sup> precipitates IO <sub>3</sub> <sup>-</sup> which pyrolyzes cleanly to O <sub>2</sub> for isotopic analysis. Dionex double mixer, t <sub>1/2</sub> 20 ms-2 s.	61

effects are less easily recognized. The quenched-flow method has been particularly effective also for the study of the transients produced in rapid reactions of certain Mo<sup>65,66</sup> and Fe<sup>67,68</sup> proteins. Epr monitoring of rapidly quenched solutions fingerprints transients. The MoFe protein of nitrogenase in the reduced form is oxidized rapidly by Fe(CN)<sub>6</sub><sup>3-</sup> and frozen at -140°C after various times have elapsed between oxidation (complete within milliseconds) and freezing. The epr examination of the frozen oxidized material of various ages allows a) the assignment of the product to a [4Fe-4S]<sup>+</sup> containing center and b) an indication of an epr signal diminishing with time after oxidation. The transient signal fades by an intramolecular process ( $k = 4.1 \pm 0.8 \text{ s}^{-1}$ ) at the same rate as that of enzyme turnover. Probably both processes are controlled by a conformational change in the protein.<sup>65</sup>

The disadvantage of the quenched-flow technique is the tedium associated with the batch method of assay. Additionally there is a relatively long reaction time limit, often >10 ms, necessitated by the extended quenching times. Offsetting these limitations are the simple equipment and the leisurely assay that are integral features of the method.

### 3.3.3 Stopped Flow

The stopped-flow technique is by far the most popular of the flow methods.<sup>69</sup> A block diagram is shown in Fig. 3.3. Stopped-flow systems have employed nearly all the usual monitoring methods and these will be discussed later (Table 3.7). The linking of the method with spectral monitoring is by far the most popular combination. A useful test reaction is the reduction of 2,6-dichlorophenol indophenol by *L*-ascorbic acid both for performance of the stopped-flow apparatus<sup>70</sup> and the double mixing arrangement.<sup>71</sup> The pseudo first-order rate constant varies linearly with the concentration of *L*-ascorbic acid, in excess, over 3 orders of magnitude. The time for mixing and moving the solution from the mixer to the observation chamber is referred to as the deadtime.<sup>72</sup> If the absorbance change accompanying a reaction is large, there may still be sufficient absorbance change after the absorbance loss due to the deadtime. The associated first-order rate constants will be large ( $>10^2 \text{ s}^{-1}$ ) but can be corrected for mixing effects.<sup>73</sup> A commercial stopped-flow apparatus can be modified so that unequal volumes of reactants (e. g. 50:1) can be mixed.<sup>74</sup> Details for mixing small amounts of organic solutions (e. g. containing dmsO) with large amounts of aqueous solution have been described. Such an approach allows the examination of the reactions of O<sub>2</sub><sup>-</sup> (stable in organic solution) with reactants (in H<sub>2</sub>O in larger syringe) in a mainly aqueous solution.<sup>75</sup> Turbidity and cavitation problems can be largely circumvented by simultaneous observation of a reaction with two detector systems set at two wavelengths and computer-subtracting the two absorbances.<sup>76</sup> *Spurious* traces can arise from mixing effects.<sup>77,78</sup> Although the majority of reported studies relate to aqueous solution in ambient conditions, the stopped-flow method has been used in nonaqueous solution,<sup>79</sup> at subzero temperatures,<sup>80</sup> and at high pressure.<sup>81-84</sup> The stopped-flow apparatus can be easily converted into a double-mixing arrangement to examine a transient intermediate,<sup>63</sup> such as VO<sub>3</sub><sup>+</sup>HO<sub>2</sub><sup>85</sup> and O<sub>2</sub><sup>-</sup> Refs. 86, 87. The double-mixer has played an important role in studying the transients in the unfolding and folding of proteins.<sup>71,88</sup>



**Fig. 3.3** Block diagram of stopped-flow apparatus. Reagents from the reservoir syringes are transferred to the 2-ml drive syringes via taps. A small portion (about 0.25 ml) of the reactants in each syringe is pushed through the mixer and observation chamber into a syringe, where the flow is abruptly stopped when A hits a mechanical stop. The progress of the reaction in the portion of stopped solution in B is monitored spectrally. The spent solution in the stop syringe is ejected through a drain tube and the process repeated. Ultraviolet, or visible, light through a monochromator passes through the observation chamber to a photomultiplier and oscilloscope or (more usually) an interfaced computer. Changing light intensity, arising from the absorbance changes in B as the reaction proceeds, is converted directly into absorbances. The design due to Q. H. Gibson and L. Milnes, *Biochem. J.* **91**, 161 (1964) has been the basis of the most successful stopped-flow apparatus, sold by Dionex.

### 3.4 Relaxation Methods

Even using the flow methods outlined in the previous sections, the reaction may still be too rapid to measure (i.e. it is complete within mixing). We must resort then to methods in which a reaction change is initiated by means other than mixing, the so-called relaxation methods.<sup>89</sup>

The amounts of species present in a chemical equilibrium may be changed by a variety of means. The rate of change of the system from the old to the new equilibrium, the *relaxation*,

is dictated by (and is therefore a measure of) the rate constants linking the species at equilibrium (Sec. 1.8). Any perturbation which changes concentrations can in principle be used. It is in the area of rapid reactions that relaxation methods are most powerful and have been most applied. The perturbation must of course be applied more rapidly than the relaxation time of the system under study. However perturbations can be imposed in much shorter times than are involved in the mixing process. Since also monitoring of very rapid processes rarely presents insuperable difficulties, reaction times in the micro-to pico second range can be measured (Fig. 3.1).

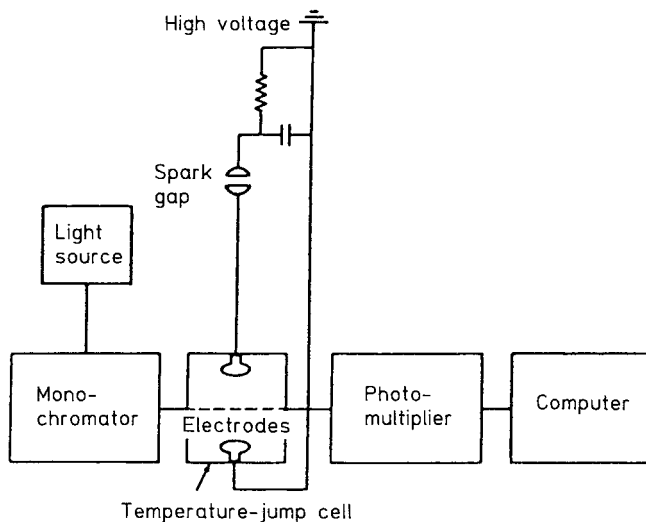
The relaxation technique does not have the wide applicability associated with the flow method since one does not usually have, nor is it easy to induce, a reasonable degree of reversibility in a system. This is essential in order that measurable changes of concentration may be induced by the perturbation, although sensitive methods for detecting very small changes are now available. Relaxation methods cover the time ranges not generally attainable by flow techniques and have permitted the measurement of large first-order rate constants associated with many fundamental elementary reactions. In addition, relatively small volumes of solution are required for most relaxation techniques and these can often be used repeatedly. The various types of relaxation techniques associated with specific perturbation modes will now be considered. These perturbations can be of two types: stepwise, meaning one abrupt change, and continuous, usually imposed as an oscillating perturbation. Regardless of the complexity of the reaction, a set of first-order kinetic equations is always obtained (Sec. 1.8.1).

### 3.4.1 Temperature Jump

The temperature jump is undoubtedly the most versatile and useful of the relaxation methods.<sup>91</sup> Since the vast majority of reactions have nonzero values for the associated  $\Delta H$ , a variation of equilibrium constant  $K$  with temperature is to be expected:

$$d \ln K/dT = \Delta H/RT^2 \quad (3.7)$$

Figure 3.4 shows a block diagram of a temperature-jump apparatus. In the original<sup>92</sup> and still most popular form of the apparatus, electric heating is supplied by discharging a capacitor through the solution.<sup>93,94</sup> Heating times are about 1  $\mu$ s but if a coaxial cable is used as the capacitor, a heating time of 10 ns – 100 ns is possible.<sup>95,96</sup> An electrically conducting solution is required, usually by adding 0.1 M  $\text{KNO}_3$  or  $\text{KCl}$ , but this is avoided when microwave heating (1  $\mu$ s) is used, although polar solvents must be employed.<sup>97</sup> Neither electrically-conducting nor polar solvents are necessary if laser heating is employed and a 1–10 ns heating time can be reached.<sup>98,99</sup> Temperature jumps of 1°–10° are commonly used, but even if a small temperature change is used, repetitive jumps on flowing solutions with computer collection can be employed effectively (e.g. with microwave heating).<sup>97</sup> The most common monitoring method is absorption spectrometry but a few others have been employed occasionally (Table 3.7). Fluorescence monitoring has the advantage of high sensitivity which means that low concentrations of reactants can be used, thus better ensuring equilibrium conditions, even with reactions which have high equilibrium constants. The most effective ways to maximize the signal-to-noise, acquire and analyze data have been fully discussed.<sup>91</sup> Temperature jump can be used for reactions involving dissolved gases, but



**Fig. 3.4** Block diagram of temperature-jump apparatus. The condenser is charged to 30–50 kilovolts and then discharged via a spark gap through the metal electrodes of the cell. This heats up a small portion of the solution some 3–10 degrees. This portion is monitored spectrally in the same manner as with the flow apparatus. An apparatus based on this arrangement was first manufactured by Messanlagen Studiengesellschaft, Göttingen, Germany.

cavitation effects may last as long as 50  $\mu\text{s}$  and thus limit its value.<sup>100</sup> The combination of the stopped-flow and temperature-jump methods for the study of the relaxation behavior of transients has not yet been extensively applied.<sup>101–104</sup> A commercial piece of equipment combines stopped flow with temperature jump and although the heating times are relatively long ( $> 50 \mu\text{s}$ ), the apparatus has been used effectively to examine the primary reaction of sodium nitroprusside with thiols before further redox reactions occur within seconds.<sup>104</sup> The temperature-jump method has been effectively combined with high pressure.<sup>91</sup>

### 3.4.2 Pressure Jump

Most chemical reactions occur with a change in volume. The equilibrium position will be therefore changed by an applied pressure, which can therefore be used as a perturbation.<sup>105</sup> Nearly always the progress of the reaction is observed at ambient pressures *after* the applied pressure has been terminated.

The expression

$$\left( \frac{d \ln K}{dP} \right)_s = \frac{-\Delta V}{RT} + \frac{\Delta H}{RT^2} \frac{\alpha T}{\rho C_p} \quad (3.8)$$

relates the variation of the equilibrium constant  $K$  with pressure  $P$  under adiabatic conditions.  $\Delta V$  = standard volume of reaction;  $\Delta H$  = enthalpy of reaction;  $\alpha$  = coefficient of thermal



expansion of the solution;  $\rho$  = density and  $C_p$  = specific heat. Normally in aqueous solution, the first term is the major contributor (>90% of total).<sup>105</sup> Usually the pressure change imposed is of the order of 50–150 atmospheres and since the response of the equilibrium constant to pressure change is much less than to temperature changes, sensitive conductivity monitoring is usually employed. Occasionally, other monitoring methods have been reported (Table 3.7). The method has the advantage that a wide range of solvents and a medium of low ionic strength can be used. The time range can be extended to long times since the pressure (unlike the temperature) remains constant after the perturbation. The method lacks the power of the temperature jump in reaching very short times (usually  $\geq 20 \mu\text{s}$ ) although attempts to shorten the working time<sup>106,107</sup> and improve the accuracy<sup>106</sup> have been made. The method has been used to study, for example, metal complex formation in solution<sup>105,108</sup> and protein self-association, using light scattering monitoring.<sup>109</sup> Pressure-jump relaxations at various (high) applied pressures allow the determination of volume of activation.<sup>110</sup> (Prob. 3.) No commercial set-up is offered but the component parts are readily available and there have been good descriptions of the system.<sup>105</sup>

### 3.4.3 Electric-Field Jump

Any reacting system occurring with a change in electric moment,  $\Delta M$ , will show a dependence of the associated equilibrium constant  $K$  on the electric-field strength  $E$ <sup>111</sup>

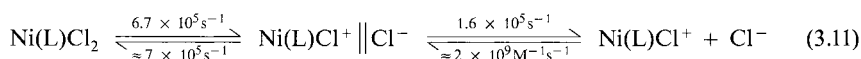
$$\left(\frac{d \ln K}{dE}\right)_{P,T} = \frac{\Delta M}{RT} \quad (3.9)$$

There is a modest increase in the electrical conductance with an increase in the electric-field gradient, an effect that operates with both strong and weak electrolytes (the first Wien effect). More important in the present context is the *marked* increase in electrical conductance of weak electrolytes when a high-intensity electric field is applied (second Wien effect). The high field promotes an increase in the concentration of ion pairs and free ions in the equilibrium



Commonly, a  $10^5$  volt/cm field will produce a 1% change in conductance of weak electrolytes. The measurement of very short relaxation times ( $\approx 50$  ns) is possible by the electric-field jump method but the technique is generally complicated and mainly restricted to ionic equilibria.<sup>111</sup>

The five-coordinate  $\text{Ni(L)Cl}_2$  ( $L = \text{Et}_2\text{N}(\text{CH}_2)_2\text{NH}(\text{CH}_2)_2\text{NEt}_2$ ) acts as a moderately weak electrolyte in acetonitrile where equilibrium with a planar form is assumed



Perturbation by an electric field jump (conductivity monitoring) produces a single relaxation. These data and other considerations give the rate constants shown in (3.11). Perturbation by a laser pulse of (3.11) using spectral monitoring (Sec. 3.5.1) gives reasonably concordant

kinetic data. Irradiation at 1.06  $\mu\text{m}$ , where  $\text{Ni(L)Cl}_2$  absorbs, increases the concentration of ion pairs and ions.<sup>112</sup>

### 3.4.4 Ultrasonic Absorption

The methods so far discussed involve a single discrete perturbation of the chemical system with direct observation of the attendant relaxation. An oscillating perturbation of a chemical equilibrium can also lead to a hysteresis in the equilibrium shift of the system. This effect can lead to the determination of a relaxation time. The process will obviously be more complex than with discrete perturbations, and there will be problems in the monitoring.<sup>113</sup>

Sound waves provide a periodic oscillation of pressure and temperature.<sup>114</sup> In water, the pressure perturbation is most important; in non-aqueous solution, the temperature effect is paramount. If  $\omega (= 2\pi f$ , where  $f$  is the sound frequency in cps) is very much larger than  $\tau^{-1}$  ( $\tau$ , relaxation time of the chemical system), then the chemical system will have no opportunity to respond to the very high frequency of the sound waves, and will remain sensibly unaffected. If  $\omega \ll \tau^{-1}$ , then the changing concentrations of chemical species demanded by the oscillating perturbation can easily follow the low frequency of the sound waves. In both cases there will be net absorption of sound. Of greatest interest is the situation in which the relaxation time is of the same order of magnitude as the periodic time of the sound wave, that is,  $\tau \approx \omega^{-1}$ . An amplitude and phase difference between the perturbation and the responding system develops and this leads to an absorption of power from the wave. It can be shown that the sound absorption is proportional to  $\omega\tau(1 + \omega^2\tau^2)^{-1}$  and that this value passes through a maximum at  $\omega\tau = 1$ . Experimentally, one has then to measure the maximum attenuation of the wave as the ultrasonic frequency is changed.

In quantitative terms, for a single equilibrium

$$\frac{\alpha}{f^2} = \frac{A}{1 + \omega^2\tau^2} + B \quad (3.12)$$

$\alpha$  = absorption coefficient in  $\text{Np cm}^{-1}$ , the experimentally determined value;  $f$  = frequency (Hz);  $\omega$  = angular frequency =  $2\pi f$ ;  $\tau$  = relaxation time;  $A$  = constant, the relaxation amplitude;  $B$  = background absorption which includes all relaxations other than due to chemical system ("classical" absorption – due to viscous and thermal losses). The plot of (3.12) is shown in Fig. 3.5. When  $\omega^2\tau^2 \gg 1$ ,  $\alpha/f^2 = B$ . When  $\omega^2\tau^2 \ll 1$ ,  $\alpha/f^2 = A + B$ . At  $\omega\tau = 1$ , there is an inflection and from this the relaxation time  $\tau$  can be obtained. As a bonus, from the value of  $A$ ,  $\Delta V$  for the reaction can be determined. There are a number of variations in the presentation of the data.<sup>113-117</sup> Computer fitting to equations such as (3.12) is increasingly popular.

A number of techniques are necessary to cover the five decades in frequency from  $10^4$  to  $10^9$  Hz corresponding to relaxation times of  $10^{-4}$  to  $10^{-9}$  s. A wide frequency range can be spanned with only two or three methods, requiring only a few ml of sample and relatively straightforward equipment. In the 10–100 kHz range considerable volumes of sample are still required (although the material is recoverable!).

Ultrasonic absorption played a major historical role in an understanding of the mechanisms of metal complex formation.<sup>118</sup> It has also been used to study stereochemical change in metal

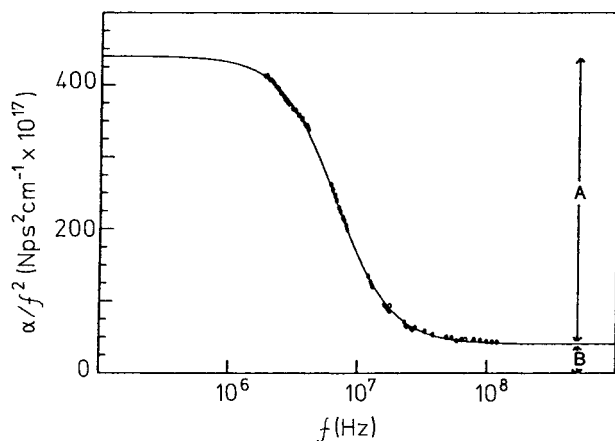


Fig. 3.5 One representation of ultrasonic data in terms of (3.12) for a single relaxation (J. K. Beattie, *Adv. Inorg. Chem.* **32**, 1 (1988)). Reproduced with permission from J. K. Beattie, *Adv. Inorg. Chem.* **32**, 1 (1988).

complexes (Sec. 7.2.3),<sup>115,116</sup> spin equilibria (Sec. 7.3),<sup>119</sup> proton transfer, aggregation phenomena, and helix-coil transitions of biopolymers.<sup>113</sup>

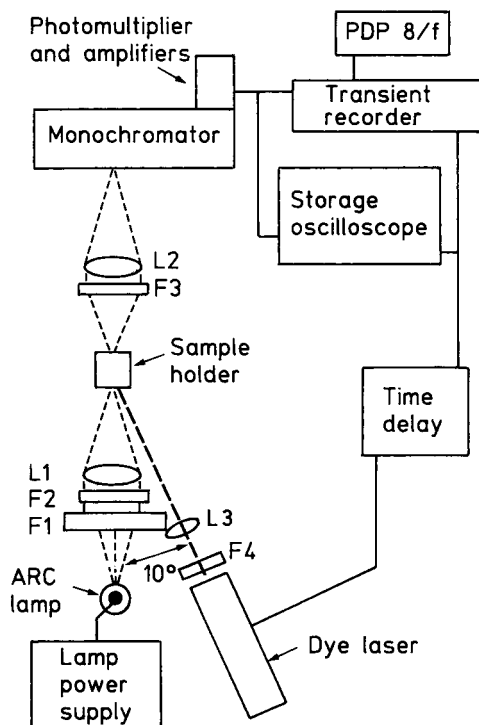
## 3.5 Large Perturbations

Photolysis and pulse radiolysis are powerful methods for producing sizeable amounts of reactive transients whose physical and chemical properties may be examined. Structural information on the transient and the characterization of early (rapid) steps in an overall reaction can be very helpful for understanding the overall mechanism in a complex reaction. Chemical equilibria may be disturbed by photolysis or radiolysis since one of the components may be most affected by the beam and its concentration thereby changed. The original equilibrium will be reestablished on removing the disturbance and the associated change can be examined just as in the relaxation methods. The approach has been more effectively used in laser photolysis and since very short perturbations are possible the rates associated with very labile equilibria may be measured.

### 3.5.1 Flash or Laser Photolysis

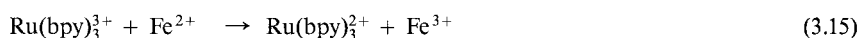
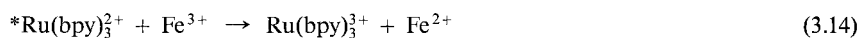
This involves the application of a pulse of high intensity light of short duration to a solution containing one or more species. In the original Nobel prize winning studies a flash lamp of a few microseconds duration was used.<sup>120</sup> Now a laser pulse is more often utilized and times as short as picoseconds or less may be attained. Several set-ups have been described.<sup>121</sup> Their complexity and cost are related to the time resolution desired. An inexpensive system using

a photographic flash lamp ( $\sim 5$  ms) and two laser systems with time resolutions of 1–5  $\mu$ s and 30 ns have been described in detail.<sup>122</sup> (See also Refs. 123–124.) One of these is shown in Fig. 3.6.<sup>122</sup> Laser photolysis in the ns-ps region is obviously very sophisticated but quite extensively used.<sup>125</sup> In Ref. 126 an apparatus for picosecond resonance Raman spectroscopy of carboxyhemoglobin is described.<sup>126</sup>



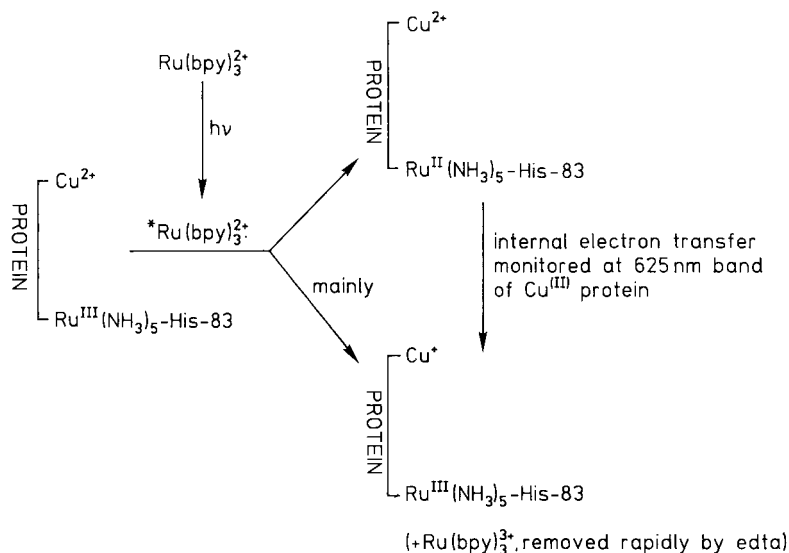
**Fig. 3.6** Schematic diagram of a dye laser photolysis set up for relaxation times  $\geq \mu$ s. The photolyzing light pulse is produced by a dye laser and enters the sample at about  $10^\circ$  to the axis of the sample beam. The observation beam originates from a 75-W xenon arc lamp. The apparatus is supplied by OLIS, Athens, Georgia USA.<sup>122</sup> Reproduced with permission from C. A. Sawicki and R. J. Morris, Flash Photolysis of Hemoglobin, in *Methods in Enzymology* (E. Antonini, L. R. Bernardi, E. Chiancone eds.), **76**, 667 (1981).

The intense pulse of light will likely produce a highly reactive excited state or states in a matter of femtoseconds. The subsequent steps that are possible can be illustrated by examining the case of  $\text{Ru}(\text{bpy})_3^{2+}$ , undoubtedly the most photochemically studied complex ion.<sup>127</sup> Irradiation at 503 nm produces the excited species  $^*\text{Ru}(\text{bpy})_3^{2+}$  which is generally believed to have the transferred electron on a single ligand. The subsequent behavior of  $^*\text{Ru}(\text{bpy})_3^{2+}$  is shown as \*A in (1.32). Of most interest to us is the strong reducing ( $E^0 = -0.86$  V) and moderate oxidizing ( $E^0 = 0.84$  V) properties of the excited species, compared with the ground state. Thus if  $\text{Fe}^{3+}$  is also present in the irradiated solution (B in scheme 1.32) the following sequence of events occurs:<sup>128</sup>



The very rapid reaction (3.15) with a large  $-\Delta G$  can thus be measured.<sup>129</sup> We therefore have an effective method for generating very rapidly *in situ* a powerful reducing or oxidizing agent. One of the most impressive applications of these properties is to the study of internal electron transfer in proteins.<sup>130, 131</sup>

The  $\text{Ru}(\text{NH}_3)_5^{2+}$  moiety can be attached to histidine-83 on the azurin surface. It can then be oxidized to Ru(III) without altering the conformation of the protein. This ruthenated protein is mixed with  $\text{Ru}(\text{bpy})_3^{2+}$  and laser irradiated. The sequence of events which occurs is shown in the scheme



In the first step, considerable amounts of the final product are produced as well as smaller amounts of a transient in which the oxidation states are “incorrect”. Internal electron transfer redresses this imbalance. The species  $\text{Ru}(\text{bpy})_3^{3+}$  produced must be removed rapidly (by scavenging with edta) so that it cannot oxidize the Ru(II) protein and interfere with the final step.<sup>130</sup> See Sec. 5.9. Some other examples of the application of the photolytic method to a variety of systems are shown in Table 3.4.<sup>132-139</sup> (See Probs. 4 and 5)

**Table 3.4** Some Transients Generated by Photolytic Methods

Irradiated System	Conditions	Results	Applications	Ref
Naphthols	pH 4-7; subnanosecond irradiation	Photoexcited naphthols with much lower $pK_a$ than in ground state dissociate <sup>133</sup>	Rapid (50 ns) pH (4 units) drop. Probe macromolecules <sup>134, 135</sup>	132
$\text{FeXsal}_2\text{trien}^+$ , X = H or $\text{OCH}_3$ . Low spin, high spin mixture	530 nm, nano-second laser; nonaqueous solvents	Transient bleaching of low spin species followed by thermal relaxation $\tau$ 's 46-192 ns at 255-205 K	Kinetics of low spin $\rightleftharpoons$ high spin Fe(III) Sec. 7.3	137

Table 3.4 (continued)

Irradiated System	Conditions	Results	Applications	Ref
Ni(pad) (H <sub>2</sub> O) <sub>4</sub> <sup>2+</sup> [See 6]	3 μs laser pulse; aqueous solution	Deactivation of excited state partly by photo-substitution and producing sizeable amounts of Ni(pada)(H <sub>2</sub> O) <sub>5</sub> <sup>2+</sup>	Direct analysis of ring closure, not possible by temperature or pressure jump	138
Oxy and carboxy-hemo proteins	Varying laser pulse times	Photodeligation to varying degrees	Measurement of combination rates of nonequilibrated forms of hemoproteins (see Eqn. 2.20)	139

### 3.5.2 Pulse Radiolysis

This technique has similarities to photolysis in that a large perturbation is involved and reactive transients can be produced and examined.<sup>140-142</sup> Van der Graff accelerators or, more popular, microwave linear electron accelerators are used to produce a high energy electron pulse typically within ns to μs. The set-up is illustrated in Figure 3.7. Reducing and oxidizing radicals result:<sup>143</sup>

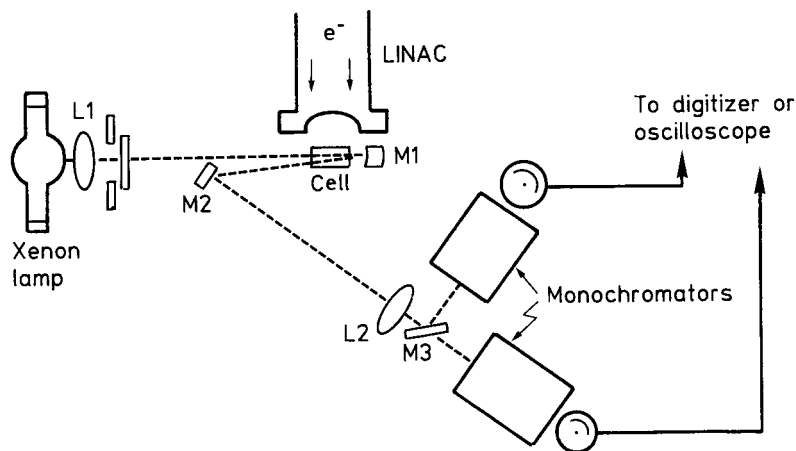
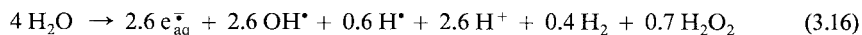
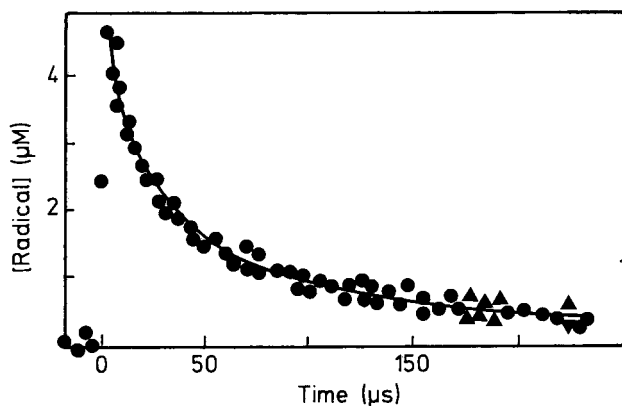


Fig. 3.7 Schematic set-up for pulse radiolysis. Electron beam and analyzing light beams are at right angles. The light beam is split for simultaneous recording at two wavelengths.<sup>142</sup>



The mixture of radicals would be difficult to examine or use. Fortunately, by the careful choice of an added substrate, some of the radicals produced in (3.16) are rapidly removed so

as to leave the desired radical for examination. For example, to examine  $e_{aq}^-$ , pulse radiolysis of solutions containing  $CH_3OH$  are used which rapidly removes  $H^\bullet$  and  $OH^\bullet$  radicals. Table 3.5 lists the more important radicals and gives references to the extensive compilation of properties and kinetic data for reactions of those radicals.<sup>144-150</sup> We thus have a means for the rapid production of highly reducing or oxidizing species. These can, in turn, be used to generate, for example, less usual oxidation states of metal ions and complexes (Chap. 8). Metastable oxidation states in polypeptides and proteins can also be produced and intramolecular electron transfer examined, just as by the photolytic method (Sect. 3.5.1).<sup>151</sup> Other examples are contained in Table 3.6. It is essential to have a concentration of substrate (S) sufficient to produce a higher rate of reaction with the radical (R),  $k[S][R]$ , than that of the spontaneous decay of R,  $k_1[R]^2$ , which occurs usually by disproportionation (Figure 3.8).<sup>149</sup>



**Fig. 3.8** Second-order decay of  $N_3^*$  ( $2N_3^* \xrightarrow{2k} 3N_2$ ) measured at 274 nm.  $2k = 8.8 \times 10^9 M^{-1} s^{-1}$ . Loss of 1–5  $\mu M$  (initial  $N_3^*$  concentrations) all conform to the solid curve. There is no evidence of any significant first-order component even at  $[N_3^*] = 0.5 \mu M$ .<sup>149</sup> Reproduced with permission from Z. B. Alfassi and R. H. Schuler, *J. Phys. Chem.* **89**, 3359 (1985). © (1985) American Chemical Society.

**Table 3.5** Some Radicals Generated by Radiolysis

Radical	Production (added substances underlined) <sup>a</sup>	Remarks
$e_{\text{aq}}^-$	$\text{CH}_3\text{OH}^{(b)} + \text{OH}^* \rightarrow \cdot\text{CH}_2\text{OH} + \text{H}_2\text{O}$ $\text{CH}_3\text{OH}^{(b)} + \text{H}^* \rightarrow \cdot\text{CH}_2\text{OH} + \text{H}_2$	Powerful reducing agent ( $E^0 = -2.9\text{V}$ ) Reacts diffusion controlled with many substrates. <sup>144,145</sup>
$\text{H}^*$	$e_{\text{aq}}^- + \text{H}^+ \rightarrow \text{H}^*$ ; $\text{CH}_3\text{OH}$ , $\text{N}_2\text{O}$	Powerful reducing agent ( $E^0 = -2.3\text{V}$ ). <sup>145,146</sup>
$\text{CO}_2^-$	$\text{N}_2\text{O} + e_{\text{aq}}^- \rightarrow \text{N}_2 + \text{OH}^- + \text{OH}^*$ $\text{HCO}_2^- + \text{OH}^* \rightarrow \text{CO}_2^- + \text{H}_2\text{O}$ $\text{HCO}_2^- + \text{H}^* \rightarrow \text{CO}_2^- + \text{H}_2$	$E^0 = -2.0\text{V}$ ; reactivity often intermediate between $e_{\text{aq}}^-$ and $\text{SO}_2^-$ Refs. 147–149.
$\text{O}_2^-$	$\text{O}_2 + \text{H} \rightarrow \text{O}_2^- + \text{H}^+$ $\text{O}_2 + e_{\text{aq}}^- \rightarrow \text{O}_2^-$ $\text{HCO}_2^- + \text{OH}^* \rightarrow \text{CO}_2^- + \text{H}_2\text{O}$ $\text{O}_2 + \text{CO}_2^- \rightarrow \text{O}_2^- + \text{CO}_2$	Often acts as one-electron slow reductant ( $E^0 = -0.33\text{V}$ ). <sup>150</sup>
$\text{OH}^*$	$\text{N}_2\text{O} + e_{\text{aq}}^- \rightarrow \text{N}_2 + \text{OH}^- + \text{OH}^*$ $\text{N}_2\text{O} + \text{H}^* \rightarrow \text{N}_2 + \text{OH}^*$	Strong oxidant ( $E^0 = 1.9\text{V}$ ). <sup>145</sup>
$(\text{SCN})_2^-$	$\text{N}_2\text{O} + e_{\text{aq}}^- \rightarrow \text{N}_2 + \text{OH}^- + \text{OH}^*$ $2\text{SCN}^- + \text{OH}^* \rightarrow (\text{SCN})_2^- + \text{OH}^-$	Ref. 148, 149. At maxm, 472 nm, $\epsilon = 7.6 \times 10^3\text{M}^{-1}\text{cm}^{-1}$ and useful for dosimetry
$\text{Br}_2^-$	$\text{N}_2\text{O} + e_{\text{aq}}^- \rightarrow \text{N}_2 + \text{OH}^- + \text{OH}^*$ $2\text{Br}^- + \text{OH}^* \rightarrow \text{Br}_2^- + \text{OH}^-$	Ref. 148, 149. Strong oxidant ( $E^0 = 1.63\text{V}$ )
$\text{N}_3^-$	$\text{N}_2\text{O} + e_{\text{aq}}^- \rightarrow \text{N}_2 + \text{OH}^- + \text{OH}^*$ $\text{N}_3^- + \text{OH}^* \rightarrow \text{N}_3 + \text{OH}^-$	Ref. 148. Rapid, selective <sup>149</sup> strong oxidant ( $E^0 = 1.30\text{V}$ )

(a) Usually 1–10  $\mu\text{M}$  radical generated in 0.2–2.0  $\mu\text{s}$ . 1% methanol or saturated  $\text{N}_2\text{O}$  or  $\approx 0.1\text{M}$   $\text{HCO}_2^-$  or halide used. Phosphate buffers.

(b)  $(\text{CH}_3)_3\text{COH}$  also used to scavenge. Radicals produced are relatively unreactive.

**Table 3.6** Examples of Use of Radicals Generated by Pulse Radiolysis

Irradiated System	Pulse Radical	Result	Ref.
(HIPIP) reduced	$e_{\text{aq}}^-$ (but not $\text{CO}_2^-$ )	First production in aqueous solution of (HIPIP) superreduced	152
Co(III) ammine complexes e.g. $\text{Co}(\text{NH}_3)_6^{3+}$ in $\text{H}^+$	$e_{\text{aq}}^-$	Production of $\text{Co}(\text{NH}_3)_6^{2+}$ Can then observe subsequent acid hydrolysis $\text{Co}(\text{NH}_3)_6^{2+} \xrightarrow{\text{H}^+} \text{Co}^{2+} + 6\text{NH}_4^+$ using conductivity monitoring	153
$\text{Co}^{\text{III}}(\text{NH}_3)_5\text{OCO}-\text{C}_6\text{H}_4\text{NO}_2^{2-}$	$\text{CO}_2^-$ or $\cdot\text{C}(\text{CH}_3)_2\text{OH}$	Formation of $\text{Co}^{\text{III}}(\text{NH}_3)_5\text{OCO}-\text{C}_6\text{H}_4\text{NO}_2^{\cdot+}$ ( $\epsilon = 2 \times 10^4\text{M}^{-1}\text{cm}^{-1}$ at 330nm). Followed by intramolecular electron transfer ( $k_{\text{et}} = 2.6 \times 10^3\text{s}^{-1}$ ), $k_{\text{et}}$ independent of $[\text{Co}(\text{III})]$ . (Sec. 5.8.2)	154 see also 155, 156



### 3.5.3 Comparison of Large Perturbation Methods

In general, photolysis induces substitutional and redox-related changes, whereas pulse radiolysis primarily promotes redox chemistry. Indeed one of the unique features of the latter method is to induce *unambiguous* one electron reduction of multi-reducible centers.<sup>157</sup> Metalloproteins can be rapidly reduced to metastable conformational states and subsequent changes monitored.<sup>158</sup>

Monitoring of events following perturbations can be achieved in much shorter times by photolysis. A variety of monitoring techniques have been linked to both methods (Table 3.7). It is valuable to obtain kinetic data by more than one method, when possible. The measurement of spin-change rates have, for example, been carried out by a variety of rapid-reaction techniques, including temperature-jump, ultrasonics and laser photolysis with consistent results (Sec. 7.3).

## 3.6 Competition Methods

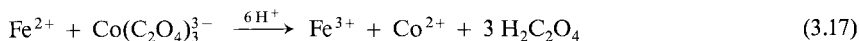
In this method, the reaction under study competes with another fast process, which may be spin relaxation (nmr and epr), fluorescence or diffusion towards an electrode. Monitoring of the competition is generally internal, making use of the characteristics of the fast process itself. This approach will be treated in some of the next sections.

## 3.7 Accessible Rate Constants Using Rapid Reaction Methods

It is the half-life of a reaction that will govern the choice of the initiation method (Fig. 3.1) and it is the character of the reaction that will dictate the monitoring procedure (Sec. 3.8 on).

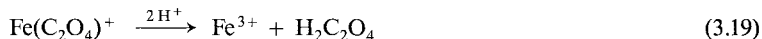
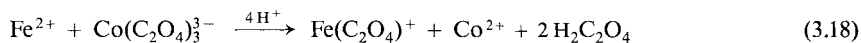
The half-life of a reaction with a kinetic order higher than one is lengthened as the concentrations of the reactants are decreased (Sec. 1.3). Provided that there is still a sufficient change of concentration during the reaction to be accurately monitored, quite large rate constants may be measured if low concentration of reactants are used, even without recourse to the specialized techniques described in the previous section.

The second-order redox reaction



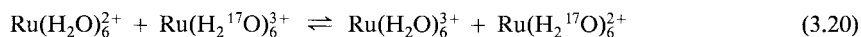
can be followed using even micromolar reactant concentrations, because of the high molar absorptivity of  $\text{Co}(\text{C}_2\text{O}_4)_3^{3-}$  ( $2.6 \times 10^4 \text{M}^{-1} \text{cm}^{-1}$  at 245 nm). The observed second-order rate constant ( $1.2 \times 10^3 \text{M}^{-1} \text{s}^{-1}$  at 25°C,  $\mu$  very low) corresponds to reaction times of minutes

with  $\mu\text{M}$  concentrations.<sup>159</sup> However if flow techniques and higher concentrations of reactants are used additional features of the reaction show up. Two steps are noted at 310 nm, a fast increase and slower decrease in absorbance corresponding to the production and loss of an intermediate  $\text{Fe}(\text{C}_2\text{O}_4)^+$ , which has a higher molar absorptivity at 310 nm than reactants or products.<sup>160</sup>



Large second-order rate constants, even diffusion controlled, can be measured by flow methods using low concentrations of reactants.<sup>161</sup> Use of pulsed accelerated flow (monitoring reaction times as low as 10  $\mu\text{s}$ ) and the large perturbation methods ( $\leq 1 \mu\text{s}$ ) can allow the measurement of rate constants  $> 10^9 \text{ M}^{-1}\text{s}^{-1}$  for *irreversible* reactions which are not amenable to relaxation methods. The concentration of a reactant and therefore the rate of a reaction may be drastically reduced by adjustment of the pH or by the addition of chelating agents.<sup>162</sup> It is worth recalling that forward and reverse rate constants are related by an equilibrium constant for the process. Relatively high rate constants for the formation of metal complexes ( $k_f$ ) can be estimated from the relationship  $k_f = k_d K$  in cases where  $K$  (the formation constant) is large and  $k_d$  is a small and easily measured dissociation rate constant. Many early data for Ni(II) were obtained in this way.<sup>163</sup>

The power of the relaxation and large perturbation methods lie in their ability to allow the measurement of large *first-order* rate constants. The half-lives of first-order reactions are concentration-independent and values  $\leq 1 \text{ ms}$  ( $k \geq 10^3 \text{ s}^{-1}$ ) are outside the ability of most flow methods. First-order rate constants ranging from  $10^4 \text{ s}^{-1}$  to as large as  $10^{11}$ – $10^{12} \text{ s}^{-1}$  can be measured by the methods shown in Fig. 3.1. This encompasses such disparate processes as conformational change, intersystem crossing, excited state deactivation and small displacements of ligands from heme centers. The rate of any reaction with a finite heat of activation will be reduced by lowering the temperature. Some reactions that are fast at normal temperatures were studied nearly forty years ago by working in methanol at  $-75^\circ\text{C}$ , when quite long reaction times were observed.<sup>164</sup> A combination of lowered temperatures (to 252 K) with fast-injection techniques has allowed the measurement of the electron self-exchange by  $^{17}\text{O}$  nmr:<sup>165</sup>



The lowered temperature approach has been linked to flow,<sup>80,166</sup> temperature jump,<sup>167</sup> photolysis,<sup>168</sup> and nmr<sup>165</sup> methods. Cryoenzymology allows the characterization of enzyme intermediates which have life-times of only milliseconds at normal temperatures, but are stable for hours at low temperatures. Mixed aqueous/organic solvents or even concentrated salt solutions are employed and must always be tested for any adverse effects on the catalytic or structural properties of the enzyme.<sup>167,169</sup>

### 3.8 The Methods of Monitoring the Progress of a Reaction

The rate of a reaction is usually measured in terms of the change of concentration, with time, of one of the reactants or products,  $-d[\text{reactant}]/dt$  or  $+d[\text{products}]/dt$ , and is usually expressed as moles per liter per second, or  $\text{M s}^{-1}$ . We have already seen how this information might be used to derive the rate law and mechanism of the reaction. Now we are concerned, as kineticists, with measuring experimentally the concentration change as a function of the time that has elapsed since the initiation of the reaction. In principle, any property of the reactants or products that is related to its concentration can be used. A large number of properties have been tried.

It is obviously advantageous from a point of view of working up the data if the reactant property and concentration are linearly related. It is much easier and more likely to be accurate to monitor the reaction continuously *in situ* without disturbing the solution than to take samples periodically from the reaction mixture and analyze these separately, in the so-called batch method. The batch method cannot, however, be avoided when an assay involves a chemical method (which “destroys” the reaction). Separation of reactants or products or both also is necessary when an assay involving radioisotopes is employed. Separation prior to analysis is sometimes helpful when the system is complicated by a number of equilibria, or when a variety of species is involved.

Methods that have been used for monitoring reactions will be discussed in the next sections. Those applicable to rapid reactions are shown in Table 3.7. Of the hundreds of possible references to the literature, only a few key ones are given. Several considerations will dictate the method chosen. If it is suspected that the reaction may be complex, then more than one method of analysis ought to be tried, so as to show up possible intermediates and characterize the reaction paths in more detail.

**Table 3.7** Monitoring Methods for Rapid Reactions

Monitoring Method	Flow	<i>T</i> -jump	<i>P</i> -jump	<i>E</i> -jump	Photolysis	Radiolysis
UV and visible spectrophotometry	46	170	171	172	122	173
Infrared	174	—	—	—	175	—
Raman	176, 177	—	—	—	178	179
Light scattering	180	181	109	—	—	—
Fluorescence	182	183	184	—	—	—
Polarimetry (cd)	185, 186	187	188	189	190	—
nmr	191, 192	—	—	—	193	194
epr	195	—	—	—	196	197
Conductivity	198, 199	200	199	201	202, 203	204
Thermal	205–207					

## 3.9 Spectrophotometry

Nearly all the spectral region has been used in one kinetic study or another to follow the progress of a chemical reaction. *In toto* it represents by far the most powerful and utilized method of monitoring.

### 3.9.1 Ultraviolet and Visible Regions

These regions are particularly useful since few, if any, reactions of transition metal complexes are unaccompanied by spectral absorption changes in these regions. We first show how optical absorbances may be substituted for the concentration changes required in deriving the rate law.

The optical absorbance  $D$  shown by a single chemical species A in solution is related to its concentration by the Beer-Lambert law:

$$D = \log \frac{I_0}{I_t} = \epsilon_\lambda \cdot l \cdot [A] \quad (3.21)$$

where  $I_0$  and  $I_t$  = incident and transmitted light intensities at wavelength  $\lambda$ .

$\epsilon_\lambda$  = molar absorptivity at a wavelength  $\lambda$ .

$l$  = light path, in cm.

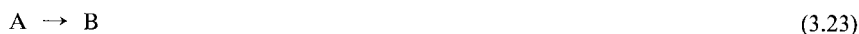
$[A]$  = molar concentration of the species A.

Mixtures of species A, B, ... usually give additive absorbances:

$$\left( \frac{D}{l} \right) = \epsilon_A [A] + \epsilon_B [B] + \dots \quad (3.22)$$

and so it is possible to analyze changes in the concentrations of specific reactants or products from absorbance changes in the reaction mixture.

It is not difficult to show that the optical absorbance, or other properties for that matter, can be used directly to measure first-order rate constants, without converting to concentrations. Consider



Omitting brackets to denote concentrations, we find:

$$\text{At zero time, } D_0 = \epsilon_A A_0 + \epsilon_B B_0 \quad (3.24)$$

$$\text{At time } t, \quad D_t = \epsilon_A A_t + \epsilon_B B_t \quad (3.25)$$

$$\text{At equilibrium } D_e = \epsilon_B B_e = \epsilon_B (A_0 + B_0) = \epsilon_B (A_t + B_t) \quad (3.26)$$

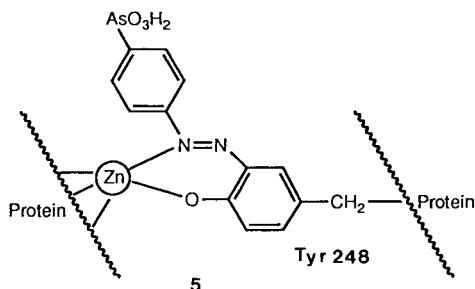
Therefore,

$$A_0 = \frac{(D_0 - D_e)}{\epsilon_A - \epsilon_B} \quad A_t = \frac{(D_t - D_e)}{\epsilon_A - \epsilon_B} \quad (3.27)$$

$$\ln \frac{A_0}{A_t} = \ln \frac{(D_0 - D_e)}{(D_t - D_e)} = kt \quad (3.28)$$

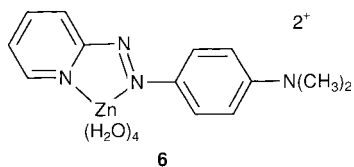
For orders of reaction other than one, a knowledge of the molar absorptivities is necessary.<sup>208</sup> See Fig. 1.3.

Commercial spectrophotometers, both in the conventional and stopped-flow mode display, usually on a computer screen, the optical absorbance changes directly. There are distinct advantages in using absorbance in the visible region since there is less likelihood of interference from buffers and added electrolytes, which are usually transparent in this region. However, the molar absorptivities of complex ions are often much higher in the ultraviolet, since they are based on charge transfer rather than on *d-d* transitions. Consequently, lower concentrations of reactants with ultraviolet monitoring will, as the reaction proceeds, give absorbance changes that are comparable with the absorbance changes when the visible region is used. A lower concentration means a greater economy in materials, but sometimes more important, a longer  $t_{1/2}$  for all but first-order reactions. We have seen the value of this already (Sec. 3.7). Even small absorbance changes can be measured accurately using the sensitive detectors and associated data acquisition equipment now available. Many runs can be accumulated and processed to obtain high signal/noise ratios even with absorbance changes as low as 0.001 units.<sup>209</sup> Small absorbance changes inherent in the system may be amplified by the introduction of a chromophoric group into one of the reactants. The modification of carboxypeptidase A by attachment of the intensely colored arsanilazo group to the tyrosine-248 residue **5** allows



the ready visualization of interactions of the enzymes with substrates and inhibitors (Sec. 1.8.2)<sup>210</sup> or of the apoenzyme with metal complexes.<sup>211</sup> Care has to be taken that the modification does not alter radically the characteristics of the unmodified reactant.<sup>212</sup> Other methods of enhancing spectral changes are to add indicators to monitor pM<sup>213,214</sup> or pH<sup>215</sup> changes.<sup>216</sup> Colored complexes may be used to probe reaction sites e.g. Zn(pad)<sup>2+</sup> **6** is a probe for two adjacent carboxylate groups of the catalytic residues of acid proteinases.<sup>217</sup>

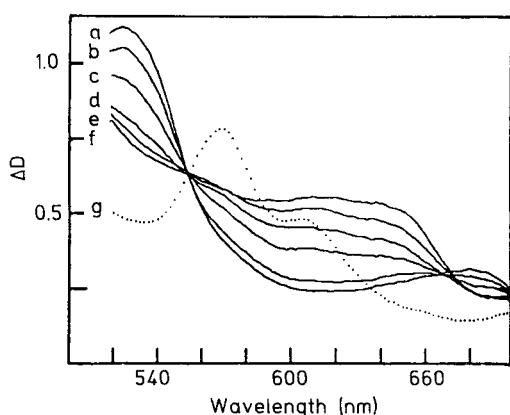
Reaction complexity can often show up (and be resolved) by studying the reaction at more than one wavelength, when different rate patterns may be observed (Sec. 3.7).<sup>218</sup> However the collection of a family of spectra directly as the reaction proceeds can be of enormous value.



As might be expected, the problem of obtaining spectra of a reacting system increases as the time resolution involved decreases. The spectral changes associated with a reaction may be constructed by wavelength point-by-point measurements. The method, although tedious and costly on materials, is still used. However rapid-scan spectrophotometry, linked to stopped-flow, is now more readily available and reliable. Two systems are used, shown schematically in (3.29)<sup>219-221</sup> and (3.30).<sup>222, 223</sup> An example of its use is shown in Fig. 3.9.<sup>222</sup> Rapid scan

white light → mixing chamber → diffraction grating → ~30 photodiodes (3.29)

white light → moving diffraction grating → mixing chamber → photomultiplier (3.30)



**Fig. 3.9** Spectra of  $\text{Fe}(\text{tpps})\text{H}_2\text{O}^{3-}$  (a),  $\text{Fe}(\text{tpps})\text{OH}^{4-}$  (f) and mixtures (curve b, pH 6.5; curve c, pH 7.0; curve d, pH 7.46, curve e, pH 7.9). Curves b–f were obtained within 3.8 ms after mixing  $\text{Fe}(\text{tpps})\text{H}_2\text{O}^{3-}$  at pH  $\approx 5$  with buffer at the designated pH. The spectrum of  $\text{Fe}(\text{tpps})\text{OH}^{4-}$  was obtained by plunging into pH 9.1. The spectrum of  $(\text{tpps})\text{Fe}-\text{O}-\text{Fe}(\text{tpps})^{8-}$  is shown in curve g. In all cases, the final concentration of iron(III) is 103  $\mu\text{M}$ . Path length in the Dionex stopped-flow instrument is 1.72 cm (fluorescence observation chamber).<sup>222</sup> Reproduced with permission from A. A. El-Awady, P. C. Wilkins and R. G. Wilkins, *Inorg. Chem.* **24**, 2053 (1985). © (1985) American Chemical Society.

spectrophotometry is valuable for obtaining spectra following radiolysis<sup>224</sup> or photolysis.<sup>225</sup> The acquiring of spectra after very rapid initiation ( $10^{-9}$  to  $10^{-14}$  s) presents large technical problems<sup>125</sup> but has been used effectively to shed light on the early events following photodeligation of oxy- and carboxyhemoproteins<sup>139</sup> (Sec. 2.1.2). A stopped-flow rapid scanning spectrophotometer for use at low temperatures has been described.<sup>226</sup> It has been used to obtain the absorbance (and epr) spectra of peptide and ester intermediates formed within 0.5 s in 4.5 M NaCl at  $-20^\circ\text{C}$  by the hydrolysis of dansyl oligopeptides and esters catalyzed by cobalt carboxypeptidase. The results indicate that the metal plays a vital but different role in the two hydrolyses.<sup>226</sup>

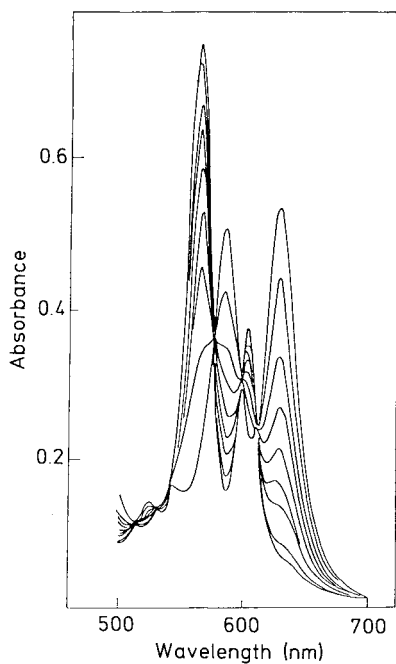
The occurrence or not of *isosbestic points* during a reaction is very informative. Isosbestic points are wavelengths at which the absorbance remains constant as the reactant and product composition changes. One (or preferably more) isosbestic points during a reaction strongly suggest that the original reactant is being replaced by *one* product, or if more than one product, that these are always in a strictly constant ratio. The occurrence of isosbestic points implies the absence of appreciable amounts of reaction intermediates, thus, for example, supporting a scheme



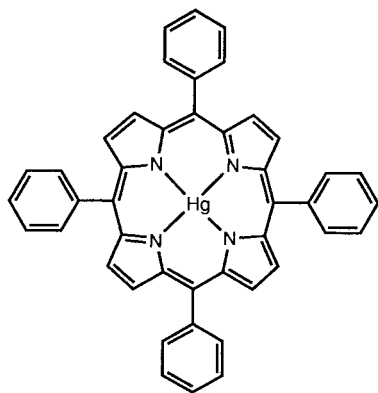
rather than



Seven isosbestic points in the relatively fast reaction of Hg(tpp) (7) with Zn(II) in pyridine (Fig. 3.10) show that Hg(tpp) converts to Zn(tpp) without formation of appreciable amounts of free tpp base, which has a different spectrum from either complex.<sup>227</sup> The occurrence of



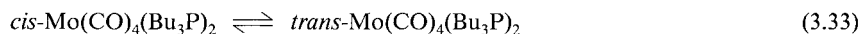
**Fig. 3.10** Seven isosbestic points observed during the reaction of Zn(II) with Hg(tpp).<sup>227</sup>



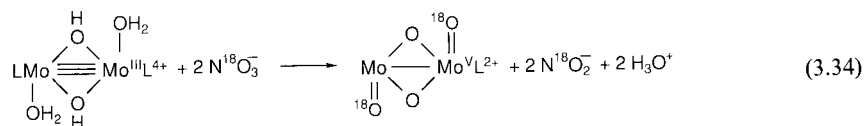
an isobestic point at 435 nm strongly suggests that Compound I is the *sole* product of the reaction between catalase and methyl hydroperoxide or peracetic acid. Compound I is only stable for a few hundred milliseconds and rapid-scan stopped-flow must be used.<sup>228</sup>

### 3.9.2 Infrared Region

Direct monitoring by infrared absorption is not commonly used for the study of complex-ion reactions in water, because the solvent and dissolved electrolytes often absorb in this region. Infrared analysis had found some use in studying H-D exchange processes in both substitution and redox reactions, using D<sub>2</sub>O as the solvent since this does not absorb extensively in the near infrared. The nmr method (Sec. 3.9.5) has largely replaced infrared for monitoring these exchanges. Infrared monitoring sometimes provides structural information not obtainable using uv-visible spectroscopy. The CO, NO and NC stretches are very sensitive to the metal environment. Therefore substitution,<sup>229</sup> including CO exchange,<sup>230,231</sup> geometrical isomerization (3.33)<sup>232</sup> and redox reactions<sup>233</sup> of organometallics have been studied in

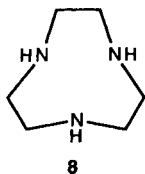


nonaqueous solvents using infrared detection. The potential for the examination of metal oxo compounds is illustrated by the demonstration of oxo-group transfer in a Mo(III) → Mo(V) transformation



(L = 1,4,7-triazacyclononane) **8**.<sup>234</sup> The rate law

$$d[\text{Mo}_2^{\text{V}}]/dt = k [\text{Mo}_2^{\text{III}}] [\text{NO}_3^-] \quad (3.35)$$

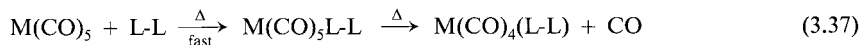
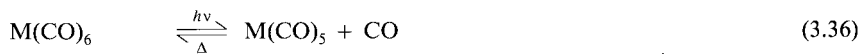


indicates that substitution of H<sub>2</sub>O by NO<sub>3</sub><sup>-</sup> is the rds. Using 90% enriched N<sup>18</sup>O<sub>3</sub><sup>-</sup> the Mo(V) product shows a predominant ν(Mo=O<sub>term</sub>) = 868 cm<sup>-1</sup> and ν<sub>as</sub>(Mo-O<sub>bridge</sub>) = 730 cm<sup>-1</sup>. Comparison with the unlabelled Mo(V) product which shows ν(Mo=O<sub>term</sub>) = 918 cm<sup>-1</sup> and ν<sub>as</sub>(Mo-O<sub>bridge</sub>) = 730 cm<sup>-1</sup> and with one terminal M=O<sub>term</sub> (ν = 887 cm<sup>-1</sup> and 730 cm<sup>-1</sup>) indicates that the terminal oxo groups in the product of (3.34) must have originated from the NO<sub>3</sub><sup>-</sup> group.<sup>234</sup>

Fast time resolved infrared attached to flow<sup>174</sup> and to uv-vis flash photolysis<sup>175</sup> has been an important development for the study of rapid substitution, e. g. in Co<sub>2</sub>(CO)<sub>8</sub> in hexane<sup>174</sup> and



for the detection of transient organometallic species, with  $\mu\text{s}$  resolution.<sup>175</sup> (Sec. 3.13.1) A unidentate intermediate is observed in the reaction of  $\text{M}(\text{CO})_6$ ,  $\text{M} = \text{Cr}, \text{Mo}$  and  $\text{W}$ , with 4,4'-dialkyl-2,2'-bipyridine (L-L) using rapid-scan Fourier transform ir.<sup>235</sup>

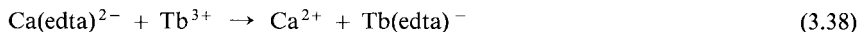


Raman, like infrared, gives sharp detailed spectra and structural information. The sensitivity is however poorer than uv-vis and the equipment more complex. By choosing an excitation frequency matching that of a strong absorption band, ordinary Raman intensities may be boosted some five orders of magnitude (resonance Raman).<sup>236</sup> Small amounts of a transient in a high solute background may be characterized. For examining some short time transients, two laser pulses are used. One photolyses the sample. The second laser acts as a resonance Raman probe. This allows picosecond imaging in very fast photochemically induced reactions.<sup>126</sup> Resonance Raman is a powerful structural tool for characterizing metallo-proteins<sup>236</sup> and has been successfully linked to flow and photolytic, but not (so far) to the relaxation methods.

### 3.9.3 Fluorescence

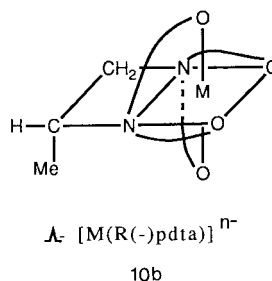
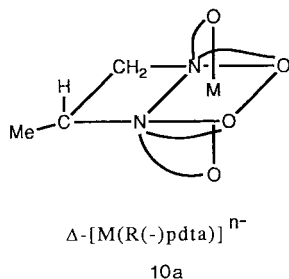
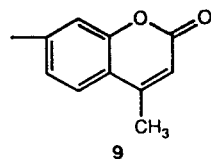
The attenuation of fluorescence can be used as a sensitive monitor for the progress of a reaction. Even reactant concentrations as low as 0.5–2.5  $\mu\text{M}$  can be detected, thus bringing the reaction rates into the stopped-flow region even although second-order rate constants as high as  $10^7 \text{ M}^{-1} \text{ s}^{-1}$  may be involved.<sup>237</sup> Fluorescence has been little used to monitor complex-ion reactions, although its enhanced sensitivity, compared with that of uv-visible should be an important consideration, not only for reactions involving aromatic-type ligands e.g. porphyrins<sup>238</sup> but also others.<sup>239</sup>

The luminescence of  $\text{Tb}^{3+}$  increases when coordinated water is replaced by a ligand such as edta. Thus the reaction



can be monitored at 545 nm at right angles to the exciting beam (360–400 nm).<sup>239</sup> Flow- and relaxation apparatus with spectral monitoring can be easily adapted to follow fluorescence changes.<sup>182,183</sup>

It is in the study of reactions involving proteins that fluorescence comes into its own.<sup>240</sup> Thus, the reaction of carbonic anhydrase with a wide variety of sulfonamides (important inhibitors) results in a substantial quenching of the fluorescence of the native protein (Sec. 1.10.2(b)) The binding of concanavalin A to certain sugars is most conveniently monitored by attaching a 4-methylumbelliferyl fluorescent label **9** to the sugar and examining by stopped-flow the fluorescence quenching of the sugar on binding.<sup>241,242</sup> See Structure **10**, Chap. 1. The kinetics of binding of “colorless” sugars can also be studied in competition with the fluorescent one.<sup>243</sup> Alternatively, the protein may be chromophorically modified. Since  $\text{Ca}^{2+}$ , an important component of many metalloproteins, can be replaced by  $\text{La}^{3+}$  without



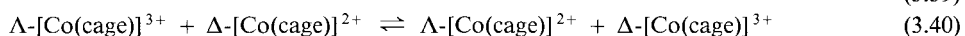
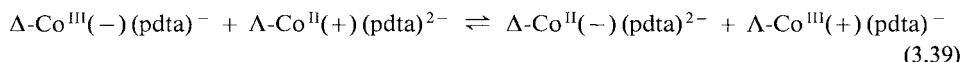
gross changes in protein structure, the La(III) derivative can be monitored by fluorescence methods, and give, indirectly, information on the native protein.<sup>244</sup>

The measurement of *fluorescence life-times* has great value for probing structural features of proteins. It requires expensive equipment since very rapid extinction of the exciting nanosecond pulse is necessary and the rapid decay of the emission must then be measured.<sup>245</sup> The decay of the tryptophan fluorescence of LADH is biphasic with  $\tau = 3.9$  and 7.2 ns and these are assigned to buried Trp-314 and exposed Trp-15, respectively.<sup>246</sup>

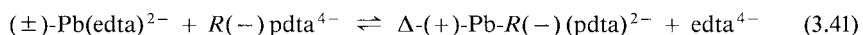
### 3.9.4 Polarimetry

The polarimetric method naturally must be used when stereochemical change involving chiral compounds is being investigated. The optical rotatory power of an optically active ligand is dependent on the environment. This fact can be used to follow the interaction of resolved ligands with metal ions.<sup>247</sup> Optical rotation changes accompanying reactions of proteins (folding, conformational changes, helix-coil transformations) are a useful monitor especially now that stopped-flow and relaxation techniques have been successfully linked with circular dichroism.<sup>185</sup>

The polarimetric method is sometimes useful for the study of exchange reactions in which large rotation changes but no net chemical change is involved:<sup>249,250</sup>



(cage = a variety of cage ligands,<sup>250</sup> See Sect. 2.2.1(a)). Even when a very slight absorbance change is involved as in (3.41)



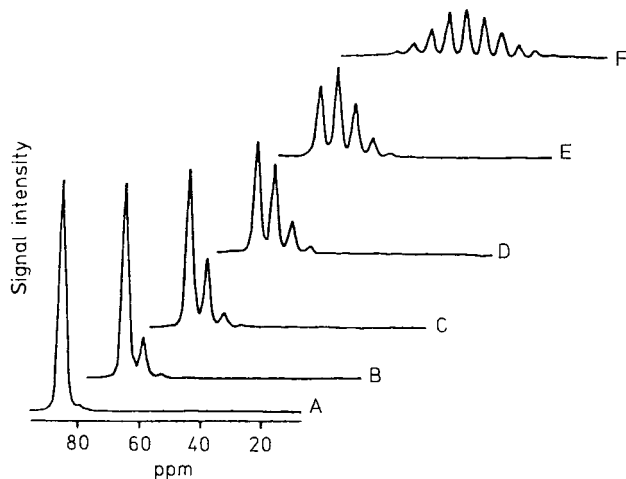
the large rotational differences between the Pb-pdta complex and the pdta ligand (**10**) at 365 nm is more sensitive and may be utilized.<sup>247</sup> Although polarimetry is rarely superior to the other spectral methods as an analytical tool, probing by more than one monitoring device can be informative. In the unfolding of apomyoglobin, monitoring by cd indicates a more rapid change than when fluorescence is examined. This is ascribed to changes in  $\alpha$ -helical structure (responding to cd) being faster than those occurring in the local environment of tryptophans which show up in fluorescence.<sup>251</sup> See also Refs. 88 and 252.

### 3.9.5 Nmr Region

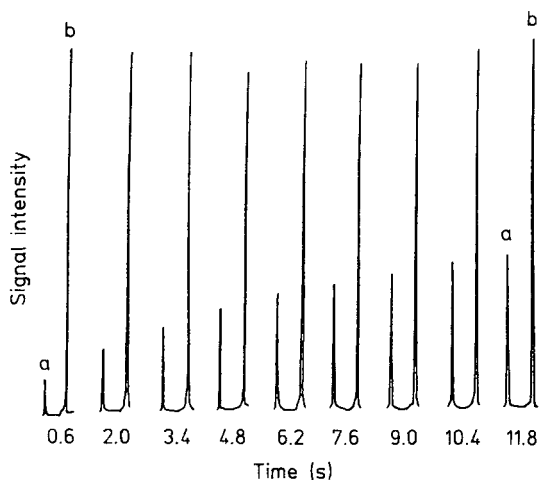
Nmr can be used simply as an analytical tool in which the strength of the signal is a measure of the concentration of a particular species. With the advent of reliable machines, more sensitive to small changes in concentration, and with the availability of multinuclear probes, the method is finding increasing use for studying a variety of reactions. One disadvantage still is the relatively high concentrations (typically 0.05–0.25 M) of solute that must be used, this posing problems of availability, solubility or stability of material. Although we saw in Chapter 1 an excellent example of the nmr analysis of the three participants in an  $A \rightarrow B \rightarrow C$  sequence,<sup>253</sup> its real advantage lies in the study of exchange processes, using both the analytical and the line broadening (next section) aspects of nmr. A selection of exchange reactions

**Table 3.8** Analytical Applications of Nmr

Type of Reaction	Example	Nucleus Used	Ref. & Notes
Water exchange in inert aqua complexes	$cis\text{-Co(en)}_2(\text{H}_2^{17}\text{O})_2^{3+} - \text{H}_2\text{O}$ exchange	$^{17}\text{O}$	254. Signal for coordinated water at 126 ppm decreases; signal for free water at 0 ppm increases.
	$\text{Pt}(\text{H}_2\text{O})_4^{2+} - \text{H}_2^{17}\text{O}$	$^{17}\text{O}$	255. High pressure probe allows determination of $\Delta V^\ddagger$ . Could also use $^{195}\text{Pt}$ , <sup>256</sup> but not as accurate.
Proton exchange in amines	$\text{Co}(\text{tren})(\text{NH}_3)_2^{3+}$ in $\text{D}_2\text{O}$	$^1\text{H}$	257. Shows H exchange of various ammine centers
	$\text{Co}(\text{NH}_3)_6^{3+}/\text{D}_2\text{O}, \text{H}_2\text{O}$	$^{59}\text{Co}$	258. Figure 3.11
Electron Transfer	$\text{C}_o^{\text{II}}\text{ttp}, \text{C}_o^{\text{III}}\text{ttp}^+$ in $\text{CDCl}_3$ (ttp = 5, 10, 15, 20 tetra-p-tolylporphine and tpp = 5, 10, 15, 20 tetraphenylporphine)	$^1\text{H}$ p-methyl peak $\text{Co}^{\text{III}}(\text{ttp})$ $\delta = 2.63$ ppm $\text{Co}^{\text{II}}(\text{ttp})$ $\delta = 4.13$ ppm (shifts from $\text{Me}_4\text{Si}$ )	259. Anions accelerate, then must use line broadening (coalescence temperature, next section)
	$\text{Ru}(\text{H}_2\text{O})_6^{3+/2+}$ electron transfer	$^{17}\text{O}$ and $^{99}\text{Ru}$	260. Injection technique. Also by line broadening with consistent results.
Substitution	$\text{VO}_3^{3-} + \text{H}_2\text{O} \rightarrow \text{VO}_4^{3-} + \text{S}^{2-}$	$^{51}\text{V}$	261. Can detect $\text{VO}_3^{3-}$ during slow reaction

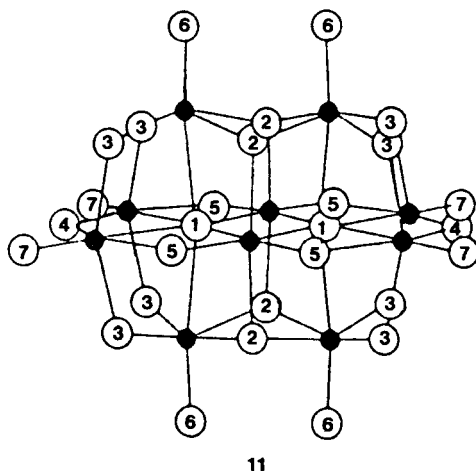


**Fig. 3.11**  $^{59}\text{Co}$  nmr spectra obtained as a function of time at 71.7 MHz and 25°C for 0.05 M  $\text{Co}(\text{NH}_3)_6\text{Cl}_3$  in  $\text{D}_2\text{O}/\text{H}_2\text{O}$  (3:1) at pH 4.0. 1.7 min (A); 18 min (B); 38 min (C); 68 min (D); 107 min (E) and 140 min (F). There is a 5.6 ppm isotope shift experienced at the Co nucleus for every proton replaced by D on the N. Each H/D isotopomer can be observed. The final distribution will depend on the H/D ratio in the solvent. A plot of the  $\text{H}_{18}$  isotopomer vs. time is first order,  $k = 3.5 \times 10^{-5} \text{s}^{-1}$ , Ref. 258. Reproduced with permission from J. G. Russell, R. G. Bryant and M. M. Kreevoy, *Inorg. Chem.* **23**, 4565 (1984). © (1984), American Chemical Society.



**Fig. 3.12** Parts of successively recorded  $^1\text{H}$  nmr spectra obtained by stopped-flow nmr after mixing  $\text{Fe}(\text{dmsO})_6^{3+}$  with  $[\text{}^2\text{H}_6]\text{dmsO}$  in  $\text{CD}_3\text{NO}_2$  solution at 243.4 K.  $\text{Fe}(\text{III}) = 10 \text{ mM}$   $[\text{}^2\text{H}_6]\text{dmsO} = 1.0 \text{ M}$ . Resonances: a = dmsO; b =  $\text{SiMe}_4$ .<sup>270</sup> Reproduced with permission from C. H. McAteer, P. Moore, *J. Chem. Soc. Dalton Trans.* 353 (1983).

studied by nmr monitoring is shown in Table 3.8<sup>254-261</sup> and illustrated in Fig. 3.11.<sup>258</sup>  $^{17}\text{O}$  can replace  $^{18}\text{O}$  in tracer applications, and continuous nmr monitoring then replaces the tedious analysis associated with the batch technique. Nowhere is this more evident than in the study of the exchange of the 7 types of O in  $\text{V}_{10}\text{O}_{28}^{6-}$  **11** with  $\text{H}_2\text{O}$ . Using  $^{18}\text{O}$ , excellent first-order traces indicating *identical* exchange rates for all O's were obtained.<sup>262</sup> The individual O's (7 types) are identified by nmr and the exchange data indicate some *very slight* differences in their exchangeability (but close to the values by  $^{18}\text{O}$ ).<sup>263</sup> For other comparative examples see Ref. 264-266. One can also examine  $^{18}\text{O}$ - $^{16}\text{O}$  exchange by using the fact that  $^{13}\text{C}$ ,<sup>267,268</sup> as well as  $^{195}\text{Pt}$ <sup>256</sup> and other nuclei show different nmr signals when adjacent to  $^{18}\text{O}$  compared with  $^{16}\text{O}$ .  $^1\text{H}$  Nmr has been extensively used for diamagnetic complexes such as those of Co(III) but there are problems with Cr(III) because of the long electron spin relaxation times associated with this paramagnetic ion. Using  $^2\text{H}$  nmr may be advantageous here since 40 fold narrower lines result.<sup>269</sup> Relatively fast processes can be examined by nmr by using fast injection techniques<sup>260</sup> or flow methods,<sup>191,192,270</sup> Fig. 3.12.<sup>270</sup>



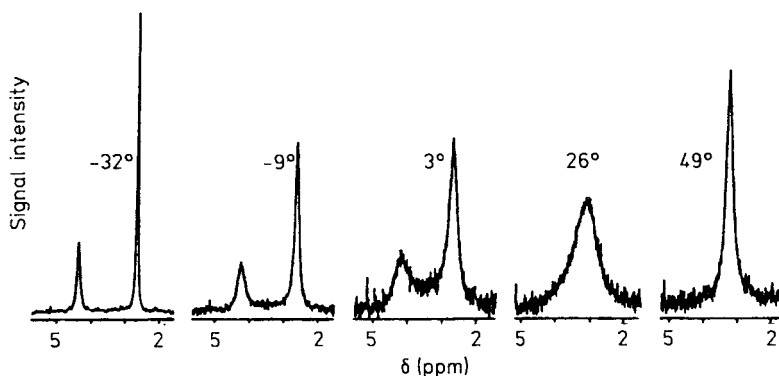
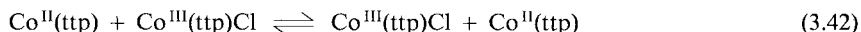
### 3.9.6 Nmr Line Broadening

The determination of the rates of fast exchange processes by nmr linebroadening experiments has been one of the most significant factors in the success in understanding the mechanisms of complex-ion reactions of all types. Among the nuclei which have now been utilized, sometimes routinely, one finds  $^1\text{H}$ ,  $^{13}\text{C}$ ,  $^{14}\text{N}$ ,  $^{17}\text{O}$ ,  $^{19}\text{F}$ ,  $^{23}\text{Na}$ ,  $^{31}\text{P}$ ,  $^{39}\text{K}$  and  $^{55}\text{Mn}$ . For exchange, the proton is most used because of the favorable 100% abundance and 1/2 spin quantum number. However the proton is invariably far from the influence of the metal site and chemical shifts between bound and free ligand are small. For this reason,  $^{13}\text{C}$ ,  $^{14}\text{N}$ ,  $^{17}\text{O}$  or  $^{31}\text{P}$  which are nearer the central atom are also used even though they are less sensitive nuclei. There have been several comprehensive accounts of the application of nmr to the measurement of exchange rates.<sup>271,272</sup>

The same nucleus (say methyl protons) in different chemical environments A and B will generally have nuclear magnetic resonances at different frequencies. If the exchange of pro-

tons between A and B is sufficiently slow, sharp lines corresponding to A and B will be recorded. As the exchange rate increases however, it is observed that at first there is an initial broadening of the signals; this is followed by their coalescing, and finally, at high exchange rates, narrowing of the single signal occurs.

This behavior is well typified in Fig. 3.13 involving the exchange<sup>259</sup>



**Fig. 3.13** Temperature dependence of the p-Me line shapes in 90-MHz  $^1\text{H}$  NMR spectra of a mixture of  $\text{Co}^{\text{II}}(\text{ttp})$  and  $\text{Co}^{\text{III}}(\text{ttp})\text{Cl}$  in  $\text{CDCl}_3$ . ttp = 5, 10, 15, 20-tetra-p-tolylporphine.<sup>259</sup> (Temperatures in  $^{\circ}\text{C}$ ). Reproduced with permission from R. D. Chapman and E. B. Fleischer, *J. Amer. Chem. Soc.* **104**, 1582 (1982). © (1982) American Chemical Society.

in  $\text{CDCl}_3$ . At temperatures around  $-30^{\circ}\text{C}$ , the spectra of mixtures are additive and exchange is too slow to affect the signals. Near  $0^{\circ}\text{C}$ , as exchange becomes important, the lines broaden until they coalesce at  $26^{\circ}\text{C}$ . Above this temperature, the methyl line appears at the average position and continually narrows as the temperature is raised, and the exchange is very fast. The region between  $-10^{\circ}\text{C}$  and near to  $26^{\circ}\text{C}$  is termed the *slow-exchange region*. That around the coalescence temperature is the *intermediate-exchange region*, and the region above about  $40^{\circ}\text{C}$  is the *fast-exchange region*. Only the temperature region between  $-10^{\circ}\text{C}$  and about  $50^{\circ}\text{C}$  can be used to assess exchange rates (see following discussion). For another example of this sequence of events see Ref. 273.

(a) *Slow-Exchange Region*. If the exchange rate is very slow, the lines due to A and B in the mixture correspond to the lines of the single components in both position and linewidth.

The broadening of the signal, say due to A, as the exchange rate increases, is the difference in full linewidth at half height between the exchange-broadened signal  $W_{\text{A}}^{\text{E}}$ , and the signal in the absence of exchange  $W_{\text{A}}^{\text{O}}$ . This difference is often denoted  $\Delta\nu_{1/2}^{\text{E}} - \Delta\nu_{1/2}^{\text{O}}$ . If the broadening of the lines is still much smaller than their separation and the widths are expressed in cps, or Hertz, then in this, *the slow-exchange region*.<sup>274</sup>

$$W_{\text{A}}^{\text{E}} - W_{\text{A}}^{\text{O}} = (\pi\tau_{\text{A}})^{-1} \quad (3.43)$$

The width  $W$  is related to the transverse relaxation time  $T_2$  by the expression

$$W = (\pi T_2)^{-1} \quad (3.44)$$

Now  $\tau_A$  is the required kinetic information, since it represents the mean lifetime of the nucleus (for example, a proton) in the environment A.

$$\tau_A = \frac{[A]}{d[A]/dt} \quad (3.45)$$

$\tau_A^{-1}$  is the first-order rate constant  $k_A$  for transfer of the nucleus out of site A. Similarly for the signal due to B,

$$W_B^E - W_B^O = (\pi \tau_B)^{-1} \quad (3.46)$$

$$\tau_B = \frac{[B]}{d[B]/dt} \quad (3.47)$$

and

$$\tau_A/\tau_B = [A]/[B] = k_B/k_A \quad (3.48)$$

The values of  $\tau_A$  and  $\tau_B$  and the manner in which they vary with the concentrations of A and B yield information on the rate law and rate constants for the exchange. (Prob. 11.)

The linewidth of the diamagnetic  $^{55}\text{MnO}_4^-$  resonance,  $W_A^O$ , is broadened on the addition of the paramagnetic  $\text{MnO}_4^{2-}$ , but there is no shift in the signal position, which is proof that we are in the slow-exchange region. The broadened line width  $W_A^E$  is a linear function of added  $\text{MnO}_4^{2-}$

$$\pi W_A^E - \pi W_A^O = k_1 [\text{MnO}_4^{2-}] = k_A \text{ (from 3.43)} \quad (3.49)$$

$$\pm d[\text{MnO}_4^-]/dt = k_A [\text{MnO}_4^-] \quad (3.50)$$

$$= k_1 [\text{MnO}_4^{2-}] [\text{MnO}_4^-] \quad (3.51)$$

indicating that the exchange is second-order with a rate constant,  $k_1$ .<sup>275</sup> This exchange has also been examined by quenched flow using radioactive manganese (see Table 3.3); there is good agreement in the results. (See Problem 13.) The slow-exchange region has been very useful for studying the rates of complex ion reactions. It has been used to study fast electron transfer processes involving the couples  $\text{Mn(VII)}-\text{Mn(VI)}$ , (above),  $\text{Cu(II)}-\text{Cu(I)}$ ,<sup>276</sup>  $\text{V(V)}-\text{V(IV)}$ ,<sup>277</sup>  $\text{Ru(III)}-\text{Ru(II)}$ ,<sup>278</sup>  $\text{Mn(II)}-\text{Mn(I)}$ ,<sup>279</sup>  $\text{Cu(III)}-\text{Cu(II)}$ ,<sup>280</sup>  $\text{Cu}(\text{taab})^{2+}/+$  (14 in Chap. 8).<sup>281</sup> The slow-exchange region has also been used in studies of the exchange of ligands between the free and complexed states,<sup>282,283</sup> ligand exchange in tetrahedral complexes,<sup>284</sup> optical inversion rates in  $\text{Co(III)}$  chelates,<sup>285,286</sup> and a most impressive series of studies of exchange of solvent molecules between solvated cations and the bulk solvent (Tables 4.1–4.6) which merit a separate section (d).

(b) *Intermediate-Exchange Region.* In the intermediate-exchange region, the separation of the peaks is still discernible. This separation  $\Delta\nu_E$  (in cps) is compared with the separation in the *absence* of exchange  $\Delta\nu_0$ . With the conditions of equal populations of A and B, that is,  $P_A = P_B$  and  $P_A + P_B = 1$ ,  $\tau_A = \tau_B$ , and no spin coupling between sites:

$$\tau^{-1} = 2^{1/2}\pi(\Delta\nu_0^2 - \Delta\nu_E^2)^{1/2} = \tau_A^{-1} + \tau_B^{-1} \quad (3.52)$$

Coalescence of lines occurs at

$$\tau^{-1} = 2^{1/2}\pi\Delta\nu_0 \quad (3.53)$$

and

$$k_A = k_B = 1/2\tau \quad (3.54)$$

The use of the intermediate region to determine rate constants is less straightforward, although it is relatively simple to obtain an approximate rate constant at the coalescence temperature.<sup>287-289</sup>

(c) *Fast-Exchange Region.* The two lines have now coalesced to a single line. Exchange is still slow enough to contribute to the width, however. Eventually, when the exchange is very fast, a limiting single-line width is reached. Under certain conditions in the fast-exchange region<sup>290-292</sup>

$$\tau^{-1} = 4\pi P_A P_B (\Delta\nu_0)^2 (W^E - W^0)^{-1} \quad (3.55)$$

where  $W^E$  and  $W^0$  are the widths of the single broadened and final lines respectively.

A number of studies have used the slow-, intermediate-, and fast-exchange regions with consistent results.<sup>282</sup> Both the slow- and the fast-exchange regions were used to analyze the exchange between  $\text{Pt}[\text{P}(\text{OEt})_3]_4$  and  $\text{P}(\text{OEt})_3$ <sup>273</sup> with very good agreement between the resultant activation parameters. The intermediate region was not useful because of serious overlap of lines.<sup>273</sup> The most reliable method involves matching observed spectra with a series of computer-calculated spectra with a given set of input parameters including  $\tau$ .<sup>293</sup> Fig. 3.14.

(d) *Exchange Involving a Paramagnetic Ion.* When the nuclei examined can exist in two environments, one of which is close to a paramagnetic ion, then the paramagnetic contribution to relaxation is extremely useful for determining the exchange rate of the nuclei between the two environments. This is undoubtedly the area on which nmr line broadening technique has had its greatest impact in transition metal chemistry, particularly in studying the exchange of solvent between metal coordinated and free (bulk) solvent. A variety of paramagnetic metal ions in aqueous and nonaqueous solvents have been studied (Tables in Ch. 4).

When a paramagnetic ion is dissolved in a solvent there will be, in principle, two resonance lines (due perhaps to  $^{17}\text{O}$  or  $^1\text{H}$ ) resulting from the two types of solvent, coordinated and free. The paramagnetic species broadens the signal due to the diamagnetic one (free solvent) via the chemical exchange. Often only the diamagnetic species will have a signal because the paramagnetic one is broadened completely by the interaction of an unpaired electron or electrons and the nucleus. The sole signal due to solvent can still be used for rate analysis, however. The broadening of the line will follow the sequence outlined above as the temperature of the



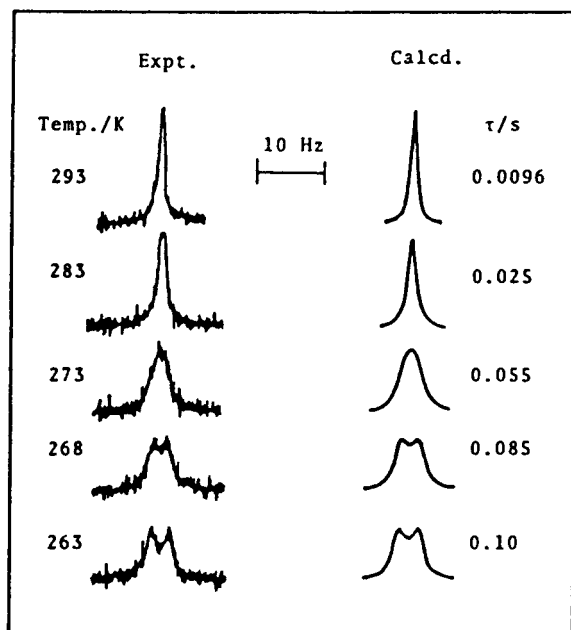


Fig. 3.14 Experimental (left) and best fit calculated  $^1\text{H}$  nmr line shapes of  $\text{UO}_2(\text{acac})_2\text{Me}_2\text{SO}$  in  $o\text{-C}_6\text{H}_4\text{Cl}_2$ . Temperature and best fit  $\tau$  values are shown at left and right sides of the figure.<sup>293</sup> Reproduced with permission from Y. Ikeda, H. Tomiyasu and H. Fukutomi, *Inorg. Chem.* **23**, 1356 (1984). © (1984) American Chemical Society.

solution is raised. A rigorous treatment of two-site exchange, considering the effects of a relaxation time and a chemical shift, has been made by Swift and Connick,<sup>294</sup> with some later modifications.<sup>295, 296</sup>

The relaxation time is given by

$$\pi (W_A^E - W_A^0) = \frac{1}{T_2} - \frac{1}{T_{2A}} = \frac{P_M}{\tau_M} \frac{\frac{1}{T_{2M}^2} + \frac{1}{\tau_M T_{2M}} + \Delta\omega_M^2}{\left[ \frac{1}{T_{2M}} + \frac{1}{\tau_M} \right]^2 + \Delta\omega_M^2} + \frac{P_M}{T_{20}} \quad (3.56)$$

where

$T_{2A}$ ,  $T_2$  = transverse relaxation times for bulk solvent nuclei alone, and with solute (concentration  $[M]$ ), respectively.

$T_{2M}$  = relaxation time in the environment of the metal.

$T_{20}$  = nuclear relaxation times of solvent molecules outside the first coordination shell.

$\tau_M$  = average residence time of the solvent molecule in the metal coordination sphere (coordination number  $n$ ).

$P_M$  = mole fraction of solvent that is coordinated to the metal  $\sim n[M]/[\text{solvent}]$  for dilute solutions;  $P_M/\tau_M = 1/\tau_A$ .

$\Delta\omega_M$  = chemical shift between the two environments in the absence of exchange, (in radians  $\text{s}^{-1}$ ).

The subscripts A and M refer to bulk and coordinated solvent. The term  $P_M/T_{20}$  is included in (3.56) when solvent exchange using  $^1\text{H}$  nmr is studied. The value  $P_M^{-1}(T_2^{-1} - T_{2A}^{-1})$  is sometimes termed  $T_{2r}^{-1}$ , the reduced line width of the free solvent.<sup>296</sup>

We can obtain the exchange regions outlined previously by considering various terms in (3.56) dominant. These might be induced by temperature changes. There are four exchange regions I–IV shown in Figure 3.15.<sup>297</sup> Only rarely is the complete behaviour displayed by a single system.<sup>297,287</sup> Although caution must be exercised in the use of approximate forms of (3.56), regions II and III can provide us with exchange rate constants.

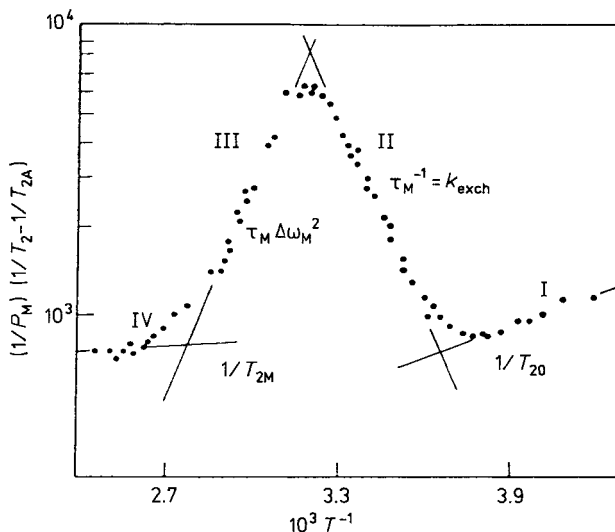


Fig. 3.15 Temperature dependence of  $(1/P_M)(1/T_2 - 1/T_{2A})$  for protons in  $\text{CH}_3\text{CN}$  solutions of  $\text{Ni}(\text{CH}_3\text{CN})_6^{2+}$  at 56.4 MHz.<sup>297</sup>

Region II. If the chemical exchange is slow compared with the relaxation mechanism (which is incorporated in the terms  $\Delta\omega_M$  or  $T_{2M}$ ), that is,

$$\tau_M^{-2}, T_{2M}^{-2} \ll \Delta\omega_M^2 \quad (3.57)$$

or

$$\tau_M^{-2}, \Delta\omega_M^2 \ll T_{2M}^{-2} \quad (3.58)$$

then in either case

$$\frac{1}{T_2} - \frac{1}{T_{2A}} = \frac{P_M}{\tau_M} \quad (3.59)$$

Relaxation is thus controlled by ligand exchange between bulk and coordinated ligand. This, the slow-exchange region (II in Fig. 3.15), is most useful for obtaining kinetic data and for studying effects of pressure.<sup>298</sup> Since  $\tau_M^{-1} = k_1$ , the pseudo first-order exchange rate con-

stant, then a semilog plot of  $1/P_M(1/T_2 - 1/T_{2A})$  vs  $1/T$  will give an Arrhenius-type plot, from which  $k_1$  at any temperature, and the activation parameters for exchange, may be directly determined.

$$\tau_M^{-1} = \frac{kT}{h} \exp\left(\frac{-\Delta H^\ddagger}{RT} + \frac{\Delta S^\ddagger}{R}\right) \quad (3.60)$$

It is clearly shown, for example, in Fig. 3.15, that at  $T = 298.2$  K ( $1/T = 3.36 \times 10^{-3}$  K<sup>-1</sup>)  $k_1 \approx 3 \times 10^3$  s<sup>-1</sup>.

Region III. If relaxation is controlled by the difference in precessional frequency between the free and coordinated states, that is, if

$$\tau_M^{-2} \gg \Delta\omega_M^2 \gg (\tau_M T_{2M})^{-1} \quad (3.61)$$

then

$$\frac{1}{T_2} - \frac{1}{T_{2A}} = P_M \tau_M \Delta\omega_M^2 \quad (3.62)$$

Now the line widths decrease rapidly with decreasing  $\tau_M$  (increasing temperature) and anti-Arrhenius behaviour is shown (Region III). Nevertheless the exchange rate constant can be determined if  $\Delta\omega_M$  is known. It is useful if data from Regions II *and* III can be used. The Ni(dmsO)<sub>6</sub><sup>2+</sup> exchange with solvent using <sup>13</sup>C was studied in the fast-exchange region.<sup>299(a)</sup> If <sup>17</sup>O nmr is used, because  $\Delta\omega_M$  is much larger, all of the data relate to the slow exchange region, since (3.57) and (3.59) apply.<sup>299(b)</sup> There is good agreement in the data from the two regions.

Region IV. If the  $T_{2M}$  process controls relaxation, that is,

$$(T_{2M} \tau_M)^{-1} \gg T_{2M}^{-2}, \Delta\omega_M^2 \quad (3.63)$$

then

$$\frac{1}{T_2} - \frac{1}{T_{2A}} = \frac{P_M}{T_{2M}} \quad (3.64)$$

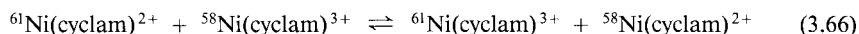
Now the linewidths no longer depend on the exchange rate and only vary slightly with temperature. The chemical shift as well as the linewidth changes as chemical exchange becomes important. Chemical shift is used less frequently to estimate exchange rates with paramagnetic systems but is important in the study of diamagnetic ones.<sup>294, 296</sup>

### 3.9.7 Epr Region

Electron paramagnetic resonance can be valuable as a monitor when paramagnetic species are being consumed or formed, as in the acid-catalyzed reaction<sup>300</sup> (see also Ref. 301)



Since there are small differences in the epr of isotopes of a particular nucleus, these may be used to study electron transfer reactions (Table 3.3)

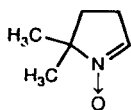


Only the Ni(III) complexes display epr signals. Those of  ${}^{61}\text{Ni}$  show a splitting of the  $g_{\parallel}$  feature owing to the nuclear spin ( $I = 3/2$ ) of  ${}^{61}\text{Ni}$ . This is missing in the corresponding  ${}^{58}\text{Ni}$  complexes.<sup>302</sup>

Epr is most effective for detecting free radicals that may occur as intermediates in oxidation and reduction reactions involving transition metal ions. Since these transients are invariably quite labile, epr is combined with continuous flow,<sup>55,303</sup> (more conveniently) stopped-flow,<sup>304-306</sup> flash photolysis,<sup>196</sup> and pulse radiolysis.<sup>197</sup>

A sharp epr signal observed 0.1 s after mixing Cr(III) (which has a broad epr spectrum) and  $\text{H}_2\text{O}_2$  in base can be assigned to a transient Cr(V) intermediate. The subsequent loss of the epr signal parallels the absorbance loss at 500 nm.<sup>305</sup>

Radicals such as  $\text{OH}^{\bullet}$  and  $\text{O}_2^{\bullet-}$  can be stabilized, and detected by epr, by spin-trapping with dmpo, **12**<sup>307,308</sup>

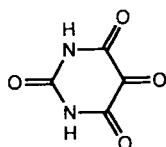
**12**

### 3.9.8 Epr Line Broadening

Another example of the use of spectral line broadening for rate measurements is by epr, although the method has been much less used than nmr. It covers a range of very short lifetimes,  $10^{-4} - 10^{-10}$  s. The very rapid interaction of ligands with square-planer complexes at the axial positions are suitable for treatment by epr line broadening.<sup>309</sup> The fast self-exchange reactions involving Cr(I) and Cr(III) complexes of bpy<sup>310</sup> and  $\eta^6$ -arenes<sup>311</sup> have also been studied by epr line broadening and full details and equations are provided.<sup>310,311</sup>

Anionic radical ligand derived from alloxan **13** shows epr which are markedly affected by coordination to diamagnetic  $\text{Mg}^{2+}$ ,  $\text{Ca}^{2+}$  and  $\text{Zn}^{2+}$  ions.

The splitting patterns due to ligand protons and  ${}^{14}\text{N}$  nuclei differ in the free ligand and the  $\text{M}^{2+}$  complexes. There is rapid intramolecular exchange of  $\text{M}^{2+}$  between two possible sites (shown in **13**) and this leads to line broadening which can be used to measure the exchange rate constants ( $5 \times 10^4 \text{ s}^{-1}$  to  $2 \times 10^7 \text{ s}^{-1}$ ).<sup>312</sup> See Table 7.4.

**13**

## 3.10 Non-Spectrophotometric Methods

Non-spectral methods are generally less useful although in specific cases, they may represent the only monitoring method.

### 3.10.1 [H<sup>+</sup>] Changes

Many complex-ion and metalloprotein reactions are accompanied by a change in the hydrogen ion concentration. This may be as a direct result of the reaction under study or because of fast concomitant secondary reactions that monitor the primary reaction. The change of [H<sup>+</sup>] with time may therefore be used *qualitatively*, to give insight into the number of changes occurring during a reaction, or as is more usual, *quantitatively*, to measure the rate of the reaction or reactions. There are basically two ways in which [H<sup>+</sup>] changes are measured in kinetic studies.

(a) *Glass Electrode*. The relationship

$$\text{pH} = -\log a_{\text{H}^+} \quad (3.67)$$

means that pH values read from a meter must usually be converted from activities into concentrations of H<sup>+</sup>, [H<sup>+</sup>], by using activity coefficients, calculated, for example, from Davies' equation

$$\log \gamma_{\pm} = \frac{-[A]z_1z_2\mu^{1/2}}{1 + \mu^{1/2}} + B\mu \quad (3.68)$$

At  $\mu = 0.1 \text{ M}$ ,  $A = 0.507$  and  $B = 0.1$ , and therefore

$$-\log [\text{H}^+] = \text{pH} - 0.11 \quad (3.69)$$

For experiments in D<sub>2</sub>O,  $\text{pD} = \text{pH} + 0.40$ ,<sup>313</sup> while for work in mixed aqueous solvents, an operational pH scale has been used.<sup>314</sup> A small correction must therefore be made in estimating [H<sup>+</sup>] or [OH<sup>-</sup>] from the pH, when these concentrations have to be used for calculating the rate constants in [H<sup>+</sup>]-dependent rate laws. However,  $d[\text{pH}]/dt$  can be used directly as a measure of  $d[\text{H}^+]/dt$  provided that only small pH changes are involved in the reaction. Since the rates of many reactions are pH-sensitive, it is obviously sensible in any case to avoid a large pH change. Specialized apparatus has been developed that will measure a change as small as 0.001 pH unit in an overall change of 0.05 pH unit during the reaction. Such equipment has been successfully employed in the study of certain enzyme reactions.<sup>315</sup> Obviously, the reaction must be sufficiently slow so that the meter or recorder response does not become rate-limiting. In certain cases, it may be necessary to add a small amount of buffer to keep the pH change reasonably small.

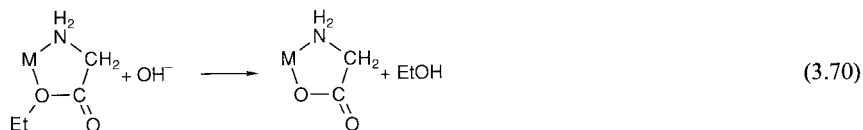
In a clever variation of the use of a pH change to monitor rate, the pH change is minimized by the controlled and registered addition of acid or base to maintain a constant pH during

the reaction. The rate of addition of reagent is thus a measure of the pH change and the reaction rate. The so-called *pH-stat method* has the decided advantage that reactions can be studied at a constant pH without recourse to buffers. It can only be used for reaction half-lives in the range 10 sec to a few hours, because of the slow response time, and possible electrode drift, over longer times.

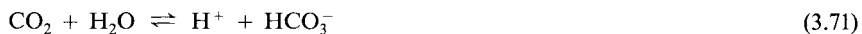
(b) *Indicators*. It may be more convenient, or even essential in certain cases, to avoid the glass electrode and register  $d[\text{H}^+]/dt$  using an appropriate acid-base indicator. This is usually necessary in the study of rapid reactions, although glass electrodes have been incorporated into continuous-flow apparatus (Sec. 3.3.1). The acid-base equilibrium involving the indicator is usually established rapidly and will not be rate-limiting with flow measurements, but may have to be considered with temperature-jump experiments, carried out at the shortest times. Some useful indicators that have been used are bromochlorophenol blue ( $\text{p}K = 4.0$ ), bromocresol green (4.7), chlorophenol red (6.0), bromothymol blue (7.1), and phenol red (7.5). The figure in parenthesis is the  $\text{p}K$ , and therefore the optimum pH value at which the indicators may be used. For a fuller list see Refs. 316 and 317. As always, one must take care that the indicator does not interfere with the system under study. Thymol blue and phenol blue, but not bromocresol green, interact with certain metals ions at pH 4.5.<sup>318</sup> The acid-base properties of certain naphthols are modified in the excited state.<sup>133</sup> Large pH changes can thereby be initiated by electronic means within nanoseconds and monitored by indicators,<sup>132</sup> (Table 3.4).

The types of reaction for which pH monitoring is useful are as follows. The mode of monitoring, (a) or (b) above, will be determined by the rate.

(1) Spontaneous and metal-ion catalyzed base hydrolysis of esters, amides, etc.<sup>319</sup>



pH changes linked to indicators have been effectively used to probe the carbonic anhydrase catalysis of the reaction<sup>317</sup>



and (indirectly) enzyme catalyzed hydrolysis of fructose biphosphate.<sup>320</sup>

Reduction of *D*-proline by *D*-amino acid oxidase at pH 8 shows two steps when monitored at 640 nm. These are interpreted as the build-up and breakdown of a reduced enzyme-imino acid charge transfer complex. If the reaction is monitored using phenol red the same two rates are observed but additionally the release of  $\approx 1$  proton for each step can be assessed and interpreted. The indicator changes are followed at 505 nm and 385 nm, which are isosbestic wavelengths for the two steps (without indicator),<sup>321</sup>

(2) Formation and dissociation of complexes containing basic ligands.<sup>322-324</sup> The polymerization of Cr(III) in basic solution is a complex reaction the kinetics of which only recently have been probed. Monitoring the pH changes using a pH-stat aids considerably in the understanding of the species involved.<sup>324</sup>

The acid-base properties of a transient can be assessed directly by placing a glass electrode in a streaming fluid that is generating that transient a few ms after the mixer. The pH is measured after the electrode has equilibrated. A series of measurements of the extent of protonation vs pH yields a  $pK_a$  value in the usual way. The  $pK_a$ 's of  $H_3VO_4$  (and lower protonated species) and  $Ni(H_2O)_6^{2+}$  could be determined, without interference by slightly slower polymerization.<sup>325</sup>

### 3.10.2 Cationic and Anionic Probes

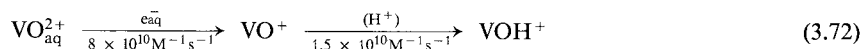
Electrodes are now available for the selective determination of the concentrations of a large number of cations and anions.<sup>33</sup> Halide-sensitive electrodes have been used to monitor reactions,<sup>326</sup> but their relatively slow response has restricted their use. They may have particular utility in the study of reactions with low spectral absorbance changes and also in an ancillary role to the kinetics determination.

Although the rate of hydrolysis of nitroammine cobalt(III) complexes can be easily measured spectrally, it proved important to monitor for loss of  $NH_3$  or  $NO_2^-$  groups in the early stages by using selective electrodes. The dominant loss of  $NH_3$  or  $NO_2^-$  in the first stage depended on the complex.<sup>327</sup>

### 3.10.3 Conductivity

The conductivity method of monitoring has occasionally been valuable for studying specific reactions. It is a colligative property and rarely shows up the fine reaction detail possible with spectral measurements. It can cope with a wide variety of rates and is convenient to use with flow, relaxation, laser photolysis and pulse radiolysis techniques (Table 3.7).<sup>198-204</sup> It has decided value in relaxation techniques since in these the changes in concentration of reactants are usually small and conductivity is a very sensitive and rapidly registered property. High concentrations of nonreacting electrolyte are to be avoided however, since otherwise the conductivity changes would be relatively small, superimposed on a large background conductivity.

Conductivity monitoring is most valuable for studying reactions which have very small spectral changes but which are accompanied by pH changes. The interaction of group 1 and 2 metal ions with cryptands and diaza-crown ethers has been studied by flow/conductivity methods.<sup>198</sup> Conductivity monitoring has been linked to reactions which may follow pulse radiolysis, for example, in examining the



rapid conductivity decrease corresponding to loss of 1  $H^+$  in the second step of (3.72)<sup>204</sup> or following laser photolysis of Cr(III) complexes.<sup>202,203</sup> (Probs. 5 and 6.) Of course, pH-indicators might also be used (Sec. 3.10.1 (b)) but might be effected by the perturbation. A conductivity cell for use at high pressures has been employed to measure  $\Delta V^\ddagger$  for substitution reactions of *cis*- and *trans*-Pt(L)<sub>2</sub>ClX with pyridine in various solvents.<sup>328</sup>

### 3.10.4 Thermal Changes

If a reaction is accompanied by a change in  $\Delta H$ , then the temperature of that reaction sensed with time is a measure of the rate. Although the method has found little use generally, it can be linked to a stopped-flow apparatus and this allows the determination of the thermal properties of a transient.<sup>205-207</sup> The heat of formation of an intermediate, which decomposes with  $k = 0.27 \text{ s}^{-1}$ , in the complicated luciferase-FMNH<sub>2</sub> reaction with O<sub>2</sub> can be measured by stopped-flow calorimetry.<sup>205</sup>

### 3.10.5 Pressure Changes

Reactions accompanied by gas evolution or absorption may be followed by measuring the change in pressure in a sealed vessel equipped with a manometer. The method has been used to study decarboxylation reactions, the decomposition of hydrogen peroxide<sup>329</sup> and the homogeneous reduction of transition metal complexes by H<sub>2</sub>.<sup>330</sup> It is essential to check that the rate of equilibration between dissolved gas in and above the solution, or that the manipulation times in using the manometer, or both, are not being measured and thus mistaken for a (faster) reaction rate. Again a combination of monitoring methods can be helpful, as in the study of the Ag(I) catalyzed decomposition of S<sub>2</sub>O<sub>8</sub><sup>2-</sup>. Both the loss of S<sub>2</sub>O<sub>8</sub><sup>2-</sup> (polarographically) and the gain of O<sub>2</sub> (Warburg meter) were monitored.<sup>331</sup>

### 3.10.6 Electrochemical Methods

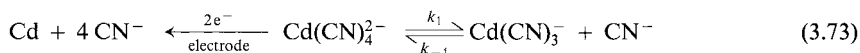
Polarography can function, like nmr and epr, in a dual manner, both as an analytical and a competitive probe. For polarography to be potentially useful analytically, one of the species in the reaction must give a polarographic wave. The limiting current at a given potential is a measure of the concentration of the species involved and so a change of waveheight with time is recorded. The polarographic method rarely has any obvious advantages over other methods, although it is straightforward to use. It is increasingly being used in laboratories where electrochemical measurements are perhaps the main thrust, and the equipment and expertise are readily available.

A graphite rotating disk electrode maintained at 0.5 V is used to monitor the reaction of Ru(NH<sub>3</sub>)<sub>6</sub><sup>2+</sup> as it is being oxidized by O<sub>2</sub> to Ru(NH<sub>3</sub>)<sub>6</sub><sup>3+</sup>. The limiting current is proportional to [Ru(NH<sub>3</sub>)<sub>6</sub><sup>2+</sup>] and there is no interference by O<sub>2</sub> or the product. The electrode is rotated at 3600 rpm to ensure rapid mixing of reactants within seconds, since reaction times are 20–30 s.<sup>332</sup> See Ref. 333. Square-wave amperometry has been linked to stopped-flow to measure reaction half-lives as short as 5 ms.<sup>334</sup>

Polarographic probes that respond specifically to concentrations of O<sub>2</sub>, CO<sub>2</sub> or SO<sub>2</sub> are very useful. They have decided advantages over the more clumsy manometric monitoring. Their use is limited to slow reactions or the continuous-flow approach, because of the relatively long response time of the probe.<sup>335</sup> An O<sub>2</sub>-electrode system for incorporation in a spectrophotometer cuvette, for simultaneous monitoring of [O<sub>2</sub>] and spectral changes, has been described.<sup>336</sup>



The polarographic technique can be used to measure the rates of rapid reactions.<sup>337</sup> Because an “internal” process is examined the problem of mixing is avoided, as it is in the relaxation and other non-flow methods. The rate of diffusion of a species (which can be oxidized or reduced) to an electrode surface competes with the rate of a chemical reaction of that species, for example



Values of  $k_1$  and  $k_{-1}$  may be extracted from the polarographic data, although the treatment is complex.<sup>338</sup> Examples of its use to measure the rate constants for certain redox reactions are given in Refs. 339 and 340 which should be consulted for full experimental details. The values obtained are in reasonable agreement with those from stopped-flow and other methods. The technique has still not been used much to collect rate constants for homogenous reactions.<sup>341</sup> The availability of ultramicroelectrodes has enabled cyclic voltammograms to be recorded at speeds as high as  $10^6 \text{ V s}^{-1}$ . Transients with very short lifetimes ( $\ll \mu\text{s}$ ) and their reaction rates may be characterised.<sup>342</sup>

### 3.11 Batch Methods

All the methods described above have been amenable to continuous monitoring as the reaction proceeded. In this section the batch procedure is described, in which aliquots of the reaction mixture are removed at various times and analyzed. Although the batch method is tedious it must be used to study certain exchange reactions and when the quenched-flow technique is used (Sec. 3.3.2). Recent events have suggested that batch analysis of a reacting system may give vital information not easily obtained by routine spectral analysis, see the next section.

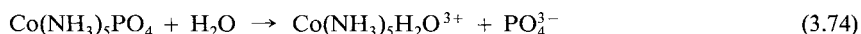
#### (a) Chemical Methods

In years past, the hydrolysis of ions such as  $\text{Co}(\text{NH}_3)_5\text{Cl}^{2+}$  or *cis*- $\text{Co}(\text{en})_2\text{F}_2^+$  has been studied by volumetric analysis of liberated chloride or fluoride ions respectively. Such purely chemical methods of assay have been largely superseded by continuous monitoring of the hydrolyzed substrate, based on some physical property. Chemical methods do have the advantage, however, of analyzing *specific* reactants, usually after a separation, and should always be used (at least in one run) to check the stoichiometry of the reaction if this is in doubt and to monitor reactions that may have irritating side reactions.<sup>343</sup> Only recently has it been realized that the reaction of  $\text{Co}(\text{NH}_3)_5\text{H}_2\text{O}^{3+}$  with  $\text{SCN}^-$  leads initially to both S-(26%) and N-bound thiocyanate cobalt(III) complexes. This can be shown by early sampling of the reaction mixture combined with ion-exchange separation. Previous kinetic studies with spectral monitoring failed to observe the S-bound isomer. Since the S-bound isomerizes completely to the N-bound form in the same time frame as the anation reaction, accurate anation rate constants are best obtained by observation at the isobestic point for  $\text{Co}(\text{NH}_3)_5\text{SCN}^{2+}$  and  $\text{Co}(\text{NH}_3)_5\text{NCS}^{2+}$ , Ref. 344.

Another classical reaction which has been reinvestigated by the batch method (with quick HPLC separation of samples withdrawn at various times) is the acid-catalyzed substitution of  $\text{Co}(\text{CN})_5\text{N}_3^{3-}$  by  $\text{SCN}^-$ . The products are  $\text{Co}(\text{CN})_5\text{H}_2\text{O}^{2-}$ ,  $\text{Co}(\text{CN})_5\text{SCN}^{3-}$  and  $\text{Co}(\text{CN})_5\text{NCS}^{3-}$ . The kinetics of these reactions are difficult to disentangle by *in situ* spectral examination alone, and indeed this procedure has led to erroneous conclusions.<sup>345</sup> Care must be observed that the separation procedure used in the batch method does not alter the conditions of the system.<sup>346</sup>

### (b) Isotopic Analysis

The use of radioisotopes as an analytical tool, although somewhat laborious, has decided value. The reaction

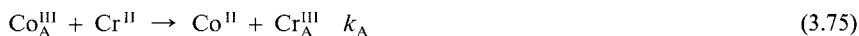


has been studied using  $^{32}\text{P}$ -labelled complexes. The spectral changes are insufficient for easy analysis.<sup>347</sup> Because of the high sensitivity of radioisotope assay,  $\mu\text{M}$  or less concentrated solutions of complexes can be examined. In this way the effect on the rate of low ionic strength (for which the Debye-Hückel treatment is most applicable) or low concentration of ions can be assessed. In using radioisotopes to study exchange reactions, we must necessarily use the batch method.

Full experimental details for assaying  $^{18}\text{O}$ , commonly used for studying exchange reactions, have been given by leading practitioners.<sup>348</sup> Usually the oxygen-containing compound is converted into a gas,  $\text{CO}_2$  or  $\text{O}_2$  for example, which is analyzed usually by mass spectrometry but also by densimetry.<sup>348</sup> The exchange reaction between  $\text{Au}(\text{NH}_3)_4^{2+}$  and  $\text{NH}_3$  has been studied<sup>349</sup> by precipitating at various times the gold complex (as phosphate) to quench the reaction, carrying out Dumas destruction of the precipitate at  $400^\circ\text{C}$  and analyzing the evolved gas by optical emission catalysis. The latter method is effective for  $^{15}\text{N}$  and  $^{13}\text{C}$  analysis.<sup>350</sup>  $^{18}\text{O}$ -sampling techniques lead to the sum of all exchanging oxygens and occasionally it is difficult to distinguish between oxygens of very similar exchangeability. In this respect the nmr method is superior, as well as representing an *in situ* technique. Nmr can be used to determine the  $^{18}\text{O}$  environment of a species (and an exchange rate) by examining the nmr signal of adjacent atoms e.g.  $^{13}\text{C}$ ,  $^{31}\text{P}$  etc. (Sec. 3.9.5).

## 3.12 Competition Methods<sup>351</sup>

Occasionally it is as useful to obtain *relative* constants for a series of reactants acting on a common substrate, as it is to have actual rate values. Relative rate constants are obtained by competition methods, which avoid the kinetic approach entirely. The method is well illustrated by considering the second-order reactions of two  $\text{Co}(\text{III})$  complexes  $\text{Co}_A^{\text{III}}$  and  $\text{Co}_B^{\text{III}}$  (which might, for example, be  $\text{Co}(\text{NH}_3)_5\text{Cl}^{2+}$  and  $\text{Co}(\text{NH}_3)_5\text{Br}^{2+}$ ), with a common reductant ( $\text{Cr}(\text{II})$  (leading in this case to  $\text{CrCl}^{2+}$  and  $\text{CrBr}^{2+}$  respectively):



If Cr(II) is used in deficiency, that is, if the starting conditions are  $[\text{Cr}^{\text{II}}]_0 < [\text{Co}_A^{\text{III}}] + [\text{Co}_B^{\text{III}}]$ , then when the reaction is complete it is clear that the ratio of Co(III) complexes remaining,  $[\text{Co}_A^{\text{III}}]_e/[\text{Co}_B^{\text{III}}]_e$ , will be related to their relative reactivities. Great care is necessary to ensure thorough mixing of all reagents particularly when, as in this example, rapid reactions are involved, otherwise fallacious results might result.<sup>352</sup> The problem of efficient mixing is circumvented by generating the scavenged material *in situ* in the presence of the two competing species. The generating process may be much slower than its scavenging and yet still be used successfully (see Prob. 17).<sup>353</sup> The approach has been particularly useful for studying certain radicals with low optical absorbancies.

The reaction of  $\mu\text{M}$  concentrations of  $\text{OH}^\bullet$  radicals (produced by pulse radiolysis) with substrates such as  $\text{Co}(\text{en})_3^{3+}$  produces very small absorbance changes. The reaction of  $\text{OH}^\bullet$  with  $\text{SCN}^-$  on the other hand ( $k = 6.6 \times 10^9 \text{ M}^{-1}\text{s}^{-1}$  at  $25^\circ\text{C}$ ) yields the highly absorbing  $(\text{SCN})_2^-$ . Competition of  $\text{Co}(\text{en})_3^{3+}$  with  $\text{SCN}^-$  for  $\text{OH}^\bullet$  can be used to measure the relative rate constants and hence the value for  $\text{OH}^\bullet$  with  $\text{Co}(\text{en})_3^{3+}$  Ref. 354, 355. This approach is useful for the study of reactions of  $\text{CO}_2^{\bullet-}$ <sup>356</sup> and  $\text{O}_2^{\bullet-}$ <sup>357</sup> with pairs of reactants.

### 3.12.1 Stern-Volmer Relationship

The decay of the excited state \*S is through a number of processes shown in Eqn (1.32) with a combined first-order rate constant  $k_0$



When a quencher Q (B in (1.32)) is added there is an additional path for deactivation



It is easy to see that if  $\tau_0$  and  $\tau$  are the excited state lifetimes in the absence and in the presence of quencher, respectively, then

$$\frac{\tau_0}{\tau} = \frac{k_0 + k_q[\text{Q}]}{k_0} = 1 + \left(\frac{k_q}{k_0}\right)[\text{Q}] \quad (3.79)$$

This is the Stern-Volmer relationship with  $K_{\text{SV}} = k_q/k_0$ , and is an important basis for determining quenching rate constants after *pulsed* excitation. The quantum yield of  $(\text{product})_0$  can be measured without  $(\phi_0)$  and with  $(\phi)$  quencher under *continuous* excitation ( $\phi = \text{moles of product/einsteins of light absorbed by system}$ ). Assuming that a steady state concentration of \*S exists in both cases,

$$\frac{\phi_0}{\phi} = 1 + K_{\text{SV}}[\text{Q}] \quad (3.80)$$

This represents a competitive, non-kinetic, method for determining relative rate constants for the photochemical system. The value of  $k_q$  may be obtained after one direct determination of  $k_0$  has been made. For an extensive compilation of quenching rate constants for excited states of metal complexes see Ref. 358.

### 3.12.2 Isotope Fractionation

Another powerful application of the competition method is in *isotope fractionation experiments*. These allow determination of the relative rates of reactants with different isotopic composition.  $\text{Co}_A^{\text{III}}$  in (3.75) might be  $\text{Co}(\text{NH}_3)_5\text{H}_2^{16}\text{O}^{3+}$  and  $\text{Co}_B^{\text{III}}$  in (3.76) might be  $\text{Co}(\text{NH}_3)_5\text{H}_2^{18}\text{O}^{3+}$ . By examining the  $^{16}\text{O}/^{18}\text{O}$  contents of the Co(III) complex remaining after all the other reactant (Cr(II) or V(II), for example) has disappeared, one can determine  $k_{16}/k_{18}$  ( $=f$ ), their relative rate constants, obtaining thereby the isotopic fractionation factor  $f$ . Since the rate constants are so close, separate studies of the two reactions could not possibly yield the ratio with the desired accuracy. The  $^{16}\text{O}/^{18}\text{O}$  ratio in the complex, converted to  $\text{H}_2\text{O}$  by heating and thence equilibrating with  $\text{CO}_2$  for assay, can however be accurately determined by mass spectrometry. An accurate value for  $f$  can thence be obtained, although the treatment and procedure are complicated.

In the reaction of a cobalt(III) aqua complex containing  $^{16}\text{O}$  and  $^{18}\text{O}$  with another reagent,<sup>359</sup>

$$f = \frac{k_{16}}{k_{18}} = \frac{d \ln [^{16}\text{O}]}{d \ln [^{18}\text{O}]} = \frac{[^{18}\text{O}]}{d [^{18}\text{O}]} \cdot \frac{d [^{16}\text{O}]}{[^{16}\text{O}]} \quad (3.81)$$

It can be shown that<sup>360</sup>

$$f = \frac{\ln \alpha (1 - N_t)/(1 - N_0)}{\ln \alpha (N_t/N_0)} \sim \frac{\log \alpha}{\log \alpha (N_t/N_0)} \quad (3.82)$$

where  $\alpha = [\text{Co(III)}]_t/[\text{Co(III)}]_0$ , the fraction of complex sample left unreduced at time  $t$ , which may conveniently be designated as that when all the other reagent is consumed.

$N_t, N_0$  = mole fractions of  $^{18}\text{O}$  in complex after partial reduction and initially.

$^{13}\text{C}$ -kinetic isotope effects have been used to determine the degree of C–C breakage in metal and non-metal catalyzed decarboxylation of oxalacetic acid.<sup>361</sup> (Sec. 2.2.2).

## 3.13 The Study of Transients

A knowledge of the properties of transients is an integral feature in understanding the rate and mechanism of reactions. We concentrate here on labile species, because the properties of

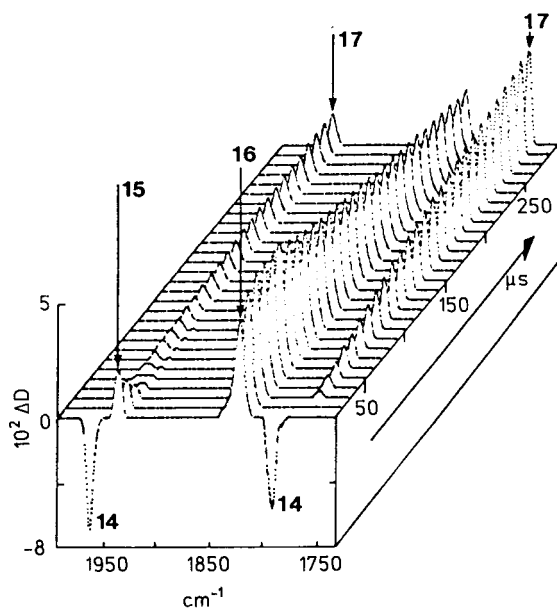
transients arising in slow reactions can be usually determined by conventional methods on equilibrated solutions. Flow and the massive perturbation techniques (but not the relaxation methods) can, as we have seen, generate sizeable amounts of reactive transients. The technique used to examine their properties depends on their reactivity. The lifetime of transients is controlled by self-reactions, reaction with solvent, buffer, etc.

### 3.13.1 Spectral Properties of Transients

The presence of intermediates suggested by a mechanism has been supported in a number of cases by rapid scan spectrophotometry. Examples include Ni(II) polyamine complexes during acid dissociation,<sup>362,363</sup> protonated and ring-opened cobalt(III) carbonate complexes during acid dissociation,<sup>364</sup> copper(III) intermediates in the oxidation of Cu(II) by  $\text{OCl}^-$ ,<sup>220</sup> and Mn(V) generated in the course of the  $\text{MnO}_4^-$ ,  $\text{SO}_3^{2-}$  reaction.<sup>221</sup> Streak camera recordings of transient spectra in 200  $\mu\text{s}$  intervals demonstrates two distinct transients in the reaction of  $\text{Cr(en)}_2(\text{SCH}_2\text{CO}_2)^+$  with  $\text{OH}^\bullet$  radicals, generated by pulse radiolysis.<sup>224</sup>

An important development for detection of transient organometallic species is fast time-resolved infrared.<sup>175</sup> The transient is generated rapidly by uv-visible flash photolysis and monitored by ir with  $\mu\text{s}$  resolution. Spectra are obtained from a series of kinetic traces recorded at about 4  $\text{cm}^{-1}$  interval.

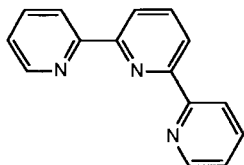
Uv-vis flash photolysis of  $[\text{CpFe}(\text{CO})_2]_2$  (**14**) and MeCN in cyclohexane at 25 °C gives the ir/time display shown in Figure 3.16. This shows that **14** is destroyed in the flash and that there are two intermediates  $\text{CpFe}(\mu\text{CO})_3\text{FeCp}$  (**16**) and in much smaller amounts,  $\text{CpFe}(\text{CO})_2^*$  (**15**). The principal intermediate reacts relatively slowly with MeCN to give  $\text{Cp}_2\text{Fe}_2(\text{CO})_3(\text{MeCN})$  (**17**) and the decay of **16** mirrors exactly the increase in **17** ( $k = 7.6 \times 10^5 \text{ M}^{-1}\text{s}^{-1}$  at 24 °C



**Fig. 3.16** Time resolved ir spectra obtained by uv flash photolysis of  $[\text{CpFe}(\text{CO})_2]_2$  (**14**) (0.6 mM) and MeCN (6mM) in cyclohexane solution at 25 °. Only ~5% of **14** is destroyed by the flash so that the concentration of **16**  $\ll$  **14**. The spectra have been reconstituted from  $\approx 70$  kinetic traces recorded at intervals of  $\sim 4 \text{ cm}^{-1}$  from 1750  $\text{cm}^{-1}$  to 1950  $\text{cm}^{-1}$ . The first three spectra correspond to the duration of the firing of the flash lamp and subsequent spectra are shown at intervals of 10  $\mu\text{s}$ . The negative peaks in the first spectrum (subsequently omitted) are due to material destroyed by the flash.<sup>365</sup> Reproduced with permission from A. J. Dixon, M. A. Healy, M. Poliakkoff and J. J. Turner, J. Chem. Soc. Chem. Comm. 994 (1986)

by separate kinetic experiments). The radical **15** disappears rapidly (probably by recombination) but does not produce much **17**.<sup>365</sup> The impact of these observations on the understanding of mechanism is self-evident.

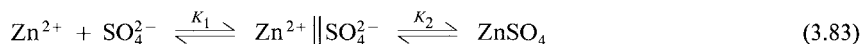
The three stages in the replacement of three dmsol molecules in  $\text{Al}(\text{dmsol})_6^{3+}$  by one terdentate ligand, trpy, (**18**) in nitromethane solution is resolved beautifully by flow/nmr. The method is effective because nmr can monitor specifically for free dmsol.<sup>366</sup> See also Fig. 3.12.



18

### 3.13.2 Thermodynamic Properties of Transients

In the equilibria



electric field jump (Sec. 3.4.3) allows the measurement of  $K_1$  ( $1.3 \times 10^3 \text{ M}^{-1}$ ). Low-field conductance measurements give an overall equilibrium constant  $K_1 K_2 = 7.5 \times 10^6 \text{ M}^{-1}$ , from which it follows that the ratio of contact to solvent separated pairs ( $K_2$ ) is  $5.8 \times 10^3$ , Ref. 367.

If a transient is formed rapidly within mixing time, but undergoes further reactions slowly, then the thermal properties of the transient may be determined using thermal monitoring. When Cr(VI) containing  $\text{HCrO}_4^-$  and  $\text{Cr}_2\text{O}_7^{2-}$  is treated with base, reaction (3.84) occurs within mixing and the associated heat change can be measured, isolated from the much slower (3.85)<sup>368</sup>



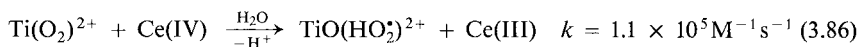
Similarly, the spectrum of a mixture of  $\text{Fe}(\text{tpps})\text{H}_2\text{O}^-$  and  $\text{Fe}(\text{tpps})(\text{OH})^{2-}$  can be measured by rapid scan/stopped-flow at various pH's within a few milliseconds after generation (Fig. 3.9). In this short time, dimerization is unimportant so that the spectrum of  $\text{Fe}(\text{tpps})\text{OH}^{2-}$  can be measured and the  $\text{p}K_a$  of  $\text{Fe}(\text{tpps})\text{H}_2\text{O}^-$  estimated.<sup>222</sup>

### 3.13.3 Chemical Reactivity of Transients

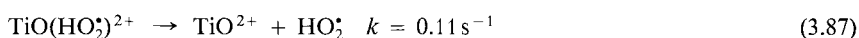
Different chemical reactivity may be used to diagnose structurally different groups. The use of flow simply widens the dimension of this use. The reactivity of the enol but not the keto

form of aldehydes as a substrate towards horseradish peroxidase I (by stopped-flow) can be used to estimate (as 0.01–0.001%) the enol form in the equilibrium mixture.<sup>369</sup>

The reactions of an unstable intermediate can be studied by the use of multiple mixers. The transient is generated in one mixer and then mixed with a reagent in a second mixer. Monitoring after the second mixer is usually by spectra.<sup>63,85</sup> The protonated superoxotitanium(IV) species  $\text{TiO}(\text{HO}_2)^{2+}$  is formed by mixing a Ce(IV) solution with one containing  $\text{H}_2\text{O}_2$  and  $\text{TiO}^{2+}$  (which gives  $\text{Ti}(\text{O}_2)^{2+}$ ).



The mixture is flowed for 0.23–0.31  $\text{s}^{-1}$  before being allowed to react in a second mixer with the examining reductant. In this time, there is a maximum production of  $\text{TiO}(\text{HO}_2)^{2+}$ , and insufficient time has elapsed for its decomposition to be marked.<sup>63</sup>



Transients such as  $\text{O}_2^{\cdot-}$  or  $\text{HO}_2^{\cdot}$  can be generated in solution by pulse radiolysis of  $\text{O}_2$ . If such solutions are contained in one syringe of a stopped-flow apparatus they may be mixed with substrate and the final mixture examined spectrally. For flow experiments these transients must, of course, have lifetimes longer than a few millisecond. For the examination of more labile transients, production may be by laser photolyses or pulse radiolysis, and the substrate under examination must be then incorporated in the pulsed solution. Care has now to be taken that substantial amounts of the substrate are not lost (by reaction) as a result of the pulse.

## References

1. A. Samuni and G. Czapski, *J. Chem. Soc. A*, 487 (1973); G. Davies and B. Warnquist, *Coordn. Chem. Revs.* **5**, 349 (1970); M. Knoblowitz, L. Miller, J. I. Morrow, S. Rich, and T. Scheinbart, *Inorg. Chem.* **15**, 2847 (1976).
2. A. C. Melnyk, N. K. Kildahl, A. R. Rendina and D. H. Busch, *J. Amer. Chem. Soc.* **101**, 3232 (1979).
3. J. Simplicio, K. Schwenzer and F. Maenpa, *J. Amer. Chem. Soc.* **97**, 7319 (1975).
4. E. L. Evers, G. G. Jayson and A. J. Swallow, *J. Chem. Soc. Faraday Trans. I* **74**, 418 (1978).
5. R. F. Evilia, *Inorg. Chem.* **24**, 2076 (1985) and references therein.
6. R. G. Khalifah, G. Sanyal, D. J. Strader and W. McI. Sutherland, *J. Biol. Chem.* **254**, 602 (1979); G. Sanyal and R. G. Khalifah, *Arch. Biochem. Biophys.* **196**, 157 (1979).
7. P. J. Connolly and E. J. Billo, *Inorg. Chem.* **26**, 3224 (1987).
8. D. J. Livingston, N. L. Davis, G. N. LaMar and W. D. Brown, *J. Amer. Chem. Soc.* **106**, 3025 (1984).
9. M. Ardon and B. Magyar, *J. Amer. Chem. Soc.* **106**, 3359 (1984); M. Ardon and A. Bino, *Structure and Bonding*, **65**, 1 (1987); P. Andersen, *Coordn. Chem. Revs.* **94**, 47 (1989). This structure persists in concentrated solution.
10. J. M. Veigel and C. S. Garner, *Inorg. Chem.* **4**, 1569 (1965).
11. C. Narayanaswamy, T. Ramasami and D. Ramasamy, *Inorg. Chem.* **25**, 4052 (1986); H. Bruce, D. Reinhard, M. T. Saliby and P. S. Sheridan, *Inorg. Chem.* **26**, 4024 (1987).
12. S. Balt and C. Dekker, *Inorg. Chem.* **15**, 1025 (1976).
13. R. Koren and B. Permuter-Hayman, *Israel J. Chem.* **8**, 1 (1970).
14. W. G. Jackson, S. S. Jurisson and B. C. McGregor, *Inorg. Chem.* **24**, 1788 (1985).

15. A. J. Thomson, A. E. Robinson, M. K. Johnson, R. Cammack, K. K. Rao and D. O. Hall, *Biochim. Biophys. Acta* **637**, 423 (1981).
16. A. J. Miralles, R. E. Armstrong and A. Haim, *J. Amer. Chem. Soc.* **99**, 1416 (1977); D. Pinnell and R. B. Jordan, *Inorg. Chem.* **18**, 3191 (1979).
17. M. G. Burnett and M. Gilfallen, *J. Chem. Soc. Dalton Trans.* 1578 (1981).
18. A. Haim, *Inorg. Chem.* **21**, 2887 (1982).
19. G. Davies and A. R. Garafalo, *Inorg. Chem.* **19**, 3543 (1980); D. H. Macartney and A. McAuley, *Inorg. Chem.* **20**, 749 (1981).
20. H. E. Toma, A. A. Batista and H. B. Gray, *J. Amer. Chem. Soc.* **104**, 7509 (1982).
21. M. W. Fuller, K.-M. F. LeBrocq, E. Leslie and I. R. Wilson, *Aust. J. Chem.* **39**, 1411 (1986).
22. K. Madlo, A. Hasnedl and S. Veprek-Siska, *Coll. Czech Chem.* **41**, 7 (1976); F. R. Duke, *Inorg. Nucl. Letters* **12**, 107 (1976).
23. D. F. Evans and M. W. Upton, *J. Chem. Soc. Dalton Trans.* 2525 (1985).
24. J. Veprek-Siska and V. Ettel, *J. Inorg. Nucl. Chem.* **31**, 789 (1969).
25. J. F. Bunnett in B5, Chap. III, directs attention to the various points that should be considered before and after a kinetic study.
26. G. A. Lawrance, *Chem. Revs.* **86**, 17 (1986).
27. A. D. Hugi, L. Helm and A. E. Merbach, *Helv. Chim. Acta* **68**, 508 (1985).
28. W. J. Ferguson, K. I. Braunschweiger, W. R. Braunschweiger, J. R. Smith, J. J. McCormick, C. C. Wasmann, N. P. Jarvis, D. H. Bell and N. E. Good, *Anal. Biochem.* **104**, 300 (1980).
29. K. Hegetschweiler and P. Saltman, *Inorg. Chem.* **25**, 107 (1986).
30. D. Masi, L. Mealli, M. Sabat, A. Sabatini, A. Vacca, F. Zanobini, *Helv. Chim. Acta* **67**, 1818 (1984).
31. F. Wang and L. M. Sayre, *Inorg. Chem.* **28**, 169 (1989).
32. R. N. Smith, *Anal. Biochem.* **93**, 380 (1979).
33. M. Kotowski and R. van Eldik, *Coordn. Chem. Revs.* **93**, 19 (1989).
34. J. R. Graham and R. J. Angelici, *Inorg. Chem.* **6**, 2082 (1967).
35. J. O. Edwards, F. Monacelli and G. Ortaggi, *Inorg. Chim. Acta* **11**, 47 (1974).
36. J. H. Swinehart and G. W. Castellani, *Inorg. Chem.* **3**, 278 (1964); J. H. Swinehart, *J. Chem. Educ.* **44**, 524 (1967), gives a full description of the study of the equilibrium  $\text{Cr}_2\text{O}_7^{2-} + \text{H}_2\text{O} \rightarrow 2\text{HCrO}_4^-$  by changing the total concentration of Cr(VI) and watching the concomitant spectral changes on a recording spectrophotometer.
37. J. F. Eccleston, R. G. Messerschmidt and D. W. Yates, *Anal. Biochem.* **106**, 73 (1980).
38. D. A. Buckingham, P. J. Cresswell, A. M. Sargeson and W. G. Jackson, *Inorg. Chem.* **20**, 1647 (1981).
39. B. F. Peterman and C.-W. Wu, *Biochemistry* **17**, 3889 (1978).
40. Z. A. Schelly in B21, p. 35-39.
41. H. Kihara, E. Takahashi, K. Yamamura and I. Tabushi, *Biochem. Biophys. Res. Commun.* **95**, 1687 (1980).
42. S. Saigo, *J. Biochem. Japan* **89**, 1977 (1981).
43. L. E. Erickson, H. L. Erickson and T. Y. Meyer, *Inorg. Chem.* **26**, 997 (1987).
44. From R. G. Wilkins, *Adv. Inorg. Bioinorg. Mechs.* **2**, 139 (1983), slightly amended.
45. B. H. Robinson in B6, Chap. 1.
46. B13, Chap. 2.
47. H. Gerischer, J. Holzworth, D. Seifert, and L. Strohmaier, *Ber. Bunsenges. Gesellschaft* **73**, 952 (1969).
48. J. F. Holzworth in B21, p. 13.
49. S. A. Jacobs, M. T. Nemeth, G. W. Kramer, T. Y. Ridley, and D. W. Margerum, *Anal. Chem.* **56**, 1058 (1984).
50. M. T. Nemeth, K. D. Fogelman, T. Y. Ridley and D. W. Margerum, *Anal. Chem.* **59**, 283 (1987).
51. J. A. Sirs, *Trans. Faraday Soc.* **54**, 207 (1958).



52. M. R. Luzzana and J. T. Penniston, *Biochim. Biophys. Acta* **396**, 157 (1975) monitor the hemoglobin-O<sub>2</sub> reaction by continuous flow combined with a Clark O<sub>2</sub> electrode and obtain a rate profile similar to that with the spectral method.
53. G. A. Rechnitz, *Anal. Chim. Acta* **180**, 289 (1986); R. L. Solsky, *Anal. Chem.* **60**, 106R (1988).
54. P. Bowen, B. Balko, K. Blevins, R. L. Berger and H. P. Hopkins Jr., *Anal. Biochem.* **102**, 434 (1980).
55. D. C. Borg, *Nature, London* **201**, 1087 (1964).
56. T. Ogura and T. Kitagawa, *J. Amer. Chem. Soc.* **109**, 2177 (1987).
57. J. C. Sheppard and A. C. Wahl, *J. Amer. Chem. Soc.* **79**, 1020 (1957).
58. P. Hurwitz and K. Kustin, *Trans. Faraday Soc.* **62**, 427 (1966).
59. W. J. Ray, Jr., and J. W. Long, *Biochemistry* **15**, 3990 (1976).
60. P. A. Benkovic, W. P. Bullard, M. M. de Maine, R. Fishbein, K. J. Schray, J. J. Steffens and S. J. Benkovic, *J. Biol. Chem.* **249**, 930 (1974).
61. H. von Felten, H. Gamsjäger and P. Baertschi, *J. Chem. Soc. Dalton Trans.* 1683 (1976).
62. S. Dahlin, B. Reinhammar and M. T. Wilson, *Biochem. J.* **218**, 609 (1984).
63. G. C. M. Bourke and R. C. Thompson, *Inorg. Chem.* **26**, 903 (1987).
64. R. K. Murmann, *Inorg. Chem.* **16**, 46 (1977).
65. B. E. Smith, D. J. Lowe, C. G. Xiong, M. J. O'Donnell and T. R. Hawkes, *Biochem. J.* **209**, 207 (1983); R. N. F. Thorneley and D. J. Lowe, *Kinetics and Mechanism of the Nitrogenase Enzyme System in Molybdenum Enzymes*, T. G. Spiro, ed. Wiley Interscience NY, 1985, Chap. 5 includes a description of the rapid freeze technique.
66. J. P. G. Malthouse, J. W. Williams and R. C. Bray, *Biochem. J.* **197**, 421 (1981).
67. P. Reisberg, J. S. Olson and G. Palmer, *J. Biol. Chem.* **251**, 4379 (1976).
68. R. Hille, G. Palmer and J. S. Olson, *J. Biol. Chem.* **252**, 403 (1977).
69. A number of stopped-flow systems are commercially available.<sup>46</sup> Three of the most used are manufactured by Atago Bussan (formerly Union Giken), Japan; Dionex (formerly Durrum), USA and Hi-Tech Scientific, UK. These also manufacture rapid scan spectrophotometers, multimixer, temperature-jump and flash photolysis equipment.
70. B. Tonomura, H. Nakatani, M. Ohnishi, J. Yamaguchi-Ito and K. Hiromi, *Anal. Biochem.* **84**, 370 (1978).
71. P. J. Hagerman, F. X. Schmid and R. L. Baldwin, *Biochemistry* **18**, 293 (1979).
72. C. Paul, K. Kirschner and G. Haenisch, *Anal. Biochem.* **101**, 442 (1980) determine the deadtime for a stopped-flow apparatus using a disulfide exchange reaction.
73. P. N. Dickson and D. W. Margerum, *Anal. Chem.* **58**, 3153 (1986), estimate that  $k_{\text{corrected}} = k_{\text{obs}}(1 - k_{\text{obs}}/k_{\text{mix}})$  and  $k_{\text{mix}} \approx 1700\text{ s}^{-1}$  and  $\approx 1000\text{ s}^{-1}$  for Dionex and Hi-Tech stopped-flow instruments respectively.
74. M. A. Abdallah, J.-F. Biellmann and P. Lagrange, *Biochemistry* **18**, 836 (1979).
75. G. J. McClune and J. A. Fee, *FEBS Lett.* **67**, 294 (1976); G. H. McClune and J. A. Fee, *Biophys. J.* **24**, 65 (1978).
76. J. T. Coin and J. S. Olson, *J. Biol. Chem.* **254**, 1178 (1979).
77. J. D. Ellis, K. L. Scott, R. K. Wharton, and A. G. Sykes, *Inorg. Chem.* **11**, 2565 (1972), who observe optical density changes when 1 M acid solutions are mixed with water in a Durrum-Gibson stopped-flow apparatus. Such traces could be incorrectly assigned to chemical reactions.
78. J. H. Sutter, K. Colquitt and J. R. Sutter, *Inorg. Chem.* **13**, 1444 (1974).
79. S. S. Hupp and G. Dahlgren, *Inorg. Chem.* **15**, 2349 (1976).
80. D. S. Auld, K. Geoghegan, A. Galdes and B. L. Vallee, *Biochemistry* **25**, 5156 (1986); C. Balny, T.-L. Saldana and N. Dahan, *Anal. Biochem.* **163**, 309 (1987) describe a high-pressure, low temperature, stopped-flow apparatus.
81. P. J. Nichols, Y. Ducommun and A. E. Merbach, *Inorg. Chem.* **22**, 3993 (1983) and references therein.
82. S. Funahashi, Y. Yamaguchi and M. Tanaka, *Inorg. Chem.* **23**, 2249 (1984).

83. R. van Eldik, D. A. Palmer, R. Schmidt and H. Kelm, *Inorg. Chim. Acta* **50**, 131 (1981) for a detailed description.
84. K. Ishihara, H. Miura, S. Funahashi and M. Tanaka, *Inorg. Chem.* **27**, 1706 (1988), describe a high-pressure, stopped-flow arrangement with conductivity monitoring.
85. J. D. Rush and B. H. J. Bielski, *J. Phys. Chem.* **89**, 1524 (1985).
86. C. Bull, G. J. McClune and J. A. Fee, *J. Amer. Chem. Soc.* **105**, 5290 (1983).
87. Z. Bradić and R. G. Wilkins, *J. Amer. Chem. Soc.* **106**, 2236 (1984).
88. P. S. Kim and R. L. Baldwin, *Ann. Rev. Biochem.* **59**, 631 (1990).
89. Selected Bibliography.
90. T.-E. Dubois, *Pure Appl. Chem.* **50**, 801 (1978); H. Kruger, *Chem. Soc. Revs.* **11**, 227 (1982).
91. D. H. Turner in B6, Chap. III.
92. G. H. Czerlinski and M. Eigen, *Z. Electrochem.* **63**, 652 (1959).
93. List of commercially available equipment (not cheap!) in Hiromi p. 159 and Bernasconi Ed. 4, p. 171.
94. A. S. Verkman, A. A. Pandiscio, M. Jennings and A. K. Solomon, *Anal. Biochem.* **102**, 189 (1980).
95. D. Porschke, *Rev. Sci. Instrum.* **47**, 1363 (1976)
96. M. F. Perutz, T. K. M. Sanders, D. H. Chenery, R. W. Noble, R. R. Pennelly, L. W.-M. Fung C. Ho, I. Giannini, D. Pörschke and H. Winkler, *Biochemistry* **17**, 3640 (1978) show relaxation of azidomethemoglobin ( $\Delta T = 4^\circ$ ,  $T = 260$  ns for human and  $< 100$  ns for carp).
97. J. Aubard, J. M. Nozeran, P. Levoir, J. J. Meyer and J. E. Dubois, *Rev. Sci. Instrum.* **50**, 52 (1979).
98. J. V. Beitz, G. W. Flynn, D. H. Turner and N. Sutin, *J. Amer. Chem. Soc.* **92**, 4130 (1970), **94**, 1554 (1972).
99. K. A. Reeder, E. V. Dose and L. J. Wilson, *Inorg. Chem.* **17**, 1071 (1978).
100. K. Kustin, I. A. Taub and E. Weinstock, *Inorg. Chem.* **5**, 1079 (1966).
101. A. J. Miralles, R. E. Armstrong and A. Haim, *J. Amer. Chem. Soc.* **99**, 1416 (1977).
102. C. F. Bernasconi and M. C. Muller, *J. Amer. Chem. Soc.* **100**, 5530 (1978).
103. A. S. Verkman, J. A. Dix and A. A. Pandiscio, *Anal. Biochem.* **117**, 164 (1981).
104. M. D. Johnson and R. G. Wilkins, *Inorg. Chem.* **23**, 231 (1984).
105. W. Knoche in B6, Chap. IV.
106. H. R. Halvorson, *Biochemistry* **18**, 2480 (1979).
107. R. M. Clegg and B. W. Maxfield, *Rev. Sci. Instrum.* **47**, 1383 (1976).
108. M. A. Lopez Quintela, W. Knoche and I. Veith, *T. Chem. Soc. Faraday Trans. I* **80**, 2313 (1984).
109. G. Kegeles, *Methods in Enzym.* **48**, 308 (1978) P-jump/light scattering arrangements are reviewed.
110. T. Inoue, K. Sugahara, K. Kojima and R. Shimozawa, *Inorg. Chem.* **22**, 3977 (1983).
111. E. M. Eyring and P. Hemmes in B6, Chap. V.
112. H. Hirohara, K. J. Ivin, J. J. McGarvey and J. Wilson, *J. Amer. Chem. Soc.* **96**, 4435 (1974).
113. J. E. Stuehr in B6, Ed. 4, Chap. VI.
114. S. Harada, Y. Uchida, M. Hiraiishi, H. L. Kuo and T. Yasunaga *Inorg. Chem.* **17**, 3371 (1978); B. Perlmutter-Hayman, *J. Chem. Educ.* **47**, 201 (1970); N. Purdie and M. F. Farrow, *Coordn. Chem. Revs.* **11**, 189 (1973) for excellent presentations.
115. Y. Funaki, S. Harada, K. Okumiya and T. Yasunaga, *J. Amer. Chem. Soc.* **104**, 5325 (1982).
116. J. K. Beattie, M. T. Kelso, W. E. Moody and P. A. Tregloan, *Inorg. Chem.* **24**, 415 (1985).
117. B22, p. 45.
118. M. Eigen and K. Tamm, *Ber. Bunsenges. Gesellschaft* **66**, 107 (1962); L. G. Jackopin and E. Yeager, *J. Phys. Chem.* **74**, 3766 (1970).
119. R. A. Binstead, J. K. Beattie, E. V. Dose, M. F. Tweedle and L. J. Wilson, *J. Amer. Chem. Soc.* **100**, 5609 (1978).
120. R. G. W. Norrish and G. Porter, *Nature London* **164**, 658 (1949).
121. M. A. West, In B6, Chap. VIII.
122. C. A. Sawicki and R. J. Morris, *Flash Photolysis of Hemoglobin, Methods in Enzym.* **76**, 667 (1981).

123. D. G. Nocera, J. R. Winkler, K. M. Yocum, E. Bordignon and H. B. Gray, *J. Amer. Chem. Soc.* **106**, 5145 (1984).
124. P. Connolly, J. H. Espenson and A. Bakac, *Inorg. Chem.* **25**, 2169 (1986); M. A. Hoselton, C.-T. Lin, H. A. Schwarz and N. Sutin, *J. Amer. Chem. Soc.* **100**, 2383 (1978).
125. G. R. Fleming, "Chemical Applications of Ultrafast Spectroscopy", Oxford Univ. Press, NY, 1986. The book covers the range  $10^{-9}$  to  $10^{-14}$  s, and full details on generating, characterizing and probing ultrashort light pulses are given.
126. J. Terner and M. A. El-Sayed, *Acc. Chem. Res.* **18**, 331 (1985).
127. A. Juris, V. Balzani, F. Barigelletti, S. Campagna, P. Belser and A. von Zelewsky, *Coordn. Chem. Revs.* **84**, 85 (1988).
128. C. R. Bock, T. J. Meyer and D. G. Whitten, *J. Amer. Chem. Soc.* **96**, 4710 (1974).
129. Since  $\text{Ru}(\text{bpy})_3^{3+}$  and  $\text{Fe}^{2+}$  must of necessity be produced in equal concentrations, (3.15) is set up for second-order conditions (Sec. 1.4.3).
130. H. B. Gray, *Chem. Soc. Revs.* **15**, 17 (1986).
131. A. G. Sykes, *Chem. in Britain* **24**, 551 (1988) and references therein.
132. S. P. Webb, S. W. Yeh, L. A. Philips, M. A. Tolbert and J. H. Clark, *J. Amer. Chem. Soc.* **106**, 7286 (1984) and references therein.
133. J. F. Ireland and P. A. H. Wyatt, *Adv. Phys. Org. Chem.* **12**, 131 (1976).
134. R. Yam, E. Nachliel and M. Gutman, *J. Amer. Chem. Soc.* **110**, 2636 (1988)
135. M. Gutman and E. Nachliel, *Biochem. Biophys. Acta* **1015**, 391 (1990).
136. G. Ferraudi, *Inorg. Chem.* **17**, 2506 (1978) generates methyl radicals photolytically.
137. I. Lawthers and J. J. McGarvey, *J. Amer. Chem. Soc.* **106**, 4280 (1984).
138. B. H. Robinson and N. C. White, *J. Chem. Soc. Faraday Trans. I* **74**, 2625 (1978).
139. Q. H. Gibson, *J. Biol. Chem.* **264**, 20155 (1989); *Biochem. Soc. Trans.* **18**, 1 (1990).
140. J. H. Baxendale and M. A. J. Rodgers, *Chem. Soc. Revs.* **7**, 235 (1978).
141. M. S. Matheson and L. M. Dorfman, *Pulse Radiolysis*, MIT Press, Cambridge, Mass. 1969.
142. L. M. Dorfman and M. C. Sauer in B6, Chap. IX.
143. G. V. Buxton and R. M. Sellers, *Coordn. Chem. Revs.* **22**, 195 (1977).
144. M. Anbar, M. Bambenek, A. B. Ross, National Bureau of Standards Publication NSRDS-NBS43 1973 and Supplement, 1975.
145. G. V. Buxton, C. L. Greenstock, W. P. Helman and A. B. Ross, *J. Phys. Chem. Ref. Data* **17**, 513 (1988).
146. M. Anbar, F. Ross and A. B. Ross, NSRDS-NBS51, 1975.
147. A. J. Swallow, *Prog. React. Kinetics* **9**, 195 (1978) – an account of reactions of free radicals (including  $\text{CO}_2^-$ ) produced by irradiation of organic compounds.
148. A. B. Ross and P. Neta NSRDS-NBS65, 1979; P. Neta, R. E. Huie and A. B. Ross, *J. Phys. Chem. Ref. Data* **17**, 1027 (1988).
149. Z. B. Alfassi and R. H. Schuler, *J. Phys. Chem.* **89**, 3359 (1985).
150. B. H. J. Bielski, D. E. Cabelli and R. L. Arudi, *J. Phys. Chem. Ref. Data* **14** 1041 (1985).
151. S. S. Isied, *Prog. Inorg. Chem.* **32**, 443 (1984).
152. J. Butler, A. G. Sykes, G. V. Buxton, P. C. Harrington and R. G. Wilkins, *Biochem. J.* **189**, 641 (1980).
153. J. Lillie, N. Shinohara and M. G. Simic, *J. Amer. Chem. Soc.* **98**, 6516 (1976).
154. M. Z. Hoffman and M. Simic, *J. Amer. Chem. Soc.* **94**, 1757 (1972).
155. K. D. Whitburn, M. Z. Hoffman, N. V. Brezniak, and M. G. Simic, *Inorg. Chem.* **25**, 3037 (1986) and references therein.
156. J. V. Beitz, J. R. Miller, H. Cohen, K. Wieghardt and D. Meyerstein, *Inorg. Chem.* **27**, 966 (1988).
157. R. G. Wilkins, *Adv. Inorg. Bioinorg. Mech.* **2**, 139 (1983).
158. L. A. Blumenfeld and R. M. Davidov, *Biochim. Biophys. Acta* **549**, 255 (1979).
159. H. Barrett and J. H. Baxendale, *Trans. Faraday Soc.* **52**, 210 (1956).

160. A. Haim and N. Sutin, *J. Amer. Chem. Soc.* **88**, 5343 (1966); R. D. Cannon and T. S. Stillman *J. Chem. Soc. Dalton Trans.* 428 (1976).
161. J. P. Candlin and J. Halpern, *Inorg. Chem.* **4**, 766 (1965).
162. M. J. Carter and J. K. Beattie, *Inorg. Chem.* **9**, 1233 (1970).
163. R. G. Wilkins, *Acc. Chem. Res.* **3**, 408 (1970); *Comments Inorg. Chem.* **2**, 187 (1983).
164. J. Bjerrum and K.G. Poulsen, *Nature London* **169**, 463 (1952).
165. P. Bernhard, L. Helm, A. Ludi and A. E. Merbach, *J. Amer. Chem. Soc.* **107**, 312 (1985).
166. D. S. Auld, *Methods in Enzym.* **61**, 318 (1979); A. Galdes, D. S. Auld and B. L. Vallee, *Biochemistry* **22**, 1888 (1983).
167. P. Douzou and G. A. Petsko, *Adv. Protein Chem.* **36**, 245 (1984); S. T. Cartwright and S. G. Waley, *Biochemistry* **26**, 5329 (1987) for a critical analysis of the technique.
168. R. H. Austin, K. W. Beeson, L. Eisenstein, H. Frauenfelder, and I. C. Gunsalus, *Biochemistry* **14**, 5355 (1975).
169. A. L. Fink, *Acc. Chem. Res.* **10**, 233 (1977).
170. A. S. Verkman, A. A. Pandiscio, M. Jennings, and A. K. Solomon, *Anal. Biochem.* **102**, 189 (1980).
171. K. Murakami, T. Sano and T. Yasunaga, *Bull. Chem. Soc. Japan* **54**, 862 (1981). This is unusual case where there are no temperature-jump relaxations. The interaction of bovine serum albumin with bromophenol blue is accompanied by four relaxations which are attributed to a fast second-order interaction followed by three first-order steps.
172. S. L. Olsen, L. P. Holmes and E. M. Eyring, *Rev. Sci. Instrum.* **45**, 859 (1974).
173. A. Raap, J. W. Van Leeuwen, H. S. Rollema and S. H. de Bruin, *Eur. J. Biochem.* **88**, 555 (1978).
174. M. Absi-Halabi, J. D. Atwood, N. P. Forbus and T. L. Brown, *J. Amer. Chem. Soc.* **102**, 6248 (1980); M. S. Corrairie and J. D. Atwood, *Inorg. Chem.* **28**, 3781 (1989).
175. M. Poliakoff and E. Weitz, *Adv. Organomet. Chem.* **25**, 277 (1986).
176. T. Ogura and T. Kitagawa, *J. Amer. Chem. Soc.* **109**, 2177 (1987).
177. M. Foster, R. E. Hester, B. Cartling and R. Wilbrandt, *Biophys. J.* **38**, 111 (1982).
178. W. K. Smothers and M. S. Wrighton, *J. Amer. Chem. Soc.* **105**, 1067 (1983); B. Cartling and R. Wilbrandt, *Biochim. Biophys. Acta* **637**, 61 (1981).
179. K. B. Lyons, J. M. Freidman, P. A. Fleury, *Nature London* **275**, 565 (1978); R. F. Dallinger, W. H. Woodruff and M. A. J. Rodgers, *J. Appl. Spectros.* **33**, 522 (1979).
180. M. Brouwer, C. Bonaventura and J. Bonaventura, *Biochemistry* **20**, 1842 (1981).
181. D. Thusius in *B23*, p. 339.
182. S. M. J. Dunn, J. G. Batchelor and R. W. King, *Biochemistry* **17**, 2356 (1978).
183. R. Rigler, C.-R. Rabl and T. M. Jovin, *Rev. Sci. Instrum.* **45**, 580 (1974).
184. M. J. Hardman, *Biochem. J.* **197**, 773 (1981) Pressure-jump combined with protein fluorescence changes are used to study LADH catalyzed reduction of acetaldehyde. The results show that the rate determining step is isomerization.
185. P. M. Bayley, *Prog. Biophys. Molec. Biol.* **37**, 149 (1981).
186. H. Nielsen and P. E. Sørensen, *Acta Chem. Scand.* **37**, 105 (1983), describe the modification of a commercial stopped-flow for polarimetry.
187. M. Anson, S. R. Martin and P. M. Bayley, *Rev. Sci. Instrum.* **48**, 953 (1977).
188. B. Gruenwald and W. Knoche, *Rev. Sci. Instrum.* **49**, 797 (1978).
189. A. L. Cummings and E. M. Eyring, *Biopolymers.* **14**, 2107 (1975).
190. X. Xie and J. D. Simons, *J. Amer. Chem. Soc.* **112**, 7802 (1990).
191. A. E. Merbach, P. Morre, O. W. Howarth, and C. H. McAteer, *Inorg. Chim. Acta* **39**, 129 (1980).
192. S. Lanza, D. Minniti, P. Moore, J. Sachinidis, R. Romeo and M. L. Tobe, *Inorg. Chem.* **23**, 4428 (1984), measure exchange of  $\text{Me}_2\text{SO}[^2\text{H}_6]$  with  $\text{cis-Pt}(\text{C}_6\text{H}_5)_2(\text{Me}_2\text{SO})_2$  in  $\text{CDCl}_3$  by stopped-flow  $^1\text{H}$  NMR. There is a steady decrease in the signal at  $\delta$  2.82 due to coordinated  $\text{Me}_2\text{SO}$  and increase at  $\delta$  2.61 (uncoordinated  $\text{Me}_2\text{SO}$ ).
193. R. J. Miller and G. L. Closs, *Rev. Sci. Instr.* **52**, 1876 (1981).

194. A. D. Trifunac, K. W. Johnson and R. H. Lowers, *J. Amer. Chem. Soc.* **98**, 6067 (1976).
195. R. C. Bray, *Adv. Enzym.* **51**, 107 (1980).
196. K.A. McLauchlan and D. G. Stevens, *Acc. Chem. Res.* **21**, 54 (1988).
197. V. Jagannadham and S. Steenken, *J. Amer. Chem. Soc.* **106**, 6542 (1984). The reaction of RCHOH, generated by pulse radiolysis, was studied with p-substituted nitrobenzenes using time-resolved optical and conductance detection. The radical anion of the nitrobenzene is produced directly and indirectly.
198. B. G. Cox, P. Firman, I. Schneider and H. Schneider, *Inorg. Chem.* **27**, 4018 (1988).
199. T. Okubo and A. Enokida, *J. Chem. Soc. Faraday Trans. I*, 1639, (1983) flow and pressure-jump with conductance.
200. H. Hoffman, E. Yaeger and J. Stuehr, *Rev. Sci. Instrum.* **39**, 649 (1968).
201. T. Sano and T. Yasunaga, *Biophys. Chem.* **11**, 377 (1980).
202. J. Lilie, W. L. Waltz, S. H. Lee and L. L. Gregor, *Inorg. Chem.* **25**, 4487 (1986).
203. W. L. Waltz, J. Lilie and S. H. Lee, *Inorg. Chem.* **23**, 1768 (1984).
204. B. Fourest, K. H. Schmidt and J. C. Sullivan, *Inorg. Chem.* **25**, 2096 (1986). For description of pulse radiolysis/conductivity see K. H. Schmidt, S. Gordon, M. Thompson, J. C. Sullivan and W. A. Mulac, *Radiat. Phys. Chem.* **21**, 321 (1983).
205. T. Nakamura, *J. Biochem. Japan* **83**, 1077 (1978); J. V. Howarth, N. C. Millar and H. Gutfreund, *Biochem. J.* **248**, 677, 683, (1987) describe the construction and testing of a thermal/stopped-flow apparatus.
206. P. Bowen, B. Balko, K. Blevens, R. L. Berger and H. P. Hopkins, Jr., *Anal. Biochem.* **102**, 434 (1980).
207. G. W. Liesegang, *J. Amer. Chem. Soc.* **103**, 953 (1981).
208. B16, Chap. 3; B12, p. 45.
209. S. Yamada, K. Ohsumi and M. Tanaka, *Inorg. Chem.* **17**, 2790 (1978).
210. L. W. Harrison and B. L. Vallee, *Biochemistry* **17**, 4359 (1978).
211. J. Hirose and R. G. Wilkins, *Biochemistry* **23**, 3149 (1984); J. Hirose, M. Noji, Y. Kidani and R. G. Wilkins, *Biochemistry* **24**, 3495 (1985).
212. D. A. Malencik, S. R. Anderson, Y. Shalitin and M. I. Schimerlik, *Biochem. Biophys. Res. Commun.* **101**, 390 (1981).
213. J. R. Blinks, W. G. Wier, P. Hess and F. G. Prendergast, *Prog. Biophys. Mol. Biol.* **40**, 1 (1982) – measurement of Ca<sup>2+</sup> in living cells.
214. P. L. Dorogi, C.-R. Rabl and E. Neumann, *Biochem. Biophys. Res. Commun.* **111**, 1027 (1983).
215. R. Koren and G. G. Hammes, *Biochemistry* **15**, 1165 (1976).
216. D. H. Devia and A. G. Sykes, *Inorg. Chem.* **20**, 910 (1981).
217. K. Nakatani, K. Kitagishiam and K. Hiromi, *J. Biochem. Japan*, **87**, 563 (1980).
218. D. Barber, S. R. Parr and C. Greenwood, *Biochem. J.* **173**, 681 (1978).
219. S. C. Koerber, A. K. H. MacGibbon, H. Dietrich, M. Zeppezauer and M. F. Dunn, *Biochemistry* **22**, 3424 (1983).
220. E.T. Gray Jr., R. W. Taylor and D. W. Margerum, *Inorg. Chem.* **16**, 3047 (1977).
221. L. I. Simándi, M. Jáky, C. R. Savage and Z. A. Schelly, *J. Amer. Chem. Soc.* **107**, 4220 (1985), which gives a detailed description of the arrangement.
222. A. A. El-Awady, P. C. Wilkins and R. G. Wilkins, *Inorg. Chem.* **24**, 2053 (1985).
223. A system which has been used successfully by a number of groups for some years is put together by On Line Instrument Systems, Jefferson, Gerogia 30549, USA.
224. J. C. Sullivan, E. Deutsch, G. E. Adams, S. Gordon, W. A. Mulac and K. H. Schmidt, *Inorg. Chem.* **15**, 2864 (1976).
225. M. Tsuda, *Biochim. Biophys. Acta* **545**, 537 (1979).

226. K. F. Geoghegan, A. Galdes, R. A. Martinelli, B. Holmquist, D. S. Auld and B. L. Vallee, *Biochemistry* **22**, 2255 (1983), give a schematic diagram of a low-temperature, stopped-flow, rapid scanning spectrometer and its use for recording spectra of intermediates in cobalt carboxypeptidase A catalyzed hydrolysis of very reactive dansyl oligo-peptides and -esters.
227. C. Grant, Jr., and P. Hambright, *J. Amer. Chem. Soc.* **91**, 4195 (1969).
228. M. M. Paleic and H. B. Dunford, *J. Biol. Chem.* **255**, 6128 (1980).
229. F. Zingales, A. Trovati and P. Uguagliati, *Inorg. Chem.* **10**, 510 (1971).
230. W. G. Jackson, *Inorg. Chem.* **26**, 3004 (1987), indicates the problems in interpreting the kinetics and stereochemistry of compounds of the type  $Mn(CO)_5X$ .
231. T. L. Brown, *Inorg. Chem.* **28**, 3229 (1989).
232. D. J. Darensbourg, *Inorg. Chem.* **18**, 14 (1979).
233. R. W. Callahan and T. J. Meyer, *Inorg. Chem.* **16**, 574 (1977).
234. K. Wieghardt, M. Woeste, P. S. Roy and P. Chaudhuri, *J. Amer. Chem. Soc.* **107**, 8276 (1985).
235. R. J. Kazlauskas and M. S. Wrighton, *J. Amer. Chem. Soc.* **104**, 5784 (1982).
236. I. D. Campbell and R. A. Dwek, *Biological Spectroscopy*, Benjamin/Cummings, Menlo Park, 1984, Chap. 9.
237. N. Capelle, J. Barbet, P. Dessen, S. Blanquet, B. P. Roques and J.-B. Le Pecq, *Biochemistry* **18**, 3354 (1979).
238. V. H. Rao and V. Krishnan, *Inorg. Chem.* **24**, 3538 (1985).
239. P. J. Breen, W. DeW. Horrocks, Jr. and K. A. Johnson, *Inorg. Chem.* **25**, 1968 (1986).
240. M. R. Eftink and C. A. Ghiron, *Anal. Biochem.* **114**, 199 (1981), review solute fluorescence quenching of proteins in the study of structure and dynamics.
241. P. C. Harrington and R. G. Wilkins, *Biochemistry* **17**, 4245 (1978).
242. R. D. Farina and R. G. Wilkins, *Biochim. Biophys. Acta* **631**, 428 (1980).
243. R. M. Clegg, F. G. Loontjens, A. V. Landschoot and T. M. Jovin, *Biochemistry* **20**, 4687 (1981).
244. P. J. Breen, K. A. Johnson and W. D. Horrocks, Jr., *Biochemistry* **24**, 4997 (1985) and references therein.
245. M. G. Badea and L. Brand. *Methods in Enzym.* **61**, 378 (1979).
246. J. B. A. Ross, C. J. Schmidt and L. Brand, *Biochemistry* **20**, 4369 (1981).
247. S. J. Simon, J. A. Boslett Jr. and K. H. Pearson, *Inorg. Chem.* **16**, 1232 (1977).
248. M. Abdullah, J. Barrett and P. O'Brien, *Inorg. Chim. Acta* **96**, L35 (1985).
249. Y. Ae Im and D. H. Busch, *J. Amer. Chem. Soc.* **83**, 3362 (1961). Models show that when the Me group of the (-)pdta ligand is equatorial (**10a**) there is less steric interaction with other hydrogens than in the axial Me group arrangement in (**10b**). The  $\Delta$ -configuration about the metal (Sec. 7.6.1) will therefore be retained regardless of the lability of the complex. A beginning net-rotation thus becomes zero at equilibrium in (3.39).
250. I. I. Creaser, A. M. Sargeson and A. W. Zanella, *Inorg. Chem.* **22**, 4022 (1983).
251. H. Kihara, E. Takahashi, K. Yamamura and I. Tabushi, *Biochem. Biophys. Res. Commun.* **95**, 1687 (1980).
252. L. F. McCoy, Jr., E. S. Rowe and K.-P. Wong, *Biochemistry* **19**, 4738 (1980).
253. P. Hendry and A. M. Sargeson, *Inorg. Chem.* **25**, 865 (1986).
254. S. Aygen, H. Hanssum and R. van Eldik, *Inorg. Chem.* **24**, 2853 (1985). The results are very similar to older data obtained by the  $^{18}O$  batch method (Sec. 3.11 (b)), W. Kruse and H. Taube, *J. Amer. Chem. Soc.* **83**, 1280 (1961).
255. L. Helm, L. I. Elding and A. E. Merbach, *Inorg. Chem.* **24**, 1719 (1985).
256. O. Gröning, T. Drakenberg and L. I. Elding, *Inorg. Chem.* **21**, 1820 (1982).
257. D. A. Buckingham, C. R. Clark and T. W. Lewis, *Inorg. Chem.* **18**, 2041 (1979).
258. J. G. Russell, R. G. Bryant and M. M. Kreevoy, *Inorg. Chem.* **23**, 4565 (1984); see also R. K. Harris and R. J. Morrow, *J. Chem. Soc. Faraday Trans. I*, **80**, 3071 (1984).
259. R. D. Chapman and E. B. Fleischer, *J. Amer. Chem. Soc.* **104**, 1575; 1582 (1982).

260. P. Bernhard, L. Helm, A. Ludi and A. E. Merbach, *J. Amer. Chem. Soc.* **107**, 312 (1985) also I. Rapaport, L. Helm, A. E. Merbach, P. Bernhard and A. Ludi, *Inorg. Chem.* **27**, 873 (1988).
261. Y. T. Hayden and J. O. Edwards, *Inorg. Chim. Acta* **114**, 63 (1986).
262. R. K. Murmann, *J. Amer. Chem. Soc.* **96**, 7836 (1974); R. K. Murmann and K. C. Giese, *Inorg. Chem.* **17**, 1160 (1978).
263. P. Comba and L. Helm, *Helv. Chim. Acta* **71**, 1406 (1988).
264. R. L. Kump and L. J. Todd, *Inorg. Chem.* **20**, 3715 (1981).
265. D. T. Richens, L. Helm, P.-A. Pittet, A. E. Merbach, F. Nicolò and G. Chapuis, *Inorg. Chem.* **28**, 1394 (1989); G. D. Hinch, D. E. Wycoff and R. K. Murmann, *Polyhedron*, **5**, 487 (1986).
266. R. van Eldik, J. von Jouanne and H. Kelm, *Inorg. Chem.* **21**, 2818 (1982).
267. J. M. Risley and R. L. Van Etten, *J. Amer. Chem. Soc.* **101**, 252 (1979).
268. T. G. Wood, O. A. Weisz and J. W. Korarich, *J. Amer. Chem. Soc.* **106**, 2222 (1984).
269. W. D. Wheeler, S. Kaizaki and J. I. Legg, *Inorg. Chem.* **21**, 3250 (1982).
270. P. Moore, *Pure Appl. Chem.* **57**, 347 (1985); C. H. McAteer and P. Moore, *J. Chem. Soc. Dalton Trans.* 353 (1983).
271. E. D. Becker, *High Resolution NMR. Theory and Chemical Applications*, Academic Press, NY, 1980.
272. G. Fraenkel in B6, Chap. X.
273. M. Meier, F. Basolo and R. G. Pearson, *Inorg. Chem.* **8**, 795 (1969).
274. These and subsequent equations are treated in: F. A. Bovey, *Nuclear Magnetic Resonance Spectroscopy*, 2nd. Edit. Academic Press, San Diego, CA, 1988, p. 118, 119, 191-203.
275. L. Spiecia and T. W. Swaddle, *Inorg. Chem.* **26**, 2265 (1987) is the more recent of a series of studies of this electron transfer.
276. H. M. McConnell and H. E. Weaver, *J. Chem. Phys.* **25**, 307 (1956).
277. C. R. Giuliau and H. M. McConnell, *J. Inorg. Nucl. Chem.* **9**, 171 (1959); K. Okamoto, W.-S. Jung, H. Tomiyasu and H. Fukutomi, *Inorg. Chim. Acta* **143**, 217 (1988) – see Prob. 5(b) Chap. 8.
278. P. J. Smolenaers and J. K. Beattie, *Inorg. Chem.* **25**, 2259 (1986).
279. R. M. Nielson, J. P. Hunt, H. W. Dodgen and S. Wherland, *Inorg. Chem.* **25**, 1964 (1986).
280. C. A. Koval and D. W. Margerum, *Inorg. Chem.* **20**, 2311 (1981).
281. E. J. Pullian and D. R. McMillan, *Inorg. Chem.* **23**, 1172 (1984).
282. D. L. Rabenstein and R. J. Kula, *J. Amer. Chem. Soc.* **91**, 2492 (1969); G. E. Glass, W. B. Schwabacher and R. S. Tobias, *Inorg. Chem.* **7**, 2471 (1968).
283. P. W. Taylor, J. Feeny and A. S. V. Burgen, *Biochemistry* **10**, 3866 (1971), employ nmr to study the binding of acetate (using  $^1\text{H}$ ) and fluoroacetate ( $^{19}\text{F}$ ) to carbonic anhydrase.
284. L. H. Pignolet and W. D. Horrocks, Jr., *J. Amer. Chem. Soc.* **90**, 922 (1968).
285. G. N. La Mar, *J. Amer. Chem. Soc.* **92**, 1806 (1970).
286. P. R. Rubini, Z. Poaty, J.-C. Boubel, L. Rodenhüser and J.-J. Delpuech, *Inorg. Chem.* **22**, 1295 (1983).
287. P. R. Rubini, L. Rodenhüser and J. J. Delpuech, *Inorg. Chem.* **18**, 2962 (1979).
288. J. M. Lehn and M. E. Stubbs, *J. Amer. Chem. Soc.* **96**, 4011 (1974).
289. G. Binsch in *Dynamic Nuclear Magnetic Resonance Spectroscopy*, L. M. Jackman and F. A. Cotton, eds. Academic Press, NY, 1975, Chap. 3.
290. A. Allerhand, H. S. Gutowsky, J. Jones and R. A. Meinzer, *J. Amer. Chem. Soc.* **88**, 3185 (1966).
291. C. B. Storm, A. H. Turner and M. B. Swann, *Inorg. Chem.* **23**, 2743 (1984).
292. M.-S. Chan and A. C. Wahl, *J. Phys. Chem.* **82**, 2542 (1978).
293. G. Binsch, *Top. Stereochem.* **3**, 97 (1968); Y. Ikeda, H. Tomiyasu and H. Fukutomi, *Inorg. Chem.* **23**, 1356 (1984) study intramolecular exchange in  $\text{UO}_2(\text{acac})_2\text{Me}_2\text{SO}$  in  $o\text{-C}_6\text{H}_4\text{Cl}_2$ .
294. T. J. Swift and R. E. Connick, *J. Chem. Phys.* **37**, 307 (1962).



295. Z. Luz and S. Meriboom, *J. Chem. Phys.* **40**, 1058, 2686 (1964); R. Murray, H. W. Dodgen and J. P. Hunt, *Inorg. Chem.* **3**, 1576 (1964); H. H. Glaeser, H. W. Dodgen and J. P. Hunt, *Inorg. Chem.* **4**, 1061 (1965); S. Funahashi and R. B. Jordan, *Inorg. Chem.* **16**, 1301 (1977); S. F. Lincoln, A. M. Hounslow and A. N. Boffa, *Inorg. Chem.* **25**, 1038 (1986); A. Kioki, S. Funahashi, M. Ishii and M. Tanaka, *Inorg. Chem.* **25**, 1360 (1986).
296. T. R. Stengle and C. H. Langford, *Coordn. Chem. Revs.* **2**, 349 (1967) and S. F. Lincoln, *Prog. React. Kinetics* **9**, 1 (1977) for comprehensive discussions of complete line shape analyses.
297. D. K. Ravage, T. R. Stengle and C. H. Langford, *Inorg. Chem.* **6**, 1252 (1967).
298. A. E. Merbach, *Pure Appl. Chem.* **59**, 161 (1987).
299. (a) P. J. Nichols and M. W. Grant, *Aust. J. Chem.* **31**, 258 (1978). (b) C. H. McAteer and P. Moore, *J. Chem. Soc. Dalton Trans.* 353 (1983).
300. J. Burgess, B. A. Goodman and J. B. Raynor, *J. Chem. Soc. A*, 501 (1968).
301. J. N. Marov, M. N. Vargaftik, V. K. Belyaeva, G. A. Evtikova, E. Hoyer, R. Kirmse and W. Dietzsch, *Russ. J. Inorg. Chem.* **25**, 101 (1980).
302. A. McAuley, D. H. Macartney and T. Oswald, *J. Chem. Soc. Chem. Commun.* 274 (1982).
303. G. Czapski, *J. Phys. Chem.* **75**, 2957 (1971).
304. J. Stach, R. Kirmse, W. Dietzsch, G. Lassmann, V. K. Belyaeva and I. N. Marov, *Inorg. Chim. Acta* **96**, 55 (1985).
305. M. Knoblowitz and J. I. Morrow, *Inorg. Chem.* **15**, 1674 (1976).
306. S. A. Jacobs and D. W. Margerum, *Inorg. Chem.* **23**, 1195 (1984).
307. E. Finkelstein, G. M. Rosen and E. J. Rauckman, *Arch. Biochem. Biophys.* **200**, 1 (1980).
308. A. J. F. Searle and A. Tomasi, *J. Inorg. Biochem.* **17**, 161 (1982).
309. B. J. Corden and P. H. Rieger, *Inorg. Chem.* **10**, 263 (1971); J. B. Farmer, F. G. Herring and R. L. Tapping, *Can. J. Chem.* **50**, 2079 (1972).
310. T. Saji and S. Aoyagui, *Bull. Chem. Soc. Japan* **46**, 2101 (1973).
311. T. T.-T. Li and C. H. Brubaker, Jr., *J. Organomet. Chem.* **216**, 223 (1981).
312. C. Daul, J.-N. Gex, D. Perret, D. Schaller and A. von Zelewsky, *J. Amer. Chem. Soc.* **105**, 7556 (1983).
313. P. K. Glasoe and F. A. Long, *J. Phys. Chem.* **64**, 188 (1960).
314. R. G. Bates, M. Paabo and R. A. Robinson, *J. Phys. Chem.* **67**, 1833 (1963); B. B. Hasinoff, H. B. Dunford and D. G. Horne, *Can. J. Chem.* **47**, 3225 (1969).
315. F. Millar, J. M. Wrigglesworth and P. Nicholls, *Eur. J. Biochem.* **117**, 13 (1981) – using glass microelectrode and pH meter followed changes of  $\pm 0.005$  pH at neutral pH.
316. B13, p. 178.
317. R. S. Rowlett and D. N. Silverman, *J. Amer. Chem. Soc.* **104**, 6737 (1982); D. N. Silverman and S. Lindskog, *Acc. Chem. Res.* **21**, 30 (1988).
318. L. S. W. L. Sokol, T. D. Fink and D. B. Rorabacher, *Inorg. Chem.* **19**, 1263 (1980).
319. R. W. Hay and P. Banerjee, *J. Chem. Soc. Dalton Trans.* 362 (1981).
320. P. A. Benkovic, M. Hegazi, B. A. Cunningham and S. J. Benkovic, *Biochemistry* **18**, 830 (1979) use continuous monitoring of inorganic phosphate product of enzyme catalyzed hydrolysis of fructose biphosphate. The pH change monitored by phenol red results from an acid, base adjustment of the liberated phosphate. This is a detailed valuable, if complicated, account.
321. P. F. Fitzpatrick and V. Massey, *J. Biol. Chem.* **257**, 9958 (1982).
322. A. K. Shamsuddin Ahmed and R. G. Wilkins, *J. Chem. Soc.* 3700 (1959).
323. R. Gresser, D. W. Boyd, A. M. Albrecht-Gary and J. P. Schwing, *J. Amer. Chem. Soc.* **102**, 651 (1980).
324. F. P. Rotzinger, H. Stünzi and W. Marty, *Inorg. Chem.* **25**, 489 (1986), use a weakish base such as ethanolamine to avoid local excesses of  $\text{OH}^-$ .
325. G. Schwarzenbach and G. Geier, *Helv. Chim. Acta* **46**, 906 (1963); G. Geier, *Chimia*, **25**, 401 (1971).
326. C. Marques and R. A. Hasty, *J. Chem. Soc. Dalton Trans.* 1269 (1980).



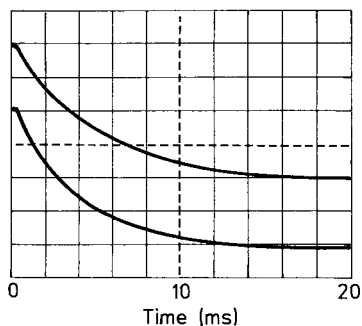
327. S. Balt and C. Dekker, *Inorg. Chem.* **15**, 2370 (1976).
328. M. Kotowski, D. A. Palmer and H. Kelm, *Inorg. Chem.* **18**, 2555 (1979).
329. L. J. Csányi, Z. M. Galbács and L. Nagy, *J. Chem. Soc. Dalton Trans.* 237 (1982).
330. R. G. Dakers and J. Halpern, *Can. J. Chem.* **32**, 969 (1954).
331. M. Kimura, T. Kawajiri and M. Tanida, *J. Chem. Soc. Dalton Trans.* 726 (1980).
332. F. C. Anson, C.-L. Ni and J. M. Saveant, *J. Amer. Chem. Soc.* **107**, 3442 (1985).
333. E. L. Yee, O. A. Gansow and M. J. Weaver, *J. Amer. Chem. Soc.* **102**, 2278 (1980).
334. B. G. Cox and W. Jedral, *J. Chem. Soc. Faraday Trans. I* **80**, 781 (1984).
335. R. F. Jameson and N. J. Blackburn, *J. Chem. Soc. Dalton Trans.* 9, (1982).
336. R. Hamilton, D. Maguire and M. McCabe, *Anal. Biochem.* **93**, 386 (1979).
337. B18, p. 42.
338. A. J. Bard and L. R. Faulkner, *Electrochemical Methods*, Wiley, NY 1980 Ch 11.
339. T. Matusinovic and D. E. Smith, *Inorg. Chem.* **20**, 3121 (1981).
340. K. Shigehara, N. Oyama and F. C. Anson, *Inorg. Chem.* **20**, 518 (1981).
341. H. Krüger, *Chem. Soc. Revs.* **11**, 227 (1982) for a short account of electrochemical (as well as other) methods for studying fast reactions.
342. R. M. Wightman and D. O. Wipf, *Acc. Chem. Res.* **23**, 64 (1990). C. P. Andrieux, P. Hapiot and J.-M. Saveant, *Chem. Revs.* **90**, 723 (1990).
343. W. E. Jones and J. D. R. Thomas, *J. Chem. Soc. A*, 1481 (1966).
344. W. G. Jackson, S. S. Jurisson and B. C. McGregor, *Inorg. Chem.* **24**, 1788 (1985).
345. M. H. M. Abou-El-Wafa, M. G. Burnett and J. F. McCullagh, *J. Chem. Soc. Dalton Trans.* 2083 (1986).
346. M. F. Perutz, *Biochem. J.* **195**, 519 (1981).
347. S. F. Lincoln and D. R. Stranks, *Aust. J. Chem.* **21**, 37; 67 (1968).
348. H. Gamsjäger and R. K. Murmann, *Adv. Inorg. Bioinorg. Chem.* **2**, 317 (1983).
349. B. Bronnum, H. S. Johansen and L. H. Skibsted, *Inorg. Chem.* **27**, 1859 (1988).
350. H. S. Johansen and V. Middelboe, *Appl. Spectrosc.* **36**, 221 (1982).
351. R. M. Noyes in B5, Chap. V (Sec. 4).
352. H. Ogino, E. Kikkawa, M. Shimura and N. Tanaka, *J. Chem. Soc. Dalton Trans.* 894 (1981).
353. A. Bakač and J. H. Espenson, *Inorg. Chem.* **20**, 953 (1981) generate  $\text{Cr}^{2+}$  slowly by the reaction  $\text{CrCH}_2\text{OH}^{2+} + \text{VO}^{2+} + \text{H}^+ \rightarrow \text{Cr}^{2+} + \text{V}^{3+} + \text{CH}_2\text{O} + \text{H}_2\text{O}$  and then the relative reaction rates with  $(\text{NH}_3)_5\text{CoX}^{2+}$  and  $\text{VO}^{2+}$  both in large excess are assessed by the  $\text{Co}^{2+}$  produced (color with  $\text{SCN}^-$ ).
354. N. Shinohara and J. Lilie, *Inorg. Chem.* **18**, 434 (1979).
355. H. Boucher, A. M. Sargeson, D. F. Sangster and J. C. Sullivan, *Inorg. Chem.* **20**, 3719 (1981).
356. M. Z. Hoffman and M. Simic, *Inorg. Chem.* **12**, 2471 (1973).
357. R. F. Pasternack and B. Halliwell, *J. Amer. Chem. Soc.* **101**, 1026 (1979).
358. M. Z. Hoffman, F. Bolleta, L. Moggi and G. L. Hug, Rate Constants for the Quenching of Excited States of Metal Complexes in Fluid Solution, *J. Phys. Chem. Ref. Data*, **18**, 219 (1989).
359. F. A. Posey and H. Taube, *J. Amer. Chem. Soc.* **79**, 255 (1957).
360. I. Dostrovsky and F. S. Klein, *Anal. Chem.* **24**, 414 (1952).
361. M. H. O'Leary, *Methods in Enzym.* **64**, 83 (1980); C. B. Grissom and W. W. Cleland, *J. Amer. Chem. Soc.* **108**, 5582 (1986).
362. T. J. Kemp, P. Moore and G. R. Quick, *J. Chem. Soc. Dalton Trans.* 1377 (1979).
363. K. J. Wannowius, K. Krimm and H. Elias, *Inorg. Chim. Acta* **127**, L43 (1987).
364. R. van Eldik, U. Spitzer and H. Kelm, *Inorg. Chim. Acta* **74**, 149 (1983).
365. A. J. Dixon, M. A. Healy, M. Poliakoff and J. J. Turner, *J. Chem. Soc. Chem. Commun.* 994 (1986).
366. A. J. Brown, O. W. Howarth, P. Moore and G. E. Morris, *J. Chem. Soc. Dalton Trans.* 1776 (1979).
367. P. Hemmes and J. J. McGarvey, *Inorg. Chem.* **18**, 1812 (1979).
368. A. Lifshitz and B. Perlmuter-Hayman, *J. Phys. Chem.* **65**, 2098 (1961).
369. C. Bohne, I. D. MacDonald and H. B. Dunford, *J. Amer. Chem. Soc.* **108**, 7867 (1986).

## Selected Bibliography

- B21. W. J. Gettins and E. Wyn-Jones (eds.) *Techniques and Applications of Fast Reactions in Solution*, D. Reidel, Boston, 1979.
- B22. D. N. Hague, *Fast Reactions*, Wiley-Interscience, New York, 1971.
- B23. I. Pecht and R. Rigler (eds.) *Chemical Relaxation in Molecular Biology*, Springer-Verlag, New York, 1977.

## Problems

- The buried Cys-212 of human carbonic anhydrase B ( $3 \mu\text{M}$ ) is virtually unreactive towards 2-chloromercuric-4-nitrophenol ( $60 \mu\text{M}$ ) at pH 9.2, but upon the addition of only  $40 \mu\text{M}$   $\text{CN}^-$ , the half-life drops to 10 minutes which is an, at least, 75-fold rate enhancement. On first analysis, this would suggest that inhibitor binding to the enzyme has produced a conformational change or altered the  $-\text{SH}$  environment of the Cys-212. This is unexpected. How would you prove by kinetic experiments that the  $\text{CN}^-$  is binding to the mercury compound and not the enzyme and that this is changing the reactivity. The rate reaches a constant value at high  $[\text{CN}^-]$ .  
R. G. Khalifah, G. Sanyai, D. J. Straker and W. McI. Sutherland, *J. Biol. Chem.* **254**, 602 (1979).
- A number of Co(III) complexes, such as  $\text{Co}(\text{edta})^-$  and  $\text{Co}(\text{phen})_3^{3+}$ , can be resolved into optical isomers and are extremely stable towards racemization. The Co(II) analogs are configurationally labile and resolution has proved impossible. Suggest how with a double mixing apparatus it might be possible to measure half-lives in the  $10^{-3}$ – $1$  s range for the first-order racemization of the Co(II) complexes.  
E. L. Blinn and R. G. Wilkins, *Inorg. Chem.* **15**, 2952 (1976).
- Figure 1 shows pressure-jump relaxation traces with conductivity monitoring at pressures,  $P$ , of  $1 \text{ kg cm}^{-2}$  (lower curve) and  $1000 \text{ kg cm}^{-2}$  for the relaxation of a  $6.06 \text{ mM}$  nickel (II) glycolate solution at  $20^\circ\text{C}$ . Time scale:  $2 \text{ ms/division}$ . Only the 1:1 complex ( $K = 210 \text{ M}^{-1}$  at  $P = 1 \text{ kg cm}^{-2}$  and  $K = 100 \text{ M}^{-1}$  at  $P = 1000 \text{ kg cm}^{-2}$ ) need be considered. Estimate the  $\Delta V^\ddagger$  value for the formation and dissociation of Ni(II) glycolate from these data, and after reading Chap. 4 account for the data.  
T. Inoue, K. Sugahara, K. Kojima and R. Shimozawa, *Inorg. Chem.* **22**, 3977 (1983).

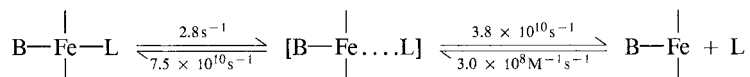


Problem 3. Reproduced with permission from T. Inoue, K. Sugahara, K. Kojima and R. Shimozawa, *Inorg. Chem.* **22**, 3977 (1983). © (1983) American Chemical Society.

4. Geminate recombination of iron(II) porphyrin with a number of isocyanides and 1-methylimidazole has been observed by T. G. Traylor, D. Magde, D. Taube and K. Jongeward, *J. Amer. Chem. Soc.* **109**, 5864 (1987).

(a) What is geminate recombination and what is its significance to the measured quantum yield?

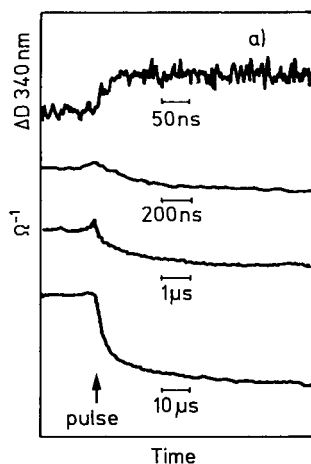
(b) The suggested mechanism (with rate constants) for the binding of MeCN(L) to the 1-methylimidazole (B) complex of protoheme dimethyl ester in toluene/B is



How are these individual rate constants determined?

5. Laser pulses of 265 nm and 20 ns duration were delivered into a quartz cell through which a solution of deaerated 0.2 mM  $[\text{Co}(\text{NH}_3)_5\text{Cl}]\text{Cl}_2$  in 5 mM HCl was flowing. Both spectral and conductivity changes could be monitored. The very fast absorbance change at 340 nm (only a slight conductivity increase) and the slower conductivity changes (no absorbance changes) are shown in Fig. 2. The absorbance at the end of (a) corresponds to  $\text{Cl}_2^-$ . Interpret the results.

J. Lilie, *J. Amer. Chem. Soc.* **101**, 4417 (1979).



Problem 5. Reproduced with permission from I. Lilie, *J. Amer. Chem. Soc.* **101**, 4417 (1979), © (1979) American Chemical Society.

6. Nitroprusside ion  $\text{Fe}(\text{CN})_5\text{NO}^{2-}$  is an important drug for the alleviation of severe hypertension. A. R. Butler and C. Glidewell, *Chem. Soc. Revs.* **16**, 361 (1987).

Radiolysis of  $\text{Fe}(\text{CN})_5\text{NO}^{2-}$  with a number of reducing radicals e.g.  $e_{\text{aq}}^-$ ,  $\text{CO}_2^-$ ,  $(\text{CH}_3)_2\dot{\text{C}}\text{OH}$ , and  $\text{H}^\bullet$  gives a common transient, A with maxima at 345 nm and 440 nm. What will be the approximate magnitude of rate constants for production of A from the radicals and what is likely to be the structure of A?

A undergoes spectral changes in the ms range by a first-order process ( $k$ ) to give a stable product (in the absence of  $\text{O}_2$  and light).  $k$  is  $2.8 \times 10^2 \text{ s}^{-1}$  from pH 4.6–8.5. Its value

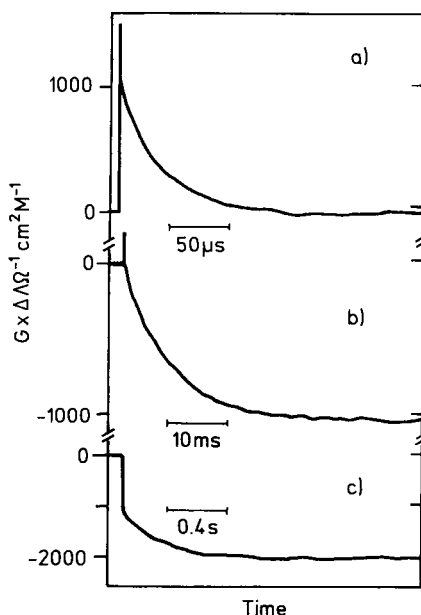
is increased if free  $\text{CN}^-$  is added to the pulse radiolyzed solution (at pH 6.7, mainly HCN). Now,

$$k_{\text{obs}} = 2.8 \times 10^2 + 4 \times 10^6 [\text{CN}^-]$$

Monitoring by conductivity shows a very rapid increase (during the reduction) and a slower decrease ( $2.6 \times 10^2 \text{ s}^{-1}$ ). Explain. R. P. Cheney, M. G. Simic, M. Z. Hoffman, I. A. Taub and K.-D. Asmus, *Inorg. Chem.* **16**, 2187 (1977).

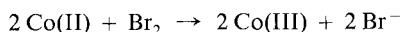
7. The conductivity changes following pulse radiolysis of a mixture of 0.5 mM  $\text{Co}(\text{acac})_3$ , 0.04 mM  $\text{HClO}_4$  and 0.1 M tert-butyl alcohol are shown in Figure 3 (the units of  $G \times \Delta\Lambda$  are (molecules/100eV)  $\Omega^{-1} \text{ cm}^2 \text{ M}^{-1}$ ). The very first increase in conductivity also appears in solutions containing no  $\text{Co}(\text{acac})_3$ . The decreases in conductivity are speeded up in acid. Account for this behavior.

D. Meisel, K. H. Schmidt and D. Meyerstein, *Inorg. Chem.* **18**, 971 (1979).

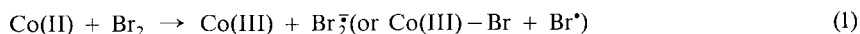


Problem 7. Reproduced with permission from D. Meisel, K.-H. Schmidt and D. Meyerstein, *Inorg. Chem.* **18**, 971 (1979), © (1979) American Chemical Society.

8. Vitamin  $\text{B}_{12}$ , a cobalt(II) complex designated  $\text{Co}(\text{II})$  is oxidized by  $\text{Br}_2$ :



Since the reaction is second-order, the rate limiting step is considered to be:



This would be followed by the faster reactions (2) or (3)



or



Show how, using pulse-radiolytically generated  $\text{Br}_2^{\cdot-}$ , you might distinguish between (2) and (3) and how you might decide whether the reaction is inner sphere.

D. Meyerstein, J. H. Espenson, D. A. Ryan and W. A. Mulac, *Inorg. Chem.* **18**, 863 (1979).

9. How would you verify that the intermediate in the  $\text{Fe}^{2+}$ ,  $\text{Co}(\text{C}_2\text{O}_4)_3^{3-}$  reaction (3.17) is the  $\text{Fe}(\text{C}_2\text{O}_4)^+$  (3.18) ion?

At high  $\text{Co}(\text{C}_2\text{O}_4)_3^{3-}$  concentrations, this reaction obeys the rate law

$$-d[\text{Fe}^{2+}]/dt = k_1[\text{Fe}^{2+}][\text{Co}(\text{C}_2\text{O}_4)_3^{3-}] + k_2[\text{Fe}^{2+}][\text{Co}(\text{C}_2\text{O}_4)_3^{3-}]^2$$

Suggest a reason for the second term.

R. D. Cannon and J. S. Stillman, *J. Chem. Soc. Dalton Trans.* 428 (1976).

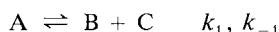
10. The second-order rate constants  $k$  for the base hydrolysis of a number of cobalt(III) complexes were measured with a simple flow apparatus using conductivity as a monitoring device. Equal concentrations ( $A_0$ ) of reactants were used. Show that a plot of  $R_t/R_e - R_t$  vs time is linear, having slope  $s$ , and that

$$k = \frac{(R_e - R_0)s}{R_0 A_0}$$

where  $R_0$ ,  $R_t$  and  $R_e$  are the resistance of the solution at times zero,  $t$  and at equilibrium, respectively.

R. G. Pearson, R. E. Meeker and F. Basolo, *J. Amer. Chem. Soc.* **78**, 709 (1956).

11. Suppose that the mechanism for exchange between A and B is a dissociative one:

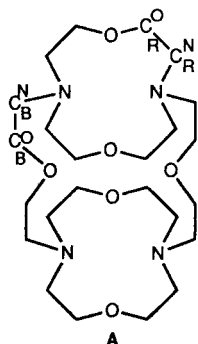


Deduce the dependence of the broadening of the lines A and B on the concentrations of the reactants and the rate constant  $k_1$ .

T. L. Brown, *Acc. Chem. Res.* **1**, 25 (1968).

12. For the 1:1  $\text{Ca}^{2+}$  complex of the ligand A, at 4°C in  $\text{D}_2\text{O}$ , two sets of four  $^{13}\text{C}$  resonances are observed arising from  $\text{C}_R^N$ ,  $\text{C}_R^O$ ,  $\text{C}_B^N$  and  $\text{C}_B^O$ . The signals for  $\text{C}_R^O$  and  $\text{C}_R^N$  have twice the intensity of the other two. When the temperature is raised, the signals of the same intensity within each set coalesce at 40°C. The separation of  $^{13}\text{C}$  signals for  $\text{C}_R^N$ ,  $\Delta\nu$ , is 48 Hz at 4°C. Excess ligand or  $\text{Ca}^{2+}$  do not affect the result. The averaged four  $^{13}\text{C}$  lines of the  $\text{Ca}^{2+}$  complex and the four  $^{13}\text{C}$  signals of free ligand (in about equal amounts) remain sharp as the temperature is raised but finally broaden and coalesce at  $\approx 105^\circ\text{C}$ . The separation of  $^{13}\text{C}$  signals for  $\text{C}_R^N$  is 21 Hz at 32°C. Calculate the exchange rate constants and free energies of activation at the two coalescent temperatures and account for the behavior.

J. M. Lehn and M. E. Stubbs, *J. Amer. Chem. Soc.* **96**, 4011 (1974).



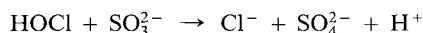
13. The  $\text{CN}^-$  exchange with  $\text{Pd}(\text{CN})_4^{2-}$  (0.117 M) was studied by  $^{13}\text{C}$  nmr complex line broadening at  $24^\circ\text{C}$  in  $\text{D}_2\text{O}$  with the following results:

$\text{CN}^-$ , M	$W_A^E - W_A^O$ , Hz
0.00	1.0
0.036	1.5
0.104	3.5
0.214	7.5
0.321	12.5
0.447	18

Estimate  $k_A$  for each  $\text{CN}^-$  concentration and hence the order of the exchange and the value of the rate constant.

J. J. Pesek and W. R. Mason, *Inorg. Chem.*, **22**, 2958 (1983).

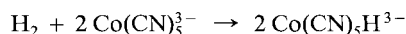
14. The mechanism for the reaction



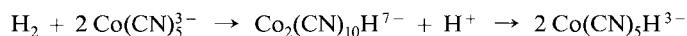
may involve either direct oxygen or  $\text{Cl}^+$  transfer. Show how by using indicators e.g. phenolphthalein ( $\text{p}K = 9.55$ ) or thymol blue ( $\text{p}K = 9.20$ ), it should be possible to differentiate between the two mechanisms.

B. S. Yiin and D. W. Margerum, *Inorg. Chem.* **27**, 1670 (1988).

15. Two plausible mechanisms for the reaction of  $\text{Co}(\text{CN})_3^{3-}$  with  $\text{H}_2$  invoke either homolytic splitting of  $\text{H}_2$ :



or heterolytic cleavage:



An attempt was made to distinguish between these by carrying out the reaction in  $\text{D}_2\text{O}$  and examining the ratio  $[\text{Co}(\text{CN})_5\text{H}^{3-}]/[\text{Co}(\text{CN})_5\text{D}^{3-}]$ . The Co–D/Co–H ir stretching intensity ratio ( $I_{1340\text{cm}^{-1}}/I_{1840\text{cm}^{-1}}$ ) R is 0.53 for an Co–D/Co–H ratio of 1.0. The following results were obtained:

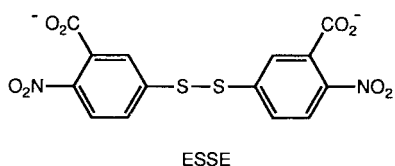
Time (mins)	R	Time (mins)	R
5	0.26	30	0.71
10	0.58	50	0.75
15	0.36	90	1.04
20	0.68 (0.43) <sup>a</sup>		

<sup>a</sup> Repeat experiment.

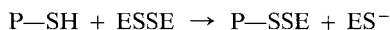
Which mechanism do these data support?

J. Halpern, *Inorg. Chim. Acta* **77**, L105 (1983).

16. The –SH group in proteins (P–SH) can be estimated by the addition of Ellmans reagent (ESSE)



which gives the colored ES<sup>-</sup> group ( $pK_{ESH} = 4.50$ )



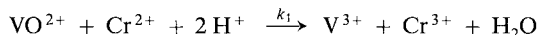
Devise a competition method which allows the determination of the rate of reaction of P–SH with another disulfide RSSR which does *not* lead to a colored species



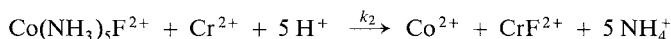
(Hint: RSH reacts rapidly with ESSE to give ES<sup>-</sup>)

J. M. Wilson, D. Wu, R. M. DeGroot and D. J. Hupe, *J. Amer. Chem. Soc.* **102**, 359 (1980).

17. The reaction of VO<sup>2+</sup> with Cr<sup>2+</sup>:



is too fast to be measured by stopped-flow. The reaction of Co(NH<sub>3</sub>)<sub>5</sub>F<sup>2+</sup> with Cr<sup>2+</sup>:

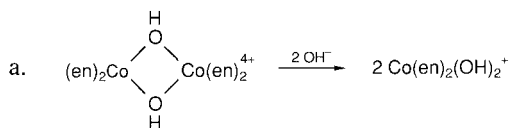


has been measured by stopped-flow, since low concentrations of reactants can be used. The relative rate constants  $k_1/k_2$  can be measured by a competition method in which a Cr<sup>2+</sup> solution is added (in fact generated *in situ*) to a well-stirred solution of a mixture of VO<sup>2+</sup> and Co(NH<sub>3</sub>)<sub>5</sub>F<sup>2+</sup> both well in excess of the Cr<sup>2+</sup> concentration. The initial concentrations are [VO<sup>2+</sup>]<sub>0</sub> and [Co(NH<sub>3</sub>)<sub>5</sub>F<sup>2+</sup>]<sub>0</sub>. After measuring, the solution was analyzed for Co<sup>2+</sup> ([Co<sup>2+</sup>]<sub>e</sub>) with the following results:

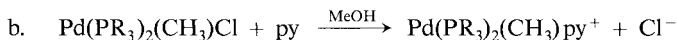
$[\text{VO}^{2+}]_0$ mM	$[\text{Co}(\text{NH}_3)_5\text{F}^{2+}]_0$ mM	$[\text{Cr}^{2+}]_0$ mM	$[\text{Co}^{2+}]_e$ mM
10.0	18.0	0.90	0.48
10.0	10.0	0.90	0.35
20.0	10.0	0.95	0.25
25.0	10.0	0.96	0.19

Estimate (preferably using a graphical method) the value of  $k_1/k_2$ . A. Bakač and J. H. Espenson, *Inorg. Chem.* **20**, 953 (1981).

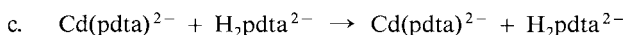
18. Suggest a suitable method (other than uv-vis spectral) for monitoring the following reactions and give details:



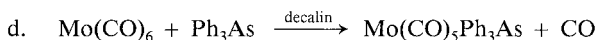
A. A. El-Awady and Z. Z. Hugus, Jr., *Inorg. Chem.* **10**, 1415 (1971).



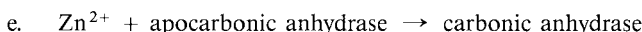
F. Basolo, J. Chatt, H. B. Gray, R. G. Pearson and B. L. Shaw, *J. Chem. Soc.* 2207 (1961).



B. Bosnich, F. P. Dwyer and A. M. Sargeson, *Aust. J. Chem.* **19**, 2213 (1966).



J. R. Graham and R. J. Angelici, *Inorg. Chem.* **6**, 2082 (1967).

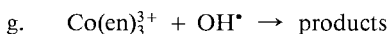


(this is the regeneration of the enzyme from the demetallated form and zinc ion).

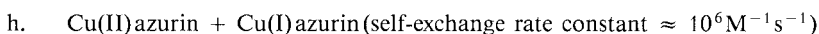
R. W. Henkens and J. M. Sturtevant, *J. Amer. Chem. Soc.* **90**, 2669 (1968).



A and B are different N,N-disubstituted dithiocarbamates (see Sec. 4.7.6(a)) M. Moriyasu and Y. Hashimoto, *Bull. Chem. Soc. Japan* **54**, 3374 (1981). J. Stach, R. Kirmse, W. Dietzsch, G. Lassmann, V. K. Belyaeva and I. N. Marov, *Inorg. Chim. Acta* **96**, 55 (1985).



N. Shinohara and J. Lilie, *Inorg. Chem.* **18**, 434 (1979).



C. M. Groeneveld, S. Dahlin, B. Reinhammer and G. W. Canters, *J. Amer. Chem. Soc.* **109**, 3247 (1987) and previous references.

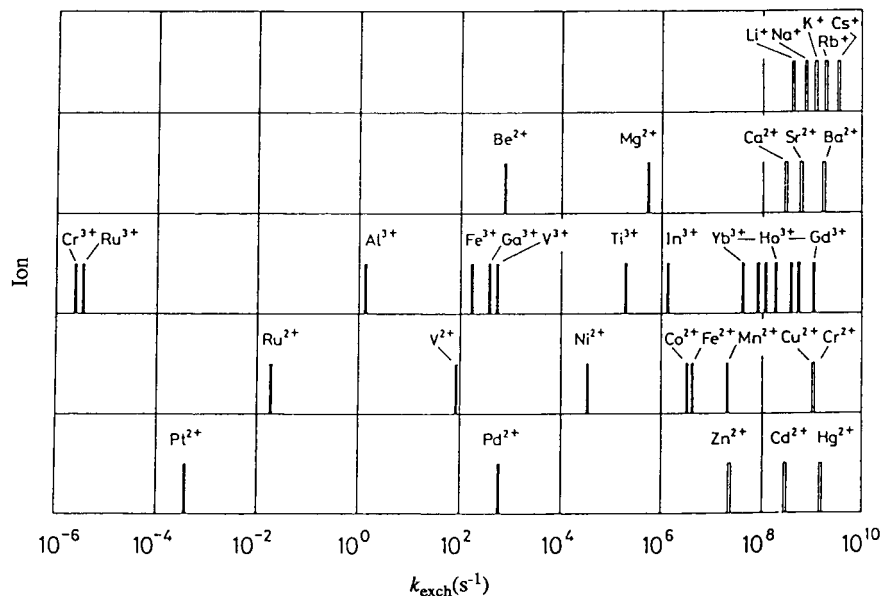


# Chapter 4

## Substitution Reactions

### 4.1 The Characteristics of Substitution Reactions

Substitution involves the replacement of a ligand coordinated to a metal by a free ligand in solution or the replacement of a coordinated metal ion by a free metal ion. No change of oxidation state of the metal occurs during the substitution, but a change may take place as a result of the substitution. The kinetics of the process have been studied for all the important stereochemistries but most intensely investigated for octahedral and square planar complexes. A very wide span of rates, almost 18 orders of magnitude, is found as indicated in Figure 4.1 which shows the water exchange rate constants for metal ions.<sup>1</sup> Thus the whole armory of

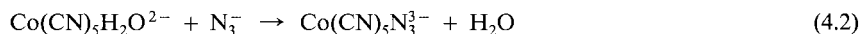
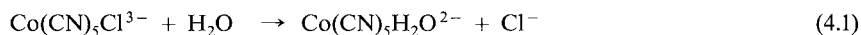


**Fig. 4.1** Rate constants ( $s^{-1}$ ) for water exchange of metal cations, measured directly by nmr or estimated from the rate constants for complex formation.<sup>1</sup> Reproduced with permission from Y. Ducommun and A. E. Merbach in *Inorganic High Pressure Chemistry* (R. von Eldik Ed), Elsevier, Amsterdam, 1986.

— nmr    □ complex formation

techniques must be used to measure substitution rate constants. Metal ions or complexes that generally react rapidly (within a matter of seconds) are termed *labile*, whereas if they substitute slowly, taking minutes or longer for completion, they are considered *inert*.<sup>2</sup>

Ligand interchange in metal complexes can occur in two ways, either (a) by a combination of solvolysis and ligation e.g.<sup>3</sup>



or (b) by simple interchange in which there is a replacement of one ligand by another without the direct intervention of solvent, e.g.



Indirect substitution of the type indicated in (4.1) and (4.2) appears to be the method much preferred by octahedral complexes,<sup>4</sup> while direct substitution is more relevant with square-planar complexes. This situation could perhaps be predicted in view of the more crowded conditions with octahedral than with planar complexes. For other geometries both routes are used.

The substitution process permeates the whole realm of coordination chemistry. It is frequently the first step in a redox reaction<sup>5</sup> and in the dimerization or polymerization of a metal ion, the details of which in many cases are still rather scanty (e.g. for Cr(III)<sup>6,7</sup>). An understanding of the kinetics of substitution can be important for defining the best conditions for a preparative or analytical procedure.<sup>8</sup> Substitution pervades the behavior of metal or metal-activated enzymes. The production of apoprotein (demetalloprotein and the regeneration of the protein, as well as the interaction of substrates and inhibitors with metalloproteins are important examples<sup>9</sup>.

### 4.1.1 Solvated Metal Ion

Before we consider substitution processes in detail, the nature of the metal ion in solution will be briefly reviewed.<sup>10</sup> A metal ion has a primary, highly structured, solvation sheath which comprises solvent molecules near to the metal ion. These have lost their translational degrees of freedom and move as one entity with the metal ion in solution. There is a secondary solvation shell around the metal ion, but the solvent molecules here have essentially bulk dielectric properties.<sup>10,11</sup> The (primary) solvation number  $n$  in  $\text{M(S)}_n^{m+}$  of many of the labile and inert metal ions has been determined, directly by x-ray or neutron diffraction of *concentrated solutions*,<sup>10,12</sup> from spectral and other considerations and by examining the exchange process



From the ratio of the areas of nmr peaks due to coordinated and free solvent, or from simple isotopic analyses, the value of  $n$  can be determined.<sup>13</sup> It may be necessary to slow the exchange process (4.4) by lowering the temperature of the solution. A variety of solvation numbers  $n$  is observed, with four and six being the most prevalent. As we have noted already, there is a wide range of labilities associated with the solvent exchanges of metal ions (Fig. 4.1).

### 4.1.2 Representation of Substitution Mechanisms

The simplest type of replacement reaction is the exchange of a coordinated ligand by an identical free ligand, an important example of which arises when the ligand is a solvent molecule.<sup>1,14</sup> The mechanisms we can visualize are presented in schematic form in Fig. 4.2.<sup>1,14</sup> The larger circle represents the total coordination sphere of the metal ion (of any geometry) and the small circle labelled E and L represents an (identical) entering and leaving ligand molecule. If we can deduce by kinetics or other tests that there is an intermediate of higher or lower coordination number than in the reactant, the mechanisms are of the extreme types, denoted associative *A* or dissociative *D* respectively.<sup>15</sup> When the interchange is concerted and there is partial, and equal, association and dissociation of the entering and leaving groups, the mechanism is termed *I*. This will rarely occur and more likely there will be a preference for *I<sub>a</sub>* or *I<sub>d</sub>*, in which the entering and leaving groups are either firmly (*I<sub>a</sub>*) or weakly (*I<sub>d</sub>*) embedded in the coordination sphere of the metal (Fig. 4.2). Microscopic reversibility considerations (Sec. 2.3.6) require that the activated complex be identical in both directions for this exchange reaction. As we have already implied, substitution in octahedral complexes is dissociatively activated, whereas with square planar complexes, associative activation is favored. Other factors, e.g. ligand crowding in the reactant, may modify these generalizations. Distinguishing mechanisms, *I<sub>d</sub>* from *D*, *I<sub>a</sub>* from *A* and particularly *I<sub>d</sub>* from *I<sub>a</sub>*, can be very difficult and it will be noted in this chapter that it is a preoccupation of the workers in this area. It is necessary to emphasize that these classifications are necessarily approximate and that there is a continuous range of behavior.<sup>16</sup>

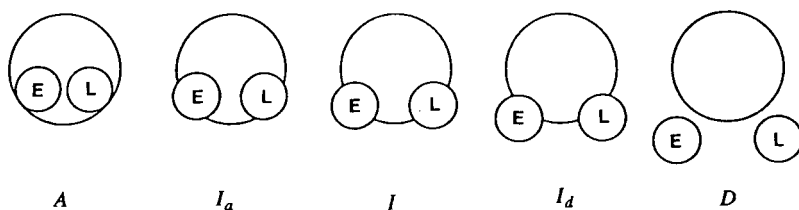


Fig. 4.2 Schematic representation of the mechanisms for substitution reactions. Based on Ref. 1.

## 4.2 Substitution in Octahedral Complexes<sup>17</sup>

The replacement of one unidentate ligand by another (particularly if the two ligands are identical) is the simplest substitution to envisage and has been used extensively to establish the rules of substitution mechanisms. This becomes handy information in order to understand substitution involving chelates and macrocycles of increased complexity. From what has been already stated, at least one of the unidentate ligands will be a solvent molecule. In (4.1) the forward direction is variously referred to as solvation, solvolysis or dissociation and the reverse reaction is termed a formation (or anation, if the entering group is anionic) process. Mechanistic information can be obtained by studying the reaction in either direction (since

these are intimately related (Sec. 2.3.6, Prob. 1) and particularly if the results are combined with those from solvent exchange studies. Substitution reactions of both labile and inert metal complexes have been investigated mainly, but not exclusively,<sup>18</sup> in aqueous solution. The earlier studies of the Werner-type complexes have been augmented by investigations of organometallic complexes, particularly of the metal carbonyls and related derivatives<sup>19</sup> although we shall not deal specifically with these.

### 4.2.1 Solvent Exchange with Metal Ions

Valuable information on mechanisms has been obtained from data on solvent exchange (4.4).<sup>1, 14, 16, 20, 21</sup> The rate law, one of the most used mechanistic tools, is not useful in this instance, unfortunately, since the concentration of one of the reactants, the solvent, is invariant. Sometimes the exchange can be examined in a "neutral" solvent, although this is difficult to find.<sup>22</sup> The reactants and products are however identical in (4.4), there is no free energy of reaction to overcome, and the activation parameters have been used exclusively, with great effect, to assign mechanism. This applies particularly to volumes of activation, since solvation differences are approximately zero and the observed volume of activation can be equated with the intrinsic one (Sec. 2.3.3).

#### (a) Divalent Metal Ions

Kinetic parameters are shown in Table 4.1<sup>23-25</sup> for the exchange of the first-row (and one second-row<sup>25</sup>) divalent transition metal ions in water. Since  $\Delta V^\ddagger$  for a *D* mechanism is  $V_{MS_5} + V_S - V_{MS_6}$  and usually  $V_{MS_5} < V_{MS_6}$ , then  $\Delta V^\ddagger$  will be less than  $V_S$ , the molar volume of the released solvent molecule.

**Table 4.1** Kinetic Parameters for Water Exchange of Divalent Transition Metal Ions,  $M(H_2O)_6^{2+}$  at 25 °C Refs. 23-25

	V <sup>2+</sup>	Mn <sup>2+</sup>	Fe <sup>2+</sup>	Co <sup>2+</sup>	Ni <sup>2+</sup>	Ru <sup>2+</sup>
$k, s^{-1}$	89	$2.1 \times 10^7$	$4.4 \times 10^6$	$3.2 \times 10^6$	$3.2 \times 10^4$	$1.8 \times 10^{-2}$
$\Delta H^\ddagger, kJ mol^{-1}$	62	33	41	47	57	88
$\Delta S^\ddagger, J K^{-1} mol^{-1}$	-0.4	+6	+21	+37	+32	+16
$\Delta V^\ddagger, cm^3 mol^{-1}$ <sup>a</sup>	-4.1	-5.4	+3.8	+6.1	+7.2	-0.4
Electronic Config.	$t_{2g}^3$	$t_{2g}^3 e_g^2$	$t_{2g}^4 e_g^2$	$t_{2g}^5 e_g^2$	$t_{2g}^6 e_g^2$	$t_{2g}^6$
Ionic Radius, Å <sup>b</sup>	0.79	0.83	0.78	0.74	0.69	0.73

<sup>a</sup> On Basis of  $\Delta\beta^\ddagger = 0$ ; <sup>b</sup> R.D. Shannon, Acta Crystallogr. Sect. A: Cryst. Phys. Diff. Theo. Gen. Crystallogr. **A32**, 751 (1976).

In aqueous solution therefore  $\Delta V^\ddagger$  will be less than  $+18 cm^3 mol^{-1}$  and probably near  $+9$  to  $+11 cm^3 mol^{-1}$  for a *D* mechanism, independent of ionic charge.<sup>11, 16, 21</sup> For an *A* mechanism  $\Delta V^\ddagger$  will be negative to the extent of about  $-11 cm^3 mol^{-1}$ . The increasingly positive values for  $\Delta V^\ddagger$  from V<sup>2+</sup> to Ni<sup>2+</sup> (Table 4.1) signify therefore an increasingly dissociative mode for substitution. It appears that the designations  $I_a$  (V<sup>2+</sup>, Mn<sup>2+</sup>)  $I$  (Fe<sup>2+</sup>) and  $I_d$  (Co<sup>2+</sup>, Ni<sup>2+</sup>) are most appropriate for water exchange with these metal ions. A strikingly similar

pattern holds for exchange in MeOH<sup>26</sup> (we can add the  $I_d$  designation for Cu<sup>2+</sup>) and CH<sub>3</sub>CN,<sup>27,28</sup> Tables 4.2 and 4.3. The increasingly dissociative activation mode of exchange from Mn to Ni is accompanied in all three solvents by slower rates and increasingly positive  $\Delta S^\ddagger$  and larger  $\Delta H^\ddagger$  values. Since it is anticipated that the entering and leaving solvent molecules will be along the three-fold axes of the octahedral complex, it might be expected that the greater the  $t_{2g}$  electron density (see Table 4.1) the less likely the associative path will be electrostatically favored, which is precisely what occurs.<sup>1,16</sup> The relative inertness (low  $k$  and large  $\Delta H^\ddagger$ ) for V<sup>2+</sup> stems from its stable  $t_{2g}^3$  electronic configuration. The high lability (large  $k$  and low  $\Delta H^\ddagger$ ) for Cu<sup>2+</sup> results from its tetragonal distortion.<sup>26</sup> When the size of the ligand (solvent) molecule increases, e.g. as in M(dmf)<sub>6</sub><sup>2+</sup>, an associative path for exchange is obviously less favored on steric grounds, all  $\Delta V^\ddagger$  values are positive (even Mn<sup>2+</sup><sup>29,30</sup>) and a dissociative activation mode is favored for all four ions. Perhaps even an extreme  $D$  mechanism is operative for Ni(dmf)<sub>6</sub><sup>2+</sup>, Table 4.4.<sup>27,29</sup> Finally, the sequence of solvent exchange rate constants H<sub>2</sub>O > dmf > CH<sub>3</sub>CN > CH<sub>3</sub>OH is metal-ion independent. Attempts to explain this sequence have so far been unsuccessful, but a relationship between  $\Delta H^\ddagger$  for solvent exchange and  $\Delta H_d$ , the heat of dissociation of solvent molecules S from MS<sub>6</sub><sup>2+</sup> has been suggested.<sup>31</sup>

**Table 4.2** Kinetic Parameters for Methanol Exchange of First-Row Divalent Transition Metal Ions, M(CH<sub>3</sub>OH)<sub>6</sub><sup>2+</sup> at 25 °C Ref. 26

	Mn <sup>2+</sup>	Fe <sup>2+</sup>	Co <sup>2+</sup>	Ni <sup>2+</sup>	Cu <sup>2+</sup>
$k, s^{-1}$	$3.7 \times 10^5$	$5.0 \times 10^4$	$1.8 \times 10^4$	$1.0 \times 10^3$	$3.1 \times 10^7$
$\Delta H^\ddagger, kJ mol^{-1}$	26	50	58	66	17
$\Delta S^\ddagger, J K^{-1} mol^{-1}$	-50	+13	+30	+34	-44
$\Delta V^\ddagger, cm^3 mol^{-1}$	-5.0	+0.4	+8.9	+11.4	+8.3

**Table 4.3** Kinetic Parameters for Acetonitrile Exchange of First-Row Divalent Transition Metal Ions, M(CH<sub>3</sub>CN)<sub>6</sub><sup>2+</sup> at 25 °C Refs. 27, 28

	Mn <sup>2+</sup>	Fe <sup>2+</sup>	Co <sup>2+</sup>	Ni <sup>2+</sup>
$k, s^{-1}$	$1.4 \times 10^7$	$6.6 \times 10^5$	$3.4 \times 10^5$	$2.8 \times 10^3$
$\Delta H^\ddagger, kJ mol^{-1}$	30	41	50	64
$\Delta S^\ddagger, J K^{-1} mol^{-1}$	-9	+5	+27	+37
$\Delta V^\ddagger, cm^3 mol^{-1}$	-7.0	+3.0	+6.7	+7.3

**Table 4.4** Kinetic Parameters for Dimethylformamide Exchange of First-Row Divalent Transition Metal Ions, M(dmf)<sub>6</sub><sup>2+</sup> at 25 °C Refs. 27, 29

	Mn <sup>2+</sup>	Fe <sup>2+</sup>	Co <sup>2+</sup>	Ni <sup>2+</sup>
$k, s^{-1}$	$2.2 \times 10^6$	$9.7 \times 10^5$	$3.9 \times 10^5$	$3.8 \times 10^3$
$\Delta H^\ddagger, kJ mol^{-1}$	35	43	57	63
$\Delta S^\ddagger, J K^{-1} mol^{-1}$	-7	+14	+53	+34
$\Delta V^\ddagger, cm^3 mol^{-1}$	+2.4	+8.5	+6.7	+9.1

## (b) Trivalent Metal Ions

The exchange of the trivalent ions of the metals Cr, Fe, Ru and Ga in water is governed by the rate law

$$k_{\text{exch}} = a + b[\text{H}^+]^{-1} \quad (4.5)$$

from which exchange data for  $\text{M}(\text{H}_2\text{O})_6^{3+}$  and  $\text{M}(\text{H}_2\text{O})_5\text{OH}^{2+}$  may be extracted (Sec. 2.1.7(b)), Tables 4.5 and 4.6.<sup>25,32,33</sup> The negative signs of  $\Delta V^\ddagger$  indicate an associative mechanistic mode for the transition metal ions  $\text{M}(\text{H}_2\text{O})_6^{3+}$ , with  $\text{Ti}(\text{H}_2\text{O})_6^{3+}$  probably  $A$ , and the others  $I_a$ -controlled. In contrast, a dissociative mechanism  $I_d$  for  $\text{M}(\text{H}_2\text{O})_5\text{OH}^{2+}$  is supported by the pressure measurements. A strong labilizing effect of coordinated  $\text{OH}^-$  in  $\text{M}(\text{H}_2\text{O})_5\text{OH}^{2+}$ , presumably on the trans  $\text{H}_2\text{O}$ , leads to a  $10^2$ – $10^3$  fold enhanced rate for the hydroxy- over the hexaaqua ion and portends an important effect of coordinated ligands on the lability of other bound ligands (Sec. 4.3.3). Again, the greater the  $t_{2g}$  electron density, the less effective is associative activation. This is shown by increasingly less negative  $\Delta V^\ddagger$ s from  $\text{Ti}^{3+}$  to  $\text{Fe}^{3+}$ . The behavior of  $\text{Ga}^{3+}$  is included for comparative purposes.<sup>32</sup> The trend is however much less pronounced than with the bivalent metal ions. A comparison between iron and ruthenium is interesting. The stable low-spin configurations of Ru(II) and Ru(III) compared with their high-spin iron counterparts lead to dramatic reductions in exchange rates.<sup>33</sup> The two  $e_g$  electrons in Fe(II) and Fe(III) are missing in Ru(II) and Ru(III) and this favors more associative character for exchange with the latter ions. This is shown by more negative  $\Delta V^\ddagger$ s for reaction of  $\text{Ru}(\text{H}_2\text{O})_6^{2+}$  and  $\text{Ru}(\text{H}_2\text{O})_6^{3+}$ . General relationships of reactivity with

**Table 4.5** Kinetic Parameters for Water Exchange of Trivalent Transition Metal Ions,  $\text{M}(\text{H}_2\text{O})_6^{3+}$  at 25°C Refs. 25, 32, 33

	$\text{Ti}^{3+}$	$\text{V}^{3+}$	$\text{Cr}^{3+}$	$\text{Fe}^{3+}$	$\text{Ru}^{3+}$	$\text{Ga}^{3+c}$
$k, \text{s}^{-1}$	$1.8 \times 10^5$	$5.0 \times 10^2$	$2.4 \times 10^{-6}$	$1.6 \times 10^2$	$3.5 \times 10^{-6}$	$4.0 \times 10^2$
$\Delta H^\ddagger, \text{kJ mol}^{-1}$	43	49	109	64	90	67
$\Delta S^\ddagger, \text{J K}^{-1} \text{mol}^{-1}$	+1	–28	+12	+12	–48	+30
$\Delta V^\ddagger, \text{cm}^3 \text{mol}^{-1a}$	–12.1	–8.9	–9.6	–5.4	–8.3	+5.0
Electronic Config.	$t_{2g}^1$	$t_{2g}^2$	$t_{2g}^3$	$t_{2g}^3 e_g^2$	$t_{2g}^5$	$t_{2g}^6 e_g^4$
Ionic Radius, Å <sup>b</sup>	0.67	0.64	0.61	0.64	0.68	0.62

<sup>a</sup> On basis of  $\Delta\beta^\ddagger = 0$ ; <sup>b</sup> R.D. Shannon, Acta Crystallogr. Sect. A: Cryst. Phys. Diffr. Theo. Gen. Crystallogr. **A32**, 751 (1976); <sup>c</sup> Included for comparative purposes.

**Table 4.6** Kinetic Parameters for Water Exchange of Trivalent Transition Metal Ions,  $\text{M}(\text{H}_2\text{O})_5\text{OH}^{2+}$  at 25°C Refs. 25, 32, 33

	$\text{CrOH}^{2+}$	$\text{FeOH}^{2+}$	$\text{RuOH}^{2+}$	$\text{GaOH}^{2+}$
$k, \text{s}^{-1}$	$1.8 \times 10^{-4}$	$1.2 \times 10^5$	$5.9 \times 10^{-4}$	$(0.6 - 2.0) \times 10^{5b}$
$\Delta H^\ddagger, \text{kJ mol}^{-1}$	110	42	96	59
$\Delta S^\ddagger, \text{JK}^{-1} \text{mol}^{-1}$	+55	+5	+15	–
$\Delta V^\ddagger, \text{cm}^3 \text{mol}^{-1a}$	+2.7	+7.0	+0.9	+6.2

<sup>a</sup> On basis of  $\Delta\beta^\ddagger = 0$ , <sup>b</sup> Range arises from the uncertainty of  $pK$  of  $\text{Ga}(\text{H}_2\text{O})_6^{3+}$

electronic configuration have been understood for some time, mainly on the basis of ligand reactions (next Section).<sup>2,34</sup> Crystal field considerations for example indicate kinetic inertness associated with the  $d^3$ , low spin  $d^4$ ,  $d^5$  and  $d^6$  and  $d^8$  electronic configurations.<sup>2, B25</sup> Undoubtedly, a much clearer picture of the intimate mechanism of reactions has emerged from the studies in the past decade of solvent exchange reactions.

### 4.2.2 The Interchange of Different Unidentate Ligands

Now we examine the replacement of a coordinated unidentate ligand L by a different unidentate ligand  $L_1$ . Either L or  $L_1$  will be  $H_2O$ . The reaction can be examined in either direction. Figure 4.2



is still generally useful for depicting mechanism. We can consider the mechanism associatively activated if the reaction characteristics (activation parameters, steric effects, etc.) are more sensitive to a change of the entering group, then they are to the leaving group.<sup>16</sup> We can now obtain a meaningful rate law, but kinetic parameters are likely to be composite and less easy to evaluate than those from solvent exchange.

The *D* mechanism is represented by the scheme



in which a five-coordinated intermediate represented by M is generated with a sufficient lifetime to discriminate between L and  $L_1$ . The full rate law governing this mechanism has been referred to in Sec. 1.6.5. If we use  $L_1$  in excess over ML and the reaction is irreversible ( $k_{-2} \approx 0$ ) then

$$-d(ML)/dt = d(ML_1)/dt = \frac{k_1 k_2 [ML] [L_1]}{k_{-1} [L] + k_2 [L_1]} \quad (4.9)$$

In the interchange mechanism, there is an interchange of L and  $L_1$  perhaps within an outer-sphere complex ( $ML \cdots L_1$ ) which is very rapidly formed from the reactants



The extent of influence of  $L_1$  on the  $k_3$  process, will dictate the applicable designation  $I_d$ ,  $I$  or  $I_a$ . For this reaction scheme,

$$d(ML_1)/dt = \frac{k_3 K_0 [ML]_0 [L_1]_0}{1 + K_0 [L_1]_0} \quad (4.13)$$

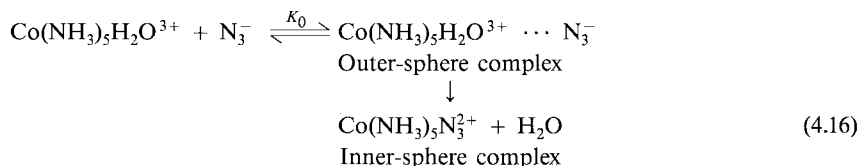
where the subscripts 0 indicate the total (starting) concentrations of the species. For an  $A$  mechanism, in which there is a seven-coordinated intermediate or activated complex, a second-order rate law obtains,



$$d[ML_1]/dt = k[ML][L_1] \quad (4.15)$$

### 4.2.3 Outer Sphere Complexes

Before considering the kinetics associated with the various mechanisms, a discussion of the outer-sphere complex is necessary, since it features so prominently in the interchange mechanism (4.10)–(4.12). The secondary interaction of an inner-sphere complex with ligands in solution to give an outer-sphere complex as depicted in (4.10) is most effective between oppositely charged species (ion pairs). The presence of an outer-sphere complex, a term first coined by Alfred Werner in 1913, is easily demonstrated in a number of systems. Rapid spectral changes in the 200–300 nm region, which can be ascribed to outer-sphere complexing, occur on addition of a number of anions to  $M(NH_3)_5H_2O^{3+}$ , where  $M = Cr$  or  $Co$ ,<sup>35</sup> long before final equilibration to the inner-sphere complex occurs. For example,



The separation of the two stages is easier to discern when the rates of the two processes are so different, but it can also be seen in the ultrasonic spectra of metal-sulfate systems (Sec. 3.4.4). Ultrasonic absorption peaks can be attributed to formation of outer-sphere complexes (at higher frequency, shorter  $\tau$ ) and collapse of outer-sphere to inner-sphere complexes (at lower frequency). In addition to uv spectral and ultrasonic detection, polarimetry and nmr methods have also been used to monitor and measure the strength of the interaction. There are difficulties in assessing the value of  $K_0$ , the outer-sphere formation constant. The assemblage that registers as an ion pair by conductivity measurements may show a blank spectroscopically.<sup>16</sup> The value of  $K_0$  at  $T$  K may be estimated using theoretically deduced expressions:<sup>36</sup>

$$K_0 = \frac{4\pi Na^3}{3000} \exp\left(-\frac{U(a)}{kT}\right) \quad (4.17)$$

where  $U(a)$  is the Debye-Hückel interionic potential

$$U(a) = \frac{z_1 z_2 e^2}{aD} - \frac{z_1 z_2 e^2 \kappa}{D(1 + \kappa a)} \quad (4.18)$$



$$\kappa^2 = \frac{8\pi Ne^2\mu}{1000DkT} \quad (4.19)$$

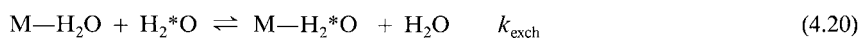
and

- $N$  = Avogadro's number.  
 $a$  = distance of closest approach of two ions (cm).  
 $k$  = Boltzmann's constant (erg).  
 $e$  = charge of an electron in esu units.  
 $D$  = bulk dielectric constant.  
 $\mu$  = ionic strength.  
 $z_1, z_2$  = charge of reactants.

To give some idea of the value of  $K_0$  – it is approximately  $14 \text{ M}^{-1}$  for interaction of  $2+$  and  $2-$  charged reactants at  $\mu = 0.1 \text{ M}$  and  $0.15 \text{ M}^{-1}$  for interaction between a cation and a zero charged species.<sup>37</sup> It is necessary to reaffirm the point that the occurrence of outer-sphere complexes, which can be observed in the studies of the  $\text{Fe(III)-Br}^-$ ,  $\text{Ni(II)-CH}_3\text{PO}_4^{2-}$  and the ultrasonics of a number of  $\text{M}^{2+} - \text{SO}_4^{2-}$  systems,<sup>38</sup> does not necessitate their being in the direct pathway for the formation of products (Sec. 1.6.4). Their appearance does not help in the deciphering of the mechanism.

#### 4.2.4 Characteristics of the Various Mechanisms

Although the rate laws derived from the three mechanisms assume distinctly different forms, (4.9), (4.13) and (4.15), the assignment of the mechanisms on the basis of these alone is difficult. If reaction (4.6) is studied using an excess of  $L_1$ , the rate laws shown in Table 4.7 will be observed for different concentrations of  $L_1$  for the  $D$  and  $I$  mechanisms. For the  $A$  mechanism the second-order rate law holds for all concentrations of  $L_1$ . At low  $[L_1]$ , all mechanisms give second-order rate behavior with composite rate constants for  $D$  and  $I$  mechanisms. Only if the mechanism is  $D$ , is the rate slowed down by  $L$  (mass law retardation). This can be used for diagnosing a  $D$  mechanism for  $L, L_1$  interchange reactions in nonaqueous solvents (see however Ref. 19) but for the ligand replacement of coordinated solvents, commonly studied,  $[L]$ , the solvent, is constant and the ability to use this feature to differentiate amongst the mechanisms is lost. For  $D$  and  $I$  mechanisms, the linear dependence of  $k_{\text{obs}}$  on  $[L_1]$  at low  $[L_1]$  may be replaced by an independence at high  $[L_1]$ . The limiting rate constants will be  $k_1$  for the breakage of the  $ML$  bond or  $k_3$ , for the interchange within the outer-sphere complex. The experimental limiting first-order rate constant is unlikely to be useful for distinguishing  $k_1$  and  $k_3$  (in an  $I_d$  mechanism) but in any case its value should be close to the value of  $k_{\text{exch}}$ .<sup>16, 39, 40</sup>



Unfortunately even a slight deviation from linearity of  $k_{\text{obs}}$  with  $[L_1]$  is rarely observed.

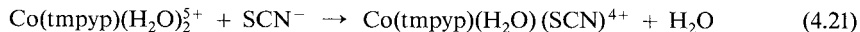
**Table 4.7** Rate Laws for Substitution Mechanisms with Different Conditions

	Low $[L_1]$	Medium $[L_1]$	High $[L_1]$
<i>D</i>	$k_2[L_1] < k_{-1}[L]$ M scavenged by L preferentially	$k_2[L_1] \sim k_{-1}[L]$	$k_2[L_1] > k_{-1}[L]$ M scavenged by $L_1$ preferentially
Rate	$\frac{k_1 k_2 [ML] [L_1]}{k_{-1} [L]}$	$\frac{k_1 k_2 [ML] [L_1]}{k_{-1} [L] + k_2 [L_1]}$	$k_1 [ML]$
<i>I</i>	$K_0 [L_1]_0 < 1$ Small build up of outer-sphere complex	$K_0 [L_1]_0 \sim 1$	$K_0 [L_1] > 1$ Formation of outer-sphere complex complete
Rate	$k_3 K_0 [ML]_0 [L_1]_0$	$\frac{k_3 K_0 [ML]_0 [L_1]_0}{1 + K_0 [L_1]_0}$	$k_3 [ML]_0$

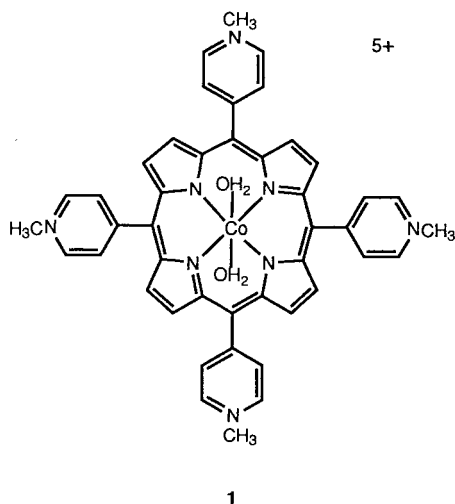
### 4.2.5 The Limiting First-Order Rate Constant

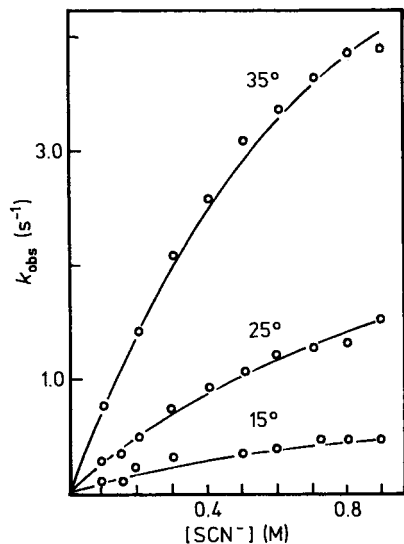
Only in a relatively few systems are deviations from constancy for the function  $k_{\text{obs}}/[L_1]$  observed and in even fewer, is a point reached in which  $k_{\text{obs}}$  is a constant, independent of  $[L_1]$ .

In the replacement of  $\text{H}_2\text{O}$  by  $\text{SCN}^-$  in the Co(III) porphyrin **1** abbreviated  $\text{CoP}^{5+}$



the pseudo first-order rate constant  $k_{\text{obs}}$  vs.  $[\text{SCN}^-]$  (used in excess) is shown in Figure 4.3.<sup>41</sup> The further replacement of the water in the product by  $\text{SCN}^-$  is very rapid. The rate law





**Fig. 4.3** The dependence of the pseudo first-order rate constants upon anion concentration for the anation of  $\text{Co}(\text{tmpyp})(\text{H}_2\text{O})_2^{5+}$  by  $\text{SCN}^-$  at 15, 25, and 35°C in 0.1 M  $\text{H}^+$ ,  $\mu = 1.0$  M.<sup>41</sup> The solid lines conform to Eqn. (4.22). Reproduced with permission from K. R. Ashley, M. Berggren and M. Cheng, *J. Amer. Chem. Soc.* **97**, 1422 (1975) © (1975) American Chemical Society.

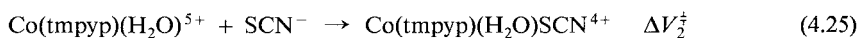
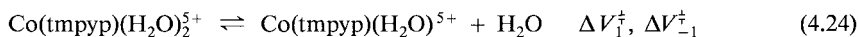
(4.22) therefore applies and an *A* mechanism is eliminated. For a *D* mechanism,  $a = k_1$  and  $b = k_{-1}/k_2$ . For an *I* mechanism,

$$-d[\text{CoP}^{5+}]_{\text{total}}/dt = \frac{a[\text{SCN}^-]}{b + [\text{SCN}^-]} [\text{CoP}^{5+}]_{\text{total}} \quad (4.22)$$

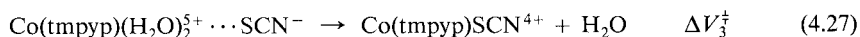
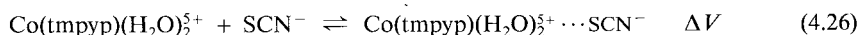
$a = k_3$  and  $b = K_0^{-1}$  (Table 4.7, Medium  $[\text{L}_1]$  Condition). The value of  $K_0$  which results from this analysis ( $0.83 \text{ M}^{-1}$  at 25°C) appears small for a +5, -1 reaction pair in an *I* mechanism, although the effective charge is probably markedly reduced from +5 since it is smeared over the whole porphyrin.<sup>41</sup> Better evidence for the *D* mechanism than simply by default, comes from studies of the pressure effect on (4.21) using the high-pressure stopped-flow technique (Sec. 3.3.3).<sup>42</sup> On the basis of the rate law (4.22), which was confirmed, the variation of  $k_{\text{obs}}$ , the pseudo first-order rate constant, with pressure  $P$  will be given by (Sec. 2.3.3)

$$k_{\text{obs}} = \frac{a \exp(-P\Delta V_a^\ddagger/RT) [\text{SCN}^-]}{b \exp(-P\Delta V_b^\ddagger/RT) + [\text{SCN}^-]} \quad (4.23)$$

For a *D* mechanism, (4.24) and (4.25) the value of  $\Delta V_a^\ddagger (= \Delta V_1^\ddagger) = 14 \pm 4 \text{ cm}^3 \text{ mol}^{-1}$  is reasonable for the loss of one  $\text{H}_2\text{O}$  molecule in the activated complex. The value of



$\Delta V_b^\ddagger (= \Delta V_{-1}^\ddagger - \Delta V_2^\ddagger) = 5 \pm 4 \text{ cm}^3 \text{ mol}^{-1}$  is also plausible. On the other hand for an  $I_d$  mechanism (4.26) and (4.27) the large value of  $\Delta V_a^\ddagger (= \Delta V_3^\ddagger)$  for the interchange step and the negative value for  $\Delta V (= -\Delta V_b^\ddagger)$  are quite unlikely.<sup>42,43</sup> See Ref. 44.



All the kinetic features expected for a *D* mechanism and rate law (4.9) i.e. marked effects of L and L<sub>1</sub> on the rate constants, are shown in the comprehensive studies in nonaqueous solution of substitution in low-spin Fe(II) complexes of the type FeN<sub>4</sub>XY where N<sub>4</sub> are planar porphyrins, phthalocyanins and macrocycles and X and Y are neutral ligands, CO, R<sub>3</sub>P, pyridines etc. Small discrimination factors (*k*<sub>-1</sub>/*k*<sub>2</sub>) suggest that the five-coordinated intermediate in these systems is very reactive.<sup>45,46</sup> There have been problems in the confirmation of curvature in the plots of *k*<sub>obs</sub>/[L<sub>1</sub>] for “classical” reactions of a number of aquapentammine complexes.<sup>47</sup>

## 4.2.6 Second-Order Rate Constants

We have to nearly always use the activation parameters from the second-order rate law to differentiate between mechanisms. For a single reaction, the kinetic parameters are of little use and it is usually necessary to compare the behavior of a number of reaction systems. The ploy then is to deduce with which mechanism the kinetic data are most consistent. Some values for *k*<sub>3</sub> for reactions of Ni<sup>2+</sup> ion with a variety of unidentate ligands, calculated from the experimental rate constant (*k*<sub>3</sub>*K*<sub>0</sub>, see Table 4.7) using an estimation of *K*<sub>0</sub>, are contained in Table 4.8<sup>40</sup>. The values of *k*<sub>3</sub> are reasonably constant, close to the water exchange rate constant (Table 4.1), and these results represent strong support for an *I*<sub>d</sub> mechanism. It was this type of evidence that Eigen used to propose the ion-pair mechanism for the reactions of a number of bivalent metal ions<sup>48</sup>. It is difficult to distinguish an *I*<sub>d</sub> from a *D* mechanism, although  $\Delta V^\ddagger$  values for solvent exchange and ligation by neutral ligands of Ni(H<sub>2</sub>O)<sub>6</sub><sup>2+</sup> also support an *I*<sub>d</sub> mechanism.<sup>49</sup> The situation appears different with the bulkier dmf ligand. The computed value of *k*<sub>3</sub> > 1.4 × 10<sup>4</sup>s<sup>-1</sup> for reaction of Ni(dmf)<sub>6</sub><sup>2+</sup> with SCN<sup>-</sup> and Et<sub>2</sub>dtc<sup>-</sup> is substantially greater<sup>50</sup> than the solvent exchange value *k*<sub>exch</sub> = 3.8 × 10<sup>3</sup>s<sup>-1</sup> (Table 4.4). An *I*<sub>d</sub> mechanism is ruled out and a *D* mechanism favored by default.<sup>51</sup> The values of  $\Delta V^\ddagger$  (+8.8 to +12.4 cm<sup>3</sup>mol<sup>-1</sup>) for reaction of a number of ligands with Ni(dmf)<sub>6</sub><sup>2+</sup> also support a dissociative mechanism.<sup>51</sup>

**Table 4.8** Computed Values for *k*<sub>3</sub> from Second-Order Rate Constants (*K*<sub>0</sub>*k*<sub>3</sub>) for the Formation of Nickel(II) Complexes from Unidentate Ligands at 25 °C Ref. 40

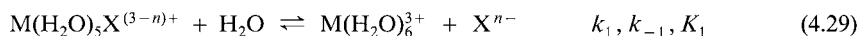
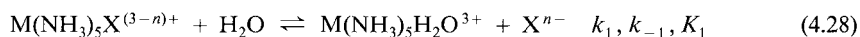
L <sup>n-</sup>	10 <sup>-3</sup> × <i>K</i> <sub>0</sub> <i>k</i> <sub>3</sub> M <sup>-1</sup> s <sup>-1</sup>	<i>K</i> <sub>0</sub> M <sup>-1</sup>	10 <sup>-4</sup> × <i>k</i> <sub>3</sub> s <sup>-1</sup>
CH <sub>3</sub> PO <sub>4</sub> <sup>2-</sup>	280	40 <sup>a</sup>	0.7 <sup>a</sup>
CH <sub>3</sub> CO <sub>2</sub> <sup>-</sup>	300	20 <sup>a</sup>	1.5 <sup>a</sup>
NH <sub>3</sub>	4.5	0.15 <sup>b</sup>	3.0
C <sub>5</sub> H <sub>5</sub> N	3.6	0.15 <sup>b</sup>	2.0
NH <sub>2</sub> (CH <sub>2</sub> ) <sub>2</sub> NMe <sub>3</sub> <sup>+</sup>	0.4	~0.02 <sup>b</sup>	~2

<sup>a</sup> These values are directly determined from relaxation data.

<sup>b</sup> Estimated values (see text).

Associative mechanisms are indicated by the second-order rate constant showing a decided dependence on the nucleophilicity (or basicity) of the entering ligand. We have already noted this in the reactions of  $\text{Fe}(\text{H}_2\text{O})_6^{3+}$  (Sec. 2.1.7) and find that a similar situation holds for  $\text{Cr}(\text{H}_2\text{O})_6^{3+}$ ,<sup>52</sup>  $\text{V}(\text{H}_2\text{O})_6^{3+}$ <sup>53</sup> and  $\text{Ti}(\text{H}_2\text{O})_6^{3+}$ <sup>33</sup> ions. The  $I_a$  assignment for substitution in these metal ions is satisfyingly consistent with their activation parameters for water exchange (Table 4.5). It has been suggested that in replacement of coordinated  $\text{H}_2\text{O}$  by  $\text{SCN}^-$  and  $\text{Cl}^-$  ions in any complex, if the ratio of their second-order rate constants ( $r$ ) exceeds 10,  $k(\text{SCN}^-)/k(\text{Cl}^-) > 10$ , an  $I_a$  mechanism is indicated.<sup>54</sup> This is a useful rule. Values of  $r$  exceeding unity are usually associated with metal ions which have negative values for  $\Delta V^\ddagger$  for water exchange again supporting associative activation. The selectivity indicated in the  $r$  value declines as the rates become faster.<sup>16</sup> Thus,  $r$  decreases in the order  $\text{Cr}(\text{H}_2\text{O})_6^{3+}$ ,  $\text{Fe}(\text{H}_2\text{O})_6^{3+}$  and probably  $\text{Mn}(\text{H}_2\text{O})_6^{2+}$ , even though solvent exchange data indicate an  $I_a$  mechanism is operative in all cases. This mild selectivity for entering ligands has caused interpretation problems in the assignment of mechanism for the most labile metal ions.<sup>16</sup>

Examining the relationship between the hydrolysis rate constants ( $k_1$ ) and the equilibrium constant ( $K_1$ ) for a series of reactions of the type (4.28) and (4.29) involving charged ligands  $\text{X}^{n-}$  has been very helpful in delineating the type of  $I$  mechanism.



For these reactions the general LFER holds

$$\log k_1 = a \log K_1 + b \quad (4.30)$$

With an  $I_d$  mechanism, the rate constants for anation ( $k_{-1}$ ) are approximately constant and any differences in the formation constants  $K_1$  reside in differing  $k_1$  values since  $K_1 = k_1/k_{-1}$ . This requires that  $a = 1.0$  as we have already seen for  $\text{Co}(\text{NH}_3)_5\text{X}^{2+}$  (Sec. 2.4).<sup>55</sup> Simple reasoning indicates that for an  $I_a$  mechanism  $a = 0.5$ .<sup>20,56</sup> The decreasing values of  $a$  for the hydrolyses of  $\text{Co}(\text{NH}_3)_5\text{X}^{2+}$  (1.0),  $\text{Cr}(\text{NH}_3)_5\text{X}^{2+}$  (0.69) and  $\text{Cr}(\text{H}_2\text{O})_5\text{X}^{2+}$  (0.58) suggest increasing associative character ( $I_a$ ) for these reactions. This is supported by the values of  $\Delta V^\ddagger$  (+1.2, -5.8 and -9.3  $\text{cm}^3 \text{mol}^{-1}$  respectively) for the water exchange of the corresponding aqua ion.<sup>20</sup> See also Ref. 57.

## 4.2.7 Summary

Since we shall not obtain the comparable amount of detailed information on the mechanisms of substitution in octahedral complexes from the studies of more complicated substitutions involving chelation and macrocycle complex formation (Secs. 4.4 and 4.5) it is worthwhile summarizing the salient features of substitution in Werner-type complexes.

Associative ( $A$ ) mechanisms are extremely rare and it is uncertain whether an authentic example exists.<sup>58</sup> Dissociative ( $D$ ) mechanisms are more common although difficult to establish. Some examples were cited in Secs. 4.2.5 and 4.2.6. Thus interchange ( $I$ ) mechanisms dominate the scene. This leads to the following generalizations:

- (a) Relatively small influence of an entering group on the rate or rate law.  
 (b) Parallel rate constants for substitution and water exchange for a large number of complexes. Equality of  $k_3$  and  $k_{\text{exch}}$ , or even better of the associated parameters  $\Delta H_{\ddagger}^{\ddagger}$  and  $\Delta H_{\text{exch}}^{\ddagger}$ , is strong evidence for an  $I_{\text{d}}$  mechanism.  
 (c) Correlation of hydrolysis rate with the binding tendencies of the leaving group, leading to a variety of LFER involving activation and reaction parameters.  
 (d) Decrease of rate with an increase in the charge of the complex (Fig. 4.1) since bond rupture is an important component, even of an  $I_{\text{a}}$  mechanism.  
 (e) Steric acceleration and deceleration effects (Sec. 2.4).

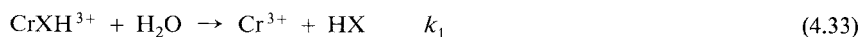
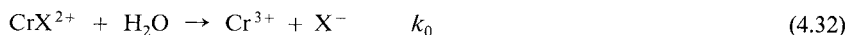
Attempts to improve the simple mechanistic classification have been made using More-O'Ferall diagrams,<sup>16</sup> or transition state bond order variations.<sup>59</sup>

### 4.3 Accelerated Substitution of Unidentate Ligands

Reagents such as  $\text{H}^+$ ,  $\text{OH}^-$ , metal ions and ligands may alter the rate of replacement of one ligand by another. These reagents act either by modifying the structure of one of the reactants, or by direct participation in the transition state (and the difference may be a subtle one and difficult to diagnose; see Sec. 2.3.6). It is important to establish that these reagents are promoting another reaction pathway and not just producing a medium effect (see Sec. 2.9.2). If the reagent is not used up in the reaction, the accelerating effect is termed *catalytic*. If on the other hand it is consumed, perhaps ending up in the product, the terms *reagent-accelerated* or *-assisted* are more appropriate. We shall deal in the next section with the catalytic and accelerated replacement of unidentate ligands and the ideas developed will be then incorporated in the discussion of chelation and macrocycle complex formation (Sec. 4.4 and 4.5).

#### 4.3.1 $\text{H}^+$ -Assisted Removal

Studies on the removal of unidentates in acid media have been made mainly with inert complexes. It might be expected that the removal of ligands that retain some basicity, even when coordinated, would be acid-promoted, e.g.



for which,

$$-d[\text{CrX}^{2+} + \text{CrXH}^{3+}]/dt = k_{\text{obs}}[\text{CrX}^{2+} + \text{CrXH}^{3+}] \quad (4.34)$$

where

$$k_{\text{obs}} = \frac{k_0 + k_1 K [\text{H}^+]}{1 + K [\text{H}^+]} \quad (4.35)$$

Sometimes appreciable amounts of  $\text{CrXH}^{3+}$  build up and the full rate law (4.35) is applicable, as with  $\text{X} = \text{CH}_3\text{CO}_2^-$ , Ref. 60. Normally however,  $K \ll [\text{H}^+]$ , and

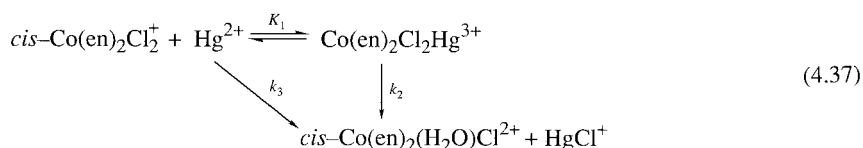
$$k_{\text{obs}} = k_0 + k_1 K [\text{H}^+] \quad (4.36)$$

Placing a proton on the X group presumably weakens the Cr-X bond. The enhanced lability is due to a reduced enthalpy of activation, compared with that associated with the  $k_0$  step.<sup>60</sup> Normally, the removal of unidentate ammonia or amine ligands from metal complexes is not accelerated by acid, since the nitrogen is coordinately saturated. This situation changes when we consider multidentates (Sec. 4.4.2).

### 4.3.2 Metal Ion-Assisted Removal

Metal ions can function much like protons, and coordinated ligands whose removal are accelerated by  $\text{H}^+$  (Sec. 4.3.1), are often ones ( $\text{N}_3^-$ ,  $\text{CN}^-$ ) whose loss are also metal ion-assisted. Metal ions can also speed up the removal of an additional type of ligand ( $\text{NCS}^-$ ,  $\text{Cl}^-$ ) that shows a strong tendency to form bridged binuclear complexes. The catalytic efficiency of a metal ion depends on a number of factors. There is a close correlation of the rate of accelerated aquation by  $\text{M}^{n+}$  with the complexing ability of  $\text{M}^{n+}$ . Hard metal ions ( $\text{Be}^{2+}$ ,  $\text{Al}^{3+}$ ), like  $\text{H}^+$ , readily remove the hard ligands, such as  $\text{F}^-$ . Soft metal ions ( $\text{Hg}^{2+}$ ,  $\text{Ag}^+$ ) are most effective when the leaving ligand is soft ( $\text{Cl}^-$ ,  $\text{Br}^-$ ).<sup>61</sup> Substitution-inert metal ions or complexes are usually ineffective.

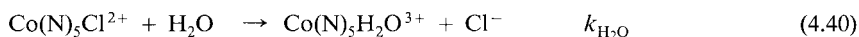
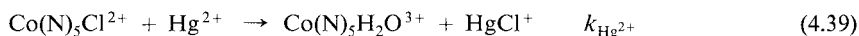
The phenomenon has been mainly explored using inert Co(III) and Cr(III) complexes with Hg(II) and Tl(III) as the accelerating ions, and the leaving groups are usually halides, pseudohalides, alkyls and carboxylates.<sup>61</sup> The majority of these induced aquations follow simple second-order kinetics. At high inducing metal ion concentration, deviations from second-order behavior might be expected with the (rapid) appearance of an adduct (exactly as might be observed with  $\text{H}^+$  catalysis) e.g.



$$V = \frac{a[\text{Hg}^{2+}][\text{Co(III)}]}{1 + K_1[\text{Hg}^{2+}]} \quad (4.38)$$

Fruitful interaction might occur via the adduct ( $a = k_2 K_1$ ) or be extraneous to adduct formation ( $a = k_3$ ).<sup>62</sup> The two mechanisms are not easily distinguished, since they lead to the same kinetics (Sec. 1.6.4). See also Ref. 63.

The Hg(II) assisted aquation of Co(III)-chloro complexes has been thoroughly studied to gain insight into the effects of solvent, ionic strength and polyelectrolytes on reaction rates and equilibria.<sup>61</sup> For the two reactions in 1.0 M  $\text{HClO}_4$  (4.39) and (4.40), ( $\text{N}$ )<sub>5</sub> representing five nitrogen donors in unidentates or multidentates or mixtures thereof,



a LFER for  $\log k_{\text{Hg}^{2+}}$  vs  $\log k_{\text{H}_2\text{O}}$  (slope 0.96) is constructable for 34 complexes, Fig. 2.6. This relationship suggests a similar 5-coordinated species as an intermediate in both these dissociatively-activated reactions.<sup>64</sup> When the removal of coordinated halides is speeded up with metal ions, products not normally obtained in aquation may result.<sup>65</sup> Mercury(II) is useful for producing chelated esters for hydrolytic examination (Sec. 6.3.1) and to probe for intermediates (Sec. 2.2.1 (b)).

### 4.3.3 Ligand-Assisted Removal

Anions can promote hydrolysis of complex cations by producing ion pairs of enhanced reactivity (see 2.178). Usually however, ligands accelerate the removal of a coordinated ligand by entering the metal coordination sphere with it and thereby labilizing it towards hydrolysis. We have already seen the effect of coordinated  $\text{OH}^-$  on the enhanced labilities of Fe(III) and Cr(III). Dissociative mechanisms and considerable acceleration are promoted by  $\text{CH}_3^-$ ,  $\text{CN}^-$ ,  $\text{SO}_3^{2-}$  and other groups on inert Cr(III), Co(III) and Pt(IV) complexes.<sup>66</sup> Nitrate ions, for example, reduce the half-life for replacement of water in  $\text{Cr}(\text{H}_2\text{O})_6^{3+}$  by dmsol from  $\sim 380$  h to 10 s!<sup>67</sup>

In some cases, the unidentate ligand is liberated at the end of the reaction. Usually, however, the ligand is found in both the reactant and the product. The effect has been most systematically examined for Ni(II).<sup>21,40</sup> Coordinated  $\text{NH}_3$  and polyamines have the largest accelerating influence. The rate acceleration induced by macrocycles resides primarily in reduced  $\Delta H^\ddagger$  values (by 15–26  $\text{kJ mol}^{-1}$ ). The 6- and 5-coordination of solvated tetramethylcyclam complexes is controlled by the conformation at the 4 N-centers, **2** and **3**. These complexes exchange by  $I_d$  and  $I_a$  mechanisms, respectively, as indicated by positive and negative  $\Delta S^\ddagger$  values (Table 4.9). Also Sec. 4.9.

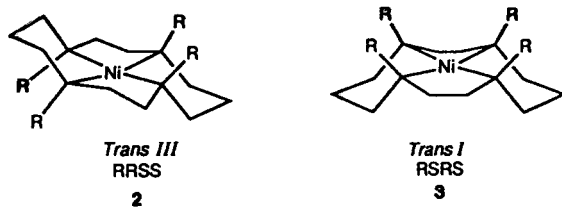
**Table 4.9** Water Exchange Rate Constants<sup>a</sup> for a Number of Nickel-(II) Complexes at 25°C. Refs. 21 and 40.

Complex	$10^{-5}k, \text{s}^{-1}$	Complex	$10^{-5}k, \text{s}^{-1}$
$\text{Ni}(\text{H}_2\text{O})_6^{2+}$	0.32	$\text{Ni}(\text{12[ane]N}_4)(\text{H}_2\text{O})_2^{2+}$	200
$\text{Ni}(\text{NH}_3)(\text{H}_2\text{O})_5^+$	2.5	$\text{Ni}(\text{Me}_4\text{cyclam})(\text{D}_2\text{O})_2^{2+ \text{ b}}$	1600
$\text{Ni}(\text{NH}_3)_2(\text{H}_2\text{O})_4^+$	6.1	$\text{Ni}(\text{Me}_4\text{cyclam})(\text{D}_2\text{O})_2^{2+ \text{ c}}$	160
$\text{Ni}(\text{NH}_3)_3(\text{H}_2\text{O})_3^+$	43	$\text{Ni}(\text{bpy})(\text{H}_2\text{O})_4^+$	0.49
$\text{Ni}(\text{2,3,2-tet})(\text{H}_2\text{O})_2^+$	40	$\text{Ni}(\text{tpy})(\text{H}_2\text{O})_3^+$	0.52

<sup>a</sup> For exchange of single solvent molecule <sup>b</sup> For *RRSS* form **2** of macrocycle,  $\Delta H^\ddagger = 37.4 \text{ kJ mol}^{-1}$  and  $\Delta S^\ddagger = +38 \text{ J K}^{-1}\text{mol}^{-1}$  <sup>c</sup> For *RSRS* **3** which forms 5-coordinated solvated species  $\Delta H^\ddagger = 27.7 \text{ kJ mol}^{-1}$  and  $\Delta S^\ddagger = -24 \text{ J K}^{-1}\text{mol}^{-1}$ .

There are linear correlations between  $\log k$  (formation) and certain properties of the ligand (number of nitrogen atoms<sup>17</sup> or electron-donor constant<sup>68</sup>). The enhanced rate resides largely





in the  $k_3$  term in (4.11). Other coordinating groups such as aminocarboxylates and heterocycles, bpy, etc. have much less labilizing influence (Table 4.9). This behavior contrasts sharply with the pronounced effect that coordinated edta and related ligands have on the rates of substitution of the waters attached to Ti(III), Cr(III), Fe(III), Ru(II) and Ru(III), Co(III) and Os(III). Factors of  $10^6$ – $10^8$  enhanced substitution rates, compared with the hexaaqua ions have been reported.<sup>69</sup> Porphyrins also accelerate dramatically the substitution of the axial unidentate group in Cr(III), Fe(III) and Co(III) complexes.<sup>70</sup>

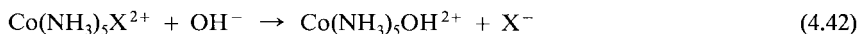
We have been concerned in this section with the formation of adducts and reactions of the type ( $S_x$  and  $S_y$  representing different ligand entities):



We are interested in the effect of  $L$ , compared with  $S_x$ , on the rate constant ( $k_1$ ) for the process. Ternary complex formation depicted in (4.41) has been actively studied, to a large extent because of the biological implications of the results.<sup>71,72</sup>

#### 4.3.4 Base-Assisted Removal

The hydroxide ion can modify the reactivity of a system in acid medium. This has been known for a long time and an example is used in Section 1.1. The ability of hydroxide to modify a reactant is probably most important in the base-assisted hydrolysis of metal ammine and amine complexes.<sup>73</sup> The overwhelming bulk of these studies have been with Co(III), for example,



and these will be considered first. The kinetics are usually second-order,

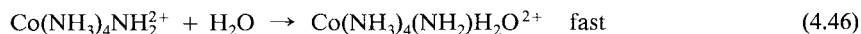
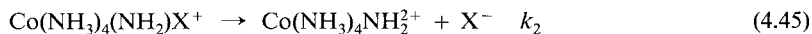
$$V = k_{\text{OH}} [\text{Co}^{\text{III}}] [\text{OH}^-] \quad (4.43)$$

a rate law which is maintained in up to 1 M  $\text{OH}^-$ , at which point flow methods must be used to follow the rapid rates. Although a number of mechanisms have been suggested to explain these simple kinetics,<sup>73</sup> there is overwhelming support for a conjugate base mechanism for the majority of systems studied.

(a) The Conjugate Base Mechanism. As originally proposed by Garrick,<sup>74</sup> base removes a proton from the ammonia or amine ligand in a rapid preequilibrium to form a substitutionally labile amide complex



Unimolecular solvolysis of this conjugate base in steps (4.45) and (4.46) produces an aqua amide complex that rapidly converts to the final product (4.47):



This mechanism termed  $D_{cb}$  (formerly  $S_N1CB$ ) was developed by Basolo and Pearson and their groups in the 1950's in the face of a good deal of healthy opposition from Ingold, Nyholm, Tobe and their co-workers who favored a straightforward  $A$  ( $S_N2$ ) attack by  $\text{OH}^-$  ion on the complex.<sup>75</sup> For a  $D_{cb}$  mechanism, in general,

$$V = d[\text{Co(III)}]/dt = k_{\text{OH}}[\text{Co(III)}][\text{OH}^-] = \frac{nk_1k_2}{k_{-1} + k_2} [\text{Co(III)}][\text{OH}^-] \quad (4.48)$$

where there are  $n$  equivalent amine protons in the cobalt reactant and assuming a steady-state concentration of the conjugate-base. Some of the evidence for the various steps proposed in the conjugate base mechanism will now be considered.

1. The base-catalyzed exchange of hydrogen between the cobalt amines and water demanded by equilibrium (4.44) has been amply demonstrated. Normally all the exchange will proceed by (4.44) but when  $k_2$  and  $k_{-1}$  are similar in magnitude, the amount of H exchange between solvent and reactant will be less than the amount of exchange between solvent and product. This rarely has been observed.<sup>76</sup> If there is a build-up of conjugate base, i.e.  $K_1[\text{OH}^-] \approx 1$ , or of an ion-pair of the Co(III) substrate with  $\text{OH}^-$ , it is easy to show that there will be a deviation from linearity of the  $V/[\text{OH}^-]$  plot. Again, this is rarely observed.<sup>73,77</sup> Normally,  $k_{-1} \gg k_2$  and  $k_1 > k_{\text{OH}}$ . With these conditions, proton-transfer in (4.44) is a preequilibrium and

$$V = nK_1k_2[\text{Co(III)}][\text{OH}^-] \quad (4.49)$$

In the unlikely event that  $k_2 \gg k_{-1}$ ,  $k_{\text{OH}} = nk_1$  and the act of deprotonation becomes rate limiting, affording powerful evidence for the necessity of (4.44) in the base reaction.<sup>78</sup> Changes of rds with conditions show up in changing values of  $\Delta H^\ddagger$  (but surprisingly not  $\Delta V^\ddagger$ ) with temperature (Sec. 2.6).

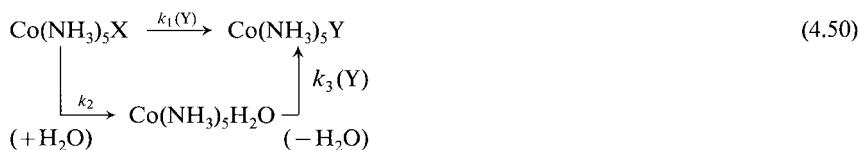
2. An intermediate of the type  $\text{Co}(\text{NH}_3)_4\text{NH}_2^{2+}$  is postulated in (4.45). The subsequent reactions of this intermediate should be independent of the nature of the X group in the starting material. The results of early experiments to verify this point have represented some of the most powerful support for the  $D_{cb}$  mechanism. Base hydrolysis of  $\text{Co}(\text{NH}_3)_5\text{X}^{2+}$  in an  $\text{H}_2^{16}\text{O}/\text{H}_2^{18}\text{O}$  mixture was found, as required, to give a constant proportion of  $\text{Co}(\text{NH}_3)_5^{16}\text{OH}^{2+}$  and  $\text{Co}(\text{NH}_3)_5^{18}\text{OH}^{2+}$ , independent of X<sup>-</sup> being Cl<sup>-</sup>, Br<sup>-</sup> or NO<sub>3</sub><sup>-</sup>.<sup>79</sup> The competition experiments described in Sec. 2.2.1 (b) support a five-coordinate intermediate which is so short lived that it retains the original ion-atmosphere of  $\text{Co}(\text{NH}_3)_5\text{X}^{(3-n)+}$  but has lost "memory" of the X group.<sup>80</sup>

3. There is strong evidence for a dissociative type of mechanism for base hydrolysis. There is an  $\approx 10^5$ -fold rate enhancement (steric acceleration) for base hydrolysis of  $\text{Co}(\text{iso-BuNH}_2)_5\text{Cl}^{2+}$  compared to  $\text{Co}(\text{NH}_3)_5\text{Cl}^{2+}$  (mainly residing in  $k_2$ <sup>73</sup>) while the corresponding factor for aquation is only  $\approx 10^2$ , emphasizing the different degrees of dissociation ( $D$  vs  $I_0$ ).<sup>81</sup> There is, incidentally, a LFER for  $\log k_{\text{OH}^-}$  vs  $\log k_{\text{H}_2\text{O}}$ , slope 1.0, for reactions of a series of  $\text{Co}(\text{III})$  complexes.<sup>82</sup> Finally, on the basis of a  $D_{\text{cb}}$  mechanism, the estimated properties of the conjugate base  $\text{Co}(\text{NH}_3)_4\text{NH}_2^{2+}$  such as heat content<sup>83</sup> and partial molar volume<sup>84</sup> (see Prob. 15, Chap. 2) are constants independent of its source. Some other characteristics of the 5-coordinated intermediate will be discussed in Sec. 4.3.5.

There is no reason to believe that the conjugate base mechanism does not apply with the other metal ions studied. Complexes of  $\text{Cr}(\text{III})$  undergo base hydrolysis, but generally rate constants are lower, often  $10^3 - 10^4$  less than for the  $\text{Co}(\text{III})$  analog,<sup>73, 85</sup> Table 4.10.<sup>86</sup> The lower reactivity appears due to both lower acidity ( $K_1$ ) and lower lability of the amido species ( $k_2$ ) in (4.49) (provided  $k_{-1}$  can be assumed to be relatively constant). The very unreactive  $\text{Rh}(\text{III})$  complexes are as a result of the very low reactivity of the amido species. The complexes of  $\text{Ru}(\text{III})$  most resemble those of  $\text{Co}(\text{III})$  but, as with  $\text{Rh}(\text{III})$ , base hydrolyses invariably takes place with complete retention of configuration.<sup>73</sup>

### 4.3.5 The Quest for Five Coordinate Intermediates

Many experiments have been performed to throw light upon, and much been written about, the existence of an intermediate in substitution reactions. Most of the work has concerned  $\text{Co}(\text{III})$  and often the complex ion  $\text{Co}(\text{NH}_3)_5\text{X}^{n+}$  has been the examining substrate of choice. Evidence rests largely on competition experiments. The existence of an intermediate  $\text{Co}(\text{NH}_3)_5^{3+}$  in the replacement of  $\text{X}$  on  $\text{Co}(\text{NH}_3)_5\text{X}$  (charges omitted) by  $\text{Y}$  is strengthened if  $\text{Co}(\text{NH}_3)_5\text{Y}$  is formed *directly* ( $k_1$  route):



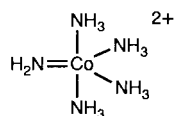
**Table 4.10** Rate Parameters for Base Hydrolysis and Exchange of  $\text{Trans-M}(\text{RRSS-cyclam})\text{Cl}_2^+$  at  $0^\circ\text{C}$  Ref. 86

M	$k_{\text{OH}^-}$ $\text{M}^{-1}\text{s}^{-1}$	$k_1$ $\text{M}^{-1}\text{s}^{-1}$	$k_2/k_{-1}$
Co	$4.1 \times 10^3$	$2.5 \times 10^{3a}$	$7.9 \times 10^{-1}$
Cr	$1.2 \times 10^{-2}$	$9.8^a$	$3.8 \times 10^{-4}$
Rh	$3.8 \times 10^{-8b}$	$6.5^{ab}$	$1.5 \times 10^{-9b}$
Ru	2.3	$1.3 \times 10^{7a}$	$4.3 \times 10^{-8}$
$\text{Co}^c$	$4.5 \times 10^5$	$5.8 \times 10^{6d}$	$4.1 \times 10^{-2}$

<sup>a</sup> Proton exchanging is *cis* to Cl. <sup>b</sup>  $20^\circ\text{C}$  <sup>c</sup> Data for *cis*- $\text{Co}(\text{RRRR-cyclam})\text{Cl}_2^+$  <sup>d</sup> Proton exchanging is *trans* to Cl.

Unfortunately, spontaneous aquation and anion-interaction with the aqua product represents another route for X-Y interchange, and it is normally difficult to separate the primary ( $k_1$ ) and secondary routes ( $k_2$  and  $k_3$ ). This problem is eased if rapidly-leaving groups X, such as  $\text{CF}_3\text{SO}_3^-$ ,  $\text{ClO}_4^-$  are employed. A comprehensive examination of 14 different complexes with  $t_{1/2}$  (hydrolysis) ranging from  $< 1\text{ s}$  to  $\approx 1$  hour, using  $\text{SCN}^-$  as a competitor, shows that there is 3–19% *direct* anion capture ( $k_1$ ) and that the values are leaving group dependent. Significantly, the ratio S-/N-bound thiocyanate in the products differs appreciably. These facts suggest that an  $I_d$  rather than a  $D$  mechanism operates.<sup>4</sup> With aquation induced by  $\text{Hg}^{2+}$  and  $\text{NO}^+$ , Ref. 87, generally dissociative activation is supported but the fine details, particularly the nature of the intermediate, has been a subject of some controversy.<sup>4,87</sup> Most work related to and the best evidence for, a 5-coordinate intermediate is in that generated in base-accelerated reactions.<sup>73</sup> The charge and nature of the leaving group  $\text{X}^{n-}$  in  $\text{Co}(\text{NH}_3)_5\text{X}^{(3-n)+}$  only slightly affects the competition ratio (it may for example vary from 8.5 to 10.6%) and when  $\text{SCN}^-$  is used as a competitor the S/N bound isomer ratios are quite constant for a large number of leaving groups (Sec. 2.2.1(b)), in contrast with the acid hydrolysis results (above.)

The consensus is for a short-lived 5-coordinated intermediate of the type  $\text{Co}(\text{NH}_3)_4\text{NH}_2^{2+}$  **4** which may react quicker than it can equilibrate with its solvent cage.<sup>88,89</sup> Experiments using competition with anions at concentrations as high as 1 M are complicated by ion-pairing.<sup>87,90</sup> Both non-aggregates and aggregates are reactive, but curiously the aggregate MY scavenges Y from solution and not from the second coordination sphere. It is not easy to arrive at any firm conclusions about the geometry of the five-coordinated intermediate of the conjugate base mechanism.<sup>73</sup> The base hydrolysis of a number of octahedral cobalt(III) and chromium(III) complexes, particularly of the type  $\text{M}(\text{en})_2\text{XY}^{n+}$  is accompanied by stereochemical change and it is reasonable to suppose that there is a rearranged trigonal-bipyramidal intermediate, although at which point along the reaction profile it appears, is uncertain.<sup>73</sup> The amido conjugate base is very labile and the manner in which the amido group labilizes is still highly speculative. It is also uncertain whether the amido group generated has to be in a specific position (*cis* or *trans* with respect to the leaving group).<sup>73</sup> It is however generally true that the presence of a meridional or “flat” sec-NH proton, *cis* to the leaving group, leads to high base hydrolysis rates. Finally, observations on the relative rates of base hydrolysis and loss of optical activity of cleverly conceived substrates have allowed reasonable conclusions about the symmetry of a relatively stable five-coordinated intermediate in base hydrolysis (Sec. 7.9).<sup>91,92</sup>

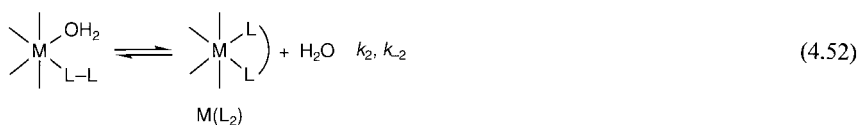
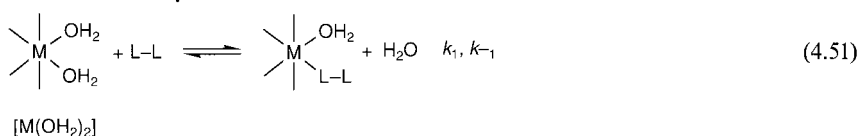
**4**

## 4.4 Replacement Reactions Involving Multidentate Ligands

There is no reason to believe that replacement of water by the donor groups of a chelating agent is fundamentally different from replacement when only unidentate ligands are involved. However, the multiplicity of steps may increase the difficulty in understanding the detailed mechanism, and mainly for this reason the simpler bidentate ligands have been most studied.

### 4.4.1 The Formation of Chelates

The successive steps in the replacement of two coordinated waters by a bidentate ligand L-L is represented as



Assuming stationary-state conditions for the intermediate, in which L-L is acting as a unidentate ligand, we find

$$d[\text{M(L}_2\text{)}]/dt = k_f[\text{M(OH}_2\text{)}_2][\text{L-L}] - k_d[\text{M(L}_2\text{)}] \quad (4.53)$$

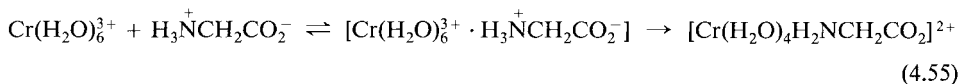
with

$$k_f = \frac{k_1 k_2}{(k_{-1} + k_2)} \quad k_d = \frac{k_{-1} k_{-2}}{(k_{-1} + k_2)} \quad (4.54)$$

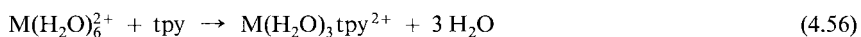
The function  $k_2/k_{-1}$  will dominate the kinetics of bidentate chelation.

(a)  $k_2 \gg k_{-1}$ . For this condition,  $k_f = k_1$  and the overall rate of chelate formation will be determined by the rate of formation of the M-L-L entity, a process we can assume is controlled by the same factors that apply with the entry of unidentates.<sup>93</sup> The relation  $k_2 \gg k_{-1}$  is anticipated when the first bond formed is relatively strong and the tendency for the intermediate to bond-break (measured by  $k_{-1}$ ) is much less than its ability to ring close ( $k_2$ ). This behavior is heralded by a single discernible rate process with rate constants for complexing by bidentate (or multidentate) ligands resembling that of the appropriate unidentate ligand. The rate constant at 25°C for complexing of Ni<sup>2+</sup> with py, bpy and tpy are within a factor of three, namely  $4 \times 10^3$ ,  $1.5 \times 10^3$  and  $1.4 \times 10^3 \text{ M}^{-1}\text{s}^{-1}$  respectively.<sup>40</sup> Complexes containing no, one and two chelate rings are formed. The reactions of Cr(H<sub>2</sub>O)<sub>6</sub><sup>3+</sup> with acetate, dicarboxylates, hydroxy- and amino acids have the common feature of a rate indepen-

dent of the concentration of ligand. All reactions obey a single first-order process with similar energies of activation (75–97 kJ mol<sup>-1</sup>) and in the suggested scheme



(with glycine for example) the outer-sphere complexing is considered complete, the rate-determining step is the expulsion of one water from the Cr(III) coordination sphere and ring closure then is rapid.<sup>94,95</sup> The volumes of activation for complexing of Mn<sup>2+</sup>, Fe<sup>2+</sup>, Co<sup>2+</sup> and Ni<sup>2+</sup> with tpy are -3.4, +3.5, +4.5 and +6.7 cm<sup>3</sup> mol<sup>-1</sup> respectively. Comparison with the water exchange data (Table 4.1) provides convincing evidence that the loss of the first H<sub>2</sub>O in (4.56) is rate-determining and that the mechanisms of replacement resemble those deduced for water exchange.<sup>96</sup>

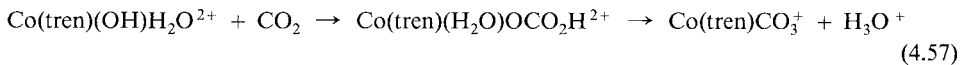


The establishment of the first bond appears to signal rapid successive ring closures with most of the multidentate ligands examined. (However, consider the Ni(II)-fad system, Sec. 1.8.2) In certain cases the later steps in chelation can be shown to be more rapid than the earlier ones, by clever experiments involving laser photolysis (Table 3.4)<sup>97</sup> or pH-adjustments of solutions containing partially formed chelates.<sup>98</sup>

The dissociation rate constant is now composite,  $k_d = k_{-1}k_{-2}/k_2$ . Following the first bond rupture ( $k_{-2}$ ) the competition between further bond rupture ( $k_{-1}$ ) and reformation ( $k_2$ ) which may lead to a small  $k_{-1}/k_2$  is the basic reason for the high kinetic stability of the chelate. The problem of complete dissociation is intensified when complexes of ligands of higher dentate character are examined. The situation is altered when the successively released donor atom(s) can be prevented from reattachment (see subject of accelerated substitution).

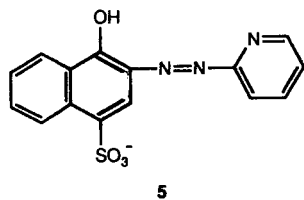
(b)  $k_2 \ll k_{-1}$ . Now,  $k_f = k_1k_2/k_{-1}$  and the rate-determining step is ring closure. The condition (b) is likely to arise in the following circumstances:

(i) If the first step is unusually rapid. The reaction of Co(tren)(OH)<sub>2</sub><sup>+</sup> and Co(tren)(OH)H<sub>2</sub>O<sup>2+</sup> with CO<sub>2</sub> at pH 7–9 is biphasic (4.57). The first step is rapid because no Co–O bond breakage is involved. This is followed by slower intramolecular chelation.<sup>99</sup> For other examples see Ref. 100.

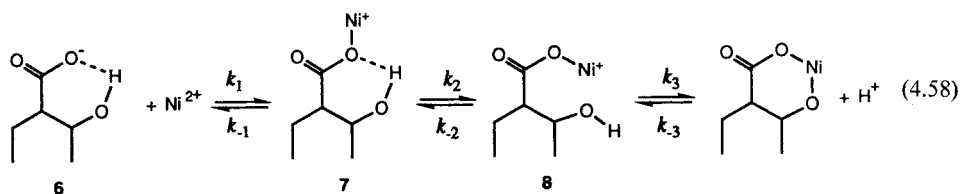


The steps in the complexing of Ni<sup>2+</sup> by the terdentate dye sulfonated 2-pyridylazo-1-naphthol (**5**) have been carefully studied. At pH = 8.0 and low [Ni<sup>2+</sup>] (<0.4 mM) the formation of the first bond is the rds. At much higher [Ni<sup>2+</sup>] ≈ 100 mM, the initial substitution is now faster than the first ring closure. The final ring closure ( $k \sim 25 \text{ s}^{-1}$  at 25°C) is abnormally slow.<sup>101</sup>

(ii) If the closing of the ring is inhibited. This may arise with the formation of certain six-membered chelate rings involving diketones<sup>102</sup> or β-aminoacids. Steric hindrance or strain may then lead to “sterically-controlled” or “chelation-controlled” substitution, which is more



important with the more labile ions.<sup>17,40</sup> If the closing arm is protonated and a proton has to be lost prior to coordination then this may inhibit ring closure. This is likely only with the more reactive metal ions, for it is only with these that substitution rate constants can be comparable to those of protonation and deprotonation.<sup>103</sup> The difficulty of ring closure from this cause is however intensified when internal hydrogen bonds need to be broken. The rate constant for reaction of  $\text{Ni}^{2+}$  with the unprotonated 3,5-dinitrosalicylate,  $\text{dnsa}^{2-}$  is  $3.1 \times 10^4 \text{ M}^{-1} \text{ s}^{-1}$  (25°C,  $I = 0.3 \text{ M}$ ), that is, a normal value. However the corresponding value is  $3.8 \times 10^2 \text{ M}^{-1} \text{ s}^{-1}$  for  $\text{dnsaH}^-$  (**6**) in which strong hydrogen bonding exists. For the scheme (4.58) the second-order formation rate constant ( $k_f$ ) is given by



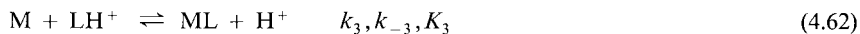
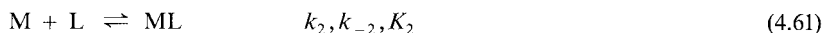
$$k_f = \frac{k_1 k_2 k_3}{k_{-1} k_{-2} + k_{-1} k_3 + k_{-2} k_3} \quad (4.59)$$

on the assumption of steady state concentrations for **7** and **8**. However it is uncertain whether the rds is opening of the H-bond in **7** or closure of the chelate ring in **8**.<sup>104,105</sup> See also Ref. 106 and 107, and Prob. 4.

The dissociation rate constant  $k_d$  measures directly the value of  $k_{-2}$  in (4.52). The strain resident in multi-ring complexes is clearly demonstrated by some hydrolysis rate studies of nickel(II) complexes. The  $\Delta H^\ddagger$  values for the *first* bond rupture for Ni(II)-polyamine complexes fall neatly into groups. They are highest for en, containing the most strain-free ring (84 kJ mol<sup>-1</sup>), about 75 kJ mol<sup>-1</sup> for complexes with terdentate ligands and only ~63 kJ mol<sup>-1</sup> for complexes of quadridentate and quinquedentate amines and with  $\text{NH}_3$  itself.<sup>108</sup> See also Ref. 109.

#### 4.4.2 Effect of $[\text{H}^+]$ on the Rates of Substitution in Chelate Complexes

Both the formation and hydrolysis rates of chelates will generally be pH-dependent. Let us compare the behavior of a chelating ligand L with its monoprotonated form  $\text{LH}^+$ . Each will exist in predominant amounts at particular pH's and usually have separate and distinct reactivities.

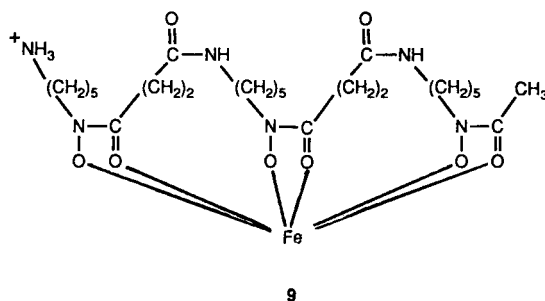


It is easy to show that

$$K_3 = K_1 K_2 \text{ and therefore } K_2 \gg K_3 \text{ since } K_1 \ll 1 \quad (4.63)$$

The smaller value of  $K_3 (= k_3/k_{-3})$  than  $K_2(k_2/k_{-2})$  will reside in  $k_3$  being less than  $k_2$  and  $k_{-3}[\text{H}^+]$  being smaller than  $k_{-2}$ . Most reported studies examine the hydrolysis of metal complexes of polyamines, particularly those of Ni(II)<sup>108,109</sup> and Cr(III).<sup>110</sup>

In the reverse direction, a proton may be effective by aiding ring-opening directly or via a reactive protonated species. It may intervene with the ring-opened species. A splendid example of these effects is shown in the acid hydrolysis of ferrioxamine B (**9**). Four stages can be separated and the kinetics and equilibria have been characterized by stopped-flow and rapid-scan spectral methods.<sup>111</sup>



#### 4.4.3 Metal Ion-Assisted Dechelation

Metal ions can assist in the dissociation (hydrolysis) of complexes containing multidentate ligands. The metal ion may not necessarily complex with the detached ligand, for example, in the metal-assisted acid-catalyzed aquation of  $\text{Cr}(\text{C}_2\text{O}_4)_3^{3-}$ . Ref. 112. Usually however the metal ion removes and complexes the ligand as in



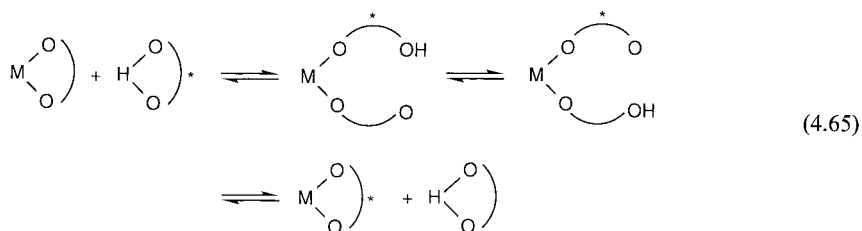
The reactions have been followed spectrally, including luminescent changes,<sup>113</sup> polarographically (when  $\text{M}_1$  is monitored) or by isotope exchange ( $\text{M}_1$  being an isotopic form of  $\text{M}$ ). They are commonly second-order reactions, with the second-order rate constant often dependent on  $[\text{H}^+]$ ,  $[\text{M}_1]$  and even  $[\text{M}]$ <sup>17,113</sup>

It is supposed that binuclear intermediates involving  $\text{M}$  and  $\text{M}_1$  occur in the various paths. The most studied systems involve edta complexes.<sup>114</sup>



### 4.4.4 Ligand-Assisted Dechelation

Interchange involving multidentate ligands is obviously even less likely to be direct than interchange involving unidentate ligands. When solvent is available on the complex (or part of the coordinated ligand is easily replaceable by solvent), the incoming ligand can gain a "coordination foothold". This can thereby lead to eventual complete ejection of the original multidentate ligand.<sup>17,115</sup> The simplest example of this is shown in the exchanges of metal chelates of  $\beta$ -diketones with free ligand which have been studied in a variety of solvents using nmr line broadening, isotopic labelling with  $^{14}\text{C}$  and spectral methods.<sup>116</sup> In the general scheme, where  $\text{OO}$  represents the diketone and the asterisk distinguishes the interchanging diketones



the rds can be (1) breaking of the  $\text{M}-\text{O}$  bond, (2) formation of an intermediate containing dangling groups or (3) intramolecular proton transfer between the dangling groups.<sup>116</sup> For exchange of  $\text{M}^{\text{III}}(\text{acac})_3$  with  $\text{acac}$  in  $\text{CH}_3\text{CN}$ , rate laws suggest that the first step is the common rds. Because  $\text{M}-\text{O}$  cleavage is involved in this step it is found that there is a LFER between ligand substitution rates of  $\text{M}(\text{acac})_3$  and water exchange of  $\text{M}(\text{H}_2\text{O})_6^{3+}$  and even  $\text{M}(\text{NH}_3)_5\text{H}_2\text{O}^{3+}$ , Fig.4.4.<sup>117</sup>

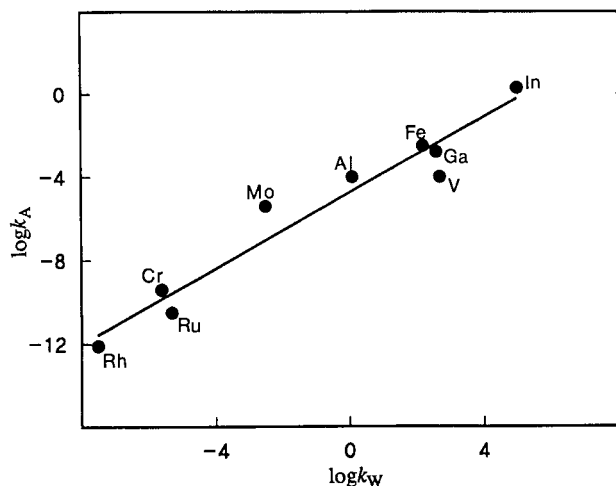
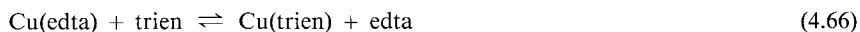
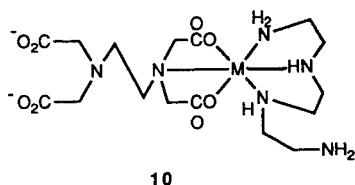


Fig. 4.4. LFER between exchange rate constants for  $\text{M}(\text{acac})_3$   $k_A$  and  $\text{M}(\text{H}_2\text{O})_6^{3+}$   $k_w$  at  $25^\circ\text{C}$ . The values are both in  $\text{s}^{-1}$  units and the former exchanges are in  $\text{acac}$ . The data for  $\text{Mo}$  are second-order rate constants for anation.<sup>117</sup>

Of course, when highly dentated ligands have to be replaced, more complicated behavior is observed. In this category, are the well-studied ligand exchange reactions of edta and polyamine complexes, a typical one of which (charges omitted) is



This may be studied in either direction by adjusting the pH and reactant concentrations. Substantial evidence exists for a mechanism in which three nitrogen atoms of the polyamine bind to the metal (**10**) before the rds of M–N cleavage, which leads to the final products.<sup>118</sup> See also Refs. 17 and 119.



The incoming ligand (or metal ion in the previous section) simulates  $\text{H}^+$  by preventing reclosing of the Ni-donor bonds as these are successively broken (see also Fig. 8.7)

## 4.5 Replacement Reactions Involving Macrocycles

The study of the complexing of macrocycle ligands should be considered for its intrinsic importance rather than for its value in illuminating the mechanism of substitution. Kinetic (but much more thermodynamic<sup>120</sup>) data are available for the reactions of the different macrocycle ligand types, shown in Fig. 4.5, including azamacrocycles,<sup>121, 122</sup> crown ethers and cryptands,<sup>123, 124</sup> and porphyrins.<sup>70, 125</sup>

Conventional, flow, temperature-jump, ultrasonic absorption, electric-field jump and nmr line broadening have all been used to measure the rates. UV-vis spectrophotometry and conductivity are the monitoring methods of choice. A variety of solvents have been used. The focus has been often on the dissociation since the dissociation rate constant appears in general to be the main controller of the overall stability.

The constraints imposed by a macrocycle on complex formation are well illustrated by a comparison of copper ion sequestering by flexible chain polyamines, 2,3,2-tet and  $\text{Me}_3\text{trien}$ , macrocycles, tetraazatetraamines, cyclam and  $(\text{N-Me}_4)\text{cyclam}$ , a bicyclic tetraamine cryptand  $2_{\text{N}}1_{\text{O}}1_{\text{O}}$  and a rigid porphyrin.<sup>121, 126–128</sup> The reactions are carried out in a strongly basic medium, where ligand protonation is unimportant, and second-order rate constants for reaction of  $\text{Cu}(\text{OH})_3^-$  and  $\text{Cu}(\text{OH})_4^{2-}$  are shown in Table 4.11. Generally it is seen that an acyclic tetraamine allows easy stepwise replacement of coordinated  $\text{H}_2\text{O}$  and  $\text{OH}$  groups and reacts  $\approx 10^8$  times faster than the rigid porphyrin, where simultaneous multiple desolvation of the metal ion is mandatory. With cyclam, twisting or folding of the ligand is possible but

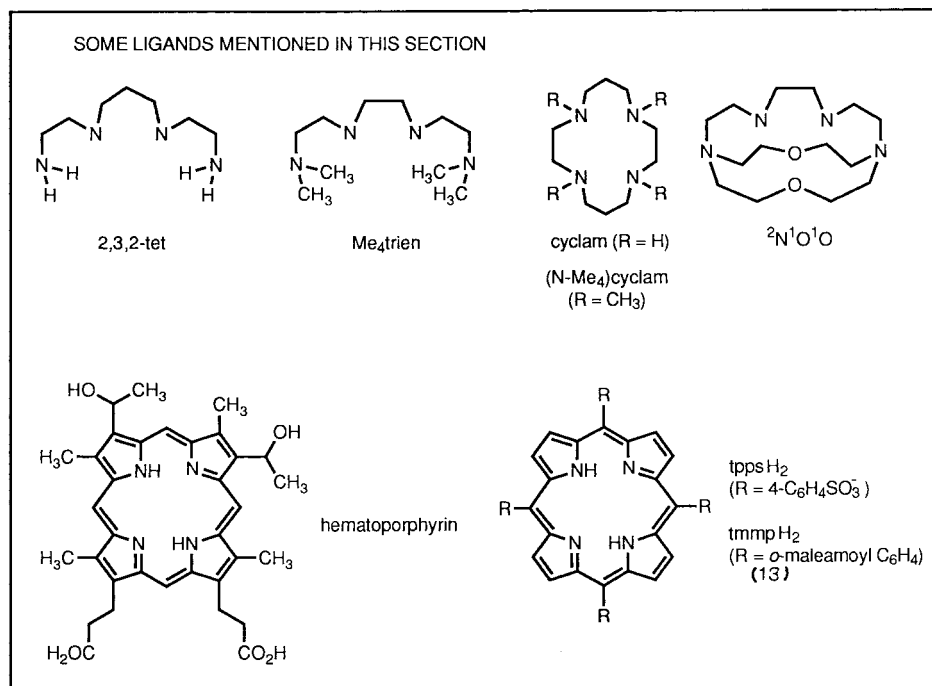


Fig. 4.5 Some ligands mentioned in this section (4.5).

(N-Me<sub>4</sub>)cyclam and <sup>2</sup>N<sup>1</sup>O<sup>1</sup>O (compare Me<sub>4</sub>trien) are more rigid and the rate constants reflect this condition. All rate constants are less than the diffusion-controlled limit and even of the anticipated axial water lability of Cu(II), Sec. 4.2.1(a). It is apparent that the mechanisms are complex and must differ appreciably (position of rds etc.) for the various types. Nevertheless there are also general similarities when the details are examined.

Table 4.11 Formation Rate Constants for Cu(II) Reactions<sup>121, 126, 127</sup>

Ligand	$k, \text{Cu(OH)}_3^-$ $\text{M}^{-1}\text{s}^{-1}$	$k, \text{Cu(OH)}_4^{2-}$ $\text{M}^{-1}\text{s}^{-1}$
2,3,2-tet	$1.0 \times 10^7$	$4.3 \times 10^6$
Me <sub>4</sub> trien	$4.1 \times 10^6$	$4.2 \times 10^5$
cyclam	$2.7 \times 10^6$	$3.8 \times 10^4$
(N-Me <sub>4</sub> )cyclam	$3.1 \times 10^3$	< 10
<sup>2</sup> N <sup>1</sup> O <sup>1</sup> O	$6.6 \times 10^4$	$3.8 \times 10^3$
hemato porphyrin	—	$\approx 2 \times 10^{-2}$

## 4.5.1 Azamacrocycles

The stepwise nature of complexing is illustrated in the suggested scheme (Fig. 4.6) for the reaction of  $\text{Cu}(\text{OH})_3^-$  and  $\text{Cu}(\text{OH})_4^{2-}$  with the cyclic tetraamines.<sup>121,127</sup> When  $\text{Cu}(\text{OH})_3^-$  and  $\text{Cu}(\text{OH})_4^{2-}$  react with similar rate constants it may be supposed that they have a common rds, which will then depend on the ligand. Indirect arguments indicate that the rds is after the first substitution of axial water. It is almost certainly before formation of the third Cu-N bond, otherwise  $\text{Cu}(\text{OH})_4^{2-}$  reacting would lead to an unlikely 7-coordinate Cu(II) complex at some point. The Jahn-Teller inversion step is an additional complication with reactions of Cu(II) and may indeed be the rds following bond formation. Differences greater than a factor of 10 for reaction of  $\text{Cu}(\text{OH})_3^-$  over  $\text{Cu}(\text{OH})_4^{2-}$  suggest a shift of rds. This is believed to be a change from the first- to the second-bond formation, respectively.<sup>121,127</sup> Formation rate constants vary little with the ring size of the tetraaza macrocycle, except that reaction with the 12-membered ring is particularly slow, perhaps because of the difficulty in folding such a ring, which would be expected to be helpful in the difficult insertion process. Conformational changes in the macrocycle can arise after metal ion incorporation. The problem of binding a metal ion to a macrocycle may be eased if the macrocycle has a pendent arm which contains a ligand center. The metal ion can bind then to the arm and from thence be pulled into the macrocycle.<sup>129</sup>

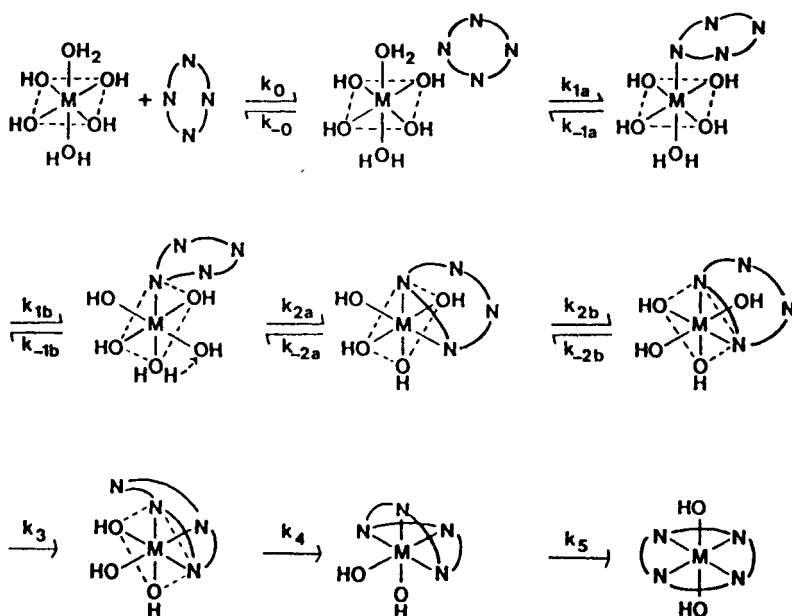


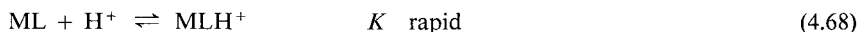
Fig. 4.6 Stepwise complexing of  $\text{Cu}(\text{OH})_4^{2-}$  by a tetradentate macrocyclic ligand. The first Cu(II)-N bond is formed by replacement of an axial solvent molecule ( $k_{1a}$ ) followed by a Jahn-Teller inversion ( $k_{1b}$ ) which brings the coordinated nitrogen into an axial position. Second-bond formation follows a similar pattern ( $k_{2a}$  and  $k_{2b}$ ).<sup>121,127</sup> Reproduced with permission from J. A. Drumhiller, F. Montavon, J. M. Lehn and R. W. Taylor, *Inorg. Chem.* **25**, 3751 (1986). © (1986) American Chemical Society.

(a) Effect of  $H^+$ 

The macrocycles are generally characterized by their extreme resistance to dissociation, (see however Prob. 6). The kinetics of acid-promoted dissociation of an extensive series of Ni(II) and Cu(II) complexes, (ML) have been reported,<sup>122</sup> The general rate law is (see Prob. 2, Chap. 2):

$$V = \{k_1 + k_2[H^+]^n\} [ML] \quad (4.67)$$

where  $n$  can vary from 1 to 3, the value of  $n$  depending on the number of preequilibria involving  $H^+$ . "Acid-limiting" kinetics are interpreted either in terms of a mechanism:



for which the first-order loss of ML is given by

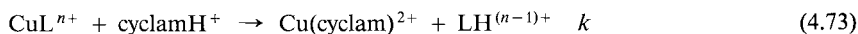
$$k_{\text{obs}} = \frac{K k_H [H^+]}{1 + K [H^+]} \quad (4.70)$$

Alternatively, they can arise as a result of the rate-determining reaction of  $H^+$  with a reactive form of ML ( $ML^*$ ) which might be an isomer originating, for example, from the chiral NH centers (Sec. 7.9).



$$k_{\text{obs}} = \left[ \frac{k_1 k_2 [H^+]}{k_{-1}} \right] \left[ 1 + \frac{k_2 [H^+]}{k_{-1}} \right]^{-1} \quad (4.72)$$

The formation of  $\text{Cu}(\text{cyclam})^{2+}$  by reaction of cyclam with a large variety of copper complexes ( $\text{CuL}^{n+}$ ) is interesting:



Provided that the stability of the  $\text{CuL}^{n+}$  is not very high ( $\log K < 10$ ), the value of  $k$  is similar to that for  $\text{Cu}_{\text{aq}}^{2+}$ . There is an inverse relationship of  $\log k$  with  $\log K$  ( $\text{CuL}^{n+}$ ) with more stable complexes (Fig. 8.7). It is also worthy of note that although the main cyclam species at the pH of the study (4-9) is  $\text{cyclamH}_2^{2+}$ , the reactive species is  $\text{cyclamH}^+$ . Ref. 130.

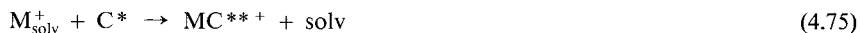
### 4.5.2 Crown-Ethers and Cryptands

Studies with these ligand systems mainly involve the Group One and Two metal ions. The suggested mechanism for the formation of complexes has a number of features in common with

those proposed for porphyrins (Sec. 4.5.3). A possible rapid pre-equilibrium involving a ligand conformational change,



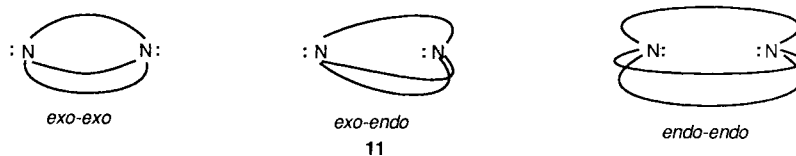
is frequently followed by a rds:



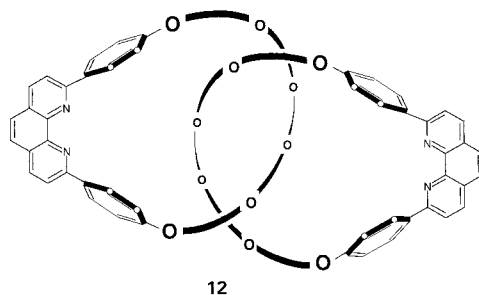
and (rapidly)



where C, C\* and C\*\* represent different conformations of the crown ether or cryptand. With for example  $2O_2O_2O_2$ , conformational changes involving endo-endo, exo-endo and exo-exo forms (**11**) have been established. Since in general there is little effect of solvents on the rates (see however Ref. 131) it is surmised that there is little desolvation in the transition state for (4.75), which thus resembles the reactants. As a corollary of this, there is a striking linear plot, slope  $-1$  over 12 orders of magnitude, for  $\log k(\text{diss})$  vs  $\log K(\text{stab})$  for a variety of systems.<sup>124</sup> Outer sphere complexing may also precede the main step as has been postulated for the first of three steps observed in the complexing, in propylene carbonate, of  $UO_2^{2+}$  by [18]crown-6 to give a 1:1 complex.<sup>132</sup> With the cryptand complexes, dissociation is only proton-promoted when easily approached donor sites are available and probably occurs through the exo-endo isomer. Dissociation of the crown-ether<sup>131</sup> and cryptand<sup>133</sup> complexes is rarely metal-ion assisted. An intriguing example of ligand-aided removal of a transition metal ion from a macrocycle, involves complexes of catenands. These are interlocked as represented in **12**. The rate law for removal of Cu(I) by  $CN^-$  from the Cu(I) complex of **12**,  $CuC^+$  (see Fig. 6.1) is



Conformers of the Cryptand (2.2.2)





The  $k_1$  term corresponds to spontaneous dissociation and the  $k_2$  term arises from cyanide-assisted dissociation:

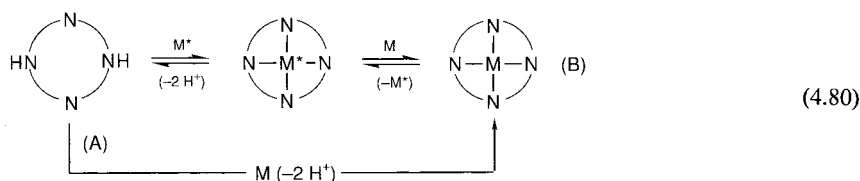


The difficulty in disengaging the two interlocked rings is seen when the values of  $k_1$  ( $2 \times 10^{-4} \text{ s}^{-1}$ ) and  $k_2$  ( $0.16 \text{ M}^{-1} \text{ s}^{-1}$ ) are compared with those for the corresponding breakdown of  $\text{Cu(dpp)}_2^+$  by  $\text{CN}^-$ ,  $k_1 = 1.3 \text{ s}^{-1}$  and  $k_2 = 14.6 \text{ M}^{-1} \text{ s}^{-1}$ , dpp = 2.9-diphenyl-1, 10-phenanthroline.<sup>134(a)</sup>

The formation of  $\text{Li}^+$ ,  $\text{Cd}^{2+}$ ,  $\text{Zn}^{2+}$  and  $\text{Co}^{2+}$  (but not  $\text{Cu}^+$ ) complexes of **12** is biphasic. The first step (overall second-order) likely represents binding of the metal ion to one of the chelating subunits of **12**. The second step (first-order) is very slow ( $k \approx 10^{-2} - 1 \text{ s}^{-1}$ ) and possibly corresponds to the gliding motion of one ring within the other while the second phenanthroline fragment attempts to bind to the metal center.<sup>134(b)</sup>

### 4.5.3 Porphyrins

Most of the studies have been carried out in nonaqueous solution. The important processes are (A) direct metal ion (M) interaction with porphyrin and (B) metal-ion  $\text{M}^*$  assisted entry (transmetallation) shown schematically in (4.80). The reactions are usually slow, easily followed spectrally because of the high characteristic absorption coefficients of the complexes and free porphyrins, and attended by beautiful isosbestic points<sup>135(a)</sup> (Fig. 3.10). The free base in (4.80) is represented as  $\text{H}_2\text{P}$  and is the reactive species.<sup>135(b)</sup> The mono- and diprotonated forms are unreactive.



#### (a) Direct Interaction

For route (A) the rate law is often second-order

$$V = k[\text{M}][\text{H}_2\text{P}] \quad (4.81)$$

The insertion steps are probably preceded by deformation of  $\text{H}_2\text{P}$  and/or outer sphere complexing.<sup>70, 135-137</sup> If these are incomplete they will introduce rapid preequilibria constants  $K_1$  and  $K_2$  into the rate expression, and by reducing the



concentrations of the reactive species, lower markedly the overall rates of reaction with the solvento complex,  $\text{MS}_6$ . Ligand dissociation and the formation of the first bond then occurs:



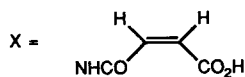
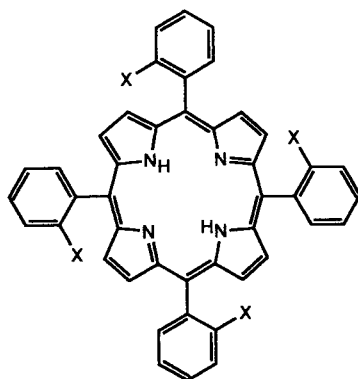
Is this the rds? There is striking correlation of the exchange rate constants for  $\text{MS}_6$  and the values of  $k$  in (4.81).<sup>135,136</sup> In addition the volumes of activation are positive for solvent exchange and interaction of  $\text{M}(\text{dmf})_6^{2+}$  ( $\text{M} = \text{Mn}, \text{Co}, \text{Ni}, \text{Zn}$  and  $\text{Cd}$ ) with N-Metpp in dmf (compare Table 4.4). In spite of these two facts however, it is considered that one of two further steps, probably the first, controls the overall rate. A sitting-atop (SAT) complex<sup>138</sup> is formed in which metal is attached by two bonds to the porphyrin and two N-H bonds remain intact.



In the final step, the SAT complex collapses to the ultimate product with a concerted release of 2 protons



This segment of the mechanism and the concept of an SAT complex<sup>138</sup> have played an important role in the understanding of the complex mechanism by which metal ions react with porphyrins.





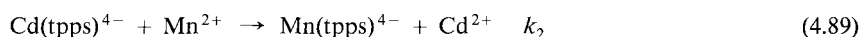
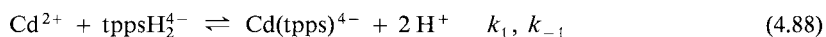
Appropriately placed groups on the porphyrin periphery can aid considerably the incorporation of metal ions into the ring. The porphyrin shown,  $H_2tmpp$ , **13** reacts rapidly with  $Co(II)$ ,  $Ni(II)$ ,  $Cu(II)$  in  $dmf/H_2O$ . The rate data indicate that an initial adduct is formed which allows the metal to more easily transfer into the porphine ring.<sup>139</sup> See also Ref. 129 for a similar behavior with an azamacrocycle.

### (b) Metal-Ion Assisted Entry

Metal ions can assist, in a novel way, the formation of a metalloporphyrin, by route (B).<sup>125</sup> Since the free porphyrin does not appear in any amount during the  $M, M^*$  interchange it is a truly associative process. The reaction of  $Mn^{2+}$  with  $tppsH_2^{4-}$  in water is very slow.



The incorporation is accelerated markedly by the presence of small amounts of  $Cd^{2+}$  ions acting as a catalyst. The following mechanism is suggested



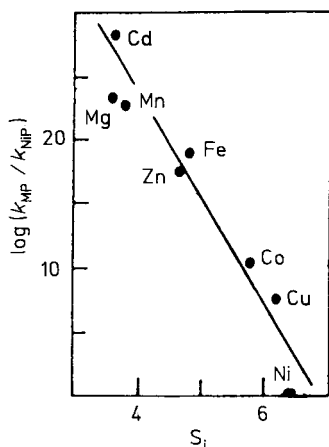
on the basis of the observed rate law,  $[Mn^{2+}] \gg [tppsH_2^{4-}]$ ,  $[Cd^{2+}]$ :

$$-d[tppsH_2^{4-}]/dt = k_{obs}[tppsH_2^{4-}] \quad (4.90)$$

where

$$k_{obs} = \frac{k_1 k_2 [Mn^{2+}] [Cd^{2+}]}{k_{-1} [H^+] + k_2 [Mn^{2+}]} \quad (4.91)$$

The reaction of  $Cd^{2+}$  with  $tppsH_2^{4-}$  is rapid, because the larger metal ion forms an out-of-plane complex. This is easily attacked, probably from the other side of the ring, by the



**Fig. 4.7** Plot of the log of the relative rates of hydrolysis of MP and the corresponding  $Ni(II)P$  vs. the stability index  $S_i$ . The parameter  $S_i$  is defined as  $100 zE_N/r_i$  where  $z$  = charge,  $r_i$  = radius and  $E_N$  = Pauling's electronegativity of the metal in the metalloporphyrin. The parameter is empirical but agrees generally with the order of stability, determined experimentally (J. W. Buchler, Ch. 5 in *Porphyrins and Metalloporphyrins*, ed. K. M. Smith, Elsevier, 1975).<sup>70</sup> Reproduced with permission from D. K. Lavalley, *Coordn. Chem. Revs.* **61**, 55 (1985).

stronger binding  $\text{Mn}^{2+}$ .<sup>140</sup> At high pH,  $k_{\text{obs}} = k_1[\text{Cd}^{2+}]$ . At 25°C,  $k_1 = 4.9 \times 10^2 \text{ M}^{-1}\text{s}^{-1}$  and  $k_{-1}/k_2 = 3.0 \times 10^{10} \text{ M}^{-1}$  ( $\mu = 0.1 \text{ M}$ ). By studying (4.89) directly,  $k_2 = 2 \times 10^2 \text{ M}^{-1}\text{s}^{-1}$  and thus  $k_{-1} = 6 \times 10^{12} \text{ M}^{-2}\text{s}^{-1}$ .<sup>125</sup> Reaction (4.89) is about  $10^4$  faster than (4.87).

Dissociation of most metal porphyrins,  $\text{M}(\text{II})\text{P}$ , is very slow. As well as metal ions,  $\text{H}^+$  accelerates the metal removal. The order of dependence on  $[\text{H}^+]$  varies from 1–3 depending on the system, with a rate law

$$V = k [\text{M}(\text{II})\text{P}] [\text{H}^+]^2 \quad (4.92)$$

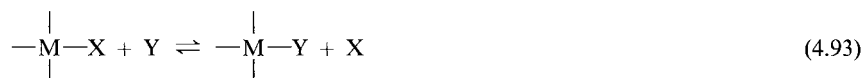
common.<sup>141</sup> This behavior suggests that a single metal-N bond is readily broken. The rate constant  $k$  parallels the instability of the porphyrin complex in a dramatic manner. Fig. 4.7.<sup>70</sup>

## 4.6 Substitution in Square-Planar Complexes

There are a number of metals, particularly with a low spin  $d^8$  configuration, that form four-coordinate square-planar complexes. Of these, the  $\text{Pt}(\text{II})$  complexes have been the most intensively investigated. They are therefore representatives of this geometry, much as  $\text{Co}(\text{III})$  complexes epitomize octahedral behavior – and for precisely the same reasons, namely that they have been previously well characterized and studied, particularly by Russian workers, and that they react slowly. There have never been any problems therefore in the initiation and the rate measurement of these reactions. With the easier access to rapid reaction techniques, particularly flow, square-planar complexes of a number of other metals,  $\text{Rh}(\text{I})$ ,  $\text{Ir}(\text{I})$ ,  $\text{Ni}(\text{II})$ ,  $\text{Pd}(\text{II})$ ,  $\text{Cu}(\text{II})$  and  $\text{Au}(\text{III})$  are being increasingly examined. Many of these metal complexes, unlike most octahedral complexes, are soluble in aprotic solvents and these have been, as well as water, examining media. The ultraviolet and nmr spectral methods, and less commonly, conductivity and radioactive isotopic exchange have been the methods most commonly employed for monitoring the rates. In many respects, substitution in square-planar complexes is one of the best understood dynamic processes in chemistry.<sup>142, 143</sup>

### 4.6.1 The Kinetics of Replacement Involving Unidentate Ligands

Most studies have again been concerned with replacement of one unidentate ligand by another, and the rules and patterns of behavior that have evolved are based mainly on this simple type of substitution reaction. Consider the substitution scheme



The rate law governing substitution in planar complexes usually consists of two terms, one first-order in the metal complex (M) alone and the other first-order in both M and the entering ligand Y:

$$V = -d[\text{MX}]/dt = k_1[\text{M}] + k_2[\text{M}][\text{Y}] \quad (4.94)$$

The experiments are invariably carried out using excess Y and therefore with pseudo first-order conditions. The experimental first-order rate constant  $k$  is given by

$$V = k[\text{M}] \quad (4.95)$$

Therefore

$$k = k_1 + k_2[\text{Y}] \quad (4.96)$$

A plot of  $k$  vs  $[\text{Y}]$  will have an intercept  $k_1$  and a slope  $k_2$ . An example is shown in Fig. 4.8.<sup>144</sup> For different nucleophiles reacting with the same complex, the value of  $k_1$  is the same, whereas the value of  $k_2$  usually will be different. Often,  $k_1 \ll k_2[\text{Y}]$  and it is then difficult to measure  $k_1$  accurately. Care has to be taken that a positive intercept in a plot of the type shown in Fig. 4.8 is not mistakenly assigned to  $k_1$  in (4.96), when it may in fact represent the reverse rate constant of (4.93) (Sec. 1.5).<sup>145,146</sup>

(a) Significance of  $k_1$ . The term containing  $k_1$  resembles octahedral complexes in their substitution behavior where it represents ligand-ligand replacement via the solvated complex:

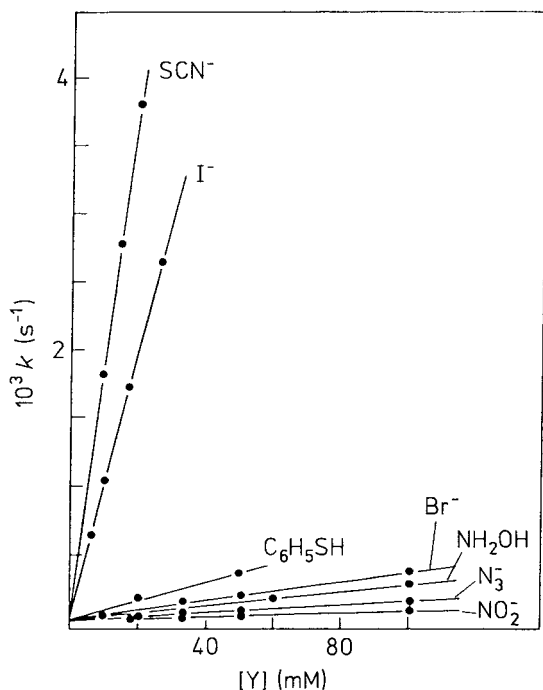
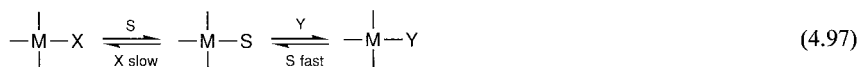
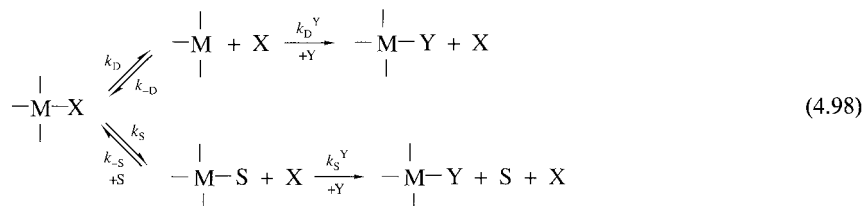


Fig. 4.8 Plots of pseudo first-order rate constants at 30°C vs [nucleophile, Y] for reaction of  $\text{trans-Pt}(\text{py})_2\text{Cl}_2$  in methanol.<sup>144</sup>



As with solvolysis reactions of octahedral complexes, the rate-determining step may be solvolytic or dissociative; in any case, it is independent of the concentration of Y:



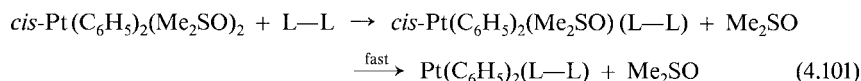
Setting up stationary-state conditions for  $\begin{array}{c} | \\ -M \\ | \end{array}$  and  $\begin{array}{c} | \\ -M-S \\ | \end{array}$  yields

$$k_1 = \frac{k_D^Y k_D [Y]}{k_D^Y [Y] + k_{-D} [X]} + \frac{k_S^Y k_S [S] [Y]}{k_S^Y [Y] + k_{-S} [X]} \quad (4.99)$$

The full equation (4.99) must be invoked when reversibility of any of the steps in (4.98) occurs.<sup>142</sup> When the step involving Y is fast, (4.99) reduces to

$$k_1 = k_D + k_S [S] \quad (4.100)$$

On the basis of either interpretation,  $k_1$  should equal the solvolysis rate constant and if MS is an isolatable intermediate, it should be shown to react rapidly with Y. Both consequences have been realized in certain systems. Although there has been some skepticism shown towards a dissociative mode of substitution ( $k_D$ ,  $k_{-D}$  in (4.98)), there is growing evidence for its existence in cases where the importance of the associatively activated pathways can be reduced. For the first step of the reaction



where L-L (a bidentate ligand) and Me<sub>2</sub>SO are used in excess, the pseudo first-order rate constant  $k$  for the loss of the Pt(II) reactant is:

$$k = \frac{a [\text{L-L}]}{b [\text{L-L}] + [\text{Me}_2\text{SO}]} + c [\text{L-L}] \quad (4.102)$$

This conforms to the usual two-term rate law (4.96), but in which the  $k_1$  term is associated with a three-coordinated intermediate in (4.99). The values of  $a = k_D k_D^Y / k_{-D}$ ,  $b = k_D^Y / k_{-D}$  and  $c = k_2$  (in (4.96)). Significantly the exchange of Me<sub>2</sub>SO with *cis*-Pt(C<sub>6</sub>H<sub>5</sub>)<sub>2</sub>(Me<sub>2</sub>SO)<sub>2</sub>, in CDCl<sub>3</sub> followed by stopped flow-nmr, yields a value for  $k_D$ , 0.08 s<sup>-1</sup> (27 °C) similar to that obtained by examining (4.101) using L-L = bpy, and other bidentate ligands in C<sub>6</sub>H<sub>6</sub>.<sup>147(a)</sup> Markedly different values of  $b$  for different entering ligands (L-L) support a *D* mechanism. The *D* mechanism might be favored in very poor nucleophilic solvents such as C<sub>6</sub>H<sub>6</sub> or

$\text{CHCl}_3$ , but its differentiation from the solvolytic path is still very difficult.<sup>142,148</sup> The  $\Delta V^\ddagger$  value of  $+5.5 \pm 0.8 \text{ cm}^3 \text{ mol}^{-1}$  for the exchange of  $\text{Me}_2\text{SO}$  with  $\text{Pt}(\text{C}_6\text{H}_5)_2(\text{Me}_2\text{SO})_2$  also strongly supports a *D* mechanism which appears favored in complexes containing a Pt-C bond.<sup>147(b)</sup>

(b) Significance of  $k_2$ . It is generally accepted that the key rate term in substitution in square-planar complexes involves nucleophilic associative attack of the entering nucleophile *Y* on the metal complex. It follows from this that the bond-making as well as the bond-breaking process will be important, and it can be expected that there will be varying degrees of participation by both. All attempts, however, to observe an intermediate in the bimolecular reactions of Pt(II) have failed, even with the most favorable situation, that is, using a strong entering ligand and a weak leaving one.<sup>145</sup>

## 4.6.2 Activation Parameters

Substitution in Pt(II) and Pd(II) complexes is invariably attended by large negative values of  $\Delta S^\ddagger$  and negative values of  $\Delta V^\ddagger$  (Table 4.12).<sup>149-152</sup> This is consistent with an associative mechanism and a net increase in bonding in an ordered and charged transition state. These considerations apply to both the  $k_1$  and the  $k_2$  terms.<sup>149</sup> Although there is strong evidence for an absolute *A* mechanism, the small value of  $\Delta V^\ddagger$  for the simple  $\text{M}(\text{H}_2\text{O})_4^{2+} - \text{H}_2\text{O}$  exchanges (Table 4.12)<sup>151</sup>, *M* = Pd(II) or Pt(II), might suggest otherwise and support an *I<sub>a</sub>* process (see also  $\text{Pt}(\text{Me}_2\text{SO})_4^{2+}$ ,  $\text{Me}_2\text{SO}$  exchange (Sec. 7.4.1)). However the formation of a fifth (equatorial) metal-water bond in the trigonal-bipyramidal intermediate or transition state (Sec. 4.7.5) may be accompanied by lengthening of the two (axial) metal-water bonds offsetting somewhat the anticipated larger negative  $\Delta V^\ddagger$ .<sup>151</sup> More data are obviously required.

**Table 4.12** Activation Parameters for Substitution in Some Square-Planar Complexes in Water at 25°C Refs. 149-152.

Complex	Reagent	$k$ $\text{M}^{-1} \text{s}^{-1}$	$\Delta H^\ddagger$ $\text{kJ mol}^{-1}$	$\Delta S^\ddagger$ $\text{J K}^{-1} \text{mol}^{-1}$	$\Delta V^\ddagger$ $\text{cm}^3 \text{mol}^{-1}$
$\text{Pd}(\text{H}_2\text{O})_4^{2+}$	$\text{H}_2\text{O}$	$5.6 \times 10^{2a}$	50	-26	-2.2
$\text{Pt}(\text{H}_2\text{O})_4^{2+}$	$\text{H}_2\text{O}$	$3.9 \times 10^{-4a}$	90	-9	-4.6
$\text{Ni}(\text{CN})_4^{2-}$	$\text{CN}^-$	$>5 \times 10^5$	—	—	—
$\text{Pd}(\text{CN})_4^{2-}$	$\text{CN}^-$	$1.2 \times 10^{2b}$	17	-178	—
$\text{Pt}(\text{CN})_4^{2-}$	$\text{CN}^-$	$26^b$	26	-143	—
$\text{Au}(\text{CN})_4^-$	$\text{CN}^-$	$3.9 \times 10^{3b}$	28	-100	—
$\text{Pt}(\text{dien})\text{Br}^+$	$\text{H}_2\text{O}$	$1.4 \times 10^{-4a}$	84	-63	-10
	$\text{Cl}^-$	$6 \times 10^{-4}$	75	-46	—
	$\text{Br}^-$	$6 \times 10^{-3}$	67	-63	—
	$\text{N}_3^-$	$6.4 \times 10^{-3}$	65	-71	-8.5
	py	$2.8 \times 10^{-3}$	46	-136	-7.7
	$\text{NO}_2^-$	$1.4 \times 10^{-3}$	72	-56	-6.4
	$\text{I}^-$	0.32	46	-104	—
	$\text{NCS}^-$	0.68	39	-112	—
	$\text{SC}(\text{NH}_2)_2$	1.3	35	-121	—

<sup>a</sup> $\text{s}^{-1}$  <sup>b</sup>No  $[\text{CN}^-]$ -independent term

## 4.7 Ligand Effects on the Rate

One of the consequences of an associative mechanism is the decided importance of all the ligands – entering, leaving and remaining – on the rate of the process. This arises because all the ligands involved are present in the five-coordinate activated complex and can therefore affect its stability and the activation energy for its production. This feature distinguishes planar from octahedral substitution. There have therefore been, mainly in the 60's and early 70's a large number of studies in which systematic variations are made in the character of all the ligands.<sup>149</sup> The interpretation of the results has been helped by the fact that complete retention of configuration during substitution has been consistently observed with the type of Pt(II) complexes studied.<sup>142</sup>

### 4.7.1 Effect of Entering Ligand

There have been extensive studies of the influence of an entering ligand on its rate of entry into a Pt(II) complex.<sup>144, 153</sup> The rate constants for reaction of a large number and variety of ligands with *trans*-Pt(py)<sub>2</sub>Cl<sub>2</sub> have been measured (Table 4.13). The large range of reactivities is a feature of the associative mechanism and differentiates it from the behavior of octahedral complexes. The rate constants may be used to set up quantitative relationships. For a variety of reactions of Pt complexes in different solvents (Sec. 2.5.4):

$$\log k_y = sn_{\text{Pt}} + \log k_s \quad (4.103)$$

**Table 4.13** Rate Constants ( $k$ ,  $\text{M}^{-1}\text{s}^{-1}$ ) for Reaction of *trans*-Pt(py)<sub>2</sub>Cl<sub>2</sub> with a Number of Nucleophiles in CH<sub>3</sub>OH<sup>144, 153</sup>

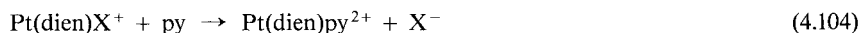
Nucleophile	$10^3 \times k$	$n_{\text{Pt}}$	Nucleophile	$10^3 \times k$	$n_{\text{Pt}}$
CH <sub>3</sub> OH	0.00027	0.0	I <sup>-</sup>	107 <sup>a</sup>	5.46
CH <sub>3</sub> O <sup>-</sup>	Very Slow	<2.4	(CH <sub>3</sub> ) <sub>2</sub> Se	148	5.70
Cl <sup>-</sup>	0.45 <sup>a</sup>	3.04	SCN <sup>-</sup>	180 <sup>a</sup>	5.75
NH <sub>3</sub>	0.47 <sup>a</sup>	3.07	SO <sub>3</sub> <sup>2-</sup>	250 <sup>a</sup>	5.79
C <sub>5</sub> H <sub>5</sub> N	0.55 <sup>a</sup>	3.19	Ph <sub>3</sub> Sb	1,810	6.79
NO <sub>2</sub> <sup>-</sup>	0.68 <sup>a</sup>	3.22	Ph <sub>3</sub> As	2,320	7.68
C <sub>3</sub> H <sub>3</sub> N <sub>2</sub>	0.74	3.44	CN <sup>-</sup>	4,000	7.14
N <sub>3</sub> <sup>-</sup>	1.6 <sup>a</sup>	3.58	SeCN <sup>-</sup>	5,150 <sup>a</sup>	7.11
N <sub>2</sub> H <sub>4</sub>	2.9 <sup>a</sup>	3.86	SC(NH <sub>2</sub> ) <sub>2</sub>	6,000 <sup>a</sup>	7.17
Br <sup>-</sup>	3.7 <sup>a</sup>	4.18	Ph <sub>3</sub> P	249,000	8.93
(CH <sub>3</sub> ) <sub>2</sub> S	21.9	4.87			

<sup>a</sup> Kinetic data at 30°C.

The term  $s$  is the nucleophile discrimination factor. The values of  $n_{\text{Pt}}$ , the nucleophilic reactivity constant, is useful for correlating kinetic data for other Pt(II) complexes.<sup>144, 149, 153</sup>

### 4.7.2 Effect of Leaving Group

Reactions of the type



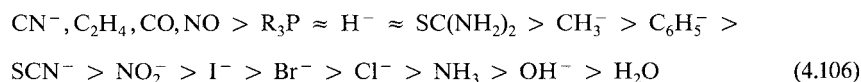
in aqueous solution have been used to study the effect of X on the rates of the reactions.<sup>149</sup> The members of the series differ in rate constants by as much as  $10^6$  from the slowest



( $\text{CN}^-$ ) to the fastest. Generally, the second-order rate constant increases with decreasing basicity of the leaving group and this gives rise to LFER. It is therefore fairly clear from these observations that metal-ligand bond breakage must be significant, even in a predominantly associative reaction.

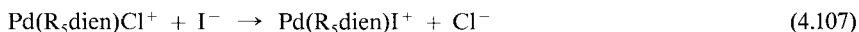
### 4.7.3 Effect of Ligands Already Present

The group *trans* to the leaving ligand appears to have a more pronounced influence than the two *cis* to it, on the rate of its departure.<sup>149</sup> It has been known for many years that a ligand can be assigned an order of *trans effect* which denotes its tendency to direct an incoming group in the position *trans* to itself. In Pt(II) complexes, this power decreases approximately in the order<sup>149</sup>



The effect has played an important role in preparing Pt(II) complexes of specific geometry. The greater *trans effect* appears to be associated with a larger rate constant for the elimination of the *trans* ligand, from a limited number of studies.<sup>154</sup> Comparison of (4.106) with (4.105) and Table 4.12 shows that the groups with a pronounced ability to *trans-labilize* are replaced the least easily and are the more powerful nucleophiles. This might be anticipated since in the five-coordinate intermediate (see 4.109) the entering nucleophile E, *trans* ligand T, and the departing ligand D, all occupy positions in the trigonal plane and all may influence the energetics of the transition state in similar ways.

In an associative mechanism, increasing the steric hindrance in the complex should lead to decreasing rates (steric retardation). This has been realised with a number of systems, that of  $\text{Pd}(\text{R}_5\text{dien})\text{X}^{n+}$  being the most explored.<sup>155,156</sup> Activation parameters for the reaction



are shown in Table 4.14.<sup>156(a)</sup> For R = H, i.e. dien itself, the usual two term rate law (4.94) is observed and the value of  $k_1$  is shown in Table 4.14. The rate constant  $k_1$ , decreases with increasing steric hindrance as a result of increases in the value of  $\Delta H^\ddagger$ . With the heavily

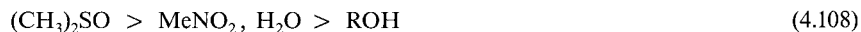
hindered complexes the rate constant  $k_1$  is almost  $10^5$  less in value than for the dien complex and now the  $k_2$  term is difficult to detect<sup>155</sup> unless large concentrations of a strong entering nucleophile are used.<sup>143,156(a)</sup> The values of  $\Delta V^\ddagger$  however throughout the series remain negative at  $-12 \pm 2$ , although rising to  $-3 \pm 1$  cm<sup>3</sup> mol when the replaced group is neutral in Pd(Et<sub>4</sub>dien)NH<sub>3</sub><sup>2+</sup>. One is forced to conclude that the solvolyses remain associative in character even in the hindered complexes although its extent may change. Similar conclusions are reached from an examination of exchange reactions of Pd(R<sub>5</sub>dien)H<sub>2</sub>O<sup>2+</sup> Ref. 156(b). In some respects then these hindered complexes, which have also been examined with Pt(II) and Au(III),<sup>149</sup> resemble their octahedral analogs and they have been termed pseudo-octahedral complexes.<sup>157</sup> They result when bulky ligands in the plane of a four-coordinate metal complex spill over and hinder the apical positions and they resemble the octahedral complexes in reactivity characteristics, while at the same time retaining some features of a square planar complex.

**Table 4.14** Activation Parameters for the Solvolysis of Pd(R<sub>5</sub>dien)Cl<sup>+</sup> in Aqueous Solution using Reaction (4.107) at 25 °C. From Ref. 156(a)

R <sub>5</sub> dien	$k_1$ s <sup>-1</sup>	$\Delta H^\ddagger$ kJ mol <sup>-1</sup>	$\Delta S^\ddagger$ J K <sup>-1</sup> mol <sup>-1</sup>	$\Delta V^\ddagger$ cm <sup>3</sup> mol <sup>-1</sup>
dien	44	43	-69	-10.0
1,4,7-Et <sub>3</sub> dien	10	41	-86	-10.8
1,1,7,7-Et <sub>4</sub> dien	$2.2 \times 10^{-3}$	66	-74	-14.9
1,1,4,7,7-Me <sub>5</sub> dien	0.28	50	-88	-10.9
1,1,4,7,7-Et <sub>5</sub> dien	$7.2 \times 10^{-4}$	59	-106	-12.8

#### 4.7.4 Effect of Solvent

The solvent is the reaction medium and as such, by solvating the ground and activated states, will influence the energetics of the activation process. In addition it acts as a nucleophile in the reaction path represented by  $k_1$ . A large value of  $k_1$  relative to  $k_2$  is observed in solvents capable of coordinating strongly to the metal so that *generally* the order



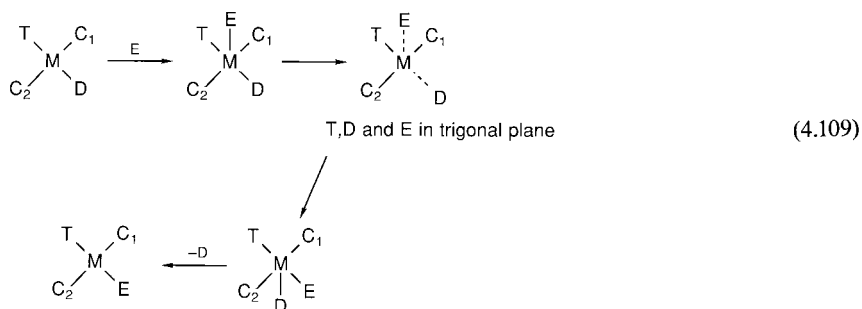
is observed.<sup>149</sup> In solvents that are poor coordinators such as C<sub>6</sub>H<sub>6</sub> and CCl<sub>4</sub>, the  $k_2$  value dominates. The order of nucleophilicities does not however change in different solvents. A linear plot of  $\Delta V^\ddagger$  vs the solvent electrostriction parameter for reaction of *trans*-Pt(py)<sub>2</sub>(Cl)NO<sub>2</sub> with py in a variety of solvents, attests to the importance of solvation in these reactions.<sup>158</sup>

#### 4.7.5 Reaction Pathways

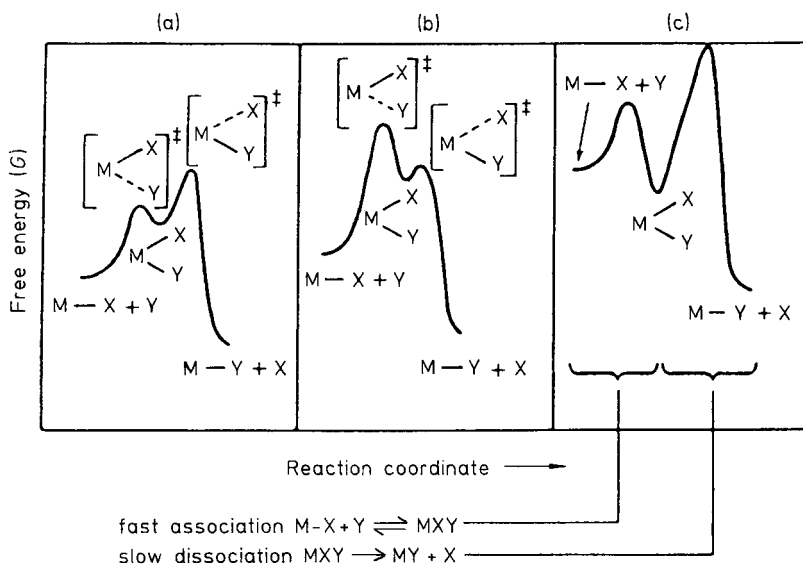
There is naturally an overriding interest in the geometry of the five-coordinate intermediate, or activated complex. General considerations of the shape in which there will be least mutual



interaction of five ligands and of the available orbitals<sup>149</sup> support a trigonal bipyramid. Much replacement behavior can be rationalized on this basis. It has been suggested, however, that both square-pyramid and trigonal-bipyramid geometries are developed in the course of the replacement:<sup>142, 149</sup>



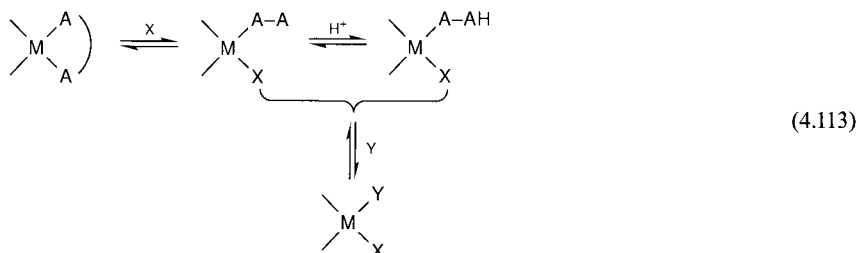
The departing ligand D is replaced by the entering E. The ligands  $C_1$  and  $C_2$  are *cis*, and T is *trans* to D. The full scheme (4.109) should therefore be represented by a reaction profile (Sec. 2.3.6) which contains 3 minima, corresponding to the 3 intermediates and 4 peaks, corresponding to the activated complexes for the four steps.<sup>142</sup> For the sake of simplicity, the reaction profile can be represented as shown in Fig. 4.9. A number of cases are depicted, exaggerating those likely to be encountered in practice. In Fig. 4.9(a) bond breaking is rate-determining and in Fig. 4.9(b) bond making is rate-determining. In both cases, the energy of



**Fig. 4.9** Simplified reaction profiles for various situations in the associative mechanism for substitution in square planar complexes, focusing attention on the replacement  $M-X + Y \rightarrow M-Y + X$  (4.93).



occur at only a slightly slower rate than cleavage of unidentates from the metal (about a factor of 10) so that the enhanced stability of  $\text{Pt}(\text{en})_2^{2+}$  over  $\text{Pt}(\text{NH}_3)_4^{2+}$  resides largely in enhanced formation rates.<sup>160</sup> A proton may aid in the removal of chelating ligands in a manner similar to that of octahedral complexes, although second-order reaction paths are possible:



X and Y may be  $\text{H}_2\text{O}$  or halide groups. A number of reactions of Pd(II) appear to fit this scheme.<sup>161</sup> Ring opening and the subsequent slower displacement of single bonded amine are kinetically separable with  $\text{M} = \text{Au}(\text{III})$ , and each step proceeds via a normal nucleophilic attack.<sup>159</sup>

#### (a) Coordination Chain Reactions

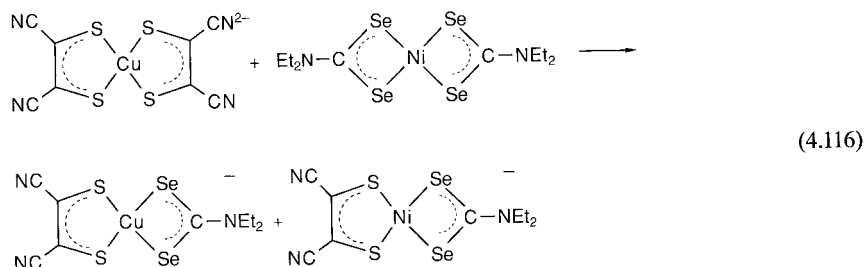
The interaction of two metal chelates,  $\text{MA}_2$  with  $\text{NB}_2$ , poses interesting mechanistic problems. Depending on the system, nature of chelating molecules A and B etc., complete exchange may occur,



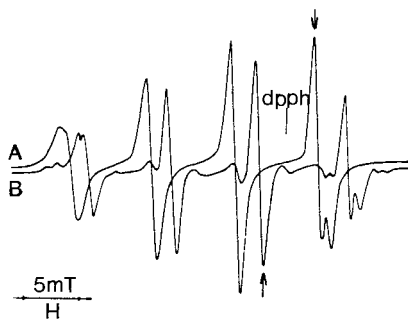
or mixed species may be partially or completely formed<sup>162-164</sup>



As an example, consider the interchange between  $\text{Cu}(\text{mnt})_2^{2-}$  and  $\text{Ni}(\text{Et}_2\text{dsc})_2$

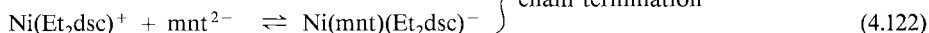
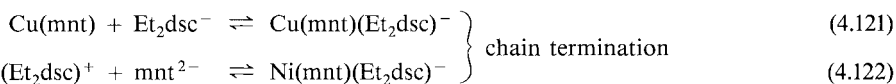
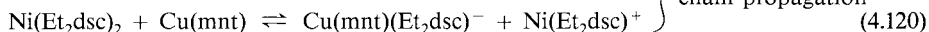
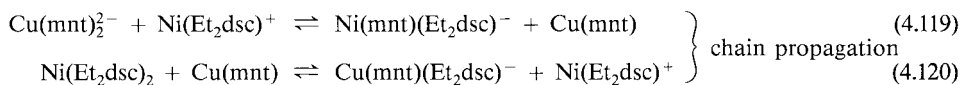
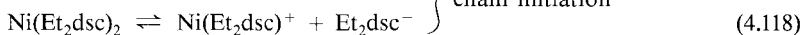
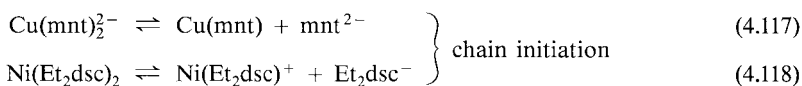


The rate has been measured in 1:1 acetone/ $\text{CHCl}_3$  by a stopped-flow/epr method.<sup>163</sup> The epr signals of  $\text{Cu}(\text{mnt})_2^{2-}$  and  $\text{Cu}(\text{mnt})(\text{Et}_2\text{dsc})^-$  are sufficiently different to allow analysis. (Fig. 4.10). A second-order rate law is usually observed, but this belies a simple mechanism,

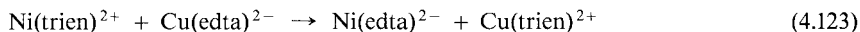


**Fig. 4.10** X-band epr spectra of  $\text{Cu}(\text{mnt})_2^{2-}$  (A) and  $\text{Cu}(\text{mnt})(\text{Et}_2\text{dsc})^-$  (B) at 25°C. The reaction is monitored at the field strengths indicated by the arrows. Full details for the mixing and accumulation of epr signals are given in Ref. 163. Reproduced with permission from J. Stach, R. Kironse, W. Dietzsch, G. Lassmann, V. K. Belyaeva and I. N. Marov *Inorg. Chim. Acta* **96**, 55 (1985).

since with some conditions an S-shaped formation of product with time is observed. In addition the rate is retarded by added ligand ( $\text{Na}_2\text{mnt}$ ) and accelerated by  $\text{Cu}(\text{II})$ . Although a full kinetic study was not reported, the observations were consistent with a chain mechanism, in which there are solvated monochelate intermediates:<sup>162,163</sup>



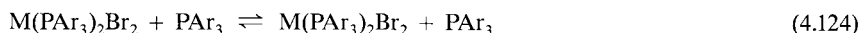
Solid evidence for this type of chain mechanism (differing only in the chain propagation steps) had been earlier obtained by Margerum and his co-workers<sup>165,166</sup> in the study of “coordination chain reactions” between two metal complexes each containing *one* multidentate ligand, edta, trien and so on, e.g.,



A number of cross reactions of the type (4.115) have been studied and, when sufficiently slow, an elegant HPLC batch method (Sec. 3.11 (a)) has been used.<sup>164</sup>

## 4.8 Substitution in Tetrahedral Complexes

The exchange reactions ( $\text{M} = \text{Fe}, \text{Co}, \text{and Ni}$ ;  $\text{Ar} = \text{Ph}$  or *p*-tolyl)



studied in  $\text{CDCl}_3$  by nmr linewidth techniques are all second-order (Table 4.15).<sup>167</sup> The lability trend  $\text{Fe} > \text{Ni} > \text{Co}$  resides mainly in a  $\Delta H^\ddagger$  effect.

**Table 4.15** Rate Constants and Activation Parameters for Ligand Exchange of  $\text{M}(\text{PPh}_3)_2\text{Br}_2$  in  $\text{CDCl}_3$  at  $25^\circ\text{C}$ <sup>167</sup>

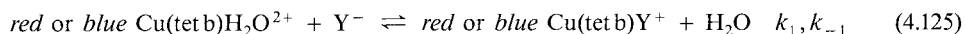
M	$k$ $\text{M}^{-1}\text{s}^{-1}$	$\Delta H^\ddagger$ $\text{kJ mol}^{-1}$	$\Delta S^\ddagger$ $\text{J K}^{-1}\text{mol}^{-1}$
Fe	$2.0 \times 10^5$	16	-92
Co	$8.7 \times 10^2$	32	-79
Ni	$6.9 \times 10^3$	20	-104

Ligand field arguments indicate that the tetrahedral  $d^6$  ground state and five-coordinate  $d^6$  transition state are both stabilized to a lesser extent than the  $d^7$  and  $d^8$  counterparts. These effects would make  $\text{Fe}(\text{II})$  more reactive and less reactive, respectively, than  $\text{Co}(\text{II})$  and  $\text{Ni}(\text{II})$ , so that presumably ground-state destabilization is the more important. For the  $\text{Co}(\text{PPh}_3)_2\text{Br}_2$  exchange with  $\text{Ph}_3\text{P}$  in  $\text{CDCl}_3$ , a value for  $\Delta V^\ddagger = -12.1 \text{ cm}^3\text{mol}^{-1}$  at  $30^\circ\text{C}$  as well as the highly negative  $\Delta S^\ddagger$ , are strong supportive evidence for an associative mechanism.<sup>168</sup> See also Ref. 169 for substitution in the tetrahedral  $\text{FeCl}_4^{2-}$  ion.

The situation is quite different with tetrahedral complexes of  $\text{Ni}(0)$ ,  $\text{Pd}(0)$  and  $\text{Pt}(0)$ . We might anticipate that an associative mechanism would be deterred, because of strong mutual repulsion of the entering nucleophile and the filled  $d$  orbitals of the  $d^{10}$  system. Thus a first-order rate law for substitution in  $\text{Ni}(0)$  carbonyls,<sup>170</sup> and  $\text{M}^0(\text{P}(\text{OC}_2\text{H}_5)_3)_4$   $\text{M} = \text{Ni}$ , (Sec. 1.4.1)  $\text{Pd}$  and  $\text{Pt}$ ,<sup>171</sup> as well as a positive volume of activation ( $+8 \text{ cm}^3\text{mol}^{-1}$ ) for the reaction of  $\text{Ni}(\text{CO})_4$  with  $\text{P}(\text{OEt})_3$  in heptane<sup>172</sup> support an associative mechanism.

## 4.9 Substitution in Five-Coordinate Complexes

Five-coordinate complexes may have either a square-pyramidal or a trigonal-bipyramidal geometry. The replacement reactions of the complexes of mainly  $\text{Co}(\text{II})$ ,  $\text{Ni}(\text{II})$  and  $\text{Cu}(\text{II})$  have been studied in both aqueous and nonaqueous media. As might be expected, the mechanisms of substitution may be associative or dissociative in character.<sup>173</sup> Axial methyl groups in macrocycles such as cyclam and tet b can impose five-coordination on metal complexes, usually square pyramidal geometry, and associative mechanisms. The complex  $\text{Ni}(\text{RSRSM}_e\text{cyclam})(\text{D}_2\text{O})^{2+}$  (**3**) exchanges with  $\text{D}_2\text{O}$  with a negative entropy of activation ( $-24 \text{ J K}^{-1}\text{mol}^{-1}$ ) whereas for *trans*- $\text{Ni}(\text{RRSSM}_e\text{cyclam})(\text{D}_2\text{O})_2^{2+}$ , **2**,  $\Delta S^\ddagger = +38 \text{ J K}^{-1}\text{mol}^{-1}$  for the corresponding exchange<sup>174</sup> (Table 4.9). For the  $\text{Co}(\text{M}_e\text{cyclam})\text{CH}_3\text{CN}^{2+}$ ,  $\text{CH}_3\text{CN}$  exchange,  $k = 6.4 \times 10^5 \text{ s}^{-1}$ ,  $\Delta H^\ddagger = 18.7 \text{ kJ mol}^{-1}$ ,  $\Delta S^\ddagger = -71 \text{ J K}^{-1}\text{mol}^{-1}$  and  $\Delta V^\ddagger = -9.6 \text{ cm}^3\text{mol}^{-1}$  all evidence for an  $I_a$  mechanism. However, for the corresponding  $\text{Ni}$  complex, a slightly positive value for  $\Delta V^\ddagger$  ( $+2.3 \text{ cm}^3\text{mol}^{-1}$ ) is interpreted in terms of a  $D$  mechanism. Significantly, an equilibrium between a 5- and 4-coordinate  $\text{Ni}(\text{II}) - \text{M}_e\text{cyclam}$  complex in  $\text{CH}_3\text{CN}$  has been established.<sup>175</sup> LFER for the reactions (for tet a and tet b see Sec. 7.9):



support the associative character for the anation (Sec. 2.5).<sup>176</sup> The value of  $k_1$  depends on the nucleophilicity of  $\text{Y}^-$  but since the effect is not as pronounced as with  $\text{Pt(II)}$ , an  $I_a$  mechanism may hold.

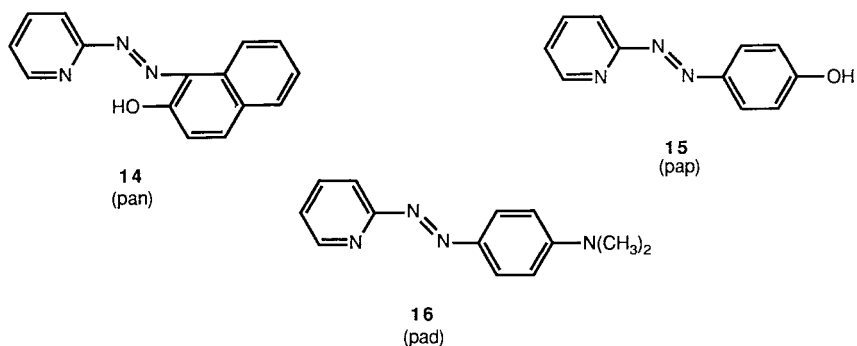
**Table 4.16** Activation Parameters for the Exchange of  $\text{M}(\text{Me}_6\text{tren})\text{dmf}^{2+}$  with  $\text{dmf}$  at  $25^\circ\text{C}$  Ref. 177

M	$k_{\text{exch}}$ $\text{s}^{-1}$	$\Delta H^\ddagger$ $\text{kJ mol}^{-1}$	$\Delta S^\ddagger$ $\text{J K}^{-1} \text{mol}^{-1}$	$\Delta V^\ddagger$ $\text{cm}^3 \text{mol}^{-1}$
Mn	$2.7 \times 10^6$	18	-61	-6
Co	51	52	-36	-2.7
Cu	$5.6 \times 10^2$	43	-47	+6.5

Substitution behavior in a trigonal-bipyramidal structure has been confined to an examination of the exchange of  $\text{M}(\text{Me}_6\text{tren})\text{dmf}^{2+}$ ,  $\text{M} = \text{Mn(II)}$ ,  $\text{Co(II)}$  and  $\text{Cu(II)}$ , with  $\text{dmf}$  (Table 4.16).<sup>177</sup> The values of  $\Delta V^\ddagger$  suggest an increasing dissociative character for the exchange with progressive filling of the  $d_{xz}$  and  $d_{yz}$  orbitals, from Mn to Cu. It is suggested that there is thereby increasing hindering of an approaching  $\text{dmf}$  to any of the three faces of the trigonal bipyramid which are adjacent to the axially-coordinated  $\text{dmf}$ .<sup>177</sup> The dissociative character for substitution in  $\text{Cu}(\text{Me}_6\text{tren})\text{dmf}^{2+}$  is supported by saturation kinetics for anation by  $\text{SCN}^-$  and an associated  $K_0 = 157 \text{ M}^{-1}$  and (as expected)  $k_3 = 5.5 \times 10^2 \text{ s}^{-1}$ . Eqns. (4.10) and (4.11). Ref. 178.

## 4.10 Substitution in Organized Surfactant Systems

The rate of metal complex formation is often modified (usually enhanced) by the presence of a charged interface in the aqueous phase. This may be provided by ionic micelles, e.g., SDS,<sup>179,180</sup> microemulsions<sup>179</sup> or polyelectrolytes.<sup>181,182</sup> The reactions of  $\text{Ni}^{2+}$  and  $\text{Co}^{2+}$  with hydrophobic ligands *pan*, *pap* and *pad* **14–16** are popular ones for examining effects, since they are well characterized in the bulk water. The simple model (4.126)





presupposes rapid interchange of species between the bulk solvent (sol) and the pseudo phase associated with surfactant (sur), compared with the complexation rate. The usual equation for complex formation is modified to allow for micelle surface concentration of  $M^{2+}$

$$k_{\text{obs}} = k_1^{\text{sur}} \frac{[M^{2+}]_T}{([\text{SDS}]_T - \text{cmc})AN} + k_{-1}^{\text{sur}} \quad (4.127)$$

cmc = critical micelle concentration

$A$  = surface area per SDS head group in  $\text{m}^2$

$N$  = Avogadro's Number

The rate constants  $k_1^{\text{sur}}$  and  $k_{-1}^{\text{sur}}$  represent rate constants for a surface reaction and have units  $\text{m}^2\text{mol}^{-1}\text{s}^{-1}$  and  $\text{s}^{-1}$  respectively. The accelerative effects are about  $10^2$ – $10^3$  fold. They indicate that both reactants are bound at the surface layer of the micelle (surfactant-water interface) and the enhanced rates are caused by enhanced reactant concentration here and *there are no other significant effects*.<sup>179</sup> Similar behavior is observed in an inverse micelle, where the water phase is now dispersed as micro-droplets in the organic phase. With this arrangement, it is possible to study anion interchange in the tetrahedral complexes  $\text{CoCl}_4^{2-}$  or  $\text{CoCl}_2(\text{SCN})_2^{2-}$  by temperature-jump. A dissociative mechanism is favored, but the interpretation is complicated by uncertainty in the nature of the species present in the water-surfactant boundary, a general problem in this medium.<sup>183</sup>

If the polyelectrolyte can coordinate strongly to a metal ion, marked deceleration effects can be noted, as, for example, in the reactions of  $\text{Ni}^{2+}$  and  $\text{Co}^{2+}$  with pad in the presence of polyphosphates.<sup>181,182</sup> Modifications of equilibria constants in these micelles must also be recognized as contributing to rate change, e.g., ligand  $pK$  or keto-enol equilibria may be altered.

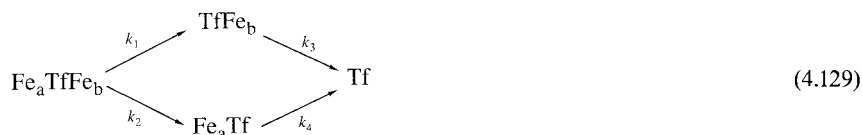
## 4.11 Substitution in Metalloproteins

Undoubtedly the most complicated milieu for a substitution process is that of a protein. However, the principles developed in this chapter for substitution in metal complexes also apply to metalloproteins.<sup>184</sup> Allowance for a role for the protein, particularly near the site, must always be made. The formation and dissociation of a metalloprotein (PM) may be represented in an undoubtedly simplified form as:



where P is a demetallated (apo) protein and ML is a metal-ligand complex. The incorporation of metal ions into proteins appears to occur post-translationally and so the forward direction probably represents the last step in the biosynthesis of many metalloproteins. The occurrence of a ternary intermediate or intermediates is deduced by the observation of “saturation kinetics” or, in rare cases, directly observed. Conformational changes may occur after the metal ion is placed in the metal site. The reverse direction has also been studied, ligand L removing metal ion M from the protein to produce the apo form. From the latter a variety of metalloforms of the protein may be prepared for useful structural analysis. For references and the study of two systems see Refs. 185 and 186. In general, formation rate constants are smaller than those for simpler ligands.

Multisites in proteins are not uncommon. The removal of metal ions from such centers is likely to be involved. This is in fact illustrated by the iron removal from serotransferrin, see also Sec. 2.6. This protein is bilobal and each lobe contains an iron-binding site. These are 35 Å apart and it is believed that direct interaction between the sites is absent. The two Fe's, designated a and b, are different and their removal is biphasic, although not markedly so.

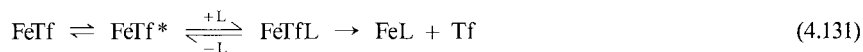


Simultaneous rate equations are complex, but solvable.<sup>187</sup> Simplifications are possible e. g.  $k_1 = k_4$  and  $k_2 = k_3$ , if the sites are non-cooperative. Strong binding ligands such as edta or synthetic siderophores effect iron removal and the two rate constants associated with the biphasic Fe removal are both curved towards saturation when plotted against [ligand].

Such behavior has been encountered in Chapter 1 and conforms to either a mechanism involving formation of a ternary species (considering just one iron):



or rate-determining transformation of a “closed” form (FeTf) to a reactive “open” one, FeTf\*:



(see Sec. 1.6.4).<sup>188-190</sup>

## References

1. Y. Ducommun and A. E. Merbach in B17, Chap. 2.
2. H. Taube, Chem. Revs. **50**, 69 (1952).
3. M. H. M. Abou El-Wafa, M. G. Burnett and J. F. McCullagh, J. Chem. Soc. Dalton Trans. 1059 (1987). Careful analysis shows no direct substitution of  $\text{Cl}^-$  by  $\text{N}_3^-$  in  $\text{Co}(\text{CN})_5\text{Cl}^{3-}$ .
4. W. G. Jackson, B. C. McGregor and S. S. Jurisson, Inorg. Chem. **26**, 1286 (1987). The reactions of 14 different complexes of the type  $\text{Co}(\text{NH}_3)_5\text{X}^{n+}$  with  $\text{SCN}^-$  show 3–19 % *direct* anion capture.



5. For example reaction of reducing ligands with trivalent metal complexes are often accompanied by complex formation.
6. J. Springborg, *Adv. Inorg. Chem.* **32**, 55 (1988).
7. F. P. Rotzinger, H. Stunzi and W. Marty, *Inorg. Chem.* **25**, 489 (1986).
8. H. A. Mottola, *Kinetic Aspects of Analytical Chemistry*, Wiley-Interscience, NY, 1988; D. P.-Bendito and M. Silva, *Kinetic Methods in Analytical Chemistry*, Ellis-Horwood, Chichester 1988.
9. A. S. Mildvan, *Metals in Enzyme Catalysis, in the Enzymes*, Chap. 9.
10. J. P. Hunt and H. L. Friedman, *Prog. Inorg. Chem.* **30**, 359 (1983). This review is concerned with the structure of hydration complexes of ions and includes a discussion of the x-ray or neutron diffraction method for determining structure of ions in solution.
11. T. W. Swaddle, *Inorg. Chem.* **22**, 2663 (1983); T. W. Swaddle and M. K. S. Mak, *Can. J. Chem.* **61**, 473 (1983).
12. J. E. Enderby, S. Cummings, G. J. Herdman, G. W. Neilson, P. S. Salmon and N. Skipper, *J. Phys. Chem.* **91**, 5851 (1987); G. W. Neilson and J. E. Enderby, *Adv. Inorg. Chem.* **34**, 195 (1989).
13. S. F. Lincoln, *Coordn. Chem. Revs.* **6**, 309 (1971); B28, Chap. 2.
14. A. E. Merbach, *Pure Appl. Chem.* **54**, 1479 (1982); **59**, 161 (1987).
15. Terms used by C. H. Langford and H. B. Gray in B31. They replace older ones,  $S_{N2}$  or  $S_{N1}$ , used in B25.
16. T. W. Swaddle, *Substitution Reactions of Divalent and Trivalent Metal Ions, in Adv. Inorg. Bioinorg. Mechs.* **2**, 95 (1983).
17. D. W. Margerum, G. R. Cayley, D. C. Weatherburn and G. K. Pagenkopf in B32, Chap. 1. A complete coverage of substitution and rate data up to 1977.
18. J. F. Coetzee, *Pure Appl. Chem.* **49**, 27 (1977); E. F. Caldin, *Pure Appl. Chem.* **51**, 2067 (1979).
19. D. Darensbourg, *Adv. Organomet. Chem.* **21**, 113 (1982); F. Basolo, *Polyhedron*, **9**, 1503 (1990).
20. L. Mønsted and O. Mønsted, *Coordn. Chem. Revs.* **94**, 109 (1989).
21. P. Moore, *Pure Appl. Chem.* **57**, 347 (1985).
22. L. S. Frankel, *Inorg. Chem.* **10**, 2360 (1971). The exchange rate constant of  $Ni(dmf)_6^{2+}$  with dmf in  $CH_3NO_2$  solution is independent of the composition of the solvent mixture. Since an  $I_d$  mechanism would require an abnormally large  $K_0$ , a  $D$  mechanism is favored.
23. Y. Ducommun, K. E. Newman and A. E. Merbach, *Inorg. Chem.* **19**, 3696 (1980).
24. Y. Ducommun, D. Zbinden and A. E. Merbach, *Helv. Chim. Acta* **65**, 1385 (1982).
25. P. Bernhard, L. Helm, I. Rapaport, A. Ludi and A. E. Merbach, *Inorg. Chem.* **27**, 873 (1988). All exchange  $k$ 's are for a particular solvent molecule (Sec. 1.9).
26. L. Helm, S. F. Lincoln, A. E. Merbach and D. Zbinden, *Inorg. Chem.* **25**, 2550 (1986) and references therein.
27. F. K. Meyer, K. E. Newman and A. E. Merbach, *Inorg. Chem.* **18**, 2142 (1979).
28. M. J. Sisley, Y. Yano and T. W. Swaddle, *Inorg. Chem.* **21**, 1141 (1982).
29. C. Cossy, L. Helm and A. E. Merbach, *Helv. Chim. Acta* **70**, 1516 (1987).
30. L. Fielding and P. Moore, *J. Chem. Soc. Chem. Commun.* **49** (1988).
31. A. Hioki, S. Funahashi, M. Ishii and M. Tanaka, *Inorg. Chem.* **25**, 1360 (1986).
32. D. H-Cleary, L. Helm and A. E. Merbach, *J. Amer. Chem. Soc.* **109**, 4444 (1987) and references therein.
33. A. D. Hugi, L. Helm and A. E. Merbach, *Inorg. Chem.* **26**, 1763 (1987).
34. J. Bjerrum and K. G. Poulsen, *Nature London*, **169**, 463 (1952).
35. T. W. Swaddle and G. Guastalla, *Inorg. Chem.* **8**, 1604 (1969).
36. R. M. Fuoss, *J. Amer. Chem. Soc.* **80**, 5059 (1958); M. Eigen, *Z. Phys. Chem. (Frankfurt)* **1**, 176 (1954).
37. By equating the exponential term to unity and setting  $a = 4 \text{ \AA}$  arbitrarily,  $K_0 = 2.5 \times 10^{21} a^3 \approx 0.15 \text{ M}^{-1}$ . See also J. E. Prue, *J. Chem. Soc.* 7534 (1965); D. B. Rorabacher, *Inorg. Chem.* **5**, 1891 (1966).

38. D. W. Carlyle and J. H. Espenson, *Inorg. Chem.* **8**, 575 (1969); H. Brintzinger and G. G. Hammes, *Inorg. Chem.* **5**, 1286 (1966); P. Hemmes and S. Petrucci, *J. Phys. Chem.* **72**, 3986 (1968).
39. The evidence available indicates that outer-sphere complexing of the  $M-H_2O$  entity does not markedly alter the value of  $k_{\text{exch}}$ . For literature see Refs. 16 and 40.
40. R. G. Wilkins, *Acc. Chem. Res.* **3**, 408 (1970); *Comments Inorg. Chem.* **2**, 187 (1983).
41. K. R. Ashley, M. Berggren and M. Cheng, *J. Amer. Chem. Soc.* **97**, 1422 (1975); K. R. Ashley and J. G. Leipoldt, *Inorg. Chem.* **20**, 2326 (1981).
42. S. Funahashi, M. Inamo, K. Ishihara and M. Tanaka, *Inorg. Chem.* **21**, 447 (1982).
43.  $\Delta V^\ddagger$  is estimated as  $\approx 0 \text{ cm}^3 \text{ mol}^{-1}$  for outer-sphere complex formation involving an uncharged species and  $\approx 3 \text{ cm}^3 \text{ mol}^{-1}$  for reactants whose charge product is  $-2.42$ .
44. J. G. Leipoldt, R. van Eldik and H. Kelm, *Inorg. Chem.* **22**, 4147 (1983).
45. X. Chen and D. V. Stynes, *Inorg. Chem.* **25**, 1173 (1986) and references therein.
46. D. V. Stynes, *Pure Appl. Chem.* **60**, 561 (1988).
47. R. van Eldik, D. A. Palmer and H. Kelm, *Inorg. Chem.* **18**, 1520 (1979).
48. M. Eigen and K. Tamm, *Ber. Bunsenges. Phys. Chem.* **66**, 107 (1962), see also M. Eigen and R. G. Wilkins, *Adv. Chem. Ser.* **49**, 55 (1965).
49.  $\Delta V^\ddagger$  values for reactions of  $Ni^{2+}$  with neutral ligands range from  $+5$  to  $+11 \text{ cm}^3 \text{ mol}^{-1}$ , Ref. 14.
50. A value of  $k_3/k_{\text{exch}}$  as low as 0.2 might arise in the  $I_d$  mechanism if the complexed anion is held randomly around the octahedral complex and only loss of water near to the anion leads to anion entry.
51. P. J. Nichols, Y. Fresard, Y. Ducommun and A. E. Merbach, *Inorg. Chem.* **23**, 4341 (1984).
52. J. H. Espenson, *Inorg. Chem.* **8**, 1554 (1969).
53. A. D. Hugi, L. Helm and A. E. Merbach, *Helv. Chim. Acta* **68**, 508 (1985).
54. Y. Sasaki and A. G. Sykes, *J. Chem. Soc. Dalton Trans.* 1048 (1975).
55. A. Haim, *Inorg. Chem.* **9**, 426 (1970). A similar pattern holds for  $Co(NH_3)_5X^+$ .
56. N. Agmon, *Int. J. Chem. Kinetics* **13**, 333 (1981).
57. N. J. Curtis, G. A. Lawrance and R. van Eldik, *Inorg. Chem.* **28**, 329 (1989).
58. Associative substitution ( $A$ ) in organometallic octahedral complexes involving  $\pi$ -type ligands is well established but not common. F. Basolo, *Inorg. Chim. Acta* **100**, 33 (1985). See Also Ref. 19.
59. S. J. Formosinho, *J. Chem. Soc. Faraday Trans. I*, **83**, 431 (1987).
60. E. Deutsch and H. Taube, *Inorg. Chem.* **7**, 1532 (1968).
61. R. Banerjee, *Coordn. Chem. Revs.* **68**, 145 (1985); G. A. Lawrance, *Adv. Inorg. Chem.* **34**, 145 (1989).
62. C. Bifano and R. G. Linck, *Inorg. Chem.* **7**, 908 (1968).
63. W. Weber, D. A. Palmer and H. Kelm, *Inorg. Chem.* **21**, 1689 (1982).
64. D. A. House, *Coordn. Chem. Revs.* **23**, 223 (1977); *Inorg. Chim. Acta* **51**, 273 (1981).
65. B. F. Anderson, J. D. Bell, D. A. Buckingham, P. J. Cresswell, G. J. Gainsford, L. G. Marzilli, G. B. Robertson and A. M. Sargeson, *Inorg. Chem.* **16**, 3233 (1977).
66. A. L. Crumbliss and W. K. Wilmarth, *J. Amer. Chem. Soc.* **92**, 2593 (1970); D. E. Clegg, J. R. Hall, and N. S. Ham, *Aust. J. Chem.* **23**, 1981 (1970) and references.
67. S.-J. Wang and E. L. King, *Inorg. Chem.* **19**, 1506 (1980).
68. S. Yamada, T. Kido and M. Tanaka, *Inorg. Chem.* **23**, 2990 (1984).
69. H. Ogino and M. Shimura, *Adv. Inorg. Bioinorg. Mechs.* **4**, 107 (1986).
70. D. K. Lavalley, *Coordn. Chem. Revs.* **61**, 55 (1985).
71. K. J. Butenhof, D. Cochenour, J. L. Banyasz and J. E. Stuehr, *Inorg. Chem.* **25**, 691 (1986) studied the rates of reaction of bpy with various Ni(II) species,  $Ni(\text{fad})^{2-}$ ,  $Ni(\text{fadH})^-$  and  $Ni(\text{fadOH})^{3-}$ , see Eqn. (8.121).
72. H. Sigel, R. M.-Balakrishnan and U. K. Häring, *J. Amer. Chem. Soc.* **107**, 5137 (1985).
73. M. L. Tobe, *Adv. Inorg. Bioinorg. Mechs.* **2**, 1 (1983) gives an authoritative and detailed account covering all aspects of base hydrolysis.
74. F. J. Garrick, *Nature London* **139**, 507 (1937).
75. R. G. Pearson, *J. Chem. Educ.* **55**, 720 (1978).

76. G. Marangoni, M. Panayotou and M. L. Tobe, *J. Chem. Soc. Dalton Trans.* 1989 (1973); J. Lichtig, M. E. Sosa and M. L. Tobe, *J. Chem. Soc. Dalton Trans.* 581 (1984).
77. D. A. Buckingham, C. R. Clark and T. W. Lewis, *Inorg. Chem.* **18**, 2041 (1979); D. A. Buckingham, C. R. Clark and W. S. Webley, *Aust. J. Chem.* **33**, 263 (1980).
78. C. Blakeley and M. L. Tobe, *J. Chem. Soc. Dalton Trans.* 1775 (1987).
79. M. Green and H. Taube, *Inorg. Chem.* **2**, 948 (1963).
80. N. E. Brasch, D. A. Buckingham, C. R. Clark and K. S. Finnie, *Inorg. Chem.* **28**, 4567 (1989).
81. D. A. Buckingham, B. M. Foxman and A. M. Sargeson, *Inorg. Chem.* **9**, 1790 (1970).
82. D. A. House, *Coordn. Chem. Revs.* **23**, 223 (1977).
83. D. A. House and H. K. J. Powell, *Inorg. Chem.* **10**, 1583 (1971).
84. Y. Kitamura, R. van Eldik and H. Kelm, *Inorg. Chem.* **23**, 2038 (1984).
85. D. A. House, *Inorg. Chem.* **27**, 2587 (1988).
86. M. E. Sosa and M. L. Tobe, *J. Chem. Soc. Dalton Trans.* 427 (1986).
87. W. G. Jackson and B. H. Dutton, *Inorg. Chem.* **28**, 525 (1989). The case has been made that all "induced" reactions are spontaneous hydrolysis of modified reactants e.g.  $(\text{NH}_3)_5\text{CoN}_3^{2+}$  is modified to  $(\text{NH}_3)_5\text{CoN}_4\text{O}^{3+}$  in the  $\text{NO}^+$  reaction.
88. N. E. Dixon, W. G. Jackson, W. Marty and A. M. Sargeson, *Inorg. Chem.* **21**, 688 (1982).
89. M. J. Gaudin, C. R. Clark and D. A. Buckingham, *Inorg. Chem.* **25**, 2569 (1986).
90. F. P. Rotzinger, *Inorg. Chem.* **27**, 772 (1988).
91. D. A. Buckingham, P. A. Marzilli and A. M. Sargeson, *Inorg. Chem.* **8**, 1595 (1969).
92. P. Comba and W. Marty, *Helv. Chim. Acta* **63**, 693 (1980). See also A. A. Watson, M. R. Prinsep and D. A. House, *Inorg. Chim. Acta* **115**, 95 (1986).
93. Higher rate constants for reactions of aliphatic diamines than expected has long been recognized and explained in terms of a conjugate base mechanism.<sup>17</sup>
94. R. E. Hamm, R. L. Johnson, R. H. Pekins, and R. E. Davis, *J. Amer. Chem. Soc.* **80**, 4469 (1958).
95. M. A. Abdullah, J. Barrett and P. O'Brien, *J. Chem. Soc. Dalton Trans.* 1647 (1984); *Inorg. Chim. Acta* **96**, L35 (1985).
96. B. Mohr and R. van Eldik, *Inorg. Chem.* **24**, 3396 (1985).
97. B. H. Robinson and N. C. White, *J. Chem. Soc. Faraday Trans. I* **74**, 2625 (1978).
98. R. L. Wilder, D. A. Kamp, and C. S. Garner, *Inorg. Chem.* **10**, 1393 (1971).
99. T. P. Dasgupta and G. M. Harris, *J. Amer. Chem. Soc.* **97**, 1733 (1975).
100. R. van Eldik, *Adv. Inorg. Bioinorg. Mechs.* **3**, 275 (1984).
101. R. L. Reeves, G. S. Calabrese and S. A. Harkaway, *Inorg. Chem.* **22**, 3076 (1983); R. L. Reeves, *Inorg. Chem.* **25**, 1473 (1986).
102. M. J. Hynes and B. D. O'Regan, *J. Chem. Soc. Dalton Trans.* 162 (1979).
103. V. S. Sharma and D. L. Leussing, *Inorg. Chem.* **11**, 138 (1972).
104. H. Diebler, F. Secco and M. Venturini, *J. Phys. Chem.* **91**, 5106 (1987).
105. S. Chopra and R. B. Jordan, *Inorg. Chem.* **22**, 1708 (1983).
106. E. Mentasti, F. Secco and M. Venturini, *Inorg. Chem.* **19**, 3528 (1980).
107. B. Perlmutter-Hayman and R. Shinar, *Inorg. Chem.* **15**, 2932 (1976).
108. G. Melson and R. G. Wilkins, *J. Chem. Soc.* 2662 (1963).
109. G. Schwarzenbach, H.-B. Burgi, W. P. Jensen, G. A. Lawrance, L. Mønsted and A. M. Sargeson, *Inorg. Chem.* **22**, 4029 (1983). For a number of Ni(II) amine complexes, the rate constant for Ni–N bond rupture decreases as the Ni–N bond length shortens.
110. D. K. Lin and C. S. Garner, *J. Amer. Chem. Soc.* **91**, 6637 (1969); L. Mønsted, *Acta Chem. Scand.* **A30**, 599 (1976).
111. B. Monzyk and A. L. Crumbliss, *J. Amer. Chem. Soc.* **104**, 4921 (1982); M. Biruš, Z. Bradić, G. Krznarić, N. Kujundžić, M. Pribanić, P. C. Wilkins and R. G. Wilkins, *Inorg. Chem.* **26**, 1000 (1987).
112. H. Kelm and G. M. Harris, *Inorg. Chem.* **6**, 1743 (1967).

113. P. J. Breen, W. DeW. Horrocks, Jr. and K. A. Johnson, *Inorg. Chem.* **25**, 1968 (1986) and extensive refs. mostly before 1980.
114. D. W. Margerum, D. L. Jones and H. M. Rosen, *J. Amer. Chem. Soc.* **87**, 4463 (1965).
115. D. B. Rorabacher and D. W. Margerum, *Inorg. Chem.* **3**, 382 (1964).
116. W.-S. Jung, H. Tomiyasu and H. Fukutomi, *Inorg. Chem.* **25**, 2582 (1986) and references therein.
117. H. Kido and K. Saito, *J. Amer. Chem. Soc.* **110**, 3187 (1988).
118. J. D. Carr, R. A. Libby and D. W. Margerum, *Inorg. Chem.* **6**, 1083 (1967).
119. K. Kumar and P. C. Nigam, *Inorg. Chem.* **20**, 1623 (1981).
120. R. M. Izatt, J. S. Bradshaw, S. A. Nielsen, J. D. Lamb, J. J. Christensen and D. Sen, *Chem. Revs.* **85**, 271 (1985).
121. J. A. Drumhiller, F. Montavon, J. M. Lehn and R. W. Taylor, *Inorg. Chem.* **25**, 3751 (1986) and references therein.
122. N. F. Curtis and S. R. Osvath, *Inorg. Chem.* **27**, 305 (1988) and extensive references.
123. H. Diebler, M. Eigen, G. Ilgenfritz, G. Maass and R. Winkler, *Pure Appl. Chem.* **20**, 93 (1969).
124. J. C. Lockhart, *Adv. Inorg. Bioinorg. Mech.* **1**, 217 (1982), extensive Tables.
125. M. Tanaka, *Pure Appl. Chem.* **55**, 151 (1983).
126. D. K. Cabbiness and D. W. Margerum, *J. Amer. Chem. Soc.* **92**, 2151 (1970).
127. C. T. Lin, D. B. Rorabacher, G. R. Cayley and D. W. Margerum, *Inorg. Chem.* **14**, 919 (1975).
128. F.-T. Chen, C.-S. Lee and C.-S. Chung, *Polyhedron* **2**, 1301 (1983).
129. F. McLaren, P. Moore and A. M. Wynn, *J. Chem. Soc. Chem. Commun.* 798 (1989). E. Kimura, Y. Kotake, T. Koike, M. Shionoya and M. Shiro, *Inorg. Chem.* **29**, 4991 (1990).
130. Y. H. Wu and T. A. Kaden, *Helv. Chim. Acta* **68**, 1611 (1985).
131. Dissociation of  $\text{Na}^+$  complex of dibenzo-[24]-crown-6 is first-order alone in acetonitrile but  $\text{Na}^+$ -assisted in nitromethane (from nmr exchange data). A full discussion of unwrapping mechanisms is given, A. Delville, H. D. H. Stöver and C. Detellier, *J. Amer. Chem. Soc.* **109**, 7293 (1987).
132. P. Fux, J. Lagrange and P. Lagrange, *J. Amer. Chem. Soc.* **107**, 5927 (1985).
133. B. G. Cox, J. Garcia-Rosas and H. Schneider, *J. Amer. Chem. Soc.* **104**, 2434 (1982).
134. (a) A.-M. Albrecht-Gary, Z. Saad, C. O. Dietrich-Buchecker and J.-P. Sauvage, *J. Amer. Chem. Soc.* **107**, 3205 (1985) (b) A.-M. Albrecht-Gary, C. Dietrich-Buchecker, Z. Saad and J.-P. Sauvage, *J. Amer. Chem. Soc.* **110**, 1467 (1988). J.-P. Sauvage, *Acc. Chem. Res.* **23**, 319 (1990).
135. (a) C. Grant Jr. and P. Hambright, *J. Amer. Chem. Soc.* **91**, 4195 (1969) (b) J. Turay and P. Hambright, *Inorg. Chem.* **19**, 562 (1980); A. Shamin and P. Hambright, *Inorg. Chem.* **22**, 694 (1983).
136. S. Funahashi, Y. Yamaguchi and M. Tanaka, *Inorg. Chem.* **23**, 2249 (1984).
137. R. F. Pasternack, G. C. Vogel, C. A. Skowronek, R. K. Harris and J. G. Miller, *Inorg. Chem.* **20**, 3763 (1981). Cu(II) incorporation into tetraphenylporphyrin in dmso shows saturation kinetics. An outer-sphere complex without appreciable distortion of the porphyrin ring is proposed to explain the kinetics.
138. E. B. Fleischer and J. H. Wang, *J. Amer. Chem. Soc.* **82**, 3498 (1960).
139. D. A. Buckingham, C. R. Clark and W. S. Webley, *J. Chem. Soc. Chem. Commun.* 192 (1981).
140. The importance of this deformation in easing metal entry is illustrated by the fact that the porphyrin N-Metraphenylporphyrin is deformed and reacts rapidly and simply with many metal ions.<sup>70,125</sup>
141. J. Nwaeme and P. Hambright, *Inorg. Chem.* **23**, 1990 (1984).
142. R. J. Cross, *Chem. Soc. Revs.* **14**, 197 (1985); *Adv. Inorg. Chem.* **34**, 219 (1989).
143. M. Kotowski and R. van Eldik, in *B17*, Chap. 4.
144. U. Belluco, L. Cattalini, F. Basolo, R. G. Pearson and A. Turco, *J. Amer. Chem. Soc.* **87**, 241 (1965).
145. P. Haake, S. C. Chan, and V. Jones, *Inorg. Chem.* **9**, 1925 (1970).
146. J. K. Beattie, *Inorg. Chim. Acta* **76**, L69 (1983).
147. (a) S. Lanza, D. Minniti, P. Moore, J. Sachinidis, R. Romeo and M. L. Tobe, *Inorg. Chem.* **23**, 4428 (1984); (b) U. Frey, L. Helm, A. E. Merbach and R. Romeo, *J. Amer. Chem. Soc.* **111**, 8161 (1989).
148. D. Minniti, G. Alibrandi, M. L. Tobe and R. Romeo, *Inorg. Chem.* **26**, 3956 (1987).

149. L. Cattalini, Mechanism of Square-Planar Substitution, in B30, p. 266.
150. U. Belluco, R. Ettorre, F. Basolo, R. G. Pearson, and A. Turco, *Inorg. Chem.* **5**, 591 (1966).
151. L. Helm, L. I. Elding and A. E. Merbach, *Helv. Chim. Acta* **67**, 1453 (1984); *Inorg. Chem.* **24**, 1719 (1985).
152. J. J. Pesek and W. R. Mason, *Inorg. Chem.* **22**, 2958 (1983).
153. R. G. Pearson, H. Sobel, and J. Songstad, *J. Amer. Chem. Soc.* **90**, 319 (1968).
154. B31
155. J. B. Goddard and F. Basolo, *Inorg. Chem.* **7**, 963; 2456 (1968).
156. (a) M. Kotowski and R. van Eldik, *Inorg. Chem.* **25**, 3896 (1986); J. J. Pienaar, M. Kotowski and R. van Eldik, *Inorg. Chem.* **28**, 373 (1989); (b) J. Berger, M. Kotowski, R. van Eldik, U. Frey, L. Helm and A. E. Merbach, *Inorg. Chem.* **28**, 3759 (1989).
157. W.H. Baddley and F. Basolo, *J. Amer. Chem. Soc.* **86**, 2075 (1964).
158. M. Kotowski, D. A. Palmer and H. Kelm, *Inorg. Chem.* **18**, 2555 (1979).
159. L. H. Skibsted, *Adv. Inorg. Bioinorg. Mechs.* **4**, 137 (1986).
160. M. J. Carter and J. K. Beattie, *Inorg. Chem.* **9**, 1233 (1970).
161. J. S. Coe and J. R. Lyons, *J. Chem. Soc. A* 829 (1971) and refs.
162. I. N. Marov, M. N. Vargaftig, V. K. Belyaeva, G. A. Evtikova, E.Hoyer, R. Kirmse and W. Dietzsch, *Russ. J. Inorg. Chem.* **23**, 101 (1980).
163. J. Stach, R. Kironse, W. Dietzsch, G. Lassmann, V. K. Belyaeva and I. N. Marov, *Inorg. Chim. Acta* **96**, 55 (1985).
164. M. Moriyasu and Y. Hashimoto, *Bull. Chem. Soc. Japan* **53**, 3590 (1980); **54**, 3374 (1981).
165. D. C. Olson and D. W. Margerum, *J. Amer. Chem. Soc.* **85**, 297 (1963).
166. D. W. Margerum and J. D. Carr, *J. Amer. Chem. Soc.* **88**, 1639, 1645 (1966).
167. L. H. Pignolet, D. Forster, and W. DeW. Horrocks, Jr., *Inorg. Chem.* **7**, 828 (1968).
168. F. K. Meyer, W. L. Earl and A. E. Merbach, *Inorg. Chem.* **18**, 888 (1979).
169. G. P. Algra and S. Balt, *Inorg. Chem.* **20**, 1102 (1981); *Acta Cryst.* **B40**, 582 (1984).
170. L. S. Meriwether and M. L. Fiene, *J. Amer. Chem. Soc.* **81**, 4200 (1959).
171. M. Meier, F. Basolo, and R. G. Pearson, *Inorg. Chem.* **8**, 795 (1969).
172. K. R. Brower and T. S. Chen, *Inorg. Chem.* **12**, 2198 (1973).
173. D. A. Sweigart, *Inorg. Chim. Acta* **18**, 179 (1976).
174. P. Moore, J. Schinidis and G. R. Willey, *J. Chem. Soc. Dalton Trans.* 1323 (1984).
175. L. Helm, P. Meier, A. E. Merbach and P. A. Tregloan, *Inorg. Chim. Acta* **73**, 1 (1983).
176. D.-T. Wu and C.-S. Chung, *Inorg. Chem.* **25**, 4841 (1986).
177. S. F. Lincoln, A. M. Hounslow, D. L. Pisaniello, B. G. Doddridge, J. H. Coates, A. E. Merbach and D. Zbinden, *Inorg. Chem.* **23**, 1090 (1984).
178. S. F. Lincoln, J. H. Coates, B. G. Doddridge and A. M. Hounslow, *Inorg. Chem.* **22**, 2869 (1983).
179. P. D. I. Fletcher and B. H. Robinson, *J. Chem. Soc. Faraday Trans. I* **80**, 2417 (1984) and refs.
180. S. Diekmann and J. Frahm, *J. Chem. Soc. Faraday Trans. I* **75**, 2199 (1979).
181. C. Tondre, *J. Chem. Soc. Faraday Trans. I* **78**, 1795 (1982).
182. N. Sbiti and C. Tondre, *J. Chem. Soc. Faraday Trans. I* **78**, 1809 (1982).
183. A. Yamagishi, T. Masui and F. Watanabe, *Inorg. Chem.* **20**, 513 (1981).
184. *Methods in Enzymology*, Vol. 158, Metallobiochemistry, Part A, eds. J. F. Riordan and B. L. Vallee Academic Press, 1988. Contains authoritative accounts of all aspects of metalloproteins.
185. J.A. Blaszkak, D.R. McMillin, A. T. Thornton and D. L. Tennent, *J. Biol. Chem.* **258**, 9886 (1983) (Cu(II) + apoazurin).
186. J. Hirose and R. G. Wilkins, *Biochemistry* **23**, 3149 (1984) (Co(II) + apoarsanilazotyrosine-248 carboxypeptidase A).
187. For a full analysis see D. Baldwin, *Biochim. Biophys. Acta* **623**, 183 (1980).
188. S. A. Kretchmar and K. N. Raymond, *J. Amer. Chem. Soc.* **108**, 6212 (1986).

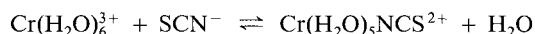
189. I. Bertini, J. Hirose, H. Kozłowski, C. Luchinat, L. Messori and A. Scozzafava, *Inorg. Chem.* **27**, 1081 (1988).  
 190. P. K. Bali and W. R. Harris, *J. Amer. Chem. Soc.* **III**, 4457 (1989).

### Selected Bibliography (Generally relevant to Chaps. 4–8)

- B24. C. F. Baes, Jr. and R. E. Mesmer, *The Hydrolysis of Cations*, Wiley-Interscience, NY, 1976.  
 B25. F. Basolo and R. G. Pearson, *Mechanisms of Inorganic Reactions*, Wiley-Interscience, NY, 1967.  
 B26. D. Benson, *Mechanisms of Inorganic Reactions in Solution*, McGraw-Hill, London, 1968.  
 B27. J. Burgess, *Metal Ions in Solution*, Ellis Horwood, Chichester, 1978.  
 B28. J. Burgess, *Ions in Solution*, Wiley-Interscience, NY, 1988.  
 B29. J. O. Edwards, *Inorganic Reaction Mechanisms*, Benjamin, NY, 1964.  
 B30. J. O. Edwards (ed) *Inorganic Reaction Mechanisms*, Wiley-Interscience, NY, 1970 (Part I); 1972 (Part 2).  
 B31. C. H. Langford and H. B. Gray, *Ligand Substitution Processes*, Benjamin, NY, 1965.  
 B32. A. E. Martell (ed) *Coordination Chemistry Vol. 2*, American Chemical Society, Washington, 1978.  
 B33. A. G. Sykes, *Kinetics of Inorganic Reactions*, Pergamon, Oxford, 1966.  
 B34. M. L. Tobe, *Inorganic Reaction Mechanisms*, Nelson, London, 1972.  
 B35. G. Wilkinson, R. D. Gillard and J. A. McCleverty (eds) *Comprehensive Coordination Chemistry*, Vol. 1. Theory and Background, Pergamon, Oxford, 1987. Chapter 7.1, M. L. Tobe (Substitution); Chapter 7.2, T. J. Meyer and H. Taube (Electron Transfer); Chap. 7.4 D. St. C. Black (Reactions of Coordinated Ligands).

### Problems

1. For the reaction



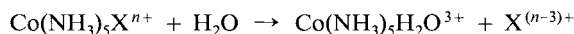
the forward direction is governed by the rate law

$$V = (k_1 + k_2[\text{H}^+]^{-1} + k_3[\text{H}^+]^{-2}) [\text{Cr}^{3+}] [\text{SCN}^-]$$

Using microscopic reversibility considerations, write down the rate law for the reverse direction and deduce the relationship between the various rate constants and thermodynamic parameters for the system.

C. Postmus and E. L. King, *J. Phys. Chem.* **59**, 1216 (1955).

2. For a large number of hydrolyses, X being anions and neutral ligands

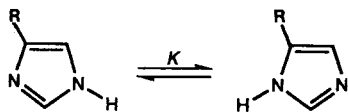


$$\Delta V^\ddagger = 0.48 \Delta V + 1.5$$

where  $\Delta V^\ddagger$  = activation volume and  $\Delta V$  = reaction volume. Discuss the significance of this equation with respect to the mechanism of the hydrolyses.

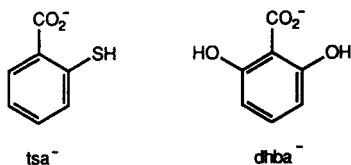
Y. Kitamura, K. Yoshitani and T. Itoh, *Inorg. Chem.* **27**, 996 (1988).

## 3. The tautomeric equilibrium



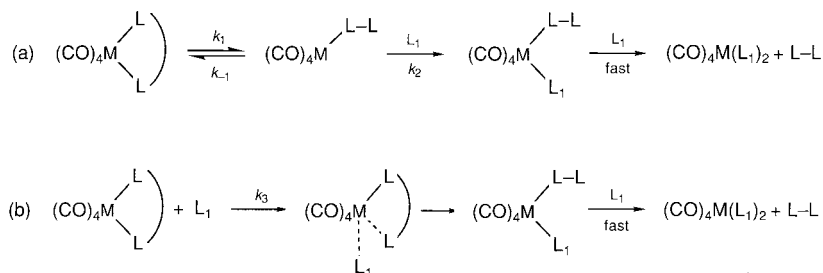
is established rapidly ( $\tau < 10^{-4}$ s). For histamine,  $R = -\text{CH}_2\text{CH}_2\text{NH}_3^+$ , the tautomeric equilibrium constant  $K$  is estimated to be 0.26 from  $^{15}\text{N}$  nmr chemical shift experiments. How might the tautomerism influence the kinetics of chelation of  $\text{Ni}^{2+}$  with histamine? P. Dasgupta and R. B. Jordan, *Inorg. Chem.* **24**, 2721 (1985).

4. (a) Show that the open form of **6** present in  $\approx 0.1\%$  in  $\text{dnsaH}^-$  cannot account for the reduced rate of reaction of  $\text{dnsaH}^-$  (Sec. 4.4.1).  
 (b) Account for the higher rate constant for reaction of  $\text{tsa}^-$  with  $\text{Ni}^{2+}$  ( $9.4 \times 10^3 \text{ M}^{-1}\text{s}^{-1}$ ) compared with that for  $\text{dhba}^-$  ( $65 \text{ M}^{-1}\text{s}^{-1}$ )



H. Diebler, F. Secco and M. Venturini, *J. Phys. Chem.* **91**, 5106 (1987).

5. There are two likely pathways for the replacement of chelates in complexes of the type  $\text{M}(\text{CO})_4(\text{L}_2)$  by an incoming unidentate nucleophile,  $\text{L}_1$



Derive the rate laws for (a) and (b) with  $\text{L}_1$  in excess, and with assumption of a steady-state concentration of the 5-coordinate species in (a) and a rds associated with  $k_3$  in (b). Under what conditions will the rate laws for (a) and (b) be identical? With these conditions in 1,2-dichloroethane  $\Delta V^\ddagger = 14.7 \text{ cm}^3\text{mol}^{-1}$  when  $\text{M} = \text{Cr}$ ,  $\text{L-L} = 3,6$ -dithiaoctane and  $\text{L}_1 = \text{P}(\text{OC}_2\text{H}_5)_3$ . Which mechanism is supported?

H.-T. Macholdt, R. van Eldik and G. R. Dobson, *Inorg. Chem.* **25**, 1914 (1986).

6. (a) The acid hydrolyses of both  $\text{Cu}(\text{12[ane]N}_4)^{2+}$  and  $\text{Cu}(\text{14[ane]N}_4)^{2+}$  are acid-dependent

$$V = k[\text{Cu(II)}][\text{H}^+]$$

Account for the value of  $k$  being  $\approx 10^4$  larger for  $\text{Cu}(\text{12[ane]N}_4)^{2+}$  than for  $\text{Cu}(\text{14[ane]N}_4)^{2+}$

R. W. Hay and M. P. Pujari, *Inorg. Chim. Acta* **100**, L1 (1985).

- (b) The rates of hydrolyses of  $\text{Cu}(\text{2}_N\text{2}_O\text{2}_O)^{2+}$  and  $\text{Cu}(\text{trans-Me}_6\text{[18]dieneN}_4)^{2+}$  are both strongly base dependent with  $n = 3$  and 2 respectively in

$$V = k[\text{Cu(II)}][\text{OH}^-]^n$$

Account for these rate laws.

J. A. Drumhiller, F. Montavon, J. M. Lehn and R. W. Taylor, *Inorg. Chem.* **25**, 3751 (1986); R. W. Hay and R. Bembi, *Inorg. Chim. Acta* **62**, 89 (1982).

7. Rationalize the following rate behavior for Ni(II) complexing with an excess of bidentate ligand, XY = en, gly or phen:

$\text{Ni}^{2+}$ , overall second order at all concentrations of XY

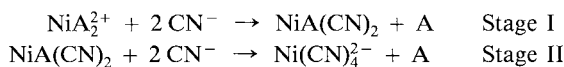
$\text{Ni}(\text{trien})(\text{H}_2\text{O})_2^{2+}$ , second-order at low concentrations of XY and first-order at high concentrations of XY (independent of [XY])

$\text{Ni}(\text{14[ane]N}_4)^{2+}$  first-order at all concentrations of XY

E. J. Billo, *Inorg. Chem.* **23**, 2223 (1984) and references therein.

8. There have been a number of studies of the kinetics of interaction of Ni(II) complexes with  $\text{CN}^-$  ion.

- (a) The square-planar complex  $\text{NiA}_2^{2+}$  reacts with  $\text{CN}^-$  to give  $\text{Ni}(\text{CN})_4^{2-}$  via a discernable intermediate  $\text{NiA}(\text{CN})_2$ , A = 2,3-diamino-2,3-dimethylbutane



At high pH, all the cyanide is present as  $\text{CN}^-$ . The rate laws are

$$\begin{array}{l} \text{Stage I} \quad d[\text{NiA}(\text{CN})_2]/dt = k_1[\text{NiA}_2^{2+}][\text{CN}^-] \\ \text{Stage II} \quad d[\text{Ni}(\text{CN})_4^{2-}]/dt = k_2[\text{NiA}(\text{CN})_2][\text{CN}^-]^2 \end{array}$$

The pH-dependence of Stage II was determined from pH 10.7 to 6.3. The order in total cyanide ion remains 2 and the rate law is

$$d[\text{Ni}(\text{CN})_4^{2-}]/dt = (k_2[\text{CN}^-]^2 + k_3[\text{CN}^-][\text{HCN}] + k_4[\text{HCN}]^2 + k_5[\text{NiA}(\text{CN})_2])$$



Suggest mechanisms for these rate laws.

J. C. Pleskowicz and E. J. Billo, *Inorg. Chim. Acta* **99**, 149 (1985).

(b) The rate law for the reaction between Ni(edda) and  $\text{CN}^-$  at pH 10.8 is

$$V = k[\text{Ni(edda)}][\text{CN}^-]^n$$

where  $n$  varies from 3 at low  $[\text{CN}^-]$  to 1 at high  $[\text{CN}^-]$ . Suggest a mechanism, and a reason why the similar reaction between Ni(cydta) $^{2-}$  and  $\text{CN}^-$  is much slower.

L. C. Coombs, D. W. Margerum and P. C. Nigam, *Inorg. Chem.* **9**, 2081 (1970).

(c) For the reaction of the binuclear chelate  $\text{Ni}_2\text{L}$  with  $\text{CN}^-$  to form  $\text{Ni}(\text{CN})_4^{2-}$  in one observable step, at high pH,

$$V = \{k_1 + k_2[\text{CN}^-]\}[\text{Ni}_2\text{L}]$$

where L = diethylenetriaminepentaacetate. Suggest a mechanism.

K. Kumar, H. C. Bajaj and P. C. Nigam, *J. Phys. Chem.* **84**, 2351 (1980).

9. (a) Account for the following two rate laws which have been observed for the incorporation of M(II) into  $\text{PH}_2$  (porphyrin)

$$(a) V = k[\text{M}]^2[\text{PH}_2]$$

$$(b) V = k_1[\text{PH}_2]$$

J. Weaver and P. Hambricht, *Inorg. Chem.* **8**, 167 (1969); C. Grant, Jr. and P. Hambricht, *J. Amer. Chem. Soc.* **91**, 4195 (1969).

(b) The structure of the porphyrin ring of both the ligand and metal complexes of N-substituted porphyrins is very similar. How would you expect the dissociation of N-substituted and unsubstituted porphyrin complexes to differ with respect to rate law, effect of  $\text{H}^+$ , rates, etc?

D. K. Lavalley, *The Chemistry and Biochemistry of N-Substituted Porphyrins*, VCH 1987 p. 112.

10. Using scheme (4.109) show how *cis*- $\text{MA}_2\text{B}_2$  could be transformed into *trans*- $\text{MA}_2\text{B}_2$  in the presence of free ligand A. See Sec. 7.7.2.

R. J. Cross, *Chem. Soc. Revs.* **14**, 197 (1985).

11. (a) What form will the rate law for substitution in square-planar complexes take if the solvolysis of the complex is rapid compared with ligand substitution? (This occurs in reactions of  $\text{PtCl}_4^{2-}$  with  $^*\text{Cl}^-$ , bpy and phen).

F. A. Palocsay and J. V. Rund, *Inorg. Chem.* **8**, 524 (1969).

(b) Predict the effects of the concentrations of  $\text{I}^-$  and  $\text{OH}^-$  on the rate constants for replacement of  $\text{Cl}^-$  in  $\text{Pd}(\text{dien})\text{Cl}^+$ ,  $\text{Pd}(1,4,7\text{-Me}_3\text{dien})\text{Cl}^+$ ,  $\text{Pd}(1,1,7,7\text{-Me}_4\text{dien})\text{Cl}^+$  and  $\text{Pd}(1,1,4,7,7\text{-Me}_5\text{dien})\text{Cl}^+$ .

J. B. Goddard and F. Basolo, *Inorg. Chem.* **7**, 936 (1968); E. L. J. Breet and R. van Eldik, *Inorg. Chem.* **23**, 1865 (1984).

12. Give a reasonable explanation for the fact that the lability of dmf in  $M(\text{Me}_6\text{tren})\text{dmf}^{2+}$  is some  $10^5$  less than in  $M(\text{dmf})_6^{2+}$  for both  $M = \text{Co}$  and  $\text{Cu}$ .

S. F. Lincoln, J. H. Coates, B. G. Doddridge and A. M. Hounslow, *Inorg. Chem.* **22**, 2869 (1983).

# Chapter 5

## Oxidation-Reduction Reactions

### 5.1 General Characteristics

Oxidation-reduction (redox) reactions of the transition metal complexes are probably the best understood of the types of processes we are concerned with. In redox reactions, the oxidation state of at least two reactants changes. A variety of such reactions are shown in Table 5.1.<sup>1-7</sup>

**Table 5.1** Some Types of Redox Reactions

Redox Reaction	Characteristics	Ref.
1. $^*Co(NH_3)_6^{2+} + Co(NH_3)_6^{3+} \rightleftharpoons$ $^*Co(NH_3)_6^{3+} + Co(NH_3)_6^{2+}$	Extremely slow, $k = (8 \pm 1) \times 10^{-6} M^{-1} s^{-1}$ at 40°C, $\mu = 2.5 M$	1
2. $^*Fe(bpy)_3^{2+} + Fe(bpy)_3^{3+} \rightleftharpoons$ $^*Fe(bpy)_3^{3+} + Fe(bpy)_3^{2+}$	$k = 3 \times 10^8 M^{-1} s^{-1}$	2
3. $^*Cr^{2+} + CrCl^{2+} \rightleftharpoons$ $^*CrCl^{2+} + Cr^{2+}$	$k = 9 M^{-1} s^{-1}$ at 0°C	3
4. $Cr^{2+} + Co(NH_3)_5Cl^{2+} + 5 H^+ \rightarrow$ $CrCl^{2+} + Co^{2+} + 5 NH_4^+$	$k = 6 \times 10^5 M^{-1} s^{-1}$ , one of earliest examples of an inner-sphere redox reaction	4, 5
5. $2 Fe^{3+} + H_2A \rightarrow$ $2 Fe^{2+} + 2 H^+ + A$	$H_2A =$ ascorbic acid. Fe(III) complexes formed. Mechanism complicated.	6
6. Horse cytochrome-c(II) + $Co(phen)_3^{3+} \rightleftharpoons$ horse cytochrome-c(III) + $Co(phen)_3^{2+}$	$k = 1.8 \times 10^3 M^{-1} s^{-1}$ . Site on protein implicated for binding, different than that used by $Fe(CN)_6^{3-}$ ( $k = 9 \times 10^5 M^{-1} s^{-1}$ )	7

A net chemical change does not necessarily occur as a result of the redox reaction. Reactions 1 and 2 (Table 5.1) involve an interchange of electrons between two similar metal complex ions. Such isotopic exchange reactions were the subject of a sizable number of studies in the late forties and fifties,<sup>8</sup> and the novelty at that time of working with radioactive isotopes attracted many physical chemists to inorganic reaction mechanisms. Reactions 1 and 2 emphasize the wide variation in rates encountered here, as in substitution. One of the challenges we must face is rationalizing these large differences in rate constants (14 orders of magnitude), as well as interpreting smaller more subtle disparities. Reaction 3 indicates that isotopic exchange may not involve merely electron transfer but also movement of atoms (chlorine in this case).

Redox reactions usually lead, however, to a marked change in the species, as reactions 4-6 indicate. Important reactions involve the oxidation of organic and metalloprotein substrates (reactions 5 and 6) by oxidizing complex ions. Here the substrate often has ligand properties, and the first step in the overall process appears to be complex formation between the metal and substrate species. Redox reactions will often then be phenomenologically associated with substitution. After complex formation, the redox reaction can occur in a variety of ways, of which a direct intramolecular electron transfer within the adduct is the most obvious.

Spectrophotometry has been a popular means of monitoring redox reactions, with increasing use being made of flow, pulse radiolytic and laser photolytic techniques. The majority of redox reactions, even those with involved stoichiometry, have second-order characteristics. There is also an important group of reactions in which first-order intramolecular electron transfer is involved. Less straightforward kinetics may arise with redox reactions that involve metal complex or radical intermediates, or multi-electron transfer, as in the reduction of Cr(VI) to Cr(III).<sup>9</sup> Reactants with different equivalences as in the noncomplementary reaction



often give rise to complicated kinetic rate laws.<sup>10</sup>

Proton-accelerated rates are often observed when the net reaction involves protons since some of these will have been lost or gained at the transition state. This is the situation with a large number of reactions of oxyions.

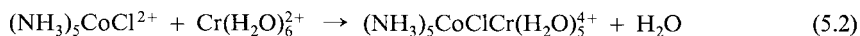
## 5.2 Classification of Redox Reactions

The most important single development in the understanding of the mechanisms of redox reactions has probably been the recognition and establishment of *outer-sphere* and *inner-sphere* processes.<sup>4</sup> Outer-sphere electron transfer involves intact (although not completely undisturbed) coordination shells of the reactants. In inner-sphere redox reactions, there are marked changes in the coordination spheres of the reactants in the formation of the activated complex.

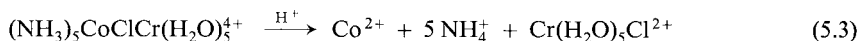
Reaction 2 in Table 5.1 must qualify for an outer-sphere redox category since the bipyridine could not become detached, even by just one end of the bidentate ligand, from the inert iron(II) or iron(III) centers during the course of the rapid redox reaction. There is thus no bond breaking or making during the electron transfer, a situation making them ideal for treatment by the theoretical chemist (Sec. 5.4).

Reaction 4 in Table 5.1, on the other hand, was one of the first-established examples of an inner-sphere redox reaction.<sup>4</sup> The rapid reaction gives  $\text{CrCl}^{2+}$  as a product, characterized spectrally after separation by ion exchange from the remainder of the species in solution. It is clear that since  $\text{CrCl}^{2+}$  could not possibly be produced from  $\text{Cr}^{3+}$  and  $\text{Cl}^-$  ions during the brief time for reaction and ion-exchanger manipulation, it must arise from the redox pro-

cess *per se*. Thus an activated complex or intermediate of the composition shown in (5.2) must arise from the penetration of the chromium(II) ion by the coordinated chloride of the cobalt(III):



Within this species, an intramolecular electron transfer from Cr(II) to Co(III) must occur, producing Cr(III) and Co(II). The adduct then breaks up and the Cr(III) takes along the chloride as the species  $\text{CrCl}^{2+}$ :



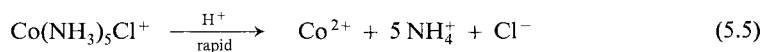
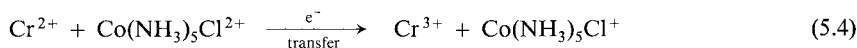
This scheme implies that at no time does chloride ion break free of the influence of at least one of the metals, and in support of this there is no incorporation of  $^{36}\text{Cl}$  in  $\text{CrCl}^{2+}$  when the reaction takes place in the presence of  $^{36}\text{Cl}^-$  ion.<sup>4</sup>

### 5.3 Characterization of Mechanism

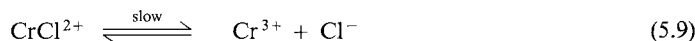
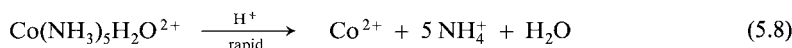
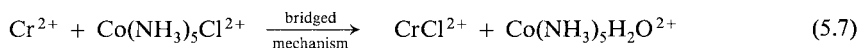
The characterization of a redox reaction as inner-sphere or outer-sphere is a primary preoccupation of the redox kineticist. The assignment is sometimes obvious, but often difficult and in certain cases impossible!

(a) From the Nature of the Products. The *eventual* products from reaction 4, Table 5.1, are  $\text{Cr}^{3+}$ ,  $\text{CrCl}^{2+}$ ,  $\text{Co}^{2+}$ ,  $\text{Cl}^-$ , and  $\text{NH}_4^+$  ions. These could arise from an outer- or an inner-sphere process:<sup>11</sup>

Outer-sphere:



Inner-sphere:



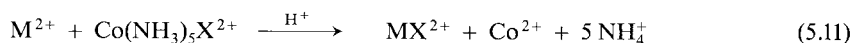
The inertness of  $\text{CrCl}^{2+}$  and the labilities of  $\text{Cr}^{2+}$  and  $\text{Co}^{2+}$  (in part responsible for the rapidity of the intermediate formation and the breakup steps) were thus cleverly exploited to provide unambiguous proof for the operation of the inner-sphere process.<sup>4</sup> Since most redox

reactions involving  $\text{Cr}^{2+}$  are rapid, and the hydrolyses of most Cr(III) complexes slow, it is not difficult to detect the intermediate  $\text{CrX}^{n+}$ , for example,



and, in so doing, characterize the reaction as inner-sphere. This has been demonstrated in the Cr(II) reduction of a large number of Co(III), Cr(III), Fe(III) and recently Rh(III)<sup>12</sup> oxidants.<sup>13</sup>

The only other common reducing agents that can lead to products leisurely characterizable, because they hydrolyze extremely slowly, are  $\text{Co}(\text{CN})_5^{3-}$ ,  $\text{Fe}(\text{CN})_5\text{H}_2\text{O}^{3-}$  and  $\text{Ru}(\text{NH}_3)_5\text{H}_2\text{O}^{2+}$ . With the other common reducing agents,  $\text{Fe}^{2+}$ ,  $\text{V}^{2+}$ ,  $\text{Eu}^{2+}$ , and  $\text{Cu}^+$ , any product will hydrolyze rapidly; for example,



**Table 5.2** Rate Parameters and Characteristics of Some Reactions of V(II) at 25°C, Refs. 15 and 16.

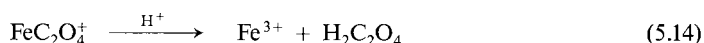
Reactant	$k$ $\text{M}^{-1}\text{s}^{-1}$	$\Delta H^\ddagger$ $\text{kJ mol}^{-1}$	$\Delta S^\ddagger$ $\text{J K}^{-1}\text{mol}^{-1}$
<i>Inner-sphere redox, intermediate detected</i>			
$\text{CrSCN}^{2+}$	8.0	54	-46
$\text{VO}^{2+}$	1.6	51	-71
$\text{Co}(\text{NH}_3)_5\text{SCN}^{2+}$	30	69	+25
$\text{Co}(\text{NH}_3)_5\text{C}_2\text{O}_4^+$	45	51	-42
<i>cis</i> - $\text{Co}(\text{en})_2(\text{N}_3)_2^+$	33	...	...
$\text{Co}(\text{CN})_5\text{N}_3^{3-}$	112	...	...
$\text{Co}(\text{CN})_5\text{SCN}^{3-}$	140	...	...
<i>Probably inner-sphere redox</i>			
$\text{Cu}^{2+}$	27	48	-59
$\text{Co}(\text{NH}_3)_5\text{N}_3^+$	13	49	-59
$\text{Co}(\text{NH}_3)_5\text{SO}_4^+$	26	49	-54
$\text{Co}(\text{NH}_3)_5\text{OCOR}^{2+}$	1-21 <sup>a</sup>	46-51 <sup>a</sup>	-54 to -71 <sup>a</sup>
$\text{Co}(\text{CN})_5\text{X}^{3-}$	120-280 <sup>b</sup>	...	...
<i>Probably outer-sphere redox</i>			
$\text{Co}(\text{NH}_3)_5\text{Cl}^{2+}$	10	31	-121
$\text{Co}(\text{NH}_3)_5\text{H}_2\text{O}^{3+}$	0.53	34	-134
$\text{Co}(\text{NH}_3)_6^{3+}$	0.004	38	-167
$\text{RuCl}^{2+}$	$1.9 \times 10^3$	...	...
$\text{Fe}^{3+}$	$1.8 \times 10^4$	...	...
$\text{FeX}^{2+}$	$(4.6-6.6) \times 10^5$ <sup>c</sup>	...	...
<i>Replacement reaction</i>			
$\text{NCS}^-$	24	67	+5
$\text{H}_2\text{O}$	89 <sup>d</sup>	62	-0.4

<sup>a</sup> Variety of R groups. <sup>b</sup> X =  $\text{Cl}^-$ ,  $\text{Br}^-$ ,  $\text{I}^-$  and  $\text{H}_2\text{O}$ . <sup>c</sup> X =  $\text{Cl}^-$ ,  $\text{N}_3^-$  and  $\text{NCS}^-$ .

<sup>d</sup> First-order rate constant ( $\text{s}^{-1}$ ) for water exchange.

It will be very difficult to detect Cu(II)X and Eu(III)X as intermediates because of their marked lability, and therefore hard to characterize  $\text{Cu}^+$  and  $\text{Eu}^{2+}$  as inner-sphere reductants by product identification. It is easier to detect Fe(III) and V(III) species, by flow methods, and a number of reactions of  $\text{Fe}^{2+}$  with Co(III) complexes<sup>14</sup> and  $\text{V}^{2+}$  with V(IV), Co(III), and Cr(III) complexes, Table 5.2,<sup>15,16</sup> have been shown to progress via the intermediate required of an inner-sphere reaction.

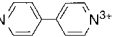
Closer examination of the reaction between  $\text{Fe}^{2+}$  and  $\text{Co}(\text{C}_2\text{O}_4)_3^{3-}$  (Sec. 3.7), for example, shows the formation and decay of an intermediate  $\text{FeC}_2\text{O}_4^+$  ion,<sup>14</sup>



Obviously, for success in this approach, the rate of the redox step producing the intermediate must be at least as fast as the decomposition of the intermediate. This can be sometimes accomplished by increasing the reactant concentrations, since the first step is second order and the second step is first order.

(b) By the Detection of a Bridged Species. The detection of a bridged complex comparable to that in (5.2) does not prove (although it may suggest) that it is an intermediate in an inner-sphere redox process. The bridged species could be in equilibrium with the reactants, but the products form directly from reactants by an outer-sphere process. This apparently occurs in the reaction of  $\text{Co}(\text{edta})^{2-}$  with  $\text{Fe}(\text{CN})_6^{3-}$  (Sec. 1.6.4). The possible oxidation states of the metals in the bridged species in (5.2) are either Cr(II) and Co(III) or Cr(III) and Co(II). In both cases, one of the components is quite labile, and the binuclear species will respectively either return to reactants or dissociate to products rather than exist independently for any length of time. When both partners in the bridged intermediate are inert, however, there is every chance that it will be detected, or at least its presence inferred from the form of the rate law, or the magnitude of the activation parameter (Sec. 5.5). A number of such systems are shown in Table 5.3.<sup>16</sup> The oxidation states of the detected species are deduced from spectral or chemical considerations. In only the last two entries are the oxidation states of the metals in the bridged complex the same as the oxidation state of the reactants. Such bridged in-

**Table 5.3** Some Bridged Species Arising from Redox Reactions.<sup>16</sup>

Reactants	Species
Cr(II) + Ru(III) chloro complexes	Cr(III)–Cl–Ru(II)
$\text{Co}(\text{CN})_5^{3-} + \text{IrCl}_6^{2-}$	Co(III)–Cl–Ir(III)
$\text{Co}(\text{edta})^{2-} + \text{Fe}(\text{CN})_6^{3-}$	Co(III)–NC–Fe(II)
Cr(II) + V(IV)	Cr(III)–(OH) <sub>2</sub> –V(III) <sup>a</sup>
Fe(II) + $\text{Co}(\text{NH}_3)_5\text{nta}$	Fe(II)–nta–Co(III) <sup>b</sup>
$\text{Fe}(\text{CN})_5\text{H}_2\text{O}^{2-} + \text{Co}(\text{NH}_3)_5$ 	$(\text{NC})_5\text{Fe}^{\text{II}}\text{N} \text{---} \text{N} \text{---} \text{NCo}^{\text{II}}(\text{NH}_3)_5^{\text{b}}$

<sup>a</sup> This is one of a number of examples in which a binuclear complex with an –O– (or (OH)<sub>2</sub>) or OH bridge results from the interaction of oxyions.<sup>18</sup>

<sup>b</sup> These species undergo intramolecular electron transfer at measurable rates (Sec. 5.8.1).

intermediates are termed precursor complexes to distinguish them from the more commonly encountered successor complexes in which electron transfer has already taken place (Sec. 5.5). In order to obtain sizeable amounts of a precursor complex it is clear that there must be a very strong affinity by the bridging ligand for the reactant partners.

(c) From Rate Data. Both inner- and outer-sphere redox reactions are usually second-order

$$V = k [\text{oxidant}] [\text{reductant}] \quad (5.15)$$

Only in a limited number of instances will the value of  $k$  and its associated parameters be useful in diagnosing mechanism. When the redox rate is faster than substitution within either reactant, we can be fairly certain that an outer-sphere mechanism holds.<sup>17</sup> This is the case with  $\text{Fe}^{3+}$  and  $\text{RuCl}_2^{2+}$  oxidation of  $\text{V(II)}$ <sup>15</sup> and with rapid electron transfer between inert partners. On the other hand, when the activation parameters for substitution and redox reactions of one of the reactants are similar, an inner-sphere redox reaction, controlled by replacement, is highly likely.<sup>18</sup> This appears to be the case with the oxidation by a number of  $\text{Co(III)}$  complexes of  $\text{V(II)}$ ,<sup>15</sup> confirmed in some instances by the appearance of the requisite  $\text{V(III)}$  complex, e. g.



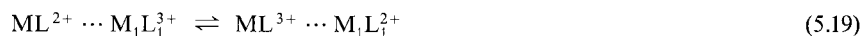
An  $[\text{H}^+]^{-1}$  term in the rate law for reactions involving an aqua redox partner strongly suggests the participation of a hydroxo species and the operation of an inner-sphere redox reaction (Sec. 5.5(a)). Methods (a) and (b) are direct ones for characterizing inner-sphere processes, analyzing for products or intermediates which are kinetically-controlled. Method (c) is indirect. Other methods of distinguishing between the two basic mechanisms are also necessarily indirect. They are based on patterns of reactivity, often constructed from data for authentic inner-sphere and outer-sphere processes. They will be discussed in a later section.

## 5.4 Outer Sphere Reactions

Consider one of the most common types of outer-sphere reactions involving bivalent and trivalent metal complexes,  $\text{ML}^{2+}$  and  $\text{M}_1\text{L}_1^{3+}$  where  $\text{L}$  and  $\text{L}_1$  represent the total ligand structure and  $\text{M}$  and  $\text{M}_1$  or/and  $\text{L}$  and  $\text{L}_1$  may be different, as in the reactant pairs,  $\text{V(H}_2\text{O)}_6^{2+}$  and  $\text{Fe(H}_2\text{O)}_6^{3+}$ ,  $\text{Fe(H}_2\text{O)}_6^{2+}$  and  $\text{Fe(bpy)}_3^{3+}$ , and  $\text{V(H}_2\text{O)}_6^{2+}$  and  $\text{Ru(NH}_3)_6^{3+}$ . The outer-sphere process can be envisaged as



proceeding in three steps





A precursor complex is very rapidly formed in (5.18). It undergoes intramolecular electron transfer (5.19) to give a successor complex, which rapidly breaks down to products (5.20). In outer sphere reactions, it is noted that the two reactants do not share at any time a common atom or group. Such reactions then are particularly suitable as a basis for the calculation of rate constants since no bond breaking or making occurs during the electron transfer. The coordination shell and immediate environment for the reactants and for the products will differ as a result of a redox reaction. However internuclear distances and nuclear velocities cannot change during the electron transition of a redox reaction (Franck-Condon principle). Therefore some "common state" must be reached for each reactant prior to electron transfer. It is the free energy  $\Delta G^*$  that is required to change the atomic coordinates from their equilibrium values to those in the activated complex, which must be calculated in any theory.

The work required to bring the ions 1 and 2 (charges  $z_1$  and  $z_2$ ) to the separation distance  $r$  ( $= a_1 + a_2$ ) is  $w_{12}$  where

$$w_{12} = \frac{z_1 z_2 e^2}{D_s r (1 + \beta r \mu^{1/2})} = \frac{4.25 \times 10^{-8} z_1 z_2}{r (1 + 3.29 \times 10^7 r \mu^{1/2})} \quad (5.21)$$

and  $\beta$  (Debye-Hückel constant) is given by

$$\beta = \left( \frac{8 \pi N^2 e^2}{1000 D_s RT} \right)^{1/2} = 0.329 \text{ \AA}^{-1} \text{ in H}_2\text{O at } 25^\circ\text{C} \quad (5.22)$$

The reorganization terms,  $\lambda_o$  and  $\lambda_i$  are given by

$$\lambda_o = (\Delta e)^2 \left( \frac{1}{2 a_1} + \frac{1}{2 a_2} - \frac{1}{r} \right) \left( \frac{1}{n^2} - \frac{1}{D_s} \right) \quad (5.23)$$

$$\lambda_i = \sum_j \frac{f_j^i f_j^p (\Delta q_j)^2}{f_j^i + f_j^p} = \frac{3 \bar{f} (\Delta d)^2}{2} \quad (5.24)$$

where  $N$  = Avogadro's number

$D_s$  = Dielectric constant of the medium

$n$  = Refractive index of the medium

$(\Delta e)$  = Charge transferred from one reactant to another

$f_j^i$  and  $f_j^p$  =  $j$ th normal mode force constants in the reactants and products respectively. Breathing vibrations are often employed and  $\bar{f}$  = mean of the breathing force constants.

$\Delta q_j$  = change in equilibrium value of the  $j$ th normal coordinate, and when breathing vibrations are employed

$\Delta d$  = the difference of the metal-ligand distance between oxidized and reduced complex.

Several workers, particularly Marcus and Hush, tackled the calculation of  $\Delta G^*$ ; for an account and comparison of the various early attempts, the reader is referred to Refs. 19 and 20. This important area has been thoroughly reviewed and representative examples in Refs. 21–25 as well as in the Selected Bibliography give accounts of the theory in varying depths as well as an entry into the vast literature.

The free energy barrier  $\Delta G^*$  is considered to consist of various components:

1. The work required to bring the reactants (assumed to be rigid spheres of radius  $a_1$  and  $a_2$ ) to their mean separation distance in the activated complex ( $r = a_1 + a_2$ ) and then remove the products to infinity. These work terms are  $w^r$  and  $-w^p$ , respectively, and incorporate electrostatic and nonpolar contributions.

2. The free energy required to reorganize the solvent molecules around the reactants (the outer coordination shell) and to reorganize the inner coordination shell of the reactants. These are termed  $\lambda_o$  and  $\lambda_i$ , respectively.

3. The standard free energy of the reaction in the conditions of the experimental medium and when the reactants are far apart. The quantity  $(\Delta G^o + w^p - w^r)$  is important since it is the standard free energy of the reaction at the separation distance (it is the work-corrected free energy of reaction). Both the  $w$  and  $\lambda_o$  terms can be fairly easily calculated. The term  $\lambda_i$  is quite difficult to estimate, requiring a knowledge of bond lengths and force constants of the reactants (see Inset).

Marcus has derived the expression (alternative forms are often seen)

$$\Delta G^* = \frac{w^r + w^p}{2} + \frac{\lambda_o + \lambda_i}{4} + \frac{\Delta G^o}{2} + \frac{(\Delta G^o + w^p - w^r)^2}{4(\lambda_o + \lambda_i)} \quad (5.25)$$

The free energy term  $\Delta G^*$  is related to the free energy of activation  $\Delta G^\ddagger$  by

$$\Delta G^* = \Delta G^\ddagger - RT \ln \left( \frac{hZ}{kT} \right) = (\Delta G^\ddagger - 2.8) \text{ kcal mol}^{-1} \quad (5.26)$$

and to the rate constant  $k$  by the expression

$$k = \kappa A r^2 \exp(-\Delta G^*/RT) \quad (5.27)$$

The transmission coefficient  $\kappa$  is approximately 1 for reactions in which there is substantial ( $>4$  kJ) electronic coupling between the reactants (adiabatic reactions).  $A r^2$  is calculable if necessary<sup>25,26</sup> but is usually approximated by  $Z$ , the effective collision frequency in solution, and assumed to be  $10^{11} \text{ M}^{-1} \text{ s}^{-1}$ . Thus it is possible in principle to calculate the rate constant of an outer-sphere redox reaction from a set of *nonkinetic* parameters, including molecular size, bond length, vibration frequency and solvent parameters (see inset). This represents a remarkable step. Not surprisingly, exchange reactions of the type



(5.28) rather than (5.17) have been examined, since  $\Delta G^o (\approx 0)$  in (5.25) can be ignored and the properties of only one redox couple ( $\text{ML}^{2+/3+}$ ) and not two ( $\text{ML}^{2+/3+}$  and  $\text{M}_1\text{L}_1^{2+/3+}$ )

need be considered. Some results are contained in Table 5.4. See also Table II in Ref. 25. The details of the calculations and references to the experimental data obtained in a variety of ways are given in Refs. 23, 25, 27–31.

**Table 5.4** Comparison of Observed Exchange Rate Constants with Values Calculated on the Basis of (5.25) at 25°C

Couple	$k_{\text{obs}}$ $\text{M}^{-1}\text{s}^{-1}$	$k_{\text{calc}}$ $\text{M}^{-1}\text{s}^{-1}$	Refs.
$\text{Ru}(\text{H}_2\text{O})_6^{2+} + \text{Ru}(\text{H}_2\text{O})_6^{3+}$	20	60	27–29
$\text{Ru}(\text{NH}_3)_6^{2+} + \text{Ru}(\text{NH}_3)_6^{3+}$	$7 \times 10^3$ (4°C)	$1 \times 10^5$	27, 30
$\text{Ru}(\text{bpy})_3^{2+} + \text{Ru}(\text{bpy})_3^{3+}$	$4 \times 10^8$	$1 \times 10^9$	25, 27
$\text{Tc}(\text{dmpe})_3^{\ddagger} + \text{Tc}(\text{dmpe})_3^{\ddagger+}$ <sup>a</sup>	$\sim 6 \times 10^5$	$3 \times 10^6$	31

<sup>a</sup> dmpe = 1,2-bis(dimethylphosphino)ethane

Everything being considered, the agreement between the calculated and the observed rate constants is excellent. The rates tend to increase with size of the ligands (see Ru entries in Table 5.4). This arises from a decrease in the value of  $\lambda_o$  as the reactant size increases. For a given ligand type, ( $\lambda_o \approx \text{constant}$ ) rate constants increase with decreasing differences in the metal-ligand distances (smaller  $\lambda_i$  term) in the two oxidation states. This is strikingly illustrated by the  $\text{M}(\text{bpy})_3^{2+/3+}$  and  $\text{M}(\text{bpy})_3^{+/2+}$  couples shown in Table 5.5.<sup>32</sup> The transfer of  $\sigma^*d$  electrons between the two oxidation states leads to larger M-N bond distance changes ( $\Delta d$ ), and slower rates than when only non-bonding  $\pi d$  electrons are involved. The varying self-exchange rate constants for a series of  $\text{M}(\text{sar})^{2+/3+}$  (Prob. 4) and Ru(II)-(III) complexes have been rationalized in a similar manner.<sup>26,33,34</sup>

**Table 5.5** Electron Transfer Rate Constants and Differences in Metal-Ligand Distances between the Oxidation States (L = bpy)<sup>32</sup>

Couple	Electron Configuration	$\Delta d(\text{\AA})$	$k_{11}, \text{s}^{-1}$
$\text{NiL}_3^{2+/3+}$	$(\pi d)^6(\sigma^*d)^2/(\pi d)^6(\sigma^*d)^1$	$\approx 0.12$	$1.5 \times 10^3$
$\text{CoL}_3^{2+/3+}$	$(\pi d)^5(\sigma^*d)^2/(\pi d)^6$	0.19	18
$\text{CoL}_3^{+/2+}$	$(\pi d)^6(\sigma^*d)^2/(\pi d)^5(\sigma^*d)^2$	-0.02	$1 \times 10^9$
$\text{FeL}_3^{2+/3+}$	$(\pi d)^6/(\pi d)^5$	0.00	$3 \times 10^8$
$\text{RuL}_3^{2+/3+}$	$(\pi d)^6/(\pi d)^5$	0.00	$4 \times 10^8$
$\text{CrL}_3^{2+/3+}$	$(\pi d)^4/(\pi d)^3$	0.00	$2 \times 10^9$

A good deal of data is required for these calculations and the theoretical ideas developed have been more usefully applied to the estimation of rate constants for net chemical changes (5.17) in terms of the free energy change,  $\Delta G^0$  and the rate constants for related reactions (LFER, Sec. 2.5). Equation (5.25) can be written

$$\Delta G^* \approx w^r + \frac{\lambda_o + \lambda_i}{4} \left( 1 + \frac{\Delta G^0 + w^p - w^r}{\lambda_o + \lambda_i} \right)^2 \quad (5.29)$$

If

$$(\Delta G^0 + w^p - w^r)(\lambda_o + \lambda_i)^{-1} < 1 \quad (5.30)$$

then

$$\Delta G^* \sim \frac{w^r + w^p}{2} + \frac{\lambda_o + \lambda_i}{4} + \frac{\Delta G^0}{2} \quad (5.31)$$

In the redox reactions of a series of *related* reagents with one *constant* reactant (so that  $\Delta G^0$  is the only important variable), a plot of  $\Delta G^*$  vs  $\Delta G^0$  would be expected to be linear with slope 0.5.

We can take the analysis still further: Consider the “cross reaction” (5.17) with the various parameters subscripted 12 (forward direction)



and the related isotopic exchange (“self-exchange”) reactions, (5.28) and (5.32) with the subscripts 11 and 22



In the first instance, we can ignore work terms. If, in addition, we can assume that the sum of  $\lambda$ 's for the cross reaction  $(\lambda_o + \lambda_i)_{12}$  is given by

$$(\lambda_o + \lambda_i)_{12} = 1/2 [(\lambda_o + \lambda_i)_{11} + (\lambda_o + \lambda_i)_{22}] \quad (5.33)$$

then combining this with (5.29) yields

$$\Delta G_{12}^\ddagger = 0.50\Delta G_{11}^\ddagger + 0.50\Delta G_{22}^\ddagger + 0.50\Delta G_{12}^0 - 1.15 RT \log f_{12} \quad (5.34)$$

or

$$k_{12} = (k_{11}k_{22}K_{12}f_{12})^{1/2} \quad (5.35)$$

where

$$\log f_{12} = \frac{(\log K_{12})^2}{4 \log (k_{11}k_{22}/Z^2)} \quad (5.36)$$

The value of  $K_{12}$  is the equilibrium constant for (5.17) in the prevailing medium, and may be determined directly (e. g. spectrally) or calculated from a knowledge of the oxidation potentials for the two self-exchanges. A relationship of the form (5.35) has been derived from a simplified nonrigorous statistical mechanical derivation<sup>35</sup> and by simple thermodynamic cycle and detailed balance considerations.<sup>36</sup> First we examine a series of reactions between a common reactant  $ML^{2+}$  (constant  $k_{11}$ ) and a number of closely related complexes  $M_1L_1^{3+}$  (there might be slight changes in the ligand structure  $L_1$ ) so that  $k_{22}$  doesn't much vary either. In addition, if the equilibrium constant for the cross-reaction  $K_{12}$  does not deviate much from unity, i. e.  $\log f_{12} \approx 0$ , then it is easily seen from (5.35) that there should be a linear relationship between  $\log k_{12}$  and  $\log K_{12}$  with a slope 0.5. In a number of systems including metalloproteins<sup>37</sup> and electronically excited reactants<sup>38,39</sup> this simple relationship has

been observed,<sup>25</sup> and an example has been already shown in Sec. 2.5. However with a large number of reactions (particularly between oppositely charged reactants and with large driving forces), work terms cannot be ignored and if the transmission coefficient  $\kappa$  is less than 1, i. e., there is an element of nonadiabaticity, then the modified Marcus expression is<sup>32,40</sup>

$$k_{12} = \left[ \frac{k_{11} k_{22} K_{12} f_{12}}{\kappa_{11} \kappa_{22}} \right]^{1/2} \kappa_{12} W_{12} \quad (5.37)$$

$$\ln f_{12} = \frac{[\ln K_{12} + (w_{12} - w_{21})/RT]^2}{4 \left[ \ln \frac{k_{11} k_{22}}{Z^2 \kappa_{11} \kappa_{22}} + \frac{w_{11} + w_{22}}{RT} \right]} \quad (5.38)$$

$$W_{12} = \exp [-(w_{12} + w_{21} - w_{11} - w_{22})/2RT] \quad (5.38a)$$

There are a number of ways of plotting the modified expression (5.37), using natural or decadic logarithms. Usually the self-exchange reactions are assumed adiabatic ( $\kappa_{11} = \kappa_{22} = 1$ ), and rearrangement of (5.37) leads to

$$2 \ln k_{12} - \ln f_{12} - 2 \ln W_{12} - \ln k_{22} = \ln (k_{11} \kappa_{12}^2) + \ln K_{12} \quad (5.38b)$$

A plot of the left-hand side of (5.38b) versus  $\ln K_{12}$  should be linear with a slope of unity and an intercept =  $\ln (k_{11} \kappa_{12}^2)$ .<sup>41</sup> Such a plot for the reactions of  $\text{Co}(\text{phen})_3^{3+}$  with  $\text{Cr}(\text{bpy})_3^{2+}$ ,  $\text{Cr}(\text{phen})_3^{2+}$  and their substituted derivatives yields a slope of 0.98 and an intercept of approximately  $-0.55$ . If  $k_{11}$ , the self-exchange rate constant for  $\text{Co}(\text{phen})_3^{3+}$  is  $30 \text{ M}^{-1} \text{ s}^{-1}$  this corresponds to  $\kappa_{12} = 0.13$ , indicating mild nonadiabaticity for reactions involving  $\text{Co}(\text{phen})_3^{3+}$ . Ref. 41. See also Fig. 8.2.

We are now in a position to understand the full implications of the plot of Fig. 2.8. The value of  $\log k_{12}$  at  $\log K_{12} = 0$  is 2 and on the basis of the simple Marcus expression this equals  $1/2(8.5 + x)$  where  $8.5 = \log k_{11}$  (for  $\text{PTZ}/\text{PTZ}^+$ ) and  $x$  is  $\log k_{22}$  (for  $\text{Fe}^{2+/3+}$ ). This leads to a value of  $x \approx -4$ , i. e.  $k_{22} = 10^{-4} \text{ M}^{-1} \text{ s}^{-1}$ . This is much smaller than the experimentally determined value of  $4 \text{ M}^{-1} \text{ s}^{-1}$ . This difference may be taken care of by using the fuller expression (5.38b) and a value of  $\kappa_{12} \approx 10^{-2}$ . See also Ref. 42.

Plots for a reaction series have been however much less used than the application of these equations, both simple (Prob. 1) and complicated, to isolated reaction systems.<sup>21,25</sup> Table 5.6

**Table 5.6** Calculated Values for the Self-Exchange Rate Constant for  $\text{Ru}(\text{H}_2\text{O})_6^{2+/3+}$  using (5.35) and Data for a Number of Cross-Reactions (from Ref. 43)

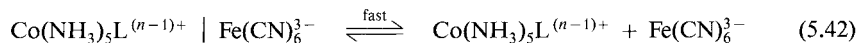
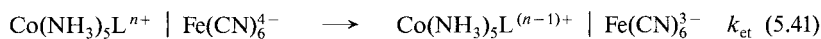
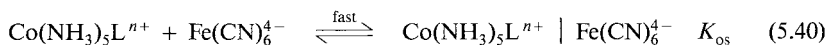
Reactions	$\Delta E^0$ V	$k_{12}$ $\text{M}^{-1} \text{ s}^{-1}$	$k_{22}$ $\text{M}^{-1} \text{ s}^{-1}$	$k_{11}$ $\text{M}^{-1} \text{ s}^{-1}$
$\text{Ru}(\text{H}_2\text{O})_6^{2+} + \text{Ru}(\text{NH}_3)_5\text{py}^{3+}$	0.082	$1.1 \times 10^4$	$4.7 \times 10^5$	15
$\text{Ru}(\text{NH}_3)_6^{2+} + \text{Ru}(\text{H}_2\text{O})_6^{3+}$	0.150	$1.4 \times 10^4$	$2 \times 10^4$	32
$\text{Ru}(\text{H}_2\text{O})_6^{2+} + \text{Ru}(\text{NH}_3)_5\text{isn}^{3+}$	0.167	$5.5 \times 10^4$	$4.7 \times 10^5$	14
$\text{V}(\text{H}_2\text{O})_6^{2+} + \text{Ru}(\text{H}_2\text{O})_6^{3+}$	0.47	$2.8 \times 10^2$	$1 \times 10^{-2}$	0.37
$\text{Ru}(\text{H}_2\text{O})_6^{2+} + \text{Co}(\text{phen})_3^{3+}$	0.15	53	40	0.24

shows the second-order rate constants  $k_{12}$  determined for a number of cross reactions involving the  $\text{Ru}(\text{H}_2\text{O})_6^{2+/3+}$  couple at 25°C and  $\mu = 1.0$  M. The difference in oxidation potentials for the two reactants,  $\Delta E^\circ$ , allows us to calculate  $\log K_{12}$  ( $= 16.9 \times \Delta E^\circ$ ) which together with  $k_{22}$ , permits an estimation of  $k_{11}$  for the  $\text{Ru}(\text{H}_2\text{O})_6^{2+/3+}$  couple using (5.35).<sup>43</sup> Inclusion of the work terms has only a small effect on the final results.<sup>40</sup> The values calculated for  $k_{11}$  using data for the highly exothermic reactions are lower than those derived from reactions with small driving forces. The higher values ( $14\text{--}32 \text{ M}^{-1}\text{s}^{-1}$ ) are satisfyingly close to those measured and calculated in Table 5.4.

If the reactants are oppositely charged, the collision complex in (5.18) takes the form of an outer-sphere complex with discernable stability. For the outer sphere redox reaction between  $\text{Co}(\text{NH}_3)_5\text{L}^{n+}$  and  $\text{Fe}(\text{CN})_6^{4-}$ , L being a series of pyridine or carboxylate derivatives, saturation kinetics are observed, with the pseudo first-order rate constant ( $k_{\text{obs}}$ ), Fe(II) in excess, being given by

$$k_{\text{obs}} = \frac{k_{\text{et}} K_{\text{os}} [\text{Fe}(\text{CN})_6^{4-}]}{1 + K_{\text{os}} [\text{Fe}(\text{CN})_6^{4-}]} \quad (5.39)$$

This behavior is consistent with the mechanism (Note however Sec. 1.6.4).



At 25°C and  $\mu = 0.1$  M, the values of  $K_{\text{os}}$  are  $10^2\text{--}10^4 \text{ M}^{-1}$  and those of  $k_{\text{et}}$  are  $10^{-4}\text{--}10^{-1} \text{ s}^{-1}$  depending on the identity of L.<sup>44</sup> The internal electron transfer rate in an outer-sphere complex can thus be analyzed<sup>45,46</sup> without considering work terms or, what is equivalent, the equilibrium controlling the formation of precursor complex.<sup>47</sup> This favorable situation is even improved when the metal centers are directly bridged. The relative orientation of the two metal centers in a well-established geometry can be better treated than in the outer-sphere complex (Sec. 5.8).

It is hardly possible to overestimate the impact that the Marcus-Hush ideas and their experimental exploitation, mainly by Sutin and his coworkers, have made on the study of redox reactions. The treatment here is necessarily brief. Other aspects have been discussed in the references cited. Some important points we have not considered are

- the application of the derived equations to other activation parameters.<sup>23</sup>
- the necessity to sometimes (not often) allow for the preexponential factor  $\kappa$  being non-unity, has been briefly alluded to. The non-adiabaticity becomes more pronounced when the standard free energy of the reaction increases (Table 5.6). Its assessment can be difficult (and controversial).<sup>48</sup>
- the occurrence of an inverted region where  $\Delta G^*$  increases (rate constant decreases) as  $\Delta G^\circ$  becomes more negative. In this region, very large driving forces are involved.<sup>23,49</sup>
- the effect of solvents.<sup>50</sup>

### 5.4.1 The Applications of the Marcus Expression

Occasionally, the successful application of the Marcus expressions (5.35) and (5.37) to a reaction can support its designation as outer-sphere. The reduction of a series of substituted benzenediazonium salts by  $\text{Fe}(\text{CN})_6^{4-}$  and  $(\text{Me}_5\text{cp})_2\text{Fe}$  conforms to the simple Marcus expression and represents supporting evidence for the formulation of these reactions as outer sphere (or non-bonded electron transfer in organic systems)



rather than inner sphere (or bonded electron transfer)<sup>51</sup>



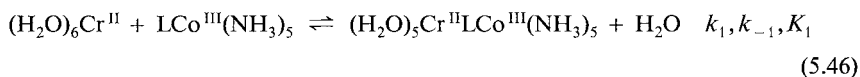
The pattern for outer-sphere oxidation by  $\text{Co}(\text{NH}_3)_6^{3+}$  compared with  $\text{Co}(\text{en})_3^{3+}$  (usually it is  $\approx 10$  times slower) towards inorganic reductants can be used<sup>52</sup> to support an estimate of the proportion of electron transfer (Marcus-dependent) and charge transfer which  $^*\text{Ru}(\text{bpy})_3^{2+}$  displays towards these oxidants (45 and 11%, respectively), Sec. 2.2.1 (b). Finally, Eqn. 5.35 can be used to determine  $K_{12}$  for a reaction in which the other kinetic parameters are known. The value of  $K_{12}$  can be used, in turn, to estimate the oxidation potential of one couple, which is normally inaccessible.<sup>53</sup> Thus the potentials of the *o*-, *m*- and *p*-benzene diol radicals  $\text{H}_2\text{A}^{\bullet}$  were determined from kinetic data for the oxidation of the diols ( $\text{H}_2\text{A}$ ) by  $\text{Fe}(\text{phen})_3^{3+}$  (5.45):<sup>53</sup>

As might be anticipated, there are exceptions to the Marcus equations (Prob. 3).<sup>25</sup>



## 5.5 Inner Sphere Redox Reactions

Just as we did with outer-sphere reactions, we can dissect an inner sphere redox process into individual steps. Specifically, let us examine the reaction of  $(\text{H}_2\text{O})_6\text{Cr}^{\text{II}}$  with  $\text{Co}^{\text{III}}(\text{NH}_3)_5\text{L}$ . The first step is the formation of the precursor complex<sup>19,20,54-56</sup>.

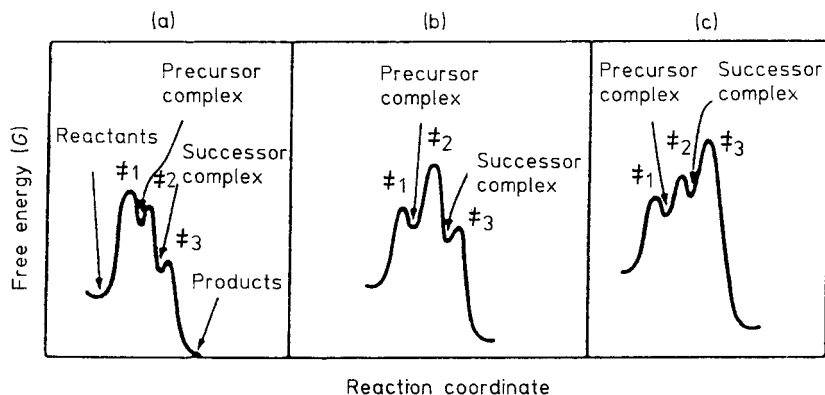


The product of intramolecular electron transfer within the precursor complex is the successor complex



which then undergoes dissociation into products





**Fig. 5.1** Reaction profiles for inner-sphere redox reactions illustrating three types of behavior (a) precursor complex formation is rate-limiting (b) precursor-to-successor complex is rate-limiting and (c) breakdown of successor complex is rate-limiting. The situation (b) appears to be most commonly encountered.

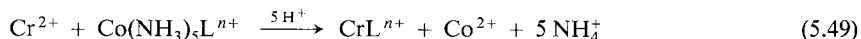
Of course the  $\text{Co}^{\text{II}}(\text{NH}_3)_5$  breaks down rapidly in acid into  $\text{Co}^{2+}$  and  $5\text{NH}_4^+$ . Precursor complex formation, intramolecular electron transfer, or successor complex dissociation may severally be rate limiting. The associated reaction profiles are shown in Fig. 5.1. A variety of rate laws can arise from different rate-determining steps.<sup>22</sup> A second-order rate law is common, but the second-order rate constant  $k_{\text{obs}}$  is probably composite. For example, (Fig. 5.1 (b)) if the observed redox rate constant is less than the substitution rate constant, as it is for many reactions of  $\text{Cr}^{2+}$ ,  $\text{Eu}^{2+}$ ,  $\text{Cu}^+$ ,  $\text{Fe}^{2+}$  and other ions, and if little precursor complex is formed, then  $k_{\text{obs}} = (k_1 k_2 k_{-1}^{-1})$ . In addition, the breakdown of the successor complex would have to be rapid ( $k_3 \gg k_{-2}$ ). This situation may even give rise to *negative*  $\Delta H_{\text{obs}}^\ddagger (= \Delta H_1^\ddagger + \Delta H_2^\ddagger)$  since enthalpies of formation of precursor complexes ( $\Delta H_1^\ddagger$ ) may be negative. Such negative values of  $\Delta H_{\text{obs}}^\ddagger$  in turn, constitutes good evidence for the existence of precursor complexes.<sup>57</sup> A good deal of effort has gone into attempting to isolate the data for the electron transfer step (5.47).<sup>22,58</sup> One way of accomplishing this might be by bulding up large concentrations of precursor complex. If this is not possible, then the experimental rate constants for reaction of a series of related complexes may still parallel the corresponding values for the intramolecular rate constants,  $k_2$ , if the values of  $k_1/k_{-1}$  remain sensibly constant. However, the possibility that this is not the case should be always recognized.

## 5.6 The Bridging Ligand in Inner-Sphere Redox Reactions

The early work of Taube and his co-workers opened several interesting avenues of approach, most of which have been fully exploited.<sup>21,22,48,B40</sup> One of the most obvious is to examine the requirements for a good bridging group and determine the effects of this bridge on the rate of the inner-sphere redox reaction. Hundreds of different bridges have been examined since



Taube's original discovery.<sup>4</sup> Attendant changes of redox rates by many orders of magnitude have been observed. Much data have been obtained on reactions of the type



and these, together with reduction of the Co(III) complexes by other metal ions and complexes, are useful for discussion purposes (Table 5.7).<sup>16</sup> Oxidation by Cr(III) and Ru(III) also provides useful information, and isotopic exchanges of the type



which cannot be outer-sphere, were early explored<sup>3</sup> (Table 5.8).

**Table 5.7** Rate Constants ( $k$ ,  $\text{M}^{-1}\text{s}^{-1}$ ) for the Reduction of  $\text{Co}(\text{NH}_3)_5\text{L}^{n+}$  by a Variety of Reductants at 25°C

L	$\text{Cr}^{2+}$	$\text{V}^{2+}$	$\text{Fe}^{2+}$ <sup>d</sup>	$\text{Eu}^{2+}$
$\text{NH}_3$	$8.0 \times 10^{-5}$	$3.7 \times 10^{-3}$		$2 \times 10^{-2}$
py	$4.1 \times 10^{-3}$	0.24		
$\text{H}_2\text{O}$	$\leq 0.1$	0.53		0.15
$\text{OCOCH}_3$	0.35	1.2	$< 5 \times 10^{-5}$	0.18
$\text{OCOCOOH}$	$1.0 \times 10^2$	12.5	$3.8 \times 10^{-3}$	
$\text{F}^-$	$2.5 \times 10^5$	2.6	$6.6 \times 10^{-3}$	$2.6 \times 10^4$
$\text{Cl}^-$	$6 \times 10^5$	10	$1 \times 10^{-3}$	$3.9 \times 10^2$
$\text{Br}^-$	$1.4 \times 10^6$	25	$7.3 \times 10^{-4}$	$2.5 \times 10^2$
$\text{I}^-$	$3 \times 10^6$	$1.2 \times 10^2$		$1.2 \times 10^2$
$\text{OH}^-$	$1.5 \times 10^6$	$< 4$		$< 2 \times 10^3$
$\text{N}_3^-$	$\sim 3 \times 10^5$	13	$8.8 \times 10^{-3}$	$1.9 \times 10^2$
$\text{NCS}^-$	19 <sup>b</sup>	0.3	$< 3 \times 10^{-6}$	0.05
$\text{SCN}^-$	$1.9 \times 10^5$ <sup>b</sup> $0.8 \times 10^5$ <sup>c</sup>	30	0.12	$3.1 \times 10^3$

L	$\text{Cu}^+$	$\text{Co}(\text{CN})_3^{3-}$	$\text{Cr}(\text{bpy})_3^{2+}$	$\text{Ru}(\text{NH}_3)_6^{2+}$	$\text{Ti}^{3+}$
$\text{NH}_3$		$8 \times 10^4$ <sup>a</sup>	$6.9 \times 10^2$	$1.1 \times 10^{-2}$	
py				1.2	
$\text{H}_2\text{O}$	$1.0 \times 10^{-3}$		$5 \times 10^4$ <sup>e</sup>	3.0	
$\text{OCOCH}_3$		$1.1 \times 10^4$ <sup>a</sup>	$1.2 \times 10^3$	$1.8 \times 10^{-2}$	
$\text{OCOCOOH}$				0.50	
$\text{F}^-$	1.1	$1.8 \times 10^3$	$1.8 \times 10^3$		$2 \times 10^2$
$\text{Cl}^-$	$4.9 \times 10^4$	$\sim 5 \times 10^7$	$8 \times 10^5$	$2.6 \times 10^2$	13
$\text{Br}^-$	$4.5 \times 10^5$		$5 \times 10^6$	$1.6 \times 10^3$	2
$\text{I}^-$				$6.7 \times 10^3$	4
$\text{OH}^-$	$3.8 \times 10^2$	$9.3 \times 10^4$	$1 \times 10^3$ <sup>c</sup>	0.04	
$\text{N}_3^-$	$1.5 \times 10^3$	$1.6 \times 10^6$	$4.1 \times 10^4$	1.8	
$\text{NCS}^-$	$\sim 1$	$1.1 \times 10^6$	$1.1 \times 10^4$	0.74	
$\text{SCN}^-$		$< 10^7$	$2.0 \times 10^6$	$3.8 \times 10^2$	

<sup>a</sup>  $\text{M}^{-2}\text{s}^{-1}$ , outer-sphere reduction by  $\text{Co}(\text{CN})_6^{3-}$ . <sup>b</sup> Remote attack. <sup>c</sup> Adjacent attack. <sup>d</sup> J. H. Espenson, *Inorg. Chem.* **4**, 121 (1965). <sup>e</sup> 4°C.

Examination of the data for (5.49) and (5.50) in Tables 5.7 and 5.8 shows that there is some general order of reactivity for the various ligands L. Containing an unshared electron pair *after coordination* appears a minimum requirement for a ligand to be potential bridging group, for it has to function as a Lewis base towards two metal cations. Thus  $\text{Co}(\text{NH}_3)_6^{3+}$  and  $\text{Co}(\text{NH}_3)_5\text{py}^{3+}$  oxidize  $\text{Cr}^{2+}$  by an outer-sphere mechanism, giving  $\text{Cr}^{3+}$  as the product, at a much slower rate than for the inner-sphere reactions.

The bridging group is often supplied by the oxidizing agent because this is invariably the inert reactant. In these cases, the bridging ligand normally transfers from oxidant to reductant during the reaction. This however is not an essential feature of an inner-sphere redox reaction. The cyanide bridge is supplied by  $\text{Fe}(\text{CN})_6^{4-}$  in some reductions and remains with the iron after electron transfer and breakup.<sup>59</sup> Such reactions, which proceed without ligand transfer, can only be shown to be inner-sphere directly, i.e. by the demonstration of a bridged intermediate.

**Table 5.8** Rate Parameters for Cr(II)–Cr(III) Exchange Reactions (5.20) at 25°C. Ref. 16.

Exchange Partners	$k$ $\text{M}^{-1} \text{s}^{-1}$	$\Delta H^\ddagger$ $\text{kJ mol}^{-1}$	$\Delta S^\ddagger$ $\text{J K}^{-1} \text{mol}^{-1}$
$\text{Cr}^{2+} + \text{Cr}^{3+}$	$\leq 2 \times 10^{-5}$	...	...
$\text{Cr}^{2+} + \text{CrOH}^{2+}$	0.7	54	–67
$\text{Cr}^{2+} + \text{CrNCS}^{2+}$	$1.4 \times 10^{-4}$	...	...
$\text{Cr}^{2+} + \text{CrSCN}^{2+}$	40	...	...
$\text{Cr}^{2+} + \text{CrN}_3^{2+}$	6.1	40	–96
$\text{Cr}^{2+} + \text{CrF}^{2+}$	$2.4 \times 10^{-3}$ (0°C)	57	–84
$\text{Cr}^{2+} + \text{CrCl}^{2+}$	9 (0°C)	...	...
$\text{Cr}^{2+} + \text{CrBr}^{2+}$	>60	...	...
$\text{Cr}^{2+} + \text{CrCN}^{2+}$	$7.7 \times 10^{-2}$	39	–134
$\text{Cr}^{2+} + \text{cis-Cr}(\text{N}_3)_2^{\ddagger}$	60	...	...

The different types of bridging ligands will now be discussed. Many of the varying patterns and theoretical bases have been built up by using the simpler bridging ligands on which we shall first concentrate. This will lead into the larger organic and protein bridges.

(a) Hydroxide and Water. With oxidants containing a coordinated water group, for example  $\text{Co}(\text{NH}_3)_5\text{H}_2\text{O}^{3+}$ , a term in the rate law containing an  $[\text{H}^+]^{-1}$  dependency for their reaction is often found. This may make a significant contribution to the rate, and mask any  $[\text{H}^+]$ -independent term.<sup>12</sup> The inverse term is usually ascribed to reduction of the hydroxy species, for example  $\text{Co}(\text{NH}_3)_5\text{OH}^{2+}$ , offering a very effective OH bridge in an inner-sphere process.<sup>60</sup> Reactions in which the aqua and hydroxy forms have similar reactivities and in which no other bridging group is present are probably outer-sphere,<sup>18</sup> and assignment of mechanism on this basis is illustrated in Table 5.7.<sup>61</sup>

There has been a continuing discussion without resolution<sup>22</sup> of whether the aqua group acts as a (weak) bridge in the situations where the corresponding hydroxo complex reacts inner-sphere.

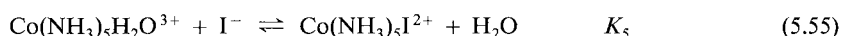
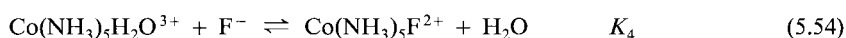
(b) Halides. The reduction of halide complexes has featured prominently in the development of redox chemistry. Rates vary monotonically from F to I but not in a consistent manner. In examining Table 5.7 it is seen that in inner-sphere reductions of  $\text{Co}(\text{NH}_3)_5\text{X}^{2+}$  by  $\text{Cr}^{2+}$ ,

the rate increases with increasing size of the halogen.<sup>62</sup> The order is inverted when reduction by  $\text{Eu}^{2+}$  is considered, even although it is probable that this is inner-sphere also. The difference has been rationalized by calculating formal equilibrium constants for halide interchange in the transition state for various redox reactions.<sup>22,64,65,B36</sup>

The equilibrium constant for



can be calculated knowing the rate and equilibrium constants for:



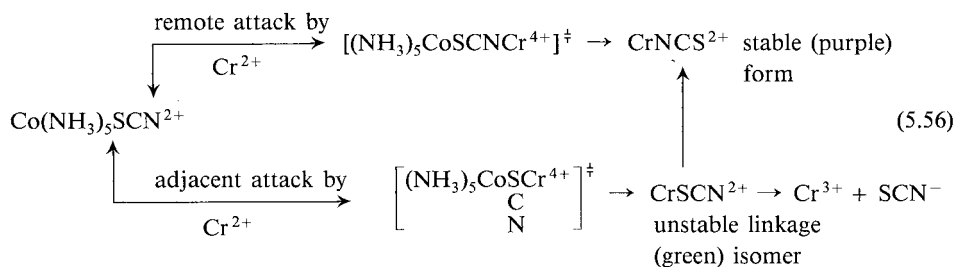
since  $K_1 = k_3 K_5 k_2 K_4 = 0.064$ .<sup>65</sup>

The value of  $K_1 < 1$  for this Cr(II) reduction, as with the reactions of Eu(II), indicates that the substitution of bridging  $\text{F}^-$  by  $\text{I}^-$  is unfavorable in the bridged transition complex in both cases. The two sets of reactivity patterns noted above thus disappear. It has been noted that  $K_1 < 1.0$  when both metal centers are hard acids, whereas  $K_1 > 1$  when one reactant is soft e.g.,  $\text{Cu}^+$ .<sup>B36</sup> These relationships have been rationalized.<sup>22</sup> The much better bridging properties of chloride than water are shown by the data in Table 5.7 and Table 5.9.

**Table 5.9** Ratio (R) of Reactivities of  $\text{Co}(\text{edta})\text{Cl}^{2-}$  and  $\text{Co}(\text{edta})\text{H}_2\text{O}^-$  towards Reductants<sup>5</sup>

Reductants	R	Mechanism
$\text{Cr}^{2+}$	$> 3 \times 10^2$	inner sphere
$\text{Fe}^{2+}$	$2 \times 10^3$	inner sphere
$\text{Fe}(\text{CN})_6^{4-}$	33	outer sphere
Ti(II)	31	outer sphere

(c) Ambidentate Ligands. The use in the oxidant of a polyatomic bridging ligand that presents more than one potential donor site towards the reducing metal ion introduces the concept of *remote* and *adjacent* attack. An authentic example of adjacent attack is rare but illustrated by the scheme<sup>66</sup>



Analysis for  $\text{CrSCN}^{2+}$  and  $\text{CrNCS}^{2+}$  in the products can be made by ion-exchange separation and spectral identification. This procedure indicates that about 30% of the reaction goes by the adjacent attack path in  $1 \text{ M}^+ \text{H}^+$  at  $25^\circ\text{C}$ . Reduction of  $\text{Co}(\text{NH}_3)_5\text{NCS}^{2-}$  by  $\text{Cr}^{2+}$ , in contrast, proceeds much more slowly and quantitatively by remote attack, leading to the unstable isomer  $\text{CrSCN}^{2+}$ . In the N-bound thiocyanate complex, the only lone pairs of electrons available for attack by the  $\text{Cr}^{2+}$  are on the sulfur. In the S-bound  $\text{Co}(\text{NH}_3)_5\text{SCN}^{2+}$  both S and N have lone pairs.<sup>22</sup> It is generally found that  $\text{MSCN}^{2+}$  is about  $10^4$  times more reactive than  $\text{MNCS}^{2+}$ ,  $\text{M} = \text{Co}(\text{NH}_3)_5$  and  $\text{Cr}(\text{H}_2\text{O})_5$ , in its reaction with Fe(II) and Cr(II), (Table 5.7) as well as with a number of other reducing ions which go by inner-sphere. With outer-sphere reductants the ratio is less, about  $10^2$ , and these ratios have been rationalized.<sup>22</sup> With V(II), the ratio is also much less, and this supports the idea that the V(II)- $\text{Co}(\text{NH}_3)_5\text{SCN}^{2+}$  reaction is substitution-controlled (Table 5.7).<sup>67</sup> Redox reactions of the type outlined above have been used to prepare linkage isomers (Sec. 7.4).

The azide bridging ligand cannot offer the interesting dual possibilities of the thiocyanate group. Because it is symmetrical and presents a nitrogen donor atom, which is favored over sulfur for most incipient trivalent metal centers,  $\text{Co}(\text{NH}_3)_5\text{N}_3^{2+}$  is likely to be a more effective oxidant than  $\text{Co}(\text{NH}_3)_5\text{NCS}^{2+}$  if the reaction goes by an inner-sphere mechanism; it is not likely to be much different in an outer-sphere reaction. This has been a useful diagnostic tool<sup>22</sup> (see Table 5.7).

Double bridges have been established for example, in the inner-sphere reaction of  $\text{Cr}^{2+}$  with *cis*- $\text{Cr}(\text{N}_3)_2^+$ .<sup>68</sup> Surprisingly, the double bridge does not offer a markedly faster route than the single bridge (a factor of only 31 in enhanced rate for the example cited<sup>68</sup>). If a chelate site presents itself to an attacking metal ion, a chelate product can result.<sup>21</sup> The oxidation of  $\text{Co}(\text{en})_2(\text{H}_2\text{O})_2^{2+}$  by  $\text{Co}(\text{C}_2\text{O}_4)_3^{3-}$  yields  $\text{Co}(\text{en})_2(\text{C}_2\text{O}_4)^+$ , probably via a double bridge, and with a very small amount of chiral discrimination (Sec. 5.7.4). Using nmr and  $^{13}\text{C}$ -enriched free oxalate ion it can be shown that there is no enriched oxalate in the  $\text{Co}(\text{en})_2(\text{C}_2\text{O}_4)^+$  product, which must therefore arise from an inner-sphere process.<sup>69</sup>

(d) Non-Bridging Ligands. We might wonder what happens to the ligands that are not involved in the bridging act during the redox process, and what influence they might have as a result on the rates of such reactions.<sup>70</sup> This is an area where theoretical predictions preceded experimental results. Orgel first drew attention to a model in which electronic states in the activated complex are matched by changing bond distances and therefore the ligand fields of the reactant ions.<sup>71</sup> For the reduction of Co(III) and Cr(III) complexes, for example, an electron from the reducing agent would appear in an unoccupied  $e_g$  say  $d_{z^2}$  orbital directed towards X (the bridging group) and Y in *trans*- $\text{Co}(\text{NH}_3)_4\text{XY}$ . The energy of this orbital will obviously be more sensitive to changes in the *trans* Y group than to changes in the *cis*  $\text{NH}_3$  ligands, and the orbital will be stabilized by a weak field ligand Y.<sup>71</sup> In general, the consequences of these happenings have been confirmed in both rate experiments and isotopic fractionation experiments. It has been shown, for example, that towards Cr(II), *trans*- $\text{Cr}(\text{NH}_3)_4(\text{H}_2^{16}\text{O})\text{Cl}^{2+}$  reacts 1.6% faster than *trans*- $\text{Cr}(\text{NH}_3)_4(\text{H}_2^{18}\text{O})\text{Cl}^{2+}$  (Sec. 3.12.2). This strongly supports the idea of stretching of the bond in the *trans*-position during the redox reaction. Stretching of the bonds in the *cis* position is less important, although not negligible, judged by the value for  $k_{16\text{O}}/k_{18\text{O}} = 1.007$  for the *cis* isomer.<sup>72</sup>

(e) The Estimation of Rate Constants for Inner-Sphere Reactions. There is evidence that a Marcus-type relationship may be applied to inner-sphere as well as outer-sphere redox reactions.<sup>25,73</sup> Varying A in *cis*- $\text{Co}(\text{en})_2(\text{A})\text{Cl}^{2+}$  has the same effect on the rate in the outer-sphere

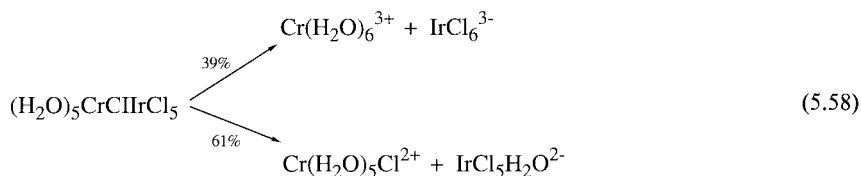
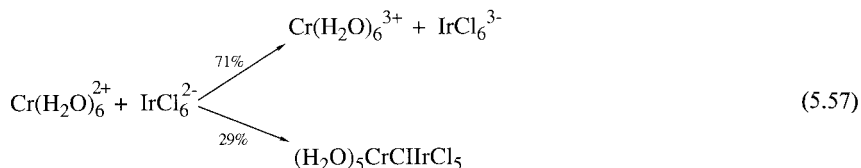
reduction by  $\text{Ru}(\text{NH}_3)_6^{2+}$  as in the inner-sphere reduction by  $\text{Fe}^{2+}$  (constant Cl bridges). Since there is a nice correlation of  $\log k$  vs  $\Delta G$  for the outer-sphere reductions, it follows that a similar LFER must also apply to the inner-sphere process.<sup>74</sup>

## 5.7 Some Other Features of Redox Reactions

We now consider some other aspects of redox reactions which might be outer- and/or inner-sphere in nature.

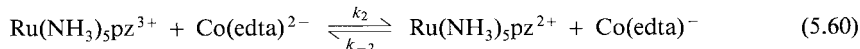
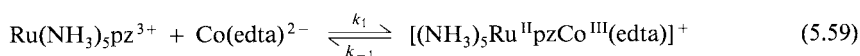
### 5.7.1 Mixed Outer- and Inner-Sphere Reactions

As might be foreseen, there are a (limited) number of systems where the energetics of the outer- and inner-sphere reactions are comparable and where therefore both are paths for the reaction. An interesting example of this behavior is the reaction of  $\text{Cr}(\text{H}_2\text{O})_6^{2+}$  with  $\text{IrCl}_6^{2-}$  which has been studied by a number of groups and is now well understood.<sup>22</sup> At 0°C, most of the reaction proceeds via an outer-sphere mechanism. The residual inner-sphere process utilizes a binuclear complex, which can undergo both Cr–Cl and Ir–Cl cleavage:



The outer-sphere rate constant for the  $\text{Cr}(\text{H}_2\text{O})_6^{2+}/\text{IrCl}_6^{2-}$  reaction can be estimated, using Marcus' equation, as  $\approx 10^9 \text{ M}^{-1} \text{ s}^{-1}$ . A value of this magnitude can obviously be competitive with that for the inner-sphere path, which is more usual with the highly labile  $\text{Cr}(\text{H}_2\text{O})_6^{2+}$  ion.<sup>22</sup>

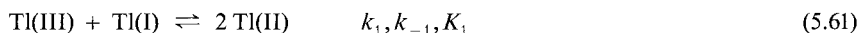
A rather involved, but interesting, example of a reaction which proceeds by both inner- and outer-sphere pathways is summarized in the scheme



The outer-sphere pathway ( $k_2$ ) produces the final products directly, as shown by a rapid increase in absorbance at 474 nm, which is a maximum for  $\text{Ru}(\text{NH}_3)_5\text{pz}^{2+}$ . At the same time, a rapid inner-sphere ( $k_1$ ) production of the binuclear complex takes place. A slower absorbance increase at 474 nm arises from the back electron transfer in the binuclear intermediate ( $k_{-1}$ ). This produces the original reactants which then undergo outer-sphere reaction ( $k_2$ ). The values of the rate constants at 25°C and  $\mu = 0.1 \text{ M}$  are  $2.5 \times 10^3 \text{ M}^{-1}\text{s}^{-1}$  ( $k_1$ ),  $16.9 \text{ s}^{-1}$  ( $k_{-1}$ ),  $1.0 \times 10^3 \text{ M}^{-1}\text{s}^{-1}$  ( $k_2$ ) and  $3.2 \text{ M}^{-1}\text{s}^{-1}$  ( $k_{-2}$ ).<sup>75</sup>

### 5.7.2 Two-Electron Transfer

In most of the discussions so far, we have been concerned with reactants undergoing one-electron transfer processes. When one or both of the participants of a redox reaction has to undergo a change of two in the oxidation state, the point arises as to whether the two-electron transfer is simultaneous or nearly simultaneous, a question that has been much discussed.<sup>21</sup> The Tl(I)–Tl(III) second-order exchange ( $k_{\text{exch}}$ ) proceeds by a two-electron transfer. One would need to postulate the equilibrium (5.61) if Tl(II) was involved in the



exchange. The value of  $k_{-1}$  can be determined by pulse radiolytic (one-electron) reduction of Tl(III) and observation of the subsequent disproportionation of the resultant Tl(II). The value of  $k_{-1}$  is  $1.9 \times 10^8 \text{ M}^{-1}\text{s}^{-1}$ . By using data for the  $\text{Fe}^{2+}$ ,  $\text{Tl}^{3+}$  reaction, involved but sound reasoning, which is well worth examining, allows the estimation of  $K_1 = 4 \times 10^{-33}$ . It follows that  $k_1 = 7.6 \times 10^{-25} \text{ M}^{-1}\text{s}^{-1}$ , and since this is very much less than  $k_{\text{exch}}$  ( $1.2 \times 10^{-4} \text{ M}^{-1}\text{s}^{-1}$ ) the exchange cannot proceed via a Tl(II) species which is free in solution.<sup>76</sup>

The immediate product of the reaction of Tl(III) with Cr(II) is the dimer  $\text{Cr}_2(\text{OH})_2^{4+}$ . This is likely to result only from an interaction of Cr(II) with Cr(IV), produced in the redox step with Tl(III). If Cr(III) (and Tl(II)) resulted directly from Cr(II) and Tl(III), it would undoubtedly be in the form of a mononuclear Cr(III) species, since this is the product of most of the oxidations of Cr(II).<sup>77</sup> Other examples are in B36 and Ref. 78.

### 5.7.3 Redox Catalyzed Substitution

Certain substitutions can be catalyzed by the operation of a redox process. It is most easily detected with inert Cr(III), Co(III) and Pt(IV). Hydrolysis, anation and anion interchange all have been accelerated in complexes of these metals by the presence of the lower oxidation state (which is more labile).

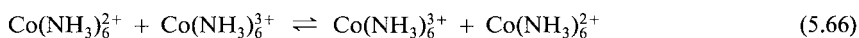
Chromium(II) catalyzes the ligation of Cr(III) by X by a mechanism:



based on a third-order rate law<sup>79</sup>

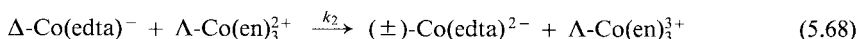
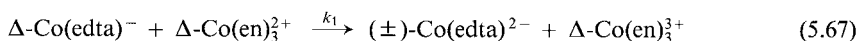
$$V = k [\text{Cr}^{\text{II}}] [\text{Cr}^{\text{III}}] [\text{X}] \quad (5.64)$$

Chromium(II) must catalyze the aquation of  $\text{Cr}^{\text{III}}\text{X}$  by the reverse of the two steps (5.62) and (5.63).<sup>80</sup> Traces of lower oxidation state may be the cause of apparent lability in the higher one e.g. Fe(II) labilising Fe(III).<sup>81,82</sup> Exchange of  $\text{Co}(\text{NH}_3)_6^{3+}$  with  $\text{NH}_3(\text{aq})$ , catalyzed by Co(II) has been examined using <sup>15</sup>N-labelled  $\text{NH}_3$  and nmr monitoring.<sup>1</sup> The treatment is complicated by side reactions.



### 5.7.4 Stereoselectivity

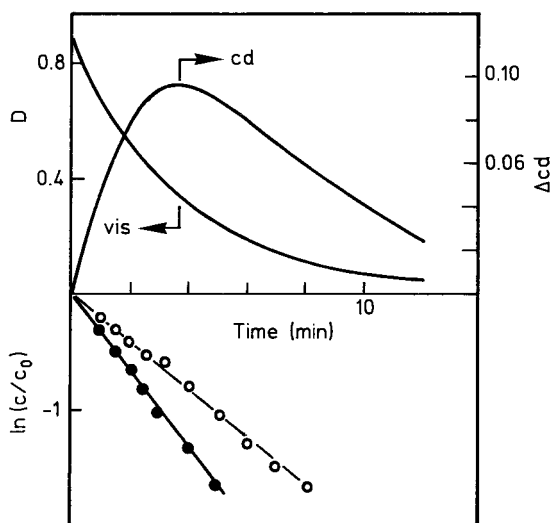
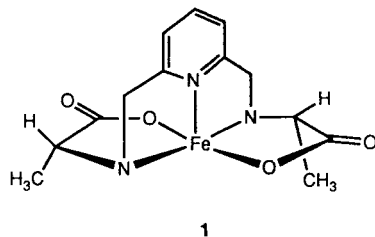
One might anticipate that there would be a rate difference for the reaction of enantiomers with a chiral compound. The first demonstration of stereoselectivity in an outer-sphere electron transfer was as recent as 1980.<sup>83</sup> Since then such asymmetric induction has been established with a number of examples, nearly all involving outer-sphere redox reactions. Thus, consider the two reactions<sup>83-85</sup>



We are looking for a difference in  $k_1$  and  $k_2$ . Since the Co(II) complex is a labile racemic mixture ( $\pm$ ), such a difference can only be demonstrated by a competition approach, searching for a preponderance in the product of one of the optical forms of  $\text{Co}(\text{en})_3^{3+}$ . In this instance a small (11%) excess of  $\Lambda\text{-Co}(\text{en})_3^{3+}$  is observed in the product, meaning that  $k_2/k_1 \approx 1.2$ . With this typical result it is clear that the kinetic approach, when applicable, is less likely to be as sensitive as that in which the product estimation is assessed by cd and optical rotation. If (5.67) and (5.68) are considered as outer-sphere redox reactions, which is highly likely, the observed rate constant  $k_1$  or  $k_2$  is composite, a product of a precursor complex formation constant and an intramolecular electron transfer rate constant (Sec. 5.4). Since there is an ion pairing selectivity between  $\text{Co}(\text{edta})^-$  and  $\text{Co}(\text{en})_3^{3+}$  which is also  $\Delta\Lambda$ , this suggests that precursor ion pair formation between  $\text{Ce}(\text{edta})^-$  and  $\text{Co}(\text{en})_3^{2+}$  is an important component of the observed electron transfer stereoselectivity. The stereoselectivity increases to 32%  $\Delta\Lambda$  preference in dmsO.<sup>85</sup> From a detailed examination of the variety of stereochemical products of reduction of  $\text{Co}(\text{edta})^-$  by a number of Co(II) complexes of the type  $\text{Co}(\text{N})_6^{2+}$ , it has been possible to make deductions about the detailed interactions, for example, that there is strong hydrogen bonding of the pseudo- $\text{C}_3$  carboxylate face of  $\text{Co}(\text{edta})^-$  with amine hydrogens on the reductant.<sup>84-86</sup>

The reductant may be optically stabilized by using optically active forms of the coordinated ligand. Such ligands may impose stereochemical restraints even with labile oxidation states

(Chap. 3, Structure 10). The *SS* form of the ligand *alamp* (chirality relating to the two asymmetric C atoms) imposes a  $\Lambda$ -configuration at the Fe(II) center in the complex  $\Lambda$ -[Fe(*SS*)-*alamp*], **1**. Treatment of this complex with the racemic mixture ( $\pm$ )-Co(*bamap*)H<sub>2</sub>O<sup>+</sup> (see 2) shows a change of cd ( $\lambda = 367$  nm) with time indicated in Fig. 5.2. The sign of the cd signal



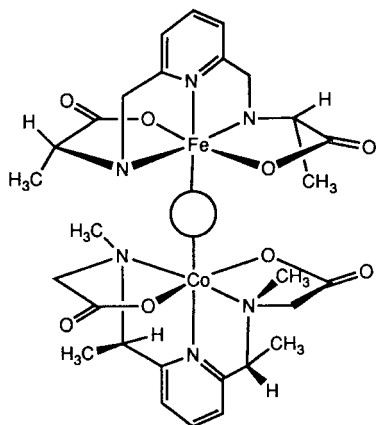
**Fig. 5.2** (a) Change in absorbance at 502 nm and in cd intensity at 367 nm on mixing ( $\pm$ )-Co(*bamap*)(H<sub>2</sub>O)<sup>+</sup> (2.5 mM) and Fe(*SS*-*alamp*) (from 2.5 mM Fe<sup>2+</sup> and 10 mM (*SS*)-*alamp*). The solution contains 0.1 M ascorbic acid.<sup>87</sup> (b)  $\ln(c/c_0)$  vs.  $t$  for reaction of (–) Co(*bamap*)(H<sub>2</sub>O)<sup>+</sup> (upper curve) and (+) Co(*bamap*)(H<sub>2</sub>O)<sup>+</sup>. The rate constants are  $3.2 \times 10^{-3} \text{ s}^{-1}$  and  $5.5 \times 10^{-3} \text{ s}^{-1}$  respectively.<sup>87</sup> pH = 4.0 and 25°C. Reproduced with permission from K. Bernauer, P. Pousaz, J. Porret and A. Jean-guenat, *Helv. Chim. Acta* **68**, 1611 (1985).

corresponds to  $\Lambda$ -(-)<sub>436</sub>-[Co(*SS*)-*bamap*(H<sub>2</sub>O)]<sup>+</sup>. This must therefore be the enantiomer building up in the residue and therefore be the one with the lower rate. This is confirmed when the two Co(III) complexes,  $\Lambda$ -(-)<sub>436</sub>-[Co(*SS*)-*bamap*(H<sub>2</sub>O)]<sup>+</sup> and  $\Lambda$ -(+)<sub>436</sub>-[Co(*RR*)-*bamap*(H<sub>2</sub>O)]<sup>+</sup> are separately examined in their rates with  $\Lambda$ -[Fe(*SS*)-*alamp*]. The ratio of rate constants is 0.6 from the cd measurements and 0.53 measured directly at 25°C and pH = 4.0. The chiral faces of the Fe(II) and Co(III) complexes fit better in a precursor complex when they show opposite chirality (**2**) and thus the  $\Lambda$ - $\Delta$  couple might be expected to react faster. An inner-sphere mechanism with a H<sub>2</sub>O bridging is proposed, although it is admitted that such a bridge is unusual (Sec. 5.5(a)).<sup>87</sup>

Both outer- and inner-sphere pathways are observed when Co(C<sub>2</sub>O<sub>4</sub>)<sub>3</sub><sup>3-</sup> reacts with Co<sup>2+</sup> in the presence of en ligand.<sup>69</sup> The outer-sphere pathway is favored in higher en concentrations and produces Co(en)<sub>3</sub><sup>3+</sup>. The  $\Delta\Lambda$  combination is preferred (9% stereospecificity). The inner



sphere pathway leads to  $\text{Co(en)}_2(\text{C}_2\text{O}_4)^+$  in only 1.5% ( $\Delta\Delta$ ) preference. It would perhaps be anticipated that inner-sphere redox processes, which lead to more intimate interactions, might be more stereoselective but in this case the bridge is extended and maintains the two cobalts some distance (5 Å) apart. There is a detailed discussion of the various interactions in the two pathways and it is clear that asymmetric induction studies have the potential for probing structural details of the mechanisms of redox reactions.<sup>69</sup>



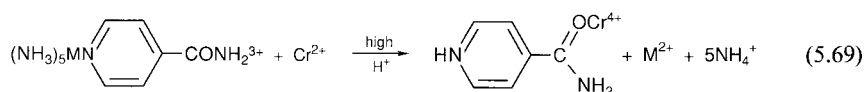
2

## 5.8 Intramolecular Electron Transfer

A major effort has been made to determine the rate of electron transfer between two well defined sites in a molecule and thus to assess the effect, on the rate, of the distance and the nature of the medium separating the points, the potential drive and so on.<sup>88</sup> Again, the pioneering work on simple complexes has laid the basis for understanding the behavior of larger molecules, especially protein systems which are attracting so much attention.

### 5.8.1 Between Two Metal Centers

The pioneering studies of Taube and his co-workers established remote attack by  $\text{Cr}^{2+}$  on an extended organic ligand attached to  $\text{M} = \text{Co(III)}, \text{Cr(III)} \text{ or } \text{Ru(III)}$ <sup>89,90</sup>



The result made it possible to begin to answer the important question as to how electron transfer from one redox center to another occurred. Was it (i) by the passage of electrons to

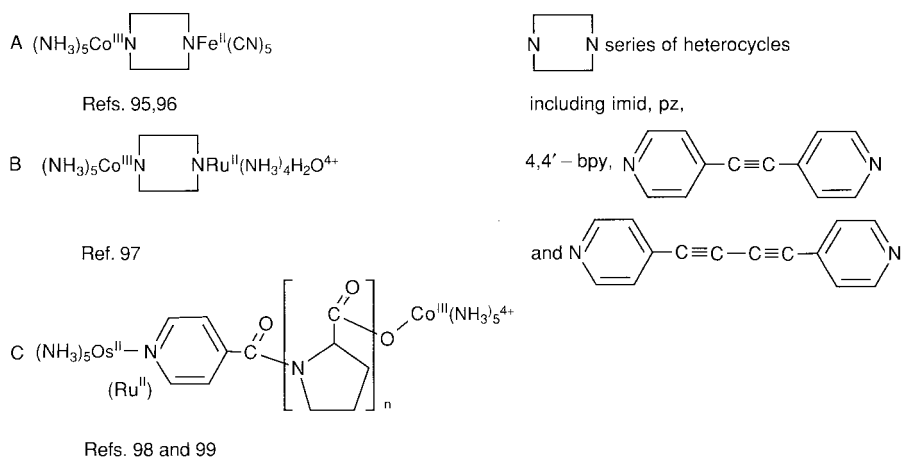
the bridging group to give a radical ion, which passes an electron further to the oxidant center?



This is called a chemical, radical or stepwise mechanism. Or was it (ii) by the action of the bridging group to increase the probability of electron transfer by tunneling, termed resonance transfer?<sup>18,56,91</sup>

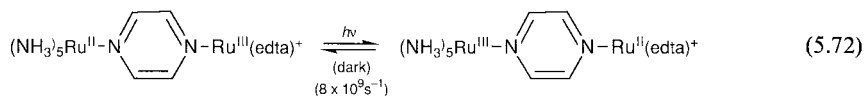
The chemical mechanism was supported for  $M = Co$  and  $Cr$ , whereas a resonance transfer was favored by  $Ru(III)$  and these differences were rationalized.<sup>89,92-94</sup> As important as these results are, they do not allow us to observe the actual electron transfer between the metal centers. Subsequent strategy has been to produce a very stable precursor complex, preferably with a versatile bridging system, and to observe the subsequent internal electron transfer. It is essential that the system is analyzed carefully kinetically, so as to obtain the internal electron transfer rate constant separated from other possible reactions also occurring (break up of precursor complex to constituents or outer-sphere electron transfer (Sec. 1.6.4(d))). For such examples see Refs. 22, 75. Examples of the types of bridging systems which have been examined are shown in Chart 5.1.<sup>95-99</sup>

Chart 5.1 Bridged Ligand Systems Within Which Electron Transfer Occurs



The bridged complexes were prepared by (a) direct interaction of the two constituents or (b) one electron reduction of the fully oxidized bridged complex (it would be the  $Co^{III}-Ru^{III}$  complex in one example shown above<sup>97</sup>). The speed with which the reduction must be carried out depends on the subsequent electron transfer rate. Both chemical reductants or rapidly generated reducing radicals have been used. The latter approach (b) has been an effective one for investigating electron transfer within proteins (Sec. 5.9). A special approach (c) involves

optical (picosecond) excitation to produce an unstable isomer, and examination of the reverse reaction<sup>100,101</sup>



An important goal using these types of bridged complexes is to determine the factors which will control the rate constants. From the previous discussions, we can guess that the important ones will include driving force, distances between redox centers and type of bridging ligand. Other more subtle influences are expected. The rate constant ( $k_{\text{et}}$ ) for intramolecular electron transfer within a ligand bridged binuclear complex (as in an inner-sphere mechanism) or in an outer-sphere complex, and in which the metal centers are separated by a distance  $r$ , is given by the expression (compare (5.27))

$$k_{\text{et}} = \nu_n \kappa_{\text{el}} \kappa_n \quad (5.73)$$

$\nu_n$  is the effective nuclear vibration frequency that destroys the activated complex configuration and is  $\approx 10^{13} \text{ s}^{-1}$ .  $\kappa_{\text{el}}$  is the electronic transmission coefficient and is approximately one for an adiabatic electron transfer, which occurs when the electronic coupling of the two redox sites is relatively strong. The value of  $\kappa_{\text{el}}$  will be, otherwise, a function of the separation and relative orientation of the two redox centers.  $\kappa_n$  is a nuclear factor<sup>23</sup> and given by (5.74); see (5.27) and (5.25), with  $w^r$  and  $w^p$  irrelevant ( $= 0$ ).

$$\kappa_n = \exp(-\Delta G^*/RT) \quad (5.74)$$

$$\Delta G^* = \frac{(\lambda_o + \lambda_i + \Delta G^\circ)^2}{4(\lambda_o + \lambda_i)} \quad (5.75)$$

$\Delta G^\circ$  is the standard free energy change for intramolecular electron transfer. Both  $\kappa_{\text{el}}$  and  $\kappa_n$  are contributory factors to a dependence of  $k$  on  $r$ , and (5.73) can be written

$$k_{\text{et}} = \nu_n \exp[-\beta(r - r_0)] \kappa_n^0 \exp(-\gamma r) \quad (5.76)$$

The term  $r_0$  is defined as that in which the value of  $\kappa_{\text{el}}$  ( $= \exp(-\beta(r - r_0))$ ) is unity when  $r = r_0$ , i.e. it is then an adiabatic reaction.

We can now consider some of the limited results which have emerged so far. In Haim's bridging systems (Chart 5.1), all reactions appear to undergo adiabatic electron transfer by a resonance mechanism with  $\kappa_{\text{el}} = 1$ . A linear plot of  $\Delta G^*$  (or  $\Delta G^\ddagger$ ) against  $1/r$  is obtained over a range of  $r$  from 6 to 16 Å for the five bridges shown. This indicates that only the solvent reorganizational term  $\lambda_o$  in (5.75) is a variable in the  $\kappa_n$  factor.<sup>22,95,96</sup> Other effects of the ligand structure are discussed (see Prob. 12). The Os(II)-L-Co(III) polyproline system has about an 0.6 V increased potential drive over the Ru(II)-L-Co(III) system (C in Chart 5.1) which is an analogous one in every other respect. A substantial increase in the rate of electron transfer results from this factor (Table 5.10). For the slower reactions ( $n = 3$  or 4) equilibra-

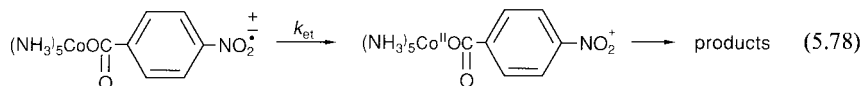
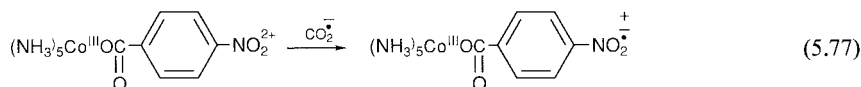
tion of *trans*- to *cis*-proline interferes with the analysis. With the Os(II)-L-Ru(III) system, both the nuclear ( $\gamma = 0.9 \text{ \AA}^{-1}$ ) and the electronic ( $\beta = 0.68 \text{ \AA}^{-1}$ ) factors are shown to contribute to the (exponential) dependence on  $r$  of  $k_{\text{et}}$ .<sup>98,99,102</sup>

**Table 5.10** Intramolecular Electron Transfer Across Oligoprolines<sup>98</sup>

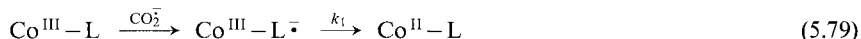
$n$ in System C (Chart 5.1)	$k_{\text{Os}}$ $\text{s}^{-1}$	$k_{\text{Ru}}$ $\text{s}^{-1}$
0	$1.9 \times 10^5$	$1.2 \times 10^{-2}$
1	$2.7 \times 10^2$	$1.0 \times 10^{-4}$
2	0.74	$6.0 \times 10^{-6}$
3	0.09	$5.6 \times 10^{-5}$
4	0.09	$1.4 \times 10^{-4}$

## 5.8.2 Metal Complexes with Reducible Ligands

Strong evidence for the feasibility of the chemical mechanism (Sec. 5.8.1) has been afforded by the production of a transient nitrophenyl radical attached to a Co(III) complex

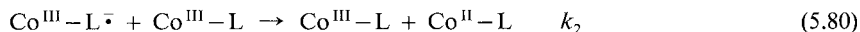


The radical undergoes first-order decay ( $k_{\text{et}}$ ) via electron transfer to Co(III).<sup>103</sup> This approach has been much employed to investigate the internal electron transfer process. Invariably Co(III) complexes have been used and since the transient radicals have strong absorbance characteristics, pulse radiolysis reduction with spectral (and occasionally) conductometric monitoring is universally employed. Since  $e_{\text{aq}}^-$  reduces both the Co(III) and the ligand centers, the use of  $\text{CO}_2^-$  and  $(\text{CH}_3)_2\dot{\text{C}}\text{OH}$ , which preferentially reduce the ligand, is preferred. In the types of systems so far examined (Table 5.11)<sup>104-106</sup> decay of the coordinated radical ligand usually occurs as in (5.78) by an intramolecular electron transfer ( $k_1$ ) leading to the cobalt(II) species.

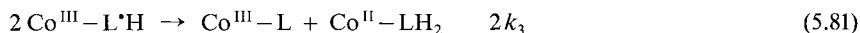


This is indicated by the observation of first-order loss of radical signal, with the rate constant  $k_1$  being independent of the concentration, both of radical complex (i. e., independent of the dose of reductant radical used) and of  $\text{Co}^{\text{III}}-\text{L}$  complex used (in excess). Only rarely is the first-order loss of  $\text{Co}^{\text{III}}-\text{L}^{\cdot-}$  directly dependent on the concentration of  $\text{Co}^{\text{III}}-\text{L}$  present,

and this is interpreted in terms of reaction (5.80). Sometimes the loss of  $\text{Co}^{\text{III}}-\text{L}^{\cdot-}$  is second-order,<sup>104</sup>


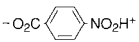
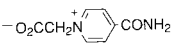
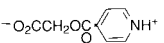
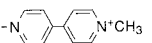


and this is attributed to a disproportionation of the protonated adduct in acid (5.81).



In all cases (5.79)–(5.81), the cobalt(II) product is expected to rapidly dissociate to constituents. The presence of (5.80) makes it difficult to determine the value of  $k_1$ , which is a small intercept on a  $k_{\text{obs}}$  vs  $[\text{Co}^{\text{III}}-\text{L}]$  plot.<sup>106</sup> The occurrence of (5.81) is usually signalled by mixed first- and second-order kinetics since as the concentration of  $\text{Co}^{\text{III}}-\text{L}^{\cdot-}$  (or  $\text{Co}^{\text{III}}-\text{L}^{\cdot}\text{H}$ ) decreases, the importance of (5.81) is superseded by (5.79) and  $k_1$  results from the (first-order) end of the decay (see Fig. 1.6). Most unusually, the complex  $(\text{NH}_3)_5\text{Co}(\text{N-Mebpy}^*)^{3+}$  undergoes all three modes of decay (Table 5.11).<sup>106</sup>

**Table 5.11** Rate Constants for Decay of  $\text{Co}(\text{NH}_3)_5(\text{L}^{\cdot})^{n+}$  at 23–25 °C

–L	$k_1, \text{s}^{-1}$	$k_2, \text{M}^{-1}\text{s}^{-1}$	$2k_3, \text{M}^{-1}\text{s}^{-1}$	Ref.
	$4.0 \times 10^5$ (o) $1.5 \times 10^2$ (m) $2.6 \times 10^3$ (p)			104
	5		$1.5 \times 10^8$	104
	$< 2.0 \times 10^4$	$1.5 \times 10^9$		105
	$2.0 \times 10^4$	$< 6 \times 10^6$		105
	$8.7 \times 10^2$	$5.4 \times 10^7$	$2.4 \times 10^8$	106

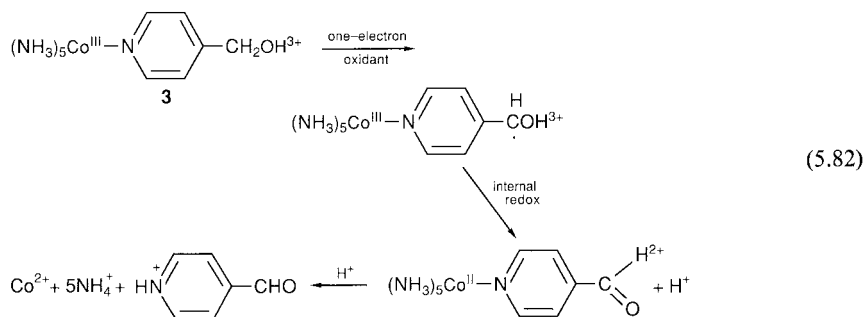
There has been nothing like the enthusiasm for the application to these systems of the theoretical equations, which we have noted in the previous sections and will encounter in the next. Nevertheless, a number of features are present which are qualitatively consistent with the discussions in Sec. 5.8.1 and which are in part illustrated in Table 5.11. There is a correlation of rate constant with the driving force of the internal electron transfer.<sup>104–108</sup> The p-nitrophenyl derivative is a poorer reducing agent when protonated and  $k_1$  is much less than for the unprotonated derivative. Consequently disproportionation ( $2k_3$ ) becomes important. Although there are not marked effects of structural variation on the values of  $k_1$ , the associated activation parameters may differ enormously and this is ascribed to the operation of different mechanisms.<sup>104</sup> The “resonance-assisted through-chain” operates with the p-

nitrophenyl derivative and has large Franck-Condon requirements, hence  $\Delta H^\ddagger = 71 \text{ kJ mol}^{-1}$  and  $\Delta S^\ddagger = +59 \text{ J K}^{-1} \text{ mol}^{-1}$ . "Direct ligand by-pass" is possible for the *o*-nitrophenyl derivative since orbital overlap of the donor and acceptor sites is now feasible. The much smaller  $\Delta H^\ddagger$  values ( $\sim 16 \text{ kJ mol}^{-1}$ ) are consistent with this, but the advantage is offset by a large negative  $\Delta S^\ddagger$  ( $= -100 \text{ J K}^{-1} \text{ mol}^{-1}$ ) which is attributed to a greatly reduced configurational flexibility which accompanies activation. Two other ways of electron transfer are suggested, namely flexible "indirect overlap" and nonadiabatic transfer with very little coupling between the centers.<sup>104</sup>

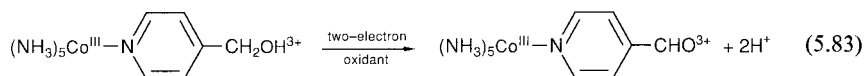
Finally, attention should be drawn to the elegant studies of Meyer and his co-workers. Metal complexes have been designed which contain both an excitable (e.g. bpy) and a quencher (e.g. *N*-Mebpy<sup>+</sup>) group. Following excitation, intramolecular electron and energy transfer occurs and the dependence of rate on distances, metal and so on, can be assessed.<sup>108</sup>

### 5.8.3 Induced Electron Transfer

Internal ligand-to-metal electron transfer may be initiated by the action of an external oxidant on the ligand. This phenomenon of induced electron transfer has received rather scant attention. In the complex **3** shown in (5.82) the one-electron oxidizing center of the Co(III) and the two-electron reducing ligand 4-pyridylcarbinol can coexist because of their redox "incompatibility". The complex is therefore relatively stable. This situation is upset when a strong one-electron oxidant such as Ce(IV) or Co(III) is added to a solution of the Co(III) complex. The oxidant attacks the carbinol function to generate an intermediate or intermediates; the intermediate in this case is oxidized *internally* by the Co(III) center; for example,



Thus, one equivalent of an external oxidant and one of the Co(III) complex are consumed in oxidizing one equivalent of the alcohol to the aldehyde. Two-equivalent oxidants, Cl<sub>2</sub>, Cr(VI), give no such radical intermediate, and therefore no Co(II), and only the Co(III) complex.<sup>109</sup>



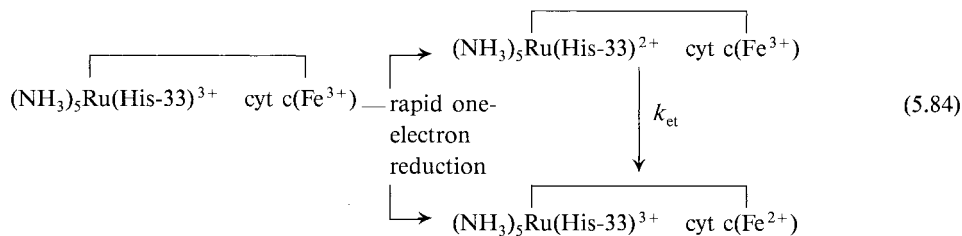
For more recent examples involving induced electron transfer linked to cobalt(III) complexes of  $\alpha$ -hydroxy acids and hydroquinone esters see Refs. 110, 111.

## 5.9 Electron Transfer in Proteins

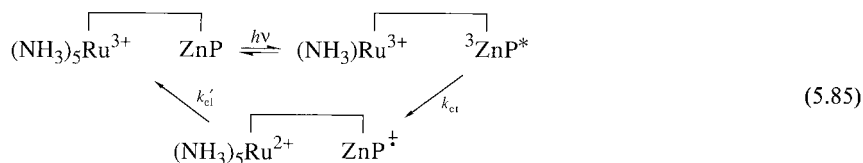
Early attempts at observing electron transfer in metalloproteins utilized redox-active metal complexes as external partners. The reactions were usually second-order and approaches based on the Marcus expression allowed, for example, conjectures as to the character and accessibility of the metal site.<sup>112,113</sup> The agreement of the observed and calculated rate constants for cytochrome c reactions for example is particularly good, even ignoring work terms.<sup>25</sup> The observations of deviation from second-order kinetics (“saturation” kinetics) allowed the dissection of the observed rate constant into the components, namely adduct stability and first-order electron transfer rate constant (see however Sec. 1.6.4).<sup>113</sup> Now it was a little easier to comment on the possible site of attack on the proteins, particularly when a number of modifications of the proteins became available.

*Protein surface “patches”* – Certain sites on the surface of proteins appear to act as conduits for electron passage. Thus in the protein azurin (*Pseudomonas aeruginosa*) a hydrophobic patch around the partly exposed His 117 (which is attached to Cu) is believed to be involved in electron transfer with nitrite reductase and in the self exchange of the Cu(I) and Cu(II) forms of azurin. The effect of specific labelling at the patch on the kinetic characteristics helps confirm this patch as playing a role in the electron transfer. Earlier, chemical modifications were employed (O. Farver, Y. Blatt and I. Pecht, *Biochemistry* **21**, 3556 (1982)). More recently the powerful technique of site-directed mutagenesis has been used. Met 44 located next to His 117 is replaced by Lys with minimum overall structural changes in the protein. The electron self-exchange measured by nmr line broadening is slower and pH-dependent for the modified protein compared with the native (wild type) protein ( $\approx 10^6 \text{M}^{-1} \text{s}^{-1}$ , which is also pH-independent). The patch is therefore implicated in the electron transfer process. (M. van de Kamp, R. Floris, F. C. Hali and G. W. Canters, *J. Amer. Chem. Soc.* **112**, 907 (1990)).

This general approach has, however, serious limitations. The position of the site for attack (and therefore the electron transfer distance involved) is very conjectural. In addition, the vexing possibility, which we have encountered several times, of a “dead-end” mechanism (Sec. 1.6.4) is always present.<sup>113</sup> One way to circumvent this difficulty, is to bind a metal complex to the protein *at a specific site*, with a known (usually crystallographic) relationship to the metal site. The strategy then is to create a metastable state, which can only be alleviated by a discernable electron transfer between the labelled and natural site. It is important to establish that the modification does not radically alter the structure of the protein. A favorite technique is to attach  $(\text{NH}_3)_3\text{Ru}^{3+}$  to a histidine imidazole near the surface of a protein. Exposure of this modified protein to a deficiency of a powerful reducing agent, will give a concurrent (partial) reduction of the ruthenium(III) and the site metal ion e.g. iron(III) heme in cytochrome c



The intramolecular electron transfer  $k_{\text{et}}$ , subsequent to the rapid reduction, must occur because the Ru(III)-Fe(II) pairing is the stable one. It is easily monitored using absorbance changes which occur with reduction at the Fe(III) heme center. Both laser-produced  $^*\text{Ru}(\text{bpy})_3^{2+}$  and radicals such as  $\text{CO}_2^-$  (from pulse radiolysis (Prob. 15)) are very effective one-electron reductants for this task (Sec. 3.5).<sup>114,115</sup> In another approach,<sup>116,117</sup> the Fe in a heme protein is replaced by Zn. The resultant Zn porphyrin (ZnP) can be electronically excited to a triplet state,  $^3\text{ZnP}^*$ , which is relatively long-lived ( $\tau = 15$  ms) and is a good reducing agent ( $E^\circ = -0.62$  V). Its decay via the usual pathways (compare (1.32)) is accelerated by electron transfer to another metal (natural or artificial) site in the protein e.g.,



The  $\text{ZnP}^\dagger$  accepts an electron from the  $\text{Ru}^{2+}$  to return the system to its initial state. Although  $k_{\text{et}}' > k_{\text{et}}$ , both can be measured.<sup>118</sup> Examples of these approaches with iron and copper proteins are shown in Table 5.12. There are a number of excellent short reviews of this subject.<sup>121-124</sup>

**Table 5.12** Intramolecular Electron Transfer Rate Constants in Metalloproteins at  $\approx 25^\circ\text{C}$

Protein	Redox Centers Involved	Initiating Mode	$k_{\text{et}}$ $\text{s}^{-1}$	Distance <sup>a</sup> $\text{\AA}$	$\Delta E$ Volts	Ref.
Cytochrome c (horse heart)	$(\text{NH}_3)_5\text{Ru}^{\text{II}}(\text{His-33})$ ; Fe(II)heme	$^*\text{Ru}(\text{bpy})_3^{2+}$	30 <sup>b</sup>	11.8	0.19	114
		$\text{CO}_2^-$	53 <sup>c</sup>	11.8	0.19	115
Plastocyanin ( <i>A. variabilis</i> )	$(\text{NH}_3)_5\text{Ru}^{\text{II}}(\text{His-59})$ ; Cu(II)	$\text{CO}_2^-$	$\leq 0.08$	11.9	0.26	119
Azurin ( <i>P. aeruginosa</i> )	$(\text{NH}_3)_5\text{Ru}^{\text{II}}(\text{His-83})$ ; Cu(II) (Sec. 3.5.1)	$^*\text{Ru}(\text{bpy})_3^{2+}$	1.9	11.8	0.28	120
		$\text{CO}_2^-$	2.5	11.8	0.28	119
Cytochrome c (horse heart)	$(\text{NH}_3)_5\text{Ru}^{\text{III}}(\text{His-33})$ ; Zn(II)	$^3\text{ZnP}^*$ ( $h\nu$ )	$7.7 \times 10^5$	11.8	0.72	118

<sup>a</sup> The shortest distance separating the delocalized metal centers, e.g. heme edge.

<sup>b</sup>  $\Delta H^\ddagger = 8-16$  kJ mol<sup>-1</sup>. <sup>c</sup>  $\Delta H^\ddagger = 15$  kJ mol<sup>-1</sup>.



Electron transfer within polypeptide material is surprisingly fast even over relatively long distances. The rate constants however are much less than the typical values of  $10^6$  to  $10^9 \text{s}^{-1}$  for electron transfer between biphenyl radical anions and organic acceptors held about  $10 \text{\AA}$  apart by a steroid frame.<sup>125</sup> In the latter case, there is generally a larger potential drive and electron transfer may be “through-bond” rather than the “through space” in proteins, although this does not now appear likely.<sup>126</sup>

We have seen that two important factors control the value of  $k_{\text{et}}$ . These are (a) the distance of separation of the two sites ( $r$ ) and (b) the driving force  $\Delta G^\circ$  for the electron transfer. Recalling (5.73) to (5.76) and setting  $r_0 = 3 \text{\AA}$ ,  $\lambda = \lambda_o + \lambda_i$ :

$$k_{\text{et}} = v_n \kappa_{\text{el}} \kappa_n = v_n \exp[-\beta(r - 3)] \exp\left[\frac{-(\Delta G^\circ + \lambda)^2}{4\lambda RT}\right] \quad (5.86)$$

For a series of Ru modified (all at His-33 so that  $r$  is constant), Fe or Zn substituted cytochrome c derivatives,  $\kappa_{\text{el}}$  and  $\lambda$  are relatively constant and  $\Delta G^\circ$  is variable. The plot of  $\ln k_{\text{et}}$  (which varies from 30 to  $3.3 \times 10^6 \text{s}^{-1}$ ) vs  $\Delta G^\circ$  ( $-0.18$  to  $-1.05 \text{V}$ ) shows the semblance of the expected parabolic shape for (5.86) and leads to  $\lambda = 1.10 \text{eV}$ .<sup>118,127</sup> Experiments directed towards the distance dependence of  $\ln k_{\text{et}}$  lead to  $\beta$  values of  $0.9$ – $1.0 \text{\AA}^{-1}$ .<sup>127</sup> Similar results are obtained with Co(III) cage modified cytochrome-c.<sup>128</sup>

More subtle factors that might affect  $k_{\text{et}}$  will be the sites structures, their relative orientation and the nature of the intervening medium.<sup>122</sup> That these are important is obvious if one examines the data for the two copper proteins plastocyanin and azurin. Despite very similar separation of the redox sites and the driving force (Table 5.12), the electron transfer rate constant within plastocyanin is very much the lesser (it may be zero).<sup>119</sup> See Prob. 16. In striking contrast, small oxidants are able to attach to surface patches on plastocyanin which are more favorably disposed with respect to electron transfer to and from the Cu, which is about  $14 \text{\AA}$  distant. It can be assessed that internal electron transfer rate constants are  $\approx 30 \text{s}^{-1}$  for  $\text{Co}(\text{phen})_3^{3+}$ ,  $> 5 \times 10^3 \text{s}^{-1}$  for  $\text{Ru}(\text{NH}_3)_3\text{imid}^{2+}$  and  $3.0 \times 10^6 \text{s}^{-1}$  for  $^*\text{Ru}(\text{bpy})_3^{2+}$ , Refs. 119 and 129. In the last case the excited state  $^*\text{Ru}(\text{bpy})_3^{2+}$  is believed to bind about  $10$ – $12 \text{\AA}$  from the Cu center. Electron transfer occurs both from this remote site as well as by attack of  $^*\text{Ru}(\text{bpy})_3^{2+}$  adjacent to the Cu site.<sup>129</sup> At high protein concentration, electron transfer occurs solely through the remote pathway.

Experimental evidence for long-range electron transfer in polypeptides and proteins had been early accrued.<sup>130</sup> The value of using a metal center as a marker is apparent from the above. The approach can be extended to electron transfer between two proteins which are physiological partners.<sup>25</sup> Metal substitution (e.g. Zn for Fe) can be used to alter the value of  $\Delta G^\circ$  and permit photoinduced initiation. The parabolic behavior predicted by (5.86) has been verified for the electron transfer rate constant vs  $\Delta G^\circ$  within the adduct between cyt c and cyt  $b_5$ .<sup>117</sup>

## 5.10 The Future

Of all the areas covered in this book, that of oxidation-reduction reactions has attracted the most attention by a variety of chemists with substantial results. Many of the future problems delineated by Taube in his book *Electron Transfer Reactions of Complex Ions in Solution* published 20 years ago, have been tackled with success. The detailed arrangement of reactants in the activated complex for both outer-sphere and inner-sphere reactions is better understood as well as the controlling factors. The calculations of outer-sphere self-exchange rate constants is likely now to be a successful exercise and the application of cross-reaction equations almost routine. Deviations are rare and lead to interesting concepts. The assessment of solvent and medium effects as well as volumes of activation still requires a good deal of examination. The observation of very short-lived transients is increasingly easier and with it comes an appreciation of an increasingly detailed mechanism, small molecule interactions with heme proteins being the best example of this. Finally, the transfer of electrons in proteins will undoubtedly attract much time and talent. The approaches that are likely to be successful have been well established in the past decade.

### References

1. A. Hammershøi, D. Geselowitz and H. Taube, *Inorg. Chem.* **23**, 979 (1984).
2. I. Ruff and M. Zimonyi, *Electrochim. Acta* **18**, 515 (1973).
3. H. Taube and E. L. King, *J. Amer. Chem. Soc.* **76**, 4053, 6423 (1954); D. L. Ball and E. L. King, *J. Amer. Chem. Soc.* **80**, 1091 (1958).
4. H. Taube, H. Myers and R. L. Rich, *J. Amer. Chem. Soc.* **75**, 4118 (1953); H. Taube and H. Myers, *J. Amer. Chem. Soc.* **76**, 2103 (1954).
5. H. Ogino, E. Kikkawa, M. Shimura and N. Tanaka, *J. Chem. Soc. Dalton Trans.* 894 (1981).
6. J. Xu and R. B. Jordan, *Inorg. Chem.* **29**, 4180 (1990); M. J. Hynes and D. F. Kelly, *J. Chem. Soc. Chem. Commun.* 849 (1988).
7. P. L. Drake, R. T. Hartshorn, J. McGinnis and A. G. Sykes, *Inorg. Chem.* **28**, 1361 (1989).
8. D. R. Stranks and R. G. Wilkins, *Chem. Rev.* **57**, 743 (1957).
9. J. H. Espenson, *Acc. Chem. Res.* **3**, 347 (1970).
10. K. G. Ashurst and W. C. E. Higginson, *J. Chem. Soc.* 3044 (1953).
11. The eventual proportions of  $\text{Cr}^{3+}$  and  $\text{CrCl}^{2+}$  formed will depend on the concentrations and formation constant of  $\text{CrCl}^{2+}$ .
12. E. F. Hills, M. Moszner and A. G. Sykes, *Inorg. Chem.* **25**, 339 (1986).
13. For tables and references see T. J. Williams and C. S. Garner, *Inorg. Chem.* **9**, 2058 (1970); D. W. Carlyle and J. H. Espenson, *J. Amer. Chem. Soc.* **91**, 599 (1969).
14. A. Haim and N. Sutin, *J. Amer. Chem. Soc.* **88**, 5343 (1966).
15. A. G. Sykes and M. Green, *J. Chem. Soc. A*, 3221 (1970); M. Green, R. S. Taylor and A. G. Sykes, *J. Chem. Soc. A*, 509 (1971); K. M. Davies and J. H. Espenson, *J. Amer. Chem. Soc.* **91**, 3093 (1969).
16. The data for this Table are taken from the compilations in B36 and in the Selected Bibliography in Chap. 4.
17. The reaction of  $\text{Fe}^{2+}$  with  $\text{Fe}(\text{phen})_3^{3+}$  is considered to be an outer-sphere reaction because of the inertness of the  $\text{Fe}(\text{III})$  complex. Marked effects of anions on the rate have been interpreted however

- in terms of nucleophilic attack of the anion on the phenanthroline ligand. Even the unaccelerated reaction has been considered as an inner-sphere process involving a water bridge, N. Sutin and A. Forman, *J. Amer. Chem. Soc.* **93**, 5274 (1971); R. Schmid and L. Han, *Inorg. Chim. Acta* **69**, 127 (1983).
18. N. Sutin, *Acc. Chem. Res.* **1**, 225 (1968).
  19. R. A. Marcus, *J. Chem. Phys.* **24**, 966 (1956); *Ann. Rev. Phys. Chem.* **15**, 155 (1964); R. A. Marcus and P. Siders in *B38*, Chap. 10.
  20. N. S. Hush, *Trans. Faraday Soc.* **57**, 557 (1961); *B38*, Chap. 13.
  21. D. E. Pennington in *B32*, Chap. 3.
  22. A. Haim, *Prog. Inorg. Chem.* **30**, 273 (1983).
  23. N. Sutin, *Acc. Chem. Res.* **15**, 275 (1982); *Prog. Inorg. Chem.* **30**, 441 (1983). N. Sutin, B. S. Brunshwig, C. Creutz and J. R. Winkler, *Pure App. Chem.* **60**, 1817 (1988).
  24. M. D. Newton and N. Sutin, *Ann. Rev. Phys. Chem.* **35**, 437 (1984).
  25. R. A. Marcus and N. Sutin, *Biochim. Biophys. Acta* **811**, 265 (1985).
  26. G. M. Brown and N. Sutin, *J. Amer. Chem. Soc.* **101**, 883 (1979).
  27. B. S. Brunshwig, C. Creutz, D. H. Macartney, T.-K. Sham and N. Sutin, *Faraday Disc. Chem. Soc.* **74**, 113 (1982).
  28. M. Kozik and L. C. W. Baker, *J. Amer. Chem. Soc.* **112**, 7604 (1990).
  29. P. Bernhard, L. Helm, I. Rapaport, A. Ludi and A. E. Merbach, *J. Chem. Soc. Chem. Commun.* 302 (1984); P. Bernhard, L. Helm, A. Ludi and A. E. Merbach, *J. Amer. Chem. Soc.* **107**, 312 (1985).
  30. P. J. Smolenaers and J. K. Beattie, *Inorg. Chem.* **25**, 2259 (1986).
  31. M. N. Doyle, K. Libson, M. Woods, J. C. Sullivan and E. Deutsch, *Inorg. Chem.* **25**, 3367 (1986).
  32. D. J. Szalda, D. H. Macartney and N. Sutin, *Inorg. Chem.* **23**, 3473 (1984). D. H. Macartney and N. Sutin, *Inorg. Chem.* **22**, 3530 (1983).
  33. P. Bernhard and A. M. Sargeson, *Inorg. Chem.* **26**, 4122 (1987).
  34. P. Bernhard and A. M. Sargeson, *Inorg. Chem.* **27**, 2582 (1988).
  35. T. W. Newton, *J. Chem. Educ.* **45**, 571 (1968).
  36. M. A. Ratner and R. D. Levine, *J. Amer. Chem. Soc.* **102**, 4898 (1980).
  37. T. E. Meyer, C. T. Przysiecki, J. A. Watkins, A. Bhattacharyya, R. P. Simondson, M. A. Cusanovich and G. Tollin, *Proc. Natl. Acad. Sci. USA* **80**, 6740 (1983).
  38. M. Z. Hoffman, F. Bolleta, L. Moggia and G. L. Hug, *J. Phys. Chem. Ref. Data* **18**, 219 (1989).
  39. T. J. Meyer, *Prog. Inorg. Chem.* **30**, 389 (1983).
  40. J. T. Hupp and M. J. Weaver, *Inorg. Chem.* **22**, 2557 (1983).
  41. U. Fürholz and A. Haim, *J. Phys. Chem.* **90**, 3686 (1986); K. Zahir, J. H. Espenson and A. Bakač, *Inorg. Chem.* **27**, 3144 (1988).
  42. W. H. Jolley, D. R. Stranks and T. W. Swaddle, *Inorg. Chem.* **29**, 1948 (1990).
  43. W. Böttcher, G. M. Brown and N. Sutin, *Inorg. Chem.* **18**, 1447 (1979).
  44. E. Kremer, G. Cha, M. Morkevicius, M. Seaman and A. Haim, *Inorg. Chem.* **23**, 3028 (1984).
  45. H.-M. Huck and K. Wiegardt, *Inorg. Chem.* **19**, 3688 (1980).
  46. A large positive  $\Delta V^\ddagger$  is associated with the internal electron transfer within the outer-sphere complex between  $\text{Co}(\text{NH}_3)_5\text{X}^{3+}$  and  $\text{Fe}(\text{CN})_6^{4-}$ . I. Krack and R. van Eldik, *Inorg. Chem.* **25**, 1743 (1986); Y. Sasaki, K. Endo, A. Nagasawa and K. Saito, *Inorg. Chem.* **25**, 4845 (1986). This value is not easy to interpret.
  47. A. Haim, *Comments Inorg. Chem.* **4**, 113 (1985).
  48. U. Fürholz and A. Haim, *Inorg. Chem.* **24**, 3091 (1985).
  49. J. R. Miller, J. V. Beitz and R. K. Huddleston, *J. Amer. Chem. Soc.* **106**, 5057 (1984). H. B. Gray, L. S. Fox, M. Kozik and J. R. Winkler, *Science*, **247**, 1069 (1990).
  50. M. J. Weaver and G. E. McManis, *Acc. Chem. Res.* **23**, 294 (1990).
  51. M. P. Doyle, J. K. Guy, K. C. Brown, S. N. Mahapatro, C. M. VanZyl and J. R. Pladziewicz, *J. Amer. Chem. Soc.* **109**, 1536 (1987). The application of Marcus ideas to organic and organometallic reactions is well covered by L. Ebersson, *Electron Transfer Reactions in Organic Chemistry*, Springer-Verlag,

- Berlin 1987 and J. K. Kochi, *Angew. Chem. Int. Ed. Engl.* **27**, 1227 (1988), where detailed accounts and comprehensive lists of references are contained.
52. K. Zahir, W. Böttcher and A. Haim, *Inorg. Chem.* **24**, 1966 (1985).
  53. M. Kimura, S. Yamabe and T. Minato, *Bull. Chem. Soc. Japan* **54**, 1699 (1981).
  54. H. Taube, *Adv. Inorg. Chem. Radiochem.* **1**, 1 (1959).
  55. N. Sutin, *Ann. Rev. Nucl. Sci.* **12**, 285 (1962).
  56. J. Halpern and L. E. Orgel, *Disc. Faraday Soc.* **29**, 32 (1960).
  57. R. C. Patel, R. E. Ball, J. F. Endicott and R. G. Hughes, *Inorg. Chem.* **9**, 23 (1970).  $\Delta H_{\text{obs}}^{\ddagger}$  is negative for the reduction of a number of complexes of the type *cis*-Co(en)<sub>2</sub>XY<sup>n+</sup> by Cr<sup>2+</sup>.
  58. A. Haim, *Pure Appl. Chem.* **55**, 89 (1983).
  59. J. P. Birk, *Inorg. Chem.* **9**, 125 (1970).
  60. R. K. Murmann, H. Taube and F. A. Posey, *J. Amer. Chem. Soc.* **79**, 262 (1957). Oxygen-18 tracer experiments have indicated that transfer of OH<sup>-</sup> to Cr<sup>2+</sup> from Co(NH<sub>3</sub>)<sub>5</sub>OH<sup>2+</sup> is quantitative.
  61. J. F. Ojo, O. Olubuyide and O. Oyetunji, *Inorg. Chim. Acta* **119**, L5 (1986).
  62. J. P. Candlin and J. Halpern, *Inorg. Chem.* **4**, 766 (1965); M. C. Moore and R. N. Keller, *Inorg. Chem.* **10**, 747 (1971). The effect is very small probably because of the extreme reactivity of Cr(II) towards these oxidants.
  63. J. P. Candlin, J. Halpern and D. L. Trimm, *J. Amer. Chem. Soc.* **86**, 1019 (1964).
  64. A. Haim, *Inorg. Chem.* **7**, 1475 (1968).
  65. A. related approach can be made to this calculation, B39, p. 51.
  66. C. Shea and A. Haim, *J. Amer. Chem. Soc.* **93**, 3055 (1971).
  67. D. P. Fay and N. Sutin, *Inorg. Chem.* **9**, 1291 (1970).
  68. R. Snellgrove and E. L. King, *J. Amer. Chem. Soc.* **84**, 4609 (1962); A. Haim, *J. Amer. Chem. Soc.* **88**, 2324 (1966).
  69. R. A. Marusak, P. Osvath, M. Kemper and A. G. Lappin, *Inorg. Chem.* **28**, 1542 (1989).
  70. J. E. Earley, *Prog. Inorg. Chem.* **13**, 243 (1970).
  71. L. E. Orgel, Report of the Tenth Solvay Conference, Brussels, 1956, p. 286.
  72. Sr. M. J. DeChant and J. B. Hunt, *J. Amer. Chem. Soc.* **90**, 3695 (1968).
  73. A. Haim and N. Sutin, *J. Amer. Chem. Soc.* **88**, 434 (1966).
  74. R. C. Patel and J. F. Endicott, *J. Amer. Chem. Soc.* **90**, 6364 (1968); D. P. Rillema, J. F. Endicott, and R. C. Patel, *J. Amer. Chem. Soc.* **94**, 394 (1972).
  75. G. C. Seaman and A. Haim, *J. Amer. Chem. Soc.* **106**, 1319 (1984).
  76. R. Dodson in B38, p. 132.
  77. M. Ardon and R. A. Plane, *J. Amer. Chem. Soc.* **81**, 3197 (1959).
  78. U. Fürholz and A. Haim, *Inorg. Chem.* **26**, 3243 (1987).
  79. R. D. Cannon and J. E. Earley, *J. Chem. Soc. A*, 1102 (1968); D. E. Pennington and A. Haim, *Inorg. Chem.* **6**, 2138 (1967), and references therein.
  80. J. Doyle, A. G. Sykes and A. Adin, *J. Chem. Soc. A*, 1314 (1968).
  81. E. M. Sabo, R. E. Shepherd, M. S. Rau and M. G. Elliott, *Inorg. Chem.* **26**, 2897 (1987).
  82. A. D. James, R. S. Murray and W. C. E. Higginson, *J. Chem. Soc. Dalton Trans.* 1273 (1974).
  83. D. A. Geselowitz and H. Taube, *J. Amer. Chem. Soc.* **102**, 4525 (1980).
  84. P. Osvath and A. G. Lappin, *Inorg. Chem.* **26**, 195 (1987).
  85. D. A. Geselowitz, A. Hammershøi and H. Taube, *Inorg. Chem.* **26**, 1842 (1987).
  86. Even the effects of chelate ring conformation in the reductants on the stereoselectivity can be assessed. Four conformational isomers are possible with M(en)<sub>3</sub><sup>n+</sup> Δ(λλλ), Δ(δλλ), Δ(δδλ) and Δ(δδδ), in which Δ refers to the chirality of the metal center and δ and λ to the chelate conformation (Secs. 7.1 and 7.6). There is a preference for ΔΔ interactions for Δ(λλλ) isomers and ΔΔ interactions for Δ(δδδ) isomers.<sup>84</sup>
  87. K. Bernauer, P. Pousaz, J. Porret and A. Jeanguenat, *Helv. Chim. Acta* **71**, 1339 (1988).

88. S. Isied, *Prog. Inorg. Chem.* **32**, 443 (1984).
89. F. Nordmeyer and H. Taube, *J. Amer. Chem. Soc.* **90**, 1162 (1968).
90. R. G. Gaunder and H. Taube, *Inorg. Chem.* **9**, 2627 (1970).
91. H. Taube and E. S. Gould, *Acc. Chem. Res.* **2**, 321 (1969).
92. M. K. Loar, Y.-T. Fanchiang and E. S. Gould, *Inorg. Chem.* **17**, 3689 (1978).
93. C. Norris and F. R. Nordmeyer, *J. Amer. Chem. Soc.* **93**, 4044 (1971).
94. C. A. Radlowski, P.-W. Chum, L. Hua, J. Heh and E. S. Gould, *Inorg. Chem.* **19**, 401 (1980).
95. A. P. Szecsy and A. Haim, *J. Amer. Chem. Soc.* **103**, 1679 (1981) and previous work.
96. G.-H. Lee, L. D. Ciana and A. Haim, *J. Amer. Chem. Soc.* **111**, 2535 (1989).
97. S. K. S. Zawacky and H. Taube, *J. Amer. Chem. Soc.* **103**, 3379 (1981).
98. S. S. Isied, A. Vassilian, R. H. Magnuson and H. A. Schwarz, *J. Amer. Chem. Soc.* **107**, 7432 (1985).
99. S. S. Isied, A. Vassilian, J. F. Wishart, C. Creutz, H. A. Schwarz and N. Sutin, *J. Amer. Chem. Soc.* **110**, 635 (1988).
100. C. Creutz, P. Kroger, T. Matsubara, T. L. Netzel and N. Sutin, *J. Amer. Chem. Soc.* **101**, 5442 (1979).
101. C. Creutz, *Prog. Inorg. Chem.* **30**, 1 (1983).
102. In a series of polypeptides of the type [TrpH-(proline)<sub>n</sub>-TyrOH] it is possible to preferentially oxidize (with N<sub>3</sub><sup>-</sup>) the trpH residue and produce [<sup>•</sup>Trp-(proline)<sub>n</sub>-TyrOH]. The rate constant for the subsequent change to [TrpH-(proline)<sub>n</sub>-TyrO<sup>•</sup>] correlates with Δ*G*<sup>o</sup>, but is only slightly sensitive to the value of *n*, M. Faraggi, M. R. DeFelippis and M. H. Klapper, *J. Amer. Chem. Soc.* **111**, 5141 (1989).
103. M. Z. Hoffman and M. Simic, *J. Amer. Chem. Soc.* **94**, 1757 (1972).
104. K. D. Whitburn, M. Z. Hoffman, N. V. Brezniak and M. G. Simic, *Inorg. Chem.* **25**, 3037 (1986) and previous references.
105. J. V. Beitz, J. R. Miller, H. Cohen, K. Wieghardt and D. Meyerstein, *Inorg. Chem.* **19**, 966 (1980).
106. K. Tsukahara and R. G. Wilkins, *Inorg. Chem.* **28**, 1605 (1989).
107. H. Cohen, E. S. Gould, D. Meyerstein, M. Nutkovich and C. A. Radlowski, *Inorg. Chem.* **22**, 1374 (1983). H. Cohen, M. Nutkovich, D. Meyerstein and K. Wieghardt, *J. Chem. Soc. Dalton Trans.* 943 (1982).
108. T. J. Meyer, *Pure Appl. Chem.* **62**, 1003 (1990).
109. B39, Chap. 4. The situation presented above is oversimplified and some puzzling features remain to be resolved. J. E. French and H. Taube, *J. Amer. Chem. Soc.* **91**, 6951 (1969).
110. V. S. Srinivasan and E. S. Gould, *Inorg. Chem.* **20**, 208 (1981).
111. R. A. Holwerda and J. D. Clemmer, *Inorg. Chem.* **21**, 2103 (1982).
112. S. Wherland and H. B. Gray in *Biological Aspects of Inorganic Chemistry*, A. W. Addison, W. R. Cullen, D. Dolphin and B. R. James, eds. Wiley, NY, 1977, p. 289.
113. A. G. Sykes, *Chem. Soc. Revs.* **15**, 283 (1986).
114. J. R. Winkler, D. G. Nocera, K. M. Yocom, E. Bordignon and H. B. Gray, *J. Amer. Chem. Soc.* **104**, 5798 (1982); **106**, 5145 (1984).
115. S. S. Isied, G. Worosila and S. J. Atherton, *J. Amer. Chem. Soc.* **104**, 7659 (1982); S. S. Isied, C. Kuehn and G. Worosila, *J. Amer. Chem. Soc.* **106**, 1722 (1984).
116. S. E. Peterson-Kennedy, J. L. McGourty, J. A. Kalweit and B. M. Hoffman, *J. Amer. Chem. Soc.* **108**, 1739 (1986).
117. G. McLendon, *Acc. Chem. Res.* **21**, 160 (1988), who also gives a short understandable account of long-distance electron transfer.
118. H. Elias, M. H. Chou and J. R. Winkler, *J. Amer. Chem. Soc.* **110**, 429 (1988).
119. M. P. Jackman, J. McGinnis, R. Pows, G. A. Salmon and A. G. Sykes, *J. Amer. Chem. Soc.* **110**, 5880 (1988). See also O. Farver and I. Pecht, *Inorg. Chem.* **29**, 4855 (1990) who find  $k_1 = 0.07 \pm 0.01 \text{ s}^{-1}$  and  $k_2 = 0$  for similar experiments with stellacyanin.
120. N. M. Kostić, R. Margalit, C.-M. Che and H. B. Gray, *J. Amer. Chem. Soc.* **105**, 7765 (1983).
121. H. B. Gray, *Chem. Soc. Revs.* **15**, 17 (1986).

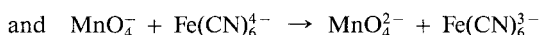
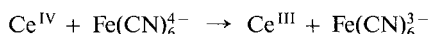
122. S. L. Mayo, W. R. Ellis, Jr., R. J. Crutchley and H. B. Gray, *Science* **233**, 948 (1986).  
 123. A. G. Sykes, *Chem. in Britain* **24**, 551 (1988).  
 124. R. A. Scott, A. G. Mauk and H. B. Gray, *J. Chem. Educ.* **62**, 932 (1985).  
 125. G. L. Closs and J. R. Miller, *Science* **240**, 440 (1988).  
 126. D. N. Beratan, J. N. Onuchic, J. N. Betts, B. E. Bowler and H. B. Gray, *J. Amer. Chem. Soc.* **112**, 7915 (1990).  
 127. A. W. Axup, M. Albin, S. L. Mayo, R. J. Crutchley and H. B. Gray, *J. Amer. Chem. Soc.* **110**, 435 (1988). T. J. Meade, H. B. Gray and J. R. Winkler, *J. Amer. Chem. Soc.* **111**, 4353 (1989).  
 128. D. W. Conrad and R. A. Scott, *J. Amer. Chem. Soc.* **111**, 3461 (1989).  
 129. B. S. Brunshwig, P. J. DeLaive, A. M. English, M. Goldberg, H. B. Gray, S. L. Mayo and N. Sutin, *Inorg. Chem.* **24**, 3743 (1985).  
 130. M. Faraggi, M. R. DeFelippis and M. H. Klapper, *J. Amer. Chem. Soc.* **111**, 5141 (1989) for references.

### Selected Bibliography

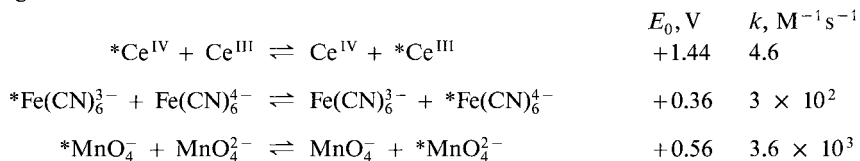
- B36. R. D. Cannon, *Electron Transfer Reactions*, Butterworth, London, 1980.  
 B37. W. L. Reynolds and R. W. Lumry, *Mechanisms of Electron Transfer*, Ronald Press, NY, 1966.  
 B38. D. B. Rorabacher and J. F. Endicott (eds.) *Mechanistic Aspects of Inorganic Reactions*, ACS Symposium Series, 198, American Chemical Society, Washington, D.C. 1982.  
 B39. H. Taube, *Electron Transfer Reactions of Complex Ions in Solution*, Academic, NY, 1970.  
 B40. J. J. Zuckerman, Ed. *Inorganic Reactions and Methods*. Vol. 15. *Electron Transfer and Electrochemical Reactions; Photochemical and other Energized Reactions*, VCH, Weinheim, 1986.

### Problems

1. Calculate the rate constants for the reactions



on the basis of the Marcus equation, (5.35). Use the following information for the isotopic exchange reactions



All values at 25°C.

2. Using the Marcus expression, the self-exchange for the couples  $\text{CO}_3^{2-}/\text{CO}_2$  and  $\text{SO}_3^{2-}/\text{SO}_2$  have been estimated as approximately  $10^{-5} \text{M}^{-1} \text{s}^{-1}$  and  $10^4 \text{M}^{-1} \text{s}^{-1}$  respectively. Suggest a reason for such a tremendous difference. H. A. Schwarz, C. Creutz and N. Sutin, *Inorg. Chem.* **24**, 433 (1985); R. J. Balahura and M. D. Johnson, *Inorg. Chem.* **26**, 3860 (1987).

3. The electron self-exchange rate constants evaluated by the Marcus expressions (using cross-reaction data) and those determined experimentally differ in the following cases. Give possible reasons for these differences.

Couple	Evaluation $M^{-1}s^{-1}$	Experimental $M^{-1}s^{-1}$	Refs.
Cu(II) peptides, Cu(III) peptides	$\sim 10^8$ <sup>a</sup>	$6 \times 10^4$	e
$Fe(H_2O)_6^{2+}$ , $Fe(H_2O)_6^{3+}$	$10^{-3}$ <sup>b</sup>	4	f, g
$O_2^-$ , $O_2$	$10^{-8}$ – $10^5$ <sup>b</sup>	$4.5 \times 10^2$	h, i
$Cu(phen)_2^+$ , $Cu(phen)_2^{2+}$	$50^c$ – $5 \times 10^7$ <sup>d</sup>	$7 \times 10^4$	j

<sup>a</sup> Using  $IrCl_6^{2-}$  <sup>b</sup> Large number of metal complex oxidants or reductants

<sup>c</sup> Using cyt-c as partner <sup>d</sup> Using  $Co(edta)^-$  as partner <sup>e–j</sup> Refs. below

(e) G. D. Owens and D. W. Margerum, *Inorg. Chem.* **20**, 1446 (1981).

(f) J. T. Hupp and M. Weaver, *Inorg. Chem.* **22**, 2557 (1983).

(g) P. Bernhard and A. M. Sargeson, *Inorg. Chem.* **26**, 4122 (1987).

(h) M. S. McDowell, J. H. Espenson and A. Bakač, *Inorg. Chem.* **23**, 2232 (1984).

(i) J. Lind, X. Shen, G. Merényi and B. Ö. Jonsson, *J. Amer. Chem. Soc.* **111**, 7654 (1989).

(j) C.-W. Lee and F. C. Anson, *Inorg. Chem.* **23**, 837 (1984).

4. The electron self-exchange rate constants ( $k$ ) have been assessed for the following couples at 25°C and  $\mu = 0.1$  M:

Couple	$k, M^{-1}s^{-1}$	$E_0$
$Mn(sar)^{2+/3+}$	17	0.52
$Fe(sar)^{2+/3+}$	$6.0 \times 10^3$	0.09
$Ru(sar)^{2+/3+}$	$1.2 \times 10^5$	0.29
$Co(sar)^{2+/3+}$	2.1	–0.43
$Co(en)_3^{2+/3+}$	$3.4 \times 10^{-5}$	–0.18
$Ni(sar)^{2+/3+}$	$1.7 \times 10^3$	0.86

Structure sar – Chap. 6, Structure 19

Correlate these data with the electronic configurations of the couples or alternatively deduce structural differences for the couples from the kinetic data.

I. I. Creaser, A. M. Sargeson and A. W. Zanella, *Inorg. Chem.* **22**, 4022 (1983).

P. Bernhard and A. M. Sargeson, *Inorg. Chem.* **26**, 4122 (1987).

5. Rationalize the relatively slow self-exchange rates for the couples involving the aqua ions,  $Ti^{3+/4+} \geq 3 \times 10^{-4} M^{-1}s^{-1}$ ;  $TiOH^{2+/3+} \approx 10^{-2} M^{-1}s^{-1}$ ;  $V^{2+/3+} = 10^{-2} M^{-1}s^{-1}$ .  
D. H. Macartney, *Inorg. Chem.* **25**, 2222 (1986) and references therein.

6. a. Explain why the rate constants for a number of  $Cr^{2+}$  reductions, although inner-sphere, do not vary much.

J. P. Candlin and J. Halpern, *Inorg. Chem.* **4**, 766 (1965); R. C. Patel, R. E. Ball, J. F. Endicott and R. G. Hughes, *Inorg. Chem.* **9**, 23 (1970); N. Sutin, *Acc. Chem. Res.* **1**, 225 (1968).

b.  $\text{Co}(\text{NH}_3)_5\text{NH}_2\text{CHO}^{3+}$  reacts rapidly with  $\text{Cr}^{2+}$  to give  $\text{Cr}(\text{H}_2\text{O})_5\text{OCHNH}_2^{3+}$ , with a rate law:

$$V = k [\text{Cr}^{\text{II}}] [\text{Co}^{\text{III}}] [\text{H}^+]^{-1}$$

whereas the linkage isomer  $\text{Co}(\text{NH}_3)_5\text{OCHNH}_2^{3+}$  only slowly reacts with  $\text{Cr}^{2+}$ , with no  $[\text{H}^+]$  dependency in the rate law. Explain.

R. J. Balahura and R. B. Jordan, *J. Amer. Chem. Soc.* **92**, 1533 (1970).

c. Discuss the probable mechanisms for  $\text{Cu}^+$  reductions from the data of Table 5.7.

O. J. Parker and J. H. Espenson, *J. Amer. Chem. Soc.* **91**, 1968 (1969); E. R. Dockal,

E. T. Everhart and E. S. Gould, *J. Amer. Chem. Soc.* **93**, 5661 (1971).

d. The reduction of nicotinic or isonicotinic acid complexes of the pentamminecobalt(III) moiety are much faster by  $\text{V}^{2+}$  than by  $\text{Cr}^{2+}$ , and this is unusual. Suggest how this might arise, bearing in mind the discussion in Sec. 5.8.1.

C. Norris and F. R. Nordmeyer, *Inorg. Chem.* **10**, 1235 (1971).

7. Comment on the rate constants,  $\text{M}^{-1}\text{s}^{-1}$  at  $25^\circ\text{C}$ , for the following pairs of reactions considering particularly the relative values:

reductant	oxidant	$k$	oxidant	$k$
$\text{Cr}^{2+}$	$\text{CrN}_3^{2+}$	6.1	$\text{FeN}_3^{2+}$	$\sim 3 \times 10^7$
	$\text{CrNCS}^{2+}$	$1.5 \times 10^{-4}$	$\text{FeNCS}^{2+}$	$3 \times 10^7$
$\text{V}^{2+}$	$\text{FeN}_3^{2+}$	$5.2 \times 10^5$	$\text{Co}(\text{CN})_5\text{N}_3^{3-}$	$1.1 \times 10^2$
	$\text{FeNCS}^{2+}$	$6.6 \times 10^5$	$\text{Co}(\text{CN})_5\text{SCN}^{3-}$	$1.4 \times 10^2$
$\text{Co}(\text{CN})_5^{3-}$	$\text{Co}(\text{NH}_3)_5\text{N}_3^{2+}$	$1.6 \times 10^6$ <sup>a</sup>		
	$\text{Co}(\text{NH}_3)_5\text{NCS}^{2+}$	$1.0 \times 10^6$ <sup>a</sup>		
$\text{TiOH}^{2+}$	$\text{Co}(\text{CN})_5\text{N}_3^{3-}$	1.5		
	$\text{Co}(\text{CN})_5\text{NCS}^{3-}$	$< 10^{-3}$		

<sup>a</sup> Inner-sphere.

O. Oyetunji, O. Olubuyide and J. F. Ojo, *Bull. Chem. Soc. Japan* **63**, 601 (1990) and references therein.

8. The reduction of a number of complexes  $\text{Co}(\text{NH}_3)_5\text{X}^{(3-n)+}$  by  $\text{Co}(\text{CN})_5^{3-}$  in solutions containing  $\text{CN}^-$  ion has been examined. With  $\text{X}^{n-} = \text{Cl}^-, \text{N}_3^-, \text{NCS}^-,$  and  $\text{OH}^-$ , the redox reactions are second-order, with a wide range of values for the second-order rate constant, and a product  $\text{Co}(\text{CN})_5\text{X}^{3-}$ . The rate law is different with  $\text{X}^{n-} = \text{NH}_3, \text{PO}_4^{3-}, \text{CO}_3^{2-}$  and  $\text{SO}_4^{2-}$ ,

$$V = k [\text{Co}^{\text{III}}] [\text{Co}^{\text{II}}] [\text{CN}^-]$$

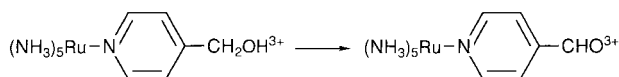
with  $k$  similar for these reductions, and the product  $\text{Co}(\text{CN})_5^{3-}$ . Give an explanation for this behavior.

J. P. Candlin, J. Halpern and S. Nakamura, *J. Amer. Chem. Soc.* **85**, 2517 (1963).



9. A strong autocatalysis is observed in the reaction of  $\text{Co}(\text{bamap})(\text{H}_2\text{O})^-$  (see 2) with  $\text{Fe}^{2+}$  in the presence of ascorbic acid,  $\text{pH} < 3.5$  (Sec. 5.7.4). The autocatalysis is eliminated if a large excess of  $\text{Zn}^{2+}$  is present and the second-order rate constant for the  $\text{Fe}^{2+}$  reaction can then be determined (as  $9.0 \times 10^{-4} \text{M}^{-1} \text{s}^{-1}$ ). What might be happening?  
K. Bernauer, P. Pousaz, J. Porret and A. Jeanguenat, *Helv. Chim. Acta* **71**, 1339 (1988).

10. Suggest why the oxidation

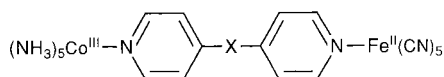


gives solely one product, whether a one- or a two-electron oxidant is used, compared with the behavior of the  $\text{Co}(\text{III})$  analog (Sec. 5.8.3).

H. Taube, *Electron Transfer Reactions of Complex Ions in Solution*, Chap. 4.

11. When the yellow-orange ion  $\text{Co}(\text{NH}_3)_5\text{py}^{3+}$  is mixed with  $\text{Fe}(\text{CN})_6^{4-}$  (in the presence of edta to prevent the precipitation of products) three color changes are observed. The solution goes orange very rapidly (within milliseconds), then turns yellow in a period of seconds and finally over hours becomes purple. Interpret these changes.  
A. J. Miralles, A. P. Szecsy and A. Haim, *Inorg. Chem.* **21**, 697 (1982).

12. Give a reasonable explanation for the intramolecular electron transfer rate constants ( $k$ ) at  $25^\circ\text{C}$  for the following precursor complexes:

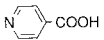


$$\text{X} = \text{CH}_2, k < 6 \times 10^{-4} \text{s}^{-1}$$

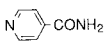
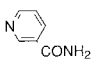
$$\text{X} = (\text{CH}_2)_2, k = 2.1 \times 10^{-3} \text{s}^{-1}$$

$$\text{X} = -\text{CH}=\text{CH}-, k = 1.4 \times 10^{-3} \text{s}^{-1}$$

A. Haim, *Prog. Inorg. Chem.* **30**, 273 (1983), p. 340.

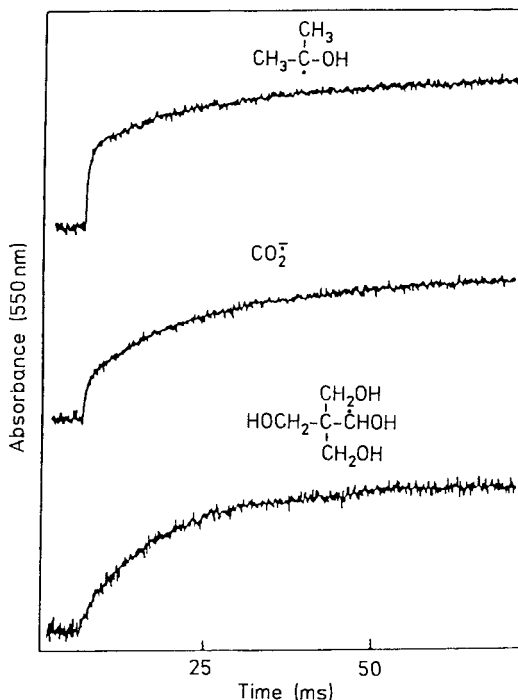
13. The rates of very sluggish outer-sphere reactions of  $\text{Eu}^{2+}$  (also  $\text{V}(\text{II})$  and  $\text{V}(\text{III})$ ) with  $\text{Co}(\text{NH}_3)_6^{3+}$  and  $\text{Co}(\text{NH}_3)_5\text{py}^{3+}$  are increased markedly by addition of small (mM) amounts of  and inhibited by  $\text{Eu}^{3+}$ . The reaction products remain unchanged. The 3-pyridine carboxylic acid is without effect. Account for this behavior.  
E. S. Gould, *Acc. Chem. Res.* **18**, 22 (1985).

14. The second-order rate constants for reaction of  $\text{Co}(\text{NH}_3)_5\text{L}^{n+}$  ( $k_{\text{H}}$ ) and  $\text{Co}(\text{ND}_3)_5\text{L}^{n+}$  ( $k_{\text{D}}$ ) with  $\text{V}^{2+}$  and  $\text{Cr}^{2+}$  have been measured. Explain the results shown

Ligand, L	$k_{\text{H}}/k_{\text{D}}(\text{V}^{2+})$	$k_{\text{H}}/k_{\text{D}}(\text{Cr}^{2+})$
py	1.54	1.48
$\text{H}_2\text{O}$	1.54	—
$\text{N}_3^-$	1.04	—
$\text{NCS}^-$	1.41	1.34
	1.16	1.07
	1.44	1.45

M. M. Itzkowitz and F. R. Nordmeyer, *Inorg. Chem.* **14**, 2124 (1975).

15. The absorbance changes shown below occur for the reaction of the radicals with pentaammine(histidine-33)ruthenium(III) ferricytochrome c,  $\text{PFe}^{\text{III}}-\text{Ru}^{\text{III}}$  (see (5.84)). The final product is  $\text{PFe}^{\text{II}}\text{Ru}^{\text{III}}$ . Absorbance increases at 550 nm are largely as a result of the step  $\text{PFe}^{\text{III}} \rightarrow \text{PFe}^{\text{II}}$ . Interpret the changes (particularly the relative absorbances associated with the very fast and slower absorbances).



Problem 15. Reduction of  $\text{Ru}(\text{III})$ -cytochrome-c- $\text{Fe}(\text{III})$  by pulse radiolysis-generated radicals. Reproduced with permission from S. S. Isied, C. Kuehn and G. Worosila, *J. Amer. Chem. Soc.* **106**, 1722 (1984).

S. S. Isied, C. Kuehn and G. Worosila, *J. Amer. Chem. Soc.* **106**, 1722 (1984).

16. The reduction of the ruthenated plastocyanin protein  $\text{PCu}^{\text{II}}\text{Ru}^{\text{III}}$  by  $\text{CO}_2^-$  results in 72%  $\text{PCu}^{\text{I}}\text{Ru}^{\text{III}}$  and 28%  $\text{PCu}^{\text{II}}\text{Ru}^{\text{II}}$ . This very fast stage is followed by a slower one in which  $\text{PCu}^{\text{II}}\text{Ru}^{\text{II}}$  is converted by a first order process into  $\text{PCu}^{\text{I}}\text{Ru}^{\text{III}}$ . For this conversion

$$d[\text{PCu}^{\text{I}}\text{Ru}^{\text{III}}]/dt = \{k_1 + k_2[\text{PCu}^{\text{II}}\text{Ru}^{\text{III}}]\}[\text{PCu}^{\text{II}}\text{Ru}^{\text{II}}]$$

$k_1 = 0.024 \pm 0.058 \text{ s}^{-1}$  and  $k_2 = 1.2 \times 10^5 \text{ M}^{-1} \text{ s}^{-1}$ . Comment on the values and the significance of  $k_1$  and  $k_2$ .

M. P. Jackman, J. McGinnis, R. Powls, G. A. Salmon and A. G. Sykes, *J. Amer. Chem. Soc.* **110**, 5880 (1988).